A genetic screen for genes involved in dendrite morphogenesis of central neurons in *Drosophila melanogaster*

Annemarie North B.Sc (Hons), M.Sc

Awarded by
Oxford Brookes University, Oxford
in collaboration with
University of Cambridge, Cambridge

August 2011

A thesis submitted in partial fulfilment of the requirements
of the award of Doctor of Philosophy

Declaration

I hereby declare that this thesis is my own work and effort and that it has not been submitted anywhere for any award. Where other sources of information have been used, they have been acknowledged.

Signature: …….

Date: …….

For Hazel and Rachel

The true delight is in the finding out rather that the knowing

Isaac Asimov

Even if you fall on your face, you're still moving forward

Victor Kiam

Abstract

In order to produce a functional nervous system, it is essential that neurons project synaptic terminals into particular regions of the developing nervous system, so as to make connections with appropriate pre- and postsynaptic partners. While axon targeting has been studied extensively, much less is known about how the postsynaptic dendrites grow and branch.

To study dendrite morphogenesis, a mosaic loss of function screen was developed and carried out in *Drosophila melanogaster* for chromosomal regions required for motor neuron dendrite development. Specifically, the Mosaic Analysis with a Repressible Cell Marker (MARCM) method was modified so that individual motor neurons can be made homozygous for a defined genomic aberration in an otherwise wild-type (heterozygous) background and visualised during early larval stages. In addition, 85 defined chromosomal deficiencies were recombined individually onto FRT-carrying chromosomes to be screened for genes involved in dendrite morphogenesis. These recombinant FRT-deficiency chromosomes provided a coverage of ~64.3% of chromosome 2 (3864 annotated genes). After analysis of ~35% of chromosome 2 (2092 annotated genes), 814 central nervous systems and 414 neurons, five genomic regions were identified that had a dendritic phenotype when absent.

One of these regions, 2R:23D2;23E, uncovered by FRT40A *Df(2L)S2590*, was studied in more detail. Overlapping deficiencies were screened to define more precisely the region of chromosome 2 where the loss of gene(s) caused a dendritic phenotype in motor neurons. Of the seven candidate genes identified in this region, only one was shown to have expression in the embryonic central nervous system – the as yet uncharacterised gene *CG34393*. Based on sequence comparisons, *CG34393* is predicted to encode a putative Ras guanyl exchange factor. Expression data from putative homologues in other species and *Drosophila* genes that are expressed in a similar developmental time course suggest that CG34393 may be involved in synapse development.

Contents

Figures

Tables

Chapter 1 Introduction

Neurons are polarised cells generally consisting of a cell body, postsynaptic dendrites and presynaptic axons. The morphology of neurons in vertebrates and invertebrates is diverse and is a reflection of the many different functions undertaken by these highly specialized cells. Invertebrate neurons are usually unipolar, where a single neurite outgrowth from the cell body branches to give rise to both axon and dendrites. In contrast, vertebrate neurons are typically multipolar, where both dendrites and axons emerge and extend from the cell body (Fig. 1.1) (Grueber & Jan 2004; Sanchez-Soriano et al 2005). Despite these organisational differences, vertebrate and invertebrate neurons share many features at the molecular and developmental level, such as: regulation of development of the nervous system by neurotrophic factors (Palgi et al 2009); development of visual circuits (Sanes & Zipursky 2010); similar structural make-up of dendrites (Sanchez-Soriano et al 2005; Takahashi et al 2007); timing of neurite outgrowth (Sanchez-Soriano et al 2005) and compartmentalisation of molecules (Katsuki et al 2011). Thus, there is some evidence that suggests that invertebrate and vertebrate neurons are homologous.

Information is passed between neurons by means of synaptic contacts (Fig. 1.1). In order to produce a functional nervous system, it is essential that neurons project synaptic terminals into particular regions of the developing nervous system, so that connections with appropriate pre- and postsynaptic partners can be made. Underlying mechanisms have been the subject of many studies that investigate, for example, the role of guidance molecules, cell adhesion and synapse formation (Baker et al 2006; Blagburn & Bacon 2004; Collins & DiAntonio 2007; Mochizuki et al 2011).

Until recently, much work focused on how axons navigate over long distances through a developing nervous system to their postsynaptic targets; much less is known about the development of dendrites, which are functionally and biochemically distinct from axons. The role of axons is to propagate signals and transmit information to another cell, whereas dendrites are mostly postsynaptic, receiving and integrating inputs from other, presynaptic neurons. One way in which axons and dendrites differ is by differential distribution of proteins. For example, early work identified *microtubule-associated protein 2* (*MAP2*) as a

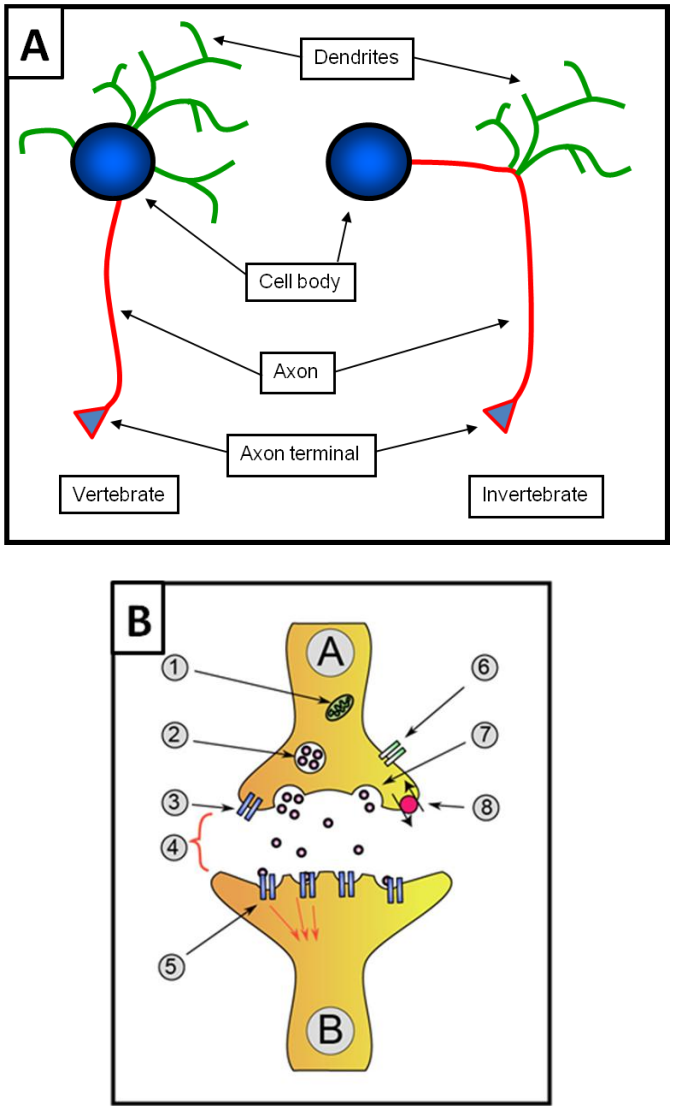

Figure 1.1 Main features of neurons and synapses

(**A**) Neurons generally consist of a cell body, postsynaptic dendrites and presynaptic axons. Dendrites in vertebrate neurons usually branch from the cell body whereas invertebrate neuron dendrites branch from the axon. (**B**) A typical chemical synapse, with neuron 'A' transmitting to neuron 'B'. Key: 1 = mitochondria; 2 = synaptic vesicle with neurotransmitters; 3 = autoreceptor; 4 = synapse with neurotransmitter released; 5 = postsynaptic receptors activated by neurotransmitter (leading to induction of a postsynaptic potential); 6 = calcium channel; 7 = exocytosis of a vesicle; 8 = recaptured neurotransmitter.

gene whose protein product is localised only in the dendrites of different types of neurons in rat brain (Bernhardt & Matus 1984). Since then, many molecules such as Neuregulin-2, Staufen and Kv2.1 (Kohrmann et al 1999; Lim et al 2000; Longart et al 2004), have been shown to be differentially expressed in, or targeted to dendrites as opposed to axons (and vice versa). As axons and dendrites extend they have to navigate through a similar environment, often at the same time and can therefore be exposed to the same cues and signals (Chiba et al 1993; Teichmann & Shen 2011). However, axons and dendrites can respond differently to the same cues (Polleux et al 2000), suggesting that structural and cytoskeletal differences between axons and dendrites might extend to differences in responsiveness to guidance cues. Moreover, the polarity of synapses also suggests that different mechanisms may be necessary for a neuron to discriminate between pre- and postsynaptic partner terminals during synapse formation. Dendrites also differ from axons in terms of structure. In axons, the arrangement of microtubules is uniform (plus end distal) whereas the polarity of microtubules in dendrites is mixed (Baas 1998). A study by Takahashi and colleagues (2007) has shown that when cultured hippocampal neuron dendrites convert to axons during a regeneration process, the microtubule orientation changes from mixed to the uniform plus end distal arrangement (Takahashi et al 2007). In *Caenorhabditis elegans*, it has been demonstrated that polarity can also be maintained by external factors. For example, Poon et al (2008) found that in loss of function mutants of UNC-6 (Netrin) and its receptor UNC-5, presynaptic components became erroneously localized to dendrites.

Features of dendrites

Dendrites are the ‘antennae’ of neurons; specialized, highly branched, tree-like projections designed to receive and integrate information from other neurons. A dendritic tree may receive thousands of inputs, which can be of different types (e.g. excitatory or inhibitory) and strengths. How dendrites are shaped into cell type-specific geometries and make connections with particular presynaptic partners remains incompletely understood. The

spatiotemporal patterns of input are integrated by the dendritic arbor into coherent signals deciding not only if an action potential is generated, but how the neuron responds to subsequent inputs (Hausser et al 2000; Spruston et al 1994). Dendrites are also capable of modulating input, by amplification or attenuation of the signal from distal dendrites to (Crandall et al 2010), and in concert with the cell body (Myoga et al 2009),

Neurons can be characterised by a number of anatomical features including cell body size and position, axonal projection and dendritic tree architecture. These features can be used to identify and distinguish types and individual neurons in populations of nerve cells, as demonstrated in *Danio rerio* (zebrafish), *D. melanogaster* and *C. elegans* (Albeg et al 2011; Bernhardt et al 1990; Landgraf et al 1997; Vonhoff & Duch 2010). Different neuronal types have characteristic dendritic branching patterns (Fig. 1.3; Fig. 1.2 describes the neuromuscular unit of the *Drosophila* larva, placing the images of labelled motor neurons herein into an anatomical context), and morphology is thought to be related to function. For example, in the mouse, a small population of retinal ganglion cells in the eye detect upward motion via asymmetric dendritic arbors aligned dorsoventrally (Kim et al 2008). Therefore, for the identification of individual neurons, dendritic morphology is a particularly good indicator.

Dendritic growth

During differentiation and maturation, neurons undergo different phases of dendritic growth in order to attain the appropriate branching pattern (reviewed in Parrish et al 2007b; Scott & Luo 2001). Live imaging of neurons in different model organisms has shown that first, there is budding and outgrowth, followed by extension and branching of dendrites (Cline 2001). Branching can take place at the growth cone (through splitting, at tips) or by interstitial branching (independent of the growth cone) (Bray 1973; Dailey & Smith 1996). With maturation, cessation of growth, refinement of branches and finally stabilisation and synapse formation with presynaptic partners occurs (Niell & Smith 2004). Dendrites are plastic structures that seem to retain the ability to remodel in response to stimuli such as activity

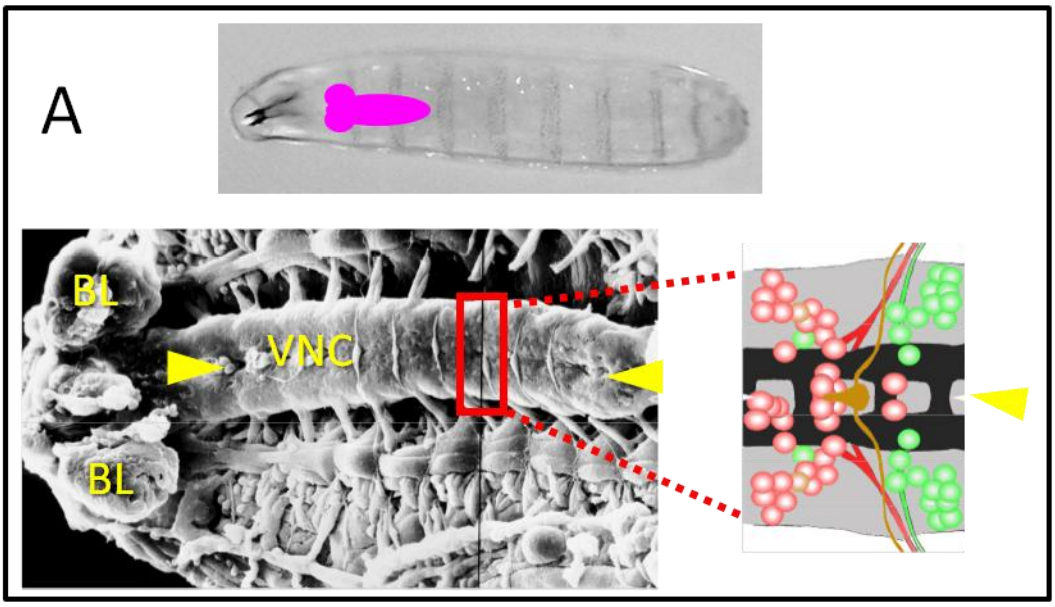
A
BL
VNC
BL

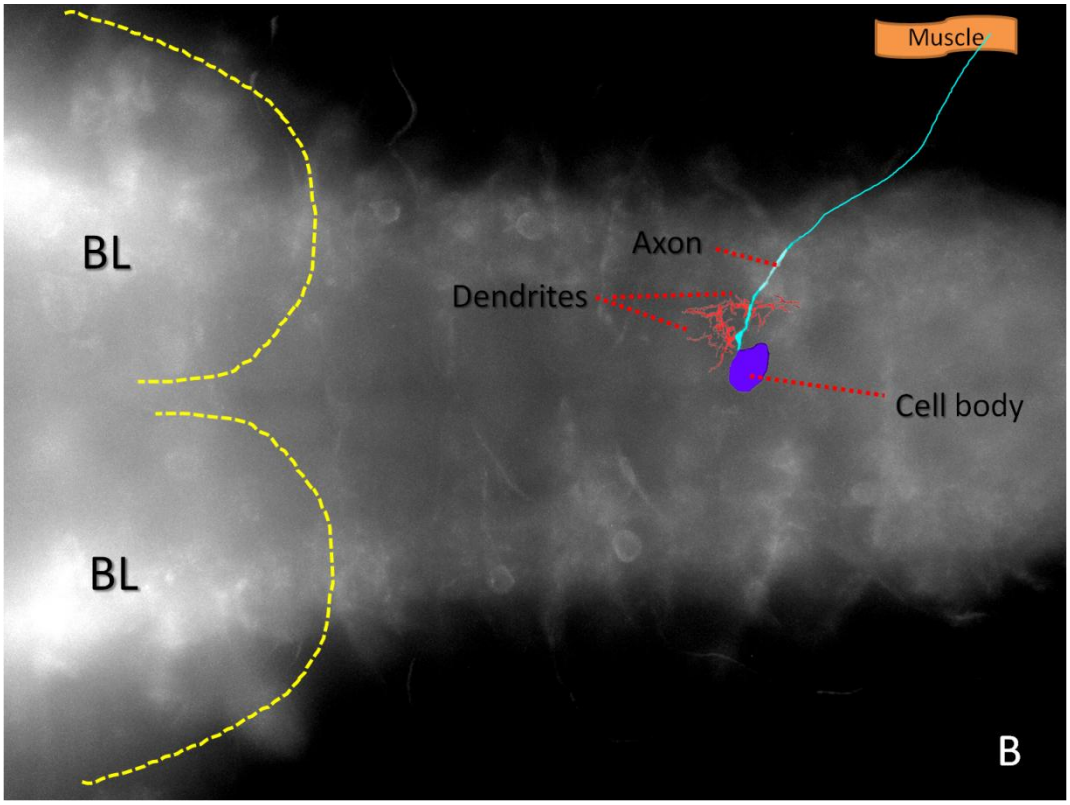
Muscle
BL
Axon
Dendrites
Cell body
BL
B

Figure 1.2 The larval *Drosophila* neuromuscular system

(**A**) *Top*: Ventral view of a first instar larva, with approximate location of the CNS highlighted in pink. Repeated vertical banding on the cuticle are the denticle belts, while anteriorly, the dark mouth hooks are plainly visible. The larva is ~1 mm in length. *Bottom left*: Scanning electron micrograph of a filleted embryo, just prior to hatching, revealing the brain lobes (BL) and ventral nerve cord (VNC). The expanded red box (*bottom right*) shows two parasegments, with cell bodies of motor neurons from the anterior segment in red, and those from the posterior segment in green. Each (abdominal) segment contains a repeated pattern of ~34 motor neurons (Landgraf et al 1997). The dark grey area is the neuropil, where axons fasciculate and synaptic connections are made. Yellow arrowheads define the midline.

(**B**) UV autofluorescence of a dissected first instar larval CNS, with an overlaid cartoon of an RP2 motor neuron highlighting the main components of a neuromuscular unit: motor neuron, comprising cell body, axon and dendrites, and out in the periphery, the target muscle.

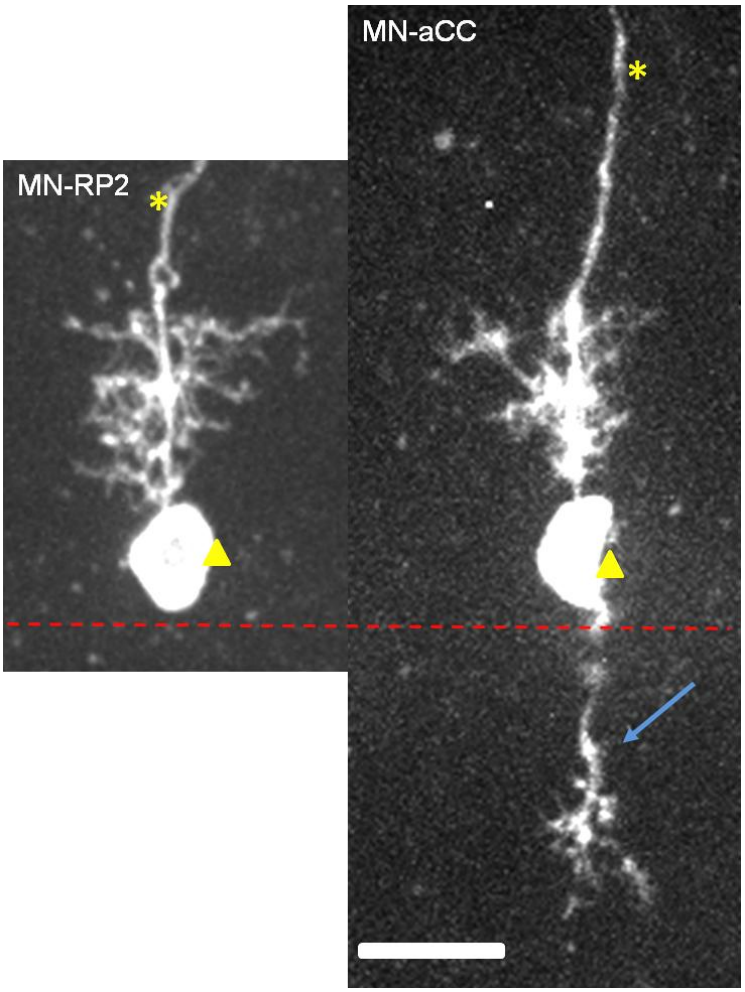

Figure 1.3 Neurons have characteristic dendritic branching patterns

(*Left*) The *Drosophila* larval RP2 motor neuron can be recognised by the dorsomedial location of the cell body and its single ipsilateral 'triangular' shaped arbor. (*Right*) The motor neuron aCC also has a dorsomedial cell body, and two dendritic arbors, one of which is contralateral (arrow). These two neuron types can be targeted by the 'RN' fractionated *eve* promoter (see main text).

Triangle = cell body; asterisk = axon; red dashed line = midline; scale bar = 10 µm.

(Lohmann & Wong 2005; Tripodi et al 2008) or changes in the environment (e.g. metamorphosis in insects) (Santos et al 2006; Williams & Truman 2005b).

There are several cellular mechanisms that regulate dendritic growth, the attainment of the correct dendritic morphology and finally synapse formation. These include the ability to sample and respond to the external environment of the cell, ultimately leading to modulation of the cytoskeleton. The cell must then be able to recognise its appropriate presynaptic partners and make synaptic connections with them. Axons essentially undergo the same process, and by looking at how axons grow, target and connect with their (postsynaptic) partner, insights can be gained into how dendrites might navigate the same complex and changing environment in order to find their (presynaptic) partners.

The molecular basis of dendrite growth

The development of dendrites (and axons) occurs in response to a complex array of cues. How a dendritic tree develops its characteristic branching pattern depends on extrinsic cues as well as the cell's intrinsic genetic identity/programme of differentiation, which determines how it responds to extrinsic cues encountered, including neuronal activity.

Parallels with axon guidance

Motor axon pathfinding has been extensively studied in both vertebrates and invertebrates (Bonanomi & Pfaff 2010; Raper & Mason 2010; Sanchez-Soriano et al 2007). As they grow, axonal growth cones are presented with a series of choices that will facilitate the axon leaving the CNS in a reproducible and stereotypical way, to join an appropriate nerve branch leading to the target in the periphery, then delineate from the nerve and terminate at the target. What mechanisms ensure that the correct choice is made at these decision points? Work in the vertebrate limb describing the mechanisms involved in motor axon decision between dorsal or ventral targets (Kania et al 2000; Sharma et al 1998) and nerve branch choice (segmental versus intersegmental), and midline crossing in *Drosophila*, (reviewed in

Sanchez-Soriano et al 2007), propose a model where growth cone guidance is controlled by signalling in different axes: mediolateral, anteroposterior and dorsolateral.

The diffusible ligands Slit and Netrin and their respective cell surface receptors, Roundabout (Robo) and Frazzled (Fra), have been intensively studied and mediate axon guidance with respect to the ventral midline (e.g. in the mediolateral axis); Slit-Robo via repulsion from the midline and Netrin-Frazzled/DCC by attraction to the midline (reviewed in Dickson & Gilestro 2006; Killeen & Sybingco 2008). Slit-Robo signalling in *Drosophila* has been shown to position motor axons in the CNS (Rajagopalan et al 2000a; Rajagopalan et al 2000b; Simpson et al 2000a; Simpson et al 2000b) and to target sensory neuron terminals to their appropriate termination zones (Zlatic et al 2003).

In *Drosophila*, one anteroposterior guidance mechanism is thought to be via the repulsion of Derailed-positive axons by the ligand Wnt oncogene analogue 5 (*Wnt5*). Since Wnt5 is enriched in the posterior commissure, growth cones of Derailed-positive axons are repulsed by this and grow anteriorly, crossing the midline by way of the anterior commissure (Yoshikawa et al 2003). Similarly in mice, Wnt1 and Wnt5a have been shown to be involved in repulsion of corticospinal tract axons via the receptor Ryk (the vertebrate homologue of Derailed) (Liu et al 2005). In contrast, *Wnt4-Frizzled3* signalling in mice has been reported to mediate attraction of post-commissural crossing axons (Lyuksyutova et al 2003).

Positioning in the dorsoventral axis is perhaps the least well studied of the three axes. Nevertheless, in *Drosophila* sensory neurons, semaphorin gradients have been shown to mediate the dorsoventral positioning of axon terminals via *Plexin* receptors (Zlatic et al 2009). Similarly, during development of the embryonic *Xenopus* visual system, dorsoventral targeting of retinal axons is controlled by the ligand *ephrin-B* through its receptor *EphB* (Mann et al 2002).

Dendritic guidance

A central question has been whether the molecular pathways that underlie axon growth cone guidance also have a role in positioning postsynaptic dendritic terminal arbors. The

signalling mechanisms that target dendrites to their correct position in the CNS are still poorly understood. Perhaps the best studied is Slit-Robo signalling, which patterns axons with respect to the ventral midline, in the mediolateral axis. One of the three *slit* genes found in mammals (*slit1*) induces more complex dendritic morphologies (increased dendritic length and branching) in cultured mouse neurons (Whitford et al 2002). In *Xenopus laevis*, Hocking et al (2010) suggest that Slit-Robo signalling can have distinct functions in axons and dendrites; Slit acting via the Robo2 receptor as a branching/growth factor in dendrites distinct from axon guidance, while Robo 2 and 3 receptors have a complementary role and function in parallel in axons during axon guidance. In *Drosophila* embryos, Slit signalling through Robo receptors has been shown to be important for setting the growth rate and branching pattern in peripheral sensory multi-dendritic dendrite arborisation neurons (Dimitrova et al 2008); in the initial outgrowth of dendrites in the central aCC motor neuron (Furrer et al 2007); and together with Netrin-Frazzled for the correct positioning of dendrites in the mediolateral axis in the embryo and larva (Mauss et al 2009), and in adult flies (Brierley et al 2009).

Less in known about the factors that control dendrite targeting in the anteroposterior and dorsoventral axes in *Drosophila*. Nevertheless, Sato and co-workers recently showed that in multidendritic sensory neurons mutant for the Rho GTPase activating protein Crossveinless-c, dendrites are unable to grow properly in the anteroposterior body axis, but still form dorsally directed branches normally (Sato et al 2010). Further, the receptor Semaphorin-1a has been shown to be required for correct targeting of olfactory projection neurons in the *Drosophila* antennal lobe in the dorsolateral and ventromedial axes (Komiyama et al 2007), though in the embryonic ventral nerve cord Semaphorin-Plexin signalling was found to have no clear effect on dendritic arbor positioning (Mauss 2008).

Intrinsic factors required for dendrite morphogenesis

Signal transduction cascades and transcription factors are intrinsic components of the cell. They are important for dendrite growth as they are the link between external cues and the

corresponding reaction to this information by the neuron, and encompass a whole range of cellular responses, from local rearrangement of the cytoskeleton to triggering cell death.

Signal transduction cascades are complex interlinked processes that form an extensive signalling network within a cell. One example, are the Rho family of GTPases, which are important regulators of the cytoskeleton (Georges et al 2008), with roles in neuronal polarity (Witte & Bradke 2008), synapse development (Tolias et al 2011) and dendritic growth (Kennedy et al 2005). In axons, guidance receptors such as Robo are thought to be linked to Rho GTPases by the acivity of guanine nucleotide exchange factors (GEFs) and GTPase activating proteins (GAPs) (Bashaw & Klein 2010; Hall & Lalli 2010). Interestingly, the *Drosophila Son of sevenless* (*Sos*) gene – a GEF capable of regulating both Rac and Rho GTPase signalling pathways – is an example that demonstrates the link between an externally derived signal and a change in dendrite growth dynamics via a signalling pathway. By forming a protein complex with the Robo receptor and an adaptor protein (Dreadlocks) at the plasma membrane, Sos has been shown to regulate Rac-dependent cytoskeletal rearrangements in response to Slit (Yang & Bashaw 2006).

A key characteristic of different neuronal types are their cell type-specific morphologies, particularly of their dendritic arbors. Thus, specification of the cell fate by transcription factor codes will impact on the development of the dendritic arbor. It is conceivable that transcription factors could specify single or multiple aspects of dendritic arbors (Komiyama et al 2003). Parrish and colleagues (2006) identified more than 70 transcription factor genes that affect sensory neuron development. Using RNAi, they screened the *Drosophila* genome for transcription factor encoding genes involved in the development of dendritic arborisation sensory neurons and identified three functional groups: genes that promote or inhibit: (i) outgrowth; (ii) branching; or (iii) routing (Parrish et al 2006b). Examples of transcription factors known to be involved in specifying different aspects of sensory neuron dendrite morphogenesis include *Hamlet, spineless* and *cut*.

Hamlet is a zinc-finger protein that functions as a binary switch during sensory neuron development. It promotes the formation of one type of sensory neuron (external sensory) as opposed to another (multidendritic) (Moore et al 2002). In *spineless* loss of function mutants,

different classes of da neurons incorrectly simplify or elaborate their dendritic arbors (Kim et al 2006). Levels of Cut in da sensory neurons were found to correlate with distinct dendritic branching patterns; high levels of Cut were observed in neurons with complex morphologies and low levels in neurons with simple dendrites (Grueber et al 2003). More recent work has suggested that combinatorial expression of transcription factors may be able to specifiy dendrite morphology. Different classes of da sensory neurons can be 'grouped' by the differential expression of Cut, Knot, Abrupt and Spineless (Matthews et al 2007). For example co-expression of Abrupt and Spineless is found in the least complex class I neurons, whereas Cut, Knot and Spineless are expressed in the most complex class IV neurons.

Partner recognition and synapse formation

Once a dendritic arbor has reached its target area, it must find and make synaptic connections with the appropriate partner. This process involves target recognition, adhesion, and induction of pre- and postsynaptic specialisations (synaptogenesis) (reviewed in Gerrow & El-Husseini 2006; Shen & Scheiffele 2010; Waites et al 2005).

Local priming factors released into the target area can help partner neurons establish synaptic connections. For example, in the developing mammalian brain, secretion of thrombospondins by immature astrocytes promotes the formation of synapses (Christopherson et al 2005). Synaptic partner choice can also be regulated intrinsically by transcription factors. The *Drosophila* transcription factor Myocyte enhancer factor 2 (Mef2) has been well studied in muscle development, but also has a role in neurons. In a screen for genes involved in *Drosophila* circadian behaviour, Mef2 was shown to be expressed in pacemaker neurons, and is required for maintaining normal circadian rhythms (Blanchard et al 2010). In rats, MEF2 has been shown to be involved in activity-dependent development of synapses (Flavell et al 2006) and in 2008, Flavell and co-workers identified the downstream targets of MEF2, which suggests that MEF2 regulates synapse number by activating mechanisms that lead to synapse loss (Flavell et al 2008). By restricting synapse number,

neurons prevent the formation of too many contacts, either with the target cell, or with inappropriate partners.

The role of activity in the regulation of dendrite development by calcium (Ca^{2+}) signalling is well documented (reviewed in Chen & Ghosh 2005; Konur & Ghosh 2005; Libersat 2005; Redmond & Ghosh 2005). cAMP response element binding (CREB) protein, NeuroD and calcium responsive transactivator (CREST) are a few of the calcium sensitive transcriptional activators involved in this process. Increased neural activity results in increased intracellular calcium levels by means of different mechanisms such as voltage gated Ca^{2+} channels, ligand gated receptors (e.g. AMPA and NMDA) (allowing entry of Ca^{2+}) and the release of Ca^{2+} from intracellular stores. Calcium ions then act as second messengers, acting on downstream targets involved in dendrite morphogenesis. One such interaction that links activity to dendrite arborisation is that of CREB and Wnt-2. In cultured hippocampal neurons, Wayman and colleagues (2006) demonstrated that neuronal activity enhanced CREB dependent transcription of Wnt-2, a molecule that stimulates dendritic arborisation (Wayman et al 2006).

Studies have shown that cell adhesion molecules such as Nectins and Down Syndrome Cell Adhesion Molecule (DSCAM) also have a role in target recognition and synaptogenesis. In vertebrates, Nectins are cell adhesion molecules that are found at adherens junctions (protein complexes that link one cell to another) and have been implicated in the formation of synapses. Nectin-1 is predominantly localised in the presynaptic membrane whereas its heterophilic partner Nectin-3, is localised in the postsynaptic membrane. Inhibition of heterophilic binding of Nectins results in smaller synaptic size, but a simultaneous increase in synapse number (Mizoguchi et al 2002). More recently it has been shown in rats that axo-dendritic recognition is facilitated by heterophilic binding of Nectin-1 and -3 in cooperation with cadherins (calcium dependent cell adhesion molecules) (Togashi et al 2006).

Drosophila Downs syndrome cell adhesion molecule (Dscam) is an extremely diverse transmembrane protein, where alternative splicing can potentially generate many thousands of isoforms. It is thought that this diversity provides a mechanism in which the identity of many neurons can be specified by only a few genes (reviewed in Millard & Zipursky 2008;

Schmucker & Flanagan 2004; Zipursky et al 2006). Dscam contributes to defining cellular identity by facilitating recognition of self, so that neurons do not make connections with themselves; it may also explain why dendrites from the same neuron spread out and do not tend to overlap each other (Schmucker & Flanagan 2004). Dscam has been shown to be necessary for self-avoidance in da sensory neurons (Soba et al 2007) and loss of Dscam in single da neurons has been shown to increase incidences of self-crossing (Hughes et al 2007). Reduction in the diversity of Dscam using mutants results in specific connection defects in sensory neurons (Chen et al 2006). Dscam homologues in vertebrates do not produce highly variant isoforms by alternative splicing but seem to function as homophilic cell adhesion molecules. For example, in the vertebrate retina, retinal ganglion cells and presynaptic partner interneurons project their synaptic terminals to, and form connections in, distinct sublaminae of the inner plexiform layer. Yamagata and Sanes (2008) have demonstrated that the cell adhesion molecules Dscam and Sidekick are expressed in subsets of interneurons and retinal ganglion cells that do not overlap, and that these subsets synapse together in discrete sublaminae defined by Dscam and Sidekick expression (Yamagata & Sanes 2008). Other studies of cell adhesion in *Drosophila* focus on the neuromuscular junction as the model synapse. Recently, Sun and colleagues (2011b) demonstrated that neuroligin 2, a cell adhesion molecule, is expressed in the embryonic and larval CNS and at the neuromuscular junction, where it binds Neurexin, and is required for postsynaptic synaptogenesis (Sun et al 2011b). Interestingly, mutations in a human neuroligin gene have been associated with schizophrenia, where synaptic dysfunction may be but one component of this multifaceted disorder (Sun et al 2011a).

Although much has been discovered so far, the mechanisms that underlie dendrite morphogenesis, particularly how the structure of dendrites is generated and maintained, remain incompletely understood. This has implications for the study of disorders and disease where dendritic structure is altered (see below).

Dendrites and disease

Anomalies in dendrites can be correlated with many disorders (Fiala et al 2002) resulting in mental retardation, and are sometimes the result of a single gene defect (Dierssen & Ramakers 2006). Studies in model organisms can help us to have a greater understanding of such conditions. Indeed, *Drosophila* has become a valuable tool for investigating nervous system disorders found in humans (Gatto & Broadie 2011). For example, Fragile-X syndrome and Oligophrenia are both caused by the misregulation of gene expression.

In Fragile-X syndrome, a trinucleotide repetition mutation in Fragile-X mental retardation protein (FMRP) silences the gene resulting in reduced levels of FMRP (Feng et al 1997; Kremer et al 1991; Pieretti et al 1991). The role of FMRP is not fully understood but it is thought to be necessary for mRNA export from the nucleus to the cytoplasm of the dendrites, thereby regulating translation. In zebrafish, morpholino (antisense oligo) knockdown of FMR1 causes abnormal axonal branching, guidance and defasciculation defects (Tucker et al 2006). A null mutant mouse model of Fragile X syndrome was found to have elongated spines (sites of synaptic connectivity in vertebrates) and enhanced long term depression (the weakening of a synapse). Mice also exhibited behavioural defects reminiscent of patients with Fragile X (Koekkoek et al 2005).

The *Drosophila* homologue of FMRP (dFMRP) has multiple roles in a variety of tissues and processes including oogenesis (Costa et al 2005), spermatogenesis (Zhang et al 2004) and more interestingly dendrite outgrowth, branching and synaptogenesis (Zhang et al 2001). In *Drosophila* dendritic arborisation (da) sensory neurons, loss of function of dFMRP results in increased number of higher order branches whereas increased levels of dFMRP generated the reverse phenotype (Lee et al 2003; Zhang et al 2001). In this study, dFMRP was also found in a ribonuclear complex containing mRNA for the small GTPase Rac1. This is an interesting finding because Rac1 is a member of the Rho family of small GTPases, which include RhoA and Cdc42. This group of molecules act downstream of environmental cues and are involved in remodelling the actin cytoskeleton (reviewed in Van Aelst & Cline 2004; Watabe-Uchida et al 2006). For example, *Drosophila* visual system neurons mutant for

Cdc42 show a variety of phenotypes including increased dendritic length, branching position and branch thickness consistency (calibre) (Scott et al 2003). dFMRP has also been shown to be involved in the regulation of the actin cytoskeleton by binding to the mRNA of the *Drosophila* homologue of *profilin* (*chickadee*) (Reeve et al 2005). Profilin is a molecule that enhances actin polymerisation, a mechanism essential for organised filopodial led migration and therefore dendritic growth (the cytoskeleton of dendritic growth cones mainly consist of actin filaments) (Dehmelt & Halpain 2004; Witke et al 1998). Further, over-expression of dFMRP in mushroom body neurons leads to decreased growth, branching and synapse formation, while downregulation leads to the converse phenotype (Pan et al 2004). More recently, Tessier et al (2011) demonstrated that dFMRP can regulate calcium signalling in mushroom body neurons, which has implications for memory formation and can affect the structural organization of dendrites (McBride et al 2005; Tessier & Broadie 2011).

A protein that has been associated with non-specific mental retardation (Oligophrenia) is Oligophrenin-1. In humans, mutations in this gene cause cerebellar hypoplasia (underdevelopment) that leads to motor and cognitive defects (Zanni et al 2005). Oligophrenin-1 codes for a Rho-GTPase activating protein, shown to be required for dendritic spine morphogenesis: spine length in CA1 neurons of rat hippocampal slices is reduced in molecular knockdown experiments (Govek et al 2004). Oligophrenin is localised to actin at the tip of growing neurites and may also have a role in dendrite morphogenesis (Fauchereau et al 2003). More recently, it has been found to locate to dendritic spines in response to NMDA receptor activation, where it stabilizes synaptic AMPA receptors, and thus, spine size (Nadif Kasri et al 2009). A *Drosophila* homologue of this gene has yet to be identified.

Genetic screens: *Drosophila melanogaster* as a genetic model system

The fruit fly *Drosophila melanogaster* is a good model for investigating how dendrites grow and find their presynaptic partners. It is easy and comparatively cheap to rear in the laboratory, has a short life cycle and produces many progeny. Various techniques and

genetic tools are in place that allow the genetic manipulation of neurons (and dendrites) and permit their visualisation with relative ease. Moreover, the embryonic and larval motor neurons have been relatively well studied and tools are available for labelling and manipulating their presynaptic cholinergic interneurons (Baines et al 2001; Landgraf et al 2003; Schmid et al 1999).

One way in which genes involved in a particular process can be identified is a genetic screen. There are several methods for carrying out genetic screens in *Drosophila*, each with its own advantages and limitations. In recent years, *P-element* screens have become an important tool with which to find genes involved in a given process. *P-elements* are a family of transposable elements in the genome of *Drosophila.* The main drawback of carrying out knockout screens is that there are hotspots in the genome to which *P-elements* are preferentially targeted (Thibault et al 2004). This means that not all genes can be targeted for analysis. Other transposable elements include *piggyBAC* and *Minos*. *PiggyBAC* has been successfully used to generate insertions in >2000 genes, and led to the identification of two Cohesin subunits required for proper axon pruning in a mosaic screen in *Drosophila* mushroom body neurons (Schuldiner et al 2008). *Minos*, has been used in a variety of model organisms to generate mutants (de Wit et al 2010; Hozumi et al 2010) either by insertional mutagenesis or by generating imprecise excisions (Metaxakis et al 2005).

Misexpression/gain of function screens have been used identify genes involved in dendrite morphogenesis in peripheral and central neurons (Ou et al 2008) although this type of screen does not necessarily demonstrate that the candidate gene(s) is/are required in the cell/tissue of interest, only that it can have an effect.

Other screens use RNA interference, where small interfering double stranded RNA (siRNA) is used to target endogenous RNA and impede normal expression of the gene of interest (reviewed in Boutros & Ahringer 2008). Studies have been carried out in cultured cells (e.g. identifying cell cycle regulators; (Lents & Baldassare 2006) and whole animals (e.g. looking for genes involved in parasitic infection; Cronin et al 2009). However, issues with using RNAi include OFF-target effects (where other genes are incorrectly targeted) and low efficiency of

knock-down leading to variable phenotypes, and false positives and negatives (Booker et al 2011).

Drosophila screens for genes involved in nervous system development

In recent years, many screens have been used to investigate how axons and dendrites grow and form connections with other neurons. However, the majority of these large scale studies screen neurons found in the *Drosophila* peripheral nervous system – more specifically the sensory da neurons (Gao et al 1999; Parrish et al 2006b). They also use techniques such as EMS mutagenesis, which generate thousands of lines and take many man-hours to analyse (Medina et al 2006). One study has looked at central neuron morphogenesis (Reuter et al 2003), but in mushroom bodies. McGovern and colleagues (2003) carried out a gain of function screen in the *Drosophila* embryonic CNS and identified many genes involved in axon guidance, regulation of the cell cycle, and embryonic patterning, including some transcription factors that had not previously been implicated (McGovern et al 2003). In addition, few studies have addressed the role of synaptogenesis in dendrite morphogenesis. In 2001 Kraut and colleagues executed a gain of function screen at the larval neuromuscular junction (NMJ) for genes involved in axon guidance and synaptogenesis (Kraut et al 2001a). More recently, Liebl and co-workers also screened the larval NMJ for genes involved in synaptogenesis using *P-element* transposon mutants (Liebl et al 2006). However, the NMJ is a presynaptic structure, whereas dendrites are postsynaptic.

These studies, although providing a great deal of data about genes involved in sensory neuron and presynaptic site morphogenesis, can only partly address how central motor neuron dendrites establish and maintain their dendritic arbors. Moreover, there is some evidence to suggest that not all genes involved in sensory neuron dendrite morphogenesis are necessarily involved in dendrite morphogenesis in motor neurons. For example, in different sensory neurons, genes are differentially expressed depending on their class. Nanos, an RNA binding protein has been shown to be required for dendrite morphogenesis in class III and IV da neurons, but not class I and II da neurons (Ye et al 2004). Furthermore,

Abrupt, a zinc finger protein is expressed in distinct subsets of MD sensory neurons (Li et al 2004). Neither gene is expressed in motor neurons.

The morphological diversity of sensory neuron dendrites is linked to their function (e.g. stretch detection) and provides a good system for the study of dendrite development: the arbors are simple, easily visualised (due to their 2D nature at the surface of the cuticle) and have characteristic class-specific arborisations. Further, the development of the PNS is relatively robust, allowing analysis of intact animals that are entirely mutant. However, the drawbacks with the sensory system are that the dendrites do not form synaptic connections with other neurons, do not have to differentiate between numerous potential partners and do not need to incorporate and interpret input from different partner neurons. Therefore, their use as a system to fully understand the development of central neurons is limited.

A screen for genes involved in dendrite morphogenesis

The overall aim of the project was to identify and characterise genes required for the morphogenesis and spatial patterning of central neuron dendritic arbors in *Drosophila melanogaster*. To achieve this, methods for mutagenizing and labelling neurons were developed from widely available existing technologies that include: GAL4/UAS (Brand & Perrimon 1993; Brand & Dormand 1995; Jones 2009); the FLP recombinase/FLP recombinase recombination target (FLP/FRT) system (Golic & Lindquist 1989; Ryder & Russell 2003; Theodosiou & Xu 1998); and mosaic analysis with a repressible cell marker (MARCM) (Lee & Luo 1999; 2001; Wu & Luo 2006). Two techniques were developed: a FLP-out system altered to target a subset of motor neurons (a gain-of-function technique), and a MARCM system modified to target and mutagenise a subset of neurons (a loss-of-function technique).

As the goal of the project was to identify intrinsic genes required for motor neuron dendrite morphogenesis, the final approach taken was a loss-of-function screen with a focus on part of the fly genome (the second chromosome) using a modified version of the MARCM technique (Chapter 2).

The screen also utilised another genetic tool: deficiency chromosomes. These are fly stocks where a defined regions of a chromosome have been deleted, excising between just a few, to hundreds of genes. Hundreds of deficiency stocks are available from the Bloomington *Drosophila* Stock Centre based at Indiana University, USA, a global *Drosophila* repository (http://flystocks.bio.indiana.edu/). Deficiencies can be generated in a number of ways including X-rays, chemical mutagens, *P-elements* and FLP/FRT-based protocols (Parks et al 2004; Ryder et al 2004; St Johnston 2002b). The main advantage of using deficiencies is that hundreds of genes can be screened relatively quickly.

Here, work to develop the screen is presented (Chapter 2), followed by the screen itself (Chapter 3), which identified five chromosomal regions of interest that have a dendritic phenotype when removed. Next, Chapter 4 concentrates on one deficiency [*Df(2L)S2590*] where a region of interest is narrowed to seven candidate genes. Finally, Chapter 5 concentrates on one of these candidates, *CG34393*, an uncharacterised gene.

Chapter 2 Method development

This Chapter describes the development of a modified version of the so-called ‘MARCM’ technique used for the loss of function screen and early experiments that identify technical issues. Efforts to improve the MARCM system through various iterations are presented along with proof of principle data. Finally, characterisation of the system in the control neurons provides the necessary foundation of cell morphology data for the screen, which is detailed in Chapter 3.

The aim of this section was to develop a method that would allow one to simultaneously knockout gene function in selected motor neurons and visualize these cells in the developing *Drosophila* CNS. The first step was to modify an already well established method for generating mosaic animals – MARCM.

Methods for visualising motor neurons in *Drosophila*

The GAL4/UAS system and visualisation of motor neuron dendrites

The introduction of the binary yeast-derived GAL4/UAS (upstream activation sequence) system revolutionised *Drosophila* research (Brand & Perrimon 1993). Proteins of interest are expressed by binding of GAL4 to upstream activation sequences (UAS). Thus, the GAL4 expression pattern determines the spatiotemporal expression profile of the transgene of interest. This binary expression system has been successfully used as a tool to visualise and investigate the role of specific genes in the nervous system of *Drosophila* (Brand & Dormand 1995; Jones 2009).

In order to investigate the morphology of neurons reliably using the GAL4/UAS system, simple expression patterns that reveal a limited number of neurons are required. By fractionating promoter regions of genes that express in the nervous system, such as *fushi tarazu* (*ftz*; (Doe et al 1988) and *even skipped* (*eve*; (Fujioka et al 1999), subsets of neurons can be targeted. One such GAL4 line commonly used in *Drosophila* nervous system investigations uses a derivative of the *eve* promoter that targets a specific subset of neurons: RN2-GAL4 drives expression in a few neurons in the embryonic CNS, aCC and RP2, both motor neurons; and pCC, an interneuron (Fujioka et al 2003). Motor neurons (MN)-RP2 and MN-aCC are well characterised structurally, electrically and developmentally (Baines 2003; Baines et al 2001; Tripodi et al 2008) and are therefore good models for studying dendrite morphogenesis in *Drosophila*. However, while this subset of cells is small compared to the number of motor neurons in the CNS, due to their location and spread of their arbors both segmentally, intersegmentally and contralaterally (aCC) their dendrites

overlap, making identification and quantification of dendritic phenotypes difficult. A method was required that could reduce the frequency of labelling in this subset, so that isolated and distinct arbors could be visualised and analysed.

Development of a FLP-out system to target individual identified motor neurons

The yeast derived FLP recombinase/FLP recombinase recombination target (FLP/FRT) system has been used extensively to study development in *Drosophila* by inducing mitotic clones whose labelled progeny reveal the cell lineage (Golic & Lindquist 1989; Ryder & Russell 2003; Theodosiou & Xu 1998). The introduction of mutations onto FRT-carrying chromosomes also allows phenotypes to be investigated in targeted cells.

The 'FLP-out system' was modified in our laboratory with the aim of developing a method that would allow single distinct neurons to be visualised in their entirety – by fractionating an already limited neuronal expression pattern. Furthermore, as this mosaic method is GAL4/UAS-based, co-expression of genes of interest can also be carried out and their resultant phenotypes examined in the labelled cells.

This variation of the FLP-out system (Fig. 2.1) uses a tandem repeat of the 'RN' (EcoRI-NheI fragment) from the *eve* regulatory region (also used in RN2-GAL4; (Fujioka et al 2003) to drive expression of the yeast enzyme FLP recombinase in three neurons per half segment: the motor neurons aCC and RP2, and the pCC interneuron. FLP recombinase acts on FRT sites, facilitating recombination between them. The FLP-out stock carries a transgene cassette, which comprises two FRT sites that flank a stop codon; the cassette is upstream of GAL4. In those neurons where FLP activity is sufficiently high (levels can be experimentally adjusted using temperature to achieve the frequency of cells targeted required), recombination between the two FRT sites takes place, the stop codon excised and as a result, GAL4 expression is initiated. Inclusion of GFP downstream of an UAS effector, enables cells to be labelled. This method has been used to good effect in a screen for gene that can influence dendrite morphogenesis in sensory and motor neurons (Ou et al 2008)

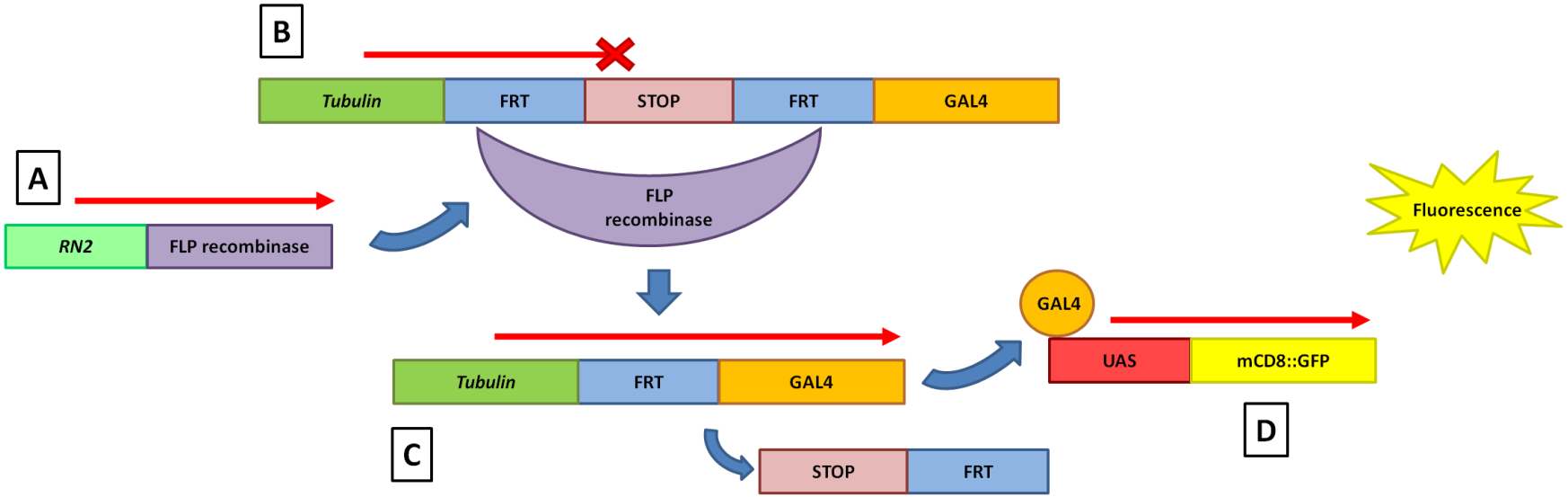

Figure 2.1 The 'FLP-out' system

(**A**) FLP recombinase is expressed in a subset of neurons targeted by the fractionated *eve* promoter 'RN2'. (**B**) Translation of GAL4 under the control of the ubiquitous and strong *tubulin* promoter is prevented by the inclusion of a stop codon upstream of the GAL4 sequence. In the targeted neurons that express FLP recombinase at sufficient levels, recombination between the two FRT sites takes place (**C**), removing the stop codon and thereby allowing expression of GAL4. (**D**) Binding of GAL4 to UAS sites drives expression of a reporter (and/or proteins of interest), which reveals the morphology of the neuron in its entirety.

and to map the changes in an olfactory neuron during transition between life stages (Roy et al 2007). However, this is a gain of function method and does not address the question of the requirement of genes that are intrinsic to neurons: a loss of function technique is needed.

Mosaic analysis with a repressible cell marker

Mosaic analysis with a repressible cell marker (MARCM) is a modification of the FLP/FRT system developed to label neurons in the *Drosophila* CNS (Lee & Luo 1999; 2001; Wu & Luo 2006) (Fig. 2.2). The main features of this technique are that: (i) the FRT sites are carried specific on homologous chromosomes at the same position; (ii) the FLP recombinase is under the control of a heat-inducible promoter; and (iii) a dominant repressor of GAL4 (GAL80), located on a homologous chromosome arm and distal to the FRT site is used to prevent expression of a marker gene (e.g. GFP). Prior to cell division, expression of the UAS reporter is prevented by GAL80 repression of GAL4. During FLP/FRT-mediated mitotic recombination, FLP recombinase facilitates recombination between the specific FRT sites carried on each homologous chromosome, resulting in genetically different daughter cells. One daughter cell is now homozygous for the GAL80 repressor, and remains unlabelled. The other daughter cell, carrying the reporter gene but lacking the GAL80 repressor, is labelled. By incorporating mutations onto FRT-carrying chromosome arms, labelled cells can be made homozygous for these mutations, while the rest of the animal remains in a heterozygous and thus, essentially wild-type state (Fig. 2.2). This method can be applied to label and genetically manipulate any small population of cells or single cell of interest and has been widely used to study neurons in *Drosophila* (Lee et al 1999; Lee & Luo 1999; 2001), e.g. in screens for genes involved in mushroom body morphogenesis (Reuter et al 2003) and neuroblast asymmetric division (Slack et al 2006).

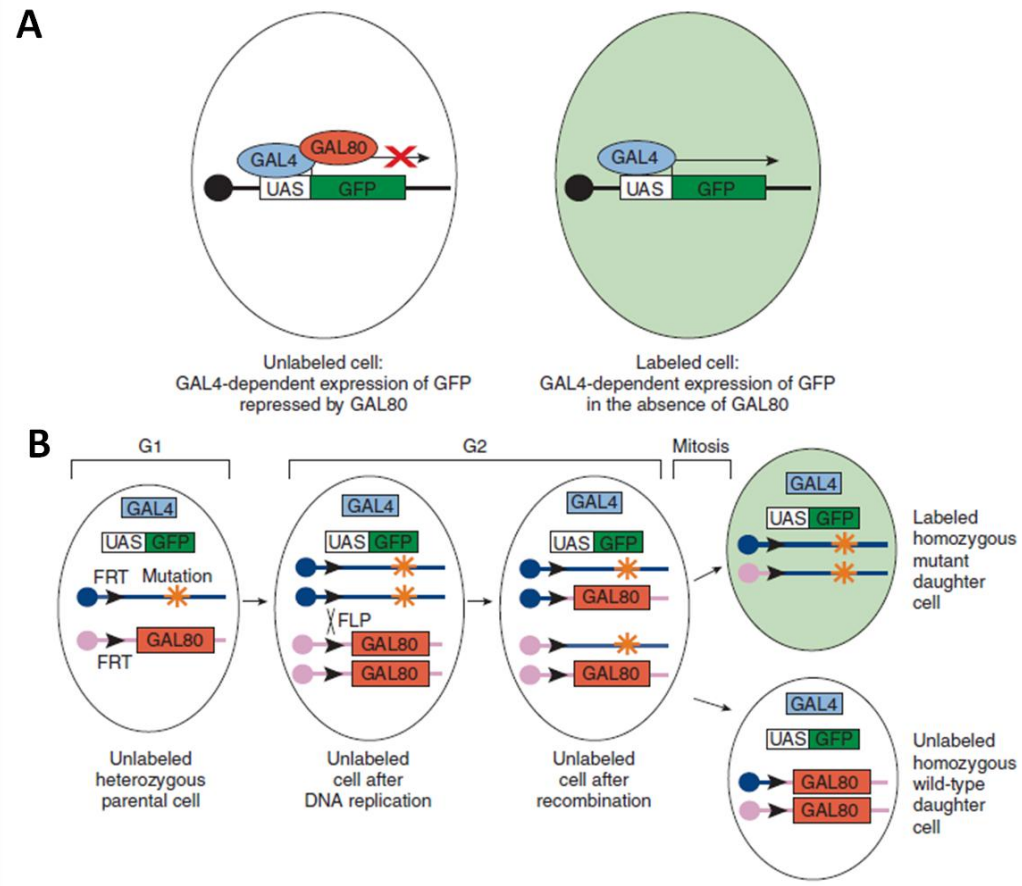

Figure 2.2 The Mosaic Analysis with a Repressible Cell Marker (MARCM) method

(**A**) In cells containing the GAL80 protein, GAL4-dependent expression of a UAS–gene (GFP) is repressed. By contrast, cells containing GAL4 but lacking GAL80 will express the UAS–gene (GFP). (**B**) MARCM requires: (i) two FRT sites located at the same position on homologous chromosomes; (ii) GAL80 located distal to one of the FRT sites; (iii) FLP recombinase located anywhere in the genome; (iv) GAL4 located anywhere in the genome except distal to the FRT site on the FRT, GAL80 recombinant chromosome arm; (v) UAS–marker located anywhere in the genome except distal to the FRT site on the FRT, GAL80 recombinant chromosome arm; and optionally (vi) a mutation distal to FRT, in *trans* to but not on the FRT, GAL80 recombinant chromosome arm. Site-specific mitotic recombination at FRT sites (black arrowheads) gives rise to two daughter cells, each of which is homozygous for the chromosome arm distal to the FRT sites. Ubiquitous expression of GAL80 represses GAL4-dependent expression of a UAS–marker (GFP) gene. Loss of GAL80 expression in homozygous mutant cells results in specific expression of GFP. Reprinted by permission from Macmillan Publishers Ltd: Nature Protocols (Wu & Luo 2006), copyright (2006).

The MARCM system is modified to target a subset of motor neurons

As described above, the MARCM system is a useful too for labelling mutant neurons, however, it is not without limitations. Firstly, perdurance of GAL80 carried over from the parent cell to the daughter cell meant that cells could not be visulaised in embryonic and early larval stages. Secondly, the use of heat-shock inducible FLP recombinase results in a random pattern of cells being labelled, whereas ideally, the same set of cells would be repeatedly labelled.

To address these issues the MARCM system was modified in several ways in order to target a specific subset of neurons, at earlier life stages. This involved expressing GAL80 under the control of a promoter that switches on early, and is restricted to, the ganglion mother cell to reduce as much as possible perdurance of the repressor. Furthermore, to target a subset of neurons, cell specific GAL4 drivers were used to initiate expression of FLP recombinase in the developing embryonic nervous system. Finally, a feedback loop was introduced to maintain reporter expression during larval life (see below for more in depth description of modified MARCM features and variations of the MARCM system trialled).

Assessment of different versions of modified MARCM systems

Prior to starting the screen, it was first necessary to carry out experiments to determine the best regime for producing mutant neurons, and to characterise the types of neurons that are targeted by the MARCM system (34 abdominal motor neurons have been identified in the fly embryo; (Landgraf et al 1997).

In initial experiments, three versions of a modified MARCM system were trialled (for genotypes see Table 2.1). Transgenes common to all three stocks included: a reporter, *UAS-mCD8::GFP*; two copies of the yeast gene encoding the enzyme Flippase under control of UAS regulatory elements, *UAS-FLP*, to catalyse FRT mediated recombination; and a GAL80 repressor of GAL4 under control of the *embryonic lethal abnormal vision* (*elav-GAL80*) promoter, located distal to FRT recombination sites.

MARCM version	Chromosome X features	Chromosome 2 features	Chromosome 3 features
elav+ftz	_	FRT40A/42D UAS-FLP *elav*-GAL80	*elav*-GAL4 *ftz*-GAL4 UAS-mCD8::GFP UAS-FLP
hs+elav+ftz	hsFLP22	FRT40A/42D UAS-FLP *elav*-GAL80	*elav*-GAL4 *ftz*-GAL4 UAS-mCD8::GFP UAS-FLP
ftz loop	_	FRT40A/42D, UAS-FLP *elav*-GAL80	*ftz*-GAL4 UAS-mCD8::GFP UAS-FLP *tubulin*-FRT-CD2-FRT-GAL4

Table 2.1 Genotypes of the three different MARCM stocks trialled

The first MARCM stock (termed 'elav+ftz') carried the following additional transgenes: two GAL4 drivers: one with the *elav* promoter, which had initially been reported to confer pan-neuronal gene expression (Robinow & White 1991); the other driver line uses the *fushi tarazu* (*ftz*) neurogenic regulatory regions, which targets GAL4 expression to a subset of ganglion mother cells and neurons (Alonso et al 2001; Hiromi et al 1985). The second MARCM stock tested (termed 'hs+elav+ftz') was the same as the first, but had a heat shock driven FLPase (*hsFLP22*) inserted on the X chromosome with the aim of increasing the number of labelled cells. Finally, a third variant (termed 'ftz loop'), had *ftz-GAL4* as the sole GAL4 driver and a *Tubulin-FRT-CD2-FRT-GAL4* transgene that served as a feedback loop, so that once mitotic recombination took place and a cell was labelled, the reporter remained switched on throughout the life of the neuron (on its own *ftz-GAL4* stops expressing during late embryonic stages). All versions were maintained over balancers and did not homozygose.

These versions of the modified MARCM were tested by crossing each stock to a line carrying the appropriate FRT site (FRT40A for the left arm of chromosome 2 and FRT42D for the right arm). To make FRT-deficiency-carrying lines, that could be screened using the modified MARCM system, appropriate FRT lines were recombined with deficiency chromosomes (see Chapter 3 Table 3.1) and maintained over a fluorescent balancer to aid selection of the appropriate genotype.

Next, the performance of these different MARCM stocks was assessed in terms of the types of neurons labelled (e.g. motor neuron, interneuron, sensory neuron or glia) and frequency of cells labelled. To this end, the left chromosome arm version (FRT40A) of each MARCM stock was crossed to an FRT-carrying stock (FRT40A, Bloomington stock number 1646) and first instar larvae of the appropriate genotype were dissected and their CNSs examined. Initially, labelled neurons were visualised using antibodies against GFP. In addition, co-staining with anti-Fasciclin 2 antibody revealed defined axon tracts as landmarks in the neuropil (Landgraf et al 2003; Lin et al 1994); specimens were examined using a confocal microscope. However, this method was time consuming and relatively few neurons could be examined per session. Processing of labelled neurons increased significantly with the

MARCM stock	CNSs examined, *n*	Neurons analysed, *n*	[a]Mean number of neurons per CNS	CNSs with no labelled neurons (%)	Advantages	Disadvantages	Most common neuron types seen (% of all neurons; top three)
elav+ftz	28	40	1.4 (0.80)	28.6	Earlier born neurons targeted	Sensory neurons are also targeted	Sensory (30); Terminal type 2PL (10); Terminal other (10)
hs+elav+ftz	39	49	1.4 (0.39)	25.6	More CNSs with labelled neurons than elav+FTZ	High frequency of sensory neurons targeted	Sensory (61.2); Other (16.3); Terminal other (10.2)
ftz loop	53	88	1.7 (1.47)	13.2	Few sensory neurons labelled; high frequency of labelled motor neurons	Glial cells are sometimes visible; greater variety of neuron types targeted	Other (22.7); Terminal other (20.5); VO4/5 (10.2) and VL2 (10.2)

Table 2.2 Comparison of three versions of the MARCM stocks trialled

Other = neurons that aren't classified due to being in a thoracic segment, overlaid by another neuron or not a type recognised.

[a]Includes all neurons (sensory, motor and interneurons); value in brackets is mean number of motor neurons per CNS examined.

realisation that they could be imaged without fixation or antibody labelling using widefield fluorescence microscopy.

The results of these MARCM system assessments are summarized in Table 2.2. The data suggested that the MARCM stock ‘ftz loop’ was the best choice for the screen for a number of reasons: (i) the frequency of labelled neurons (including sensory, motor and interneurons) was higher (‘ftz loop’ = 1.7 neurons per CNS compared to 1.4 with ‘hs+elav+ftz’ an ‘elav+ftz’); (ii) more CNSs had at least one neuron labelled (‘ftz loop’ = 86.8% compared to 74.4% for ‘hs+elav+ftz’, and 72.4% for ‘elav+ftz’); (iii) the frequency of sensory neurons targeted was low (‘ftz loop’ = 1.1% of neurons per CNS examined compared to 30% for ‘elav+ftz’ and 61.2% for ‘hs+elav+ftz’).

However, the ‘ftz loop’ did have some disadvantages compared to ‘elav+ftz’ and ‘hs+elav+ftz’ in that a greater variety of neurons were labelled, thereby increasing the number of neurons needed to screen a deficiency stock sufficiently. Furthermore, in contrast to earlier born neurons seen with ‘elav+ftz’ and ‘hs+elav+ftz’ MARCM stocks, later born neurons were targeted, making the targeting of the well characterised MN-RP2 neurons less likely. Glial cells were also occasionally labelled; these cells have the potential to obscure the dendrites of labelled motor neurons due to their surface location and morphology. Nevertheless, the disadvantage of having glial cells labelled, which can obscure neuronal cell morphologies, was outweighed by alternative versions (‘elav+ftz’ and ‘hs+elav+ftz’) labelling a large number of sensory neurons that were more likely to obscure the dendrites of labelled motor neurons due to their location and higher intensity of reporter expression.

Interneurons were also labelled in all three MARCM stocks and had the potential to obscure motor neuron morphology, though the frequency was comparable between ‘ftz loop’, ‘elav+ftz’ and ‘hs+elav+ftz’ (10.2, 7.5 and 12.8% of labelled neurons, respectively).

During neurogenesis, neurons are sequentially born in a columnar fashion from the ventrally located neuroblasts, such that older, early born neurons have more dorsally located cell bodies in the CNS than younger, later born cells, which reside ventrally. Thus, relative birth time can be estimated based on cell body location in the dorsoventral axis. Analysis of 77

control neurons using the FRT40A variants of ‘ftz loop’, ‘elav+ftz’ and ‘hs+elav+ftz’ showed that motor neurons born relatively late in neuroblast lineages (i.e. with ventral cell bodies) were preferentially targeted by the system. Only 7% of motor neuron clones had dorsally located cell bodies, indicative of early lineage products.

About seven distinct motor neurons are frequently labelled by the ‘ftz loop’ MARCM stock. Although the identity of these neurons has not been confirmed, previous work in the embryo (Landgraf et al 1997) and early first instar larva (Mauss et al 2009) suggests likely identities for some. They include neurons innervating the following body wall muscles: ventral oblique 4/5 (VO4/5), ventral lateral 2 (VL2), dorsal oblique 5 (DO5), a ventral lateral transverse (VT); unidentified motor neurons include a group of terminal ganglion motor neurons and the group of motor neurons classed as ‘L-shape’. The most frequently observed identified motor neurons were VO4/5 and MN-VL2, both with a frequency of 10.2% of all neurons. Others included MN-DO5 (2.3%), MN-VT (3.4%), unidentified neurons in the terminal ganglion (20.5%) and the unidentified group of motor neurons classed as ‘L-shape’ (Fig 2.3).

Attempts were made early on to identify the labelled cells using a combination of fluorescence microscopy to identify CNSs with labelled motor neurons, and antibody labelling against the reporter mCD8::GFP to follow the axons of labelled motor neurons to their target muscles. However, this approach was abandoned as it was unsuccessful, mainly due to attenuation of the mCD8::GFP signal along the distal axon, so that it was undetectable in the muscle field.

The fact that labelled neurons are generated indicates that the modified MARCM system works. The data generated also provided an archive of control images necessary for direct comparison with mutant cells produced in the screen. However, it should be noted that the data collected was from the left (FRT40A) arm of chromosome 2 versions of MARCM stocks as at the time; versions for the right (FRT42D) arm were still under construction.

Figure 2.3 Examples of neurons frequently targeted by the 'ftz loop' MARCM method

(**A**–**F**) All neurons are controls, obtained from the 'ftz loop' MARCM stock crossed to the FRT40A-carrying Bloomington fly line 1646. For all figures: triangle = cell body; asterisk = axon; dashed red line = midline; scale bar = 10 µm; anterior is left.

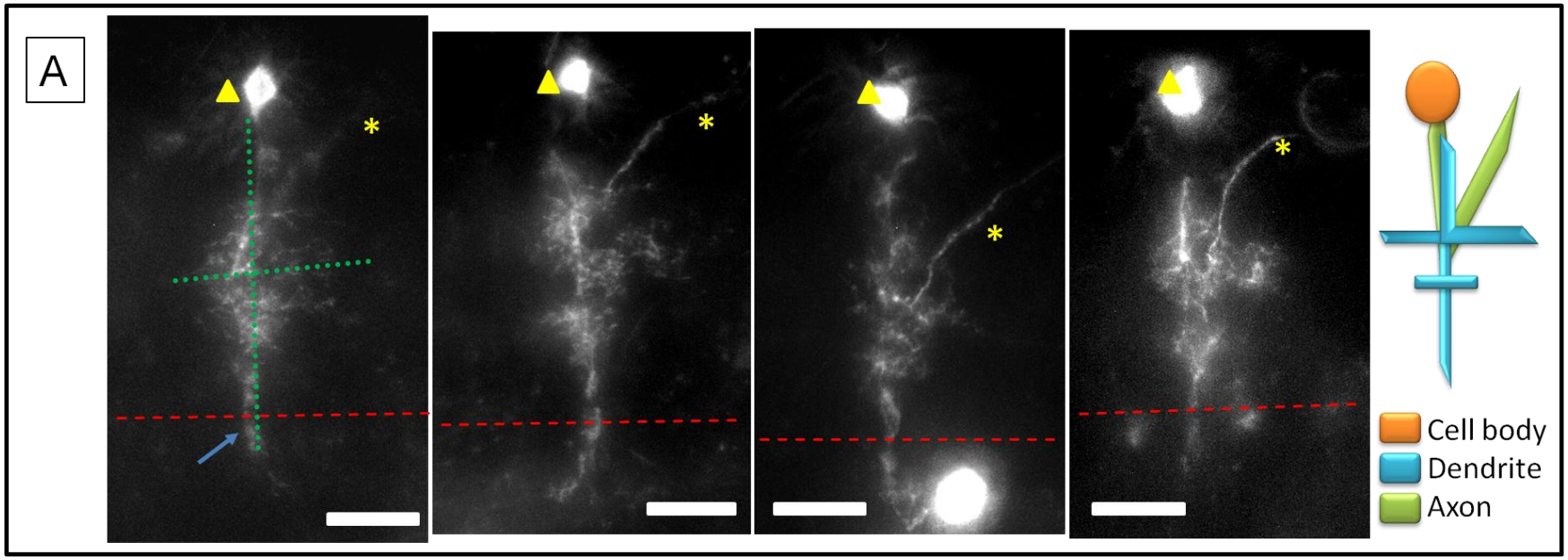

(**A**) MN-VO4/5. These intersegmental neurons target some of the ventral oblique motor neurons in the periphery and are easily identified by the characteristic cross-like shape of their primary dendritic branches (highlighted by dotted green line). The most medial branch, perpendicular to the anterior/posterior axis, only just crosses the midline. The cell body is ventral. (*Right*) Simple cartoon depicting the basic structure of MN-VO4/5.

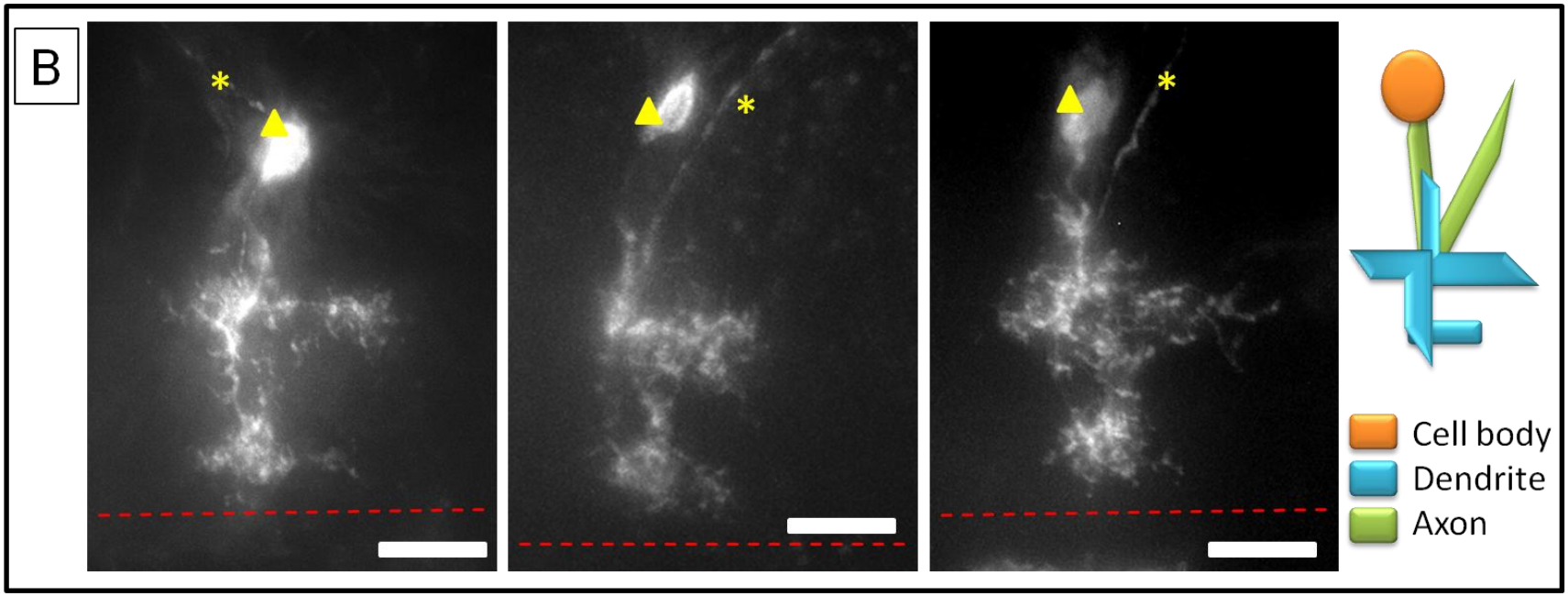

(**B**) MN-VL2. With a similar arbor structure to MN-VO4/5, these intersegmental neurons generally have two dendritic sub-arbors. In these examples, the branch that in MN-VO4/5 crosses the midline is absent, and there is a posterior extension to the most lateral arbor. (*Right*) Simple cartoon depicting the basic structure of MN-VL2.

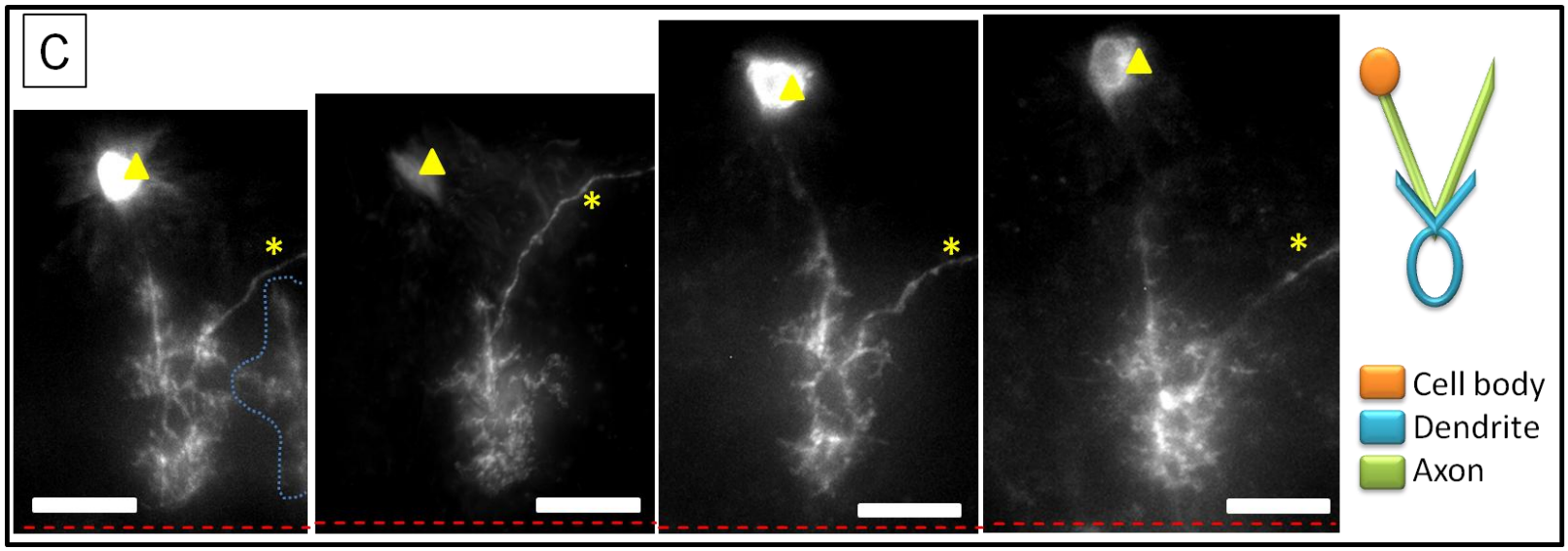

(**C**) An intersegmental motor neuron that targets one of the dorsal oblique muscles is DO5. This neuron is characterised by a ventral cell body and a dendritic arbor with a typical looping shape when viewed as a *z*-stack. (*Left*) Dotted blue line demarcates the arbor of a neighbouring labelled neuron. (*Right*) Simple cartoon depicting the basic structure of MN-DO5.

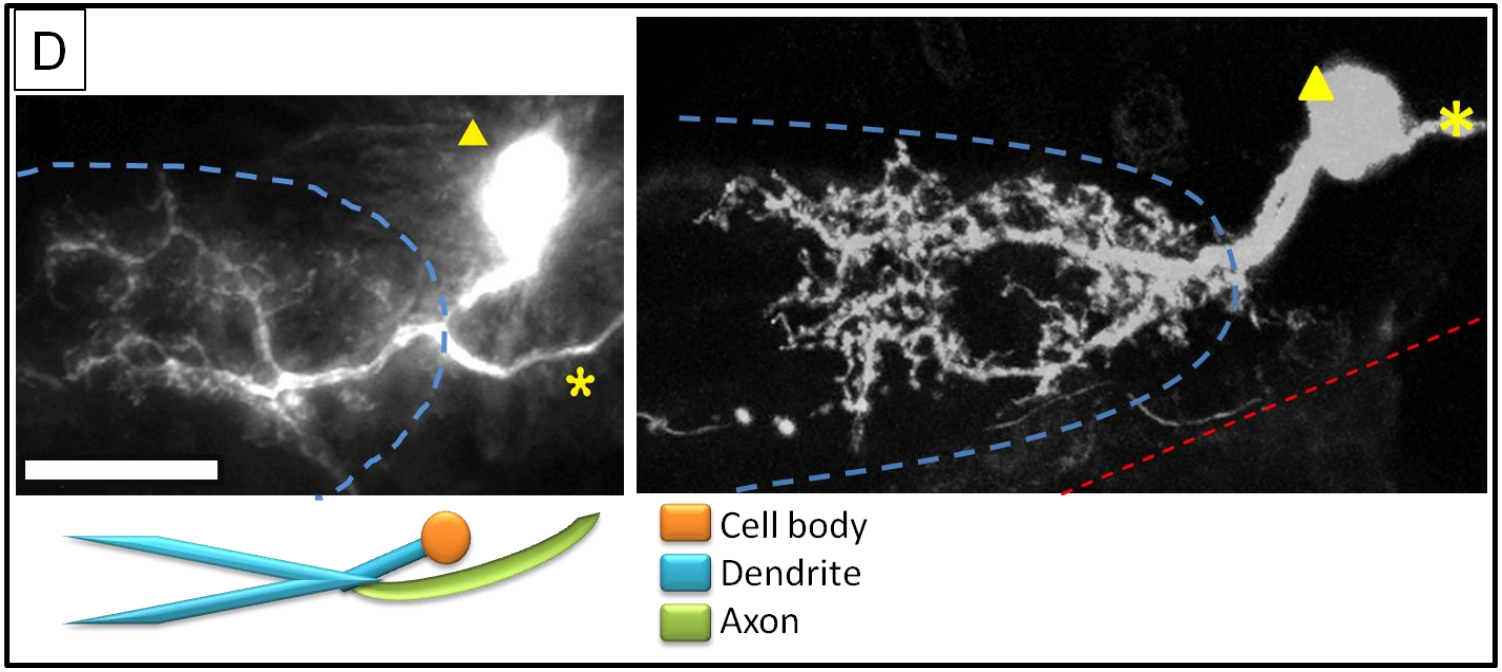

(**D**) Some of the most common motor neurons that are seen in the posterior part of the CNS are terminal ganglion neurons, which are thought to innervate one of the muscles that control the posterior part of the animal. The cell body is ventral and the axon exits the CNS posteriorly. These two examples are not the same type of neuron, but share branching characteristics in that the arbors consist of two main branches that extend anteriorly into the neuropil. (*Right*) Simple cartoon depicting the basic structure of terminal ganglion neurons.

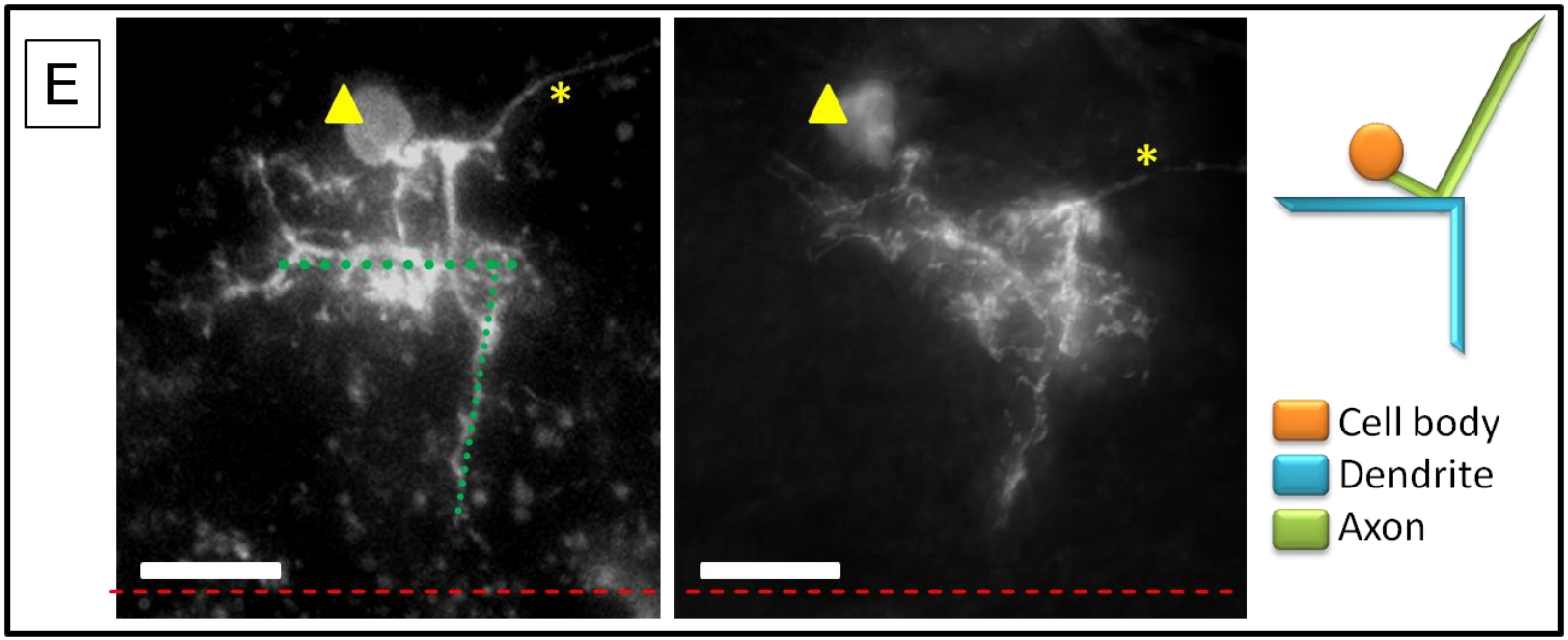

(**E**) The identity of these intersegmental motor neurons has not been determined. Based on their characteristic arborisation arrangement, they have therefore been classed as 'L-type' neurons (green dotted line). Although the configuration of the neurons can vary with regards to the location of the secondary branches, cell body and the exiting axon, there are common features that can be used to identify them. In particular, these neurons have two characteristic main branches that extend anteriorly and medially perpendicular to one another forming a reverse 'L' shape. (*Right*) Simple cartoon depicting the basic structure of 'L-type' neurons.

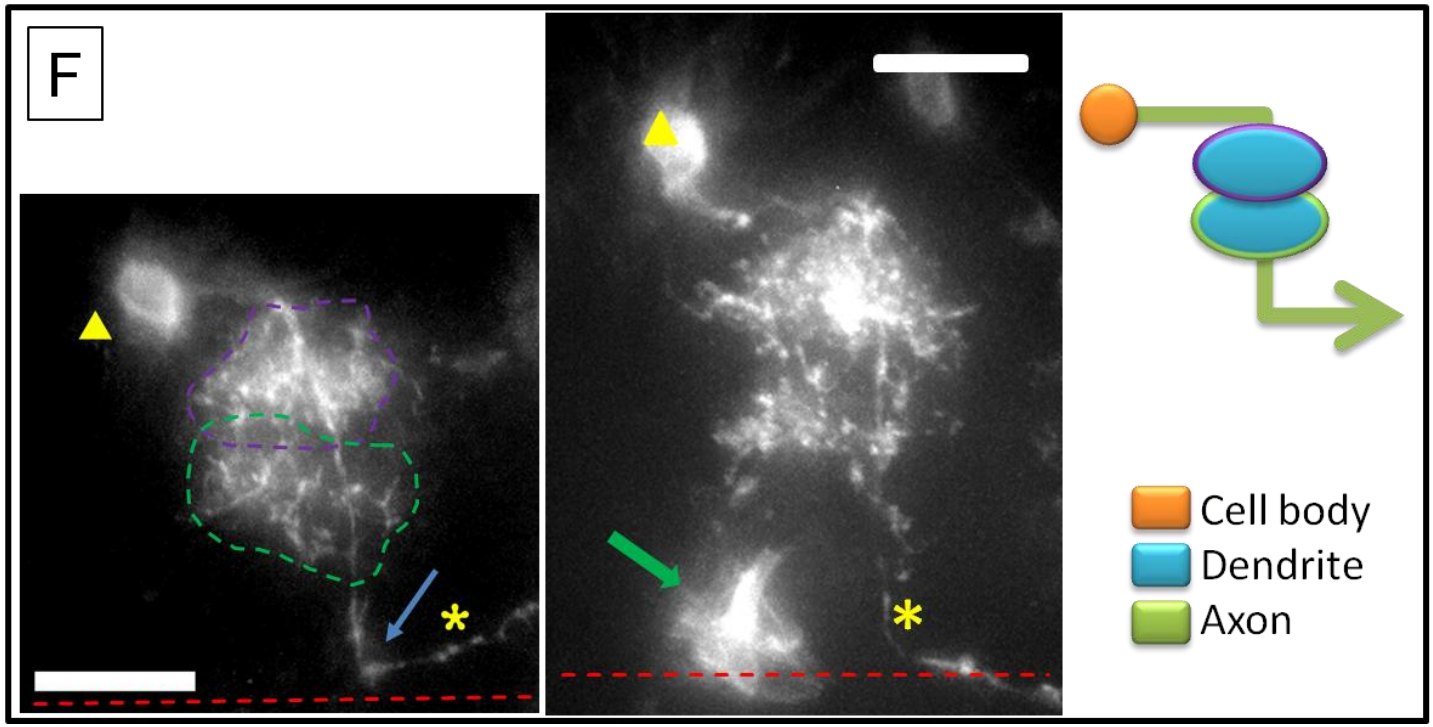

(**F**) The ventral transverse (VT) motor neuron is easily identified due to its typical axonal trajectory, as it is the only motor neuron where the axon exits the CNS dorsally via the transverse nerve (blue arrow). The VT neuron has two arborisations, one medial (purple dashed line) and one lateral (green dashed line). Green arrow indicates a glial cell wrapped around the medial edge of the neuropil. (*Right*) Simple cartoon depicting the basic structure of VT motor neurons.

Experiments using mutations known to affect dendrite development confirm the function of the modified MARCM system

To prove that the modified MARCM system does work, fly lines with mutations known to give rise to dendritic phenotypes were used to generate homozygous mutant motor neurons. One was a loss of function allele of *short stop* (*shot*^{2}), the only spectraplakin found in *Drosophila.* Spectraplakins are highly conserved large actin–microtubule linker proteins that have roles in various processes – a feature that reflects their diverse functional domains (Bottenberg et al 2009). Shot has been shown to be necessary for local growth of motor and sensory neuron dendrites (Gao et al 1999; Prokop et al 1998) and for correct axonal growth (Lee et al 2000a) and has recently been shown to control the formation of filopodia via the actin cytoskeleton and regulation of microtubules during axonal growth (Sanchez-Soriano et al 2009). Another loss of function allele is *robo*^{GA285}, a gene coding for a receptor required for midline repulsion of axons and dendrites (Furrer et al 2003; Mauss et al 2009). Once recombined with the appropriate FRT chromosome (FRT42D), the mutants were screened using the appropriate FRT variant of the 'ftz loop' MARCM stock. Thirty-eight and 33 CNSs were visualised for *shot*^{2} and *robo*^{GA285}, respectively. The frequency of labelled motor neurons for the *shot*^{2} and *robo*^{GA285} experiments was very low, with almost half of all nerve cords analysed containing no labelled motor neurons. Nevertheless, phenotypes characteristic for these mutations were seen, albeit with varying degrees of penetrance. Figure 2.4 shows examples of the phenotypes seen in 'ftz loop' MARCM labelled neurons mutant for *shot*^{2} and *robo*^{GA285}*.* In a muscle VO4/5 motor neuron mutant for *shot*^{2} (Fig. 2.4B), the majority of the fine dendrites are absent, and only the primary branches remain. This fits with data from experiments with other alleles of *shot* that show reduced dendritic complexity in developing aCC and RP2 motor neurons (Bottenberg et al 2009). Lack of such an important component of the cytoskeleton in structures undergoing rapid growth and retraction (as in the fine branches of dendrites that are exploring their territories to find appropriate presynaptic partners) will likely cause the failure of the dendrites to grow. The fact that primary branches are present suggests that sufficient wild-type protein might be

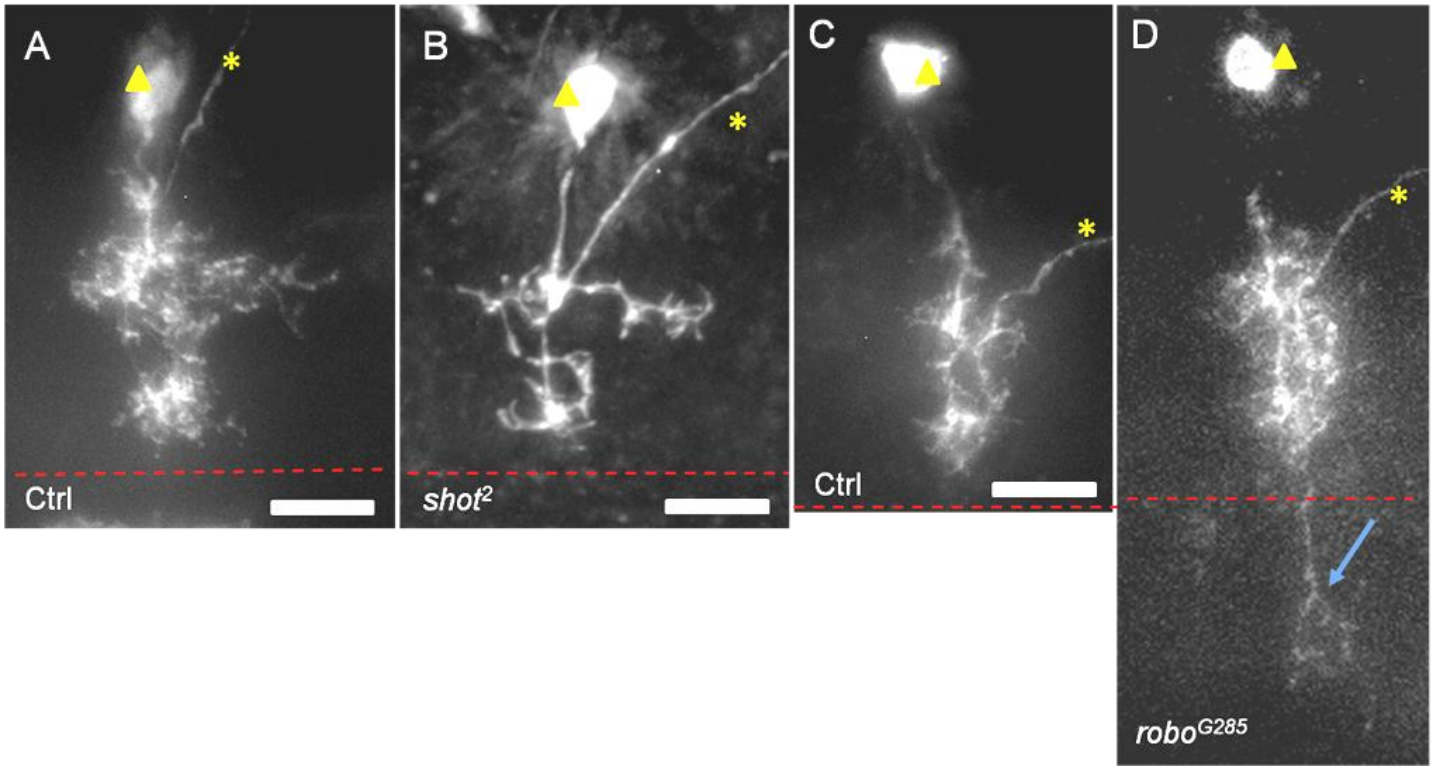

Figure 2.4 Loss of function mutations visualised by the 'ftz loop' MARCM method

(**A** and **B**) Characteristic loss of higher order branches in *shot*^{2} mutant MN-VL2 neurons (**B**) compared to a control neuron (**A**). (**C** and **D**) Aberrant midline crossing (**D**, arrow) of MN-DO5 neurons mutants for *robo*^{GA285} not normally seen in control neurons (**C**).

Scale bar = 10 μm; asterisk = axon; triangle = cell body; red dashed line = midline; anterior is to the left.

carried over during precursor cell division to build and maintain those, but not enough is present to allow the production and/or maintenance of secondary branches. Figure 2.4D shows an example of the phenotype seen in muscle DO5 motor neurons mutant for *robo*^{GA285}. Dendrites proximal to the midline aberrantly crossed the midline and formed a small contralateral arbor. This phenotype closely resembles that seen in axons and dendrites lacking proper *robo* function. Furrer and colleagues (2003) demonstrated that in *robo* mutant RP2 and RP3 motor neurons, dendrites grow closer to the midline, and often extend beyond the midline and into the contralateral side of the CNS (Furrer et al 2003). Further, while investigating the formation of a neural map in the mediolateral axis of the embryonic CNS, Mauss and colleagues (2009) also showed that a single dendrite branch aberrantly crosses the midline in DA3 and LL1 motor neurons deficient in *robo* protein function (Mauss et al 2009).

In summary, these tests confirmed that the experimental approach works, and that mutant dendritic phenotypes could be identified based on dendritic morphology.

Variations of the 'ftz loop' MARCM stock

In ongoing efforts to improve and develop the 'ftz loop' MARCM stock throughout the project, different neuroblasts drivers, fluorescent reporters and GAL80 transcriptional repressors were trialled. The aims were to reduce background from glia, interneuron and sensory neurons, and to improve phenotypic penetrance while maintaining strong expression of reporter in MARCM-labelled motor neurons.

Neuroblast GAL4 drivers

The experiments using *shot*^{2} and *robo*^{GA285} revealed that phenotypes seen with the 'ftz loop' MARCM can be very variable, with some neurons only mildly affected. One possible reason for this is that wild-type proteins present in the ganglion mother cell are distributed to the daughter cells via the cytoplasm when the cell divides. How much protein is carried over into

the daughter cell and the stability of the protein are two factors that could account for the variability of phenotypes seen. Any wild-type protein present in the daughter cell must be degraded before the phenotype can potentially become visible; if the majority of dendrite development has already occurred by this time then a phenotype might not be seen. The young developmental stage (first instar larva) when analysis of neurons takes place might also mean that there is not enough time for a phenotype to become apparent after the protein has run out. For example, a dendrite may begin to degrade once a protein necessary for maintaining the cell membrane is used up, but unless time is allowed for this, a phenotype will not be seen.

To address the issue of protein perdurance, experiments to induce mitotic recombination earlier in development, namely in neuroblasts, so as to more effectively dilute out wild-type gene products inherited from the progenitor cell and thus result in more severe mutant phenotypes, were carried out. A variety of neuroblast drivers were tested; altogether, 11 GAL4 drivers were tested by crossing to the appropriate 'ftz loop' variant of the MARCM to test that: (i) the 'ftz loop' MARCM still functioned and (ii) to look for variations in the pattern of neurons targeted by the 'ftz loop' MARCM. Table 2.3 summarizes the 11 GAL4 drivers examined. The most promising alternative GAL4 driver is *worniu-GAL4* as it has the highest frequency of labelled motor neuron cells compared to the other GAL4 drivers.

Red fluorescence protein

UAS-mCD8::GFP is a good reporter for the MARCM system in that it is visible using widefield fluorescence microscopy, it is non-toxic to the cell and it does not bleach quickly. However, it is flawed in that it does not diffuse well along membranes of dendrites and axons, as demonstrated in the experiments to identify MARCM labelled neurons with antibody labelling against GFP as discussed above. This failing would make 3D reconstruction and subsequent quantification of dendritic trees difficult. Towards the end of the project, the use of *UAS-myr-mRFP1* (Chang 2003) became more common in the lab as

GAL4 driver (ftz loop chromosomearm)	Reference	Expression pattern in nervous system	CNSs examined (*n*)	CNSs with motor neurons labelled (*n*)	CNSs with interneurons/glia labelled (*n*)	CNSs with no labelled cells (*n*)	Other comments
1407 (FRT40A)	(Luo et al 1994; Sweeney et al 1995)	Early NB CNS, PNS, NMJ	6	0	0/4	2	Insufficient numbers screened
Asense (FRT40A)	(Zhu et al 2006)	All actively dividing NBs	36	0	1/7	24	Three CNSs had labelled cells in the brain lobes
Eagle (FRT42D)	(Dittrich et al 1997)	NB 7-3 and all progeny until stage 17	1	0	0	1	Insufficient numbers screened
Engrailed (FRT42D)	(Brand 1997)	Subset of NBs, some PNS in *Kruppel* domain	3	1	1/1	1	2-3 sensory neurons per CNS; hard to pick correct genotype

Kruppel (FRT40A)	**(Castelli-Gair et al 1994)**	**early NB stages in CNS; also in neurectodermal cells**	**14**	**0**	**0**	**0**	**14 labelled neurons that innervate Bolwigs organ**
Nkx6 (*HGTX*) (FRT40A)	(Broihier et al 2004; Uhler et al 2002)	Midline precursors, ventral intermediate column NBs, later in neurons but not glia	8	0	0	0	
Patched (FRT42D)	(Hooper & Scott 1989; Shyamala & Bhat 2002)	Subset of NBs	26	1	0	0	One NB clone; two sensory; high GFP background
Scabrous (FRT40A)	(Graba et al 1992; Mlodzik et al 1990)	PNS, CNS, NBs	19	2	3/11	4	Three CNSs had labelling in tracheal cells
Wingless (FRT40A)	(Chu-LaGraff & Doe 1993)	Neurectoderm, from which NBs are derived	23	3	11/7	8	
Worniu (FRT40A)	(Albertson et al 2004; Albertson & Doe 2003)	NB-specific, expresses from the time of NB formation	23	10	10/9	13	Expect only 50% of CNSs to have labelled cells; one NB clone seen

Table 2.3 Assessment of different neuroblast drivers for use in MARCM NB = neuroblast

the myristoylation tag allows better diffusion within neuronal membranes than the CD8 transmembrane protein; and MARCM versions using *UAS-myr-mRFP1* rather than *UAS-mCD8::GFP* as a reporter were generated.

Alternative GAL80 expression constructs

For the majority of the project, the transcriptional repressor of GAL4, GAL80, was driven under the control of the pan-neuronal *elav* promoter. Based on previously published reports it was assumed that *elav* expression was post-mitotic (Robinow & White 1991), i.e. after ganglion mother cells have divided. This is important because expression of GAL80 earlier in ganglion mother cells or even neuroblasts could interfere with the proper function of the *ftz-GAL4* driver for inducing mitotic recombination events. Evidence from experiments presented above, where late born neurons are preferentially labelled in the 'ftz loop' MARCM (and also in 'elav+ftz' and 'hs+elav+ftz' versions) and data from others show that *elav* is transiently expressed in glial cells and embryonic neuroblasts (Berger et al 2007). For example, the observations that neurons born late in neuroblast lineages are preferentially targeted by the modified MARCM system is compatible with the possibility that GAL80, under control of the *elav* promoter, is not only expressed post-mitotically, but also transiently in neuroblasts and perhaps also in ganglion mother cells.

In light of this, GAL80 transgenes under the control of different promoters were assessed for suitability to either complement *elav*-GAL80 or for its replacement.

Four different insertions lines of *n-synaptobrevin* driving GAL80 (*n-syb*-GAL80) were tested by generating 'ftz loop' MARCM stocks with them (carried out by a colleague, M.L.), and crossing to a FRT-carrying chromosome, with mixed results. One line (A6) had a high frequency of strongly labelled neurons and low background, but also labelled glial cells, particularly a subset of perineurial glia that form part of the blood–brain barrier; no early born neurons were seen. The second line (A1) gave poorer contrast, and labelled fewer neurons and more glial cells than insertion A6. Insertion B6, was the worst performing insertion with no labelled neurons, high background fluorescence and strong mCD8::GFP expression in the brain lobes.

Finally, insertion B2A6 a recombinant of two different *n-syb*-GAL80 lines, produced the desired result of a high frequency of labelled neurons, some of which were early born, with no glial cells labelled. However, the contrast in this line was poor as labelled neurons did not express GFP strongly. These results support the idea that the labelling of glia (except some perineurial glia not seen with *elav*-GAL80), and the targeting of later born neurons is a consequence of using *elav*-GAL80 to repress GAL4 expression.

To try and prevent mCD8::GFP expression in perineurial glia labelled by *n-syb*-GAL80 'ftz loop' MARCM, another GAL80 was tested. Reversed polarity (repo) is a homeodomain protein expressed in all glial cells except the midline glia (Awad & Truman 1997; Halter et al 1995). In order to reduce the background expression of GFP in glia, *repo*-GAL80 (Awasaki et al 2008) was recombined with a FRT40A-carrying chromosome and crossed to the A6 *n-syb*-GAL80 'ftz loop' MARCM stock. However, this made no difference and glial cells were still labelled.

Concluding remarks

Despite some of the drawbacks of the 'ftz loop' MARCM (glial cells and interneurons also labelled, late born neurons targeted and wide variety of neurons labelled) it was felt that the system was robust enough to begin a pilot screen, which is described in the next chapter. In the meantime, modifications of the MARCM would continue in efforts to improve its performance.

Chapter 3 Loss of function screen

Chapter 3 summarizes the data obtained from the loss of function screen including: recombination of deficiency chromosomes with lines carrying FRT sites; chromosome 2 coverage; identification of five regions of chromosome 2 where deletions give a dendritic phenotype. Four of the regions identified [deleted in *Df(2L)al*, *Df(2L)TE35BC-24*, *Df(2R)Np5* and *Df(2R)Px2*] are then discussed while the fifth [*Df(2L)S2590*] is the subject of Chapter 4.

Generation of a fly stock collection for FLP/FRT mediated mitotic recombination with defined chromosome 2 deficiencies

In order to carry out a mosaic loss of function screen based on mitotic recombination, chromosomes with defined deletions and with FRT sites were recombined together. These permit mitotic recombination to take place at the FRT sites (FRT40A, FRT42D) located near the centromere of chromosome 2. Briefly, fly lines carrying a deletion, maintained in heterozygous condition over a *CyO* balancer chromosome, were crossed to flies homozygous for an FRT site on the same chromosome arm as the deficiency, additionally carrying a *P-element* insertion that confers eye colour distal to the FRT site. Female virgin offspring with a deficiency chromosome over an FRT chromosome were then crossed to second chromosome balancer males (w^-; *If* / *CyO*) so that recombinants could be recovered. To select for FRT-deficiency recombinants larvae produced by the cross were maintained on media containing 50 µg/ml Geneticin® antibiotic (a neomycin analogue) (Xu & Rubin 1993) at 25°C and subjected to heat shocks at 37°C on consecutive days to strongly activate the heat-shock inducible neomycin resistance gene that is part of the FRT site containing *P-elements*. Once eclosed, flies were screened for loss of eye colour indicating that recombination in the right part of the chromosome had taken place. With one further cross, the resulting white-eyed FRT-deficiency recombinant chromosomes were balanced over a fluorescently marked *CyO* balancer, which would aid selection of the appropriate genotype when subsequently crossed to the 'ftz loop' MARCM stock (see Materials and methods and Fig. 3.1 for a more detailed explanation of the crossing scheme).

In the interest of efficiency, deficiencies that failed to recombine onto FRT chromosome were discarded after two attempts. Some of these deficiencies that did not readily recombine onto FRT chromosomes as well as those that produced dendritic phenotypes when homozygous were broken up into sets of overlapping deficiencies. The rationale was to circumvent potential synthetic lethal effects associated with larger deficiencies and the recombination onto FRT chromosomes. For the deficiencies causing a dendritic phenotype when homozygous, this allowed more precise mapping of the chromosome regions responsible for the phenotype.

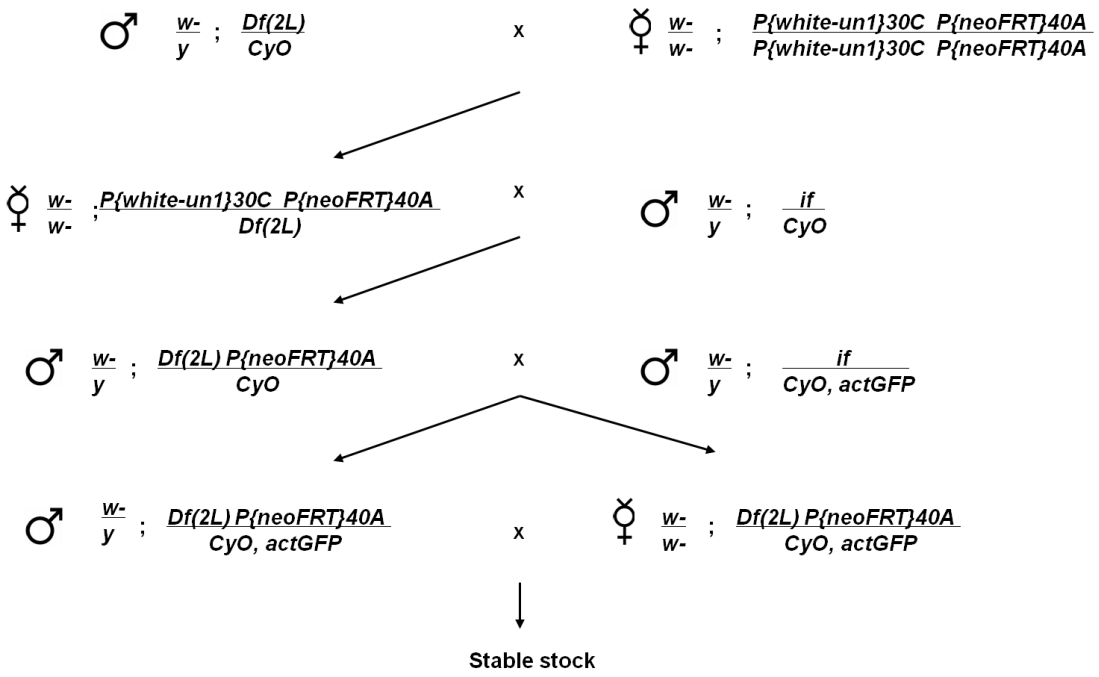

Figure 3.1 Crossing scheme for making FRT/Deficiency recombinants, illustrated for the left arm of chromosome 2

(**Line 1**, *top*) Males carrying the deficiency in a heterozygous condition were crossed to females homozygous for the FRT site. Eye colour is conferred by a second *P*-element insertion distal to the FRT site. (**Line 2**) Female progeny were selected based on absence of the *CyO* balancer and eye colour, and were crossed to a second chromosome balanced stock. (**Line 3**) Male progeny with no eye colour, indicating recombination had taken place during which the second P-element had been lost and concomitantly the deficiency probably recombined on, were selected on Geneticin® food (only *hs-neo*^{R} carriers survive) and crossed to females carrying a fluorescently marked balancer (*CyO*, *actGFP*). (**Line 4**, *bottom*) Males and virgin females carrying the fluorescently marked *CyO* balancer (as determined by eye colour) were crossed together to generate a stable stock. Only stocks that maintained the *CyO* balancer in subsequent generations were kept, signifying the presence of lethal mutations on the second chromosome and indicative of the deficiency having been successfully recombined onto the FRT chromosome.

One hundred and nineteen fly lines were included at the start of the project: 116 deficiencies and three with mutations in a single gene. Of these, 116 lines went on to be recombined with FRT-carrying chromosomes; three of the deficiency lines had already been recombined with FRT-carrying chromosomes (Fig 3.2). At the conclusion of the project 150 such recombinations had been carried out: recombination onto FRT-carrying chromosomes was successful for 79 lines at the first attempt (= 79 recombinations); a further 34 lines were attempted a second time (= 68 recombinations); and one line was attempted a third time (= 3 recombinations). Of the 116 lines that required recombination with a FRT-carrying chromosome, 22 lines failed to recombine at all. Among these, four lines were selected to be covered by overlapping deficiencies: *In(2LR)DTD16^{L}DTD42^{R}* was replaced with *Df(2L)BSC28*; *Df(2L)cl-h3* with *Df(2L)2801* and *Df(2L)cl2*; *Df(2R)Jp1* with *Df(2R)knSA4* and *Df(2R)Jp4*; and *Df(2R)Egfr5* with *Df(2R)PK1*, *Df(2R)Egfr3* and *Df(2R)01D01Y-R21*. At this stage, 90 recombinant FRT lines were available for screening. However, two recombinant stocks died before they could be tested [FRT40A *Df(2L)net-PMF* and FRT40A *Tp(2;Y)J54*] and three were later removed from the screen following a re-evaluation of their breakpoints, which deviated significantly from those originally described (Bloomington stock numbers 3090, 3157 and 7913). For the final screen, 85 recombinant stocks survived and were available for testing.

Table 3.1 shows stock and deficiency/gene deletion data obtained from Flybase (versions FB2011_03, released March 21st, 2011 to FB2011_04, released April 22nd, 2011) and Bloomington stock centre (http://flystocks.bio.indinana.edu/), and results of screening with the 'ftz loop' MARCM line at the end of the project. The results are discussed below.

Coverage of chromosome 2 by recombinant FRT-deficiency stocks

The coverage of both arms of chromosome 2 by deficiencies used in the screen is summarized in Table 3.2 and also detailed in Appendix 1 (see Supplementary CD). These data were derived from Flybase (v FB2011_04) using the 'Genes' dataset, field 'Map:location arm' and either '2L' or 2R' in the SearchText box. This search for the left arm

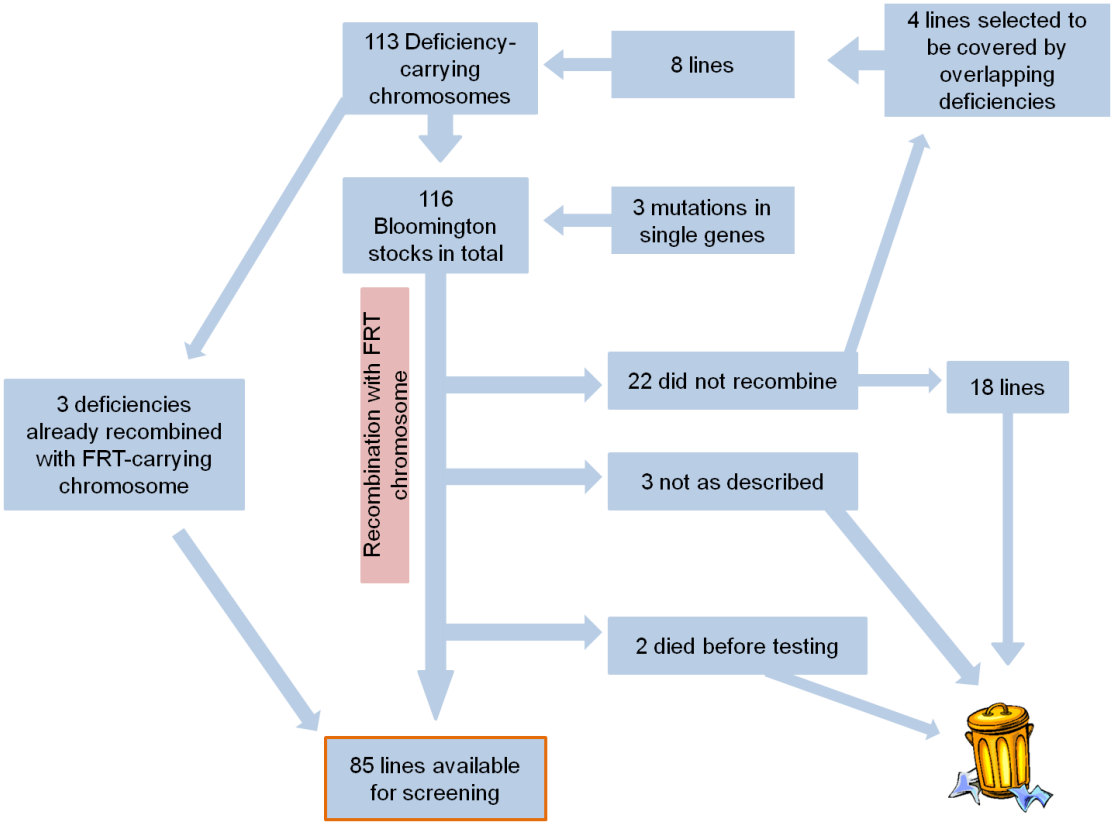

Figure 3.2 Flowchart describing the process of generating a fly stock collection for FLP/FRT mediated mitotic recombination with defined chromosome 2 deficiencies

Of the 116 lines obtained from the Bloomington stock centre, 85 recombinant FRT deficiency/single gene mutation fly lines were available for screening using ftz loop MARCM.

Table 3.1 Summary of Deficiency lines in the screen

Deficiency	Bloomington stock number	FRT stock	Deletion cytological and (sequence) coordinates	Rec. (*n*)	Genes deleted (*n*)	CNSs analysed (*n*)	Motor neurons observed (*n*)	Phenotype seen	Average neurons per CNS
Df(2L)BSC4	6283	1646	21B7;21C3	1	37	45	33	–	0.73
Df(2L)al	3548	1646	21C1;21C7	1	20	17	20	+	**1.18**
Df(2L)BSC107	8673	1646	21C2;21E2 (2L:431096;574741)	1	21	nd	nd	–	–
Df(2L)BSC16	6608	1646	21C3;21C8	1	1	34	30	–	0.88
Df(2L)S2	6697	1646	21C8; 22B1	1	140	33	10	–	0.30
Df(2L)ast2	3084	1646	21D1;22B3	1	153	52	21	?	0.40
Df(2L)C144	90	1646	22F3;23C5 (2L:2517598;2961962)	1	63	6	8	–	**1.33**
Df(2L)JS32	97	1646	23C3;23D2	1	32	nd	nd	–	–
Df(2L)BSC162	9597	1646	23C5;23D4 (2R:3046634;3164472)	1	11	41	22	–	0.54

Deficiency	Bloomington stock number	FRT stock	Deletion cytological and (sequence) coordinates	Rec. (*n*)	Genes deleted (*n*)	CNSs analysed (*n*)	Motor neurons observed (*n*)	Phenotype seen	Average neurons per CNS
Df(2L)BSC28	6875	1646	23C5;23E2	1	29	12	16	+	**1.33**
Df(2L)S2590	4954	1646	23D2;23E3	1	22	47	25	+	0.53
Df(2L)Exel8008	7786	1646	23E3;23E5 (2R:3302636;3354858)	1	10	13	12	–	0.92
Df(2L)tim-02	6502	1646	23F2;24A1	1	27	33	25	–	0.76
Df(2L)drm-P2	6507	1646	23F3;24A2	1	29	27	1	–	**0.04**
Df(2L)ed1	5330[#]	1646	24A2;24D4	1	53	19	18	–	0.95
Df(2L)cl2	6224	1646	25D2;25F4	1	68	7	4	–	0.57
Df(2L)2802	1712	1646	25F2; 25F5	1	27	16	8	–	0.50
Df(2L)E110	490[#]	1646	25F3;26D11	1	125	5	5	–	1.00
Df(2L)BSC7	6374[#]	1646	26D10;27C1	1	51	7	9	–	**1.29**
Df(2L)J-H	1357	1646	27C5;28B4	1	72	20	17	–	0.85

Deficiency	Bloomington stock number	FRT stock	Deletion cytological and (sequence) coordinates	Rec. (*n*)	Genes deleted (*n*)	CNSs analysed (*n*)	Motor neurons observed (*n*)	Phenotype seen	Average neurons per CNS
Df(2L)spd	3077[#]	1646	27E1;28B3	1	41	22	12	–	0.55
Df(2L)XE-2750	4955	1646	28A5;28C9	1	39	nd	nd	–	–
Df(2L)Trf-C6R31	140	1646	28DE (putative 2L:8071809;8110561)	1	5	nd	nd	–	–
Df(2L)TE29Aa-11	179	1646	28E4;029C1	1	78	10	2	?	0.20
Df(2L)N22-5	384	1818	29C3;30C9	1	157	nd	nd	–	–
***PKA-C1^{H2}* loss of function allele, point mutation**	4101[$]	1646	30C1	1	1	15	18	–	**1.20**
Df(2L)BSC17	6478	1818	30C3;30F1	1	52	5	0	–	0.00
Df(2L)Mdh	1045	1818	30D;031F	1	169	nd	nd	–	–
Df(2L)BSC32	7142	1818	32A1;32D1	1	76	nd	nd	–	–
Df(2L)FCK-20	5869[#]	1818	32D1;32F3	1	54	12	5	–	0.42

Deficiency	Bloomington stock number	FRT stock	Deletion cytological and (sequence) coordinates	Rec. (*n*)	Genes deleted (*n*)	CNSs analysed (*n*)	Motor neurons observed (*n*)	Phenotype seen	Average neurons per CNS
Df(2L)Prl	3079	1818	32F1;33F2	1	130	nd	nd	–	–
Df(2L)prd1.7	3344[#]	1818	33B3;34A2	1	86	5	4	–	0.80
Df(2L)Sco^{rv10}	6084	1818	35B1;35B2 + 35D1;35E1	1	77	nd	nd	–	–
Df(2L)Sco^{rv14}	6085	1818	35B1;35B4 + 35D1;35E2	1	90	nd	nd	–	–
Df(2L)TE35BC-24	3588[#]	1818	35B4;035E2	1	124	10	13	+	**1.30**
Df(2L)TE35BC-34	6244	1818	35B4;35D5	1	108	nd	nd	–	–
Df(2L)Exel8034	7830	1818	35C5;35D2 (2L:15264714;15439965)	1	12	nd	nd	–	–
Df(2L)Sco^{rv25}	6086	1818	35D1;35D5	1	47	nd	nd	–	–
Df(2L)r10	1491	1818	35D1;36A7	1	114	nd	nd	–	–
Df(2L)Exel7063	7831	1818	35D2;35D4 (2L:15426051;15744445)	1	21	nd	nd	–	–
Df(2L)RA5	6915	1818	35E1;36A1	1	48	nd	nd	–	–

Deficiency	Bloomington stock number	FRT stock	Deletion cytological and (sequence) coordinates	Rec. (*n*)	Genes deleted (*n*)	CNSs analysed (*n*)	Motor neurons observed (*n*)	Phenotype seen	Average neurons per CNS
Df(2L)cact-255^{rv64}	2583	1818	35F6036D	2	134	nd	nd	–	–
Df(2R)cn9	3368	2120	42E;44C1	1	225	22	7	–	0.32
Df(2R)H3C1	198	2120	43F;44D8	1	130	4	0	–	0.00
Df(2R)H3E1	201	2120	44D1;45A1	1	99	18	7	–	0.39
Df(2R)G75	6090	2120	44F4;44F11	1	15	23	3	–	**0.13**
Df(2R)Np5	3591	2120	44F8;045E3 (2R:4848845;5411775)	1	87	12	9	+	0.75
Df(2R)w45-30n	4966	2120	45A6;045E3	1	51	18	10	–	0.56
Df(2R)G53	6227	2120	45A9;45A6	1	8	31	5	–	**0.16**
Df(2R)w73-2	6247	2120	45A9;45D8	1	50	21	0	–	**0.00**
Df(2R)w73-1	6246	2120	45A9;45D8	2	50	nd	nd	–	–
Df(2R)wun-GL	68	2120	45C8;45D8	1	17	nd	nd	–	–

Deficiency	Bloomington stock number	FRT stock	Deletion cytological and (sequence) coordinates	Rec. (*n*)	Genes deleted (*n*)	CNSs analysed (*n*)	Motor neurons observed (*n*)	Phenotype seen	Average neurons per CNS
Df(2R)w45-19g	6245	2120	45C8;45E1	1	19	nd	nd	–	–
Df(2R)BSC29	6917	2120	45D3;45F6	1	35	nd	nd	–	–
Df(2R)B5	1743	2120	46A1;46C12	1	49	nd	nd	–	–
Df(2R)X1	1702	2120	46C2;47A1	1	68	nd	nd	–	–
Df(2R)stan1	447*	1928	46D7;47F16	0†	214	2	0	–	0.00
Df(2R)stan2	596	1928	46F1;47B9	0†	70	nd	nd	–	–
Df(2R)en30	1145	1928	48A3;48C8	1	45	13	8	–	0.62
Df(2R)BSC3	5879	1928	48E12;49B6	2	75	nd	nd	–	–
Df(2R)vg-c	754	1928	49B2;49E2	2	62	nd	nd	–	–
Df(2R)CX1	442	1928	49C1;50D5 (2R:8587926;9950134)	2	199	nd	nd	–	–
Df(2R)BSC18	6516	1928	50D1;50D7	1	4	11	10	–	0.91

Deficiency	Bloomington stock number	FRT stock	Deletion cytological and (sequence) coordinates	Rec. (*n*)	Genes deleted (*n*)	CNSs analysed (*n*)	Motor neurons observed (*n*)	Phenotype seen	Average neurons per CNS
Df(2R)knSA4	6380	1928	51C3;51D6	1	30	nd	nd	–	–
Df(2R)Jp4	3517	1928	51F13;52F9	2	117	nd	nd	–	–
Df(2R)Jp8	3520	1928	52E1;53C1	2	69	nd	nd	–	–
Rho1 **loss of function allele (point mutation)**	3176[$]	1928	52E3;4	1	1	2	0	–	0.00
Df(2R)P803-Delta15	6404	1928	53E;53F11	2	37	nd	nd	–	–
Df(2R)k10408	5574	1928	54B16;54B16	2	9	nd	nd	–	–
Df(2R)robl-c	5680	1928	54B17;54C4	1	28	nd	nd	–	–
Df(2R)Pcl7B	3064	1928	54E08;55C1	1	95	11	2	–	0.18
Df(2R)P34	757	1928	55E6;56C1	1	59	20	3	–	**0.15**

Deficiency	Bloomington stock number	FRT stock	Deletion cytological and (sequence) coordinates	Rec. (*n*)	Genes deleted (*n*)	CNSs analysed (*n*)	Motor neurons observed (*n*)	Phenotype seen	Average neurons per CNS
Df(2R)017	543	1928	56F5;56F15	2	22	nd	nd	–	–
Df(2R)AA21	3467	1928	57B19;57E6	2	114	nd	nd	–	–
Df(2R)PK1	3469	1928	57C5;57F6	3	91	nd	nd	–	–
Df(2R)Egfr3	6276	1928	57E1;57F10	2	61	nd	nd	–	–
Df(2R)01D01Y-R21	6859	1928	57F9;58D2	1	81	18	6	–	0.33
Df(2R)or-BR6	1682	1928	59D5;60B8	2	183	nd	nd	–	–
Df(2R)Exel6082	7561	1928	60C4;60C7 (2R:20145420;20257300)	1	8	12	0	–	0.00
Df(2R)Px2	2604	1928	60C6;60D9	1	60	16	9	+	0.56
Df(2R)ED4061	9068	1928	60C8;60D13 (2R:20290110;20560724)	1	64	nd	nd	–	–
Df(2R)Exel7185	7914	1928	60C8;60D3	1	29	33	0	–	**0.00**
Df(2R)ED4071	8028	1928	60C8;60E7	1	102	1	0	–	0.00

Deficiency	Bloomington stock number	FRT stock	Deletion cytological and (sequence) coordinates	Rec. (*n*)	Genes deleted (*n*)	CNSs analysed (*n*)	Motor neurons observed (*n*)	Phenotype seen	Average neurons per CNS
			(2R:20290189;20830362)						
Df(2R)Kr10	4961	1928	60E10;60F5	1	29	nd	nd	–	–
P*-element insertion in *zipper	11215[$]	1928	60E12	1	1	13	7	–	0.54
			TOTAL	**150**	**3864**	**814**	**424**		

[$]single gene targets; *Bloomington stock no longer available (Kyoto stock number = 108904); [†]Stock already carries FRT site; [#]tested by Katsiarina Belaya; nd = not determined; FRT stock indicates the FRT-carrying Bloomington stock the deficiency was recombined in, 1646 and 1818 = FRT40A, 2120 and 1928 = FRT42D; red = deficiencies where >20 CNSs have been screened but the ratio of motor neurons per CNS is <0.1; orange = deficiencies where >20 CNSs have been screened but the ratio of motor neurons per CNS is between 0.1 and 0.2; green = deficiencies with a ratio of motor neurons per CNS >1; Rec. = number of attempts to recombine the deficiency onto the FRT chromosome; deletion = the maximum cytological breakpoints of the deficiency.

Chromosome arm	CG and CR entries in Flybase	CG and CR genes deleted by deficiencies	Deletion coverage (% of annotated genes)
2L	2857	1825	63.9
2R	3149	2039	64.8
Total	6006	3864	64.3

Table 3.2 Summary of coverage of chromosome 2 by deletions in the screen

Data derived from Flybase (v FB2011_4); see Appendix 1 in Supplementary material. Almost two-thirds of the protein-coding (CG) and non-protein-coding genes (CR) annotated on chromosome 2 are deleted by the 85 recombinant FRT-deficiency fly stocks.

(2L) of chromosome 2 generated a hit-list of 2857 protein-coding (CG) and non-protein coding (CR) entries, while for the right arm (2R) the search resulted in a hit-list of 3149 entries; a total of 6006 (CG and CR) entries were downloaded. The coverage for each deficiency, based on the maximum reported cytological breakpoints or, where known, sequence coordinates, were then entered into the data set. The largest deletion, *Df(2R)cn9*, removed 225 genes; the smallest, *Df(2R)BSC18*, deleted four. The mean number of genes deleted per deficiency stock, averaged over the collection of recombinant stocks available for screening, was 76. The library of FRT-deficiency chromosome recombinant stocks generated covered 1825 genes (63.9% of the total annotated) on chromosomal arm 2L and 2039 (64.8%) on chromosomal arm 2R. Thus, the screen had the potential to cover ~3864 (64.3%) of coding and non-coding genes on the second chromosome.

In addition, three lines carrying mutations in individual genes (rather than deficiencies) were also included in the screen. Bloomington stock 4101 is a loss of function allele in one of the three catalytic subunits of *cAMP-dependent protein kinase* (*Pka-C1*^{H2}), (Lane & Kalderon 1993). Other alleles, *Pka-C1*^{X4} and *Pka-C1*^{B3} are known to have a phenotype at the neuromuscular junction in motor neurons (Margulies et al 2005; Renger et al 2000), and Pka is involved in memory formation in *Drosophila* (Tanaka et al 2007). Bloomington stock 3176 is a loss of function allele of *Rho1* (*Rho1*$^{E3.10}$) (Halsell et al 2000), and is thought to have a role in neuroblast proliferation; lack of Rho1 has been shown to cause overextension of mushroom body dendrites (Lee et al 2000b). Bloomington fly stock 11215 is a *P*-element insertion in *zipper*, a gene that is expressed in the embryonic CNS and is required for normal axonal patterning (Zhao et al 1988).

Screening chromosome 2 using the 'ftz loop' MARCM method and FRT-deficiency recombinants

Using the protocol developed in Chapter 2 (see also Materials and methods section), early first instar larvae were selected based on genotype, dissected and their CNSs viewed immediately under UV widefield fluorescence. Table 3.1 shows the number of CNSs and

motor neurons analysed for each deficiency. By the completion of the project, 45 of the 85 available FRT-deficiency stocks had been tested, and 814 CNSs and 424 motor neurons examined. However, of the FRT-deficiency stocks tested, 24 had either ≤20 CNSs or ≤10 motor neurons analysed due to time constraints and therefore confidence in the final result of these lines is reduced.

Effects of lethality in neurons homozygous for recombinant FRT-deficiencies

It would be expected that as more genes are deleted by a deficiency, the more likely a gene or combination of genes necessary for cell survival would be lost (synthetic lethal affects). This would be expected to result in a reduced number of neurons labelled when the deficiency is screened with the 'ftz loop' MARCM stock. To test this idea, the average number of motor neurons labelled by the 'ftz loop' MARCM method for each deficiency was calculated. The average number of motor neurons per CNS varied from almost zero (suggestive of a deficiency where genes essential for cell survival were lost) to relatively high (approaching wild-type). For example, three deficiencies where >20 CNSs have been examined, have a ratio of <0.1 motor neurons per CNS: FRT42D *Df(2R)w73-2* (ratio = 0), FRT42D *Df(2R)Exel6082* (0) and FRT40A *Df(2L)drm-P2* (0.04). Another three deficiencies have a low ratio of 0.1–0.2 motor neurons per CNS: FRT42D *Df(2R)G75* (0.13), FRT42D *Df(2R)P34* (0.15) and FRT42D *Df(2R)G53* (0.16). At the other end of the scale, the deficiencies with the highest ratio (>1) of motor neurons per CNS were: FRT40A *Df(2L)al* (1.18), the *Pka-C1*^{H2} allele FRT40A 4101 (1.2), FRT40A *Df(2L)BSC7* (1.29), FRT40A *Df(2L)TE35BC-24* (1.30), FRT40A *Df(2L)C144* (1.33) and FRT40A *Df(2L)BSC28* (1.33). The ratio obtained with controls with the 'ftz loop' MARCM stock was 1.47 motor neurons per CNS. Does the likelihood of generating motor neuron MARCM 'clones' correlate with the number of genes deleted? The number of genes deleted slightly inversely correlated with the number of motor neurons labelled per CNS (r = -0.07994, n = 45) (Fig. 3.3), suggesting that as more genes are deleted, the chances of seeing a labelled motor neuron was reduced to a

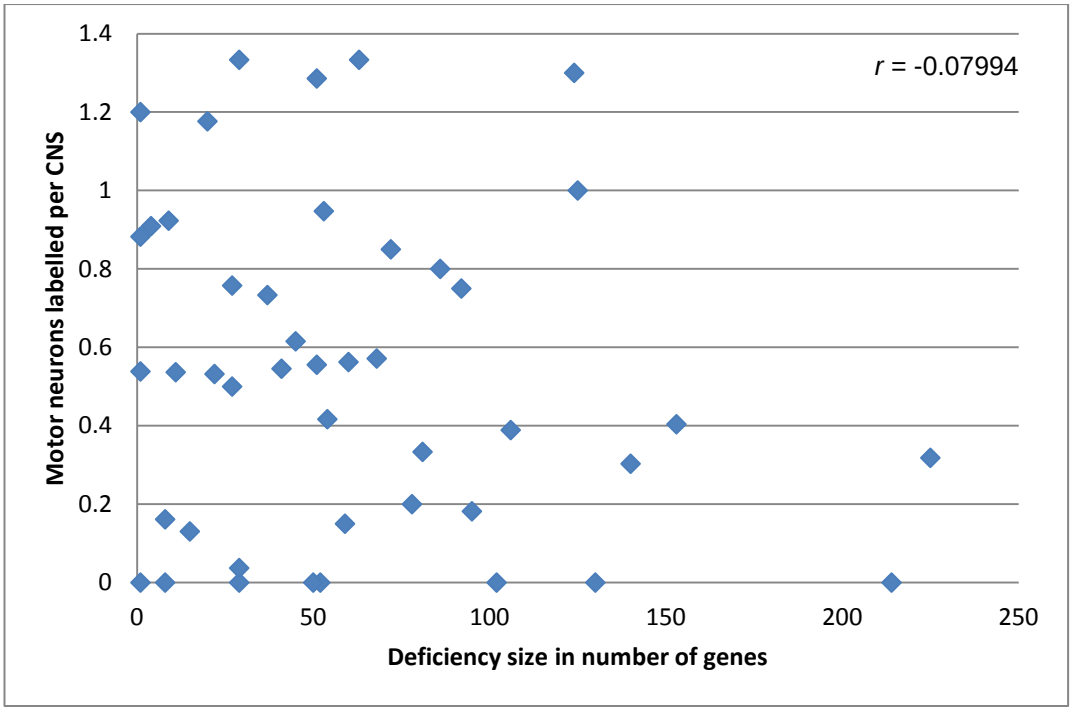

Figure 3.3 Correlation between MARCM labelling efficiency and deficiency size in terms of number of genes deleted

To see if larger deletions increased cell lethality when neurons were made homozygous for them using the ftz loop MARCM method, the number of genes deleted was plotted against the average number of motor neurons per CNS for a given deficiency. Each data point represents the average number of motor neurons per CNS for those deficiency lines where >20 CNSs or >10 motor neurons were analysed (n = 45). The number of genes deleted in a deficiency inversely correlated with the average number of motor neurons labelled per CNS to a small degree (r = -0.07994), suggesting that the size of a deletion, as determined by the number of genes deleted, does not affect the frequency of motor neurons labelled.

small degree. This was unexpected as the more genes that are deleted, the more likely a gene or combination of genes necessary for cell survival would be lost. However, although the data are limited, there is some indication that the chromosomal arm being tested affects the number of motor neurons that are labelled. This affect could be due to either the result of recombination of the deficiency chromosome with the FRT-carrying chromosome, having the deficiency in combination with the arm variant of the 'ftz loop' MARCM stock (left arm, FRT40; right arm, FRT42D) during screening, or both. When the average number of motor neurons labelled per CNS when using deficiencies on the left arm of chromosome 2 (0.78, *n* = 16) was compared with that of the right arm (0.28, *n* = 8), it suggested that the chromosomal arm being screened in some way affects the likelihood of seeing labelled motor neurons. The simplest explanation is that this difference is due to the FRT insertion sites, but other differences in genetic background and transgene composition could also be the cause. The 'ftz loop' MARCM stock for screening the right arm of chromosome 2 by necessity carries transgenes (e.g. *elav-GAL80* and FRT42D) on a different chromosomal arm to the 'ftz loop' MARCM stock for the left arm of chromosome 2. Further, the 'ftz loop' MARCM stock was put together after the left arm and was not tested with an FRT42D-carrrying control as rigorously as the right arm was with a FRT40A-carrying control.

Regions of chromosome 2 that cause a motor neuron dendrite phenotype when homozygous

Out of the 45 deficiency lines screened, phenotypes were observed with five deficiencies and one of the three single gene targets. These are described below and in Fig 3.4. As the penetrance of phenotypes was known to vary (e.g. proof of principle experiments with $shot^{1}$ and $robo^{GA285}$) the criterion for deciding if a recombinant deficiency would be taken forward for further investigation was simply dendritic arbors that looked unusual in terms of spread, positioning, decreased or increased branching, blebbing, but also axonal phenotypes if they were seen.

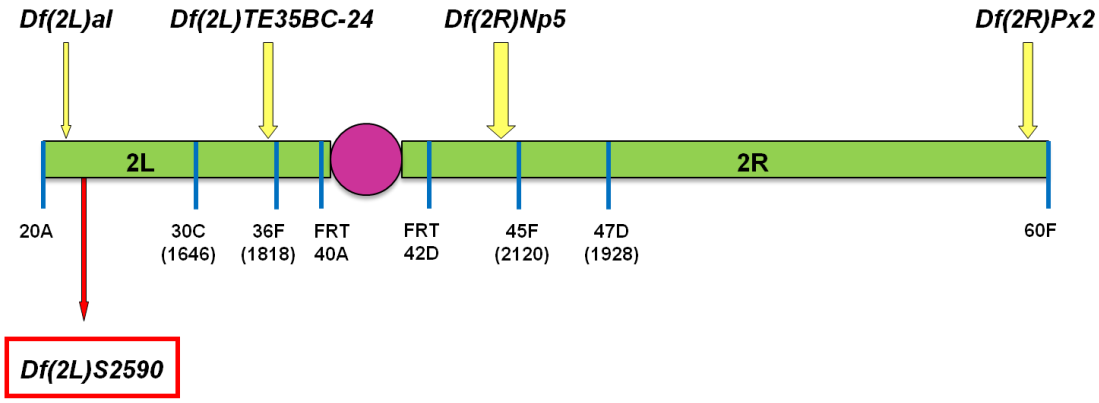

Figure 3.4 Five regions of chromosome 2 generate a dendritic phenotype in motor neurons

Representation of chromosome 2 with locations of five deficiencies (*Df*; yellow arrows) identified in the screen that cause abnormal dendritic development in motor neurons homozygous for the deficiency. *Df(2L)S2590* (red arrow) is the subject of further study. Blue lines indicate cytological points on each chromosome arm that correspond to FRT and other *P*-element insertion sites in the four stocks used for recombinations with deficiency chromosomes – Bloomington stock numbers are given in parentheses below; for example, on the left arm, stock 1646 carries the FRT site at 40A and a [w+] *P*-element insertion at 30C. Purple circle = centromere; 20A and 60F mark the cytological extremes of chromosome 2.

Df(2L)al

Df(2L)al was the most distal region on the left arm of chromosome 2 to be examined, with the first breakpoint thought to be ~300 kbp from the telomere (Brentrup et al 2000). It was also the smallest region uncovered in the screen to give a phenotype, removing ~134 kbp of genomic sequence and 20 genes. Seventeen CNSs and 20 identified motor neurons were examined and loss of secondary branching and blebbing of fine dendrites were observed (Fig. 3.5).

The recombinant FRT40A *Df(2L)al* was analysed further by looking at a subset of five overlapping FRT40A recombinant deficiencies: *Df(2L)net-PMF*, *Df(2L)BSC4*, *Df(2L)BSC16*, *Df(2L)S2* and *Df(2L)BSC107* (Fig. 3.6 and Appendix 2). FRT40A *Df(2L)BSC4* completely overlaps this region, and after analysing 33 neurons (45 CNSs) no phenotype was observed. Analysis of the overlapping recombinant deficiencies FRT40A *Df(2L)S2* and FRT40A *Df(2L)BSC16* also failed to recapitulate the phenotype observed. FRT40A *Df(2L)BSC107* and FRT40A *Df(2L)net-PMF* were not tested; the FRT40A *Df(2L)net-PMF* stock died prior to testing and the region covered by *Df(2L)BSC107* had already been screened using FRT40A *Df(2L)BSC4* (Appendix 3). These results suggested that the phenotypes seen with FRT40A *Df(2L)al* might be artefacts. The loss of branching phenotype appeared in only one of three MN-VO4/5 neurons examined and one possible reason for the blebbing phenotype observed is damage to the dendrites during preparation of the CNS. This aspect is discussed in the discussion section.

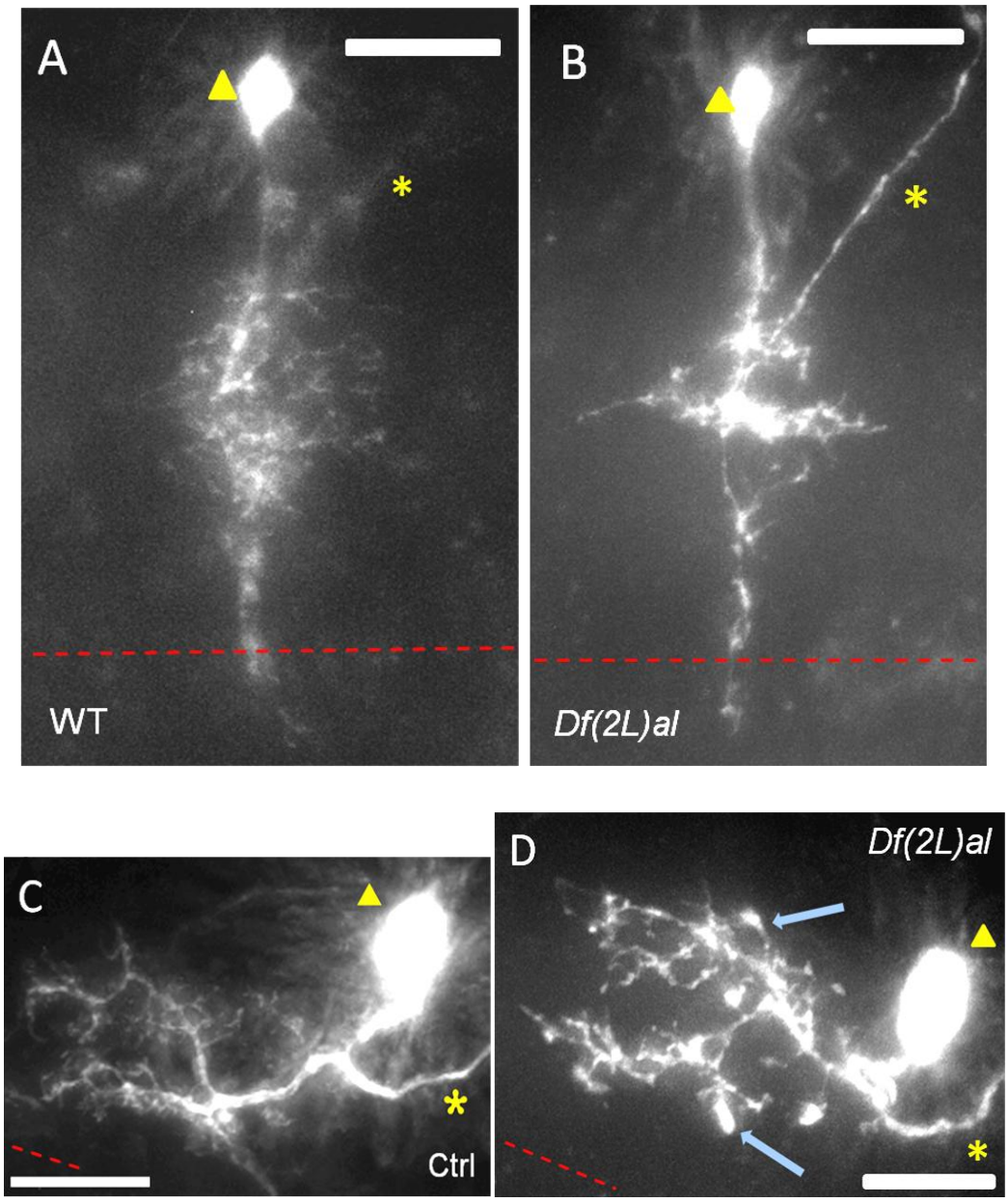

Figure 3.5 Examples of phenotypes seen in neurons homozygous for FRT40A *Df(2L)al*

(**A**) Control VO4/5 motor neuron. (**B**) VO4/5 motor neuron homozygous for *Df(2L)al* showing reduced higher order branching. (**D**) Motor neuron from the terminal ganglion with blebbing (arrows), and slight loss of higher order branching compared to control (Ctrl; **C**). Triangle = cell body; asterisk = axon; dashed red line = midline; scale bar = 10 µm; blue arrow in **D** = blebbing; anterior is left.

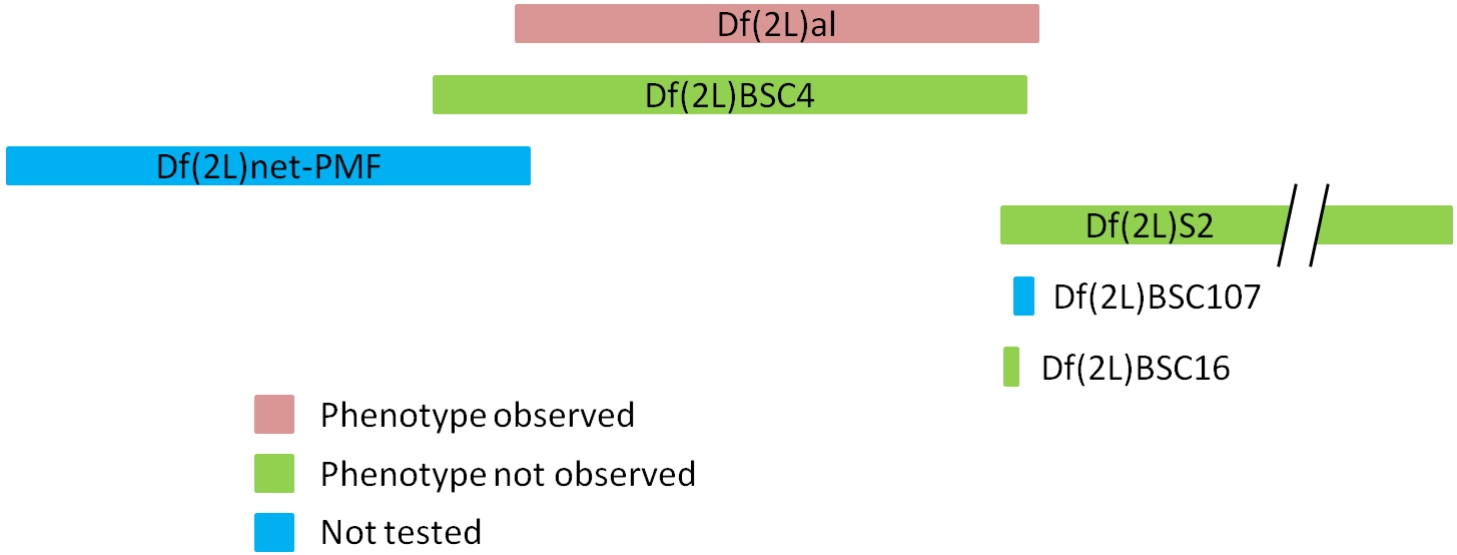

Figure 3.6 Regions of overlap between *Df(2L)al* and surrounding deficiencies

Df(2L)net-PMF was not tested as the stock died; *Df(2L)BSC107* was not tested as the region was completely overlapped by other deficiencies. The loss of branching and blebbing phenotypes observed with *Df(2L)al* were not recapitulated in any of the overlapping deficiencies tested, suggesting the phenotypes were artefacts. Sizes of deficiencies are approximate and are relative to one another. More detail of the overlaps can be found in Appendix 2 (see Supplementary CD).

Df(2L)TE35BC-24

Df(2L)TE35BC-24 was the largest deletion to give a phenotype identified in the screen. Approximately 1476 kbp and 124 genes are removed. Ten CNSs and 13 neurons were examined by another investigator (Katsiarina Belaya) and an overgrowth of dendritic arbors, with aberrant midline crossing and positioning defects in both anteroposterior and mediolateral axes were observed (Fig. 3.7). After reviewing the data, the phenotype was confirmed by me; however, because of the strong anomalies it was particularly difficult to identify the identities of the affected neurons, to compare them to equivalent control cells.

Df(2L)TE35BC-24 overlapped with nine other recombinant FRT-deficiency lines that were available in the screen fly stock collection (Fig. 3.8 and Appendix 2). At the close of the project, all nine had yet to be tested (Appendix 3).

Of the many genes deleted by *Df(2L)TE35BC-24*, several are known to be expressed in the CNS of *Drosophila* and are potential candidates. For example, *moladietz* (*mol*) encodes a molecule involved in asymmetric protein localisation and was identified in a behavioural screen for defects in memory in adult flies, where long term memory performance is reduced when compared to wild-type adults (Dubnau et al 2003). Its expression and requirement in the developing CNS are unknown. *Snail, worniu and escargot* are members of the Snail family of transcriptional regulators that are involved in several developmental processes including neurogenesis (Ashraf et al 2004; Ashraf et al 1999). Removal of all three genes has also been shown to cause disruption of asymmetric division in neuroblasts (Cai et al 2001). *Shuttle craft* (*stc*) encodes a zinc finger transcription factor that is required zygotically later in development for the correct migration of axons as they exit the CNS into the periphery (Tolias & Stroumbakis 1998). It was also identified in an embryonic head screen for novel *Drosophila* neural precursor genes (Brody et al 2002). *Cyclin E* is a well characterised gene known to be involved in regulating asymmetric cell division in neuroblasts independently of its role in the cell division cycle (Berger et al 2010). Finally, *beaten path 1a* encodes an immunoglobulin-like neural cell adhesion protein that is involved in the defasciculation of motor axons from nerves at decision points in the periphery

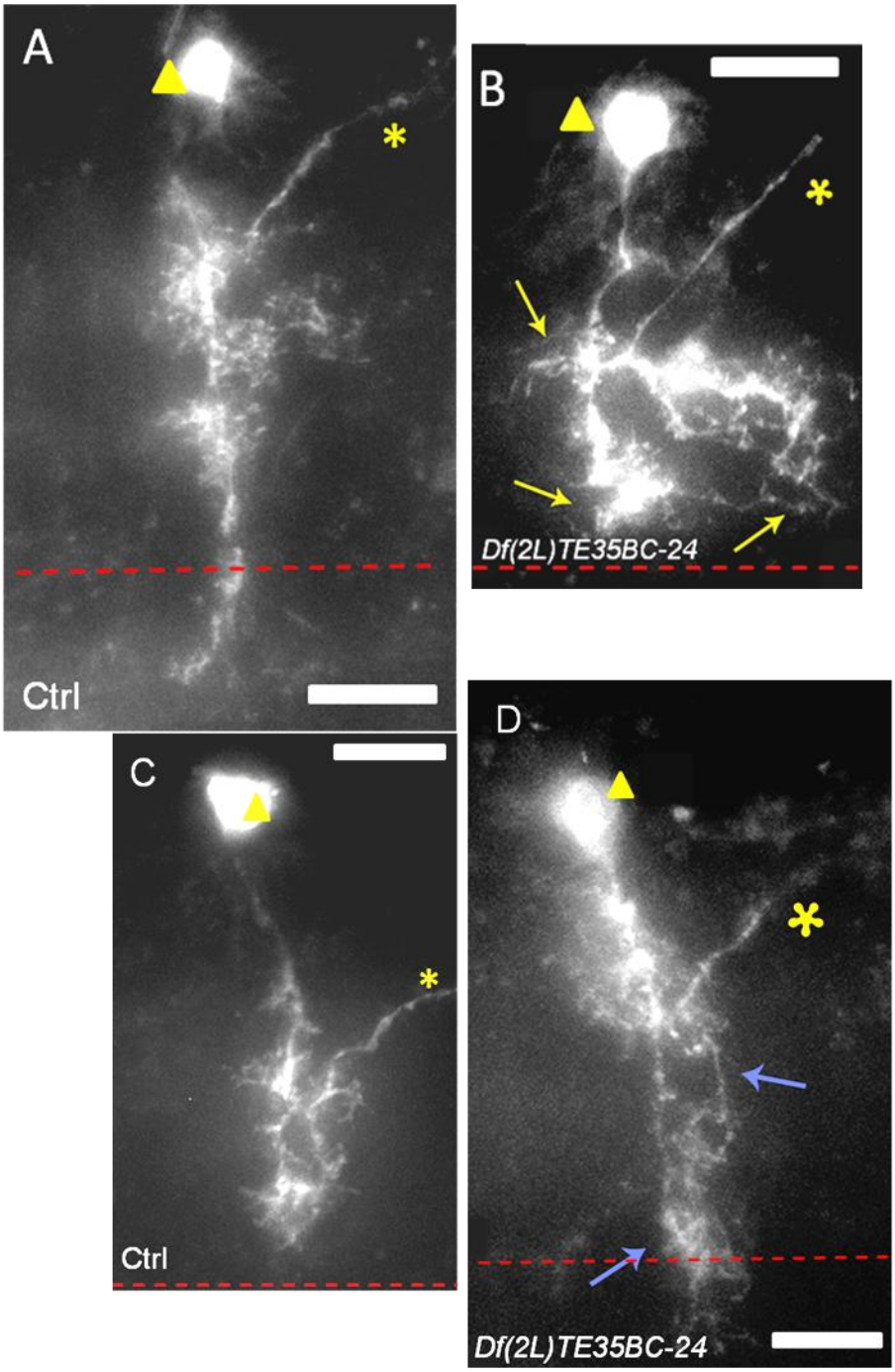
A
Ctrl
B
Df(2L)TE35BC-24
C
Ctrl
D
Df(2L)TE35BC-24

Figure 3.7 Motor neurons homozygous for FRT40A *Df(2L)TE35BC-24*

(**A**, **C**) Control MN-VO4/5 (**A**) and MN-DO5 (**C**) neurons. (**B**, **D**) MN-VO4/5 (**B**) and MN-DO5 (**D**) neurons homozygous for *Df(2L)TE35BC-24* show aberrant targeting and overgrowth of dendrites (arrows), affecting both primary and higher order branches. Motor neuron VO4/5 dendrites fail to cross the midline (**B**), while motor neuron DO5 dendrites cross abnormally (**D**).

Yellow triangle = cell body; asterisk = axon; red dashed line = midline; scale bar = 10 μm; anterior is left.

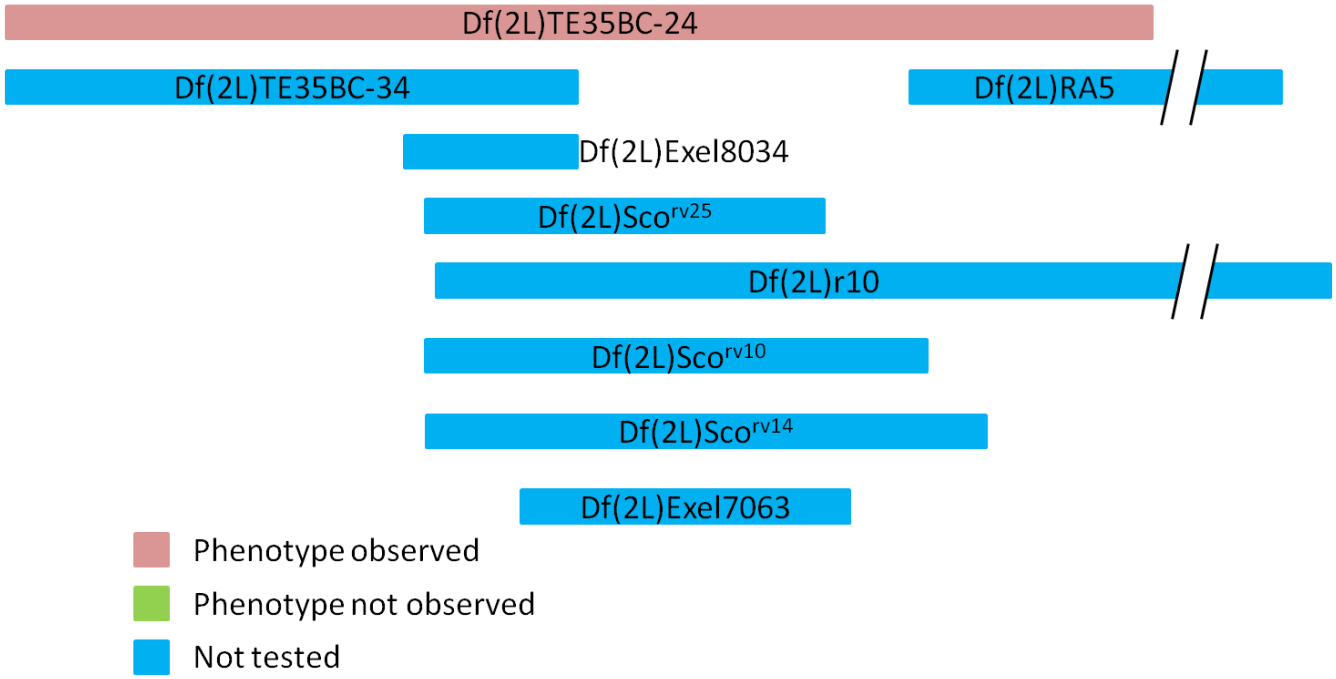

Figure 3.8 Regions of overlap between *Df(2L)TE35BC-24* and surrounding deficiencies

All of the deficiencies that overlap with *Df(2L)TE35BC-24* have yet to be tested. Sizes of deficiencies are approximate and are relative to one another. More detail of the overlaps can be found in Appendix 2 (see Supplementary CD).

(Fambrough & Goodman 1996). The role, if any, of these genes in dendrite morphogenesis has not been determined.

Df(2R)Np5

Df(2R)Np5 was the most proximal deficiency region on the right arm of chromosome 2 found to have a phenotype when absent. Approximately 562 kbp and 87 genes are deleted. The phenotype identified during the screen after examining nine motor neurons from a total of 12 CNSs was a positioning defect of dendrites in the mediolateral axis and axon misrouting (Fig. 3.9). The phenotype was identified in a FRT42D *Df(2R)Np5* homozygous ventral transverse (VT) motor neuron, which is easily identified by the characteristic way in which the axon exits the CNS dorsally at the midline.

The region deleted by FRT42D *Df(2R)Np5* was analysed further by screening eight smaller and overlapping deficiencies available from the FRT-deficiency library: FRT42D *Df(2L)H3E1*, FRT42D *Df(2L)w73-1*, FRT42D *Df(2L)w73-2*, FRT42D *Df(2L)w45-30n*, FRT42D *Df(2L)G53*, FRT42D *Df(2L)wun-GL*, FRT42D *Df(2L)w45-19g* and FRT42D *Df(2L)BSC29* (Fig. 3.10 and Appendix 2). Of these, three had been screened by the end of the project. FRT42D *Df(2L)H3E1*, covering the most proximal part of FRT42D *Df(2R)Np5* did not recapitulate the phenotype after screening 18 CNSs and seven motor neurons. Similarly, FRT42D *Df(2L)w45-30n* and FRT42D *Df(2L)G53* that overlapped the most distal part of FRT42D *Df(2R)Np5*, also failed to produce the phenotype seen with FRT42D *Df(2R)Np5* after screening 18 and 31 CNSs, and 10 and five motor neurons, respectively (Appendix 3).

The genes uncovered in *Df(2R)Np5* include many candidate genes already known to be expressed in the CNS, with diverse roles including: remodelling of dendrites during pupation (*baboon*; Zheng et al 2003), sensory neuron dendrite morphogenesis (*shrub*; Gao et al 1999), cell adhesion (*hikaru genki*; Hoshino et al 1996; Kurusu et al 2008), synapse formation (*wunen*/*wunen2*; Kraut et al 2001b) and synaptic plasticity and maintenance (*bruchpilot*; Kittel et al 2006; Wagh et al 2006). Although deletion of any one or more of these genes has the potential to cause the phenotype seen with FRT42D *Df(2R)Np5*, none

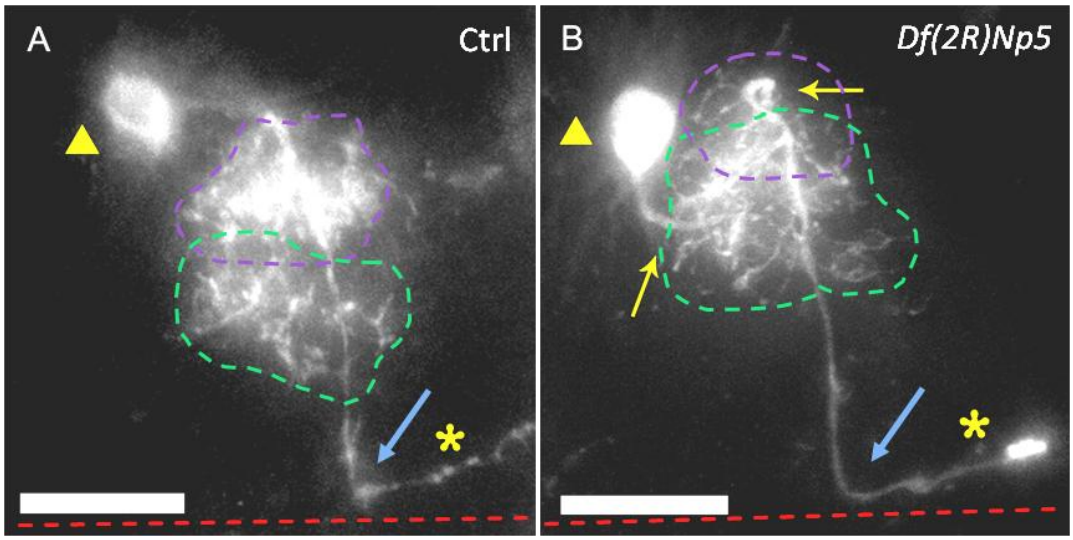

Figure 3.9 Phenotype in a VT motor neuron homozygous for FRT42D *Df(2R)Np5*

(**A**) Control VT motor neuron with distinctive dendrite and axon morphology. The VT motor neuron normally has two separate dendritic sub-arbors, one at a ventrolateral location (purple dashed line) and the other in a dorsomedial position (green dashed line); both sub-arbors emerge from the primary neurite. The axon has a characteristic trajectory, exiting the CNS dorsally at the midline (blue arrows). (**B**) Axon targeting and aberrant dendritic positioning phenotypes in a VT motor neurons homozygous for *Df(2R)Np5* (*n* = 1). The axon branches from the cell body medially rather than posteriorly, and twists (yellow arrows); however, it still succeeds in following its normal trajectory out of the CNS. The mediolateral sub-arbor is shifted laterally so that in a *z*-projection image, both sub-arbors overlay each other. It is not known whether this phenotype is reproducible for this neuron type. As MARCM events for VT neurons are relatively rare, (frequency of 3.4% of all neurons with the 'ftz loop' MARCM method) another example was not obtained during the screen with this deficiency.

Yellow triangle = cell body; red dashed line = midline; asterisk = axon; scale bar = 10 µm; anterior is left.

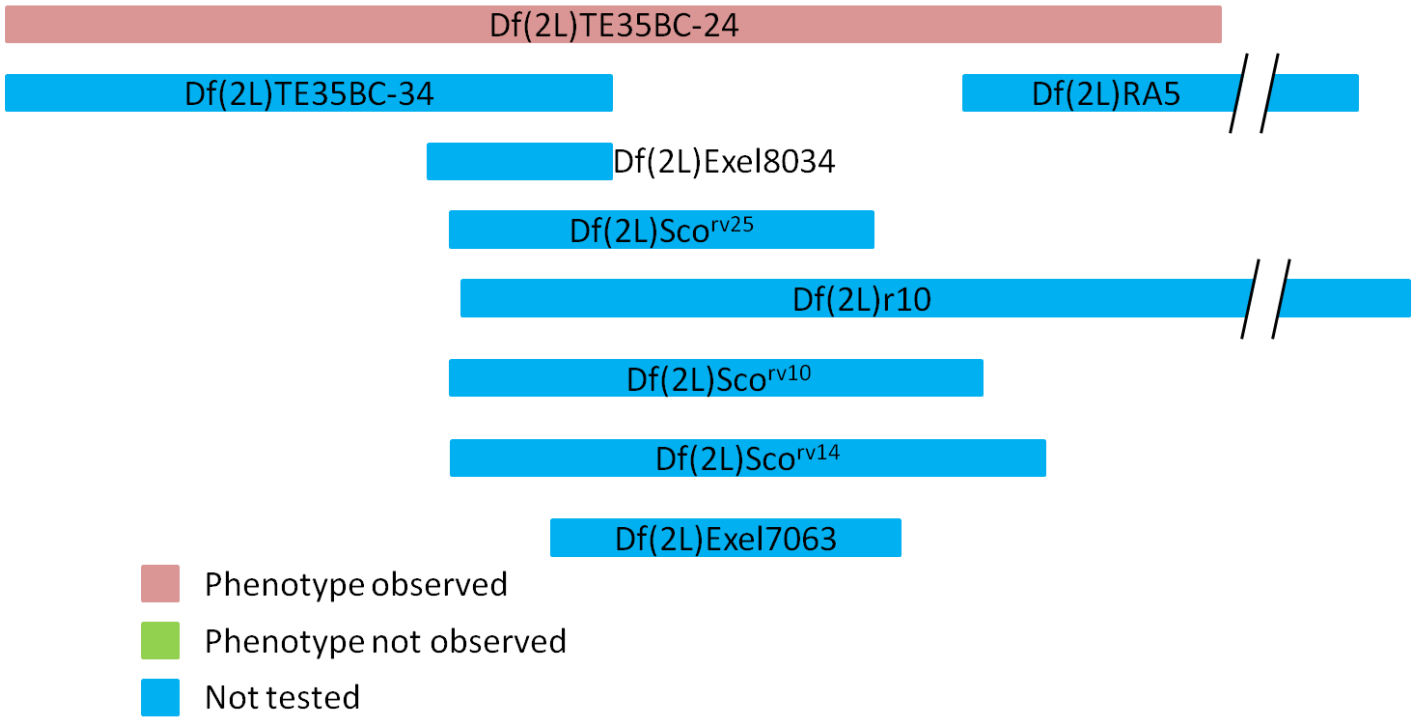

Figure 3.10 Regions of overlap between *Df(2L)TE35BC-24* and surrounding deficiencies

All of the deficiencies that overlap with *Df(2L)TE35BC-24* have yet to be tested. Sizes of deficiencies are approximate and are relative to one another. More detail of the overlaps can be found in Appendix 2 (see Supplementary CD).

are contained within the 12 genes deleted by the deficiency that were not overlapped by other deficiencies that were screened. Of these 12 genes, several are small nucleolar RNAs (snoRNAs); non-coding RNAs involved in post-transcriptional modification of other RNAs. Their requirement in dendrite morphogenesis has not been established. However, it has been shown that such molecules are involved in neuroblast division, where neuroblasts mutant for a snoRNA coding gene, *wicked*, produce fewer neurons (Fichelson et al 2009).

Df(2R)Px2

Df(2R)Px2 deletes a very distal part of the right arm of chromosome 2, quite close to the telomere. Removal of this region resulted in two different phenotypes: blebbing (irregular bulges of the cell membrane) and mistargeting of secondary dendrites (Fig. 3.11). About 345 kbp and 42 genes are deleted by this deficiency, which was further analysed by screening four overlapping recombinant deficiencies lines: FRT42D *Df(2L)Exel6082*, FRT42D *Df(2L)Exel7185*, FRT42D *Df(2L)ED4071* and FRT42D *Df(2L)ED4061* (Fig. 3.12). Of these, only two stocks have been tested sufficiently thus far: FRT42D *Df(2L)Exel6082* and FRT42D *Df(2L)Exel7185*, with 12 and 33 CNSs analysed, respectively. However, neither deficiency produced any labelled motor neurons from those CNSs tested. For FRT42D *Df(2L)ED4071*, only one CNS was tested, also with no labelled motor neurons, and this is not enough data to draw any conclusions and further testing of this line is necessary. The final deficiency, FRT42D *Df(2L)ED4061* had not been tested at the conclusion of the project.

Candidate genes include *nervy* (*nvy*), muscarinic acetylcholine receptor 60C (mAcR-60C) and beta 3 tubulin (βTub60D). *Nvy* is a zinc finger transcription factor known to be involved in regulating Semaphorin 1a axon repulsion. In loss of function mutants motor neuron axons are defasciculated and have inappropriate projections (Terman & Kolodkin 2004). It is also involved in dendrite morphogenesis of sensory neurons, where RNAi knockdown of the transcript resulted in increased dendritic branching (Parrish et al 2006a).

mAcR-60C is a *Drosophila* homologue of vertebrate muscarinic acetylcholine receptor. It belongs to the G protein coupled receptor family and its functions in the CNS include

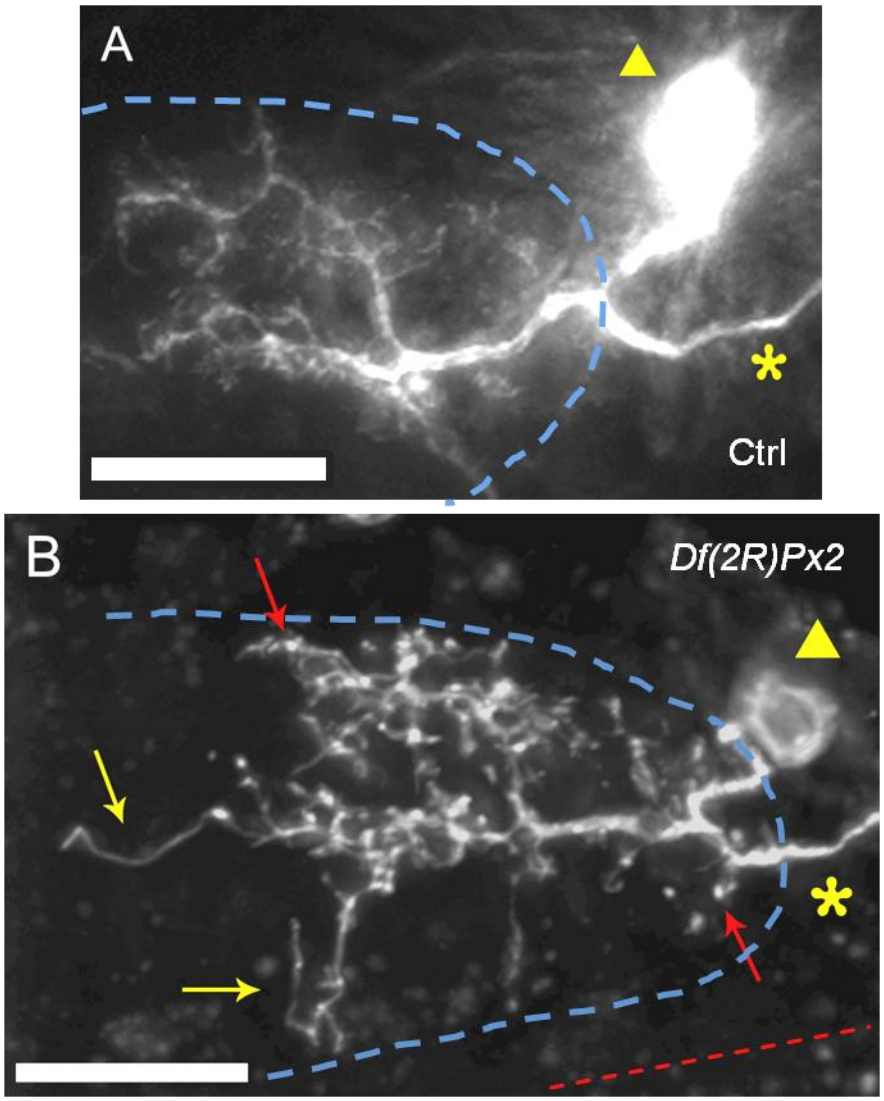

Figure 3.11 Motor neurons homozygous for FRT42D *Df(2R)Px2*

(**A**) Control motor neuron in the terminal ganglion. (**B**) Neurons homozygous for FRT42D *Df(2R)Px2* have a phenotype consisting of blebbing (red arrows) and overgrowth of long unbranched dendritic segments (yellow arrows). Midline is not visible in **A** and is to the lower left as in **B**. Blue dashed line demarcates the posterior end of one of the two neuropils.

Yellow triangle = cell body; red dashed line = arrowhead = midline; asterisk = axon; scale bar = 10 µm; anterior is left.

Figure 3.12 Regions of overlap between *Df(2R)NPx2* and surrounding deficiencies

Two deficiencies that overlap *Df(2R)NPx2* have been tested, with negative results. Limited screening of *Df(2R)ED4071* was carried out, however, too few motor neurons had been analysed at the close of the project to give a conclusive result. Sizes of deficiencies are approximate and are relative to one another. More detail of the overlaps can be found in Appendix 2 (see Supplementary CD).

acetylcholine receptor signalling and the muscarinic pathway (Grumbling & Strelets 2006). In rats, nicotinic receptors have been shown to have a role in neurite outgrowth (Coronas et al 2000). Although *Drosophila* motor neurons express nicotinic acetylcholine receptors (another type of acetylcholine receptor) and are receptive to acetylcholine (Baines & Bate 1998; Fayyazuddin et al 2006), it is not known if they express muscarinic acetylcholine receptors.

βTub60D is a well characterised component of the cytoskeleton required for many and varied processes in *Drosophila*. These include viability and fertility (Kimble et al 1990), mistargeting of axons in the optic lobe (Hoyle et al 2000) and light avoidance in the larva (Dettman et al 2001).

Bloomington stock 4101

As detailed above, Bloomington stock 4101 is a loss of function allele of *Pka-C1* (*Pka-C1*^{H2}), known to have multiple roles in the CNS at different life stages. At the time that this line was screened, its identity was unknown and it was tested as for any of the other deficiencies. Nevertheless, after analysis of 18 motor neurons from 15 CNSs, an increase in higher order branching phenotype was observed (Fig. 3.13). This result also provided added reassurance that phenotypes could be identified with the 'ftz loop' MARCM method, even when blinded to the predicted result (in contrast to the positive control experiments with *shot*^{2} and *robo*^{GA285} as detailed in Chapter 2 where it was already known that these mutants would likely produce a dendritic phenotype).

This result coincided with other work in the lab by colleagues interested in the growth of dendrites in response to changes in synaptic activity. In their paper, Tripodi and colleagues investigated the changes in dendritic structure that take place when connections are first made during embryonic development (Tripodi et al 2008) and how neurons maintain homeostasis. They showed that a reduction of Pka activity (using a dominant negative regulatory subunit) resulted in an induction of dendritic overgrowth.

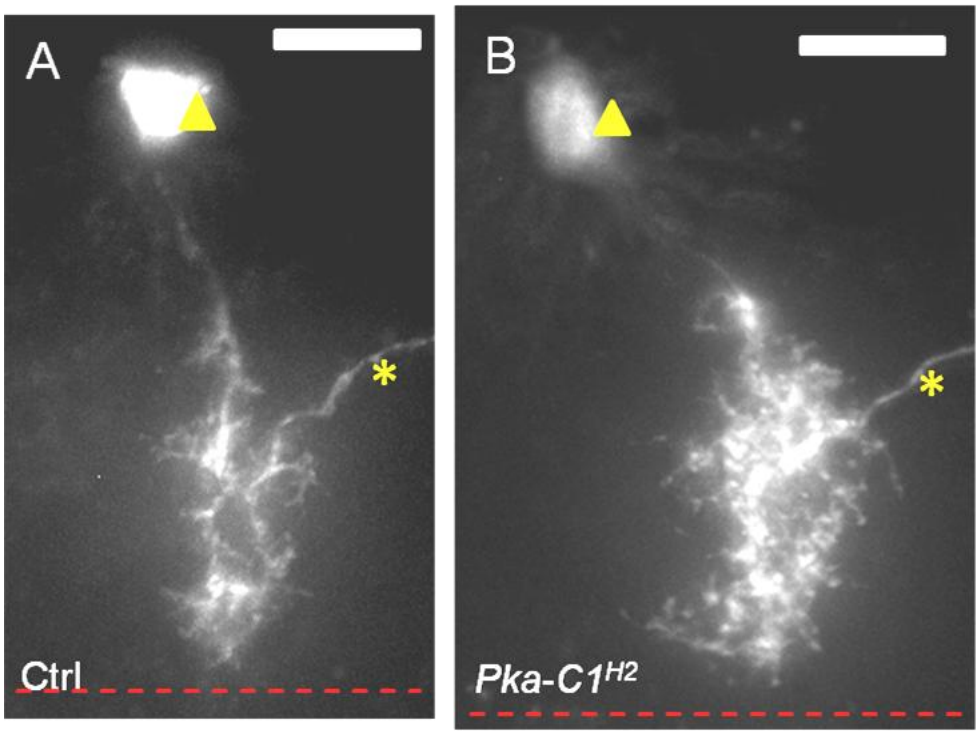

Figure 3.13 Phenotype in motor neurons homozygous for FRT40A, *Pka-C1^{H2}*

DO5 motor neuron homozygous for FRT40A *Pka-C1^{H2}*, a loss of function mutation in the *cAMP-dependent protein kinase 1* gene (**B**), have increased higher order branching when compared to an equivalent control neuron (**A**).

Red dashed line = midline; yellow triangle = cell body; asterisk = axon; scale bar = 10 µm; anterior is to the left.

As a consequence of this overlap between projects, it was decided that further experiments with Pka-C1, as part of this project, would be abandoned.

Df(2L)S2590

The rest of the project concentrated on identifying the gene(s) responsible for the phenotype observed in *Df(2L)S2590*, and is presented in the following chapters.

Chapter 4 Df(2L)S2590

Chapter 4 presents the analysis of *Df(2L)S2590*. The presence of the deficiency is confirmed and overlapping deficiencies are used to isolate the region of the chromosome containing the gene(s) responsible for the phenotype. Expression analysis of seven candidate genes is presented and identifies *CG34393*, a previously uncharacterised gene as the most likely candidate.

Previously, in Chapter 3, the results of four regions identified in the screen that have a phenotype when deleted were presented. The fifth region to be identified was *Df(2L)S2590* and is the subject of the work described below.

Df(2L)S2590 is a relatively small chromosomal deletion that was generated by x-ray mutagenesis. Its breakpoints have been mapped to lie at cytological locations 2L:23D2 and 2L:23E3. In total, ~197 kbp are deleted, disrupting 21 genes mapped to this region (Flybase version FB2011_05). The dendritic phenotype seen in motor neurons made homozygous for this deficiency is characterised by positioning defects in the mediolateral axis. As can be seen in Fig. 4.1, dendrites are abnormally drawn towards the midline and/or cross the midline; conversely, in neurons whose dendrites would normally cross the ventral midline, failure to cross is observed. These phenotypes suggested that a gene or genes is/are deleted by *Df(2L)S2590* that is/are necessary for correctly interpreting midline signals, which have been shown as critical in positioning motor neuron dendrites in the mediolateral axis and for gating midline crossing (Brierley et al 2009; Kim & Chiba 2004; Mauss et al 2009; Ou et al 2008).

Twenty-five motor neurons were analysed from 47 CNSs; the types of motor neurons examined are summarized in Appendix 3. A strong midline phenotype was identified in one of the five VO4/5 motor neurons and a reduction in the number of higher order branches was observed in another VO4/5 motor neuron. The penetrance of these phenotypes seemed low (a phenotype was seen in 4% of all motor neurons analysed) compared to the penetrance of similar strength phenotypes seen with the positive control experiments with $shot^{2}$ and $robo^{GA285}$ (a phenotype was seen in 7.7% of all labelled $shot^{2}$ mutant motor neurons and 16.7% of all labelled $robo^{GA285}$ mutant motor neurons). Nevertheless, *Df(2L)S2590* was put forward for further analysis using overlapping deficiencies.

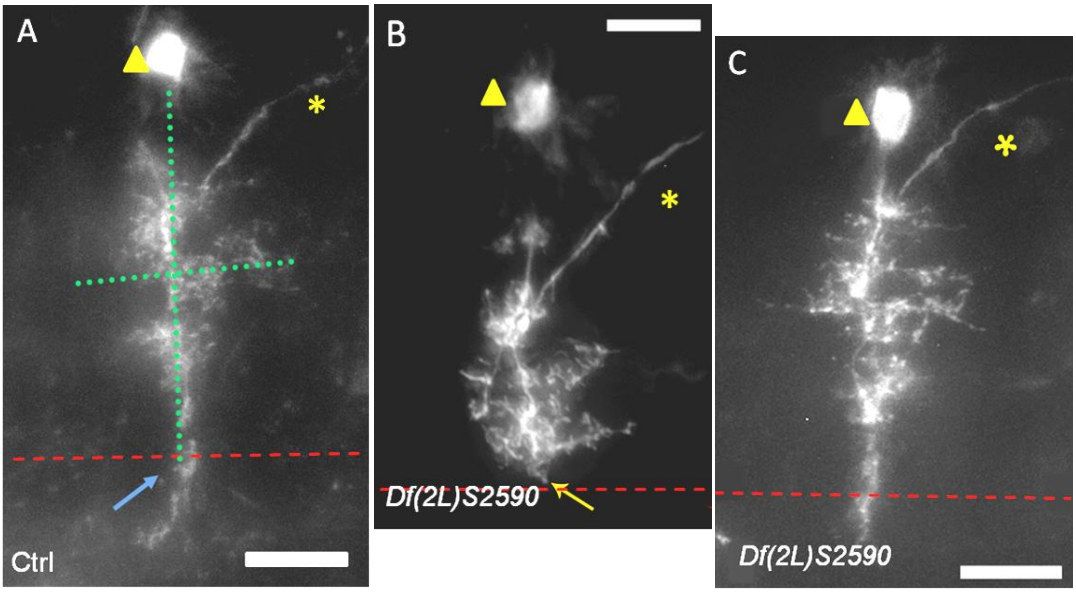

Figure 4.1 Examples of dendritic phenotypes in motor neurons homozygous for FRT40A *Df(2L)S2590*

(**A**) Control VO4/5 motor neurons have a characteristic cross-shaped arbor (green dashed line) with one branch that extends just over the midline (blue arrow). (**B**) Dendrites of neurons homozygous for the recombinant deficiency FRT40A *Df(2L)S2590* failed to branch in the typical way and did not cross the midline (yellow arrow in **B**). The phenotype is not 100% penetrant, as shown in the example in **C** (see main text). The midline phenotype was repeated in a different neuron type homozygous for the overlapping deficiency FRT40A *Df(2L)BSC28*, (see Fig. 4.3)

Triangle = cell body; asterisk = axon; red dashed line = midline; scale bar = 10 µm; anterior is left.

Analysis of deletions overlapping with *Df(2L)S2590* refines the genomic area containing candidate genes for dendritic development

In order to narrow down the area containing the gene(s) responsible for this dendritic phenotype, deficiencies overlapping with *Df(2L)S2590* were identified using Flybase. Figure 4.2 shows the relative positions of the four deficiencies identified from Flybase whose aberrations overlap with *Df(2L)S2590*. More detail of the overlaps can be found in Appendix 2 (see Supplementary CD).

Df(2L)BSC28 is a deletion generated using *P-element* recombination and distally overlaps with the majority of *Df(2L)S2590*. It deletes and disrupts 29 genes between the cytological location 2L:23C5 and 2L:23E2; all except four of these genes are also deleted in *Df(2L)S2590*.

The small deficiency *Df(2L)BSC162* was also generated by FLPase mediated recombination of *P-elements* (Christensen & Cook 2006; Thibault et al 2004). The breakpoints have been mapped accurately molecularly, showing that this deficiency removes 11.8 kbp containing 11 genes, seven of which are also deleted by *Df(2L)S2590*.

At its proximal end *Df(2L)S2590* overlaps with *Df(2L)Exel8008*, also generated by FLPase mediated recombination. *Df(2L)Exel8008* deletes 52 kbp containing 10 genes, five of which are also deleted in *Df(2L)S2590*.

Two genes deleted by *Df(2L)S2590* are also deleted by *Df(2L)JS32*, however, FRT40A *Df(2L)JS32* was not tested as the genes deleted were already covered by FRT40A *Df(2L)BSC28* and FRT40A *Df(2L)BSC162*, and motor neurons made homozygous for these deficiencies appeared normal. Further, FRT40A *Df(2L)BSC162* was later found not to repeat the phenotype seen in motor neurons homozygous for FRT40A *Df(2L)S2590*.

The recombinant deficiency lines FRT40A *Df(2L)BSC28*, FRT40A *Df(2L)BSC162* and FRT40A *Df(2L)Exel8008* were analysed using the ‘ftz loop’ MARCM method, as described previously; results are presented below.

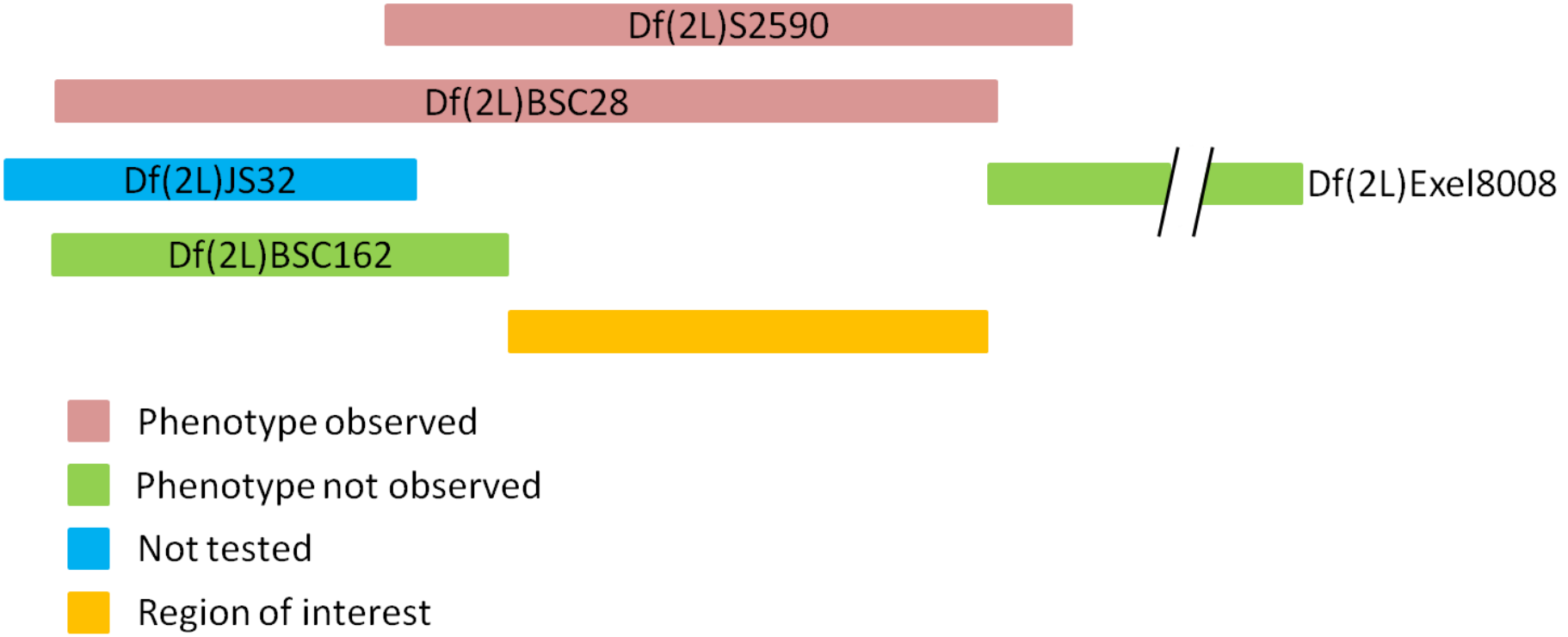

Figure 4.2 Regions of overlap between *Df(2L)S2590* and surrounding deficiencies

The midline attraction/repulsion phenotype observed in neurons deficient for the region deleted in *Df(2L)S2590* was recapitulated by *Df(2L)BSC28*, but not in *Df(2L)BSC162* and *Df(2L)Exel8008*, suggesting that gene(s) of interest would lie in the region highlighted in orange. *Df(2L)JS32* was not tested, however, the part that overlaps with *Df(2l)S2590* is already covered by *Df(2L)BSC162*. More detail of the overlaps can be found in Appendix 2 (see Supplementary CD).

MARCM analysis of dendritic phenotypes deficiencies that overlap with Df(2L)S2590

Df(2L)BSC28

In total 12 CNSs were examined for FRT40A *Df(2L)BSC28*. Of these, nine had labelled motor neurons (*n* = 16 neurons) suitable for analysis, the remainder having no labelled motor neurons, or containing only glia, interneurons or motor neurons in thoracic segments. The 15 abdominal motor neurons analysed consisted of five identifiable types, which are summarized in Appendix 3. One motor neuron identified as 'L-shape' aberrantly crossed the midline (Fig. 4.3A). In addition to the 15 identified neurons, one other cell could not be identified unambiguously, though its primary branch structure suggests it to be another 'L-shape' motor neuron with particularly strongly affected dendrites (Fig. 4.3B). In this example, some dendrite branches were attracted to the midline as normal, but continued to grow and appeared to 'rebound' away from the midline while remaining on the ipsilateral side. Furthermore, other branches that would normally grow in the anteroposterior axis were attracted to the midline.

In summary, of the 15 motor neurons analysed, two had a dendritic phenotype related to midline attraction and/or repulsion – a similar phenotype to that seen in neurons homozygous for FRT40A *Df(2L)S2590*. The penetrance of the phenotype seen in motor neurons homozygous for FRT40A *Df(2L)BSC28* was higher (a phenotype was seen in 13.3% of all motor neurons analysed) and was observed in a different neuronal type ('L-shape' as opposed to MN-VO4/5 motor neurons); the three MN-VO4/5 motor neurons homozygous for FRT40A *Df(2L)BSC28* appeared normal. This is not unusual as three out of five MN-VO4/5 neurons analysed with FRT40A *Df(2L)S2590* also appeared normal.

Interestingly, the decrease in higher order branching, as observed in some motor neurons made homozygous for FRT40A *Df(2L)S2590*, was not recapitulated in cells made homozygous for FRT40A *Df(2L)BSC28*. It is conceivable that the decreased branching phenotype was cell type-specific to MN-VO4/5 motor neurons or that in *Df(2L)S2590*, this

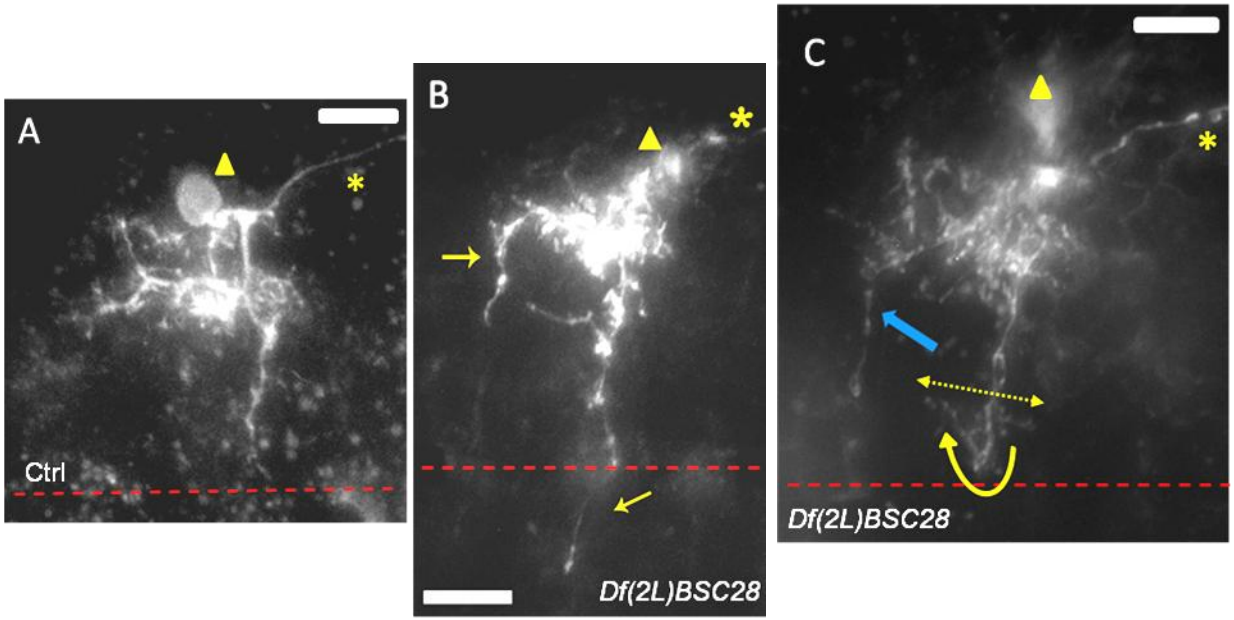

Figure 4.3 The midline crossing phenotype seen in FRT40A *Df(2L)S2590* is recapitulated with FRT40A *Df(2L)BSC28*

(**A**) Control 'L-shape' neurons have a characteristic reverse 'L-shape' with two main dendritic branches perpendicular to one another, one projecting anteriorly and the other medially. In one mutant 'L-shape' neuron (**B**), the medial branch extended over the midline, while the anteriorly extending branch changed direction after leaving the cell body, moving towards the midline (arrows). In another example (**C**), the medial branch appeared to 'rebound' away from the midline (yellow arrow) and then branched as shown (dashed yellow arrow). Further, the anterior branch (blue arrow), similar to **B**, is drawn first diagonally in an anteromedial direction, before turning and heading towards the midline.

Triangle = cell body; asterisk = axon; dashed red line = midline; scale bar = 10 µm; anterior is left.

particular feature of the dendritic phenotype was synthetic: caused by loss of a combination of genes; four genes covered by *Df(2L)S2590* are not covered by *Df(2L)BSC28*.

Df(2L)BSC162

For FRT40A *Df(2L)BSC162*, 41 CNSs were dissected, yielding a total of 13 motor neurons suitable for analysis of dendritic phenotypes. A further nine neurons were discounted as they were thoracic or not unambiguously identifiable. The distribution is summarized in Appendix 3 and representative examples are shown in Fig. 4.4. No midline phenotype was observed in neurons homozygous for FRT40A *Df(2L)BSC162*. However, a loss of fine, higher order branching seemed to occur in some neurons, though it is unclear whether this reflects slight differences in age, GFP expression, imaging or image processing artefacts.

Df(2L)Exel8008

For FRT40A *Df(2L)Exel8008*, 13 CNSs were dissected giving 14 motor neurons for analysis as summarized in Appendix 3. Two other neurons that were marked were not included due to their location in thoracic segments of the CNS. Representative examples are shown in Fig. 4.5. No dendritic midline phenotype was observed in neurons made homozygous for FRT40A *Df(2L)Exel8008*.

To summarize, phenotypic analysis of 'ftz loop' MARCM method labelled motor neurons showed that: (i) motor neurons homozygous for FRT40A *Df(2L)BSC28* recapitulated the midline phenotype seen with FRT40A *Df(2L)S2590*; and (ii) no obvious dendritic phenotypes were seen when cells were made homozygous for, FRT40A *Df(2L)BSC162* or FRT40A *Df(2L)Exel8008*, thus defining the regions of overlap between FRT40A *Df(2L)S2590* and FRT40A *Df(2L)BSC28* as containing candidate gene or genes required for dendrite development.

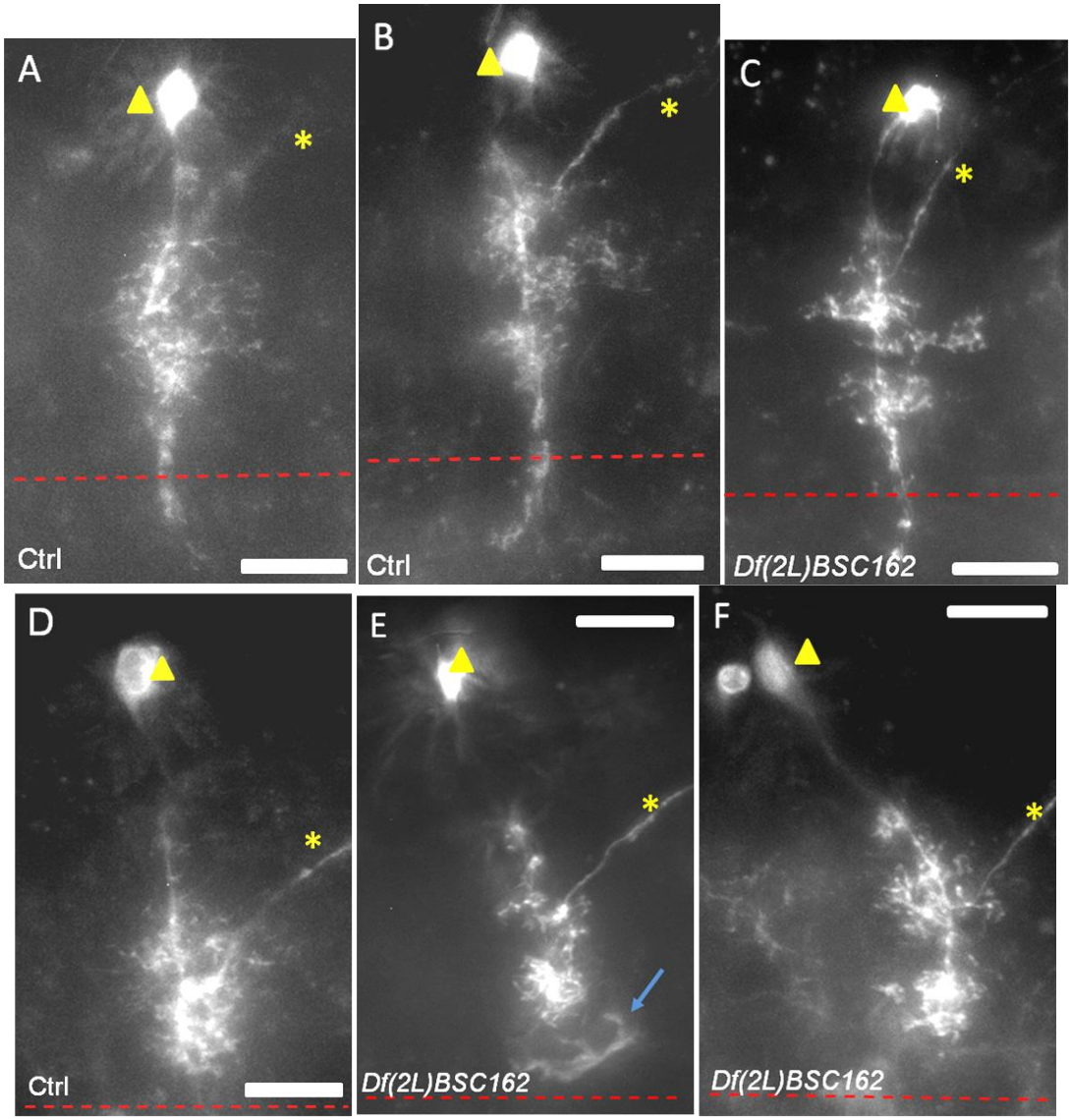

Figure 4.4 Motor neurons homozygous for FRT40A *Df(2L)BSC162* have normal dendrites

Control (**A**, **B** and **D**) and neurons homozygous for FRT40A *Df(2L)BSC162* (**C**, **E** and **F**): MN-VO 4/5 (**C**) and MN-DO5 (**E**, **F**). No dendritic midline phenotype was visible in mutant neurons compared to controls and therefore the phenotype seen in motor neurons homozygous for FRT40A *Df(2L)S2590* was not recapitulated in FRT40A *Df(2L)BSC162*.

Triangle = cell body; asterisk = axon; dashed red line = midline; scale bar = 10 µm; anterior is left; blue arrow in **E** = glial cell wrapped around the medial edge of the neuropil.

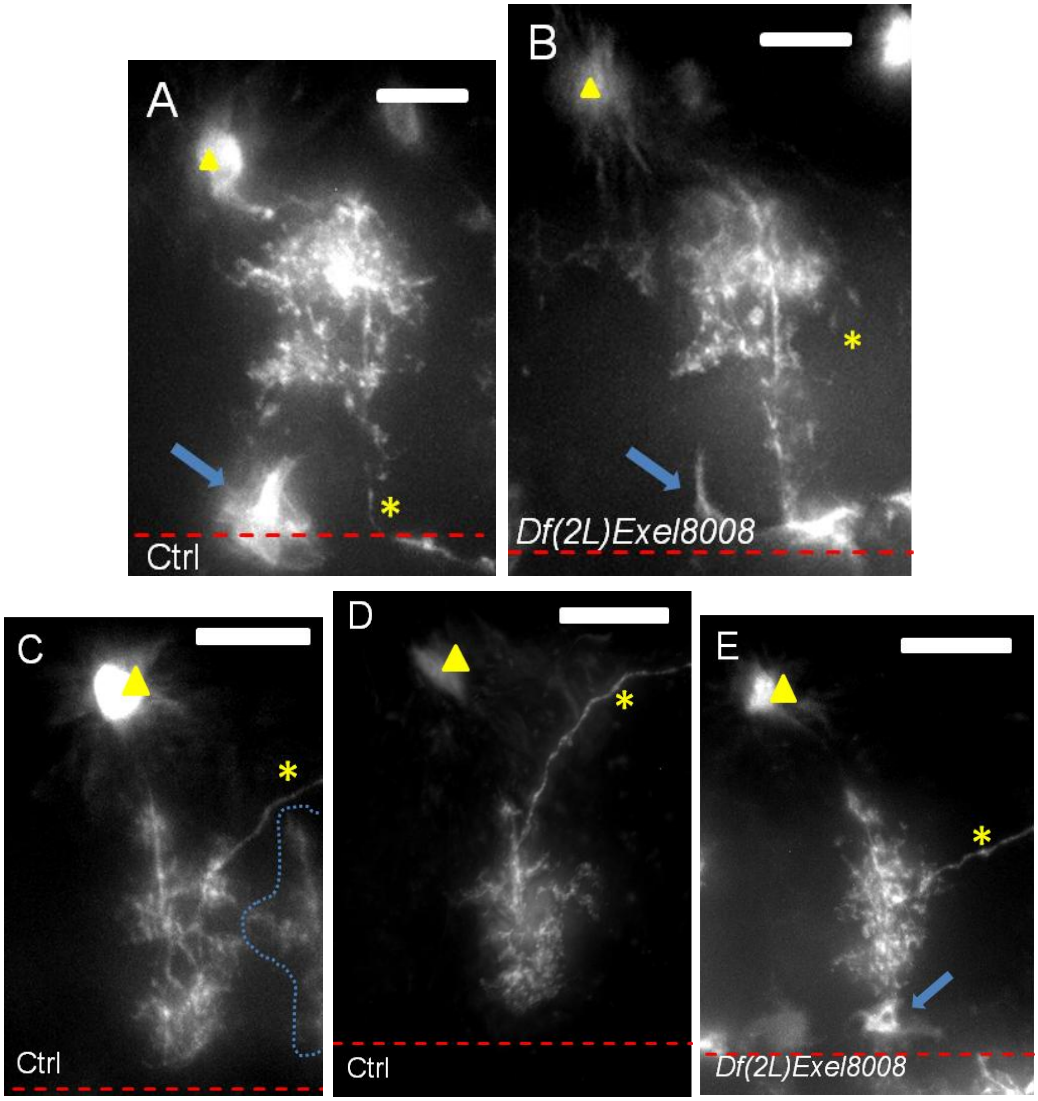

Figure 4.5 Motor neurons homozygous for FRT40A *Df(2L)Exel8008* have normal dendrites

Control (**A**, **C** and **D**) and neurons homozygous for FRT40A *Df(2L)Exel8008* (**B, E**); MN-VT (**A**, **B**) and MN-DO5 (**C**, **D** and **E**). (**A** and **B**) Both characteristic axon trajectory and dendritic arborizations in the mutant neuron were similar to controls. (**C, D** and **E**) MN-DO5 made homozygous for FRT40A *Df(2L)Exel8008* (**E**) appears to have normal dendritic arbors in terms of mediolateral patterning. These results suggest that there is no midline phenotype in FRT40A *Df(2L)Exel8008* mutant neurons.

Triangle = cell body; asterisk = axon; red dashed line = midline; scale bar = 10 µm; anterior is left; blue arrows in **A**, **B** and **E** = glial cell wrapped around the medial edge of the neuropil; blue dashed line demarcates dendrites of a neighbouring neuron.

This region thus identified spans 13.8 kbp and contains the seven protein-coding genes: *CG34406*, *CG31698*, *CG15404*, *CG34393*, *CG3347*, *CG3332* and *CG9664* (Fig. 4.6). At the most distal and proximal ends of the region, the two genes *alpha/beta hydrolase2* (*Hydr2*) and *CG9663* are truncated by *Df(2L)BSC162* and *Df(2L)Exel8008*, respectively. The breakpoint in *Df(2L)BSC162* at sequence coordinates 2L:3164472 deletes about the first 800 bp of *Hydr2*. Similarly the breakpoint at 2L:3302636 deletes about the first 500 bp of CG9663. These fore-shortened genes were assumed non-functional and since not associated with dendritic phenotypes were not included in the candidate shortlist.

Two additional genes in this 13.8 kbp region are transfer RNAs, tRNA:s7:23Ea and tRNA:s7:23Eb, which are thought to be copies of one another (Leung et al 1991). According to Flybase, there are six tRNA:ser genes that are located on chromosomes 2, 3 and X. Although some transfer RNA genes are known to be required during development (e.g. in *Xenopus*; Stutz et al 1989), these two transfer RNAs were not included in the shortlist due to redundancy in the genome (Leung et al 1991; Tweedie et al 2009).

Complementation analysis confirms that *Df(2L)S2590* is contiguous with FRT40A and does not cause dendritic phenotypes in a heterozygous condition

To ensure that the deficiency carried in Bloomington stock number 4954, which carries the deficiency *Df(2L)S2590* is actually responsible for the observed dendritic phenotype, a range of experiments were carried out.

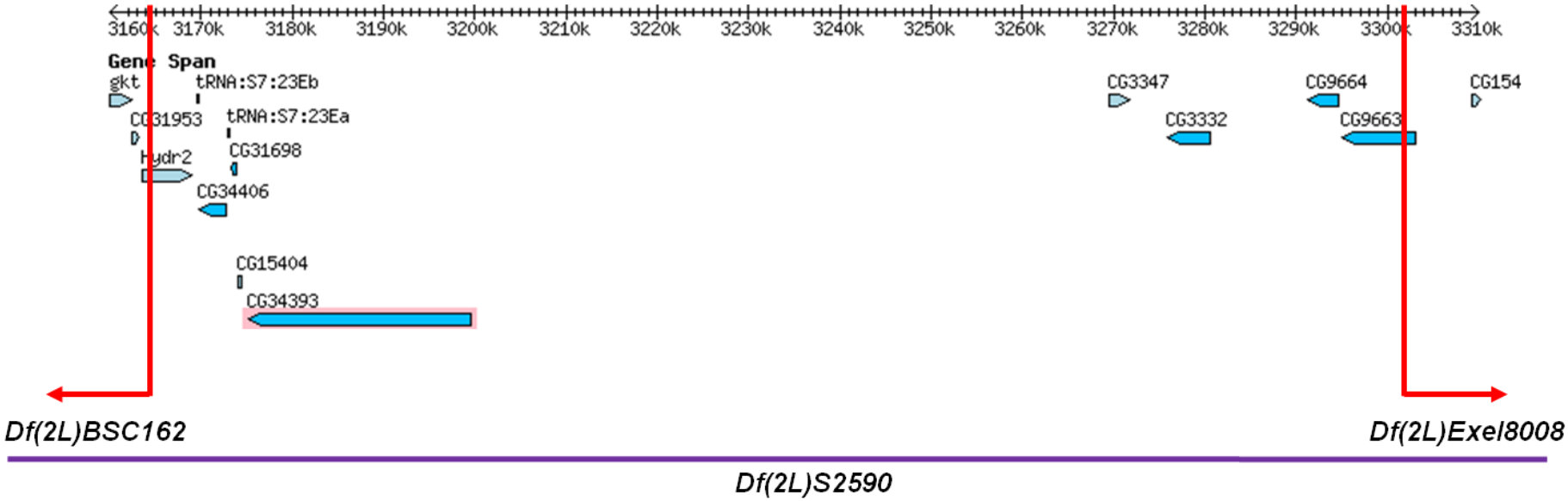

Figure 4.6 Genomic region containing candidate gene(s) required for dendrite development

Nine genes, comprising seven protein coding and two non-protein coding genes (transfer RNAs) were identified by MARCM analysis of deficiencies overlapping with FRT 40A *Df(2L)S2590*. *Hydr2* and *CG9663* are truncated by FRT40A *Df(2L)BSC162* and FRT40A *Df(2L)Exel8008*, respectively. The first 800 bp of *Hydr2* and 500 bp of *CG9663* are deleted and as dendritic phenotypes were not observed in neurons homozygous for FRT40A *Df(2L)BSC162* and FRT *Df(2L)Exel8008*, the genes were not included in the candidate shortlist. The region containing candidate genes covers ~13.8 kbp.

First, confirmation that *Df(2L)S2590* was contiguous with the FRT40A site was demonstrated by:

- Survival of the fly line on selective media containing neomycin
- Generation of labelled cells only when crossed to the FRT40A ftz loop MARCM fly line
- When crossed to Bloomington Stock 5615, which carries *eyeless*-FLP; FRT40A, adult progeny have clones in the eye.

The presence of the deficiency was confirmed by:

- Failure to complement itself (i.e. balancer was always maintained)
- Failure to complement overlapping deficiencies *Df(2L)BSC162* and *Df(2L)BSC28*. However, unexpectedly FRT40A *Df(2L)S2590* did complement FRT40A *Df(2L)Exel8008*; furthermore FRT40A *Df(2L)Exel8008* failed to complement FRT40A *Df(2L)BSC28*, both of which are reported to overlap by only one gene: *CG9663*.
- Failure to complement a FRT42D *Df(2L)S2590* line, where the deficiency was recombined with a different FRT site (FRT42D) on the right as opposed to the left chromosome arm. This also served to confirm that FRT40A *Df(2L)S2590* does not produces a similar phenotype when heterozygous: motor neurons heterozygous for FRT40A *Df(2L)S2590* appeared to have normal dendritic arbors (CNSs n = 40; motor neurons n = 18).

In situ hybridisations identify candidate genes contained within *Df(2L)S2590* with embryonic central nervous system expression

At the time of analysis, according to Flybase release 5.1, nine genes were located in the genomic region within *Df(2L)S2590* identified with overlapping deficiencies and shown to have a dendritic phenotype. A later release (5.2) merged four of these genes into two different genes (*CG18555* and *CG3485* became *CG34406*; *CG15405* and *CG8829* became

CG34393). The *in situ* hybridisation experiments outlined below were based on the earlier release, so that two different probes were generated for both *CG34406* and *CG34393*.

To determine which of the candidate genes are normally expressed in the CNS during its development and therefore potentially have a role in dendrite morphogenesis, *in situ* hybridisations were carried out as described in the materials and methods. Digoxigenin labelled probes were made for each gene using the largest exon as a template (some of the genes are relatively small). Where more than one transcript was indicated by Flybase, more than one probe was made; as was the case for *CG9664*, which had three transcripts predicted by Flybase release 5.1 at the time. Probes were used at three different concentrations (1:100, 1:1000 and 1:5000) to determine the optimum dilution; for those genes with CNS expression, hybridisations were repeated to confirm results. All probes were made simultaneously from agarose gel verified PCR products (for size) and quantified using a Nanodrop spectrophotometer (yield); hybridisation steps included a *robo* positive control probe, made and confirmed as functional by a colleague (B.C.)

Table 4.1 summarises the results for the *in situ* hybridisations. Where available, data from the BDGP *in situ* database are also included.

Anti-sense probes generated for detection of transcripts of genes *CG31698*, *CG15404* and *CG9664* gave no staining in embryos (Figs 4.7 and 4.8). For *CG9664*, two probes against exons 3 and 6 were used to detect and distinguish between the three transcripts predicted in Flybase release 5.1.

The *in situ* results for *CG31698* correlated with data from the BDGP *in situ* database. At the time of writing, Flybase (release FB 2011_05) high-throughput expression pattern data for both *CG31698* and the adjacent gene *CG15404* showed extremely high expression in third instar larval salivary gland (Gelbart & Emmert 2010); their function is unknown.

The same Flybase dataset showed *CG9664* to have very high expression levels in late larval fat body and moderate expression levels in larval midgut, Malpighian tubules, adult fat body, and virgin spermatheca. *CG9664* is predicted to have ABC transporter activity – proteins that are involved in the import and export of molecules in and out of cells.

Gene	*In situ* staining	BDGP *in situ* data
CG34406 (CG3485)	Yolk cells (weak – likely background)	No data
CG34406 (CG18555)	Yolk cells (weak – likely background)	No staining seen at any stage
CG31698	No staining	No staining seen at any stage
CG15404 (Exon 1)	No staining	No data
CG34393 (CG15405)	CNS (strong) Stage 14 onwards	No data
CG34393 (CG8829)	CNS (weak)	No data
CG3347	Yolk cells (weak – likely background)	No data
CG3332	Hindgut, rectum	Stage 13-16; embryonic rectum and anal pad
CG9664 (Exon 3, present in Transcript A, B and C)	No staining	No data
CG9664 (Exon 6, present in Transcript A and B)	No staining	No data

Table 4.1 Summary of *in situ* hybridisations of candidate genes

Additional data was obtained from the Berkley *Drosophila* Genome Project *in situ* database [http://insitu.fruitfly.org/cgi-bin/ex/insitu.pl; (Tomancak et al 2002)].

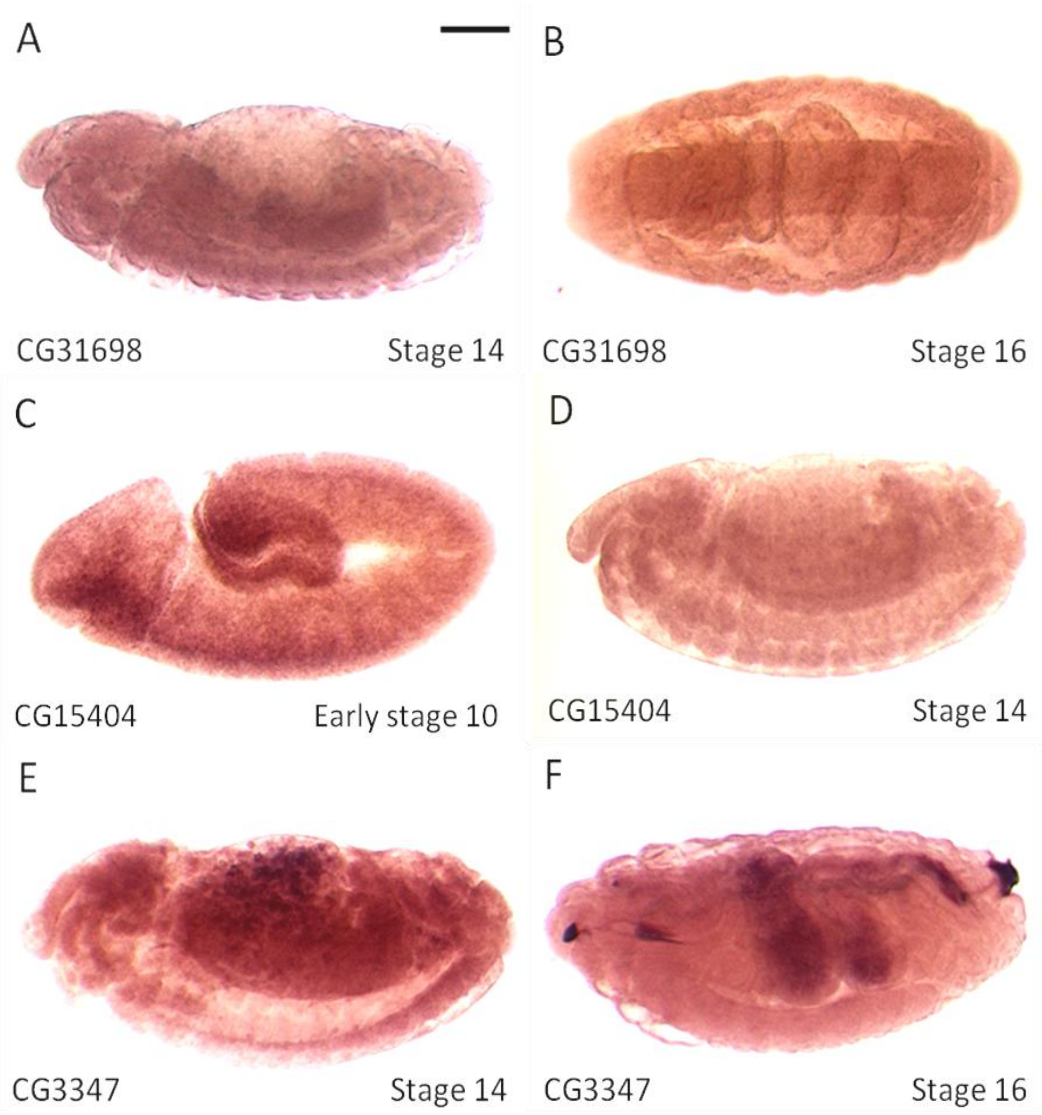

Figure 4.7 *In situ* hybridisation results for *CG31698*, *CG15404* and *CG3347*

Oregon-R wild-type embryos hybridised with digoxigenin labelled anti-sense probe against *CG31698* (**A** and **B**) and *CG15404* (**C** and **D**). No obvious staining was seen. (**E** and **F**) Embryos hybridised with probe against *CG3347*. Some staining can be seen in yolk cells (**E**) and in the gut of older embryos (**F**), however this is likely to be non-specific background staining, which is also evident in trachaea and spiracles (arrow heads). Scale bar = 100 µm. Anterior is left and dorsal is up except **B**, which is viewed ventrally.

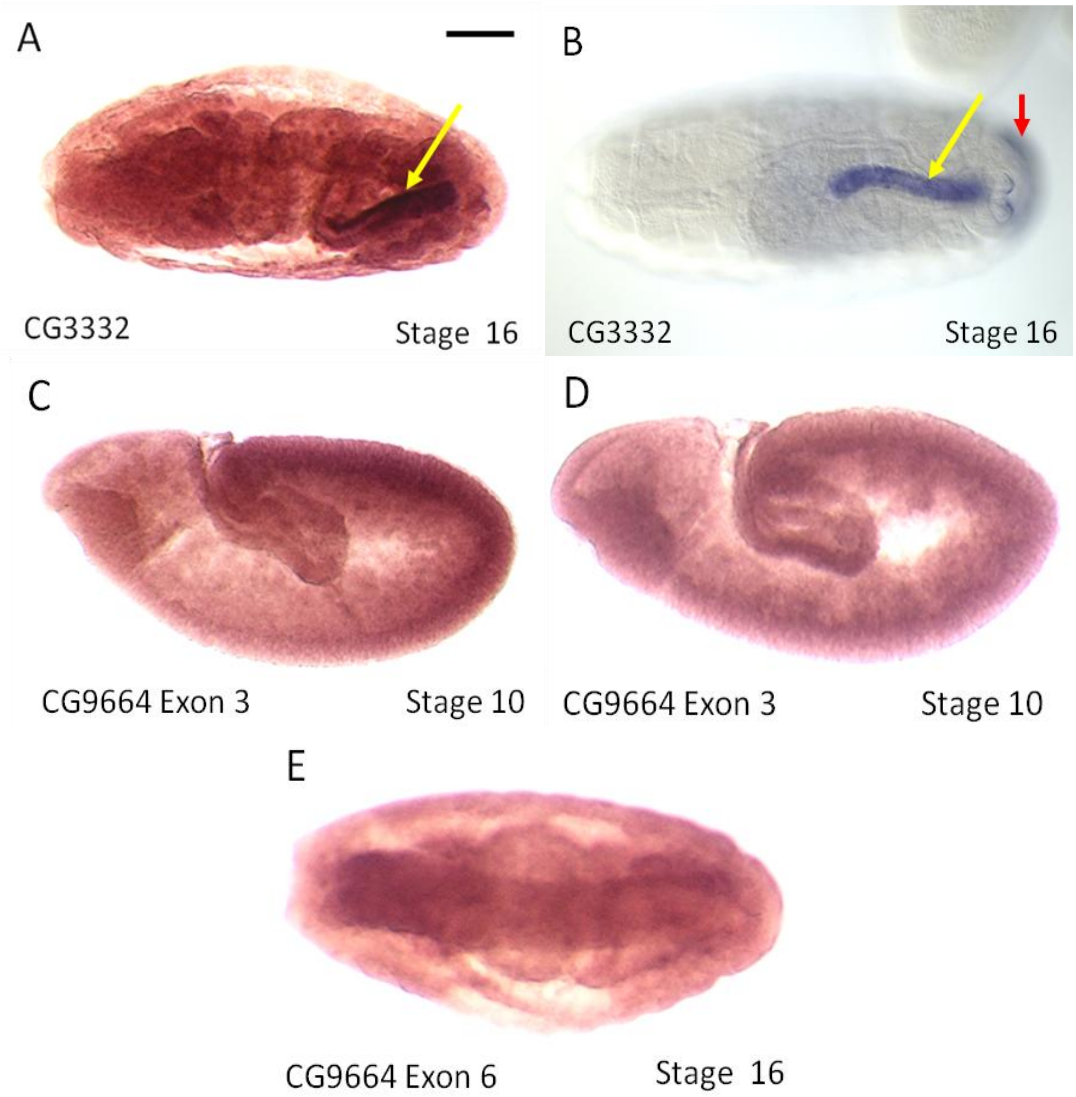

Figure 4.8 *In situ* hybridisation results for *CG3332* and *CG9664*

(**A**) Wild-type embryos hybridised with *CG3332* digoxigenin labelled anti-sense probe. Strong expression was seen in the hindgut/rectum (yellow arrows) that corresponds with the BDGP result shown in **B**, which also had staining in the anal pads (red arrow) not seen in **A** (Tomancak et al 2002). No specific staining was evident in embryos hybridised with anti-sense probes against Exon 6 (**C**) or Exon 3 (**D** and **E**) of *CG9664*.

Scale bar = 100 µm. In all images, anterior is left. In **A** and **B**, images are dorsal views; in **C** and **D** dorsal is up; and in **E**, image is a ventral view.

CG34406 and *CG3347* appeared to have weak *in situ* staining in yolk cells (Figs 4.7 and 4.9); however, this was probably background staining as yolk staining normally occurs during early developmental stages (stages 4–6). Two probes for *CG33406*, made from templates of *CG3485* and *CG18555* prior to them being merged into a single gene gave similar results. CG34406 is a predicted zinc-finger protein with moderate expression levels in embryos up to 12 hours of age (~stage 15); no expression was detected in larval or adult life stages (high-throughput expression pattern data from Flybase; Gelbart & Emmert 2010) and its function is currently unknown.

CG3332 had a strong expression signal in the developing hindgut/rectum of the embryo (Fig 4.8). This result correlates with data from the BDGP *in situ* database, although the BDGP *in situ* also revealed expression in the anal pads. High-throughput expression data suggests a moderate level of expression in later embryonic stages (18–24 hours) and high levels of expression in larval midgut and adult hindgut. CG3332 function has not yet been determined.

In situ hybridisation of *CG34393*, comprising probes made against *CG15405* and *CG8829* (subsequently merged into a single gene, *CG34393*), shows expression in the CNS (Fig. 4.10). Small groups of cells are moderately labelled in a segmentally repeated pattern in both the ventral nerve cord and the brain lobes. High-throughput data suggest that CG34393 is expressed at low levels from 12–24 hours of embryonic development, and at low levels in the larval CNS, and adult brain and thoracicoabdominal ganglion. It is predicted to have Ras guanine nucleotide exchange factor activity, a family of proteins that regulate Ras – membrane bound molecular switches – by promoting the uptake of fresh guanine triphosphates (GTP).

In summary, the *in situ* experiments suggest that the most likely candidate gene, whose loss in FRT40A *Df(2L)S2590* causes a dendritic phenotype, is *CG34393* as it is the only gene in the chromosomal region of interest with demonstrated expression in the embryonic CNS. However, this does not completely rule out those genes for which *in situ* probes revealed no or no convincing staining (e.g. *CG31698*, *CG15404*, *CG34406*, *CG3347* and *CG9664*). Different probe designs might yield different results and it may be that levels of expression of these genes are below the detection limit of the assay.

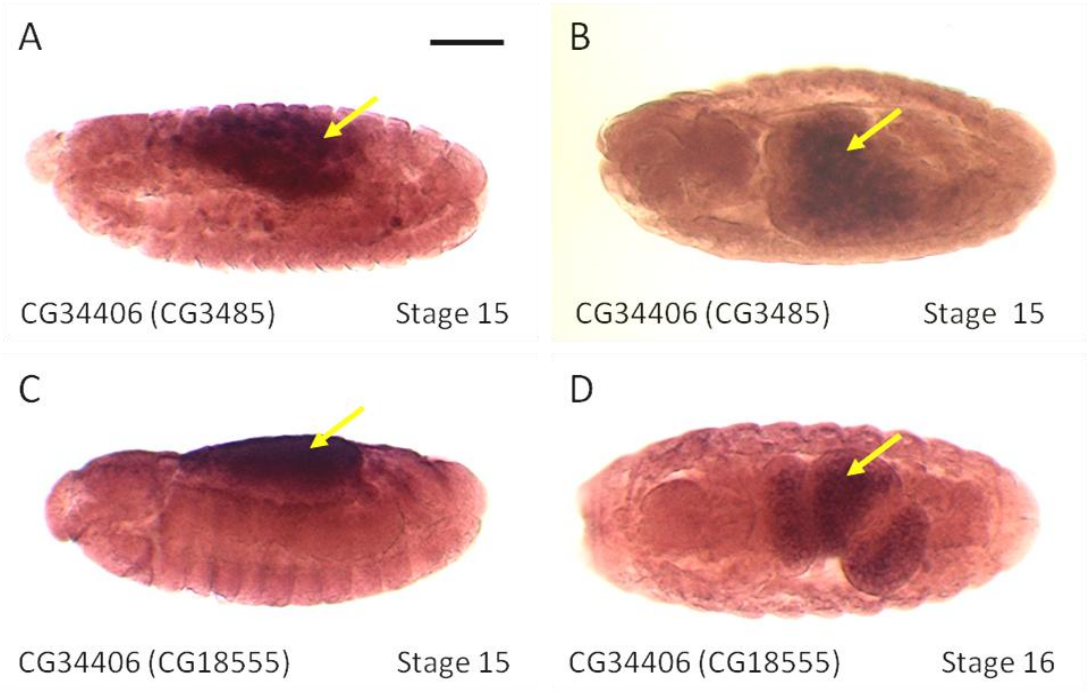

Figure 4.9 *In situ* hybridisation results for *CG34406*

In Flybase release 5.2, *CG3485* and *CG18555* were merged as they are now thought to be part of a single gene, *CG34406*. No specific staining was evident for *CG34406* with either anti-sense probes against *CG3485* (**A** and **B**) or *CG18555* (**C** and **D**). Non-specific background staining was seen in yolk cells and later in the gut (arrows).

Scale bar = 100 µm. Anterior is left; **A** and **C,** dorsal is up; **B** and **D**, dorsal view.

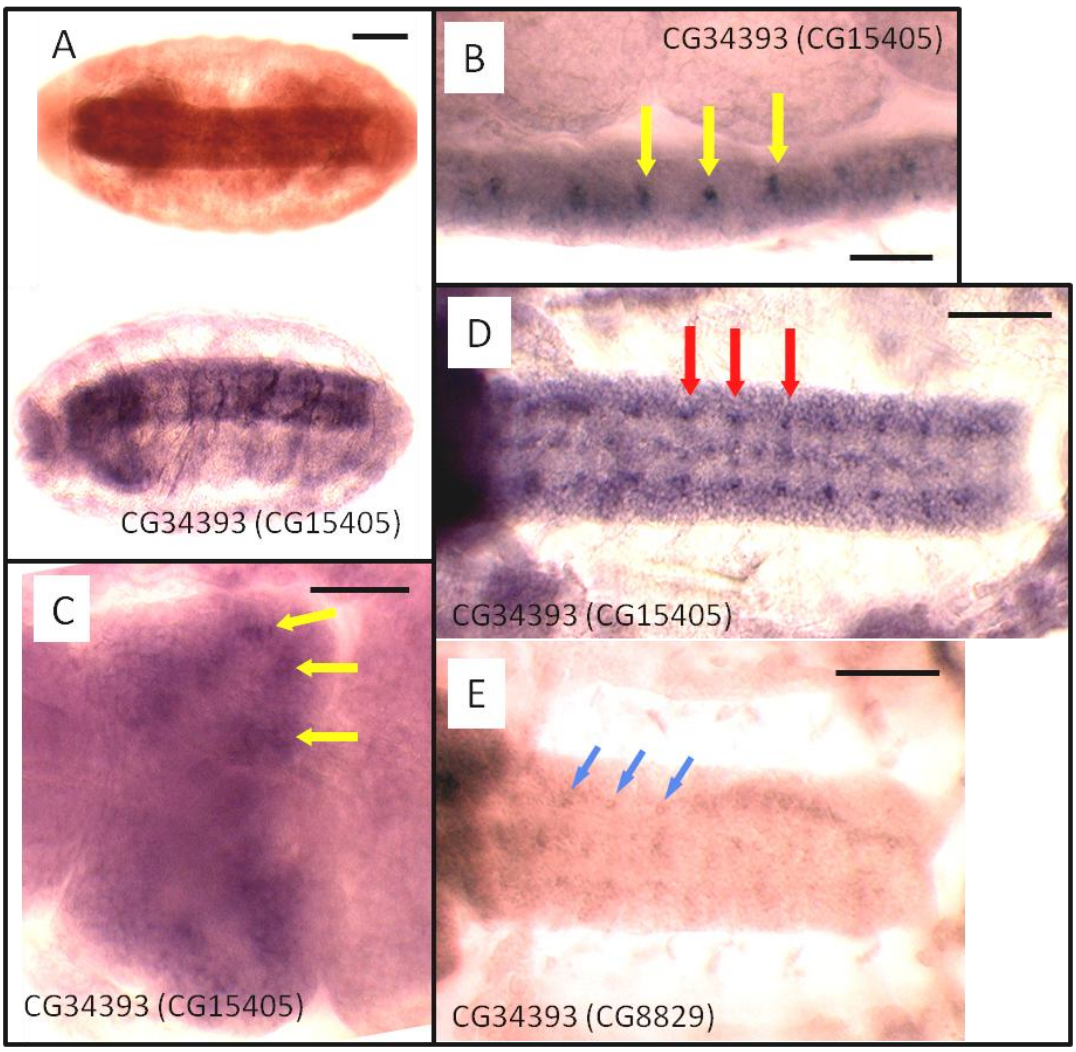

Figure 4.10 *In situ* hybridisation results for *CG34393*

In Flybase release 5.2, *CG15405* and *CG8829* were merged as they are now thought to be part of a single gene, *CG34393*. (**A**–**D**) Stage 16 wild-type embryos hybridised with digoxigenin labelled anti-sense probes against *CG15405* and *CG8829*. Differences in colour are due to post-hybridisation processing with methanol in some embryos (*bottom* **A**, **B**, **C**, **D**). (**A**) Ventral view of embryos with staining in the CNS. (**B**) Sagittal view of the ventral nerve cord showing *CG15405* expression in small groups of cells in a segmentally repeated pattern (arrows), also seen in the brain lobes (arrows, **C**). (**D** and **E**) Dorsal view of nerve cords with staining in a subset of cells (**D**). A similar but weaker expression pattern is seen in the ventral nerve cord of embryos hybridised with anti-sense probes against *CG8829* (**E**). Scale bars A, D, E = 100 µm; B, C = 50 µm. Anterior is to the left.

Chapter 5 CG34393

In this Chapter, experiments to ascertain if *CG34393* has a role in dendrite morphogenesis are presented. These include efforts to generate a loss of function mutant using *Minos* transposase and RNAi experiments in MN-RP2 using the FLP-out method. The chapter concludes with data mining that suggests CG34393 could have a role in the CNS, possibly at the synaptic level.

Detailed analysis of *Df(2L)S2590*, as outlined in the previous chapter, suggested that gene *CG34393* might be required for normal dendrite development in motor neurons. Specifically, among the seven candidate genes identified by virtue of overlapping deficiencies, *CG34393* was the only gene with proven expression in the CNS. However, it is not clear if the *in situs* for those genes where no staining was seen either have expression in the CNS below detection limits or indeed, if the *in situ* hybridisation worked for those particular probes.

To determine if loss of CG34393 is indeed responsible for the dendritic phenotype when motor neurons are made homozygous for the overlapping deficiencies *Df(2L)S2590* or *Df(2L)BSC28* (see also Fig. 4.1) one would ideally test a specific loss of function allele for CG34393. The objectives of this chapter were to generate mutant alleles for CG34393, as none were publicly available, and to study whether there is a requirement for CG34393 during dendrite development.

Generation of a *CG34393* loss of function mutant using the Minos transposase

According to online sources (Flybase, Bloomington and Kyoto Stock Centres), no mutant alleles were available for *CG34394* (or its predecessors *CG15405* and *CG8829*). Mutant alleles can be generated in a number of different ways e.g. with X-rays or chemicals (EMS), FLPase mediated recombination and imprecise excision using transposable elements (St Johnston 2002a). X-ray and chemical mutagenesis were not considered as they are time consuming to perform. To assess the potential of using FLPase mediated recombination or imprecise excision using transposable elements, the genomic area that contains *CG34393* was examined using the GBrowse tool in Flybase. A cluster of *piggyBac* insertions were reported downstream of *CG34393*, mainly located in the *CG34406* gene, which is ~2.6 kbp distant; however, these were not considered as *piggyBac* insertions are known to excise precisely (Bellen et al 2011; Ding et al 2005). Two *Minos* insertions were identified in the region where *CG34393* is located. One was sited ~12.7 kbp upstream of *CG34393* and was

not considered as (i) it was thought to be too distant from *CG34393*; and (ii) no stocks were publicly available. The other *Minos* insertion is discussed below.

Figure 5.1 shows the genomic region where *CG34393* is located, it's gene structure, and the location of a *Minos* insertion at position 2L:3193677. Mobilisation of *Minos,* a transposable element found in another species of fruit fly, *D. hydei*, has been demonstrated by Metataxis and colleagues (2005) to be an efficient way of generating imprecise excisions in *D. melanogaster*. The authors generated a large collection of fly lines that carry *Minos* transgene insertions and made these insertion lines publicly available (Bloomington Stock Centre, Indiana). One such line, 23180, is located in the first intron of the pre-mRNA transcript, 566 bp upstream of the intron/exon junction and only 790 bp upstream of the ATG start codon. This proximity to the start codon and its location in the intron, made 23180 an ideal candidate for generating an imprecise excision using *Minos* transposase and thus, potentially, a loss of function allele.

The *Minos* transgene contains a 7.5 kb dominant marker cassette consisting of three Pax6 regulatory region repeats that target expression of EGFP to the adult eye, flanked at either end by *Minos* transposable element repeats. *Minos* transposase can mobilise the *Minos* insertion cassette and in a small fraction of cases, this excision will be imprecise, deleting or disrupting some of the surrounding genomic DNA (via 'hit and run' events that cause small genomic deletions/insertions or by leaving some of the *Minos* insertion itself behind). If DNA necessary for the correct expression of a gene, for example, regulatory elements or coding sequence is deleted or changed in some way, a mutant allele for that gene will be produced.

Imprecise excisions using *Minos* have been reported to be produced with an efficiency of up to 2%, with >1 kb deleted in some examples (Metaxakis et al 2005). Given these published figures, 200 single pair matings of 23180/*Minos* transposase flies were set up. Of these, 186 crosses produced progeny to be processed further as described in the Materials and methods section. Briefly, flies were screened for excisions by loss of the *Minos* flanked EGFP expressing transgene, which expresses in the adult eye. These lines were balanced and then screened for imprecise excisions by PCR. None of the 110 lines with excisions

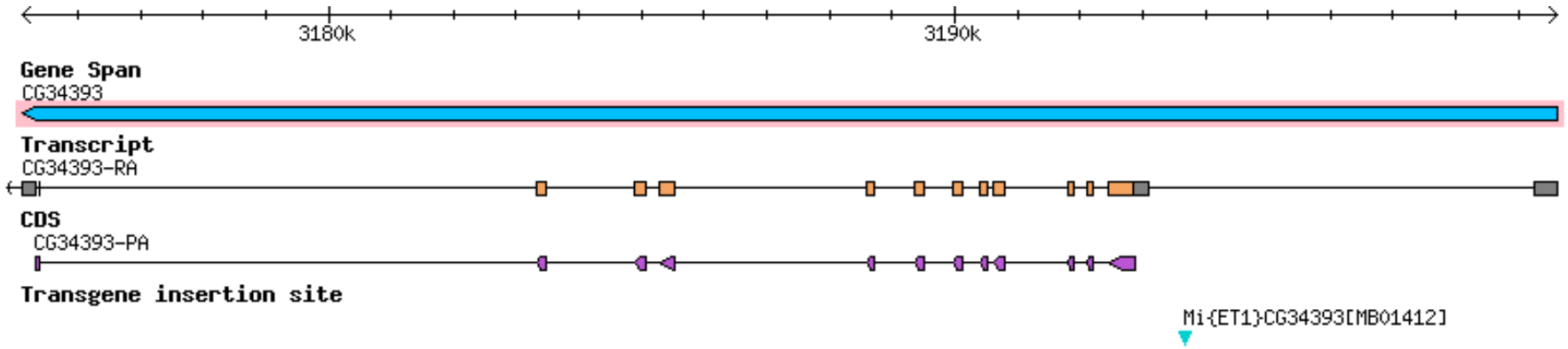

Figure 5.1 The gene structure of *CG34393* and location of a *Minos* insertion

Genomic region 2L:3175112–3199620 showing the predicted gene model of *CG34393*. The pale blue arrowhead indicates the insertion site of the transposable element *Mi{ET1}cCG34393*^{MB01412}.

The gene span is presented in light blue and depicts the total extent of the transcribed region of the gene, with direction of transcription indicated. Messenger RNA is shown in orange and shows the exon (wider bars) and intron (narrow bars) structure of the coding transcript. Untranslated regions are in grey. The coding sequence (CDS) of CG34393 is in purple and represents the extent of sequence encoding each specific polypeptide, with direction of transcription indicated. Introns are indicated as narrow lines.

Image taken from Flybase version FB2010_7.

(59% of the original 186 crosses) were homozygous lethal, suggesting that: (i) no imprecise excisions might have taken place; and/or (ii) mutations in CG34393 are not lethal.

Figure 5.2 shows the location of the *Minos* transgene insertion and the PCR primers used in the analysis of excision events. Details of primer pairs and PCR conditions are in the Materials and methods section; however, most lines were screened using primer pair OL193/OL194 that gave a wild-type PCR band of 1.938 kb. The limitation of this was that if the excision event produced small deletions or insertions, these might not necessarily be spotted when the PCR products were separated by size on an agarose gel. Similarly, very large insertions or deletions would cause the PCR reaction for that line to fail, as parameters would not be ideal (e.g. too short an extension time, or primer binding site had been deleted). Nevertheless, imprecise excisions causing alterations of >100 bp of the 1.938 kb wild-type PCR band should easily be detected when products were run on an agarose gel.

In total, 103 lines where an excision took place (56% of the original 186 crosses) were events where the jump out was precise as determined by PCR. This left seven lines (3.7%) that needed further investigation (lines 33, 40, 92, 93, 170, 192 and D).

Three lines (lines 33, 92 and 93) were excluded after they were found to be still carrying the full-length Minos insertion. However, the GFP marker contained in the insertion was not functional, as there was no EGFP expression in adult eyes, which in turn meant that these lines were processed as if they represented excision events. PCR analysis as described above using primers OL193/OL194 failed to produce a PCR product and it was initially thought that a large deletion event had taken place outside the binding region of one or both of the primers OL193/OL194. The reason for the PCR failure was identified when a long template polymerase (LongAmp Taq, NEB) and primers OL153/OL220, were used and the PCR products compared with that of the line carrying the *Minos* transgene (23180). The PCR products were a similar size and suggested that complete excision events had not taken place and the *Minos* insertion was still present. Sequencing of the 5’ and 3’ ends of the 10.464 kb PCR product did not identify why the EGFP marker was not functional. It is possible that a mutation in a region that was not sequenced was generated during the excision process, thereby silencing the expression of EGFP.

Four lines were classed as carrying imprecise excisions (lines 40, 170, 192 and D). Of these, two were cases where the *Minos* insertion was incompletely excised, leaving some of the transgene insertion behind (lines 192 and D). PCRs using primers OL197 and OL194 revealed larger than wild-type PCR products. Sequencing of these PCR products revealed that 103 bp and 870 bp of the insertion was retained at the insertion site for lines D and 192, respectively.

Last, lines 40 and 170 were identified as being cases where imprecise excision had taken place and genomic DNA had been deleted. PCR analysis using primer pairs OL153/OL220 revealed bands that were smaller than wild-type (2645 bp), ~1.3 to 1.4 kb in size. Sequence analysis of these PCR products showed that 1277 and 1285 bp had been deleted from the genomic DNA of lines 40 and 170, respectively. However, sequence alignment using Vector NTI (Invitrogen) showed that the deletions were 5', or upstream from the insertion site and away from the intron/exon boundary and the ATG start codon. Although this was not the desired result, it is as yet unclear as to whether these excision events compromise normal expression of *CG34393*. Further testing is needed to ascertain if the regions deleted in lines 40 and 170 are important for the proper expression of *CG34393*.

In summary, while the objective of generating a loss of function mutant for *CG34393* was not achieved, the method of creating deletion mutants using imprecise excision with *Minos* transposable elements was successful. The rate of imprecise excisions was similar (2 out of 186 fly lines generated, 1.08%) to those published by Metataxis et al. (2005).

Knockdown of *CG34393* using small interfering RNA

When the generation of a mutant using imprecise excisions proved unsuccessful, another alternative was considered whereby the expression of *CG34393* could be reduced in specific neurons by RNA interference (RNAi) and resultant phenotypes investigated. In RNAi, endogenous messenger RNA for a gene of interest is targeted for degradation by the expression of sequence-specific double stranded small interfering RNA (siRNA). Exogenous RNA is designed to generate a double stranded hairpin loop that once expressed in a cell,

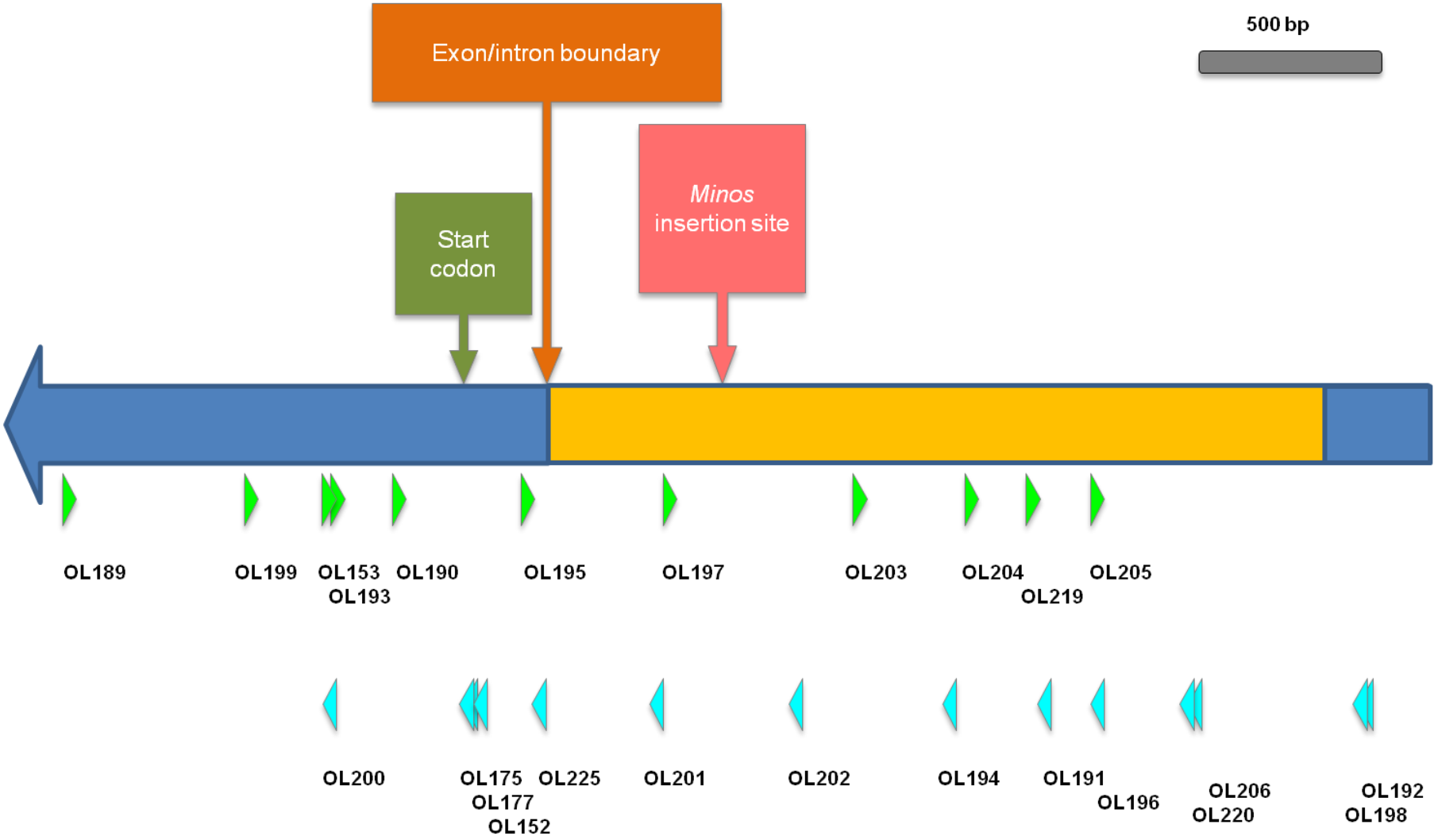
Exon/intron boundary
500 bp
Start codon
Minos insertion site
OL189
OL199
OL153
OL193
OL190
OL195
OL197
OL203
OL204
OL219
OL205
OL200
OL175
OL177
OL152
OL225
OL201
OL202
OL194
OL191
OL196
OL206
OL220
OL192
OL198

Figure 5.2 Features of *CG34393* in relation to the *Minos* insertion transposable element and PCR primers used for the analysis of excision events

The large arrow represents the first 4 kbp of the genomic region of the 24.5 kbp gene *CG34393*, including introns (orange), and exons (blue); 5' is to the right. The location of the *Minos* insertion in relation to the intron/exon boundary, the start codon of the gene and primers used for the analysis of excision events are also shown. Light blue arrowheads represent the position of forward primers, while green arrowheads represent reverse primers. The start codon is 224 bp downstream from the intron/exon boundary and 790 bp downstream of the *Minos* insertion site.

harnesses the cells intrinsic post-transcriptional gene silencing capabilities. These mechanisms are thought to be used for many RNA-mediated processes in a cell such as combating viruses, transgene silencing and endogenous transpositions (reviewed in Kavi et al 2008). The double stranded RNA is processed into small 21–23 nucleotide long fragments by enzymes [e.g. Dicer-2 (*Dcr2*)], one strand of which is then incorporated into an RNA induced silencing complex (e.g. the *argonaute* family members; Miyoshi et al 2005). Guided by the anti-sense RNA strand, the target RNA is recognised, cleaved and destroyed; thus endogenous messenger RNA levels of the gene of interest are reduced.

RNAi is a technique applied in many model organisms, both *in vitro* and *in vivo*, and for studying nervous system development – the focus of this work. For example, in cultured rat dorsal root ganglion cells, RNAi was used to knockdown *RhoA* mRNA in axons (and not dendrites) and consequently prevent semaphorin-mediated growth cone collapse (Hengst et al 2006). In the mouse, RNAi was used to study spinal interneuron neurogenesis (Misra et al 2008). Since its use in *Drosophila* cell lines to investigate signal transduction pathways (Clemens et al 2000), RNAi has also been widely applied as a tool to study various components of nervous system development in *Drosophila*. For example, mushroom body neurons in brain development (Lin et al 2009), axon guidance and pioneer neurons (Ostrowski et al 2008), synapse formation in mechanosensory neurons (Neufeld et al 2011), ion channel function in adult flight motor neurons (Ryglewski & Duch 2009) and in a screen for neural outgrowth genes (Sepp et al 2008). In *Drosophila* dendrites, RNAi has been used to study transcription factors required for correct sensory neuron morphogenesis (Parrish et al 2006a), gene regulation in olfactory projection neurons (Hillebrand et al 2010), neurodegenerative disease homologues in sensory neurons (Lu et al 2009), and in cultured *Drosophila* neural cells to study RNAi silencing *in vitro* (Sharma & Nirenberg 2007). In fact, at the time of writing, in 30 different published RNAi screens (http://flight.icr.ac.uk), looking at a range of cellular processes, CG34393 has not had a positive hit. Although RNAi has been used to study peripheral nervous system dendrite development (Parrish et al 2006a), thus far, no studies that use RNAi in the *Drosophila* embryo to study motor neuron dendrite

development have been published; hence, using RNAi in this context would be interesting in itself.

UAS-RNAi fly lines are commercially available from the Vienna *Drosophila* RNAi centre (Dietzl et al 2007). These lines carry inducible RNAi expression constructs based on the GAL4/UAS binary system (Enerly et al 2002). A variety of GAL4 drivers are available that allow expression of the UAS-RNAi line(s) in the embryonic and larval nervous system: cell specifically (e.g. MN-RP2), neuron subtype specifically (e.g. motor neuron) or pan-neuronally (PNS and CNS).

To avoid potentially lethal artefacts of driving RNAi expression pan-neuronally, RNAi experiments were carried out using a cell-specific FLP-out method that selectively targets expression to a subset of neurons (Ou et al 2008; Roy et al 2007). RN2-FLP directs expression of yeast derived FLPase, via a tandem repeat of regulatory regions derived from the *even-skipped* locus, specifically to the aCC and RP2 motor neurons and also the pCC interneuron. During FLPase mediated recombination, FLPase targets FRT sites carried in the transgene *Tub-FRT-CD2-FRT-GAL4* such that after removal of the stop codon (contained within the FRT-CD2-FRT cassette) the *Tubulin* promoter strongly drives the expression of GAL4. GAL4 in turn, drives expression of the reporter *UAS-myr-mRFP1* (two copies of myristoylated monomeric RFP), and at the same time, drives expression of *UAS-Dcr2*. *Dcr2* is an endoribonuclease that helps to process the double stranded RNA produced by the RNAi transgene, and is thought to improve the efficacy of target gene knockdown (Dietzl et al 2007; Preall et al 2006). The VDRC holds two UAS-RNAi libraries (GD and KK), which differ in the method used to generate the insertion lines. The lines discussed below were obtained from both libraries. Controls (w^{1118}) were included for comparison; this fly line is the same genetic background as was used by the VDRC to generate the UAS-RNAi lines.

Four UAS-RNAi fly lines were obtained from the VDRC. Two lines have the UAS-RNAi insertion on the second chromosome (stock numbers 40330 and 101816) and two lines on the third chromosome (stock numbers 23471 and 23472). Three of the lines (VDRC stock numbers 23471, 23472 and 40330) are generated from the same transgenic construct and inserted ‘randomly’ into the genome (GD library, VDRC reference 13529). The fourth line

(VDRC stock number 101816) was made using a different transformation vector, which inserts into the genome at a specific place (KK library, VDRC reference 109767). In total, there were eight UAS-RNAi lines available for *CG34393*; these four were chosen as they had the fewest number of predicted OFF targets. OFF targets are genes that may be inadvertently targeted by the siRNA generated from the UAS-RNAi lines during experiments and have the potential to cause phenotypes that mask that of the intended target gene. All four UAS-RNAi lines had one OFF target gene in common, *Translocase of outer membrane 70* (*Tom70*). Data from the BDGP *in situ* and FlyAtlas databases suggest that *Tom70* is expressed in the CNS at similar developmental stages to *CG34393* (i.e. late embryogenesis). Is it feasible that knockdown of *Tom70* could interfere with interpretation of results if the UAS-RNAi lines from the VDRC have a dendritic phenotype?

Tom70 acts as a receptor and is one of seven subunits that form the TOM mitochondrial membrane complex, which has been shown to have a role in the insertion of pro-apoptotic proteins into the outer membrane of mitochondria (Colin et al 2009). Apoptotic genes have been implicated in neurite remodelling due to developmental changes (e.g. pruning during metamorphosis; Williams et al 2006; Williams & Truman 2005a; b) and Wallerian degeneration (after injury or during disease; Coleman & Freeman 2010); although in *Drosophila* dendrites pruning and degeneration are thought to be mediated by different processes (Tao & Rolls 2011). Loss of function of Tom70 has been shown to reduce the apoptotic phenotype seen in *Drosophila* cells that express the mouse BCL2-associated X protein (Bax) (Colin et al 2009), which is a gene that is required for developmental elimination of aberrantly projected sensory axons in the mouse (Schoenmann et al 2010). These results suggest that knockdown of Tom70 could have an effect on dendrites where initiation of pruning/apoptosis pathways is reduced or prevented, theoretically resulting in aberrant overgrowth or ectopic branches. However, as discussed below (and in Figs 5.5 and 5.6) the phenotype seen is the opposite.

In order to increase the levels of siRNA in the RNAi experiments, additional RNAi lines were generated by crossing together RNAi lines on different chromosomes so as to be able to co-express two UAS-RNAi lines simultaneously (e.g. VDRC stock numbers 101816;23471 and

101816;23472). It was not possible to generate such double insertion stocks with VDRC stock 40330 due to time limitations.

As frequency of FLP-out events correlates with incubation temperature during embryogenesis, (higher temperatures give rise to more FLP-out labelled cells) initial experiments were carried out with the aim of generating ventral nerve cords containing few physically separate labelled neurons. The protocol used is described in the Materials and methods section.

RNAi in early first instar larvae

In total, 42 MN-RP2 neurons were analysed: w^{1118} (control, *n* = 8 neurons), VDRC stock number 23471 (*n* = 11), VDRC stock number 101816 (*n* = 7) and the double insertion lines 101816;23471 (*n* = 6) and 101816;23472 (*n* = 10). *Z*-projections of both control and RNAi expressing MN-RP2 motor neurons were produced using ImageJ. Images were cropped to a standard size and labelled randomly with a number for blind testing. They were then viewed independently by two colleagues (M.L and J.F.E) familiar with the RP2 motor neuron and its dendritic arbor at several developmental stages, who scored the neurons for severity of phenotype. Six neurons were excluded during the analysis due to poor quality imaging or because they were thought to be too old. The results are summarized in Table 5.1 and Figs. 5.3–4. Neurons in the strong phenotype class appear to have a more compact dendritic arbor than those neurons in the wild-type class, probably due to reduced branching and shorter dendritic processes.

The distribution of control and UAS-RNAi expressing neurons across the phenotypic spectrum (wild-type-like to strong phenotype) initially suggested that RNAi knockdown of *CG34393* was not successful as the assessors were unable to distinguish between control (w^{1118}) and RNAi neurons. For example, only 13% of control neurons were classed as phenotypically wild-type and the double RNAi lines (VDRC stock numbers 101816;23471 and 101816;23472), which might be expected to have a more severe phenotype, accounted

for 63% of neurons classed as phenotypically wild-type. There also appeared to be no obvious trend in phenotypic score between larvae carrying one or two RNAi transgenes.

Furthermore, the phenotype seen in neurons homozygous for FRT40A *Df(2L)S2590* (positioning defects in the mediolateral axis and aberrant midline crossing) was not recapitulated in this experiment. However, the fact that control neurons were not scored as wild-type-like was interesting as it suggested that other factors might be having an effect on the development of dendrites in these MN-RP2 neurons. These results raised two questions: (i) what was affecting the growth of dendrites in control neurons such that they would be classed as non-wild-type; and (ii) in the *CG34393* knockdown neurons, why were some neurons classed as wild-type?

Firstly, the expression of *UAS-Dcr2*, in addition to any endogenous Dcr2 protein, has the potential to affect the expression of other genes in the cell, including those necessary for correct dendrite morphogenesis in control neurons. However, Berdnik and colleagues (2008) demonstrated in rescue experiments that Dcr2 is not required for correct targeting of projection neuron dendrites in the larval olfactory system (Berdnik et al 2008). Nevertheless, over-expression of Dcr2 in motor neurons could still affect endogenous RNAi processes. Secondly, the penetrance of phenotypes seen in UAS-RNAi expressing neurons may be inherently variable due to perdurance of wild-type proteins passed on from the ganglion mother cell to the target neuron or because the CG34393 protein is stable and long-lived. Such variability was observed in motor neurons made homozygous mutant for deficiencies and defined genes (see Chapters 2 and 3). Further, the potency of these RNAi lines has not been established; although insertions were validated at VDRC, only a sample were functionally tested and it is estimated that >80% of RNAi lines from the VDRC library provide effective silencing (Dietzl et al 2007).

To investigate this further, the UAS-RNAi experiments were repeated, with and without co-expression of *UAS-Dcr2*, and with analysis at a later developmental stage to allow for a longer period of action of the manipulation.

RNAi in young third instar larvae, 48 h after hatching

The RNAi experiments were repeated to analyse effects at later developmental stages, after prolonged expression, as described in the Materials and methods section. Firstly, RNAi was carried out using two versions of the FLP-out stock: (i) with co-expression of *UAS-Dcr2*; and (ii) without. In total, 29 CNSs were screened using the FLP-out method with *UAS-Dcr2*: w^{1118} (control), *n* = 5; VDRC stock number 23471, *n* = 11; stock 101816, *n* = 7; stock 40330, *n* = 4; and co-expression of two UAS-RNAi insertions, numbers 101816;23472, *n* = 2. Eleven CNSs were similarly tested using the FLP-out method without co-expression of *UAS-Dcr2*: control, *n* = 1; VDRC stock number 23471, *n* = 1; and stock number 101816, *n* = 9.

To address the question of whether expression of the UAS-RNAi constructs causes a phenotype in RP2 motor neuron dendrites, the data set was split into neurons that were tested with (Fig. 5.5) and without (Fig. 5.6) co-expression of *UAS-Dcr2*. Fig. 5.5 shows that RNAi knockdown of *CG34393* with co-expression of *UAS-Dcr2* appears to have a variable effect, as also seen at the first instar larval stage (Fig. 5.4). In the most severely affected neurons, a reduction in arbor size is evident (Fig. 5.5C and D). Less affected neurons appear to have a similar dendritic span as their control counterparts, but dendrites appear comparatively stunted and possibly also less branched. Further, control neurons (expressing *UAS-Dcr2* but not UAS-RNAi) appear normal, no obvious phenotype was seen in the five neurons examined (two are presented in Fig. 5.5). Figure 5.6 shows the limited results of *CG34393* knockdown in MN-RP2 neurons without co-expression of *UAS-Dcr2*. These are hard to evaluate, as only one control neuron was visualised, and it was damaged during preparation. However, the overall impression in the few neurons analysed is that no phenotype is apparent, perhaps with the exception of the example shown in Fig 5.6C, which may have a reduced dendritic arbor. This result is not entirely unexpected as *Dcr2* is thought to increase the potency of UAS-RNAi gene knockdown (Dietzl et al 2007; Preall et al 2006), and it is conceivable that without co-expression of *UAS-Dcr2* the efficiency of *CG34393* knockdown is not sufficient to cause a dendritic phenotype.

Table 5.1

Wild-type-like	Mild phenotype	Medium phenotype	Strong phenotype	Removed from analysis
15	5	16	24	25
47	28	10	35	11
34	45	3	37	41
12	8	21	9	32
14	36	30	27	13
19	23	26	4	38
22	40	1	31	
20	46	17		
		18		
		6		
		42		
		7		
		33		

Fig. 5.3

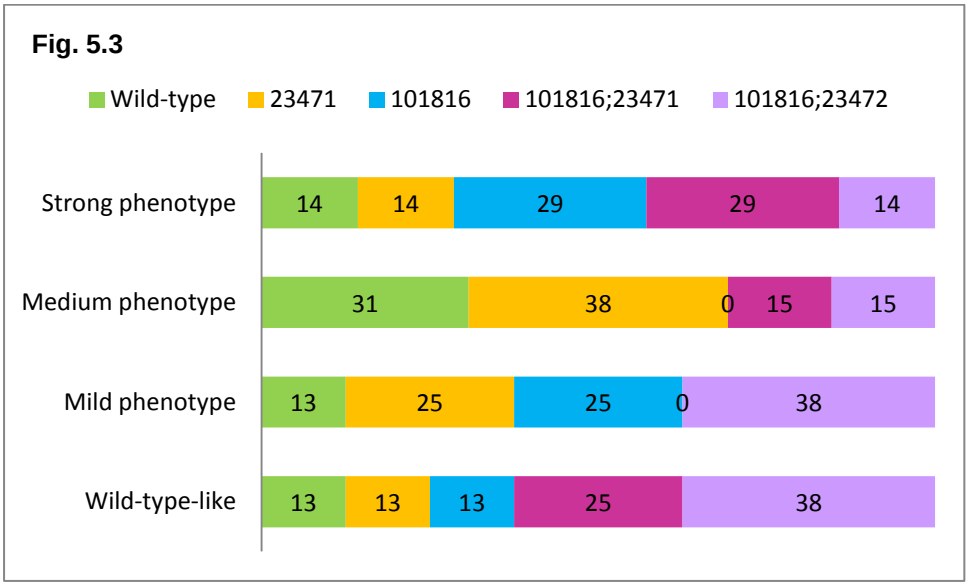

Table 5.1 and Figure 5.3 Phenotype scores in MN-RP2 motor neurons with RNAi knockdown of *CG34393* in first instar larvae

Images were evaluated blind by two colleagues and classed according to severity of dendritic arbor phenotype. Numbers in Table 5.1 refer to the randomly applied image number. Representative images for wild-type-like and the strong phenotype are shown in Fig. 5.4. Colour key for genotypes is shown in Fig 5.3. In Fig.5.3, the distribution for each RNAi line and the wild-type is shown for each phenotype class; values are per cent of neurons in that phenotypic class. Interestingly, only 13% of control neurons were classed as having wild-type arbors. Further, the double RNAi lines (stock numbers 101816;23471 and 101816;23472) accounted for 63% of neurons classed as phenotypically wild-type.

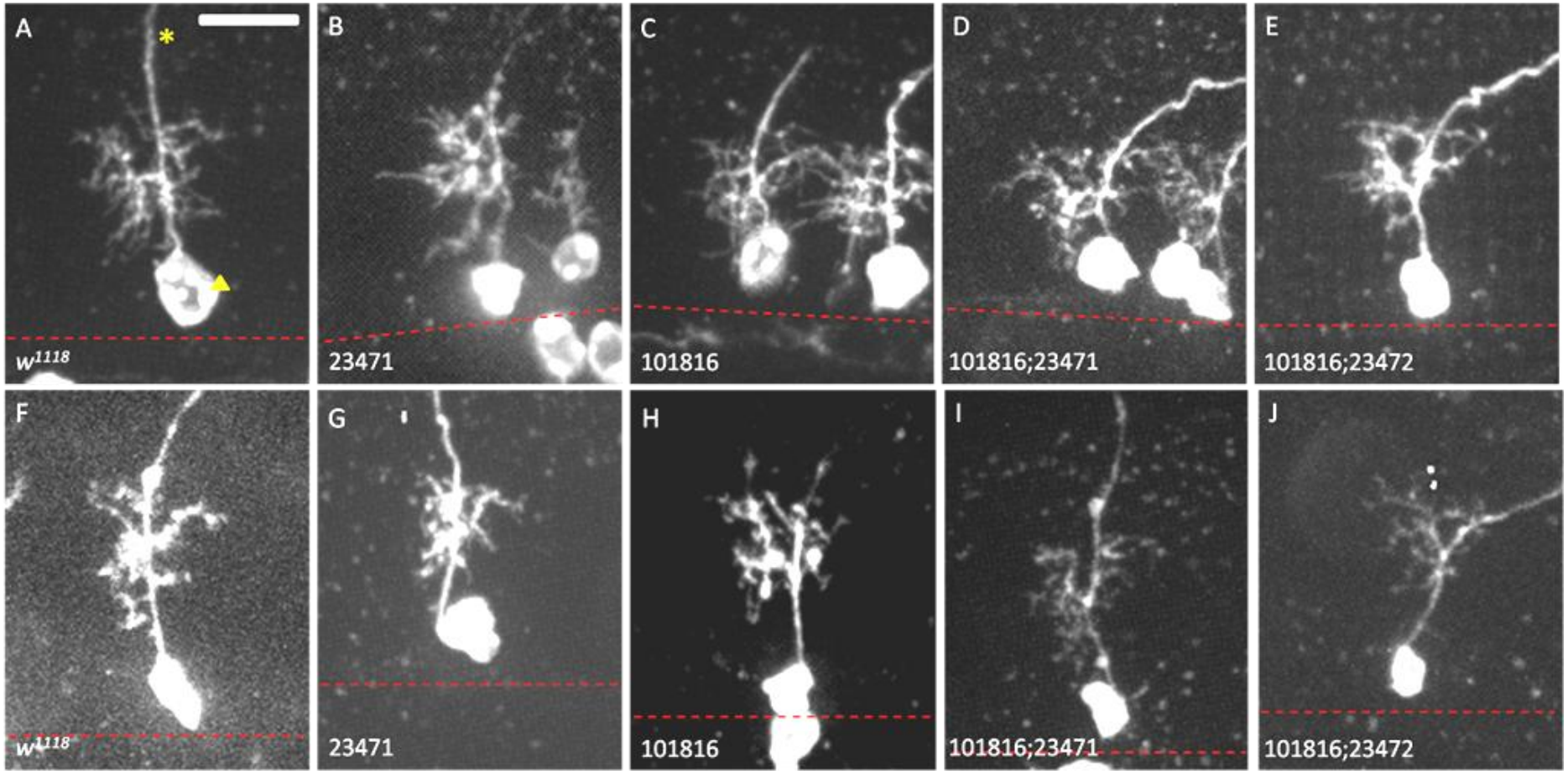
A
B
C
D
E
w^{1118}
23471
101816
101816;23471
101816;23472
F
G
H
I
J
w^{1118}
23471
101816
101816;23471
101816;23472

Figure 5.4 RNAi knockdown of *CG34393* in first instar larvae

(*Top*) MN-RP2 neurons in the wild-type-like class and (*bottom*) in the strong phenotype class, labelled using the FLP-out method and carrying *UAS-Dcr2* and the following UAS-RNAi transgenes against *CG34393*: (**A**, **F**) w^{1118} (control); (**B**, **G**) VDRC stock number 23471; (**C**, **H**) stock number 101816; (**D**, **I**) double insertion stock numbers 101816;23471; and (**E**, **J**) 101816;23472. Neurons in the strong phenotype class have a compact dendritic arbor, with reduced branching and short processes when compared to the wild-type-like class. Triangle = cell body; asterisk = axon; red dashed line = midline; scale bar = 10 µm; anterior is left.

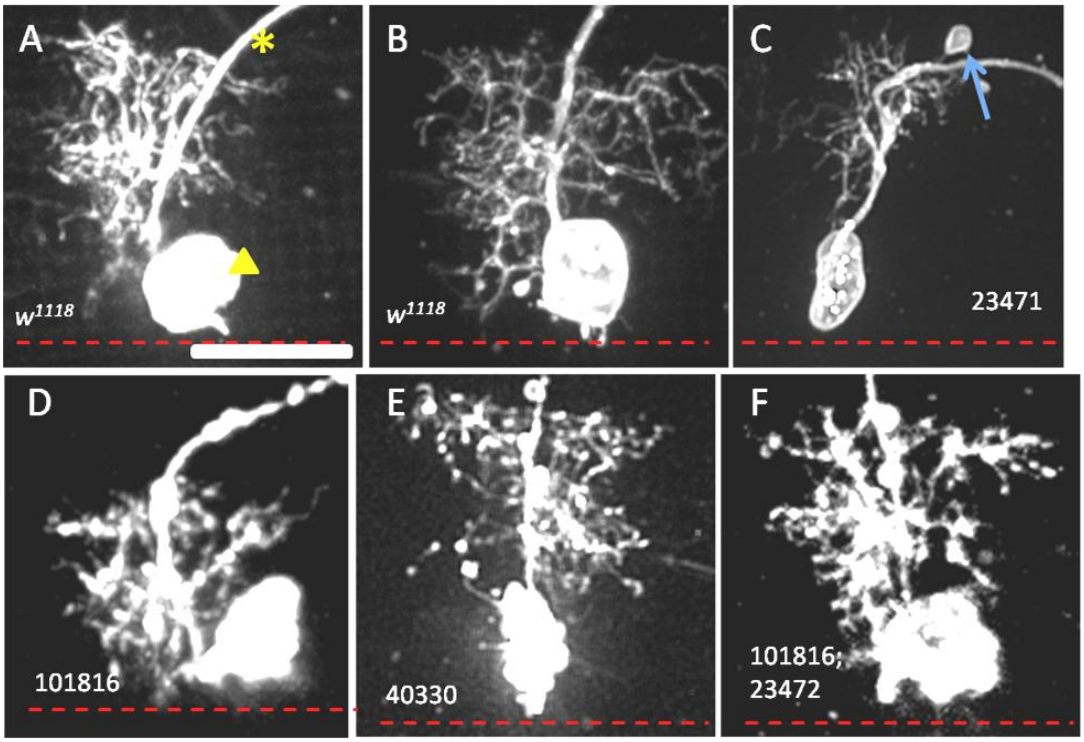

Figure 5.5 MN-RP2 motor neurons 48 h ALH, expressing UAS-RNAi against *CG34393* and co-expressing *UAS-Dcr2*

MN-RP2 motor neurons labelled with *UAS-myr-mRFP1* using the FLP-out method. (**A** and **B**) Control neurons co-expressing *UAS-Dcr2* in an otherwise w^{1118} background. (**C**–**F**) Experimental neurons that also co-express UAS-RNAi against *CG34393*: (**C**) VDRC stock number 23471, (**D**) stock number 101816, (**E**) stock number 40330 and (**F**) double insertion stock numbers 101816;23472. All UAS-RNAi lines target *CG34393*, but differ in chromosomal location and transformation vector. MN-RP2 neurons are arranged with descending phenotype severity from **C** to **F**. (**C**) Neuron with severely reduced dendritic arbor. Arrow indicates blebbing, likely an artefact caused by handling during sample preparation. (**D**) Neuron with reduced dendritic arbor. (**E** and **F**) The spread of the arbors are essentially wild-type, however, dendrites appear stunted and less branched.

Triangle = cell body; asterisk = axon; scale bar for all images = 10 µm; red dashed line = midline; anterior is left.

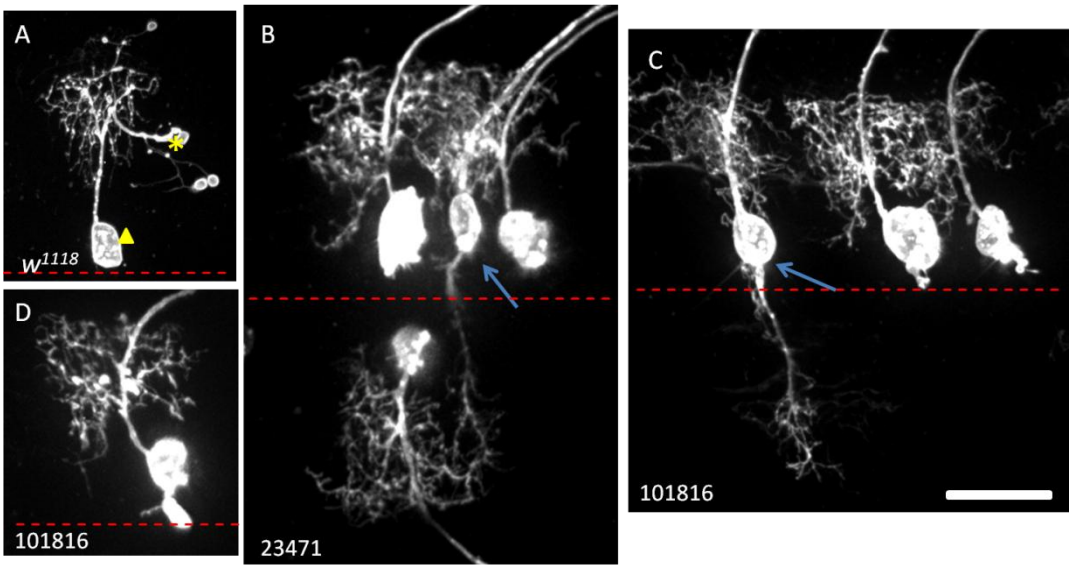

Figure 5.6 MN-RP2 and MN-aCC motor neurons 48 h ALH, expressing UAS-RNAi against *CG34393* and not co-expressing *UAS-Dcr2*

MN-RP2 motor neurons labelled with *UAS-myr-mRFP1* using the FLP-out method that do not co-express *UAS-Dcr2*. (**A**) Control neuron in an otherwise w^{1118} background. This example was damaged during preparation; only one control cell was labelled in this series of experiments. (**B**) VDRC stock number 23471; these neurons appear relatively normal, but it is difficult to assess the phenotype due to dendrites overlapping. (**C** and **D**) Stock number 101816; on the whole, the dendritic arbors appear normal in **C**, however, in **D** there is some suggestion of reduced branching and/or stunted dendrites.

Blue arrow indicates aCC motor neuron, which has two dendritic arbors, one of which is contralateral; triangle = cell body; asterisk = axon; scale bar for all images = 10 µm; dashed red line = midline; anterior is left.

To conclude, these results in older animals suggest that knockdown of *CG34393* using RNAi causes a dendritic phenotype (albeit a variable one), where the finer processes are shorter and stunted, and branching and the span of the arbor is reduced compared to control neurons. The question of whether expression of *UAS-Dcr2* in these neurons causes a dendritic phenotype, as suggested in the RNAi experiments in first instar larvae, remains unanswered; a larger sample size of control neurons without co-expression of *UAS-Dcr2* is required. Furthermore, the midline targeting phenotype seen in neurons homozygous for *Df(2L)S2590*, was not evident in the MN-RP2 neurons 48h after larval hatching, which express a UAS-RNAi transgene designed to knock down *CG34393*. This discrepancy is explored in the Discussion chapter.

Data mining provides clues as to the possible role of CG34393 in dendrite morphogenesis

In light of the uncertain experimental results for *CG34393* thus far, how can its presumptive role in dendrite morphogenesis be investigated further? Numerous online databases and tools are available that can be used to provide clues and evidence for the function and role of *CG34393* – an uncharacterised gene. These include data from expression profiles, e.g. developmental time-course (modENCODE) and tissue expression (BDGP *in situ* database, FlyAtlas); prediction algorithms, e.g. similarity searches (blastn, blastp); and access to additional data via dedicated *Drosophila* databases (Flybase, Flymine).

What is CG34393?

CG34393 is an uncharacterised gene that is predicted to code for a protein 691 amino acids long. It has one predicted transcript, 2874 bp in length comprising 12 introns and 13 exons (Fig 5.1). It has been predicted to have guanyl-nucleotide exchange factor activity and to be involved in the regulation of small GTPase mediated signal transduction (Flybase).

In terms of expression, *in situ* data of *CG34393* expression in the CNS of *Drosophila* is supported by other data (www.flyatlas.org; Chintapalli et al 2007) derived from the third instar larva, cultured cells and the adult, though not the embryo. Table 5.2 summarizes the database entry for *CG34393* in FlyAtlas in adult and larval tissues. FlyAtlas data indicate in which tissues a gene is expressed, its relative abundance (signal) and level of expression (enrichment) compared to the whole fly. The Affymetrix value (present call) was generated from microarrays that show how often the mRNA was detectably expressed (out of four independent biological replicates and hence, four arrays). Enrichment above a value of five is considered significant. As highlighted in Table 5.2, *CG34393* was found to be upregulated in the adult brain (enrichment of 9.40 and 13.20), the adult thoracicoabdominal ganglion (enrichment of 8.90 and 6.50) and in the third instar larval CNS (enrichment of 2.15 and 3.20). Data were also available for cultured S2 cells (the product of disassociated 20–24 hour old embryos) but *CG34393* was not detected (present calls of 0 of 4 for both probes). This may be due to restricted expression of CG34393 in a subset of cells in the CNS as suggested by the *in situ* hybridisation carried out as part of this work (Fig. 4.10).

In summary, the FlyAtlas data suggested that mRNA expression of *CG34393* is enriched in the adult and larval CNS compared with other tissues and cultured cells, thus providing supporting evidence for the *in situ* data that shows CG34393 to be expressed in the CNS.

Similarly expressed genes

One feature available in Flybase is the ability to search for genes that are expressed in a similar profile to the gene of interest. The similarly expressed profile search is a useful tool because it could provide information about genes whose regulation is similarly coordinated and may therefore take place in the same process. In other words, genes that are vital for a particular process, at a certain time and are perhaps part of the same pathway, may share a similar expression profile. However, without experimental validation these relationships are in the main theoretical.

Figure 5.7 shows the expression profile for *CG34393* from the modENCODE temporal expression data set obtained from Flybase (Celniker et al 2009; Gelbart & Emmert 2010). According to these data, CG34393 is expressed at low levels during development – likely due to a CNS restricted expression pattern, (see *in situ,* Fig. 4.10 and FlyAtlas data, Table 5.2). Two peaks of almost moderate expression occur during late embryogenesis and the pupal stage; time points where dendrites are growing and making new connections. There is also a peak in males throughout their adult lifespan; however, the source of this is not clear as the FlyAtlas expression data does not show any significant upregulation of *CG34393* in either sex of the adult fly.

In the case of *CG34393*, this search was based on the levels of expression during development from the early embryo, through larval stages and pupation to adult from the modENCODE dataset (Celniker et al 2009; Gelbart & Emmert 2010; mod et al 2010), which is distinct from the tissue expression data from FlyAtlas, detailed above. The results are presented as a summary of the top 100 similarly expressed genes, with correlation value, molecular function and biological process the genes are involved in [based on Gene Ontology (GO) terms]. By refining the hit list of genes for controlled vocabulary terms, the genes are subdivided into different categories based on their biological function. The 20 most frequent biological function terms (out of 102) are presented in Table 5.3. Thirty-nine related records have no data available, and most of these represent uncharacterized genes where no biological function has been predicted. An interesting feature of these results is the number of biological functions that are implicated in nervous system development, such as synaptic transmission, neurotransmitter secretion and signalling (G-protein coupled receptor protein signalling pathway and G-protein coupled receptor protein signalling pathway).

If the data are analysed in greater detail, by looking specifically at the top 10 similarly expressed genes by examining their Flybase entries in full, some interesting associations become apparent (Table 5.4). Firstly, all 10 genes are >90% similar in expression profile, indicating good matches. Secondly, of the 10 genes, four are linked to synapse formation: *nervous wreck* (Coyle et al 2004); *Ankyrin2* (*Ank2*; Koch et al 2008); *sif* (Collins & DiAntonio 2004; Packard et al 2003); and *Neurexin-1* (*Nrx-1*; Zeng et al 2007); two with

dendrite.morphogenesis: *Ank2* (Yamamoto et al 2006) and *CG42613* (Brenman et al 2001; Parrish et al 2006a); and two with the cytoskeleton: *Ank2* (Koch et al 2008; Pielage et al 2008) and *sif* (Ng & Luo 2004a), while one, *tipE homologue 1*, is an auxiliary subunit of the sodium channel *paralytic* (Derst et al 2006) and two others are known to have CNS expression: *Ca-beta* (Chintapalli et al 2007) and *stanley-cup* (Barreau et al 2008). Only two genes in the top 10 are not involved with the nervous system: *CG15464*, which is uncharacterised and has no reliable expression data; and *CG42541*, which is thought to be involved in phagocytosis and engulfment (Stroschein-Stevenson et al 2006). These data show that the expression profile of *CG34393* corresponds with several interesting genes that are involved in processes important in the development of dendrites, such as synapse formation, and stability and modulation of the cytoskeleton.

Homology to other genes

An online protein similarity search using blastp (http://blast.ncbi.nlm.nih.gov/Blast.cgi?PAGE=Proteins), identified a conserved RasGEF domain in the predicted *CG34393* gene product in three separate protein annotation databases: conserved domain database (Marchler-Bauer et al 2011); pfam (http.//pfam.sanger.ac.uk; Bateman et al 2004); and smart (simple modular architecture research tool: Letunic et al 2009; Schultz et al 1998). Furthermore, the database entries in pfam and prosite (Sigrist et al 2010) using the CG34393 protein annotation ID – Q9VQM8 – showed that CG34393 is predicted to contain two motifs: RasGEF_NTER and RasGEF_CAT. Further exploration of the pfam and prosite databases places CG34393 into a group of 358 and 547 genes with similar domain architecture, respectively (i.e. RasGEF_N–RasGEF; Fig. 5.8), which includes genes from a wide range of species from yeast to humans.

Tissue	mRNA Signal ± SEM	Present call	Enrichment	Affy call
Adult brain	67 ± 3	4 of 4	9.40	Up
	45 ± 3	4 of 4	13.20	Up
Adult head	15 ± 2	3 of 4	2.20	Up
	9 ± 1	2 of 4	2.90	Up
Adult eye	5 ± 0	0 of 4	0.83	None
	6 ± 1	1 of 4	1.75	None
Adult thoracicoabdominal ganglion	46 ± 5	4 of 4	6.50	Up
	30 ± 2	4 of 4	8.90	Up
Adult salivary gland	7 ± 4	0 of 4	1.10	None
	6 ± 3	0 of 4	1.73	None
Adult crop	5 ± 1	0 of 4	0.70	None
	8 ± 1	1 of 4	2.40	Up
Adult midgut	3 ± 1	0 of 4	0.40	Down
	9 ± 1	1 of 4	2.90	Up
Adult tubule	7 ± 0	0 of 4	1.00	None
	3 ± 0	0 of 4	1.10	None
Adult hindgut	6 ± 2	0 of 4	0.90	None
	5 ± 2	0 of 4	1.70	None
Adult heart	4 ± 1	0 of 4	0.56	None
	4 ± 1	0 of 4	1.40	None
Adult fat body	9 ± 3	0 of 4	1.36	None
	5 ± 4	1 of 4	1.55	None
Adult ovary	3 ± 0	0 of 4	0.50	Down
	3 ± 1	0 of 4	0.90	None
Adult testis	7 ± 0	0 of 4	1.00	None
	2 ± 0	1 of 4	0.80	None
Adult male accessory glands	3 ± 1	0 of 4	0.40	Down
	6 ± 1	0 of 4	1.80	None
Adult virgin spermatheca	7 ± 2	1 of 4	0.97	None
	4 ± 2	0 of 4	1.32	None
Adult mated spermatheca	11 ± 0	1 of 4	1.57	Up
	5 ± 1	0 of 4	1.51	None
Adult carcass	7 ± 2	0 of 4	1.10	None
	8 ± 4	1 of 4	2.30	None
Larval CNS	15 ± 2	4 of 4	2.15	Up
	11 ± 1	4 of 4	3.20	Up
Larval salivary gland	7 ± 2	0 of 4	1.07	None
	8 ± 1	0 of 4	2.59	Up
Larval midgut	3 ± 1	0 of 4	0.51	None
	12 ± 2	1 of 4	3.48	Up
Larval tubule	6 ± 1	0 of 4	0.90	None
	6 ± 0	0 of 4	1.90	None
Larval hindgut	4 ± 1	0 of 4	0.62	None
	3 ± 1	0 of 4	0.91	None
Larval fat body	6 ± 1	0 of 4	1.00	None
	0 ± 0	0 of 4	0.20	None
Larval trachea	4 ± 1	1 of 4	0.58	Down
	5 ± 3	1 of 4	1.64	None
Larval carcass	6 ± 1	1 of 4	0.96	None
	4 ± 1	0 of 4	1.16	None

Tissue	mRNA Signal ± SEM	Present call	Enrichment	Affy call
S2 cells (growing)	6 ± 0 5 ± 0	0 of 4 0 of 4	0.86 1.70	None None
Whole fly	7 ± 0 3 ± 1	0 of 4 0 of 4		

Table 5.2 Summary of mRNA expression of *CG34393* in non-embryonic tissues

Data from FlyAtlas (www.flyatlas.org) showing for each tissue, the relative abundance (signal) and level of expression of the *CG34393* transcript compared to the whole fly (enrichment). The Affymetrix value (present call) is generated from microarrays that show how often the mRNA was detectably expressed (out of four arrays). The affy call is the concluding result for that tissue, whether the gene transcript is upregulated, downregulated or no significant change detected (none). The two data sets for each tissue represent two different probes for *CG34393* (against the two genes, *CG15405* and *CG8829*, which were merged in a later release of Flybase to form *CG34393*). Adult tissues were derived from 1-week-old Canton S wild-type flies, while larval tissues were from feeding (i.e. non-wandering) third instar larvae. S2 cells from Invitrogen were grown in Schneiders medium and assayed before confluence (Chintapalli et al 2007). Highlighted data are considered interesting as the transcripts were detected in four out of four independent biological replicates (and thus four different arrays) and are enriched compared to the whole fly, suggesting expression of CG34393 is tissue specific.

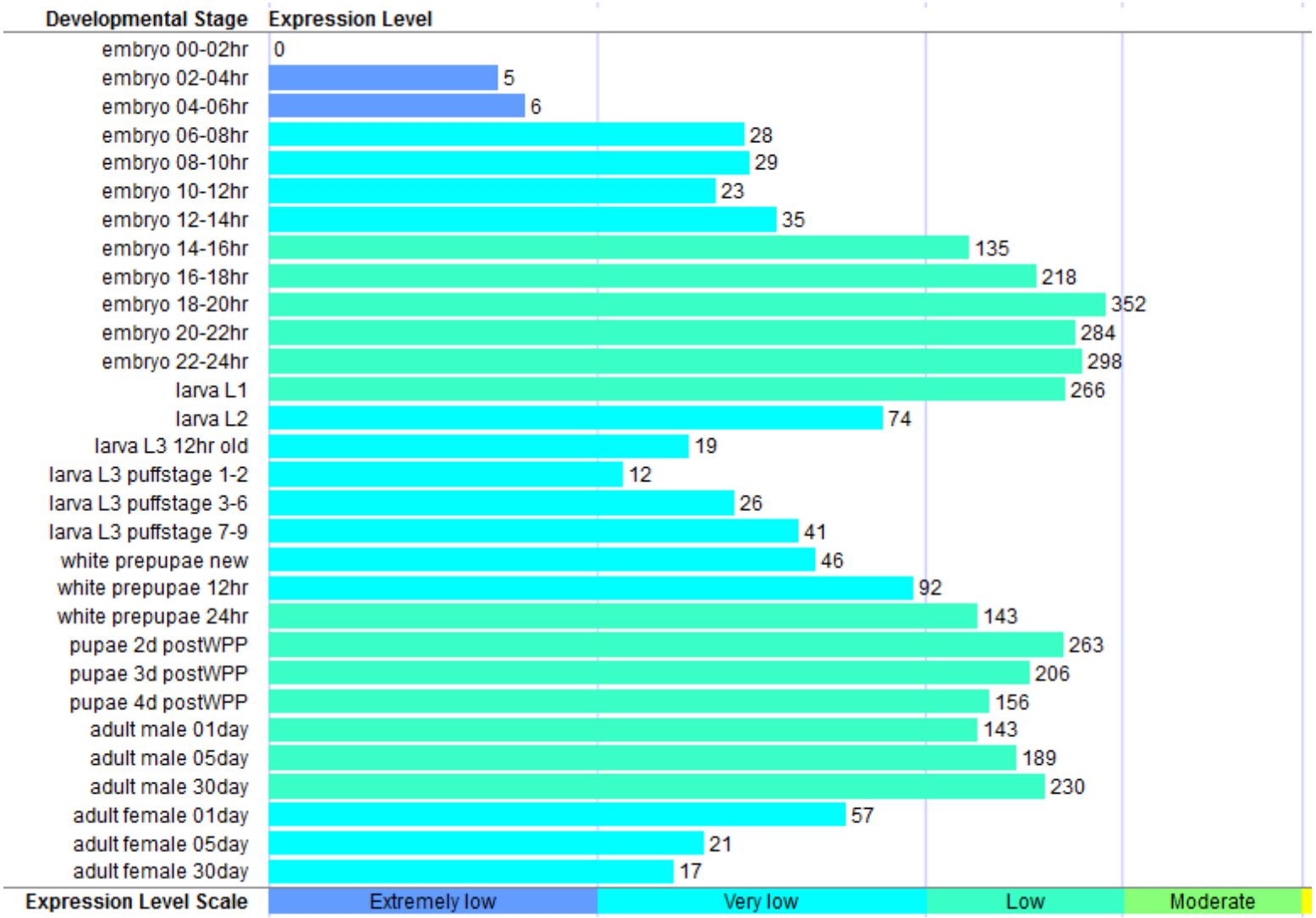
Developmental Stage
Expression Level
embryo 00-02hr 0
embryo 02-04hr 5
embryo 04-06hr 6
embryo 06-08hr 28
embryo 08-10hr 29
embryo 10-12hr 23
embryo 12-14hr 35
embryo 14-16hr 135
embryo 16-18hr 218
embryo 18-20hr 352
embryo 20-22hr 284
embryo 22-24hr 298
larva L1 266
larva L2 74
larva L3 12hr old 19
larva L3 puffstage 1-2 12
larva L3 puffstage 3-6 26
larva L3 puffstage 7-9 41
white prepupae new 46
white prepupae 12hr 92
white prepupae 24hr 143
pupae 2d postWPP 263
pupae 3d postWPP 206
pupae 4d postWPP 156
adult male 01day 143
adult male 05day 189
adult male 30day 230
adult female 01day 57
adult female 05day 21
adult female 30day 17
Expression Level Scale
Extremely low
Very low
Low
Moderate

Figure 5.7 Expression profile of *CG34393* from embryonic to adult stages

CG34393 is expressed from extremely low to almost moderate levels, with peaks during late embryogenesis and early larval life, post white prepupae (wpp) and in adult males. These data were taken from the modENCODE Temporal Expression Data for CG34393 available from Flybase (FBgn0085422) (Celniker et al 2009; Gelbart & Emmert 2010).

Values reflect average coverage per kb per gene derived from modENCODE RNA-seq temporal expression data for each developmental stage that was then intersected with Flybase exons from release 5.26 to generate a single value.

Most frequent controlled vocabulary terms	Number of related records	Genes
[empty field - no data available]	39	[a] –
biological process; GO:0008150	6	*CG9164*, *CG32132*, *CG32544*, *CG42613*, *dpr14*, *munin*
transmembrane transport; GO:0055085	5	*narrow abdomen*, *Shaker cognate b*, *Shaker cognate w*, *Shaw-like*, *slowpoke*
proteolysis; GO:0006508	5	*CG5282*, *CG6154*, *mind-meld*, *Neprilysin 4*, *slamdance*
G-protein coupled receptor protein signalling pathway; GO:0007186	5	*Octβ3R*, *CG33639*, *Dromysuppressin receptor 1*, *Dopamine/Ecdysteroid receptor*, *metabotropic GABA-B receptor subtype 2*
synaptic transmission; GO:0007268	4	*CG1909, Neurexin 1, Shaker cognate b, still life*
potassium ion transport; GO:0006813	4	*Shaker cognate b, Shaker cognate w, Shaw-like, slowpoke*
small GTPase mediated signal transduction; GO:0007264	3	*CG8500, CG42541, Rgk2*
vesicle-mediated transport; GO:0016192	3	*CG6208, n-synaptobrevin, Synaptotagmin 1*
ion transport; GO:0006811	3	*Glu1α, narrow abdomen, nicotinic Acetylcholine Receptor beta 64B,*
protein phosphorylation; GO:0006468	3	*CG7236, Pas kinase, Tie-like receptor tyrosine kinase*
GTP catabolic process; GO:0006184	3	*CG800, CG42541, Rgk2*
neurotransmitter secretion; GO:0007269	3	*n-synaptobrevin, Synapsin, Synaptotagmin 1*

larval locomotory behaviour; GO:0008345	3	*Shaker cognate b, Synaptotagmin 1, Tyramine β hydroxylase*
synaptic vesicle exocytosis; GO:0016079	3	*complexin, Synapsin, Synaptotagmin 1*
male courtship behaviour; GO:0008049	2	*Quick-to-court, Tyramine β hydroxylase*
neuromuscular synaptic transmission; GO:0007274	2	*nervous wreck, straightjacket*
cell adhesion; GO:0007155	2	*alpha-catenin related, hikaru genki*
circadian behaviour; GO:0048512	2	*narrow abdomen, slowpoke*
ATP hydrolysis coupled proton transport; GO:0015991	2	*CG131030, Vacuolar H^+ ATPase subunit 68-1*

Table 5.3 Most frequent controlled vocabulary terms from genes with a similar expression profile to *CG34393*

The top 20 terms (out of 102) from the GO: biological process data of 100 similarly expressed genes to *CG34393*.

[a]Mostly uncharacterized genes; too many to include in the table.

Gene	Profile (selected subsets only)	Correlation (%)	Molecular function	Biological process
CG34393		100.00	guanyl-nucleotide exchange factor activity	regulation of small GTPase mediated signal transduction
s-cup		93.09		
nwk	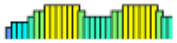	91.84	SH3/SH2 adaptor activity	negative regulation of synaptic growth at neuromuscular junction neuromuscular synaptic transmission regulation of synaptic growth at neuromuscular junction
CG42613	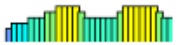	91.61	molecular_function	biological_process
Ank2		90.89	cytoskeletal protein binding structural constituent of cytoskeleton	axon extension cytoskeletal anchoring at plasma membrane microtubule cytoskeleton organization neuromuscular junction development signal transduction
CG42541		90.79	GTP binding GTPase activity	GTP catabolic process phagocytosis, engulfment small GTPase mediated signal transduction
sif		90.39	Rho guanyl-nucleotide exchange factor activity guanyl-nucleotide exchange factor activity receptor signaling protein activity	actin cytoskeleton organization regulation of Rho protein signal transduction regulation of axonogenesis regulation of synapse structure and activity synaptic transmission
Nrx-1	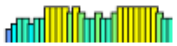	90.21		associative learning synapse assembly synapse organization synaptic transmission
Teh1		90.21		positive regulation of sodium ion transport via voltage-gated sodium channel activity
Ca-beta		90.15	voltage-gated calcium channel activity	calcium ion transport regulation of calcium ion transport via voltage-gated calcium channel activity
CG15464		90.07		

Table 5.4 The top 10 genes with a similar expression profile to *CG34393*

Many similarly expressed genes have roles at the synapse and are involved in regulating the actin cytoskeleton. *Ank2*, a cytoskeletal linker protein and *sif*, a guanyl exchange factor (like *CG34393*) are two such examples.

Source	Domain	Start	End
Pfam A	RasGEF_N	190	278
Pfam A	RasGEF	328	484
low_complexity		37	65
low_complexity		74	97
low_complexity		215	228
low_complexity		239	255
low_complexity		506	519
low_complexity		557	584
Pfam B	Pfam-B_13575	485	690
Pfam B	Pfam-B_16273	1	169

Figure 5.8 Domain architecture of CG34393 as predicted by pfam and prosite

In the pfam database (http.//pfam.sanger.ac.uk), 358 genes are predicted to have a similar domain architecture (*top*); prosite (http://www.expasy.org/prosite/) identifies 547 (*bottom*). That is, they have a RasGEF_N domain followed by a RasGEF domain. The RasGEF_N domain is thought have a structural role that helps to stabilise and correctly place the helical hairpin structure contained within the catalytic domain, important for nucleotide exchange, thus mediating the switch from inactive GDP-bound Ras to the active GTP-bound form during interaction with Ras family proteins, small G proteins upstream of signalling pathways that control many cellular functions. Pfam A families are manually curated and are predictions of higher quality than Pfam-B families; low-complexity regions are regions that can cause false positives in alignments as they contain short repetitive sequences, and are often filtered out before alignment algorithms are run.

Looking at the online generated distance tree of the blastp results (Fig. 5.9; which is a rough guide and is not meant to be used as a definitive phylogenetic reconstruction), seems to suggest that *CG34393* is a highly conserved gene in *Drosophila* species [where the significance value (E-value) approaches zero] and other invertebrates (e.g. mosquito, bee, ants and beetles). According to another online resource (orthoDB; Waterhouse et al 2011), CG34393 belongs to an orthologous group of 16 genes in 15 species comprising 12 *Drosophila*, and three mosquito species (*Culex quinuefasciatus*, *Anopheles gambiae* and *A. aegypti*). The distance tree also suggests that CG34393 is related to some vertebrate genes (Fig. 5.9) (Grishin 1995; Saitou & Nei 1987). For example, the *D. rerio* gene *rasgef1B* has an E-score of 2e-34 and 60% of high-scoring pairs matched between the two genes (blastp results), suggesting the two genes are related. The expression pattern of *rasgef1B* has been published and interestingly, as seen in the *in situ* against *Drosophila* gene *CG34393*, it too has a segmentally repeated pattern in the developing brain in zebrafish (Fig 5.10) (Epting et al 2007). *Rasgef1B* is thought to be regulated by Nodal and FGF signalling pathways, which are important for the development of the nervous system in vertebrates (reviewed in Gomes et al 2005; Kiecker & Niehrs 2001).

Furthermore, a summary of data for *CG34393* in FLIGHT (http://flight.icr.ac.uk) yields additional information, e.g. Homologene (http://www.ncbi.nlm.nih.gov/homologene) identifies an *Anopheles gambiae* gene with 47% identity, and Ensembl compara homology data (http://www.ensembl.org) yields 11 genes in vertebrates with between 25–28% identity in rat, mouse and humans.

CG34393* is homologous to the *C. elegans* gene *R05G6.10

According to Flymine v.28, *CG34393* is homologous to the *C. elegans* gene *R05G6.10*, a RasGEF that is expressed in the nematode CNS (Von Stetina et al 2007). When the entry for *R05G6.10* was viewed in WormBase (http://www.wormbase.org, release WS225), *R05G6.10* was also found to be homologous to two additional *Drosophila* genes: *CG7369* and *CG4853*. *CG7369* is a RasGEF thought to be involved in the regulation of cell shape

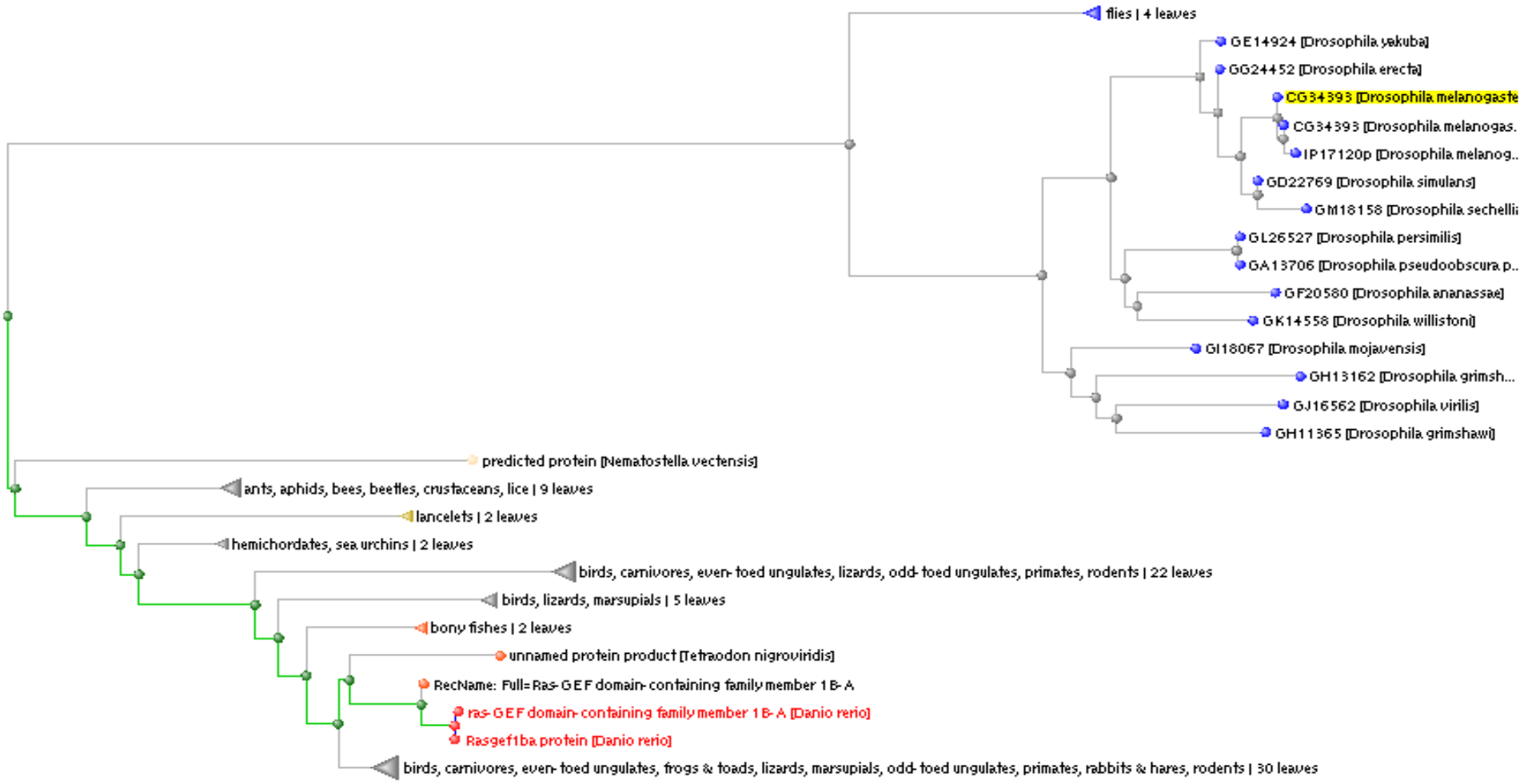
flies | 4 leaves
GE14924 [Drosophila yakuba]
GG24452 [Drosophila erecta]
CG34393 [Drosophila melanogaste
CG34393 [Drosophila melanogas.
IP17120p [Drosophila melanog..
GD22769 [Drosophila simulans]
GM18158 [Drosophila sechelli
GL26527 [Drosophila persimilis]
GA13706 [Drosophila pseudoobscura p..
GF20580 [Drosophila ananassae]
GK14558 [Drosophila willistoni]
GI18067 [Drosophila mojavensis]
GH13162 [Drosophila grimsh...
GJ16562 [Drosophila virilis]
GH11365 [Drosophila grimshawi]
predicted protein [Nematostella vectensis]
ants, aphids, bees, beetles, crustaceans, lice | 9 leaves
lancelets | 2 leaves
hemichordates, sea urchins | 2 leaves
birds, carnivores, even-toed ungulates, lizards, odd-toed ungulates, primates, rodents | 22 leaves
birds, lizards, marsupials | 5 leaves
bony fishes | 2 leaves
unnamed protein product [Tetraodon nigroviridis]
RecName: Full=Ras-GEF domain-containing family member 1B-A
ras-GEF domain-containing family member 1B-A [Danio rerio]
Rasgef1ba protein [Danio rerio]
birds, carnivores, even-toed ungulates, frogs & toads, lizards, marsupials, odd-toed ungulates, primates, rabbits & hares, rodents | 30 leaves

Figure 5.9 A simple phylogenetic distance tree for CG34393 and related genes

This tree is based on pairwise alignments generated from a blastp similarity search using CG34393 amino acid sequence as a template. CG34393 is highlighted in yellow, and a distantly related zebrafish gene *rasgef1ba* is shown in red. *CG34393* is a putative RasGEF protein that is closely related to genes in other species of *Drosophila*, and also shares similarity to genes in other phyla.

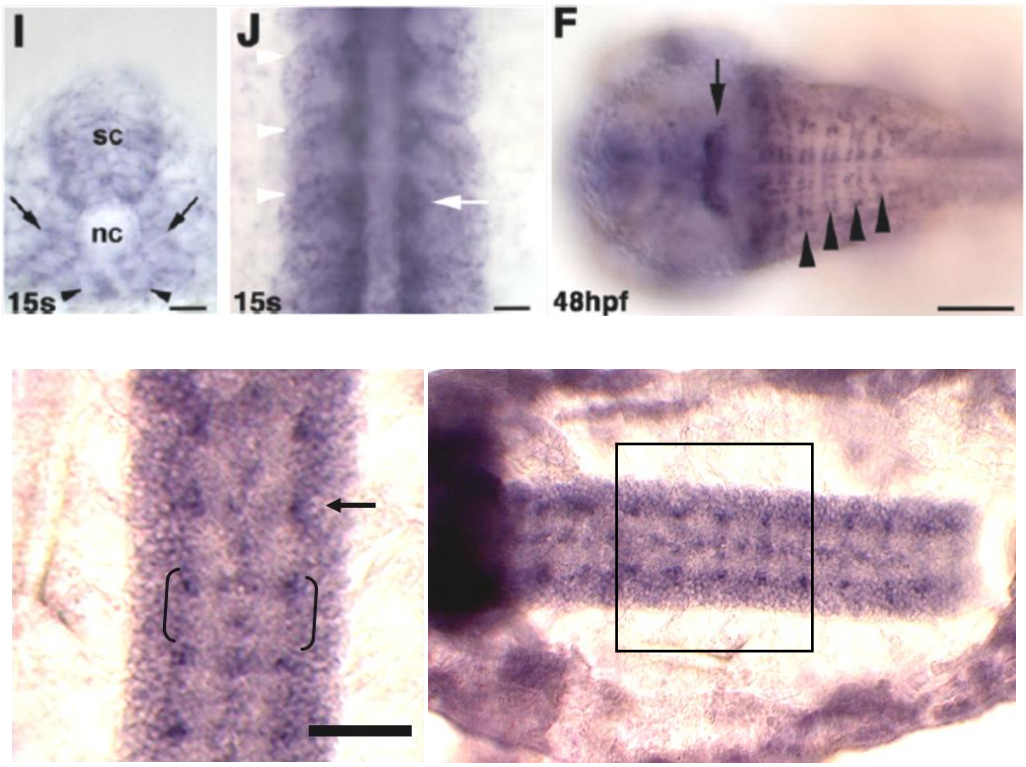

Figure 5.10 *CG34393*, in *Drosophila,* and *rasgef1b*, in zebra fish, are expressed in the nerve cord in a segmentally repeated pattern

(*Top left*) Expression of *D. rerio rasgef1b* at the 15-somite stage of development, with expression in the spinal cord (sc), and (*centre*) with stronger expression in the anterior part of the somite (white arrow). (*Top right*) Forty-eight hours post-fertilization, expression is seen in the ventral part of the mid-hindbrain (arrow) and in lines of cells adjacent to rhombomere boundaries, one line at the anterior border, and one at the posterior (arrowheads mark rhombomere boundaries). Reprinted from Gene Expression Patterns, 7, Expression of *rasgef1b* in zebrafish, Copyright (2007), with permission from Elsevier. (*Bottom*, *left*) Close up of area outlined in *right*, of an *in situ* against *CG34393*. Brackets approximately define one segment, anterior is up, scale bar = 20 µm. Although it is uncertain if the bulk of CNS expression is low-level expression or background, a small group of cells express *CG34393* more strongly, and they are located at the anterior part of the segment.

(Kiger et al 2003) and *CG4853* is also a RasGEF thought to be involved in mushroom body development in the *Drosophila* brain (Kobayashi et al 2006). Wormbase also provides data from yeast two hybrid screens that identify three genes that *R05G6.10* interacts with: *Unc-57*, *add-1* and *ehs-1. Unc-57* (or *endophilin*) is expressed in all neurons, at synapses (including the neuromuscular junction) and is required for synaptic vesicle endocytosis (Schuske et al 2003). Add-1 is a cell membrane associated protein expressed in the ventral nerve cord that mediates localized changes in the cytoskeleton in response to signal transduction cascades (Moorthy et al 1996) – the Ras signalling pathway perhaps? Finally, *ehs-1* is expressed in the nervous system of *C. elegans*, particularly synapse rich structures such as the nerve ring, and dorsal and ventral nerve cord processes, and is involved in synaptic vesicle recycling (Salcini et al 2001).

Concluding remarks

Efforts to further investigate the dendritic phenotype of CG34393 by generating a loss of function with *Minos* transposase, and RNAi knockdown in identified cells gave mixed results. Although the imprecise excision method was successful in itself, it remains to be seen whether the two imprecise excision lines made affect expression of *CG34393*. The RNAi results suggest that knockdown of *CG34393* mRNA can cause a reduced dendritic branching/stunting of higher order branches phenotype, particularly evident in larvae 48 h ALH. However, the UAS-RNAi expression induced phenotypes are variable, possibly due to inter-cell differences in RNAi expression and perdurance of wild-type protein; perhaps due to an inherent variability in the efficacy of RNAi knockdowns induced in this way. Further work is necessary to clarify this phenotype, particularly as it is different to the midline phenotype seen in neurons homozygous for the recombinant deficiency line FRT40A *Df(2L)S2590*.

In addition to these experimental results, several lines of evidence suggest that *CG34393* is a conserved gene, with expression in the CNS in many organisms. Based on data on homologous genes, and genes that are expressed in a similar developmental time course, *CG34393* may similarly be involved with synapse development. This line of investigation needs to be pursued further.

Chapter 6 Discussion

The *Drosophila* embryo develops into a larva capable of complex behaviours within 21 hours. During this rapid embryogenesis it forms a complete nervous system, including sensory systems in the periphery that provide information about environmental stimuli, internal (e.g. nutritional) states and posture, central networks that integrate these inputs, and the motor system, which generates corresponding behavioural outputs. All these systems have to make appropriate connections within and between each other to ultimately ensure the survival of the animal. The processes that neurons – the functional unit of the nervous system – undergo to project synaptic terminals (axons and dendrites) into appropriate regions of the developing nervous system, and make connections with pre- and postsynaptic partners is the subject of much study, ultimately aimed to help us understand how our own highly complex nervous system is put together, and how it can fail in neurological diseases and disorders. Most of what is known about nervous system development in *Drosophila*, derives from work on (the more accessible and less complex) structures in the periphery (e.g. development of the sensory system, axon pathfinding and neuromuscular junction formation) and cells grown in culture; much less is known about the development of central neurons in the CNS, particularly motor systems and how the dendrites of neurons achieve their characteristic shapes and make connections with their presynaptic partners.

Ideally, to identify cell autonomous components that are required for dendrite morphogenesis within motor neurons, a loss-of-function screen is required; further, this screen should be mosaic so that secondary, non-autonomous effects are avoided, which can occur when large parts of the CNS are made mutant.

In this study, a novel modification of the commonly used MARCM technique was developed to allow the identification of intrinsic genes required for correct patterning of motor neuron dendrites in the *Drosophila* embryo and first instar larva. The efficacy of this system (termed 'ftz loop' MARCM) as a way of studying motor neuron dendritogenesis was tested using mutations known to have a dendritic phenotype, $robo^{GA285}$ and $shot^{2}$, which demonstrated that mutant motor neurons labelled using this method could be identified based on their dendritic morphology.

The next stage of the project was to carry out a limited genetic loss of function screen. This was achieved by generating a library of fly lines in which deletions of defined regions of chromosome 2 were recombined onto FRT-carrying chromosomes. While the Bloomington Stock Centre in Indiana, USA holds a collection totalling some 2974 deficiency-carrying stocks, 1159 of which are deletions of regions of chromosome 2, only 15 carry a FRT site that could be used in a mosaic system such as MARCM. The library of 83 FRT-deficiency recombinant stocks generated as part of this work (two stocks obtained from the Bloomington Stock Centre were already recombined with FRT) provides a valuable resource for any project using a mosaic loss-of-function approach, in any tissue of interest.

Appraisal of the loss-of-function screen

Comparison with other screens

Fifty-three per cent (45/85) of the FRT/deficiency recombinant stocks were screened using 'ftz loop' MARCM and from these, five lines were identified as having a dendritic phenotype, and although the screen is not fully complete, it is likely that one novel gene has been identified that has a role in dendrite morphogenesis. How does this compare to other MARCM-based screens in the *Drosophila* nervous system?

Reuter and colleagues (2003) used the MARCM system in third instar larval mushroom body neurons to screen 4600 independent lines mutagenized with EMS on the right arm of chromosome 2. They identified 33 mutations that cause defects in neuronal morphogenesis, five of which caused abnormal axon and dendrite morphogenesis; two of these genes were novel (Reuter et al 2003). Another screen, also in the third instar larval brain, used MARCM to identify genes on the left arm of chromosome 3 that are involved in neuroblast division (Slack et al 2006). Of 2300 EMS mutagenized lines, 1923 were screened for phenotypes in MARCM neuroblast clones, identifying four mutations involved in neuroblast asymmetric division, and 78 mutations affecting cell division, 12 of which had already been described. At a later stage during metamorphosis, Schuldiner and co-workers (2008) generated 1803

piggyBAC insertion mutagenized fly lines and screened with MARCM to identify 128 genes involved in the proliferation of mushroom body neurons

How successful are other screens that do not use a MARCM-based approach, such as those that use RNAi or the GAL4/UAS system? Parrish and colleagues (2006) screened 730 transcription factors by injection of double stranded RNA into embryos expressing GFP in class I sensory neurons, and looked during late embryogenesis for dendritic phenotypes; 78 genes were identified (Parrish et al 2006a). In cultured neurons, Sepp and co-workers (2008) carried out a genome-wide RNAi screen of 21,300 double stranded RNAs and identified 2442 that produced morphological phenotypes (Sepp et al 2008). In two papers based on the same screen, 3314 double stranded RNAs were used to knockdown gene function by injection in the developing embryo and the CNS and PNS revealed by antibody staining. The authors report the identification of 43 genes in the initial screen (Ivanov et al 2004) and a further 22 additional genes in a follow-up paper (Koizumi et al 2007). Medina et al (2006) identified 13 genes with dendritic phenotypes from 4000 EMS mutagenized lines in a subset of second instar larval sensory neurons revealed by GAL4/UAS expression of GFP (Medina et al 2006). Finally, McGovern et al (2003) used a combination of the GAL4/UAS system to reveal the axonal morphology of embryonic central neurons and 4100 *P-element* insertion mutagenized lines and found 18 genes with an axonal phenotype; two were previously uncharacterised (McGovern et al 2003).

In terms of the number of genes identified per number of lines screened (one gene from 45 lines screened; 2.2%), the present study was as successful as the MARCM-based screens described above (0.7–7%), less successful than those studies that use RNAi (10–11%) and much better than those that use a GAL4/UAS-based system (0.325–0.4%). However, if the number of genes identified out of the number of genes screened so far is calculated (1 out of 2745; 0.03%) the success rate is very low. This may be due to nature of the method used, in that the version of the MARCM system developed and used in this screen is inherently variable to some extent and prone to the effects of protein perdurance for example. It remains to be seen whether the other three regions of chromosome 2 identified in the screen will yield more genes involved in dendrite morphogenesis in the present study.

The screen presented here has some advantages over the screens described above in that analysis of labelled cells takes place at an earlier developmental stage in the present screen, in contrast to the many days required for animals to reach the third instar or metamorphosis stages. Further it is less labour intensive (at least initially), an issue that was acknowledged by Reuter and colleagues (2003). The use of deficiencies readily available from Bloomington Stock Center, means that many genes can be screened at one time. The deficiencies are defined and complementation experiments are not required to identify the region containing the phenotype causing mutation. However, at later stages of the screen, a significant amount of time was required to analyse sufficient numbers of CNSs to confirm and in some cases disprove that a deficiency caused a phenotype in homozygous mutant motor neurons..

Despite its limited success thus far, this study is the first screen to investigate intrinsic genes required for the development of motor neuron dendrites in the early larval stages of *Drososphila*.

Synthetic phenotypes

One of the concerns associated with this kind of genetic screen using deficiencies (the present study), is the possibility of synthetic phenotypes. These are phenotypes caused by the cumulative loss of two or more genes. The loss-of-function of any one of the genes is not sufficient to cause a phenotype, but loss of several of them (i.e. in a deficiency) has an effect. Synthetic phenotypes are interesting as they can lead to the identification of genes that are involved in the same biochemical pathway or process, and some screens have been based on the similar idea of synthetic lethality, particularly for identification of pathways involved in tumour development (Brough et al 2011). However, these types of genetic effects are not the focus of this work.

Of the five chromosomal regions identified in the screen, two of them were fully investigated using overlapping deficiencies: *Df(2L)al* and *Df(2L)S2590*. With *Df(2L)al*, the results suggested that the loss of secondary branching and blebbing phenotype was a synthetic

phenotype, as the dendrites in neurons homozygous for overlapping deficiencies appeared normal. A possible, though unlikely alternative explanation for the blebbing might be that it is an imaging artefact caused by damage during preparation and imaging of the nerve cord; if the case such an artefact would not explain the loss in secondary branching and it one would have expected it to occur more frequently and likely show a fair degree of lack of reproducibility.

In *Df(2L)S2590*, the midline targeting phenotype was recapitulated in an overlapping deficiency. However, during RNAi knockdown of a single candidate gene contained in this deficiency, *CG34393*, a different phenotype was observed. It is conceivable that the midline phenotype is synthetic, and may have masked the more subtle reduced branching and stunting phenotype seen in neurons with RNAi-mediated knockdown of *CG34393*.

Protein perdurance

Another issue associated with the screen was protein perdurance. Wild-type proteins are carried over to the daughter cell as the parental cell divides to generate one wild-type and one daughter cell that is homozygous 'mutant' for genes contained in a deficiency. This passing on of wild-type gene products from the mother cell has the potential to reduce the penetrance of any phenotypes seen. It may have also resulted in some deficiencies having been overlooked that may have produced phenotypes over time, with the disappearance of wild-type protein. The variation in phenotype severity seen in both the screen using the 'ftz loop' MARCM technique and the RNAi experiments, suggests that protein perdurance had a significant impact in the screen. This is particularly true if the wild-type protein is stabile and has a long half-life before it is degenerated.

Protein perdurance has been documented in many reports where MARCM has been used to label single cells (Lee & Luo 2001; Parrish et al 2007a; Wu & Luo 2006). Lee and Luo (2001) report that MARCM is not useful for analysis of events that occur shortly after mitotic recombination, Parrish and colleagues (2007a) were limited to clonal analysis after 48 h AEL, and in their MARCM protocol paper, Wu and Luo (2006) report that the MARCM

system can only be used to label single cells 24–48 hours after mitotic recombination is induced; all due to perdurance of GAL80 protein. In these published MARCM systems, GAL80 is driven by the strong and ubiquitous tubulin promoter, thus levels in all cells are comparatively high. Further, it has been suggested that maternally contributed proteins prevent the use of MARCM in the embryo (Wu & Luo 2006), and that mutant clones have milder phenotypes than homozygous mutant animals due to protein perdurance in MARCM clones (Parrish et al 2007a). The results of the screen in the present study complement and support some aspects of these conclusions.

In this study, to address the issue of GAL80 perdurance, one of the modifications made to the MARCM system was to limit the expression of GAL80 to post-mitotic cells using the *elav* promoter. However, evidence that *elav* is not strictly expressed post-mitotically was published after the screen was well underway (Berger et al 2007). The impact that transient expression of GAL80 under the control of *elav* would have on the modified MARCM system is that expression of GAL4 (using the *ftz* promoter) would be repressed, and thus the likelihood of *FLPase*-mediated recombination taking place is reduced. This would result in decreased numbers of labelled cells than the system can potentially generate. This works to the advantage of the screen though, as too many labelled cells makes interpretation of results difficult due to dendritic arbors overlapping.

The expression of GFP was also a limiting factor of the screen as it was necessary to wait until the late first instar larva stage and GFP levels to subside, before animals of the appropriate genotype that carried GAL80 could be selected. Thus, the MARCM in this project was also not suitable for use in the embryo, but for a different reason. In addition, at this life stage, it was thought that maternally derived proteins would not be an issue, but this does not preclude the possibility that wild-type proteins carried over from the ganglion mother cell could persist in the daughter cell; Reuter and co-workers (2003) report in their screen that more mutations were identified in neuroblast clones, which likely dilute proteins carried over more rapidly than do single-cell clones, which were generated in the present screen.

Perdurance of wild-type protein, and also of the UAS-RNAi double stranded RNAs may have contributed towards the variable phenotype seen in neurons with RNAi-mediated knockdown of the candidate gene CG34393. Protein perdurance of target proteins present prior to induction or introduction of double stranded RNAi is an acknowledged issue with RNAi (Sepp et al 2008; Ying et al 2006). Furthermore, the stability of the interfering double stranded RNA itself may also play a part in variability of phenotypes, particularly if it is rapidly degraded, expressed at low levels, or fails to completely knockdown the target.

Labelling frequency and identification of targeted neurons

Screening recombinant FRT-deficiency lines was not as efficient as it was initially thought. The initial 'wild-type' experiments where the 'ftz loop' MARCM stock was crossed to FRT-carrying lines yielded an average of 1.47 motor neurons per CNS. However, this frequency was not achieved with FRT/deficiency recombinant lines, and indeed varied depending on which chromosomal arm was being analysed – the underlying reasons remain unclear, but surprisingly it is not a consequence of deletion size (i.e. number of genes deleted).

Another factor that affected screening efficiency was the number of different motor neurons that could be targeted by the system. In contrast to the FLP-out method (Ou et al 2008; Roy et al 2007), which targets a small subset of neurons (i.e. aCC, pCC and RP2), the 'ftz loop' MARCM method has the potential to label any motor neuron whose ganglion mother cell expresses *ftz* during embryogenesis. In the control experiments, seven motor neuron types were most frequently targeted (with a frequency of between 2–10% depending on the motor neuron type); the remainder, ~27% of motor neurons labelled could not be identified, as they did not appear frequently enough during either control, or screening experiments. While a greater variety of neuronal types that can be targeted in a genetic screen increases the chances of identifying genes required for specific cell types, it makes the screening procedure much less effective. Moreover, in instances of severe phenotypes, as occurred with *Df(2L)TE35BC-24*, the identity of affected neurons may be impossible to pin down.

In the end, more CNSs for each deficiency had to be screened to ensure that enough motor neurons were analysed: (i) so that they could be compared to their equivalent control neuron and (ii) to allow for any differences in phenotype penetrance.

Phenotypic classes identified in the screen

The phenotypes seen in the initial proof of principle experiments with *robo*^{GA285} and *shot*^{2}, and in the deficiency lines identified in the screen, can be broadly classified into two types: (i) growth and branching, which include loss or overgrowth of secondary branches and blebbing (e.g. loss of secondary branches in *shot*^{2} mutant neurons); and (ii) targeting, where dendrites are delivered to inappropriate areas (e.g. *robo*^{GA285}). One limitation of the imaging method used was that data were reviewed as a maximum projection of a *z*-stack, which means that phenotypes only in the anteroposterior and/or mediolateral axes would be evident.

Growth and branching

Blebbing is a phenomenon usually associated with apoptotic cells where bulbous extrusions form in membranes under the contractile forces of actin-myosin cytoskeletal structures. In neurons, it can also occur during growth cone collapse and is typically observed as thickenings in the membrane as it is degraded (for review see Negishi et al 2005). Blebbing may be due to genes involved directly in producing and maintaining the cytoskeleton being removed, or indirectly as a result of loss of gene(s) required for partner recognition e.g. receptors and the subsequent redundant dendrite retracting (Parrish et al 2007b; Williams & Truman 2005b).

Blebbing was seen in two of the deficiency lines, *Df(2R)Px2* and *Df(2R)al*. Despite later being found to be a synthetic phenotype, an interesting result with *Df(2R)al* is that loss of secondary branching was also observed. This loss may be correlated with the blebbing in that neurons with loss of secondary branching may have already undergone a stage of

dendritic retraction and are left with the primary branches. There may be a separate mechanism for the growth of higher order branches than that responsible for producing and maintaining the primary branches; alternatively, higher order branches are more susceptible to degradation than core components of the arbor, which have a more stable tubulin-based cytoskeleton. The positive control test with the mutant *shot*^{2}, a gene known to be involved in maintaining the cytoskeleton also has the loss in higher order branching phenotype, but without any evidence of blebbing. This is not so at earlier stages, however, as embryonic neurons mutant for *shot* have been shown to have a blebbing phenotype (Prokop et al 1999). It is conceivable that at earlier stages, blebbing due to lack of an important component of the cytoskeleton causes the development of higher order dendrites to fail.

Targeting defects

Four of the five deficiency lines identified so far have dendritic targeting defects illustrating how complex and important this aspect of dendrite development is. Also interesting is that different deficiencies have targeting phenotypes in different axes. This suggests that there is more than one guidance mechanism at work and that targeting in different axes may require genetically distinct mechanisms. For example, *Df(2L)TE35BC-24* had defects in both mediolateral and anteroposterior axes, whereas *Df(2L)S2590* and *Df(2L)Np5* had defects in the mediolateral axes only (similar to *robo*^{GA285} mutant neurons). Indeed, during axon guidance and presynaptic terminal positioning in the *Drosophila* CNS, different signal/receptor mechanisms are used to target growth cones in anteroposterior, dorsoventral and mediolateral axes independently (Mauss 2008; Simpson et al 2000a; Yoshikawa et al 2003; Zlatic et al 2003; Zlatic et al 2009).

Motor neurons homozygous for *Df(2L)S2590* and with RNAi-mediated knockdown of *CG34393* have different phenotypes.

Defects in mediolateral positioning were seen in dendrites of neurons lacking the region uncovered with deficiencies *Df(2L)S2590* and *Df(2L)BSC28*. However, the phenotype seen in neurons expressing RNAi against CG34393 was different: smaller arbors, reduced branching and stunted dendrites. As discussed earlier, these two phenotypes are representative of two different phenotypic classes uncovered in the screen: (i) growth and branching and (ii) targeting. How can this discrepancy in phenotypes be explained? One possibility is that the midline targeting phenotype could be synthetic, caused by loss of more than one gene in the deficiency [i.e. in *Df(2L)S2590* and *Df(2L)BSC28*]; and deletion of *CG34393* may or may not contribute to the mediolateral positioning defect. This hypothesis might be supported by the fact that it remains uncertain whether or not the other candidate genes identified by this and overlapping deficiencies (*CG31698*, *CG9664*, *CG3332*, *CG3347*, *CG15404*, *CG34406*) are expressed in the CNS; their expression levels may be below detection limits or the design of the *in situ* probes may not have been optimal.

Another reason might be that different neurons may have different intrinsic requirements to achieve their characteristic shape, (e.g. dendritic length, number of branch points; Mauss et al 2009); the phenotype displayed could depend on neuronal type. The mediolateral phenotype was most prominent in MN-VO4/5 and 'L-shape' neurons, whereas in MN-RP2 neurons (in which the RNAi knockdown was carried out), reduced arbor size and branching, and stunted dendrites were seen. Simply, this may be because RP2 motor neurons do not cross the midline, whereas MN-VO4/5 dendrites do and 'L-shape' neurons have a strong mediolateral arbor that almost reaches the midline.

How might a reduction in CG34393 levels result in the phenotypes seen?

As discussed in Chapter 5, CG34393 is predicted to be a RasGEF. It is therefore important to discuss the role of RasGEFs in neurons in this context.

The Ras superfamily and regulation by RasGEFs

RasGEFs are a group of proteins (termed guanine exchange factors or guanine nucleotide releasing factors) that in partnership with GTPase-activating proteins (GAPs) catalyse activation of the small G-protein Ras to control cellular functions. Ras proteins are molecular switches that cycle between a RasGEF mediated GTP-bound activated state and an inactivated GDP-bound state, mediated by RasGAPs (Donovan et al 2002; Downward 1998). Originally identified as proto-oncogenes (rat sarcoma), Ras heads a superfamily of proteins, which includes Ras, Rho, Rab, Rap, Rheb, Rad, Rit Arf and Ran families (Wennerberg et al 2005) and more recently the Miro family (Reis et al 2009); proteins that 'specialise' in the control of a variety of cellular processes. For example, the Miro family of GTPases are regulators of mitochondria morphogenesis and trafficking along microtubules (Reis et al 2009), Rab and Arf families are involved in vesicle-associated processes, Rho members control aspects of cytoskeletal rearrangements and Ras family members regulate signalling pathways that regulate cell proliferation and differentiation (Bos et al 2007). Ras is also involved in signalling in non-dividing cells such as neurons, where it is important for synaptic transmission, plasticity and memory (Thomas & Huganir 2004).

RasGEFs, the proteins that activate Ras, can be generally divided into families based on different motifs that are incorporated into their structure. *Son of sevenless* (*Sos*) members contain pleckstrin homology domains (has multiple functions including binding inositol phosphates and other proteins) and Dbl homology domains (for Rho and Rac GTPase interaction) (Nimnual et al 1998). EPAC (exchange protein directly activated by cyclic AMP) family members have cyclic nucleotide binding domain motifs that bind cAMP, which when

bound, enables them to activate Rap (de Rooij et al 1998); C3G members have (SH)2-containing motifs (recognize phosphorylated tyrosine on target proteins) and are also thought to activate Rap GTPases (Pannekoek et al 2009). Finally the RasGRF family RasGEFs have calcium-binding EF hand and diacylglycerol (DAG)-binding motifs and activate Ras in response to calcium and DAG signalling (Ebinu et al 1998).

All RasGEFs also contain 'core' motifs necessary for their Ras activation activity: a 'RasGEF' catalytic domain for guanyl nucleotide exchange factor activity; and many also contain the RasGEF_N N-terminal motif, which is thought to play a purely structural role (Boriack-Sjodin et al 1998).

As shown in Fig. 5.8 CG34393 is predicted to contain the two RasGEF and RasGEFN motifs (Pfam, Bateman et al 2004; prosite, Sigrist et al 2010), and none of the other motifs associated with the RasGEF families as discussed above. However, this is not unusual as many RasGEFs have no obvious signalling domains other than the 'core' motifs. Examples of these were reported in the social amoeba *Dictyostelium discoidiem*, where a comprehensive analysis of the genome was carried out with the aim of identifying all RasGEFs and their likely biological roles (Wilkins et al 2005). The authors identified 25 RasGEF genes that contained at least the RasGEF and RasGEFN domains; eight of these genes only had the two 'core' motifs – similar to CG34393. Looking at many species that have been studied, from yeast to humans, 358 genes have a similar RasGEF–RasGEFN architecture with no other obvious motifs (Pfam, Bateman et al 2004), including the zebrafish gene *rasgef1b*, which has similarities with CG34393 in the pattern of CNS expression (Fig. 5.10).

RasGEFs are expressed in vertebrate and invertebrate neurons, where their function, regulation and mechanisms of action are largely unknown (Chen et al 2011). Flybase (release FB2011_07, released July 21st, 2011) reports 59 genes with guanyl-nucleotide exchange factor activity in *Drosophila*, 33 of which are thought to have Ras guanyl-nucleotide exchange factor activity and of those that have been characterised, many are expressed in the nervous system.

The role of RasGEFs in *Drosophila* neurons

In *Drosophila*, several RasGEFs have been implicated in nervous system development and some have been shown to have a role in axon growth and guidance, for example, *Sos*, *vav*, *Gef64C*, *trio* and *pebble* (*pbl*).

In *Drosophila* neurons, *Sos* has multiple functions and has been shown to regulate both Ras (Bonfini et al 1992) and Rho family (Rac, Rho and CDC42) GTPases in *Drosophila* (Luo 2000; Yuan et al 2003). Interestingly, it has been reported to be involved in Robo/Slit-mediated axon repulsion via its Rac-GEF activity. Sos is thought to form a complex with the Robo receptor and the adapter protein *Dreadlocks* at the cell membrane and regulates Rac-dependant cytoskeletal rearrangements in response to the midline secreted signal slit (Yang & Bashaw 2006). *Drosophila* vav is another member of the Rho/Rac GTPase family, and has been shown to be required in at least three different stages of nervous system development, where it prevents longitudinal axons crossing the midline during embryogenesis, is required in larval photoreceptors for correct targeting of axons to the optic lobe, and in adult, where vav loss-of-function causes axon growth defects in the brain (Malartre et al 2010). Trio, has been reported to regulate embryonic midline crossing of axons downstream of the Fra receptor and in concert with Abelson tyrosine kinase and Enabled (Forsthoefel et al 2005). It has also been suggested that Vav, Trio and Sos cooperate in the CNS of the developing embryo to regulate Rac activity (Malartre et al 2010). Gef64C, a RhoGEF, is reported to promote axon attraction to the midline (Bashaw et al 2001) and Pbl positively regulates the Rho1/Rok/LIMK1 pathway, to inhibit axon growth (Ng & Luo 2004b).

GEFs in *Drosophila* have been shown to be involved in other aspects of development in the CNS. For example, *Ephexin* (*Exn*) at the presynaptic membrane of the neuromuscular junction binds Eph receptor, and via Cdc42 couples Eph signalling to the control of presynaptic channels during synaptic homeostasis (Frank et al 2009), an important component of synapse formation at the neuromuscular junction. Epac has also been shown to have a role at the synapse, where it is involved in cAMP-dependent potentiation independently of cAMP-dependent protein kinase (Cheung et al 2006).

Protostome-specific GEF (*PsGEF*) and *CG4853* have been reported to have a role in mushroom body development in the *Drosophila* brain. PsGEF is expressed in a subset of cells in the ventral nerve cord and in the brain, and interacts with Rac1 for proper axon development in mushroom bodies (Higuchi et al 2009). RNAi knockdown of CG4853, caused mushroom body defects in the adult brain (Kobayashi et al 2006).

These reports show that RasGEFs expressed in the nervous system perform a variety of functions in different types of neurons and subcellular compartments. The evidence from *Sos*, *vav* and *trio* shows that GEFs can play a key role in the mediolateral guidance of axons. Other GEFs (Epac and Ephexin) are found at presynaptic sites and help the neuron integrate and respond to synaptic signalling. Based on its predicted structure, it is unlikely that CG34393 can be linked directly to the activation of a receptor (i.e. like Sos or Epac) as it lacks the necessary motifs. Consequently, it is doubtful that loss of CG34393 in neurons homozygous for Df(2L)S2590 is the cause of the midline targeting phenotype observed, and the phenotype is probably synthetic.

The putative role of CG34393 in *Drosophila* neurons

How might loss of CG34393 cause reduced branching and dendritic stunting as seen in the RNAi knockdown experiments? The data mining carried out in Chapter 5 showed that the expression profile of CG34393 is similar to other genes that are involved in nervous system development in *Drosophila*, particularly at the synapse. Recently, human RASGEF1B, which is highly expressed in the human brain and shares a similar domain structure to CG34393, has been implicated in a new syndrome with mental retardation (Bonnet et al 2010). The authors speculate that loss of RASGEF1B interferes with cytoskeletal dynamics during dendrite and spine plasticity. This is interesting as three of the genes that share a similar expression time course with *CG34393* are *Ank2*, *sif* and *Nrx-1*, which are involved in synapse formation and/or regulation of the cytoskeleton. Ankyrins link membrane proteins to the underlying spectrin-actin cytoskeleton, and in *Drosophila* are required for maintaining the stability of the neuromuscular junction. In mutants for the long isoforms of Ank2, the synaptic

microtubule cytoskeleton disintegrates leading to a reduction in terminal size (Koch et al 2008). Ank2 interacts with the cytoplasmic domain of the cell adhesion molecule Neuroglian (Bouley et al 2000) and Sif (a RhoGEF that activates Rac, a known regulator of the actin cytoskeleton; Ng & Luo 2004b) has been shown to act in the same pathway as Fasciclin II (FasII) a cell adhesion molecule that is required for maintenance of synapses after they have formed (Schuster et al 1996). Interestingly, the downregulation of FasII is controlled by the activation of the Ras1-MAPK pathway during the process of new synapse formation (Koh et al 2002). Nrx-1 is a cell adhesion molecule that is enriched in the brain and ventral nerve cord and is required for synapse formation and function at the neuromuscular junction and during memory formation in the brain (Chen et al 2010a; Li et al 2007; Zeng et al 2007).

Until CG34393 is fully characterised in the developing CNS its precise role remains speculative. A preliminary hypothesis can be formulated based on a combination of the reports above and clues from the data mining whereby loss of CG34393 in dendrites leads to failure to activate a signalling pathway that regulates control of cell adhesion molecules at the synapse and hence, the cytoskeleton. If new synapses are not formed, or extra synapses not removed, then the dendrites may stop growing as the amount of appropriate input is achieved prematurely. This type of effect has been documented in motor neurons where postsynaptic dendrites adjust their growth to compensate for changes in the activity and density of synapses with presynaptic partners in order to maintain an appropriate level of input (Tripodi et al 2008). Synapses could influence the amount of growth a dendrite undergoes by stabilising the exploratory filopodia on which they form – a synaptotropic model (Niell 2006). Recently in *Xenopus*, the cell adhesion molecule binding partners β-Neurexin and Neuroligin-1 have been used to demonstrate cell adhesion molecule-mediated stabilization of synapses that directs normal dendritic arbor development (Chen et al 2010b).

The phenotype seen in CG34393 RNAi knockdown is subtle and incompletely penetrant. Apart from perdurance of wild-type protein and efficacy of knockdown by the UAS-RNAi transgene, this can be explained by redundancy, not only in signalling pathways (e.g. Rac and Rho) but between the regulators of these pathways (e.g. *vav* and *trio*). It is unknown if CG34393 is complemented by another protein capable of activating a similar pathway to

achieve the same end in dendrites. Work in *Dictyostelium* suggests that all GEFs have precise roles (Wilkins et al 2005); however, *Dictyostelium* is a simpler organism and has fewer GEFs than *Drosophila*. Moreover, redundancy between GEFs in *Drosophila* has already been demonstrated (Malartre et al 2010).

The role of CG34393 in dendrite morphogenesis may be small, and neurons are plastic and adaptable cells that may be able to function even in its absence. Nevertheless, it is a conserved gene, particularly among *Drosophila* species and must therefore be of some importance. Further investigation of this previously uncharacterised gene to fully understand its role in nervous system development will be interesting and will provide another piece of the puzzle towards better understanding of how dendrites achieve their characteristic branching patterns.

Conclusion

Here, a loss of function screen for genes involved in dendrite morphogenesis is presented. The development and then execution of modified MARCM method-based loss-of-function screen identified a previously uncharacterised gene and also has:

- generated a library of recombinant FRT/deficiency fly stocks that provide a useful tool for any MARCM-based project wishing to use a loss-of-function approach.
- shown that the process of going from screen to single gene using this method, was possible and provides a foundation for further work.
- shown that in terms of lines screened, but not numbers of genes screened results so far are comparable to other, more labour-intensive larger-scale screens.
- overcome the main shortfall with the current MARCM system in that it can be used at an earlier developmental stage (first instar larva); more recently this system developed in this work has been improved by the use myrisolylated mRFP as a reporter, and can now be used in the early first instar larva (M.L. personal communication)

- *CG34393*, a previously uncharacterised gene is implicated in the development of dendrites.
- The presence of *UAS-Dcr2* in first instar larvae seems to mask or cause a phenotype.

Future directions

Completion of the screen

With the discovery that the phenotype seen in motor neurons homozygous for *Df(2L)S2590* was recapitulated with *Df(2L)BSC28* but not *Df(2L)BSC162* or *Df(2L)Exel8008*, screening ceased as the focus of the project shifted toward the identification of candidate genes.

Consequently, analysis of overlapping deficiencies for *Df(2L)TE35BC-24*, *Df(2R)Np5* and *Df(2R)Px2* in order to narrow down the region containing the gene(s) responsible for phenotypes is incomplete. Further, 40 FRT/deficiency recombinant lines have yet to be screened. The screening of these lines and analysis of any new discoveries could form the basis of further work.

CG34393

There are a number of avenues yet to be explored with the previously uncharacterised gene, CG34393. It would be interesting and informative to: (i) properly explore the expression pattern of CG34393 alongside landmarks (e.g. *engrailed*) with the aim of identifying the small subset of cells in which it expresses strongly, for example by generating expression constructs or by better quality *in situs* that use larger intronic probes, which would generate a nuclear signal and help to distinguish between CG34393 expression, and labelling by landmark probes; (ii) further study the loss-of-function phenotype by reattempting the generation of mutant lines e.g. using *Minos* tranposase or by better use of RNAi technology, concentrating on dendrite morphology and synapse formation either in the dendrites or at the NMJ; and (iii) explore the phenotype associated with RNAi knockdown of CG34393 in

concert with other members of the Ras pathway to try and fully understand its role in neuron development.

Identification of neurons most frequently targeted

It would be beneficial in any future work if the identity of motor neurons most frequently labelled in the 'ftz loop' MARCM method could be established with greater accuracy. In Chapter 2, an attempt to identify the neurons targeted by the 'ftz loop' MARCM method was described whereby anti-mCD8 labelling was combined with fluorescent microscopy in order to follow the axons of MARCM labelled neurons to their muscle target. This was unsuccessful as the signal attenuated along the axon. More recently, however, a better technique to address this question has become available after the development of fly lines that express GFP in the z-bands of their muscles (Crisp et al 2008). Myristolated monomeric red fluorescent protein (myr-mRFP) is a highly diffusible membrane-targeted fluorescent protein reporter that is particularly good for visualising fine processes and distal membranes of dendrites (Mauss et al 2009). An exon trap line that labels muscles with GFP was introduced into a variation of the 'ftz loop' MARCM line that used myr-mRFP as a reporter, thus enabling the simultaneous visualisation of both muscles and labelled motor neurons in flat-prepped larvae. This modification could provide more clear-cut evidence for motor neuron identity. This line of investigation needs exploring further.

Continuing development of the MARCM method

Recently, a useful tool for the specific visualisation of the somatodendritic compartment (i.e. does not label axons) has been developed. By generating a hybrid of the mouse cell adhesion molecule ICAM5/Telencephalin and the red fluorescent protein mCherry, termed DenMark, the authors have developed a way of revealing entire dendritic arbors that previously were not visible using other reporters (Nicolai et al 2010). It would be interesting to incorporate this marker into the modified MARCM system used in this project, and

rescreen the recombinant FRT-deficiency chromosomes for genes that specify the dendritic compartment as opposed to the axonal compartment; thereby reporting issues with cell polarity as the reporter spreads outside the somatodendritic domain into axons.

Materials and methods

Fly stocks

Experiment	Stock number	Source	Genotype	Notes
RNAi	40330	Vienna *Drosophila* RNAi Centre	w^{1118}; *P{GD13529v40330*	
	23471	Vienna *Drosophila* RNAi Centre	w^{1118}; *P{GD13529}v23471*	
	23472	Vienna *Drosophila* RNAi Centre	w^{1118}; *P{GD13529}v23472*	
	101816	Vienna *Drosophila* RNAi Centre	w^{1118}; *P{KK109767}v101816*	
		Generated in the lab	*UAS-Dcr2*;*RN2-Flp*, *Tubulin84b-FRT-CD2-FRT-GAL4*, *2 × UAS-myr-mRFP* / *Tm6b*, *DfdYFP*, *Sb*	
		Generated in the lab	*RN2-Flp*, *Tubulin84b-FRT-CD2-FRT-GAL4*, *2 × UAS-myr-mRFP* / *TM6B*, *P{Dfd-EYFP}3*, Sb^1 Tb^1 ca^1	
MARCM	1818	Bloomington Stock Centre, Indiana	w^{1118}; *P{*w^{+mC}*=piM36F P{*$ry^{+t7.2}$*=neoFRT}40A*	
	2120	Bloomington Stock Centre, Indiana	w^{1118}; *P{*$ry^{+t7.2}$*=neoFRT}Sca42D P{*w^{+mC} *=piM}45F*	
	1928	Bloomington Stock Centre, Indiana	w^{1118}; *P{*$ry^{+t7.2}$*=neoFRT}42D P{*w^{+t*} ry^{+t*}*=white-un1}47A*	

	1646	Bloomington Stock Centre, Indiana	*w^{1118}*; *P{w^{+t*} ry^{+t*}=white-un1}30C P{ry$^{+t7.2}$=neoFRT}40A*	
		Bloomington Stock Centre, Indiana	*w^{-}* ; *If/CyO*, *actGFP*	
		Generated in the lab	*w^{-}* ; *If/CyO*, *wgLacZ*	
		Generated in the lab	*w^{-}*; *elav-GAL80-1*, *FRT42D*, *UAS-FLP / CyO*;*Tubulin84b-FRT-CD2-FRT-GAL4*, *UAS-mCD8::GFP*, *UAS-FLP*, *ftz-GAL4 / TM6B*	
		Generated in the lab	*w^{-}*; *elav-GAL80-2*, *FRT42D*, *UAS-FLP / CyO* ; *Tubulin84b-FRT-CD2-FRT-GAL4*, *UAS-mCD8::GFP*, *UAS-FLP*, *ftz-GAL4 / TM6B*	
Minos	23180	Bloomington Stock Centre, Indiana	*y^{1} w^{67c23}*; *Mi{ET1}CG34393^{MB01412}*	
	24613	Bloomington Stock Centre, Indiana	*w^{1118}*; *noc^{Sco}/SM6a*, *P{hsILMiT}2.4*	
Neuroblast GAL4 drivers		Chu-LaGraff & Doe 1993		wingless-*GAL4*
		Zhu et al 2006	*P{ase-GAL4}*	asense-GAL4
		Hooper & Scott 1989; Shyamala & Bhat 2002		*patched-GAL4*
		Castelli-Gair et al 1994		*Kruppel-GAL4*
		Dittrich et al 1997		*eagle-GAL4*

		Brand 1997		*engrailed-GAL4*
		Broihier et al 2004; Uhler et al 2002		*Nkx6-GAL4*
		Albertson et al 2004; Albertson & Doe 2003	*P{wor.GAL4.A}*	*worniu-GAL4*
	6479	Graba et al 1992; Mlodzik et al 1990	*y1 w**; *P{w+mW.hs=GawB}sca109-68/CyO*	*scabrous-GAL4*
	8751	Luo et al 1994; Sweeney et al 1995	w^{*}; *P{GawB}1407*	*1407-GAL4*
Other		Bloomington Stock Centre, Indiana	*If/CyO*, *wgLacZ*;*Tm6b/MKRS*	
	5	Bloomington Stock Centre, Indiana	*Oregon-R*	
	3605	Bloomington Stock Centre, Indiana	w^{1118}	
	5615	Bloomington Stock Centre, Indiana	$y^{d2}w^{1118}P\{ry[^{+t7.2}]=ey\text{-}FLP.N\}2\ P\{GMR\text{-}lacZ.C(38.1)\}TPN1$; $P\{r^{[+t7.2}=neoFRT\}40A$	
	5616	Bloomington Stock Centre, Indiana	$y^{d2}\ w^{1118}\ P\{ry^{+t7.2}=ey\text{-}FLP.N\}2\ P\{GMR\text{-}lacZ.C(38.1)\}TPN1$; $P\{ry^{+t7.2}=neoFRT\}42D$	

Fly husbandry

Fly stocks were maintained at 18°C or room temperature on standard cornmeal agar food and supplemented with dried bakers yeast as required. Fly stocks and recombinant chromosomes were generated using standard procedures at 25°C (Greenspan 1997) unless otherwise stated.

Recombination of deficiencies and FRT-carrying chromosomes

Deficiency stocks were crossed to the appropriate FRT stock. Female virgin progeny were crossed to male w^-; *If*/*CyO*, *wg-lacZ* flies and grown on selective cornmeal agar food containing 50 µg/ml Geneticin® (Invitrogen). After four days adult flies were tipped to fresh food and the progeny heat shocked at 37°C for 45 minutes. This heat shock regime was repeated for two further consecutive days. Recombination events were identified by a white eye phenotype (loss of an insert due to recombination) and survival on selective media (heat-shock inducible neomycin resistance gene associated with the FRT site). Stocks were generated by crossing white eyed males to female virgin w^-; *If*/ *CyO*, *actGFP* and progeny with genotype w^-; *Df(2L or R)*, FRT/*CyO*, *actGFP* selfed to make the final stock. As deficiency chromosomes are homozygous lethal, those lines that maintained the *CyO*, *actGFP* balancer were considered true recombinants between the deficiency and the FRT site.

Modified mosaic analysis with a repressible cell marker

Male recombinant FRT/deficiency-carrying lines were crossed to MARCM virgin females and placed into a laying pot with apple juice agar and enough yeast for the adults to feed on. Crosses were incubated at 29°C. Agar plates were changed in the morning and evening. Plates with eggs laid during the day were kept and maintained at 29°C for a further 48 h. Normally, after 48 h, the eggs would have hatched and moulted into a second instar larva, but larvae were maintained under starvation conditions to enable better visualisation during

selection of the appropriate genotype. Larvae typically have to grow a certain amount before moulting can take place and my observations and those in studies in *Drosophila* and other insects indicate starvation slows body growth and delays larval moulting and puparium formation (Davidowitz et al 2003; Nijhout 2003; Zhou et al 2004).

Late first instar larvae with the appropriate genotype were selected using a Leica MZFLIII fluorescence stereo microscope. The appropriate genotype was distinguished from other larvae by expression of GFP only in the salivary glands. This is a result of the presence of:

- GFP – *UAS-mCD8::GFP*
- *ftz.ng20-GAL4* – expression in the salivary glands
- *elav-GAL80* – repression of ubiquitous expression in the ventral nerve cord
- *Tubulin84b-FRT-CD2-FRT-GAL4* – in combination with a GAL4 line (e.g. *ftz.ng20-GAL4*) and *UAS-FLP* a 'feedback loop' is generated that maintains expression in the late embryo and larva

And absence of:

- *CyO*, *actGFP* – expression in the visceral musculature of the midgut.

Taken together, this indicates that the larvae are:

w^{-}; *elav-GAL80*, FRT40A/42D, *UAS-FLP* / FRT40A/42D, deficiency ; *Tubulin84B-FRT-CD2-FRT-GAL4*, *UAS-mCD8::GFP*, *UAS-FLP*, *ftz.ng20-GAL4* / +

and therefore have the potential to have GFP labelled mitotic clones in their ventral nerve cords.

The ventral nerve cords of selected larvae were dissected out under PBS and adhered to poly-L-lysine coated coverslips, ventral side down and imaged immediately (unfixed) using a Zeiss Axiophot widefield fluorescence microscope. If mitotic clones were visible, *Z*-stacks were taken with an AxioCam MR camera operated by Axiovision 4 software (Zeiss). Images were processed and assessed for dendritic phenotypes using ImageJ (http://rsbweb.nih.gov/ij/).

Generation of imprecise excisions using *Minos* transposase

Imprecise excisions were generated as described (Metaxakis et al 2005) with the following exceptions: heat shocks were carried out in an incubator; and 200 single pair matings of virgin females of the genotype y^{1} w^{67c23}; *Mi{ET1}CG34393*^{MB01412} / w^{1118}; *noc*^{Sco}/ *SM6a*, *P{hsILMiT}2.4* crossed to male w^{-} ; *If/CyO* were set up. Excision events were identified by loss of GFP expression and eye colour in adult eyes, indicating that the *Minos* transgene (which contains a 7.5 kb dominant marker cassette consisting of three Pax6 regulatory region repeats that target expression of EGFP to the adult eye) was not present. Imprecise excisions were identified by PCR of genomic DNA across the *Minos* insertion site.

FLP-out targeted RNAi expression

RNAi of early first instar larvae

Male flies of the genotype: *UAS-Dcr2* ; *RN2-Flp*, *Tubulin84b-FRT-CD2-FRT-GAL4*, 2 × *UAS-myr-mRFP* / Tm6b, DfdYFP, Sb were crossed to female virgin flies carrying one or two of the four *UAS-RNAi* transgenes selected for testing. Flies were maintained on apple juice agar plates with minimal amounts of bakers yeast at 28°C. Plates were changed after 24 h and kept at 28°C. Newly hatched first instar larvae were screened under widefield fluorescence illumination and larvae without the EYFP balancer chromosome were selected for analysis. One to three hours after selection, ventral nerve cords were dissected out under saline and adhered to poly-L-lysine coated cover slips, ventral side down, then imaged live using a spinning discs confocal microscope (see 'Microscopy' section below). Images were processed using ImageJ.

UAS-RNAi in larvae 48 h after larval hatching

The same protocol was used as described above for RNAi in first instar larvae with the following modifications: male flies of the genotype: (i) *UAS-Dcr2* ; *RN2-Flp*, *Tubulin84b-FRT-*

CD2-FRT-GAL4, 2 × *UAS-myr-mRFP* / *Tm6b*, *DfdEYFP*, *Sb*; or (ii) *RN2-Flp*, *Tubulin84b-FRT-CD2-FRT-GAL4*, 2 × *UAS-myr-mRFP* / *TM6B*, *P{Dfd-EYFP}3*, Sb^1 Tb^1 ca^1 (i.e. with and without *UAS-Dcr2*) were crossed to female virgin flies as before; flies and larvae were maintained at 25°C; and once selected, larvae were aged for 48 h prior to dissection and imaging on a spinning discs microscope.

Microscopy

Spinning disc confocal microscope setup

Unfixed nerve cords were imaged with a Yokogawa CSU22 field scanning confocal scan head, mounted on an Olympus BX51WI fixed stage compound microscope equipped with a motorised stage (Prior). A Sutter external filter wheel was used for specific fluorophore emission detection and fast band switching. The laser launch was from Visitech and the camera was a back-thinned, back-illuminated EMCCD (electron multiplication charge coupled device) camera (Photometrics CascadeII) with 512 × 512 pixels. To illuminate for myr-mRFP detection, a Melles Griot 561nm DPSS laser was used and for GFP, the 488 nm line from an Argon-Ion laser also from Melles Griot.

Widefield UV Microscopy

Central nervous systems were imaged using an Olympus ×60 water immersion objective with 1.2 NA, on a Zeiss Axiophot microscope. Images were acquired using Axiovision 4 software.

.

In situ hybridisation

In situ hybridisation was carried out as described in (Patel 1996) with the modification that 0.3% sodium dodecyl sulphate was used in the hybridisation solution. Probes were generated from PCR templates made from the following sources: cDNA clones (DGRC), EST clones (DGRC) and genomic DNA. The appropriate T3 or T7 Megascript kit (Ambion) was used to generate antisense probe labelled with DIG-UTP (Roche). Alkaline phosphatase conjugated anti-DIG followed by a NBT/BCIP reaction was used to visualise probe localisation in embryos. As a positive control a probe against *Robo*, known to work well, was used to verify that the hybridisation had worked successfully and that the embryos were of good enough quality

Gene	**5' Oligo (Tail added for PCR amplification)**	**3' Oligo (Tail added for making RNA probe and PCR amplification)**	**Source**	**Expected PCR and probe size**	**Additional Notes**
CG15404 (Exon 1)	OL154 (T3)	OL155 (T7)	Genomic DNA	288 bp	
CG15405 (CG34393)	OL152 (T3)	OL153 (T7)	Genomic DNA	464 bp	
CG8829 (CG34393)	OL156 (T3)	OL157 (T7)	GH08314 (DGRC)	282 bp	pOT2 vector backbone Is not a cDNA insert
CG9664 (Exon 3, present in transcript A, B and C)	OL158 (T3)	OL159 (T7)	GH02377 (DGRC)	423 bp	pOT2 vector backbone Is not a cDNA insert

Gene	5’ Oligo (Tail added for PCR amplification)	3’ Oligo (Tail added for making RNA probe and PCR amplification)	Source	Expected PCR and probe size	Additional Notes
CG9664 (Exon 6, present in transcripts A and B)	OL160 (T3)	OL161 (T7)	GH02377 (DGRC)	885 bp	pOT2 vector backbone Is not a cDNA insert
CG3347	BC12 (T3)	BC11 (T7)	IP13916 (DGRC)	2253 bp	pOT2 vector backbone
CG3332	BC12 (T3)	BC11 (T7)	Gold collection (DGRC)	2702 bp	pOT2 vector backbone
CG31698	BC12 (T3)	BC11 (T7)	Gold collection (DGRC)	536 bp	pOT2 vector backbone
CG3485 (CG34406)	BC12 (T3)	BC11 (T7)	IP01409 (DGRC)	1717 bp	pOT2 vector backbone
CG18555 (CG34406)	pBS-T7 (T7)	pBS-T3 (T3)	LD10416 (DGRC)	1049 bp	pBluescript vector backbone

Large scale screening of *Minos* imprecise excision events using ball bearings

This protocol is essentially as described on the following website with minor modifications: http://flypush.imgen.bcm.tmc.edu/pscreen/GDP_iPCRProtocol_10272009.pdf

Briefly, 15 homozygous flies for each *Minos* excision line were frozen in a 1.5ml eppendorf tube, and disrupted in buffer A with three small ball bearings by vigorous shaking. After incubation at 65°C for 30 min, addition of 5 M LiCl/6 M KAc solution and centrifugation to remove proteins, contaminating RNA was removed with an RNase A incubation step (RNase A 100 µg/ml, add 1 µl to 100 µl of DNA preparation; incubate 37°C for 30 mins; heat inactivate at 65°C for 20 min). Genomic DNA was precipitated, pelleted by centrifugation and washed with ethanol before final storage at -20°C. In this way many lines could be processed relatively quickly in batches.

The genomic DNA was then analysed by PCR using primers designed to amplify across the *Minos* insertion site. Those with wild type sized bands, where the *Minos* transgene cassette has been excised precisely were deemed negative, and the fly lines discarded.

Those lines that gave PCR products of a different size to wild-type bands or were difficult to PCR were tested using different combinations of PCR primers based around the *Minos* insertion site (Fig. 5.2) and greater amounts of better quality genomic DNA prepared as follows: 50 flies were disrupted using an eppendorf pestle in homogenisation buffer (1 ml 5 M NaCl, 2.5 ml 2M Tris HCl pH 8, 10 ml 0.25 M EDTA, 1.25 µl 20% SDS; made up to 50 ml with sterile distilled water). To 10 ml of homogenisation buffer, 1.1 µl RNase A (10 mg/ml) and 40 µl Proteinase K (10 mg/ml) was added prior to use. Disrupted flies were incubated at 68°C for 30 min, then 75 µl 8 M potassium acetate was added, mixed gently and incubated at 0°C for 30 min in a thermal cycler. After centrifugation, the supernatant was retained and DNA precipitated with ethanol. After washing with 70% ethanol, the pellet was resuspended in Tris-EDTA buffer and an RNase A incubation step carried out as before for 10 min. After addition of 3 M sodium acetate, two phenol:chloroform:iso-amyl alcohol extractions were

carried out and the aqueous supernantant retained. DNA was washed with ethanol and resuspended in sterile distilled water.

Polymerase chain reaction

PCR reactions were carried out as described in the data sheet for each brand of polymerase used. Polymerases used were:

BioTaq™ DNA Polymerase (Bioline, London, UK)

Taq DNA Polymerase (Roche Applied Science, Burgess Hill, UK)

LongAmp® Taq (New England Biolabs, Hitchin, UK)

The table below describes PCR parameters for primer pairs used and their application.

5' Primer	3' Primer	Wild-type band size (bp)	Annealing temp (°C)	Extension time	Enzyme used	Application
OL153	OL152	464	55	45 s	Bioline	Minos; *In situ*
OL193	OL194	1938	50	5 min 3 min 10 s	Bioline Roche	Minos
OL189	OL192	4026	44	6 min	Bioline	Minos
OL189	OL194	2766	44	6 min	Bioline	Minos
OL193	OL192	3242	44	6 min	Bioline	Minos
OL158	OL159	423	56	45 s	Bioline	Minos; *In situ*
OL197	OL194	893	50	1 min 20 s	Bioline	Minos

				1 min 45 s	Roche	
OL199	OL200	270	45	45 s	Bioline	Minos
OL193	OL177	455	45	45 s	Bioline	Minos
OL195	OL201	392	45	45 s	Bioline	Minos
OL197	OL202	414	45 50	45 s	Bioline; Roche	Minos
OL203	OL194	301	45	45 s	Bioline	Minos
OL204	OL196	409	45	45 s	Bioline	Minos
OL205	OL206	327	45	45 s	Bioline	Minos
OL195	OL194	1386	50	3 min 10 s	Roche	Minos
OL153	OL220	2645	50	8 min 5 s	NEB LongAmp	Minos

Sequencing

Sequencing of PCR products was carried out externally by GeneServices: http://www.lifesciences.sourcebioscience.com/

Sequences were analysed using Vector NTI software (Invitrogen) or ApE: http://www.biology.utah.edu/jorgensen/wayned/ape/

Oligonucleotides for PCR and sequencing

Oligonucleotides were sourced from Invitrogen, rehydrated to 1 µl/µg with sterile distilled water and stored at -20°C.

OL152 AATTAACCCTCACTAAAGGGATGGCGATGTATTTTATGCCAGC

OL153 TAATACGACTCACTATAGGGCTCTAATTGCTGAAACCCCATTTC

OL154 AATTAACCCTCACTAAAGGGATGGTTGCCAAGATTCTGCTGAGCC

OL155 TAATACGACTCACTATAGGGTTAGCTTATTTCTCTTGTCGCGCAC

OL156 AATTAACCCTCACTAAAGGGATGAGCAGCAGGAGGGTCTCAAG

OL157 TAATACGACTCACTATAGGGCGCATTGCATTAGTACCGGAAATGC

OL158 AATTAACCCTCACTAAAGGGGACGATATTATCGACATACTGCAGC

OL159 TAATACGACTCACTATAGGGCCGAAATCCGCGGGATTGTAGTACTG

OL160 AATTAACCCTCACTAAAGGGGCTGTCCAAATGCGTCTGGTGATGC

OL161 TAATACGACTCACTATAGGGGTTTAACAATCGTAACACTTTATTAGCC

OL177 CGAACGTGACACATGGCGATGTAC

OL189 AATTAACCCTCACTAAAGGGGCATACGATGGAATTTATGAAATATG

OL190 AATTAACCCTCACTAAAGGGCCCGATTCGCCCAACTCCAGGCCGC

OL191 TAATACGACTCACTATAGGGCGATTTATTTACTGACTCGCCAAGG

OL192 TAATACGACTCACTATAGGGGAAAGCGTAGACAAGGGCGTTTGG

OL193 TTTCAGGAAGTTTCACTCAC

OL194 GGCATTGACATTGATTTTCT

OL195 ACGTCAATTACGATAGGGAT

OL196 TTGCCATAGTTCAACATACA

OL197 TGCGGTCAATCGCAGCACATTACT

OL198 GGGCATTGAAACGAAATAAAATGTC

OL199 GCCCAACCGATATTGTGGTG

OL200 GTGAGTGAAACTTCCTGAAA

OL201 CGCCGCGCGACCCATTGAGC

OL202 AGCCATTTAAGTTATTTCCC

OL203	CGGCAACGGCGGAAGTTGGC
OL204	CCTGATTCATTCACCCTGAC
OL205	TTGTATGTTGAACTATGGC
OL206	GTTTGAGTTATTGCTTAAGTC
OL220	TAAAACTACGCCACATAACA

Appendices

Appendices can be found on a CD attached to the inside cover of this thesis. Appendix 1 contains an Excel file detailing all of the genes on chromosome 2 from Flybase (v FB2011_4), and the corresponding coverage of the 85 stocks that make up the recombinant FRT-deficiency library used in the screen. In Appendix 2, another Excel file provides more deficiency overlap detail of the five deficiencies uncovered in the screen. Finally, in Appendix 3, a Word file, tables summarise the raw data from the five deficiencies whose loss affects dendrite morphology.

Acknowledgements

I would like to acknowledge and thank the following people for their help, support and friendship during the course of my PhD studies:

Matthias Landgraf my supervisor, for his encouragement, invaluable advice and the original idea behind the whole project; Mike Bate, Director of Studies who gave me the opportunity to study for a Ph.D while simultaneously working as a research assistant; Soeren Diegelmann for road trips, small talk and all things molecular – including pITA-vectors; Jan Felix Evers for lively conversation and help with imaging; Barabara Chwalla my *in situ* mentor; Anne Mackay for making such good fly food that my sick deficiency stocks could live to be tested, mooching, and most of all a life-long friendship; and everyone else in the basement for making my many years in the basement 'fly' by so quickly – including Vicky Jeffery and Sara Pasalodos for putting the idea of doing a PhD into my head in the first place.

I would also like to thank Isabel Bermudez-Diaz, my supervisor at Oxford Brookes for agreeing to take me on as her student, and help with administration.

Finally, I would like to thank my husband for his understanding, unwavering support and the uninterrupted time to write up; and my two daughters for making sure that there is life away from the laptop.

References

Albeg A, Smith CJ, Chatzigeorgiou M, Feitelson DG, Hall DH, et al. 2011. C. elegans multi-dendritic sensory neurons: morphology and function. *Mol Cell Neurosci* 46:308-17

Albertson R, Chabu C, Sheehan A, Doe CQ. 2004. Scribble protein domain mapping reveals a multistep localization mechanism and domains necessary for establishing cortical polarity. *J Cell Sci* 117:6061-70

Albertson R, Doe CQ. 2003. Dlg, Scrib and Lgl regulate neuroblast cell size and mitotic spindle asymmetry. *Nat Cell Biol* 5:166-70

Alonso CR, Maxton-Kuechenmeister J, Akam M. 2001. Evolution of Ftz protein function in insects. *Current Biology* 11:1473-8

Ashraf SI, Ganguly A, Roote J, Ip YT. 2004. Worniu, a snail family zinc-finger protein, is required for brain development in drosophila. *Developmental Dynamics* 231:379-86

Ashraf SI, Hu X, Roote J, Ip YT. 1999. The mesoderm determinant snail collaborates with related zinc-finger proteins to control Drosophila neurogenesis. *EMBO J* 18:6426-38

Awad TA, Truman JW. 1997. Postembryonic development of the midline glia in the CNS of Drosophila: proliferation, programmed cell death, and endocrine regulation. *Dev Biol* 187:283-97

Awasaki T, Lai SL, Ito K, Lee T. 2008. Organization and postembryonic development of glial cells in the adult central brain of Drosophila. *J Neurosci* 28:13742-53

Baas PW. 1998. The role of motor proteins in establishing the microtubule arrays of axons and dendrites. *J Chem Neuroanat* 14:175-80

Baines RA. 2003. Postsynaptic protein kinase A reduces neuronal excitability in response to increased synaptic excitation in the Drosophila CNS. *J Neurosci* 23:8664-72

Baines RA, Bate M. 1998. Electrophysiological development of central neurons in the *Drosophila* embryo. *J. Neurosci.* 18:4673-83

Baines RA, Uhler JP, Thompson A, Sweeney ST, Bate M. 2001. Altered electrical properties in *Drosophila* neurons developing without synaptic transmission. *J. Neurosci.* 21:1523-31

Baker KA, Moore SW, Jarjour AA, Kennedy TE. 2006. When a diffusible axon guidance cue stops diffusing: roles for netrins in adhesion and morphogenesis. *Curr Opin Neurobiol* 16:529-34

Barreau C, Benson E, Gudmannsdottir E, Newton F, White-Cooper H. 2008. Post-meiotic transcription in Drosophila testes. *Development* 135:1897-902

Bashaw GJ, Hu H, Nobes CD, Goodman CS. 2001. A novel Dbl family RhoGEF promotes Rho-dependent axon attraction to the central nervous system midline in Drosophila and overcomes Robo repulsion. *J Cell Biol* 155:1117-22

Bashaw GJ, Klein R. 2010. Signaling from axon guidance receptors. *Cold Spring Harb Perspect Biol* 2:a001941

Bateman A, Coin L, Durbin R, Finn RD, Hollich V, et al. 2004. The Pfam protein families database. *Nucleic Acids Res* 32:D138-41

Bellen HJ, Levis RW, He Y, Carlson JW, Evans-Holm M, et al. 2011. The Drosophila gene disruption project: progress using transposons with distinctive site specificities. *Genetics* 188:731-43

Berdnik D, Fan AP, Potter CJ, Luo L. 2008. MicroRNA processing pathway regulates olfactory neuron morphogenesis. *Curr Biol* 18:1754-9

Berger C, Kannan R, Myneni S, Renner S, Shashidhara LS, Technau GM. 2010. Cell cycle independent role of Cyclin E during neural cell fate specification in Drosophila is mediated by its regulation of Prospero function. *Developmental Biology* 337:415-24

Berger C, Renner S, Lüer K, Technau GM. 2007. The commonly used marker ELAV is transiently expressed in neuroblasts and glial cells in the Drosophila embryonic CNS. *Developmental Dynamics* 236:3562-8

Bernhardt R, Matus A. 1984. Light and electron microscopic studies of the distribution of microtubule-associated protein 2 in rat brain: a difference between dendritic and axonal cytoskeletons. *J Comp Neurol* 226:203-21

Bernhardt RR, Chitnis AB, Lindamer L, Kuwada JY. 1990. Identification of spinal neurons in the embryonic and larval zebrafish. *J Comp Neurol* 302:603-16

Blagburn JM, Bacon JP. 2004. Control of central synaptic specificity in insect sensory neurons. *Annu Rev Neurosci* 27:29-51

Blanchard FJ, Collins B, Cyran SA, Hancock DH, Taylor MV, Blau J. 2010. The transcription factor Mef2 is required for normal circadian behavior in Drosophila. *J Neurosci* 30:5855-65

Bonanomi D, Pfaff SL. 2010. Motor axon pathfinding. *Cold Spring Harb Perspect Biol* 2:a001735

Bonfini L, Karlovich CA, Dasgupta C, Banerjee U. 1992. The Son of sevenless gene product: a putative activator of Ras. *Science* 255:603-6

Bonnet C, Andrieux J, Beri-Dexheimer M, Leheup B, Boute O, et al. 2010. Microdeletion at chromosome 4q21 defines a new emerging syndrome with marked growth

restriction, mental retardation and absent or severely delayed speech. *J Med Genet* 47:377-84

Booker M, Samsonova AA, Kwon Y, Flockhart I, Mohr SE, Perrimon N. 2011. False negative rates in Drosophila cell-based RNAi screens: a case study. *BMC Genomics* 12:50

Boriack-Sjodin PA, Margarit SM, Bar-Sagi D, Kuriyan J. 1998. The structural basis of the activation of Ras by Sos. *Nature* 394:337-43

Bos JL, Rehmann H, Wittinghofer A. 2007. GEFs and GAPs: critical elements in the control of small G proteins. *Cell* 129:865-77

Bottenberg W, Sanchez-Soriano N, Alves-Silva J, Hahn I, Mende M, Prokop A. 2009. Context-specific requirements of functional domains of the Spectraplakin Short stop in vivo. *Mech Dev* 126:489-502

Bouley M, Tian MZ, Paisley K, Shen YC, Malhotra JD, Hortsch M. 2000. The L1-type cell adhesion molecule neuroglian influences the stability of neural ankyrin in the *Drosophila* embryo but not its axonal localization. *J. Neurosci.* 20:4515-23

Boutros M, Ahringer J. 2008. The art and design of genetic screens: RNA interference. *Nat Rev Genet* 9:554-66

Brand A. 1997. P{GawB} insertions.

Brand A, Perrimon N. 1993. Targeted gene expression as a means of altering cell fates and generating dominant phenotypes. *Development* 118:401-15

Brand AH, Dormand EL. 1995. The GAL4 system as a tool for unravelling the mysteries of the Drosophila nervous system. *Curr Opin Neurobiol* 5:572-8

Bray D. 1973. Branching patterns of individual sympathetic neurons in culture. *J Cell Biol* 56:702-12

Brenman JE, Gao FB, Jan LY, Jan YN. 2001. Sequoia, a tramtrack-related zinc finger protein, functions as a pan-neural regulator for dendrite and axon morphogenesis in Drosophila. *Dev Cell* 1:667-77

Brentrup D, Lerch HP, Jackle H, Noll M. 2000. Regulation of Drosophila wing vein patterning: net encodes a bHLH protein repressing rhomboid and is repressed by rhomboid-dependent Egfr signalling. *Development* 127:4729-41

Brierley DJ, Blanc E, Reddy OV, Vijayraghavan K, Williams DW. 2009. Dendritic targeting in the leg neuropil of Drosophila: the role of midline signalling molecules in generating a myotopic map. *PLoS Biol* 7:e1000199

Brody T, Stivers C, Nagle J, Odenwald WF. 2002. Identification of novel Drosophila neural precursor genes using a differential embryonic head cDNA screen. *Mech Dev* 113:41-59

Broihier HT, Kuzin A, Zhu Y, Odenwald W, Skeath JB. 2004. Drosophila homeodomain protein Nkx6 coordinates motoneuron subtype identity and axonogenesis. *Development* 131:5233-42

Brough R, Frankum JR, Costa-Cabral S, Lord CJ, Ashworth A. 2011. Searching for synthetic lethality in cancer. *Curr Opin Genet Dev* 21:34-41

Cai Y, Chia W, Yang X. 2001. A family of Snail-related zinc finger proteins regulates two distinct and parallel mechanisms that mediate Drosophila neuroblast asymmetric divisions. *The EMBO Journal* 20:1704-14

Castelli-Gair JE, Greig S, Micklem G, Akam ME. 1994. Dissecting the temporal requirements for homeotic gene function. *Development* 120:1983-95

Celniker SE, Dillon LA, Gerstein MB, Gunsalus KC, Henikoff S, et al. 2009. Unlocking the secrets of the genome. *Nature* 459:927-30

Chang H. 2003.

Chen BE, Kondo M, Garnier A, Watson FL, Puettmann-Holgado R, et al. 2006. The molecular diversity of Dscam is functionally required for neuronal wiring specificity in Drosophila. *Cell* 125:607-20

Chen K, Gracheva EO, Yu SC, Sheng Q, Richmond J, Featherstone DE. 2010a. Neurexin in embryonic Drosophila neuromuscular junctions. *PLoS One* 5:e11115

Chen L, Fu Y, Ren M, Xiao B, Rubin CS. 2011. A RasGRP, C. elegans RGEF-1b, couples external stimuli to behavior by activating LET-60 (Ras) in sensory neurons. *Neuron* 70:51-65

Chen SX, Tari PK, She K, Haas K. 2010b. Neurexin-neuroligin cell adhesion complexes contribute to synaptotropic dendritogenesis via growth stabilization mechanisms in vivo. *Neuron* 67:967-83

Chen Y, Ghosh A. 2005. Regulation of dendritic development by neuronal activity. *J Neurobiol* 64:4-10

Cheung U, Atwood HL, Zucker RS. 2006. Presynaptic effectors contributing to cAMP-induced synaptic potentiation in Drosophila. *J Neurobiol* 66:273-80

Chiba A, Hing H, Cash S, Keshishian H. 1993. Growth cone choices of Drosophila motoneurons in response to muscle fiber mismatch. *J Neurosci* 13:714-32

Chintapalli VR, Wang J, Dow JA. 2007. Using FlyAtlas to identify better Drosophila melanogaster models of human disease. *Nat Genet* 39:715-20

Christensen S, Cook K. 2006. Isolation and characterization of Df(2L)BSC162.

Christopherson KS, Ullian EM, Stokes CC, Mullowney CE, Hell JW, et al. 2005. Thrombospondins are astrocyte-secreted proteins that promote CNS synaptogenesis. *Cell* 120:421-33

Chu-LaGraff Q, Doe CQ. 1993. Neuroblast specification and formation regulated by wingless in the *Drosophila* CNS. *Science* 261:1594-7

Clemens JC, Worby CA, Simonson-Leff N, Muda M, Maehama T, et al. 2000. Use of double-stranded RNA interference in Drosophila cell lines to dissect signal transduction pathways. *Proc Natl Acad Sci U S A* 97:6499-503

Cline HT. 2001. Dendritic arbor development and synaptogenesis. *Curr. Opin. Neurobiol.* 11:118-26

Coleman MP, Freeman MR. 2010. Wallerian degeneration, wld(s), and nmnat. *Annu Rev Neurosci* 33:245-67

Colin J, Garibal J, Mignotte B, Guénal I. 2009. The mitochondrial TOM complex modulates bax-induced apoptosis in Drosophila. *Biochemical and Biophysical Research Communications* 379:939-43

Collins CA, DiAntonio A. 2004. Coordinating synaptic growth without being a nervous wreck. *Neuron* 41:489-91

Collins CA, DiAntonio A. 2007. Synaptic development: insights from Drosophila. *Curr Opin Neurobiol* 17:35-42

Coronas V, Durand M, Chabot JG, Jourdan F, Quirion R. 2000. Acetylcholine induces neuritic outgrowth in rat primary olfactory bulb cultures. *Neuroscience* 98:213-9

Costa A, Wang Y, Dockendorff TC, Erdjument-Bromage H, Tempst P, et al. 2005. The Drosophila fragile X protein functions as a negative regulator in the orb autoregulatory pathway. *Dev Cell* 8:331-42

Coyle IP, Koh YH, Lee WCM, Slind J, Fergestad T, et al. 2004. Nervous wreck, an SH3 adaptor protein that interacts with Wsp, regulates synaptic growth in Drosophila. *Neuron* 41:521-34

Crandall SR, Govindaiah G, Cox CL. 2010. Low-threshold Ca2+ current amplifies distal dendritic signaling in thalamic reticular neurons. *J Neurosci* 30:15419-29

Crisp S, Evers JF, Fiala A, Bate M. 2008. The development of motor coordination in Drosophila embryos. *Development* 135:3707-17

Cronin SJ, Nehme NT, Limmer S, Liegeois S, Pospisilik JA, et al. 2009. Genome-wide RNAi screen identifies genes involved in intestinal pathogenic bacterial infection. *Science* 325:340-3

Dailey ME, Smith SJ. 1996. The dynamics of dendritic structure in developing hippocampal slices. *J Neurosci* 16:2983-94

Davidowitz G, D'Amico LJ, Nijhout HF. 2003. Critical weight in the development of insect body size. *Evol Dev* 5:188-97

de Rooij J, Zwartkruis FJ, Verheijen MH, Cool RH, Nijman SM, et al. 1998. Epac is a Rap1 guanine-nucleotide-exchange factor directly activated by cyclic AMP. *Nature* 396:474-7

de Wit T, Dekker S, Maas A, Breedveld G, Knoch TA, et al. 2010. Tagged mutagenesis by efficient Minos-based germ line transposition. *Mol Cell Biol* 30:68-77

Dehmelt L, Halpain S. 2004. Actin and microtubules in neurite initiation: are MAPs the missing link? *J Neurobiol* 58:18-33

Derst C, Walther C, Veh RW, Wicher D, Heinemann SH. 2006. Four novel sequences in Drosophila melanogaster homologous to the auxiliary Para sodium channel subunit TipE. *Biochemical and Biophysical Research Communications* 339:939-48

Dettman RW, Turner FR, Hoyle HD, Raff EC. 2001. Embryonic expression of the divergent Drosophila beta3-tubulin isoform is required for larval behavior. *Genetics* 158:253-63

Dickson BJ, Gilestro GF. 2006. Regulation of commissural axon pathfinding by slit and its Robo receptors. *Annu Rev Cell Dev Biol* 22:651-75

Dierssen M, Ramakers GJ. 2006. Dendritic pathology in mental retardation: from molecular genetics to neurobiology. *Genes Brain Behav* 5 Suppl 2:48-60

Dietzl G, Chen D, Schnorrer F, Su KC, Barinova Y, et al. 2007. A genome-wide transgenic RNAi library for conditional gene inactivation in Drosophila. *Nature* 448:151-6

Dimitrova S, Reissaus A, Tavosanis G. 2008. Slit and Robo regulate dendrite branching and elongation of space-filling neurons in Drosophila. *Dev Biol* 324:18-30

Ding S, Wu X, Li G, Han M, Zhuang Y, Xu T. 2005. Efficient transposition of the piggyBac (PB) transposon in mammalian cells and mice. *Cell* 122:473-83

Dittrich R, Bossing T, Gould AP, Technau GM, Urban J. 1997. The differentiation of the serotonergic neurons in *Drosophila* ventral nerve cord depends on the combined function of the zinc finger proteins Eagle and Huckebein. *Development* 124:2515-25

Doe CQ, Hiromi Y, Gehring WJ, Goodman CS. 1988. Expression and function of the segmentation gene *fushi tarazu* during *Drosophila* neurogenesis. *Science* 239:170-5

Donovan S, Shannon KM, Bollag G. 2002. GTPase activating proteins: critical regulators of intracellular signaling. *Biochim Biophys Acta* 1602:23-45

Downward J. 1998. Ras signalling and apoptosis. *Curr Opin Genet Dev* 8:49-54

Dubnau J, Chiang AS, Grady L, Barditch J, Gossweiler S, et al. 2003. The staufen/pumilio pathway is involved in Drosophila long-term memory. *Curr Biol* 13:286-96

Ebinu JO, Bottorff DA, Chan EY, Stang SL, Dunn RJ, Stone JC. 1998. RasGRP, a Ras guanyl nucleotide- releasing protein with calcium- and diacylglycerol-binding motifs. *Science* 280:1082-6

Enerly E, Larsson J, Lambertsson A. 2002. Reverse genetics in Drosophila: from sequence to phenotype using UAS-RNAi transgenic flies. *Genesis* 34:152-5

Epting D, Vorwerk S, Hageman A, Meyer D. 2007. Expression of rasgef1b in zebrafish. *Gene Expr Patterns* 7:389-95

Fambrough D, Goodman CS. 1996. The Drosophila beaten path gene encodes a novel secreted protein that regulates defasciculation at motor axon choice points. *Cell* 87:1049-58

Fauchereau F, Herbrand U, Chafey P, Eberth A, Koulakoff A, et al. 2003. The RhoGAP activity of OPHN1, a new F-actin-binding protein, is negatively controlled by its amino-terminal domain. *Mol Cell Neurosci* 23:574-86

Fayyazuddin A, Zaheer MA, Hiesinger PR, Bellen HJ. 2006. The nicotinic acetylcholine receptor Dalpha7 is required for an escape behavior in Drosophila. *PLoS Biol* 4:e63

Feng Y, Absher D, Eberhart DE, Brown V, Malter HE, Warren ST. 1997. FMRP associates with polyribosomes as an mRNP, and the I304N mutation of severe fragile X syndrome abolishes this association. *Mol Cell* 1:109-18

Fiala JC, Spacek J, Harris KM. 2002. Dendritic spine pathology: cause or consequence of neurological disorders? *Brain Res Brain Res Rev* 39:29-54

Fichelson P, Moch C, Ivanovitch K, Martin C, Sidor CM, et al. 2009. Live-imaging of single stem cells within their niche reveals that a U3snoRNP component segregates asymmetrically and is required for self-renewal in Drosophila. *Nat Cell Biol* 11:685-93

Flavell SW, Cowan CW, Kim TK, Greer PL, Lin Y, et al. 2006. Activity-dependent regulation of MEF2 transcription factors suppresses excitatory synapse number. *Science* 311:1008-12

Flavell SW, Kim TK, Gray JM, Harmin DA, Hemberg M, et al. 2008. Genome-wide analysis of MEF2 transcriptional program reveals synaptic target genes and neuronal activity-dependent polyadenylation site selection. *Neuron* 60:1022-38

Forsthoefel DJ, Liebl EC, Kolodziej PA, Seeger MA. 2005. The Abelson tyrosine kinase, the Trio GEF and Enabled interact with the Netrin receptor Frazzled in Drosophila. *Development* 132:1983-94

Frank CA, Pielage J, Davis GW. 2009. A presynaptic homeostatic signaling system composed of the Eph receptor, ephexin, Cdc42, and CaV2.1 calcium channels. *Neuron* 61:556-69

Fujioka M, Emi-Sarker Y, Yusibova GL, Goto T, Jaynes JB. 1999. Analysis of an even-skipped rescue transgene reveals both composite and discrete neuronal and early blastoderm enhancers, and multi-stripe positioning by gap gene repressor gradients. *Development* 126:2527-38

Fujioka M, Lear BC, Landgraf M, Yusibova GL, Zhou J, et al. 2003. Even-skipped, acting as a repressor, regulates axonal projections in Drosophila. *Development* 130:5385-400

Furrer MP, Kim S, Wolf B, Chiba A. 2003. Robo and Frazzled/DCC mediate dendritic guidance at the CNS midline. *Nat Neurosci* 6:223-30

Furrer MP, Vasenkova I, Kamiyama D, Rosado Y, Chiba A. 2007. Slit and Robo control the development of dendrites in Drosophila CNS. *Development* 134:3795-804

Gao F-B, Brenman JE, Jan LY, Jan YN. 1999. Genes regulating dendritic outgrowth, branching, and routing in *Drosophila*. *Genes Dev.* 13:2549-61

Gatto CL, Broadie K. 2011. Drosophila modeling of heritable neurodevelopmental disorders. *Curr Opin Neurobiol*

Gelbart WM, Emmert DB. 2010. FlyBase High Throughput Expression Pattern Data Beta Version. www.flybase.org

Georges PC, Hadzimichalis NM, Sweet ES, Firestein BL. 2008. The yin-yang of dendrite morphology: unity of actin and microtubules. *Mol Neurobiol* 38:270-84

Gerrow K, El-Husseini A. 2006. Cell adhesion molecules at the synapse. *Front Biosci* 11:2400-19

Golic KG, Lindquist S. 1989. The FLP recombinase of yeast catalyzes site-specific recombination in the Drosophila genome. *Cell* 59:499-509

Gomes FC, Sousa Vde O, Romao L. 2005. Emerging roles for TGF-beta1 in nervous system development. *Int J Dev Neurosci* 23:413-24

Govek EE, Newey SE, Akerman CJ, Cross JR, Van der Veken L, Van Aelst L. 2004. The X-linked mental retardation protein oligophrenin-1 is required for dendritic spine morphogenesis. *Nat Neurosci* 7:364-72

Graba Y, Aragnol D, Laurenti P, Garzino V, Charmot D, et al. 1992. Homeotic control in Drosophila; the scabrous gene is an in vivo target of Ultrabithorax proteins. *EMBO J.* 11:3375-84

Greenspan RJ. 1997. *Fly pushing: The theory and practice of Drosophila genetics*. Cold Spring Harbor New York: Cold Spring Harbor Laboratory Press

Grishin NV. 1995. Estimation of the number of amino acid substitutions per site when the substitution rate varies among sites. *J Mol Evol* 41:675-9

Grueber WB, Jan LY, Jan YN. 2003. Different levels of the homeodomain protein cut regulate distinct dendrite branching patterns of Drosophila multidendritic neurons. *Cell* 112:805-18

Grueber WB, Jan YN. 2004. Dendritic development: lessons from Drosophila and related branches. *Curr Opin Neurobiol* 14:74-82

Grumbling G, Strelets V. 2006. FlyBase: anatomical data, images and queries. *Nucleic Acids Res* 34:D484-8

Hall A, Lalli G. 2010. Rho and Ras GTPases in axon growth, guidance, and branching. *Cold Spring Harb Perspect Biol* 2:a001818

Halsell SR, Chu BI, Kiehart DP. 2000. Genetic analysis demonstrates a direct link between rho signaling and nonmuscle myosin function during Drosophila morphogenesis. *Genetics* 155:1253-65

Halter DA, Urban J, Rickert C, Ner SS, Ito K, et al. 1995. The homeobox gene *repo* is required for the differentiation and maintenance of glia function in the embryonic nervous system of *Drosophila melanogaster*. *Development* 121:317-32

Hausser M, Spruston N, Stuart GJ. 2000. Diversity and dynamics of dendritic signaling. *Science* 290:739-44

Hengst U, Cox LJ, Macosko EZ, Jaffrey SR. 2006. Functional and selective RNA interference in developing axons and growth cones. *J Neurosci* 26:5727-32

Higuchi N, Kohno K, Kadowaki T. 2009. Specific retention of the protostome-specific PsGEF may parallel with the evolution of mushroom bodies in insect and lophotrochozoan brains. *BMC Biol* 7:21

Hillebrand J, Pan K, Kokaram A, Barbee S, Parker R, Ramaswami M. 2010. The Me31B DEAD-Box Helicase Localizes to Postsynaptic Foci and Regulates Expression of a

CaMKII Reporter mRNA in Dendrites of Drosophila Olfactory Projection Neurons. *Front Neural Circuits* 4:121

Hiromi Y, Kuroiwa A, Gehring WJ. 1985. Control elements of the Drosophila segmentation gene fushi tarazu. *Cell* 43:603-13

Hocking JC, Hehr CL, Bertolesi GE, Wu JY, McFarlane S. 2010. Distinct roles for Robo2 in the regulation of axon and dendrite growth by retinal ganglion cells. *Mech Dev* 127:36-48

Hooper JE, Scott MP. 1989. The Drosophila patched gene encodes a putative membrane protein required for segmental patterning. *Cell* 59:751-65

Hoshino M, Suzuki E, Nabeshima Y-i, Hama C. 1996. Hikaru genki protein is secreted into synaptic clefts from an early stage of synapse formation in *Drosophila*. *Development* 122:589-97

Hoyle HD, Turner FR, Raff EC. 2000. A transient specialization of the microtubule cytoskeleton is required for differentiation of the Drosophila visual system. *Dev Biol* 221:375-89

Hozumi A, Kawai N, Yoshida R, Ogura Y, Ohta N, et al. 2010. Efficient transposition of a single Minos transposon copy in the genome of the ascidian Ciona intestinalis with a transgenic line expressing transposase in eggs. *Dev Dyn* 239:1076-88

Hughes ME, Bortnick R, Tsubouchi A, Baumer P, Kondo M, et al. 2007. Homophilic dscam interactions control complex dendrite morphogenesis. *Neuron* 54:417-27

Ivanov AI, Rovescalli AC, Pozzi P, Yoo S, Mozer B, et al. 2004. Genes required for Drosophila nervous system development identified by RNA interference. *Proc Natl Acad Sci U S A* 101:16216-21

Jones WD. 2009. The expanding reach of the GAL4/UAS system into the behavioral neurobiology of Drosophila. *BMB Rep* 42:705-12

Kania A, Johnson RL, Jessell TM. 2000. Coordinate roles for LIM homeobox genes in directing the dorsoventral trajectory of motor axons in the vertebrate limb. *Cell* 102:161-73

Katsuki T, Joshi R, Ailani D, Hiromi Y. 2011. Compartmentalization within neurites: its mechanisms and implications. *Dev Neurobiol* 71:458-73

Kavi HH, Fernandez H, Xie W, Birchler JA. 2008. Genetics and biochemistry of RNAi in Drosophila. *Curr Top Microbiol Immunol* 320:37-75

Kennedy MB, Beale HC, Carlisle HJ, Washburn LR. 2005. Integration of biochemical signalling in spines. *Nat Rev Neurosci* 6:423-34

Kiecker C, Niehrs C. 2001. The role of prechordal mesendoderm in neural patterning. *Curr Opin Neurobiol* 11:27-33

Kiger AA, Baum B, Jones S, Jones MR, Coulson A, et al. 2003. A functional genomic analysis of cell morphology using RNA interference. *J Biol* 2:27

Killeen MT, Sybingco SS. 2008. Netrin, Slit and Wnt receptors allow axons to choose the axis of migration. *Dev Biol* 323:143-51

Kim IJ, Zhang Y, Yamagata M, Meister M, Sanes JR. 2008. Molecular identification of a retinal cell type that responds to upward motion. *Nature* 452:478-82

Kim MD, Jan LY, Jan YN. 2006. The bHLH-PAS protein Spineless is necessary for the diversification of dendrite morphology of Drosophila dendritic arborization neurons. *Genes Dev* 20:2806-19

Kim S, Chiba A. 2004. Dendritic guidance. *Trends Neurosci* 27:194-202

Kimble M, Dettman RW, Raff EC. 1990. The beta 3-tubulin gene of Drosophila melanogaster is essential for viability and fertility. *Genetics* 126:991-1005

Kittel RJ, Wichmann C, Rasse TM, Fouquet W, Schmidt M, et al. 2006. Bruchpilot promotes active zone assembly, Ca2+ channel clustering, and vesicle release. *Science* 312:1051-4

Kobayashi M, Michaut L, Ino A, Honjo K, Nakajima T, et al. 2006. Differential microarray analysis of Drosophila mushroom body transcripts using chemical ablation. *Proceedings of the National Academy of Sciences* 103:14417-22

Koch I, Schwarz H, Beuchle D, Goellner B, Langegger M, Aberle H. 2008. Drosophila ankyrin 2 is required for synaptic stability. *Neuron* 58:210-22

Koekkoek SK, Yamaguchi K, Milojkovic BA, Dortland BR, Ruigrok TJ, et al. 2005. Deletion of FMR1 in Purkinje cells enhances parallel fiber LTD, enlarges spines, and attenuates cerebellar eyelid conditioning in Fragile X syndrome. *Neuron* 47:339-52

Koh YH, Ruiz-Canada C, Gorczyca M, Budnik V. 2002. The Ras1-mitogen-activated protein kinase signal transduction pathway regulates synaptic plasticity through fasciclin II-mediated cell adhesion. *J. Neurosci.* 22:2496-504

Kohrmann M, Luo M, Kaether C, DesGroseillers L, Dotti CG, Kiebler MA. 1999. Microtubule-dependent recruitment of Staufen-green fluorescent protein into large RNA-containing granules and subsequent dendritic transport in living hippocampal neurons. *Mol Biol Cell* 10:2945-53

Koizumi K, Higashida H, Yoo S, Islam MS, Ivanov AI, et al. 2007. RNA interference screen to identify genes required for Drosophila embryonic nervous system development. *Proc Natl Acad Sci U S A* 104:5626-31

Komiyama T, Johnson WA, Luo L, Jefferis GS. 2003. From lineage to wiring specificity. POU domain transcription factors control precise connections of Drosophila olfactory projection neurons. *Cell* 112:157-67

Komiyama T, Sweeney LB, Schuldiner O, Garcia KC, Luo L. 2007. Graded expression of semaphorin-1a cell-autonomously directs dendritic targeting of olfactory projection neurons. *Cell* 128:399-410

Konur S, Ghosh A. 2005. Calcium signaling and the control of dendritic development. *Neuron* 46:401-5

Kraut R, Menon K, Zinn K. 2001a. A gain-of-function screen for genes controlling motor axon guidance and synaptogenesis in *Drosophila*. *Curr Biol* 11:417-30

Kraut R, Menon K, Zinn K. 2001b. A gain-of-function screen for genes controlling motor axon guidance and synaptogenesis in Drosophila. *Current Biology* 11:417-30

Kremer EJ, Pritchard M, Lynch M, Yu S, Holman K, et al. 1991. Mapping of DNA instability at the fragile X to a trinucleotide repeat sequence p(CCG)n. *Science* 252:1711-4

Kurusu M, Cording A, Taniguchi M, Menon K, Suzuki E, Zinn K. 2008. A screen of cell-surface molecules identifies leucine-rich repeat proteins as key mediators of synaptic target selection. *Neuron* 59:972-85

Landgraf M, Bossing T, Technau GM, Bate M. 1997. The origin , location and projections of the embryonic abdominal motorneurons in *Drosophila*. *J. Neurosci.* 17:9642-55

Landgraf M, Sánchez-Soriano N, Technau G, Urban J, Prokop A. 2003. Charting the *Drosophila* neuropile: a strategy for the standardised characterisation of genetically amenable neurites. *Dev Biol 260*:207-25

Lane ME, Kalderon D. 1993. Genetic investigation of cAMP-dependent protein kinase function in Drosophila development. *Genes & Development* 7:1229-43

Lee A, Li W, Xu K, Bogert BA, Su K, Gao FB. 2003. Control of dendritic development by the Drosophila fragile X-related gene involves the small GTPase Rac1. *Development* 130:5543-52

Lee S, Harris KL, Whitington PM, Kolodziej PA. 2000a. short stop is allelic to kakapo, and encodes rod-like cytoskeletal-associated proteins required for axon extension. *J Neurosci* 20:1096-108

Lee T, Lee A, Luo L. 1999. Development of the Drosophila mushroom bodies: sequential generation of three distinct types of neurons from a neuroblast. *Development* 126:4065-76

Lee T, Luo L. 1999. Mosaic analysis with a repressible cell marker for studies of gene function in neuronal morphogenesis. *Neuron* 22:451-61

Lee T, Luo L. 2001. Mosaic analysis with a repressible cell marker (MARCM) for Drosophila neural development. *Trends Neurosci* 24:251-4

Lee T, Winter C, Marticke SS, Lee A, Luo L. 2000b. Essential roles of Drosophila RhoA in the regulation of neuroblast proliferation and dendritic but not axonal morphogenesis. *Neuron* 25:307-16

Lents NH, Baldassare JJ. 2006. RNA interference takes flight: a new RNAi screen reveals cell cycle regulators in Drosophila cells. *Trends Endocrinol Metab* 17:173-4

Letunic I, Doerks T, Bork P. 2009. SMART 6: recent updates and new developments. *Nucleic Acids Res* 37:D229-32

Leung J, Sinclair DA, Hayashi S, Tener GM, Grigliatti TA. 1991. Informational redundancy of tRNA(4Ser) and tRNA(7Ser) genes in Drosophila melanogaster and evidence for intergenic recombination. *J Mol Biol* 219:175-88

Li J, Ashley J, Budnik V, Bhat MA. 2007. Crucial role of Drosophila neurexin in proper active zone apposition to postsynaptic densities, synaptic growth, and synaptic transmission. *Neuron* 55:741-55

Li W, Wang F, Menut L, Gao FB. 2004. BTB/POZ-zinc finger protein abrupt suppresses dendritic branching in a neuronal subtype-specific and dosage-dependent manner. *Neuron* 43:823-34

Libersat F. 2005. Maturation of dendritic architecture: lessons from insect identified neurons. *J Neurobiol* 64:11-23

Liebl FL, Werner KM, Sheng Q, Karr JE, McCabe BD, Featherstone DE. 2006. Genome-wide P-element screen for Drosophila synaptogenesis mutants. *J Neurobiol* 66:332-47

Lim ST, Antonucci DE, Scannevin RH, Trimmer JS. 2000. A novel targeting signal for proximal clustering of the Kv2.1 K+ channel in hippocampal neurons. *Neuron* 25:385-97

Lin DM, Fetter RD, Kopczynski C, Grenningloh G, Goodman CS. 1994. Genetic analysis of Fasciclin II in drosophila: Defasciculation, refasciculation, and altered fasciculation. *Neuron* 13:1055-69

Lin S, Huang Y, Lee T. 2009. Nuclear receptor unfulfilled regulates axonal guidance and cell identity of Drosophila mushroom body neurons. *PLoS One* 4:e8392

Liu Y, Shi J, Lu CC, Wang ZB, Lyuksyutova AI, et al. 2005. Ryk-mediated Wnt repulsion regulates posterior-directed growth of corticospinal tract. *Nat Neurosci* 8:1151-9

Lohmann C, Wong RO. 2005. Regulation of dendritic growth and plasticity by local and global calcium dynamics. *Cell Calcium* 37:403-9

Longart M, Liu Y, Karavanova I, Buonanno A. 2004. Neuregulin-2 is developmentally regulated and targeted to dendrites of central neurons. *J Comp Neurol* 472:156-72

Lu Y, Ferris J, Gao FB. 2009. Frontotemporal dementia and amyotrophic lateral sclerosis-associated disease protein TDP-43 promotes dendritic branching. *Mol Brain* 2:30

Luo L. 2000. Rho GTPases in neuronal morphogenesis. *Nat Rev Neurosci* 1:173-80

Luo L, Liao YJ, Jan LY, Jan YN. 1994. Distinct morphogenetic functions of similar small GTPases: Drosophila Drac1 is involved in axonal outgrowth and myoblast fusion. *Genes & Development* 8:1787-802

Lyuksyutova AI, Lu CC, Milanesio N, King LA, Guo N, et al. 2003. Anterior-posterior guidance of commissural axons by Wnt-frizzled signaling. *Science* 302:1984-8

Malartre M, Ayaz D, Amador FF, Martin-Bermudo MD. 2010. The guanine exchange factor vav controls axon growth and guidance during Drosophila development. *J Neurosci* 30:2257-67

Mann F, Ray S, Harris W, Holt C. 2002. Topographic mapping in dorsoventral axis of the Xenopus retinotectal system depends on signaling through ephrin-B ligands. *Neuron* 35:461-73

Marchler-Bauer A, Lu S, Anderson JB, Chitsaz F, Derbyshire MK, et al. 2011. CDD: a Conserved Domain Database for the functional annotation of proteins. *Nucleic Acids Res* 39:D225-9

Margulies C, Tully T, Dubnau J. 2005. Deconstructing memory in Drosophila. *Curr Biol* 15:R700-13

Matthews BJ, Kim ME, Flanagan JJ, Hattori D, Clemens JC, et al. 2007. Dendrite self-avoidance is controlled by Dscam. *Cell* 129:593-604

Mauss A. 2008. *Development and patterning of motoneuron dendrites in the Drosophila embryo*. University of Cambridge, Cambridge

Mauss A, Tripodi M, Evers JF, Landgraf M. 2009. Midline signalling systems direct the formation of a neural map by dendritic targeting in the Drosophila motor system. *PLoS Biol* 7:e1000200

McBride SM, Choi CH, Wang Y, Liebelt D, Braunstein E, et al. 2005. Pharmacological rescue of synaptic plasticity, courtship behavior, and mushroom body defects in a Drosophila model of fragile X syndrome. *Neuron* 45:753-64

McGovern VL, Pacak CA, Sewell ST, Turski ML, Seeger MA. 2003. A targeted gain of function screen in the embryonic CNS of Drosophila. *Mech Dev* 120:1193-207

Medina PM, Swick LL, Andersen R, Blalock Z, Brenman JE. 2006. A novel forward genetic screen for identifying mutations affecting larval neuronal dendrite development in Drosophila melanogaster. *Genetics* 172:2325-35

Metaxakis A, Oehler S, Klinakis A, Savakis C. 2005. Minos as a genetic and genomic tool in Drosophila melanogaster. *Genetics* 171:571-81

Millard SS, Zipursky SL. 2008. Dscam-mediated repulsion controls tiling and self-avoidance. *Curr Opin Neurobiol* 18:84-9

Misra K, Gui H, Matise MP. 2008. Prox1 regulates a transitory state for interneuron neurogenesis in the spinal cord. *Dev Dyn* 237:393-402

Miyoshi K, Tsukumo H, Nagami T, Siomi H, Siomi MC. 2005. Slicer function of Drosophila Argonautes and its involvement in RISC formation. *Genes Dev* 19:2837-48

Mizoguchi A, Nakanishi H, Kimura K, Matsubara K, Ozaki-Kuroda K, et al. 2002. Nectin: an adhesion molecule involved in formation of synapses. *J Cell Biol* 156:555-65

Mlodzik M, Baker NE, Rubin GM. 1990. Isolation and expression of scabrous, a gene regulating neurogenesis in Drosophila. *Genes Dev* 4:1848-61

Mochizuki H, Toda H, Ando M, Kurusu M, Tomoda T, Furukubo-Tokunaga K. 2011. Unc-51/ATG1 Controls Axonal and Dendritic Development via Kinesin-Mediated Vesicle Transport in the Drosophila Brain. *PLoS One* 6:e19632

mod EC, Roy S, Ernst J, Kharchenko PV, Kheradpour P, et al. 2010. Identification of functional elements and regulatory circuits by Drosophila modENCODE. *Science* 330:1787-97

Moore AW, Jan LY, Jan YN. 2002. hamlet, a binary genetic switch between single- and multiple- dendrite neuron morphology. *Science* 297:1355-8

Moorthy S, Chen LS, Bennett V. 1996. A Novel C.Elegans Adducin: A Whole New Can of Worms. In *East Coast Worm Meeting*. Howard Hughes Medical Institute and Departments of Biochemistry and Cell Biology, Duke University, Durham , NC 27710

Myoga MH, Beierlein M, Regehr WG. 2009. Somatic spikes regulate dendritic signaling in small neurons in the absence of backpropagating action potentials. *J Neurosci* 29:7803-14

Nadif Kasri N, Nakano-Kobayashi A, Malinow R, Li B, Van Aelst L. 2009. The Rho-linked mental retardation protein oligophrenin-1 controls synapse maturation and plasticity by stabilizing AMPA receptors. *Genes Dev* 23:1289-302

Negishi M, Oinuma I, Katoh H. 2005. Plexins: axon guidance and signal transduction. *Cell Mol Life Sci* 62:1363-71

Neufeld SQ, Hibbert AD, Chen BE. 2011. Opposing roles of PlexinA and PlexinB in axonal branch and varicosity formation. *Mol Brain* 4:15

Ng J, Luo L. 2004a. Rho GTPases regulate axon growth through convergent and divergent signaling pathways. *Neuron* 44:779-93

Ng J, Luo L. 2004b. Rho GTPases Regulate Axon Growth through Convergent and Divergent Signaling Pathways. *Neuron* 44:779-93

Nicolai LJ, Ramaekers A, Raemaekers T, Drozdzecki A, Mauss AS, et al. 2010. Genetically encoded dendritic marker sheds light on neuronal connectivity in Drosophila. *Proc Natl Acad Sci U S A* 107:20553-8

Niell CM. 2006. Theoretical analysis of a synaptotropic dendrite growth mechanism. *J Theor Biol* 241:39-48

Niell CM, Smith SJ. 2004. Live optical imaging of nervous system development. *Annu Rev Physiol* 66:771-98

Nijhout HF. 2003. The control of body size in insects. *Dev Biol* 261:1-9

Nimnual AS, Yatsula BA, Bar-Sagi D. 1998. Coupling of Ras and Rac guanosine triphosphatases through the Ras exchanger Sos. *Science* 279:560-3

Ostrowski K, Bauer R, Hoch M. 2008. The Drosophila innexin 7 gap junction protein is required for development of the embryonic nervous system. *Cell Commun Adhes* 15:155-67

Ou Y, Chwalla B, Landgraf M, van Meyel DJ. 2008. Identification of genes influencing dendrite morphogenesis in developing peripheral sensory and central motor neurons. *Neural Dev* 3:16

Packard M, Mathew D, Budnik V. 2003. FASt remodeling of synapses in Drosophila. *Curr Opin Neurobiol* 13:527-34

Palgi M, Lindstrom R, Peranen J, Piepponen TP, Saarma M, Heino TI. 2009. Evidence that DmMANF is an invertebrate neurotrophic factor supporting dopaminergic neurons. *Proc Natl Acad Sci U S A* 106:2429-34

Pan L, Zhang YQ, Woodruff E, Broadie K. 2004. The Drosophila fragile X gene negatively regulates neuronal elaboration and synaptic differentiation. *Curr Biol* 14:1863-70

Pannekoek WJ, Kooistra MR, Zwartkruis FJ, Bos JL. 2009. Cell-cell junction formation: the role of Rap1 and Rap1 guanine nucleotide exchange factors. *Biochim Biophys Acta* 1788:790-6

Parks AL, Cook KR, Belvin M, Dompe NA, Fawcett R, et al. 2004. Systematic generation of high-resolution deletion coverage of the Drosophila melanogaster genome. *Nat Genet* 36:288-92

Parrish JZ, Emoto K, Jan LY, Jan YN. 2007a. Polycomb genes interact with the tumor suppressor genes hippo and warts in the maintenance of Drosophila sensory neuron dendrites. *Genes Dev* 21:956-72

Parrish JZ, Emoto K, Kim MD, Jan YN. 2007b. Mechanisms That Regulate Establishment, Maintenance, and Remodeling of Dendritic Fields. *Annu Rev Neurosci*

Parrish JZ, Kim MD, Jan LY, Jan YN. 2006a. Genome-wide analyses identify transcription factors required for proper morphogenesis of Drosophila sensory neuron dendrites. *Genes & Development* 20:820-35

Parrish JZ, Kim MD, Jan LY, Jan YN. 2006b. Genome-wide analyses identify transcription factors required for proper morphogenesis of Drosophila sensory neuron dendrites. *Genes Dev* 20:820-35

Patel NH. 1996. In situ hybridization to whole-mount Drosophila embryos. In *A Laboratory Guide to RNA: Isolation, Analysis and Synthesis.*, ed. PA Krieg. New York: Wiley-Liss

Pielage J, Cheng L, Fetter RD, Carlton PM, Sedat JW, Davis GW. 2008. A presynaptic giant ankyrin stabilizes the NMJ through regulation of presynaptic microtubules and transsynaptic cell adhesion. *Neuron* 58:195-209

Pieretti M, Zhang FP, Fu YH, Warren ST, Oostra BA, et al. 1991. Absence of expression of the FMR-1 gene in fragile X syndrome. *Cell* 66:817-22

Polleux F, Morrow T, Ghosh A. 2000. Semaphorin 3A is a chemoattractant for cortical apical dendrites. *Nature* 404:567-73

Poon VY, Klassen MP, Shen K. 2008. UNC-6/netrin and its receptor UNC-5 locally exclude presynaptic components from dendrites. *Nature* 455:669-73

Preall JB, He Z, Gorra JM, Sontheimer EJ. 2006. Short interfering RNA strand selection is independent of dsRNA processing polarity during RNAi in Drosophila. *Curr Biol* 16:530-5

Prokop A, Uhler J, Roote J, Bate M. 1999. The *kakapo* mutation affects terminal arborisation and central dendritic sprouting of *Drosophila* motorneurons (Abstract 7th European Symposium on *Drosophila* Neurobiology). *J. Neurogenet.*:, in press

Prokop A, Uhler J, Roote J, Bate MC. 1998. The *kakapo* mutation affects terminal arborisation and central dendritic sprouting of *Drosophila* motorneurons. *J. Cell Biol.* 143:1283-94

Rajagopalan S, Nicolas E, Vivancos V, Berger J, Dickson BJ. 2000a. Crossing the midline: roles and regulation of Robo receptors. *Neuron* 28:767-77

Rajagopalan S, Vivancos V, Nicolas E, Dickson BJ. 2000b. Selecting a longitudinal pathway: Robo receptors specify the lateral position of axons in the Drosophila CNS. *Cell* 103:1033-45

Raper J, Mason C. 2010. Cellular strategies of axonal pathfinding. *Cold Spring Harb Perspect Biol* 2:a001933

Redmond L, Ghosh A. 2005. Regulation of dendritic development by calcium signaling. *Cell Calcium* 37:411-6

Reeve SP, Bassetto L, Genova GK, Kleyner Y, Leyssen M, et al. 2005. The Drosophila fragile X mental retardation protein controls actin dynamics by directly regulating profilin in the brain. *Curr Biol* 15:1156-63

Reis K, Fransson A, Aspenstrom P. 2009. The Miro GTPases: at the heart of the mitochondrial transport machinery. *FEBS Lett* 583:1391-8

Renger JJ, Ueda A, Atwood HL, Govind CK, Wu CF. 2000. Role of cAMP cascade in synaptic stability and plasticity: ultrastructural and physiological analyses of individual synaptic boutons in Drosophila memory mutants. *J Neurosci* 20:3980-92

Reuter JE, Nardine TM, Penton A, Billuart P, Scott EK, et al. 2003. A mosaic genetic screen for genes necessary for Drosophila mushroom body neuronal morphogenesis. *Development* 130:1203-13

Robinow S, White K. 1991. Characterization and spatial distribution of the ELAV protein during Drosophila melanogaster development. *J Neurobiol* 22:443-61

Roy B, Singh AP, Shetty C, Chaudhary V, North A, et al. 2007. Metamorphosis of an identified serotonergic neuron in the Drosophila olfactory system. *Neural Dev* 2:20

Ryder E, Blows F, Ashburner M, Bautista-Llacer R, Coulson D, et al. 2004. The DrosDel collection: a set of P-element insertions for generating custom chromosomal aberrations in Drosophila melanogaster. *Genetics* 167:797-813

Ryder E, Russell S. 2003. Transposable elements as tools for genomics and genetics in Drosophila. *Brief Funct Genomic Proteomic* 2:57-71

Ryglewski S, Duch C. 2009. Shaker and Shal mediate transient calcium-independent potassium current in a Drosophila flight motoneuron. *J Neurophysiol* 102:3673-88

Saitou N, Nei M. 1987. The neighbor-joining method: a new method for reconstructing phylogenetic trees. *Mol Biol Evol* 4:406-25

Salcini AE, Hilliard MA, Croce A, Arbucci S, Luzzi P, et al. 2001. The Eps15 C. elegans homologue EHS-1 is implicated in synaptic vesicle recycling. *Nat Cell Biol* 3:755-60

Sanchez-Soriano N, Bottenberg W, Fiala A, Haessler U, Kerassoviti A, et al. 2005. Are dendrites in Drosophila homologous to vertebrate dendrites? *Dev Biol*

Sanchez-Soriano N, Tear G, Whitington P, Prokop A. 2007. Drosophila as a genetic and cellular model for studies on axonal growth. *Neural Dev* 2:9

Sanchez-Soriano N, Travis M, Dajas-Bailador F, Goncalves-Pimentel C, Whitmarsh AJ, Prokop A. 2009. Mouse ACF7 and drosophila short stop modulate filopodia formation and microtubule organisation during neuronal growth. *J Cell Sci* 122:2534-42

Sanes JR, Zipursky SL. 2010. Design principles of insect and vertebrate visual systems. *Neuron* 66:15-36

Santos JG, Pollak E, Rexer KH, Molnar L, Wegener C. 2006. Morphology and metamorphosis of the peptidergic Va neurons and the median nerve system of the fruit fly, Drosophila melanogaster. *Cell Tissue Res* 326:187-99

Sato D, Sugimura K, Satoh D, Uemura T. 2010. Crossveinless-c, the Drosophila homolog of tumor suppressor DLC1, regulates directional elongation of dendritic branches via down-regulating Rho1 activity. *Genes Cells* 15:485-500

Schmid A, Chiba A, Doe CQ. 1999. Clonal analysis of *Drosophila* embryonic neuroblasts: neural cell types, axon projections and muscle targets. *Development* 126:4653-89

Schmucker D, Flanagan JG. 2004. Generation of recognition diversity in the nervous system. *Neuron* 44:219-22

Schoenmann Z, Assa-Kunik E, Tiomny S, Minis A, Haklai-Topper L, et al. 2010. Axonal degeneration is regulated by the apoptotic machinery or a NAD+-sensitive pathway in insects and mammals. *J Neurosci* 30:6375-86

Schuldiner O, Berdnik D, Levy JM, Wu JS, Luginbuhl D, et al. 2008. piggyBac-based mosaic screen identifies a postmitotic function for cohesin in regulating developmental axon pruning. *Dev Cell* 14:227-38

Schultz J, Milpetz F, Bork P, Ponting CP. 1998. SMART, a simple modular architecture research tool: identification of signaling domains. *Proc Natl Acad Sci U S A* 95:5857-64

Schuske KR, Richmond JE, Matthies DS, Davis WS, Runz S, et al. 2003. Endophilin is required for synaptic vesicle endocytosis by localizing synaptojanin. *Neuron* 40:749-62

Schuster CM, Davis WD, Fetter RD, Goodman CS. 1996. Genetic dissection of structural and functional components of synaptic plasticity. I. Fasciclin II controls synaptic stabilisation and growth. *Neuron* 17:641-54

Scott EK, Luo L. 2001. How do dendrites take their shape? *Nat Neurosci* 4:359-65

Scott EK, Reuter JE, Luo L. 2003. Small GTPase Cdc42 is required for multiple aspects of dendritic morphogenesis. *J Neurosci* 23:3118-23

Sepp KJ, Hong P, Lizarraga SB, Liu JS, Mejia LA, et al. 2008. Identification of neural outgrowth genes using genome-wide RNAi. *PLoS Genet* 4:e1000111

Sharma K, Sheng HZ, Lettieri K, Li H, Karavanov A, et al. 1998. LIM homeodomain factors Lhx3 and Lhx4 assign subtype identities for motor neurons. *Cell* 95:817-28

Sharma SK, Nirenberg M. 2007. Silencing of genes in cultured Drosophila neurons by RNA interference. *Proc Natl Acad Sci U S A* 104:12925-30

Shen K, Scheiffele P. 2010. Genetics and cell biology of building specific synaptic connectivity. *Annu Rev Neurosci* 33:473-507

Shyamala BV, Bhat KM. 2002. A positive role for patched-smoothened signaling in promoting cell proliferation during normal head development in Drosophila. *Development* 129:1839-47

Sigrist CJ, Cerutti L, de Castro E, Langendijk-Genevaux PS, Bulliard V, et al. 2010. PROSITE, a protein domain database for functional characterization and annotation. *Nucleic Acids Res* 38:D161-6

Simpson JH, Bland KS, Fetter RD, Goodman CS. 2000a. Short-range and long-range guidance by Slit and its Robo receptors: a combinatorial code of Robo receptors controls lateral position. *Cell* 103:1019-32

Simpson JH, Kidd T, Bland KS, Goodman CS. 2000b. Short-range and long-range guidance by slit and its Robo receptors. Robo and Robo2 play distinct roles in midline guidance. *Neuron* 28:753-66

Slack C, Somers WG, Sousa-Nunes R, Chia W, Overton PM. 2006. A mosaic genetic screen for novel mutations affecting Drosophila neuroblast divisions. *BMC Genet* 7:33

Soba P, Zhu S, Emoto K, Younger S, Yang SJ, et al. 2007. Drosophila Sensory Neurons Require Dscam for Dendritic Self-Avoidance and Proper Dendritic Field Organization. *Neuron* 54:403-16

Spruston N, Jaffe DB, Johnston D. 1994. Dendritic attenuation of synaptic potentials and currents: the role of passive membrane properties. *Trends Neurosci* 17:161-6

St Johnston D. 2002a. The art and design of genetic screens: Drosophila melanogaster. *Nat Rev Genet* 3:176-88

St Johnston D. 2002b. The Art and design of Genetic Screens: Drosophila Melanogaster. *Nature Reviews Genetics* 3:176-88

Stroschein-Stevenson SL, Foley E, O'Farrell PH, Johnson AD. 2006. Identification of Drosophila gene products required for phagocytosis of Candida albicans. *PLoS Biol* 4:e4

Stutz F, Gouilloud E, Clarkson SG. 1989. Oocyte and somatic tyrosine tRNA genes in Xenopus laevis. *Genes Dev* 3:1190-8

Sun C, Cheng MC, Qin R, Liao DL, Chen TT, et al. 2011a. Identification and functional characterization of rare mutations of the neuroligin-2 gene (NLGN2) associated with schizophrenia. *Hum Mol Genet*

Sun M, Xing G, Yuan L, Gan G, Knight D, et al. 2011b. Neuroligin 2 is required for synapse development and function at the Drosophila neuromuscular junction. *J Neurosci* 31:687-99

Sweeney ST, Broadie K, Keane J, Niemann H, O'Kane CJ. 1995. Targeted expression of tetanus toxin light chain in *Drosophila* specifically eliminates synaptic transmission and causes behavioral defects. *Neuron* 14:341-51

Takahashi D, Yu W, Baas PW, Kawai-Hirai R, Hayashi K. 2007. Rearrangement of microtubule polarity orientation during conversion of dendrites to axons in cultured pyramidal neurons. *Cell Motil Cytoskeleton* 64:347-59

Tanaka Y, Takase M, Gamo S. 2007. Relationship between general anesthesia and memory in Drosophila involving the cAMP/PKA pathways and adhesion-related molecules. *Curr Med Chem* 14:1479-88

Tao J, Rolls MM. 2011. Dendrites have a rapid program of injury-induced degeneration that is molecularly distinct from developmental pruning. *J Neurosci* 31:5398-405

Teichmann HM, Shen K. 2011. UNC-6 and UNC-40 promote dendritic growth through PAR-4 in Caenorhabditis elegans neurons. *Nat Neurosci* 14:165-72

Terman JR, Kolodkin AL. 2004. Nervy links protein kinase a to plexin-mediated semaphorin repulsion. *Science* 303:1204-7

Tessier CR, Broadie K. 2011. The fragile X mental retardation protein developmentally regulates the strength and fidelity of calcium signaling in Drosophila mushroom body neurons. *Neurobiol Dis* 41:147-59

Theodosiou NA, Xu T. 1998. Use of FLP/FRT system to study Drosophila development. *Methods* 14:355-65

Thibault ST, Singer MA, Miyazaki WY, Milash B, Dompe NA, et al. 2004. A complementary transposon tool kit for Drosophila melanogaster using P and piggyBac. *Nat Genet* 36:283-7

Thomas GM, Huganir RL. 2004. MAPK cascade signalling and synaptic plasticity. *Nat Rev Neurosci* 5:173-83

Togashi H, Miyoshi J, Honda T, Sakisaka T, Takai Y, Takeichi M. 2006. Interneurite affinity is regulated by heterophilic nectin interactions in concert with the cadherin machinery. *J Cell Biol* 174:141-51

Tolias KF, Duman JG, Um K. 2011. Control of synapse development and plasticity by Rho GTPase regulatory proteins. *Prog Neurobiol* 94:133-48

Tolias PP, Stroumbakis ND. 1998. The Drosophila zygotic lethal gene shuttle craft is required maternally for proper embryonic development. *Dev Genes Evol* 208:274-82

Tomancak P, Beaton A, Weiszmann R, Kwan E, Shu S, et al. 2002. Systematic determination of patterns of gene expression during Drosophila embryogenesis. *Genome Biol* 3:RESEARCH0088

Tripodi M, Evers JF, Mauss A, Bate M, Landgraf M. 2008. Structural homeostasis: compensatory adjustments of dendritic arbor geometry in response to variations of synaptic input. *PLoS Biol* 6:e260

Tucker B, Richards RI, Lardelli M. 2006. Contribution of mGluR and Fmr1 functional pathways to neurite morphogenesis, craniofacial development and fragile X syndrome. *Hum Mol Genet* 15:3446-58

Tweedie S, Ashburner M, Falls K, Leyland P, McQuilton P, et al. 2009. FlyBase: enhancing Drosophila Gene Ontology annotations. *Nucleic Acids Res* 37:D555-9

Uhler J, Garbern J, Yang L, Kamholz J, Mellerick DM. 2002. Nk6, a novel Drosophila homeobox gene regulated by vnd. *Mechanisms of Development* 116:105-16

Van Aelst L, Cline HT. 2004. Rho GTPases and activity-dependent dendrite development. *Curr Opin Neurobiol* 14:297-304

Von Stetina SE, Watson JD, Fox RM, Olszewski KL, Spencer WC, et al. 2007. Cell-specific microarray profiling experiments reveal a comprehensive picture of gene expression in the C. elegans nervous system. *Genome Biol* 8:R135

Vonhoff F, Duch C. 2010. Tiling among stereotyped dendritic branches in an identified Drosophila motoneuron. *J Comp Neurol* 518:2169-85

Wagh DA, Rasse TM, Asan E, Hofbauer A, Schwenkert I, et al. 2006. Bruchpilot, a protein with homology to ELKS/CAST, is required for structural integrity and function of synaptic active zones in Drosophila. *Neuron* 49:833-44

Waites CL, Craig AM, Garner CC. 2005. Mechanisms of vertebrate synaptogenesis. *Annu Rev Neurosci* 28:251-74

Watabe-Uchida M, Govek EE, Van Aelst L. 2006. Regulators of Rho GTPases in neuronal development. *J Neurosci* 26:10633-5

Waterhouse RM, Zdobnov EM, Tegenfeldt F, Li J, Kriventseva EV. 2011. OrthoDB: the hierarchical catalog of eukaryotic orthologs in 2011. *Nucleic Acids Res* 39:D283-8

Wayman GA, Impey S, Marks D, Saneyoshi T, Grant WF, et al. 2006. Activity-dependent dendritic arborization mediated by CaM-kinase I activation and enhanced CREB-dependent transcription of Wnt-2. *Neuron* 50:897-909

Wennerberg K, Rossman KL, Der CJ. 2005. The Ras superfamily at a glance. *J Cell Sci* 118:843-6

Whitford KL, Marillat V, Stein E, Goodman CS, Tessier-Lavigne M, et al. 2002. Regulation of cortical dendrite development by Slit-Robo interactions. *Neuron* 33:47-61

Wilkins A, Szafranski K, Fraser DJ, Bakthavatsalam D, Muller R, et al. 2005. The Dictyostelium genome encodes numerous RasGEFs with multiple biological roles. *Genome Biol* 6:R68

Williams DW, Kondo S, Krzyzanowska A, Hiromi Y, Truman JW. 2006. Local caspase activity directs engulfment of dendrites during pruning. *Nat Neurosci* 9:1234-6

Williams DW, Truman JW. 2005a. Cellular mechanisms of dendrite pruning in Drosophila: insights from in vivo time-lapse of remodeling dendritic arborizing sensory neurons. *Development* 132:3631-42

Williams DW, Truman JW. 2005b. Remodeling dendrites during insect metamorphosis. *J Neurobiol* 64:24-33

Witke W, Podtelejnikov AV, Di Nardo A, Sutherland JD, Gurniak CB, et al. 1998. In mouse brain profilin I and profilin II associate with regulators of the endocytic pathway and actin assembly. *Embo J* 17:967-76

Witte H, Bradke F. 2008. The role of the cytoskeleton during neuronal polarization. *Curr Opin Neurobiol* 18:479-87

Wu JS, Luo L. 2006. A protocol for mosaic analysis with a repressible cell marker (MARCM) in Drosophila. *Nat Protoc* 1:2583-9

Xu T, Rubin GM. 1993. Analysis of genetic mosaics in developing and adult Drosophila tissues. *Development* 117:1223-37

Yamagata M, Sanes JR. 2008. Dscam and Sidekick proteins direct lamina-specific synaptic connections in vertebrate retina. *Nature* 451:465-9

Yamamoto M, Ueda R, Takahashi K, Saigo K, Uemura T. 2006. Control of axonal sprouting and dendrite branching by the Nrg-Ank complex at the neuron-glia interface. *Curr Biol* 16:1678-83

Yang L, Bashaw GJ. 2006. Son of sevenless directly links the Robo receptor to rac activation to control axon repulsion at the midline. *Neuron* 52:595-607

Ye B, Petritsch C, Clark IE, Gavis ER, Jan LY, Jan YN. 2004. Nanos and Pumilio are essential for dendrite morphogenesis in Drosophila peripheral neurons. *Curr Biol* 14:314-21

Ying SY, Chang DC, Miller JD, Lin SL. 2006. MicroRNA protocols. Perspectives. *Methods Mol Biol* 342:351-8

Yoshikawa S, McKinnon RD, Kokel M, Thomas JB. 2003. Wnt-mediated axon guidance via the Drosophila Derailed receptor. *Nature* 422:583-8

Yuan XB, Jin M, Xu X, Song YQ, Wu CP, et al. 2003. Signalling and crosstalk of Rho GTPases in mediating axon guidance. *Nat Cell Biol* 5:38-45

Zanni G, Saillour Y, Nagara M, Billuart P, Castelnau L, et al. 2005. Oligophrenin 1 mutations frequently cause X-linked mental retardation with cerebellar hypoplasia. *Neurology* 65:1364-9

Zeng X, Sun M, Liu L, Chen F, Wei L, Xie W. 2007. Neurexin-1 is required for synapse formation and larvae associative learning in Drosophila. *FEBS Lett* 581:2509-16

Zhang YQ, Bailey AM, Matthies HJ, Renden RB, Smith MA, et al. 2001. *Drosophila* fragile X-related gene regulates the MAP1B homolog Futsch to control synaptic structure and function. *Cell* 107:591-603

Zhang YQ, Matthies HJ, Mancuso J, Andrews HK, Woodruff E, 3rd, et al. 2004. The Drosophila fragile X-related gene regulates axoneme differentiation during spermatogenesis. *Dev Biol* 270:290-307

Zhao DB, Cote S, Jahnig F, Haller J, Jaeckle H. 1988. Zipper encodes a putative integral membrane protein required for normal axon patterning during Drosophila neurogenesis. *The EMBO Journal* 7:1115-9

Zheng X, Wang J, Haerry TE, Wu AY, Martin J, et al. 2003. TGF-beta signaling activates steroid hormone receptor expression during neuronal remodeling in the Drosophila brain. *Cell* 112:303-15

Zhou X, Zhou B, Truman JW, Riddiford LM. 2004. Overexpression of broad: a new insight into its role in the Drosophila prothoracic gland cells. *J Exp Biol* 207:1151-61

Zhu S, Lin S, Kao CF, Awasaki T, Chiang AS, Lee T. 2006. Gradients of the Drosophila Chinmo BTB-zinc finger protein govern neuronal temporal identity. *Cell* 127:409-22

Zipursky SL, Wojtowicz WM, Hattori D. 2006. Got diversity? Wiring the fly brain with Dscam. *Trends Biochem Sci* 31:581-8

Zlatic M, Landgraf M, Bate M. 2003. Genetic specification of axonal arbors: atonal regulates robo3 to position terminal branches in the Drosophila nervous system. *Neuron* 37:41-51

Zlatic M, Li F, Strigini M, Grueber W, Bate M. 2009. Positional cues in the Drosophila nerve cord: semaphorins pattern the dorso-ventral axis. *PLoS Biol* 7:e1000135

ANNOTATION SYMBOL	CYTOGENETIC MAP	NAME	LOCATION MAX	LOCATION MIN	COVERED BY DELETION STOCK NUMBER	COVERED BY DELETION STOCK NUMBER 2	COVERED BY DELETION STOCK NUMBER 3	COVERED BY DELETION STOCK NUMBER 4	COVERED BY DELETION STOCK NUMBER 5	COVERED BY DELETION STOCK NUMBER 6	COVERED BY DELETION STOCK NUMBER 7	COVERED BY DELETION STOCK NUMBER 8	TOTAL COVERAGE
CG40006	-	-	22649081	22515149									
CG40439	-	-	22690967	22690251									
CG43266	-	-	22736254	22735486									
CG17715	-	-	22747273	22736958									
CG18028	-	light	22833492	22817519									
CG40005	-	-	22843012	22842025									
CG17678	-	concertina	22885080	22874534									
CG18140	-	Chitinase 3	22918647	22892290									
CG17540	-	Spf45	22961179	22959606									
CR43242	-	-	22963456	22961737									
CG11023	21A5-21A5	-	9484	7529			3638						
CG2671	21A5-21A5	lethal (2) giant larvae	21372	9839			3638						
CG2657	21A5-21B1	Ionotropic receptor 21a	25151	21919			3638						
CG31973	21B1-21B1	Chitin deacetylase-like 5	59242	25402			3638						
CG11371	21B1-21B1	debra	71390	66721			3638						
CG11372	21B1-21B1	galectin	76211	71757			3638						
CG11374	21B1-21B1	-	77785	76326			3638						
CG11450	21B1-21B1	net	87382	82456			3638						
CG11376	21B1-21B2	-	102086	94752			3638						
CG11377	21B2-21B2	-	104142	102382			3638						
CG12178	21B2-21B2	Na[+]/H[+] hydrogen exchanger 1	106718	103962			3638						
CG2674	21B2-21B2	S-adenosylmethionine Synthetase	114433	106903			3638						
CG13694	21B2-21B2	-	116488	115365			3638						
CG4822	21B2-21B2	-	121974	117079			3638						
CG3164	21B2-21B2	-	130791	122624			3638						
CG2718	21B2-21B3	Glutamine synthetase 1	134472	132060			3638						
CG31975	21B3-21B3	-	140992	138384			3638						
CG31976	21B3-21B3	-	140992	138384			3638						
CG31974	21B3-21B3	-	142978	141077			3638						
CG11454	21B3-21B3	-	144227	143309			3638						
CG42399	21B3-21B3	-	153288	144231			3638						
CG3709	21B3-21B3	-	155321	153539			3638						
CG11455	21B3-21B3	-	156030	114842			3638						
CG3436	21B3-21B3	-	157666	156029			3638						
CG33635	21B3-21B3	-	158664	157836			3638						
CG18497	21B3-21B4	split ends	203250	159034			3638						
CG11488	21B4-21B4	mitochondrial ribosomal protein L10	204782	203784			3638						
CG11617	21B4-21B4	-	207297	204738			3638						

CG11490	21B4-21B4	-	210506	207399			3638				
CG3696	21B4-21B5	kismet	250795	210732			3638				
CG13693	21B5-21B5	-	233965	232514			3638				
CR42959	21B5-21B5	mir-965 stem loop	243141	243035			3638				
CG11606	21B5-21B5	RNaseP protein p30	252331	251163			3638				
CG3645	21B5-21B7	-	271732	252589	6283		3638				
CG17075	21B6-21B6	-	266688	263782	6283		3638				
CG3345	21B7-21B7	-	271626	269088	6283		3638				
CG11604	21B7-21B7	mushroom body miniature	274096	271912	6283		3638				
CG11555	21B7-21B7	-	274766	273955	6283		3638				
CG17078	21B7-21B7	-	277212	274740	6283		3638				
CG11561	21B7-21B7	smoothened	282167	277588	6283		3638				
CG11601	21B7-21B7	-	283281	281970	6283		3638				
CG11592	21B7-21B7	-	288919	287252	6283		3638				
CG3625	21B7-21B7	-	291010	283385	6283		3638				
CG11562	21B7-21B7	-	293222	292466	6283		3638				
CG3582	21B7-21B8	U2 small nuclear riboprotein auxiliary factor 38	294679	293337	6283		3638				
CG2720	21B8-21B8	Hsp70/Hsp90 organizing protein homolog	297413	295109	6283		3638				
CG2699	21B8-21B8	Pi3K21B	303955	297882	6283		3638				
CG11912	21B8-21B8	-	319254	318362	6283		3638				
CG11911	21B8-21B8	-	321246	320279	6283		3638				
CG33127	21B8-21B8	-	323091	322101	6283		3638				
CG4574	21B8-21C1	Phospholipase C at 21C	346549	305941	6283	3548	3638				
CG33992	21C1-21C1	-	328518	327429	6283	3548					
CG31920	21C1-21C1	-	329761	325520	6283	3548					
CG31921	21C1-21C1	-	332335	329991	6283	3548					
CG11907	21C1-21C1	Equilibrative nucleoside transporter 1	357868	355559	6283	3548					
CG3935	21C1-21C1	aristaless	387439	378116	6283	3548					
CG4213	21C2-21C2	-	402181	396595	6283	3548					
CG4033	21C2-21C2	RNA polymerase I 135kD subunit	407969	404305	6283	3548					
CG4260	21C2-21C2	alpha-Adaptin	414775	408030	6283	3548					
CG4063	21C2-21C2	ebi	418536	415069	6283	3548					
CG13690	21C2-21C2	-	419642	418434	6283	3548					
CG4087	21C2-21C2	Ribosomal protein LP1	420706	419931	6283	3548					
CG11885	21C2-21C2	-	421407	420887	6283	3548					
CG13692	21C2-21C2	-	422435	421800	6283	3548					
CG13691	21C2-21C2	BBS8	425291	423452	6283	3548					
CG4114	21C2-21C2	expanded	448701	431253	6283	3548				8673	
CG4280	21C2-21C2	croquemort	453023	448254	6283	3548				8673	
CG4164	21C2-21C2	-	454654	453111	6283	3548				8673	
CR43080	21C2-21C2	-	455313	454754	6283	3548				8673	
CG4133	21C2-21C8	-	458745	455543	6283	3548		6608	6697	8673	
CG4297	21C8-21D1	-	465607	460515			3084		6697	8673	

CG4184	21D1-21D1	Mediator complex subunit 15	476176	473021	3084	6697	8673	
CG4427	21D1-21D1	cabut	479682	476437	3084	6697	8673	
CG2762	21E1-21E2	u-shaped	540541	523467	3084	6697	8673	
CG3018	21E2-21E2	lesswright	542572	541235	3084	6697	8673	
CG11840	21E2-21E2	Signal peptide protease	544627	542776	3084	6697	8673	
CG11822	21E2-21E2	nicotinic acetylcholine receptor beta 21C	547096	545148	3084	6697	8673	
CG2914	21E2-21E2	Ets at 21C	552454	547414	3084	6697	8673	
CG11838	21E2-21E2	reduced mechanoreceptor potential A	560310	553742	3084	6697	8673	
CG2789	21E2-21E2	-	560523	559611	3084	6697	8673	
CG11835	21E2-21E2	-	563303	560794	3084	6697	8673	
CG2794	21E2-21E2	-	566472	564170	3084	6697	8673	
CG2863	21E2-21E2	Notchless	568162	566366	3084	6697	8673	
CG2807	21E2-21E2	-	572716	568337	3084	6697	8673	
CG13688	21E2-21E2	Ipk2	574232	573033	3084	6697	8673	
CG2813	21E2-21E2	coiled	575734	574486	3084	6697	8673	
CG13687	21E2-21E2	Prothoracicotropic hormone	576896	575711	3084	6697		
CG2819	21E2-21E2	PvuII-PstI homology 13	579549	577488	3084	6697		
CG2851	21E2-21E2	Goosecoid	594810	583540	3084	6697		
CG13689	21E2-21E2	-	603562	602813	3084	6697		
CG13686	21E2-21E2	lectin-21Cb	621540	620433	3084	6697		
CG2826	21E2-21E2	lectin-21Ca	625556	624617	3084	6697		
CG2839	21E2-21E2	-	628143	625663	3084	6697		
CG17941	21E2-21E2	dachsous	714968	640021	3084	6697		
CG2830	21E2-21E2	Heat shock protein 60 related	730564	728412	3084	6697		
CG3159	21E2-21E2	Excitatory amino acid transporter 2	744395	737212	3084	6697		
CG3022	21E2-21E2	metabotropic GABA-B receptor subtype 3	762142	752800	3084	6697		
CG12506	21E2-21E2	-	774020	773575	3084	6697		
CG13946	21E2-21E2	-	776892	776536	3084	6697		
CG13947	21E2-21E2	-	779655	779201	3084	6697		
CG13948	21E2-21E2	Gustatory receptor 21a	782885	780482	3084	6697		
CG3544	21E2-21E2	-	786161	784336	3084	6697		
CG3324	21E2-21E2	cGMP-dependent protein kinase 21D	790795	786153	3084	6697		
CG31658	21E2-21E2	Nnf1b	811531	810586	3084	6697		
CG3561	21E2-21E2	KH1	813380	811609	3084	6697		
CG3883	21E2-21E2	SAGA factor-like TAF6	815951	813314	3084	6697		
CG3639	21E2-21E2	peroxin 12	817032	816023	3084	6697		
CG15880	21E2-21E2	-	818445	817046	3084	6697		
CG3876	21E2-21E2	-	819520	818079	3084	6697		
CG3642	21E2-21E2	Clipper	821209	819964	3084	6697		
CG3662	21E2-21E2	-	824337	821418	3084	6697		
CG3862	21E2-21E2	-	825861	824329	3084	6697		
CG3727	21E2-21E2	dreadlocks	833245	825964	3084	6697		
CG3365	21E2-21E2	drongo	851096	833584	3084	6697		

CG4291	21E2-21E2	-	852709	851316	3084		6697		
CG3943	21E2-21E2	kraken	854539	852767	3084		6697		
CG13949	21E2-21E2	-	856236	855337	3084		6697		
CR42884	21E2-21E2	mir-375 stem loop	857632	857542	3084		6697		
CG13950	21E2-21E2	-	861806	860309	3084		6697		
CR34660	21E2-21E2	-	865493	865366	3084		6697		
CG4276	21E2-21E2	arouser	868352	861849	3084		6697		
CG4258	21E2-21E2	dribble	869911	868675	3084		6697		
CG33526	21E2-21E2	PNUTS	877050	870464	3084		6697		
CG3966	21E2-21E2	neither inactivation nor afterpotential A	878270	877293	3084		6697		
CG15824	21E2-21E2	-	885052	878175	3084		6697		
CG4178	21E2-21E2	Larval serum protein 1 beta	901320	898647	3084		6697		
CR31656	21E2-21E2	small nuclear RNA U1 at 21D	901654	901491	3084		6697		
CG4226	21E2-21E2	Glutamate receptor IIC	917805	914090	3084		6697		
CG4341	21E2-21E2	-	958098	922795	3084		6697		
CG4375	21E3-21E3	-	1026897	1026107	3084		6697		
CG4415	21E3-21E3	-	1038685	1037275	3084		6697		
CG31795	21E3-21E3	IA-2 ortholog	1048053	1011421	3084		6697		
CG4385	21E4-21E4	Star	1077811	1050877	3084		6697		
CG4426	21E4-21E4	asteroid	1080809	1077980	3084		6697		
CG4428	21E4-21E4	Autophagy-specific gene 4	1083378	1080913	3084		6697		
CG4629	21E4-21F1	-	1102506	1083090	3084		6697		
CG4644	21F1-21F1	mitochondrial RNA polymerase	1108369	1103483	3084		6697		
CG14339	21F1-21F1	-	1112702	1108539	3084		6697		
CG14340	21F1-21F1	-	1114140	1112988	3084		6697		
CG4710	21F1-21F1	Pinocchio	1128953	1114652	3084		6697		
CG4552	21F1-21F1	-	1132413	1129235	3084		6697		
CG4715	21F1-21F1	Iris	1134120	1132330	3084		6697		
CG4577	21F1-21F1	-	1141156	1134702	3084		6697		
CG4726	21F1-21F1	-	1147395	1143203	3084		6697		
CG4749	21F1-21F1	-	1149454	1147833	3084		6697		
CG5041	21F1-21F1	Tfb4	1150673	1149445	3084		6697		
CG4764	21F1-21F1	-	1151764	1150783	3084		6697		
CG33979	21F1-21F1	capulet	1158264	1151678	3084		6697		
CG4775	21F1-21F1	Transport and Golgi organization 14	1160221	1158679	3084		6697		
CG5080	21F1-21F1	-	1163882	1160290	3084		6697		
CG4785	21F1-21F1	-	1166432	1164470	3084		6697		
CG14341	21F1-21F1	-	1167211	1166514	3084		6697		
CG5105	21F1-21F1	Phospholipase A2 activator protein	1170079	1167172	3084		6697		
CG31922	21F1-21F2	-	1170789	1170181	3084		6697		
CG5118	21F2-21F2	-	1172745	1170753	3084		6697		
CG4887	21F2-21F2	-	1177496	1173011	3084		6697		
CG4896	21F2-21F2	-	1182454	1177706	3084		6697		

CG5126	21F2-21F2	-	1184021	1182297		3084	6697	
CG4947	21F2-21F2	tRNA-guanine transglycosylase	1185698	1184088		3084	6697	
CG5001	21F2-21F2	-	1196806	1186256		3084	6697	
CG5139	21F2-21F2	-	1199204	1198465		3084	6697	
CG43348	21F2-21F2	-	1199709	1199412		3084	6697	
CG43349	21F2-21F2	-	1200580	1200205		3084	6697	
CG5011	21F2-21F2	-	1201220	1200237		3084	6697	
CG14342	21F2-21F2	-	1205254	1204241		3084	6697	
CR43263	21F2-21F2	-	1217785	1216854		3084	6697	
CG42329	21F2-21F2	-	1229802	1219318		3084	6697	
CG5397	21F3-21F3	-	1242205	1240038		3084	6697	
CG5423	21F3-21F4	robo3	1294687	1256426		3084	6697	
CG5430	22A1-22A1	antennal protein 5	1329904	1329161		3084	6697	
CG5440	22A1-22A1	-	1334932	1334245		3084	6697	
CG33923	22A1-22A1	-	1342095	1341365		3084	6697	
CG33922	22A1-22A1	-	1344171	1343443		3084	6697	
CG5450	22A1-22A1	Cytoplasmic dynein light chain 2	1345144	1344480		3084	6697	
CG5556	22A1-22A1	-	1352869	1351805		3084	6697	
CG5561	22A1-22A1	-	1354109	1352970		3084	6697	
CG31924	22A1-22A1	-	1354919	1354101		3084	6697	
CG5565	22A1-22A1	-	1355924	1354911		3084	6697	
CG31659	22A1-22A1	-	1359784	1358925		3084	6697	
CG33126	22A1-22A1	Neural Lazarillo	1361732	1359983		3084	6697	
CG14346	22A1-22A1	-	1369047	1368102		3084	6697	
CG5481	22A1-22A1	leak	1420449	1380086		3084	6697	
CR31927	22A2-22A2	small nuclear RNA U3 at 22A	1432921	1432711	3133	3084	6697	
CG31928	22A2-22A2	-	1493645	1492295	3133	3084	6697	
CG33128	22A2-22A2	-	1495456	1494090	3133	3084	6697	
CG31926	22A2-22A2	-	1496979	1495747	3133	3084	6697	
CG31661	22A2-22A2	-	1498435	1497254	3133	3084	6697	
CG18131	22A2-22A2	-	1500760	1498455	3133	3084	6697	
CG7420	22A2-22A2	-	1502903	1500835	3133	3084	6697	
CG18132	22A2-22A2	-	1517478	1516790	3133	3084	6697	
CG7428	22A2-22A2	halo	1518184	1517532	3133	3084	6697	
CG12193	22A2-22A2	Odorant receptor 22a	1522151	1520613	3133	3084	6697	
CG4231	22A2-22A2	Odorant receptor 22b	1524259	1522691	3133	3084	6697	
CG10869	22A3-22A3	-	1587155	1584864	3133	3084	6697	
CG14351	22A3-22A3	hattifattener	1607617	1555159	3133	3084	6697	
CG31935	22A3-22A3	-	1611125	1595043	3133	3084	6697	
CG14352	22A3-22A3	-	1612579	1611421	3133	3084	6697	
CG7361	22A3-22A3	Rieske iron-sulfur protein	1614182	1612686	3133	3084	6697	
CG31666	22A5-22A8	Chronologically inappropriate morphogenesis	1698617	1651260	3133	3084	6697	
CG17158	22B1-22B1	capping protein beta	1706962	1704904	3133	3084	6697	

CG17660	22B1-22B1	-	1710415	1707132	3133		3084	6697	
CG17642	22B1-22B1	mitochondrial ribosomal protein L48	1711466	1710466	3133		3084	6697	
CG17657	22B1-22B1	fritz	1715861	1711299	3133		3084	6697	
CG18317	22B1-22B1	-	1724391	1716244	3133		3084	6697	
CG31938	22B1-22B1	-	1729575	1728735	3133		3084	6697	
CG17654	22B1-22B1	Enolase	1729629	1724974	3133		3084	6697	
CG31937	22B1-22B1	-	1731070	1729946	3133		3084	6697	
CG17652	22B1-22B1	-	1732356	1731358	3133		3084	6697	
CG17646	22B1-22B2	-	1750613	1732526	3133		3084	6697	
CG17712	22B2-22B2	-	1752116	1750687	3133		3084		
CG17648	22B2-22B2	-	1752851	1752349	3133		3084		
CG31932	22B2-22B2	Gustatory receptor 22f	1756451	1755253	3133		3084		
CG17650	22B2-22B2	-	1759078	1758286	3133		3084		
CG31936	22B2-22B2	Gustatory receptor 22e	1785286	1784062	3133		3084		
CR31930	22B2-22B2	Gustatory receptor 22d	1790361	1789141	3133		3084		
CG31929	22B2-22B2	Gustatory receptor 22c	1791823	1790617	3133		3084		
CG31931	22B2-22B2	Gustatory receptor 22b	1793268	1792057	3133		3084		
CG31662	22B2-22B2	Gustatory receptor 22a	1794917	1793668	3133		3084		
CG31933	22B3-22B3	-	1823331	1821256	3133		3084		
CG31664	22B3-22B3	-	1826378	1824273	3133		3084		
CR42982	22B3-22B3	mir-2280 stem loop	1831799	1831685	3133		3084		
CG15623	22B3-22B3	calcutta cup	1832557	1831627	3133		3084		
CG31665	22B3-22B4	weary	1858550	1836630	3133		3084		
CG7295	22B4-22B4	-	1870956	1869867	3133				
CG31663	22B4-22B4	-	1880644	1858609	3133				
CG15358	22B4-22B4	-	1884056	1882415	3133				
CG7337	22B4-22B6	-	1943818	1884984	3133				
CR31667	22B6-22B6	transfer RNA:gly3:22BCa	1938159	1938089	3133				
CG15357	22B6-22B6	-	1945709	1945225	3133				
CG33673	22B6-22B6	-	1947359	1945840	3133				
CG31670	22B6-22B7	earmuff	1954519	1950235	3133				
CR31942	22B8-22B8	transfer RNA:CR31942	1965498	1965426	3133				
CG10908	22B8-22B8	Derlin-1	1975413	1974126	3133				
CG15356	22B8-22B8	-	1980755	1976236	3133				
CG15362	22B8-22B8	-	1982099	1981176	3133				
CG7289	22B8-22B8	-	1984514	1982220	3133				
CG4233	22B8-22B8	Glutamate oxaloacetate transaminase 2	1987788	1984512	3133				
CG7291	22B8-22B8	Niemann-Pick type C-2a	1988940	1988264	3133				
CR42874	22B8-22B8	-	1990600	1989450	3133				
CG31941	22B8-22B8	Odorant-binding protein 22a	1992152	1991705	3133				
CG33543	22B8-22B8	-	2006307	1997102	3133				
CG15353	22B8-22B8	-	2007193	2006763	3133				
CG15361	22B8-22B8	Neuropeptide-like precursor 4	2008966	2008460	3133				

CR31943	22B8-22B8	transfer RNA:CR31943	2009226	2009155	3133
CR31944	22B8-22B8	transfer RNA:CR31944	2009609	2009538	3133
CR31939	22B8-22B8	transfer RNA:CR31939	2010717	2010646	3133
CR31940	22B8-22B8	transfer RNA:CR31940	2010940	2010869	3133
CR31669	22B8-22B8	transfer RNA:CR31669	2013250	2013179	3133
CG4238	22B8-22C1	-	2030536	2010118	3133
CR31945	22C1-22C1	transfer RNA:gly3:22BCb	2031762	2031692	3133
CG42296	22C1-22C1	-	2035936	2032635	3133
CG42295	22C1-22C1	lectin-22C	2037247	2036456	3133
CG4244	22C1-22C1	Suppressor of deltex	2044373	2037802	3133
CG31672	22C1-22C1	-	2048054	2045525	3133
CG15377	22C1-22C1	Odorant receptor 22c	2057967	2054589	3133
CG33516	22C1-22C3	dpr3	2109878	2058859	3133
CG12674	22C2-22C2	-	2081286	2079977	3133
CG4259	22C3-22C3	-	2129211	2128215	3133
CG7254	22C3-22D1	Glycogen phosphorylase	2137296	2130815	3133
CG31671	22D1-22D1	tho2	2145175	2137350	3133
CG11723	22D1-22D1	-	2147287	2145497	3133
CG7261	22D1-22D1	-	2151664	2147519	3133
CG7263	22D1-22D1	Apoptosis inducing factor	2155390	2151664	3133
CG15382	22D1-22D1	-	2156791	2155760	3133
CG3166	22D1-22D1	anterior open	2178749	2156484	3133
CR31946	22D1-22D1	transfer RNA:CR31946	2187079	2187007	3133
CG10874	22D1-22D1	-	2192372	2189913	3133
CG34172	22D1-22D1	-	2193010	2192525	3133
CG31668	22D1-22D4	-	2206028	2203904	3133
CG33124	22D4-22D4	-	2208906	2206796	3133
CG15385	22D4-22D4	-	2212571	2209574	3133
CG4265	22D4-22D4	Ubiquitin carboxy-terminal hydrolase	2214179	2212738	3133
CG34174	22D4-22D4	-	2215167	2214305	3133
CG10880	22D4-22D4	-	2216304	2214972	3133
CG15386	22D4-22D4	-	2217231	2216503	3133
CG42371	22D4-22D4	-	2217231	2216503	3133
CG7074	22D4-22D4	missing oocyte	2220625	2217363	3133
CG7082	22D4-22D4	-	2225555	2220767	3133
CG15387	22D4-22D4	-	2226840	2225549	3133
CG7085	22D4-22D4	lethal (2) s5379	2231096	2226523	3133
CG10882	22D4-22D5	ghost	2236826	2231777	3133
CG31679	22D5-22D5	-	2238251	2237076	3133
CG32463	22D5-22D5	-	2239384	2238304	3133
CG31682	22D5-22D5	-	2240593	2239414	3133
CG4267	22D5-22D5	-	2244415	2242379	3133
CG31686	22D5-22D5	-	2245352	2244637	3133

CR42859	22D5-22D5	-	2245901	2245330	3133		
CG17240	22D5-22D5	Serine protease 12	2251275	2250431	3133		
CG17239	22D5-22D5	-	2252341	2251572	3133		
CG17234	22D5-22D5	-	2253834	2253079	3133		
CG17012	22D5-22D5	-	2255050	2254176	3133		
CG4270	22D6-22D6	-	2264241	2263464	3133		
CG34049	22D6-22D6	-	2265321	2264231	3133		
CG17242	22D6-22D6	-	2269119	2268299	3133		
CG43099	22D6-22D6	-	2280818	2280534	3133		
CG4271	22D6-22D6	-	2285926	2285174	3133		
CG31681	22D6-22D6	-	2286873	2285925	3133		
CG42658	22D6-22D6	-	2287933	2287025	3133		
CG17237	22D6-22D6	-	2289370	2288503	3133		
CG10838	22D6-22D6	robl22E	2290673	2290224	3133		
CG31949	22E1-22E1	-	2300888	2300103	3133		
CG16995	22E1-22E1	-	2308671	2307948	3133		
CG9967	22E1-22E1	-	2357332	2308758	3133		
CG33955	22E1-22E1	eyes shut	2358181	2311693	3133		
CG3664	22E1-22E1	Rab-protein 5	2365362	2359546	3133		
CG4272	22E1-22E1	-	2370114	2365335	3133		
CG3597	22E1-22E1	-	2371524	2370152	3133		
CG3609	22E1-22E1	-	2374553	2372455	3133		
CG15390	22E1-22E1	-	2375697	2374689	3133		
CG9866	22E1-22E1	-	2380514	2375894	3133		
CG9867	22E1-22E1	-	2383077	2381140	3133		
CG9870	22E1-22E1	-	2384731	2383299	3133		
CG3557	22E1-22E1	-	2385792	2384761	3133		
CG9887	22E1-22E1	Vesicular glutamate transporter	2410668	2400306	3133		
CG18641	22E1-22E1	-	2412129	2410884	3133		
CG31948	22E1-22E1	-	2416720	2415434	3133		
CG34448	22E1-22E1	-	2417965	2416809	3133		
CG34447	22E1-22E1	-	2420010	2418422	3133		
CG9886	22E1-22E1	-	2422915	2420808	3133		
CG9885	22F1-22F3	decapentaplegic	2459609	2428454			
CR31986	22F3-22F3	transfer RNA:tyr1:22Fb	2460044	2459924			
CR31987	22F3-22F3	transfer RNA:tyr1:22Fa	2462686	2462593			
CG15393	22F3-22F3	-	2490119	2489754			
CG3539	22F3-22F4	SLY-1 homologous	2492666	2490205			
CG9884	22F4-22F4	out at first	2498846	2492955			
CG3528	22F4-22F4	-	2518037	2517102	90		
CG3515	22F4-22F4	-	2552844	2551144	90		
CG9964	22F4-23A1	Cyp309a1	2564848	2562885	90		
CG18559	23A1-23A1	Cyp309a2	2573047	2564882	90		

CG3240	23A1-23A1	Radiation insensitive 1	2575080	2573424	90
CG34314	23A1-23A1	-	2575080	2573424	90
CG3227	23A1-23A1	-	2577006	2575276	90
CG9883	23A1-23A1	-	2579180	2577671	90
CG3214	23A1-23A1	-	2580056	2579217	90
CG9881	23A1-23A1	p16-ARC	2581114	2580291	90
CG3210	23A1-23A1	Dynamin related protein 1	2585448	2581437	90
CG15394	23A1-23A1	-	2592775	2588854	90
CG15395	23A1-23A1	-	2611285	2610146	90
CG9962	23A2-23A2	-	2647720	2646577	90
CG33125	23A2-23A2	-	2652291	2648440	90
CG17301	23A2-23A2	Proteasome beta4R1 subunit	2653931	2653112	90
CG9880	23A2-23A2	Odorant receptor 23a	2655461	2654125	90
CG17302	23A2-23A2	Proteasome beta4R2 subunit	2660830	2655394	90
CG9879	23A2-23A2	-	2666195	2665110	90
CG15396	23A2-23A2	Gustatory receptor 23a	2672159	2669823	90
CG15398	23A2-23A2	-	2696437	2695375	90
CG31690	23A2-23A2	-	2719431	2674825	90
CG31689	23A3-23A3	-	2739833	2730106	90
CG2903	23A3-23A3	Hepatocyte growth factor regulated tyrosine kinase substrate	2743377	2739986	90
CG9961	23A3-23A3	-	2744934	2743366	90
CG2843	23A3-23A3	Cwc25	2746944	2745102	90
CG9894	23A3-23A3	-	2756606	2752799	90
CG9960	23A3-23A3	-	2759710	2758427	90
CG9958	23A3-23A3	snapin	2759710	2758427	90
CG2848	23A3-23A5	Transportin-Serine/Arginine rich	2763610	2759915	90
CG3127	23A3-23B1	Phosphoglycerate kinase	2748522	2746880	90
CG3077	23A5-23A5	-	2765686	2764067	90
CG2855	23A5-23A5	anterior pharynx defective 1	2767154	2766235	90
CG3069	23A5-23A5	TBP-associated factor 10b	2768166	2767281	90
CG2859	23A5-23A5	TBP-associated factor 10	2768612	2767902	90
CG3057	23A5-23A5	congested-like trachea	2770066	2768590	90
CG2862	23A5-23A5	-	2770904	2770136	90
CG15399	23A5-23A5	-	2771776	2770884	90
CG3139	23A6-23B1	Synaptotagmin 1	2799970	2780741	90
CG16987	23B1-23B2	dawdle	2812147	2805518	90
CG2964	23B2-23B2	-	2814429	2812437	90
CG15400	23B2-23B2	-	2815760	2814336	90
CG3123	23B2-23B2	-	2825506	2823546	90
CG3131	23B2-23B3	Dual oxidase	2830236	2815970	90
CG3119	23B3-23B3	-	2837831	2834887	90
CG2973	23B3-23B3	Cuticular protein 23B	2839547	2838414	90
CG2975	23B4-23B4	-	2842638	2840124	90

CG18558	23B4-23B4	-	2844513	2842589	90			
CG18557	23B4-23B4	-	2845711	2844601	90			
CG3117	23B4-23B5	-	2847197	2846084	90			
CG2983	23B5-23B5	-	2848997	2847632	90			
CG3104	23B5-23B5	-	2855749	2849732	90			
CG2986	23B5-23B6	Ribosomal protein S21	2857041	2856070	90			
CG2991	23B6-23B7	-	2868553	2857159	90			
CG8813	23B7-23B8	-	2870649	2869652	90			
CG31694	23B7-23B8	-	2874518	2868627	90			
CG8814	23B8-23C1	-	2877168	2874872	90			
CG3083	23C1-23C1	Peroxiredoxin 6005	2878232	2877091	90			
CG31950	23C1-23C1	-	2879001	2878520	90			
CG18627	23C1-23C1	beta subunit of type II geranylgeranyl transferase	2880708	2879124	90			
CG3059	23C1-23C1	NTPase	2885850	2880704	90			
CG8817	23C1-23C3	lilliputian	2953077	2885952	90	97		
CG3157	23C1-23C4	gamma-Tubulin at 23C	2974862	2972892		97		
CG3151	23C3-23C3	RNA-binding protein 9	2968434	2954762	90	97		
CG3181	23C3-23C3	Ts	2969620	2968293		97		
CG3178	23C3-23C4	Recombination repair protein 1	2972676	2969773		97		
CG9641	23C4-23C4	-	2976859	2974859		97		
CG3165	23C4-23C4	-	2978500	2977132		97		
CG9643	23C4-23C4	-	2979410	2978526		97		
CG3733	23C4-23C4	Chromodomain-helicase-DNA-binding protein 1	2987677	2979699		97		
CG18642	23C4-23C4	Bem46	2990094	2988135		97		
CG3736	23C4-23C4	okra	2992761	2989594		97		
CG3558	23C4-23C4	-	2998614	2992964		97		
CG17265	23C4-23C4	-	3016069	3013501		97		
CG17224	23C4-23C4	-	3018304	3016591		97		
CG17264	23C4-23C4	-	3021506	3018508		97		
CG17223	23C4-23C4	alpha4GT1	3023169	3021309		97		
CG3542	23C4-23C4	-	3026439	3023235		97		
CG3605	23C4-23C4	-	3029189	3026533		97		
CG17219	23C4-23C5	-	3030616	3029251	6875	97		
CG17257	23C5-23C5	beta4GalNAcTB pilot	3032300	3030562	6875	97		
CG17258	23C5-23C5	-	3035348	3032210	6875	97		
CG17259	23C5-23C5	-	3037403	3035493	6875	97		
CG17260	23C5-23C5	-	3038793	3037411	6875	97		
CG17262	23C5-23C5	cornichon related	3039812	3038826	6875	97		
CG17221	23C5-23C5	-	3041626	3039976	6875	97		
CG17261	23C5-23C5	-	3043593	3042919	6875	97		
CR32999	23C5-23C5	small nuclear RNA U5 at 23DE	3048831	3048701	6875	97	9597	
CG3524	23C5-23C5	v(2)k05816	3055601	3043973	6875	97	9597	
CG3523	23C5-23D1	-	3068184	3056615	6875	97	9597	

CG8822	23D1-23D1	Protein phosphatase D6	3110998	3109672	6875	97		9597			
CG9660	23D1-23D2	toucan	3144613	3068339	6875	97	4954	9597			
CG15403	23D2-23D2	-	3129464	3128720	6875	97	4954	9597			
CG12400	23D3-23D3	-	3145719	3145125	6875		4954	9597			
CG12399	23D3-23D3	Mothers against dpp	3159630	3146484	6875		4954	9597			
CG8825	23D4-23D4	glaikit	3162403	3159956	6875		4954	9597			
CG31953	23D4-23D4	-	3163147	3162515	6875		4954	9597			
CG3488	23D4-23D4	alpha/beta hydrolase2	3168999	3163647	6875		4954	9597			
CR31734	23D4-23D4	transfer RNA:ser7:23Eb	3169663	3169582	6875		4954				
CG34406	23D4-23D4	-	3172751	3169813	6875		4954				
CR31951	23D4-23D4	transfer RNA:ser7:23Ea	3173084	3173003	6875		4954				
CG31698	23D4-23D4	-	3173826	3173283	6875		4954				
CG15404	23D4-23D4	-	3174442	3173989	6875		4954				
CG34393	23D5-23D5	-	3199620	3175112	6875		4954				
CG3347	23E1-23E1	-	3271806	3269437	6875		4954				
CG3332	23E1-23E1	-	3280533	3275794	6875		4954				
CG9664	23E1-23E1	-	3294706	3291245	6875		4954				
CG9663	23E1-23E3	-	3303129	3294926	6875		4954	7786			
CG15406	23E3-23E3	-	3311684	3309222			4954	7786			
CG3277	23E3-23E3	-	3317086	3313347			4954	7786			
CG3326	23E3-23E3	-	3319872	3317476			4954	7786			
CG8837	23E3-23E4	-	3323141	3320255			4954	7786			
CG33281	23E4-23E4	-	3326637	3324234				7786			
CG33282	23E4-23E4	-	3329792	3327903				7786			
CG3285	23E4-23E4	-	3332876	3330930				7786			
CG15408	23E4-23E4	-	3334790	3332814				7786			
CG3327	23E4-23E5	Early gene at 23	3355000	3334871				7786			
CG8838	23E5-23E5	-	3358618	3357684							
CG34394	23E5-23E6	-	3373047	3358640							
CG15412	23F1-23F1	-	3375711	3373567							
CG9662	23F1-23F1	-	3376686	3375883							
CG3289	23F1-23F1	Phosphotyrosyl phosphatase activator	3378586	3377008							
CG42459	23F1-23F1	Seminal fluid protein 23F	3387743	3387392							
CG42460	23F1-23F1	-	3388496	3387898							
CG34175	23F1-23F1	-	3398684	3398023							
CG8840	23F1-23F1	-	3411199	3410610							
CG31952	23F1-23F1	-	3417869	3416693							
CG3254	23F1-23F1	polypeptide GalNAc transferase 2	3426642	3404460							
CG2772	23F3-23F3	-	3447591	3445997	6502	6507					
CG2774	23F3-23F3	-	3452106	3449686	6502	6507					
CG12795	23F3-23F3	-	3453596	3452451	6502	6507					
CG3248	23F3-23F3	Cog3	3457058	3453697	6502	6507					
CG8843	23F3-23F3	sec5	3460371	3457329	6502	6507					

CG3246	23F3-23F3	-	3461975	3460315	6502	6507			
CG3241	23F3-23F3	male-specific lethal 2	3466111	3462213	6502	6507			
CG8844	23F3-23F3	Pdsw	3467326	3466162	6502	6507			
CG3238	23F3-23F3	-	3470007	3467416	6502	6507			
CG31776	23F3-23F3	-	3472368	3470182	6502	6507			
CG31956	23F3-23F3	polypeptide GalNAc transferase 4	3475338	3472735	6502	6507			
CG8846	23F3-23F6	Thor	3479612	3478434	6502	6507			
CG15414	23F3-23F6	-	3491048	3480755	6502	6507			
CG3234	23F6-23F6	timeless	3507754	3493986	6502	6507			
CG31954	23F6-23F6	-	3510082	3509058	6502	6507			
CG33123	23F6-23F6	-	3514662	3510477	6502	6507			
CG17593	23F6-23F6	-	3517111	3514737	6502	6507			
CG3213	23F6-23F6	-	3519697	3517273	6502	6507			
CG8851	23F6-23F6	-	3522555	3520262	6502	6507			
CG3212	23F6-23F6	Scavenger receptor class C, type IV	3523960	3522594	6502	6507			
CG8852	23F6-24A1	-	3527588	3525133	6502	6507			
CG15415	24A1-24A1	Spindly	3530317	3527387	6502	6507			
CG8853	24A1-24A1	-	3532526	3530903	6502	6507			
CG10016	24A1-24A1	drumstick	3548086	3539251	6502	6507			
CG3242	24A1-24A1	sister of odd and bowl	3580766	3578010	6502	6507			
CG3851	24A1-24A1	odd skipped	3606748	3604222	6502	6507			
CG2788	24A1-24A2	Dorothy	3621573	3619191	6502	6507	5330		
CG15418	24A2-24A2	-	3621681	3621090		6507	5330		
CG10033	24A2-24A4	foraging	3656951	3622071		6507	5330		
CG34340	24A5-24B1	-	3691737	3662745			5330		
CG42461	24B1-24B1	Seminal fluid protein 24Ba	3668551	3667977			5330		
CG42463	24B1-24B1	-	3669134	3668691			5330		
CG42462	24B1-24B1	Seminal fluid protein 24Bb	3669775	3669261			5330		
CG42602	24B1-24B1	Seminal fluid protein 24Bc	3670581	3670131			5330		
CG16704	24B1-24B1	-	3692588	3692138			5330		
CG3513	24B1-24B1	-	3693182	3692699			5330		
CG31779	24B1-24B1	Acp24A4	3693889	3693184			5330		
CR43364	24B2-24B2	-	3694371	3694105			5330		
CG43165	24B2-24B2	-	3694938	3694204			5330		
CG16713	24B2-24B3	-	3695406	3695032			5330		
CG16712	24B3-24B3	-	3696661	3696240			5330		
CG3604	24B3-24B3	-	3697872	3697242			5330		
CG10031	24B3-24C1	-	3699091	3698451			5330		
CG42464	24C1-24C1	-	3699819	3699493			5330		
CG42465	24C1-24C1	-	3700658	3700195			5330		
CG42466	24C1-24C1	Seminal fluid protein 24C1	3701092	3700674			5330		
CG42467	24C1-24C1	-	3701699	3701307			5330		
CG43145	24C1-24C1	-	3702131	3701848			5330		

CG2816	24C1-24C1	-	3704253	3703659	5330		
CG31778	24C1-24C1	-	3705462	3704106	5330		
CG31777	24C1-24C1	-	3707060	3706543	5330		
CG33122	24C1-24C1	cutlet	3711722	3707230	5330		
CG31955	24C1-24C1	-	3712862	3712154	5330		
CG2818	24C1-24C1	-	3716810	3713374	5330		
CG3410	24C1-24C1	lectin-24A	3717773	3716800	5330		
CG2822	24C1-24C2	Shaker cognate w	3727587	3718187	5330		
CG10019	24C2-24C3	-	3752309	3745692	5330		
CG31959	24C3-24C3	-	3759212	3757631	5330		
CR42926	24C3-24C3	mir-1004 stem loop	3767688	3767621	5330		
CG31772	24C3-24C3	-	3768191	3760068	5330		
CG10021	24C3-24C4	brother of odd with entrails limited	3784129	3771706	5330		
CG31960	24C4-24C4	-	3785515	3784946	5330		
CG31958	24C4-24C4	-	3786292	3785819	5330		
CG3921	24C5-24C5	-	3802245	3790663	5330		
CG3920	24C5-24C5	lethal (2) k16918	3809064	3803581	5330		
CG3407	24C5-24C5	-	3813407	3810799	5330		
CG16738	24C6-24C6	sloppy paired 1	3827137	3825680	5330		
CG2939	24C7-24C7	sloppy paired 2	3839201	3836842	5330		
CG3964	24C8-24C8	-	3867507	3862681	5330		
CG3980	24C8-24C8	-	3871425	3867714	5330		
CG31957	24C8-24C8	-	3872458	3871480	5330		
CG3399	24C8-24C9	cappuccino	3902860	3872658	5330		
CG31773	24C9-24D1	-	3914288	3911790	5330		
CG31774	24C9-24D1	friend of echinoid	3947160	3905524	5330		
CG34176	24D3-24D3	-	4004480	4004080	5330		
CG15422	24D3-24D3	-	4005670	4004984	5330		
CG15423	24D3-24D3	-	4006606	4006041	5330		
CG10039	24D3-24D3	-	4008999	4007690	5330		
CG12676	24D4-24D6	echinoid	4115059	4031379	5330		
CR34661	24D5-24D5	-	4086005	4085890			
CG31962	24D6-24D6	Scavenger receptor class C, type III	4121442	4120363			
CG4099	24D6-24D6	Scavenger receptor class C, type I	4124002	4121721			
CG2955	24D6-24D6	-	4151203	4149279			
CG11767	24D7-24D7	Odorant receptor 24a	4166134	4164689			
CG31961	24D8-24D8	-	4187789	4186245			
CG2958	24D8-24D8	lectin-24Db	4189285	4188123			
CG3714	24D8-24D8	-	4198058	4189497			
CG3352	24D8-24D8	fat	4217852	4198402			
CG3702	24D8-24E1	-	4227097	4224650			
CG2960	24E1-24E1	Ribosomal protein L40	4228563	4227642			
CG15425	24E1-24E1	-	4258425	4257572			

CG3675	24E1-24E1	Arginine methyltransferase 2	4279315	4277696
CG15427	24E1-24E1	turtle	4321233	4283147
CG16857	24E1-24E1	-	4331837	4324573
CR42895	24E1-24E1	mir-1005 stem loop	4343756	4343696
CG2969	24E1-24E1	ABC transporter expressed in trachea	4345776	4333926
CG15429	24E1-24E1	-	4354030	4352975
CG3048	24E1-24E4	TNF-receptor-associated factor 4	4380725	4362549
CG17612	24E4-24E4	-	4382719	4380508
CG3338	24E4-24E4	-	4386062	4382920
CG4104	24E4-24E5	Trehalose-6-phosphate synthase 1	4392788	4388321
CG3652	24E5-24E5	-	4393851	4392770
CG3054	24E5-24F1	lethal (2) k05819	4400105	4394198
CG18013	24F1-24F1	Psf2	4387046	4386176
CG33003	24F1-24F1	-	4403091	4400953
CG3058	24F1-24F1	Dim1	4403955	4403255
CG43055	24F1-24F1	-	4411824	4411157
CG15431	24F1-24F2	-	4439547	4406129
CR31963	24F2-24F2	transfer RNA:CR31963	4419048	4418977
CG34177	24F2-24F2	-	4435057	4433908
CG34178	24F2-24F2	-	4435057	4433908
CG43056	24F2-24F2	-	4438201	4437787
CG42468	24F2-24F2	Seminal fluid protein 24F	4442060	4441429
CG15432	24F2-24F2	-	4442985	4442429
CG15437	24F2-24F2	modifier of rpr and grim, ubiquitously expressed	4444677	4442870
CG15433	24F2-24F2	Elongator complex protein 3	4446765	4444732
CG15438	24F2-24F3	-	4448637	4446662
CG15439	24F3-24F3	-	4453004	4449289
CG15440	24F3-24F3	-	4454457	4453167
CG15434	24F3-24F3	-	4455207	4454664
CG15441	24F3-24F3	GS1-like	4456822	4455193
CR33674	24F3-24F3	-	4457674	4457603
CG33002	24F3-24F3	mitochondrial ribosomal protein L27	4459602	4458980
CG15435	24F3-24F3	-	4461746	4459835
CG15443	24F3-24F3	-	4462994	4461657
CG15436	24F3-24F4	-	4465075	4463642
CG17840	24F4-24F4	-	4468022	4465200
CG15444	24F4-24F4	inebriated	4477024	4468000
CG33196	24F4-25A1	dumpy	4591963	4479471
CG15442	24F8-24F8	Ribosomal protein L27A	4458373	4457186
CG15636	25A1-25A1	Heterochromatin protein 6	4578201	4577719
CG34102	25A2-25A2	BG642163	4642747	4641296
CG15635	25A2-25A2	-	4646472	4642998
CG3355	25A2-25A2	-	4652877	4651403

CG12205	25A3-25A3	Blastoderm-specific gene 25A	4684459	4683050
CG11929	25A3-25A3	-	4687235	4682677
CG15634	25A3-25A3	-	4688956	4687513
CG3251	25A3-25A3	-	4690702	4688965
CG15632	25A3-25A3	TBP-associated factor 30kD subunit alpha-2	4701588	4700941
CG34351	25A3-25A3	-	4722468	4694721
CG15631	25A4-25A4	-	4734458	4732413
CG42523	25A4-25A4	-	4763537	4762937
CG15630	25A4-25A6	-	4794040	4734592
CG3294	25A6-25A6	-	4796576	4794549
CG3244	25A6-25A6	C-type lectin 27kD	4801923	4796584
CG15629	25A6-25A6	-	4815891	4813025
CG3225	25A6-25A7	-	4818210	4815613
CG15628	25A7-25A8	-	4828552	4821776
CG2976	25A8-25A8	-	4830686	4829381
CG15627	25A8-25A8	Ionotropic receptor 25a	4835300	4830846
CG15626	25A8-25A8	-	4837996	4835333
CG12194	25A8-25A8	-	4841465	4839219
CG2950	25A8-25B1	-	4847292	4842086
CG11927	25B1-25B1	-	4849499	4847748
CG2937	25B1-25B1	mitochondrial ribosomal protein S2	4850418	4849439
CG11926	25B1-25B1	-	4852640	4850639
CG31660	25B1-25B1	poor gastrulation	4875233	4852865
CG11924	25B1-25B1	Chorion factor 2	4883341	4876890
CG3008	25B1-25B1	-	4885669	4883171
CG15625	25B1-25B1	-	4891378	4889995
CG3036	25B1-25B2	-	4903889	4892115
CG2837	25B2-25B3	-	4906761	4904068
CG12787	25B3-25B3	hoepel1	4932296	4908745
CG15624	25B4-25B4	hoepel2	4936582	4933047
CG3047	25B4-25B4	Salivary gland secretion 1	4941424	4937409
CG14044	25B4-25B4	-	4944305	4942748
CG8849	25B4-25B4	mitochondrial ribosomal protein L24	4945343	4944256
CG3469	25B4-25B4	beta subunit of type I geranylgeranyl transferase	4948321	4945598
CG8873	25B4-25B4	jetlag	4949751	4948202
CG8871	25B4-25B4	Jonah 25Biii	4950763	4949947
CG8869	25B4-25B4	Jonah 25Bii	4953134	4952250
CG8867	25B4-25B4	Jonah 25Bi	4955353	4954071
CG3753	25B4-25B4	Marcal1	4958292	4955519
CG34124	25B4-25B5	-	4965432	4958411
CG34125	25B5-25B5	-	4966400	4965694
CG8882	25B5-25B5	Trip1	4967778	4966367
CG8885	25B5-25B5	Synthesis of cytochrome c oxidase	4968936	4967832

CG3756	25B5-25B5	-	4970216	4969004
CG8886	25B5-25B5	lethal (2) 05714	4971453	4970135
CG14043	25B5-25B5	-	4973687	4971704
CG3782	25B5-25B5	mitochondrial ribosomal protein L28	4975284	4973978
CG8890	25B5-25B5	GDP-mannose 4,6-dehydratase	4977018	4975300
CG3792	25B5-25B5	-	4978567	4977266
CG8891	25B5-25B5	-	4979339	4978484
CG8892	25B5-25B5	-	4981588	4979513
CG34126	25B5-25B9	-	4992436	4981646
CG33113	25B9-25C1	Rtnl1	5009744	4993641
CR33915	25C10-25C10	small non-messenger RNA 128	5196097	5196035
CR34569	25C10-25C10	snoRNA:Psi18S-525k	5202522	5202383
CR33749	25C10-25C10	small non-messenger RNA 158	5206361	5206205
CG6081	25C10-25C10	Cyp28d2	5209345	5207308
CG10833	25C10-25C10	Cyp28d1	5212445	5210461
CG7742	25C10-25D1	-	5214730	5212395
CG31917	25C1-25C1	-	5010825	5009931
CG42373	25C1-25C1	-	5010825	5009931
CG3887	25C1-25C1	-	5012127	5011081
CG16858	25C1-25C1	viking	5027412	5012144
CG4145	25C1-25C1	Collagen type IV	5037114	5029615
CG14042	25C1-25C1	-	5040816	5038053
CG14041	25C1-25C1	SP555	5040818	5038053
CG31650	25C1-25C1	-	5044712	5040648
CG31919	25C1-25C1	-	5048366	5043269
CG33995	25C1-25C1	-	5048366	5043269
CG9121	25C1-25C3	-	5050877	5047818
CG9124	25C3-25C3	Eukaryotic initiation factor 3 p40 subunit	5053209	5051193
CG14040	25C3-25C3	-	5054575	5052846
CG14036	25C3-25C3	-	5055004	5054579
CG5825	25C3-25C3	Histone H3.3A	5055995	5055058
CG31918	25C3-25C3	-	5058241	5055982
CG18174	25C3-25C3	Rpn11	5059816	5058404
CG14039	25C3-25C4	quick-to-court	5070750	5060832
CR42920	25C4-25C4	mir-2495 stem loop	5068684	5068570
CG5827	25C4-25C4	Ribosomal protein L37A	5072055	5070957
CG31651	25C4-25C6	polypeptide GalNAc transferase 5	5093590	5072156
CG42768	25C6-25C10	Muscle-specific protein 300	5205690	5100877
CG5828	25C6-25C6	-	5095439	5094021
CG4230	25C6-25C6	-	5098613	5096227
CG8680	25C6-25C6	-	5100214	5099500
CR34568	25C9-25C9	snoRNA:Psi28S-2263	5187922	5187778
CR33789	25C9-25C9	small non-messenger RNA 765	5193516	5193471

CG14034	25D1-25D1	-	5216533	5215211	
CG6514	25D1-25D1	Troponin C at 25D	5219059	5218260	
CG14026	25D1-25D2	thickveins	5271353	5218996	6224
CR31971	25D2-25D2	transfer RNA:CR31971	5240837	5240766	6224
CR31914	25D2-25D2	transfer RNA:CR31914	5241177	5241106	6224
CR14033	25D2-25D2	-	5244239	5242707	6224
CG14032	25D2-25D2	Cyp4ac1	5265899	5264001	6224
CG17970	25D2-25D2	Cyp4ac2	5268455	5266392	6224
CG14031	25D2-25D2	Cyp4ac3	5270329	5268517	6224
CG14025	25D2-25D3	Blastoderm-specific gene 25D	5278558	5271728	6224
CG14030	25D3-25D3	Bub1 homologue	5283002	5279051	6224
CG14029	25D4-25D5	vrille	5310996	5299647	6224
CG14024	25D5-25D5	-	5314885	5312136	6224
CG14023	25D5-25D6	-	5324936	5316240	6224
CG14028	25D6-25D6	cyclope	5328000	5327241	6224
CG14022	25D6-25D6	-	5328870	5327978	6224
CG14027	25D6-25D6	Turandot M	5330466	5329857	6224
CG14021	25D6-25D6	fuseless	5338053	5330468	6224
CG12512	25D6-25D6	-	5342349	5339132	6224
CG11020	25D6-25D7	no mechanoreceptor potential C	5365039	5342321	6224
CG42850	25E1-25E1	-	5381054	5379433	6224
CG6604	25E1-25E1	H15	5415928	5404342	6224
CR34662	25E2-25E2	-	5437749	5437634	6224
CG31647	25E2-25E2	-	5439277	5435582	6224
CG6634	25E2-25E2	midline	5467609	5461641	6224
CG14020	25E5-25E5	-	5518949	5517823	6224
CG7382	25E5-25E5	-	5519889	5518893	6224
CG11024	25E5-25E5	clot	5521382	5520235	6224
CG7371	25E5-25E5	-	5523877	5521281	6224
CG6907	25E5-25E5	-	5525809	5524139	6224
CG31648	25E5-25E5	-	5527854	5526962	6224
CG31915	25E5-25E5	-	5530682	5528087	6224
CG7277	25E5-25E5	-	5532195	5530620	6224
CG14016	25E5-25E5	tombola	5536726	5535933	6224
CG31989	25E5-25E5	Chromosome associated protein D3	5537108	5525905	6224
CG14015	25E5-25E6	-	5539169	5536850	6224
CG7269	25E6-25E6	Helicase at 25E	5542310	5539326	6224
CG6944	25E6-25E6	Lamin	5546642	5542527	6224
CG6957	25E6-25E6	Oscillin	5549614	5547203	6224
CG14014	25E6-25E6	-	5550835	5549707	6224
CG18269	25E6-25E6	-	5552648	5552046	6224
CG14013	25E6-25E6	-	5553848	5552843	6224
CG14017	25E6-25E6	-	5555137	5553897	6224

CG6992	25E6-25E6	Glutamate receptor IIA	5558994	5555074	6224		
CG7234	25E6-25E6	Glutamate receptor IIB	5563502	5559342	6224		
CR32998	25E6-25E6	snRNA:U4:25F	5565766	5565619	6224		
CG14011	25F1-25F1	-	5581116	5579580	6224		
CG7251	25F1-25F1	-	5588414	5587149	6224		
CG18266	25F1-25F1	-	5598636	5596833	6224		
CG14010	25F1-25F1	-	5617747	5602958	6224		
CR7249	25F1-25F1	Cyp6a16Psi	5623760	5621602	6224		
CG31646	25F1-25F2	-	5658553	5626291	6224	1712	
CR42963	25F2-25F2	mir-959 stem loop	5641037	5640940	6224	1712	
CR43028	25F2-25F2	mir-960 stem loop	5641155	5641063	6224	1712	
CR42946	25F2-25F2	mir-961 stem loop	5641279	5641191	6224	1712	
CR42907	25F2-25F2	mir-962 stem loop	5641389	5641298	6224	1712	
CR43040	25F2-25F2	mir-963 stem loop	5642078	5641990	6224	1712	
CR42950	25F2-25F2	mir-964 stem loop	5642201	5642102	6224	1712	
CG7235	25F2-25F2	Hsp60C	5670838	5662849	6224	1712	
CG12511	25F2-25F2	-	5679223	5678638	6224	1712	
CG7236	25F3-25F3	-	5713648	5708449	6224	1712	490
CG14007	25F3-25F3	-	5716650	5715491	6224	1712	490
CG34011	25F3-25F3	-	5718067	5716819	6224	1712	490
CG11149	25F3-25F3	-	5720896	5718121	6224	1712	490
CG7238	25F3-25F3	septin interacting protein 1	5723791	5721039	6224	1712	490
CG11030	25F3-25F4	-	5760047	5724658	6224	1712	490
CG14006	25F4-25F4	-	5728811	5727221	6224	1712	490
CG11147	25F4-25F4	-	5741244	5733675	6224	1712	490
CG11029	25F4-25F4	-	5747620	5746277	6224	1712	490
CG11142	25F4-25F4	obstructor-E	5766141	5762553	6224	1712	490
CG31913	25F4-25F4	-	5784893	5784031	6224	1712	490
CG9171	25F4-25F5	-	5800204	5768250	6224	1712	490
CG14005	25F5-25F5	-	5801969	5800517		1712	490
CG7239	25F5-25F5	-	5804030	5802255		1712	490
CG11034	25F5-25F5	-	5808858	5805395		1712	490
CG43307	25F5-25F5	-	5811925	5811574		1712	490
CG31644	25F5-25F5	-	5818393	5817890		1712	490
CG34381	25F5-26A1	-	5856757	5824842		1712	490
CG8965	26A1-26A1	-	5879481	5859762			490
CG42469	26A1-26A1	Seminal fluid protein 26Ac	5884774	5884350			490
CG43185	26A1-26A1	-	5885457	5884932			490
CG9029	26A1-26A1	-	5886609	5886016			490
CG9024	26A1-26A1	Accessory gland-specific peptide 26Ab	5892862	5892298			490
CG8982	26A1-26A1	Accessory gland-specific peptide 26Aa	5893896	5892883			490
CG9021	26A1-26A1	-	5904674	5903359			490
CG14000	26A1-26A1	-	5910289	5908906			490

CG14001	26A1-26A1	blue cheese	5921242	5907180	490		
CG9016	26A1-26A1	-	5923646	5922904	490		
CG9019	26A1-26A2	dissatisfaction	5938767	5925937	490		
CG42603	26A3-26A3	Seminal fluid protein 26Ad	5943263	5942781	490		
CG9042	26A3-26A3	Glycerol 3 phosphate dehydrogenase	5949092	5943682	490		
CG9044	26A3-26A3	-	5955238	5949484	490		
CG13999	26A3-26A3	-	5956466	5955312	490		
CG13998	26A3-26A3	-	5956805	5956512	490		
CG9046	26A3-26A3	Vitelline membrane 26Ab	5957628	5957004	490		
CG13997	26A3-26A3	Vitelline membrane 26Aac	5958631	5958005	490		
CG9048	26A3-26A3	Vitelline membrane 26Aa	5960340	5959700	490		
CG9050	26A4-26A4	palisade	5964322	5963087	490		
CG13992	26A4-26A4	-	5967632	5965519	490		
CG9064	26A4-26A5	Ucp4C	5969761	5968597	490		
CG18340	26A5-26A5	Ucp4B	5971025	5969871	490		
CG9553	26A5-26B2	chickadee	5981025	5972900	490		
CG34380	26B11-26B11	-	6209477	6179514	490		
CG9481	26B11-26B11	UDP-glycosyltransferase 37b1	6226842	6225050	490		
CG9075	26B2-26B2	Eukaryotic initiation factor 4a	5985572	5981759	490		
CG9078	26B2-26B2	infertile crescent	5988858	5986324	490		
CG9088	26B2-26B2	little imaginal discs	5999483	5990441	490		
CG9093	26B2-26B2	Tetraspanin 26A	6003740	6000231	490		
CG9092	26B2-26B2	beta galactosidase	6006791	6003574	490		
CG9098	26B2-26B2	-	6012338	6007364	490		
CG11607	26B2-26B3	Homeodomain protein 2.0	6019398	6013057	490		
CG13996	26B3-26B3	-	6021672	6020850	490		
CG9107	26B3-26B3	-	6024545	6022951	490		
CG9109	26B3-26B3	-	6034423	6025870	490		
CG9115	26B3-26B3	myotubularin	6036937	6034796	490		
CG9117	26B3-26B3	-	6037902	6036997	490		
CG31643	26B3-26B3	-	6041283	6038161	490		
CR43024	26B3-26B3	mir-966 stem loop	6045713	6045627	490		
CG9127	26B3-26B3	adenosine 2	6045970	6041178	490		
CG9131	26B3-26B3	slowmo	6048702	6046646	490		
CG34179	26B3-26B3	-	6048702	6046650	490		
CG12393	26B3-26B3	-	6050474	6047999	490		
CG9135	26B3-26B3	-	6053498	6050829	490		
CG13995	26B3-26B4	-	6060169	6054307	490		
CG34180	26B4-26B4	-	6060940	6060510	490		
CG9140	26B4-26B4	-	6062757	6060835	490		
CG13994	26B4-26B4	-	6063676	6063018	490		
CG9144	26B4-26B4	-	6065949	6063562	490		
CG9147	26B4-26B4	-	6067635	6066186	490		

CG9150	26B4-26B4	-	6068635	6067668	490		
CG13993	26B4-26B4	-	6069838	6069079	490		
CG9154	26B4-26B4	-	6070646	6069790	490		
CG9159	26B4-26B4	Kruppel homolog 2	6073961	6070990	490		
CG9162	26B4-26B4	-	6079737	6078453	490		
CG18783	26B5-26B5	Kruppel homolog 1	6096498	6081808	490		
CG9175	26B5-26B5	-	6098964	6096698	490		
CG31641	26B5-26B7	stathmin	6124412	6100378	490		
CG31642	26B7-26B7	-	6120522	6118512	490		
CG5972	26B7-26B7	Arc-p20	6125911	6125138	490		
CG9226	26B7-26B7	WD repeat domain 79 homolog	6127762	6125889	490		
CG42730	26B7-26B8	-	6130659	6127872	490		
CG42731	26B7-26B8	tectonic	6130659	6127872	490		
CG9222	26B8-26B8	-	6132484	6131023	490		
CG13991	26B8-26B8	-	6145011	6139461	490		
CG13990	26B8-26B8	Mucin 26B	6153701	6151971	490		
CG31639	26B8-26B9	-	6155088	6153840	490		
CG13989	26B9-26B9	-	6161082	6160444	490		
CG9486	26C1-26C1	-	6256715	6255859	490		
CG13983	26C1-26C1	-	6264487	6263557	490		
CG42735	26C1-26C1	-	6271511	6271200	490		
CG33531	26C1-26C2	Discoidin domain receptor	6322251	6253123	490		
CG13984	26C2-26C2	-	6309475	6308819	490		
CG9491	26C2-26C3	Gef26	6331552	6323767	490		
CG9493	26C3-26C3	Pez	6338493	6332876	490		
CG11567	26C3-26C3	Cytochrome P450 reductase	6346282	6338772	490		
CG9497	26C3-26C3	-	6348151	6346542	490		
CG9498	26C3-26C3	-	6351028	6349393	490		
CG9499	26C3-26C3	pickpocket 7	6354331	6352324	490		
CG9501	26C3-26C3	pickpocket 14	6356498	6354956	490		
CG9500	26C3-26C3	-	6358235	6357251	490		
CG9505	26C4-26C4	-	6370195	6367884	490		
CG9506	26C4-26C4	slow as molasses	6377287	6372415	490		
CG9507	26C4-26C4	-	6383421	6381266	490		
CG42370	26C4-26D1	-	6385512	6383545	490		
CG42368	26C4-26D1	-	6411306	6377767	490		
CG42369	26D1-26D1	-	6397249	6395853	490		
CG13982	26D1-26D1	-	6415344	6412315	490		
CG11527	26D1-26D1	Tiggrin	6423308	6415257	490		
CG9523	26D1-26D1	-	6426373	6424337	490		
CG9527	26D1-26D1	-	6448016	6445070	490		
CG9528	26D4-26D5	real-time	6455934	6448801	490		
CG9526	26D5-26D5	farjavit	6459008	6456106	490		

CG16947	26D5-26D6	-	6463843	6459079		490	
CG9531	26D7-26D7	-	6467700	6466217		490	
CG9535	26D7-26D7	mummy	6473919	6468538		490	
CG9536	26D7-26D7	-	6476972	6474438		490	
CG9539	26D7-26D8	Sec61alpha	6480489	6477182		490	
CG9537	26D8-26D9	Daxx-like protein	6487585	6480956		490	
CG9542	26D9-26D9	-	6488615	6487562		490	
CG9543	26D9-26D9	epsilonCOP	6490195	6489092		490	
CG9548	26D9-26D9	-	6490828	6490151		490	
CG9547	26D9-26D9	-	6494527	6492972		490	
CG31638	26D9-26D9	-	6496986	6491122		490	
CG9550	26D9-26D9	-	6498455	6497053		490	
CG31637	26D9-26E1	-	6526996	6498642	6374	490	
CG9554	26E1-26E2	eyes absent	6546972	6527447	6374		
CG9595	26E3-26E3	osm-6	6557359	6555811	6374		
CG11015	26E3-26E3	-	6559308	6557800	6374		
CG11043	26E3-26E3	-	6560133	6559431	6374		
CG9596	26E3-26E3	-	6561660	6560131	6374		
CG31911	26E3-26E3	Equilibrative nucleoside transporter 2	6564396	6562318	6374		
CG13766	26E3-26E3	-	6566587	6564363	6374		
CG11319	26E3-26F1	-	6601066	6568390	6374		
CG11050	26F1-26F1	-	6617117	6611023	6374		
CG11320	26F1-26F3	-	6621700	6617134	6374		
CG34345	26F3-26F3	-	6625361	6623123	6374		
CG31634	26F3-26F3	Organic anion transporting polypeptide 26F	6632404	6625128	6374		
CG31635	26F3-26F3	-	6649088	6634549	6374		
CG11098	26F3-26F5	Transport and Golgi organization 1	6654574	6649430	6374		
CG31633	26F5-26F5	-	6656315	6654760	6374		
CG31636	26F5-26F5	-	6657879	6656459	6374		
CG11070	26F5-26F6	-	6662033	6658507	6374		
CG13771	26F6-26F6	-	6663614	6662060	6374		
CG9232	26F6-26F6	-	6668031	6666264	6374		
CG11331	26F6-26F6	Serpin 27A	6673344	6671778	6374		
CG34310	26F6-26F7	-	6674525	6673963	6374		
CG11181	26F6-26F7	cup	6674790	6663965	6374		
CG11330	26F7-26F7	cortex	6676635	6674637	6374		
CG11329	26F7-26F7	-	6677606	6676729	6374		
CG11328	26F7-26F7	Na[+]/H[+] hydrogen exchanger 3	6684357	6677835	6374		
CG11327	26F7-26F7	-	6686995	6684845	6374		
CG11326	26F7-27A1	Thrombospondin	6709085	6686786	6374		
CG11325	27A1-27A1	Gonadotropin-releasing hormone receptor	6716183	6711286	6374		
CG11188	27A1-27A1	-	6719389	6717627	6374		
CG11324	27A1-27A1	homer	6723355	6720395	6374		

CG11199	27A1-27A2	Liprin-alpha	6731346	6723907	6374		
CG11201	27A2-27A2	Tubulin tyrosine ligase-like 3B	6736049	6732866	6374		
CG11323	27A2-27A2	Tubulin tyrosine ligase-like 3A	6740176	6736449	6374		
CR34663	27A2-27A2	-	6745078	6745000	6374		
CG31910	27A2-27A2	-	6745609	6744656	6374		
CG11221	27A2-27B1	-	6755686	6742508	6374		
CG11322	27B1-27B1	-	6759628	6757864	6374		
CG11321	27B1-27B1	-	6770949	6760527	6374		
CG17378	27B1-27B1	-	6778456	6774039	6374		
CG9258	27B1-27B1	nervana 1	6786856	6778554	6374		
CG9261	27B1-27B2	nervana 2	6798864	6789761	6374		
CR31631	27B2-27B2	transfer RNA:CR31631	6799816	6799744	6374		
CG17376	27B2-27B3	-	6800834	6799946	6374		
CG17377	27B3-27B3	-	6802830	6801363	6374		
CG11236	27B3-27B3	-	6804372	6803033	6374		
CG17375	27B3-27B3	-	6805792	6804619	6374		
CG31632	27B4-27B4	senseless-2	6839005	6822317	6374		
CG10800	27C1-27C1	Regulator of cyclin A1	6853876	6852324	6374		
CG10806	27C1-27C1	Na[+]/H[+] hydrogen antiporter 1	6870387	6860903	6374		
CG10805	27C1-27C2	lethal (2) k09022	6860864	6854170	6374		
CR42912	27C3-27C3	mir-932 stem loop	6902152	6902062			
CG13772	27C3-27C4	neuroligin	6906661	6896830			
CG13773	27C4-27C4	-	6907817	6906918			
CG10354	27C4-27C4	-	6911432	6908087			
CG4488	27C4-27C4	wee	6914137	6911338			
CG32829	27C4-27C4	-	6916387	6915683			
CG10206	27C4-27C4	nop5	6918741	6916753			
CG10203	27C4-27C4	xl6	6920274	6914300			
CG10377	27C4-27C4	Heterogeneous nuclear ribonucleoprotein at 27C	6926046	6920693			
CG43232	27C4-27C4	-	6932552	6932244			
CG18304	27C4-27C6	-	6942814	6932685	1357		
CG10158	27C6-27C6	-	6945284	6943740	1357		
CG9211	27C6-27C6	interference hedgehog	6948778	6945458	1357		
CG9207	27C6-27C6	Gas41	6950135	6949310	1357		
CG3423	27C7-27C7	Stromalin	6954590	6950440	1357		
CG13775	27C7-27C7	-	6956872	6954585	1357		
CG3430	27C7-27C7	-	6959104	6957010	1357		
CG9200	27C7-27C7	ATAC component 1	6960285	6959099	1357		
CG10399	27C7-27C7	-	6961552	6960426	1357		
CG9188	27C7-27C7	septin interacting protein 2	6964073	6961516	1357		
CG3433	27C7-27C7	Coproporphyrinogen oxidase	6965812	6964390	1357		
CG4494	27C7-27C7	smt3	6967593	6966776	1357		
CG8749	27C7-27D1	small ribonucleoprotein particle U1 subunit 70K	6971736	6969825	1357		

CR43142	27D1-27D1	-	6972796	6972243	1357		
CG9138	27D1-27D3	uninflatable	7009888	6972828	1357		
CG43321	27D4-27D4	-	7012742	7012311	1357		
CG43322	27D4-27D4	-	7014737	7013396	1357		
CG3440	27D4-27D4	Pupal cuticle protein	7022473	7021682	1357		
CG31628	27D4-27D4	adenosine 3	7023940	7014861	1357		
CG31908	27D4-27D4	-	7027295	7024825	1357		
CG3476	27D5-27D5	-	7028959	7027594	1357		
CG9100	27D5-27D5	Rab30	7032603	7030480	1357		
CG11266	27D5-27D5	-	7037620	7032713	1357		
CG43227	27D5-27D7	milton	7056010	7037998	1357		
CG31907	27D7-27D7	-	7060851	7059318	1357		
CG13778	27D7-27D7	Menin 1	7063406	7056306	1357		
CG13779	27D7-27D7	-	7064467	7063985	1357		
CG8902	27D7-27D7	Nuf2	7065833	7064431	1357		
CG11289	27D7-27E1	-	7069546	7067983	1357	3077	
CG13780	27E1-27E1	PDGF- and VEGF-related factor 2	7084634	7069578	1357	3077	
CG34378	27E2-27E3	PDGF- and VEGF-related factor 3	7156701	7099692	1357	3077	
CG4495	27E4-27E4	-	7185530	7182236	1357	3077	
CG4496	27E4-27E4	-	7188068	7185461	1357	3077	
CG4497	27E4-27E4	-	7194588	7190431	1357	3077	
CG4502	27E4-27E4	-	7204259	7194908	1357	3077	
CG13784	27E4-27E5	-	7220029	7205250	1357	3077	
CG4567	27E5-27F2	iconoclast	7223079	7220272	1357	3077	
CG42253	27E6-27E5	Na[+]-driven anion exchanger 1	7240500	7224851	1357	3077	
CG13786	27E7-27E7	-	7252772	7250719	1357	3077	
CG31909	27E7-27E7	-	7258205	7257512	1357	3077	
CG4698	27E7-27E8	Wnt oncogene analog 4	7277168	7255460	1357	3077	
CG4889	27F1-27F1	wingless	7316255	7307161	1357	3077	
CG4969	27F2-27F2	Wnt6	7352542	7334801	1357	3077	
CG4971	27F2-27F3	Wnt10	7377528	7364820	1357	3077	
CG5125	27F3-27F3	neither inactivation nor afterpotential C	7384344	7377718	1357	3077	
CG5149	27F3-27F3	-	7388248	7384486	1357	3077	
CG5155	27F3-27F3	-	7390902	7388537	1357	3077	
CG5160	27F3-27F3	-	7398403	7390984	1357	3077	
CG5171	27F3-27F3	-	7404526	7395832	1357	3077	
CG5177	27F3-27F3	-	7408475	7405214	1357	3077	
CG5181	27F3-27F3	-	7409779	7408533	1357	3077	
CG15818	27F3-27F3	-	7412229	7410934	1357	3077	
CG5229	27F3-27F4	chameau	7422389	7412453	1357	3077	
CR43020	27F4-27F4	mir-275 stem loop	7425892	7425795	1357	3077	
CR43032	27F4-27F4	mir-305 stem loop	7426044	7425972	1357	3077	
CG5261	27F4-27F4	-	7430329	7426866	1357	3077	

CG5958	27F4-27F4	-	7433480	7430529	1357	3077			
CG5973	27F4-27F4	-	7445269	7437506	1357	3077			
CG12789	28A1-28A1	scavenger receptor acting in neural tissue and majority of rhodopsin is absent	7451165	7445345	1357	3077			
CG13787	28A1-28A1	Gustatory receptor 28a	7454169	7452525	1357	3077			
CG13788	28A1-28A1	Gustatory receptor 28b	7462247	7454825	1357	3077			
CG6055	28A1-28A1	-	7472493	7466546	1357	3077			
CG6441	28A1-28A1	-	7476952	7474704	1357	3077			
CG42533	28A1-28A3	-	7495618	7472505	1357	3077			
CG6641	28A4-28A4	Pheromone-binding protein-related protein 5	7497360	7496785	1357	3077			
CG34374	28B1-28B1	Rapgap1	7576604	7497805	1357	3077	4955		
CG13791	28B1-28B2	-	7578559	7578233	1357	3077	4955		
CG6717	28B3-28B3	Serine protease inhibitor 7	7583334	7581932	1357	3077	4955		
CG6730	28B4-28B4	Cyp4d21	7607703	7605600	1357		4955		
CG6739	28B4-28B4	-	7616528	7608390	1357		4955		
CG13792	28B4-28C1	-	7645997	7643527	1357		4955		
CG6772	28C1-28C1	Slowpoke binding protein	7675078	7647053			4955		
CG6976	28C1-28C1	Myo28B1	7689459	7666047			4955		
CG18585	28C1-28C1	-	7691057	7689376			4955		
CG7025	28C1-28C1	-	7692683	7691109			4955		
CG43235	28C1-28C1	-	7693821	7693030			4955		
CG7052	28C1-28C1	Thiolester containing protein II	7701585	7693800			4955		
CG7068	28C1-28C1	Thiolester containing protein III	7710697	7702807			4955		
CR31905	28C1-28C1	transfer RNA:tyr1:28C	7711661	7711476			4955		
CG7075	28C1-28C1	Neurotransmitter transporter-like	7714032	7711020			4955		
CG33296	28C1-28C1	-	7716645	7714069			4955		
CG13793	28C1-28C1	-	7719487	7716972			4955		
CG13794	28C2-28C2	-	7722823	7719847			4955		
CG13795	28C2-28C2	-	7726298	7723310			4955		
CG13796	28C2-28C2	-	7732668	7727150			4955		
CG31904	28C2-28C2	-	7738795	7734411			4955		
CG7216	28C2-28C2	Adult cuticle protein 1	7741542	7740552			4955		
CG7214	28C2-28C2	-	7744841	7743677			4955		
CG7211	28C2-28C2	-	7747874	7747343			4955		
CG7203	28C2-28C2	-	7753156	7752168			4955		
CG14538	28C2-28C2	-	7756934	7756317			4955		
CG7196	28C2-28C2	-	7765716	7754191			4955		
CG7191	28C3-28C3	-	7775033	7767649			4955		
CG7179	28C3-28C3	-	7778027	7775804			4955		
CG7171	28C3-28C3	Urate oxidase	7781415	7780085			4955		
CG7164	28C3-28C3	-	7782627	7781503			4955		
CG7154	28C3-28C3	-	7786063	7782857			4955		
CG7149	28C3-28C4	-	7790557	7786157			4955		
CG7144	28C4-28C4	lysine ketoglutarate reductase	7795958	7791406			4955		

CG14536	28C4-28C4	Homocysteine-induced endoplasmic reticulum protein	7799846	7796308			4955		
CG7138	28C4-28C4	r2d2	7802008	7800167			4955		
CG7134	28C4-28C4	cdc14	7810697	7802415			4955		
CG7123	28C4-28D1	LanB1	7820771	7811440			4955		
CG14472	28D11-28E1	purity of essence	8071591	8054322	140		4955		
CG7115	28D1-28D1	-	7825350	7821534					
CG7111	28D1-28D1	Receptor of activated protein kinase C 1	7827252	7825626					
CG7109	28D1-28D2	microtubule star	7832745	7827743					
CG43100	28D2-28D2	-	7840332	7839874					
CG14537	28D2-28D2	-	7841262	7840481					
CG14535	28D2-28D2	-	7855255	7844905					
CG7106	28D2-28D2	lectin-28C	7857931	7857090					
CG14534	28D2-28D2	TweedleE	7860838	7857957					
CG7105	28D2-28D2	Proctolin	7871432	7864639					
CR31903	28D2-28D2	transfer RNA:gly3:28D	7872919	7872849					
CG7104	28D2-28D2	spatzle 3	7879550	7873495					
CG18591	28D2-28D2	Small ribonucleoprotein particle protein SmE	7885425	7884932					
CG34132	28D2-28D2	-	7886014	7885649					
CG7102	28D2-28D2	-	7887489	7883468					
CG31902	28D2-28D2	Serpin 28Da	7889129	7887693					
CG33121	28D2-28D2	Serpin 28Db	7890530	7889371					
CG7466	28D3-28D11	-	8054328	8043715					
CG34421	28D3-28D3	Sno oncogene	7984158	7892316					
CG7231	28D3-28D3	-	7986785	7984720					
CG7228	28D3-28D3	peste	7994182	7987113					
CG7227	28D3-28D3	-	7998150	7994837					
CG7224	28D3-28D3	-	7999743	7998934					
CG7221	28D3-28D3	WW domain containing oxidoreductase	8004313	7999670					
CG7219	28D3-28D3	Serpin 28D	8007253	8004548					
CG12560	28D3-28D3	-	8009477	8008321					
CG34010	28D3-28D3	-	8010635	8009603					
CG7356	28D3-28D3	Transglutaminase	8026901	8011407					
CG7380	28D3-28D3	barrier to autointegration factor	8030150	8029464					
CG7392	28D3-28D3	Connector of kinase to AP-1	8039598	8030722					
CG7367	28D3-28D3	-	8039788	8026914					
CG7429	28D3-28D3	-	8041879	8041115					
CR33693	28D3-28D3	-	8042350	8042189					
CG7424	28D3-28D3	Ribosomal protein L36A	8042856	8041880					
CG18780	28E1-28E1	Mediator complex subunit 20	8072844	8071809	140				
CG7562	28E1-28E1	TBP-related factor	8073949	8072897	140				
CG7586	28E1-28E3	Macroglobulin complement-related	8082969	8074109	140				
CG31605	28E3-28E5	Basigin	8110561	8083422	140	179			
CG8683	28E6-28E7	-	8124001	8116965		179			

CG8673	28E7-28E7	-	8125799	8124329	179		
CG12375	28E7-28E7	-	8126876	8125668	179		
CG8668	28E7-28E7	-	8133989	8127024	179		
CG42762	28E7-28E7	-	8144027	8143488	179		
CG42763	28E7-28E7	-	8145088	8144456	179		
CG31606	28E7-28E7	-	8148279	8147630	179		
CG31607	28E7-28E7	-	8155603	8148950	179		
CG8552	28E7-28E9	-	8159575	8134247	179		
CG31900	28E8-28E9	-	8158711	8156827	179		
CG8506	28E9-28E9	Rabenosyn-5	8161800	8159840	179		
CG8498	28E9-28E9	-	8162389	8161794	179		
CG8486	28E9-28F1	-	8190044	8163298	179		
CG18103	28F1-28F1	fos-related gene at 28F	8181331	8180222	179		
CG34134	28F1-28F1	-	8190781	8190297	179		
CG8475	28F1-28F1	-	8196893	8190954	179		
CG8460	28F1-28F1	-	8198813	8197196	179		
CG8455	28F1-28F1	-	8200652	8198959	179		
CG8451	28F1-28F1	-	8205128	8200465	179		
CG8419	28F1-28F2	-	8209639	8206206	179		
CG8409	28F2-28F3	Suppressor of variegation 205	8211133	8209626	179		
CG8396	28F3-28F3	Single stranded-binding protein c31A	8211938	8211347	179		
CG8372	28F3-28F3	-	8212881	8212039	179		
CG8360	28F3-28F3	-	8214135	8213179	179		
CG8353	28F3-28F3	-	8215239	8214305	179		
CG8349	28F3-28F3	-	8216901	8215915	179		
CG8292	28F3-28F3	-	8218017	8216851	179		
CG8282	28F3-28F3	Snx6	8220737	8218071	179		
CG8222	28F4-28F5	PDGF- and VEGF-receptor related	8239875	8220980	179		
CG8137	28F5-28F5	Serine protease inhibitor 2	8241839	8240414	179		
CR43262	28F5-28F5	-	8242435	8242055	179		
CG14277	28F5-28F5	-	8243426	8242659	179		
CG43057	28F5-28F5	-	8243988	8243513	179		
CG8086	28F5-29A1	-	8257502	8244160	179		
CR42893	29A1-29A1	mir-2b-1 stem loop	8258692	8258616	179		
CG8049	29A1-29A3	Btk family kinase at 29A	8301072	8259504	179		
CR31899	29A2-29A2	transfer RNA:lys5:29A	8290799	8290727	179		
CG7870	29A3-29A3	wollknaeuel	8302983	8301345	179		
CG7851	29A3-29A3	Sarcoglycan alpha	8305376	8303433	179		
CG7840	29A3-29A3	-	8306743	8305590	179		
CG7830	29A3-29A3	-	8308188	8306684	179		
CG7818	29A3-29A3	-	8309963	8308440	179		
CG7810	29A3-29A3	-	8311144	8309869	179		
CG7806	29A3-29A4	-	8317017	8311419	179		

CG7795	29A4-29A4	mitoshell	8319920	8316889		179	
CG7787	29A4-29A4	-	8321285	8320324		179	
CG7781	29A4-29A4	-	8325299	8321276		179	
CG14275	29A5-29A5	-	8332911	8327458		179	
CG14274	29A5-29B1	-	8342056	8338312		179	
CG14273	29B1-29B1	-	8344378	8342764		179	
CG7778	29B1-29B1	-	8350197	8346621		179	
CG31901	29B1-29B1	Mucin related 29B	8355173	8352200		179	
CG7627	29B1-29B1	-	8361198	8355674		179	
CG13389	29B2-29B2	Ribosomal protein S13	8364609	8363699		179	
CG42522	29B2-29B2	COP9 complex homolog subunit 8	8365663	8364832		179	
CG17291	29B2-29B2	Protein phosphatase 2A at 29B	8370082	8366009		179	
CG17292	29B2-29B2	-	8374250	8370513		179	
CG17293	29B2-29B3	-	8375549	8374481		179	
CG13390	29B3-29B3	-	8376777	8375501		179	
CG17294	29B3-29B3	-	8378206	8377051		179	
CG13391	29B3-29B3	Alanyl-tRNA synthetase	8381756	8378262		179	
CG13392	29B3-29B4	-	8382723	8381905		179	
CG17295	29B4-29B4	Reduction in Cnn dots 4	8383657	8382815		179	
CG13393	29B4-29B4	-	8384132	8383612		179	
CG13384	29B4-29C1	-	8388804	8384430		179	
CG42819	29C1-29C1	-	8389304	8388728		179	
CR32989	29C1-29C1	U6atac snRNA at 29B	8389820	8389724		179	
CG42820	29C1-29C1	-	8392398	8389881		179	
CG17797	29C1-29C1	Accessory gland-specific peptide 29AB	8393239	8392466		179	
CG17799	29C1-29C1	lectin-29Ca	8394280	8393489		179	
CG31893	29C1-29C1	Peritrophin-15b	8394897	8394510		179	
CG17814	29C1-29C1	Peritrophin-15a	8396084	8395661		179	
CG13385	29C1-29C1	-	8397886	8396713		179	
CG13386	29C1-29C1	-	8399972	8399044		179	
CG31898	29C1-29C1	-	8401477	8400457		179	
CG13396	29C1-29C1	fuzzy	8403442	8401446		179	
CG13387	29C1-29C3	embargoed	8408853	8403575	384	179	
CG13397	29C3-29C3	-	8411868	8409051	384		
CG13398	29C3-29C3	-	8415245	8412411	384		
CG13388	29C3-29C4	A kinase anchor protein 200	8430984	8415690	384		
CG17610	29C4-29C4	gurken	8433598	8431086	384		
CG13400	29C4-29C4	D12	8437346	8434058	384		
CG10890	29C4-29C5	mutagen-sensitive 201	8442352	8437411	384		
CG13399	29C4-29C5	Chrac-14	8442352	8437411	384		
CG31897	29C5-29C5	-	8445660	8442447	384		
CG13401	29C5-29C5	U26	8449571	8445861	384		
CG17608	29C5-29D1	fu12	8463990	8449691	384		

CG9233	29D1-29D1	fu2	8466529	8464491	384		
CG33194	29D1-29D1	Chemosensory protein A 29a	8478088	8477349	384		
CR31896	29D1-29D1	transfer RNA:CR31896	8481848	8481777	384		
CR31892	29D1-29D1	transfer RNA:CR31892	8482155	8482084	384		
CG42840	29D1-29D1	dachs	8488671	8466830	384		
CG13088	29D1-29D1	-	8490546	8488959	384		
CG13094	29D1-29D3	Diuretic hormone 31	8506845	8491868	384		
CG13095	29D2-29D2	beta-site APP-cleaving enzyme	8496304	8495108	384		
CG13096	29D3-29D3	-	8511844	8509251	384		
CG13097	29D3-29D4	-	8514864	8512169	384		
CG13089	29D4-29D4	-	8516756	8515098	384		
CG13098	29D4-29D4	mitochondrial ribosomal protein L51	8517377	8516754	384		
CG13090	29D4-29D4	-	8519180	8517446	384		
CG13091	29D4-29D4	-	8521733	8519690	384		
CG10593	29D4-29D4	Angiotensin-converting enzyme-related	8524991	8521899	384		
CG34441	29D4-29D5	-	8528618	8525663	384		
CG34440	29D4-29D5	lemming	8528618	8525663	384		
CG17834	29D5-29E1	-	8541462	8529143	384		
CR31604	29E1-29E1	transfer RNA:CR31604	8541623	8541552	384		
CR31603	29E1-29E1	transfer RNA:CR31603	8541832	8541761	384		
CG18405	29E1-29E3	Sema-1a	8671276	8542009	384		
CR31895	29E2-29E2	transfer RNA:CR31895	8570960	8570888	384		
CR31602	29E2-29E2	transfer RNA:CR31602	8620099	8620028	384		
CG9280	29E3-29E3	Glutactin	8676811	8672043	384		
CR31889	29E3-29E3	transfer RNA:CR31889	8679187	8679116	384		
CG9287	29E3-29E3	-	8679782	8676848	384		
CR31890	29E3-29E3	transfer RNA:CR31890	8683522	8683451	384		
CR31888	29E3-29E3	transfer RNA:CR31888	8683877	8683806	384		
CG9289	29E3-29E3	-	8684350	8681403	384		
CG9296	29E3-29E3	Prenyl-binding protein	8685954	8684815	384		
CG9298	29E3-29E4	-	8687052	8686231	384		
CG9314	29E4-29E4	-	8707440	8705572	384		
CG9310	29E4-29E4	Hepatocyte nuclear factor 4	8709038	8687281	384		
CG12437	29E4-29E6	raw	8740660	8709880	384		
CG12438	29E6-29E6	-	8753209	8752305	384		
CG9463	29F1-29F1	-	8768708	8765361	384		
CG9465	29F1-29F1	-	8772344	8769175	384		
CG9466	29F1-29F1	-	8776257	8772948	384		
CG9468	29F1-29F1	-	8781251	8777661	384		
CG42710	29F1-29F1	-	8782494	8781897	384		
CG42712	29F1-29F1	-	8810032	8809400	384		
CG18024	29F2-29F2	SoxNeuro	8829670	8825625	384		
CG32986	29F3-29F3	-	8863743	8862776	384		

CG32987	29F3-29F3	-	8864847	8863811	384		
CG32988	29F3-29F3	-	8865692	8864864	384		
CG32983	29F3-29F3	-	8866659	8865850	384		
CG9483	29F3-29F3	-	8867686	8866767	384		
CG42713	29F3-29F3	-	8892180	8891489	384		
CG34398	29F3-29F4	-	8933382	8898804	384		
CG9494	29F4-29F4	Tetraspanin 29Fa	8936096	8933964	384		
CG9496	29F5-29F5	Tetraspanin 29Fb	8939746	8937390	384		
CG9510	29F5-29F5	-	8943264	8939780	384		
CG9515	29F5-29F5	-	8943264	8939780	384		
CG9520	29F5-29F5	Core 1 Galactosyltransferase A	8951200	8943454	384		
CG31886	29F5-29F5	-	8958977	8953481	384		
CG9525	29F5-29F6	-	8962354	8960318	384		
CG32985	29F6-29F6	-	8964628	8962617	384		
CG32984	29F6-29F6	-	8967028	8965134	384		
CG18088	29F6-29F6	-	8970259	8967537	384		
CG9541	29F6-29F6	-	8974976	8970801	384		
CG18662	29F6-29F6	-	8981437	8980680	384		
CG13101	29F6-29F6	-	8984870	8977882	384		
CG9552	29F6-29F7	rolling stone	8989287	8985932	384		
CG9555	29F7-29F7	-	8993632	8991989	384		
CG17906	29F7-29F7	-	8995546	8994463	384		
CG9556	29F7-29F7	alien	8997375	8994669	384		
CG18661	29F7-29F7	-	8998544	8997641	384		
CG9564	29F7-29F7	Trypsin 29F	8999468	8998537	384		
CG9568	29F7-29F7	-	9011342	9010586	384		
CG13102	29F7-29F7	-	9012890	9012193	384		
CG9573	29F7-29F7	-	9014070	9012885	384		
CG9582	29F8-29F8	-	9025404	9024450	384		
CG31708	29F8-30A1	-	9071162	9051631	384		
CG12439	30A1-30A1	-	9077988	9077121	384		
CG18241	30A1-30A1	Toll-4	9089440	9084107	384		
CG31609	30A1-30A1	-	9098176	9097627	384		
CG13106	30A1-30A1	Odorant receptor 30a	9113285	9111814	384		
CG32982	30A2-30A2	-	9163721	9125751	384		
CG13108	30A2-30A2	-	9165426	9164235	384		
CG9586	30A2-30A2	-	9166543	9165421	384		
CG13109	30A2-30A6	taiman	9247187	9166802	384		
CR31885	30A6-30A6	transfer RNA:CR31885	9236594	9236521	384		
CG17009	30A6-30A6	australin	9251042	9250088	384		
CG4454	30A6-30A6	borealin-related	9253116	9251472	384		
CG17011	30A6-30A7	lectin-30A	9254854	9254076	384		
CG3694	30A6-30A7	G protein gamma30A	9291798	9253037	384		

CG42844	30A8-30A8	-	9305007	9304437	384	
CG17005	30A8-30A8	-	9330067	9327744	384	
CG3738	30A8-30A8	Cyclin-dependent kinase subunit 30A	9331981	9330767	384	
CG3747	30A8-30A8	Excitatory amino acid transporter 1	9341925	9333568	384	
CG3748	30A8-30A8	-	9344491	9342832	384	
CG43350	30A9-30A9	-	9349875	9349557	384	
CG13110	30A9-30A9	-	9350996	9350470	384	
CG31883	30B10-30B10	-	9529648	9528515	384	
CG3811	30B10-30B10	Organic anion transporting polypeptide 30B	9540060	9521214	384	
CG17855	30B10-30B10	-	9542480	9540631	384	
CG3818	30B10-30B10	Cuticular protein 30B	9543478	9542878	384	
CG13113	30B10-30B10	-	9544792	9544175	384	
CG13114	30B10-30B10	-	9547424	9545811	384	
CG4405	30B10-30B12	junctophilin	9566750	9547720	384	
CG3838	30B12-30B12	-	9573572	9568892	384	
CG4389	30B12-30B12	-	9576768	9573563	384	
CG31709	30B12-30B12	-	9579638	9578536	384	
CG12245	30B12-30B12	glial cells missing	9581742	9579449	384	
CG3841	30B12-30C1	-	9591783	9589476	384	
CG34181	30B1-30B1	-	9368434	9367640	384	
CG34366	30B1-30B1	Shaw-like	9384845	9373025	384	
CG3752	30B1-30B1	Aldehyde dehydrogenase	9391679	9387389	384	
CG4438	30B1-30B1	-	9397988	9397110	384	
CG3759	30B2-30B3	-	9426342	9416593	384	
CG3763	30B3-30B3	Fat body protein 2	9427835	9426860	384	
CG42847	30B3-30B3	-	9428740	9427912	384	
CG4435	30B3-30B3	FucTB	9431029	9428771	384	
CG3766	30B3-30B3	scattered	9435341	9431403	384	
CG3769	30B3-30B3	-	9436842	9435510	384	
CG34182	30B3-30B3	Ribosomal protein S28-like	9437227	9436953	384	
CG3779	30B3-30B5	numb	9463293	9437513	384	
CG33723	30B4-30B4	-	9440740	9440011	384	
CG33298	30B5-30B10	-	9520696	9495472	384	
CG4422	30B5-30B5	GDP dissociation inhibitor	9494855	9491176	384	
CG4382	30C1-30C1	-	9600853	9598940	384	
CG3858	30C1-30C1	gcm2	9612706	9608479	384	
CG31884	30C1-30C1	thioredoxin-2	9616048	9613165	384	
CG3881	30C1-30C1	GlcAT-S	9623109	9616469	384	
CG31882	30C1-30C1	-	9625285	9624452	384	
CG15828	30C2-30C2	-	9656026	9634201	384	
CG33299	30C2-30C2	-	9657347	9656600	384	
CG4379	30C5-30C5	cAMP-dependent protein kinase 1	9699293	9682315	384	6478
CG3949	30C5-30C5	hoi-polloi	9700459	9699791	384	6478

CG31710	30C5-30C5	-	9705944	9702964	384	6478		
CG3959	30C5-30C5	pelota	9708883	9700796	384	6478		
CG4364	30C5-30C6	-	9711269	9708921	384	6478		
CG13116	30C6-30C6	-	9730945	9729940	384	6478		
CG13117	30C6-30C6	-	9737329	9736645	384	6478		
CG18660	30C6-30C7	Nckx30C	9746483	9712583	384	6478		
CG4105	30C7-30C7	Cytochrome P450-4e3	9750071	9747839	384	6478		
CG3998	30C7-30C7	Zinc finger protein 30C	9762375	9758338	384	6478		
CG4079	30C7-30C7	TBP-associated factor 11	9763244	9762364	384	6478		
CG4008	30C7-30C7	uninitiated	9765338	9763345	384	6478		
CG13120	30C7-30C8	-	9766912	9765357	384	6478		
CG4017	30C8-30C8	-	9768727	9767059	384	6478		
CG17633	30C8-30C8	-	9770409	9769067	384	6478		
CG13121	30C8-30C8	-	9770996	9770395	384	6478		
CG34059	30C8-30C8	pickpocket 16	9773044	9771155	384	6478		
CG34058	30C8-30C9	pickpocket 11	9775030	9773108	384	6478		
CG4026	30C9-30D1	Inositol 1,4,5-triphosphate kinase 1	9788499	9782390	384	6478	1045	
CR18854	30D1-30D1	-	9790745	9787279		6478	1045	
CG4036	30D1-30D1	-	9791958	9790667		6478	1045	
CG13123	30D1-30D1	-	9793097	9791961		6478	1045	
CG4128	30D1-30E1	nicotinic Acetylcholine Receptor alpha 30D	9886214	9796948		6478	1045	
CG4535	30E1-30E1	FK506-binding protein FKBP59	9890119	9888034		6478	1045	
CG34183	30E1-30E1	-	9890787	9890061		6478	1045	
CG4537	30E1-30E1	-	9891336	9890885		6478	1045	
CG5924	30E1-30E1	-	9893419	9891255		6478	1045	
CR32876	30E1-30E1	snoRNA:U14:30Eb	9894026	9893946		6478	1045	
CR32875	30E1-30E1	snoRNA:U14:30Ea	9894285	9894205		6478	1045	
CR32874	30E1-30E1	-	9894544	9894477		6478	1045	
CR31877	30E1-30E1	-	9894907	9894795		6478	1045	
CR32873	30E1-30E1	U snoRNA host gene 2	9895003	9893805		6478	1045	
CG4539	30E1-30E1	Bekka	9896104	9895289		6478	1045	
CG5920	30E1-30E1	Ribosomal protein S2	9897542	9896265		6478	1045	
CG33300	30E1-30E1	Mucin 30E	9903128	9897953		6478	1045	
CG13124	30E1-30E1	-	9908649	9903379		6478	1045	
CG5899	30E1-30E4	Etl1 homologue	9912585	9908830		6478	1045	
CG4602	30E4-30E4	Srp54	9915044	9912907		6478	1045	
CG4600	30E4-30E4	yippee interacting protein 2	9917220	9915220		6478	1045	
CG5885	30E4-30E4	-	9918165	9917221		6478	1045	
CG4598	30E4-30E4	-	9919901	9918636		6478	1045	
CG4594	30E4-30F1	-	9921459	9920161		6478	1045	
CG4592	30F1-30F1	-	9922766	9921639		6478	1045	
CG13125	30F1-30F1	-	9924860	9922737		6478	1045	
CG42366	30F1-30F1	-	9930378	9926613		6478	1045	

CG42367	30F1-30F1	-	9930999	9930446	6478	1045		
CG31876	30F1-30F1	Cuticular protein 30F	9933092	9932587	6478	1045		
CG31712	30F1-30F1	-	9938142	9934767	6478	1045		
CG31713	30F1-30F1	diadenosine tetraphosphate hydrolase	9938787	9938170	6478	1045		
CG4619	30F1-30F1	-	9941099	9938865	6478	1045		
CG5853	30F1-30F1	-	9947442	9940769	6478	1045		
CR42983	30F1-30F1	mir-87 stem loop	9950516	9950418	6478	1045		
CG13126	30F2-30F2	-	9954180	9952428		1045		
CG4709	30F2-30F2	-	9956179	9954449		1045		
CG5846	30F2-30F2	-	9957019	9956148		1045		
CG4658	30F2-30F2	-	9960168	9957287		1045		
CG5850	30F2-30F2	-	9963767	9960450		1045		
CG5838	30F2-30F3	DNA replication-related element factor	9967455	9964147		1045		
CG4651	30F3-30F3	Ribosomal protein L13	9968495	9967312		1045		
CG13130	30F5-30F5	-	9984657	9983661		1045		
CG4722	30F5-30F5	big brain	9995545	9984647		1045		
CG31755	30F5-30F5	-	10001433	9996932		1045		
CG31875	30F5-30F5	-	10002446	9995561		1045		
CG4747	30F5-30F5	-	10008889	10003825		1045		
CG4758	30F5-30F5	Translocation protein 1	10013170	10009386		1045		
CG13131	30F5-30F5	-	10017463	10013271		1045		
CG13127	30F6-30F6	-	10029299	10026740		1045		
CG4778	30F6-31A1	obstructor-B	10038954	10032694		1045		
CG33301	31A1-31A1	-	10050956	10049482		1045		
CG33302	31A1-31A1	Cuticular protein 31A	10055935	10054215		1045		
CG4799	31A1-31A2	Pendulin	10060095	10056906		1045		
CG4804	31A2-31A2	Serpin 31A	10063925	10060871		1045		
CG31714	31A2-31A2	-	10087884	10064322		1045		
CG13133	31A2-31A2	-	10092419	10091208		1045		
CG13135	31A2-31A2	-	10122771	10122196		1045		
CG34109	31A2-31A2	-	10125736	10094088		1045		
CG42843	31A3-31A3	-	10137552	10096805		1045		
CG4839	31A3-31A3	-	10155510	10144850		1045		
CG13137	31B1-31B1	-	10174090	10172702		1045		
CG31874	31B1-31B1	-	10191496	10189820		1045		
CG5772	31B1-31B1	Sulfonylurea receptor	10199112	10182557		1045		
CG18145	31B1-31B1	RPA-interacting protein alpha	10200972	10199396		1045		
CG4897	31B1-31B1	Ribosomal protein L7	10202145	10201101		1045		
CG34159	31B1-31B1	-	10204320	10202520		1045		
CG5734	31B1-31B1	-	10206961	10204757		1045		
CG5731	31B1-31B1	-	10209737	10207085		1045		
CG5727	31B1-31B1	-	10210700	10209853		1045		
CG4901	31B1-31B1	-	10213721	10211183		1045		

CG5722	31B1-31B1	Niemann-Pick type C-1a	10220957	10213892	1045		
CG4904	31B1-31B1	Proteasome 35kD subunit	10222503	10221353	1045		
CG4908	31B1-31B1	-	10224442	10222658	1045		
CG5708	31B1-31B1	-	10226808	10224664	1045		
CG5694	31B1-31B1	-	10231689	10227760	1045		
CG4912	31B1-31B1	eEF1delta	10234450	10232493	1045		
CG31720	31B1-31B1	-	10238317	10234585	1045		
CG4916	31B1-31B1	maternal expression at 31B	10242172	10239326	1045		
CG5686	31B1-31B1	chico	10247064	10242512	1045		
CG5680	31B1-31B1	basket	10250479	10247502	1045		
CG31717	31B1-31B1	-	10251594	10250737	1045		
CG4926	31B1-31B1	Ror	10254686	10251838	1045		
CG5676	31B1-31B1	-	10255884	10254610	1045		
CG5671	31B1-31B1	Pten	10261017	10256319	1045		
CG5655	31B1-31B1	Repressor splicing factor 1	10263582	10262426	1045		
CG18619	31B1-31B1	-	10265229	10264131	1045		
CG4946	31B1-31B1	-	10266570	10265339	1045		
CG4953	31B1-31B1	-	10268748	10266705	1045		
CG4957	31B1-31B1	-	10269904	10268875	1045		
CG5619	31B1-31B1	trunk	10272223	10271443	1045		
CG34043	31B1-31C4	-	10280846	10278951	1045		
CG5604	31C4-31C6	-	10292278	10281943	1045		
CG18144	31C6-31C7	Hand	10295299	10292781	1045		
CG5640	31C7-31C7	-	10278811	10272627	1045		
CG5603	31C7-31D1	cylindromatosis	10299827	10295856	1045		
CG34367	31D10-31D10	-	10353631	10347851	1045		
CG5367	31D10-31D10	-	10356597	10354743	1045		
CG5045	31D10-31D10	-	10357876	10356743	1045		
CG5366	31D10-31D10	-	10362703	10358162	1045		
CG5052	31D10-31D10	pimples	10364046	10362989	1045		
CG13139	31D10-31D10	lowfat	10366410	10364465	1045		
CG5056	31D10-31D10	-	10367946	10366698	1045		
CG33304	31D10-31D11	rhomboid-5	10373900	10368134	1045		
CG33303	31D11-31D11	-	10375790	10374186	1045		
CG13140	31D11-31D11	dpr19	10379908	10376492	1045		
CG5091	31D11-31D11	-	10382865	10380118	1045		
CG5096	31D11-31D11	-	10384730	10382253	1045		
CG5363	31D11-31D11	cdc2	10386263	10384739	1045		
CG5108	31D11-31D11	mitochondrial ribosomal protein S7	10387524	10386664	1045		
CG5102	31D11-31E1	daughterless	10392786	10388078	1045		
CG13138	31D1-31D1	-	10301955	10300222	1045		
CG5395	31D1-31D1	no mitochondrial derivative	10303945	10302592	1045		
CG5390	31D1-31D1	-	10306594	10304063	1045		

CG4968	31D1-31D1	-	10308050	10306903	1045		
CG5387	31D1-31D3	Cdk5 activator-like protein	10310736	10308124	1045		
CG31873	31D-31D	-	10271465	10270067	1045		
CG5385	31D4-31D4	-	10312069	10311169	1045		
CG5384	31D4-31D5	-	10314396	10312316	1045		
CG4972	31D5-31D6	-	10317569	10314795	1045		
CG5381	31D6-31D7	-	10321800	10317497	1045		
CG4995	31D7-31D8	-	10324990	10322476	1045		
CG5371	31D8-31D8	Ribonucleoside diphosphate reductase large subunit	10327986	10325018	1045		
CG5375	31D8-31D9	-	10331116	10328347	1045		
CG5037	31D9-31D9	-	10333134	10331463	1045		
CG5034	31D9-31D9	GATAd	10338441	10333914	1045		
CG5029	31D9-31D9	S-adenosylmethionine decarboxylase	10341505	10339471	1045		
CG31715	31D9-31D9	-	10342527	10341621	1045		
CG5025	31D9-31D9	Selenophosphate synthetase 2	10344228	10342594	1045		
CG5022	31D9-31D9	-	10347706	10344459	1045		
CG31716	31E1-31E1	-	10402882	10396711	1045		
CG17768	31E1-31E1	-	10405175	10403197	1045		
CG33677	31E1-31E1	Like Sm protein 4	10405175	10403197	1045		
CG31718	31E1-31E1	Ionotropic receptor 31a	10408011	10406075	1045		
CG5277	31E1-31E1	Intronic Protein 259	10409604	10408353	1045		
CG5271	31E1-31E1	Ribosomal protein S27A	10410467	10408351	1045		
CG5355	31E1-31E1	-	10413572	10410537	1045		
CG5300	31E1-31E1	Klp31E	10418991	10414034	1045		
CG5313	31E1-31E1	Replication factor C subunit 3	10420612	10419190	1045		
CG5354	31E1-31E1	pineapple eye	10422781	10420711	1045		
CG5168	31E1-31E1	-	10425482	10423291	1045		
CG5183	31E1-31E1	KDEL receptor	10428159	10426867	1045		
CG5188	31E1-31E1	-	10429988	10428833	1045		
CG5343	31E1-31E1	-	10430914	10429920	1045		
CG5352	31E1-31E2	Small ribonucleoprotein particle protein SmB	10426791	10425483	1045		
CG5362	31E1-31F2	Malate dehydrogenase 1	10396299	10393847	1045		
CG5193	31E2-31E2	Transcription factor IIB	10432999	10431344	1045		
CG5337	31E2-31E2	-	10435679	10432677	1045		
CG5198	31E2-31E2	-	10437317	10435991	1045		
CG5203	31E2-31E2	CHIP	10439244	10437551	1045		
CG13142	31E2-31E2	-	10440886	10439440	1045		
CG6232	31E3-31E3	-	10450080	10442727	1045		
CG34042	31E3-31E4	pickpocket 10	10452201	10450134	1045		
CG5322	31E4-31E4	-	10456044	10452677	1045		
CG6206	31E5-31E5	-	10462475	10457656	1045		
CG31719	31E6-31F1	RluA-1	10474347	10463336	1045		
CG6187	31F1-31F1	RluA-2	10482975	10477114	1045		

CG6176	31F1-31F1	Grip75	10485857	10483285		1045	
CG7456	31F1-31F1	-	10488623	10485538		1045	
CG6144	31F1-31F1	-	10490461	10488745		1045	
CG13144	31F1-31F1	-	10491429	10489900		1045	
CG7438	31F1-31F4	Myosin 31DF	10506778	10491682		1045	
CG6094	31F4-31F4	-	10507918	10507117		1045	
CG7384	31F4-31F4	-	10510461	10507859		1045	
CG7400	31F4-31F5	Fatty acid (long chain) transport protein	10517216	10511252		1045	
CG6098	31F5-31F5	Leucine-rich repeat 47	10518991	10517337		1045	
CG6113	31F5-31F5	Lipase 4	10531560	10529418		1045	
CG18301	31F5-31F5	-	10533647	10531821		1045	
CG18302	31F5-31F5	-	10536545	10534322		1045	
CG31721	31F5-32A2	Trim9	10627374	10544881	7142	1045	
CG6138	32A1-32A1	-	10568012	10567290	7142		
CG7363	32A1-32A1	world cup	10577792	10575860	7142		
CG34160	32A1-32A1	-	10580324	10579809	7142		
CG34161	32A1-32A1	-	10581662	10580966	7142		
CG7329	32A2-32A2	-	10631053	10629352	7142		
CG31872	32A2-32A2	-	10643492	10639946	7142		
CG18284	32A2-32A2	-	10645812	10643985	7142		
CG17097	32A2-32A2	-	10650152	10646435	7142		
CG17098	32A2-32A2	-	10654499	10651978	7142		
CG31871	32A2-32A3	-	10671489	10662087	7142		
CG17104	32A3-32A3	-	10679525	10677370	7142		
CG17105	32A4-32A4	-	10681358	10681047	7142		
CG17107	32A4-32A4	-	10682383	10681975	7142		
CG7299	32A4-32A4	-	10684407	10683767	7142		
CG7296	32A4-32A4	-	10686988	10686391	7142		
CG7294	32A4-32A4	-	10689269	10688734	7142		
CG17108	32A4-32A4	-	10694103	10692940	7142		
CG7300	32A4-32A4	-	10698024	10695209	7142		
CG7279	32A4-32A4	Lipase 1	10701458	10699408	7142		
CG6415	32A4-32A4	-	10704935	10703621	7142		
CG17116	32A4-32A4	Lipase 2	10706190	10702235	7142		
CG6431	32A5-32A5	-	10728740	10724274	7142		
CG6443	32A5-32A5	-	10730302	10728975	7142		
CG17118	32A5-32A5	-	10731356	10730255	7142		
CG6750	32A5-32A5	-	10732406	10731400	7142		
CG6444	32A5-32A5	Dpy-30-like 1	10733307	10732749	7142		
CG6743	32A5-32A5	Nucleoporin 107	10736077	10733293	7142		
CG6737	32A5-32A5	Vacuolar H[+] ATPase subunit 16-5	10737576	10736319	7142		
CG12299	32A5-32A5	-	10740762	10737345	7142		
CG6729	32A5-32A5	-	10743934	10740786	7142		

CG17124	32A5-32A5	-	10756316	10744075	7142		
CG6495	32A5-32A5	-	10764972	10761147	7142		
CG6720	32A5-32A5	Ubiquitin conjugating enzyme 2	10768005	10765562	7142		
CG6724	32A5-32A5	-	10769964	10768234	7142		
CG17127	32A5-32A5	-	10771370	10770867	7142		
CG31869	32A5-32B1	-	10801107	10772038	7142		
CG31870	32B1-32B1	-	10790776	10790242	7142		
CG6508	32B1-32B1	-	10820394	10819123	7142		
CG17134	32B1-32B1	-	10821968	10820710	7142		
CG6713	32B1-32B1	Nitric oxide synthase	10838448	10804269	7142		
CG6700	32B1-32B1	-	10842603	10837732	7142		
CG17140	32B1-32B1	-	10845664	10843014	7142		
CG17139	32B1-32B1	-	10845664	10843014	7142		
CG17137	32B1-32B1	Porin2	10847044	10845783	7142		
CG6647	32B1-32B1	porin	10850868	10847227	7142		
CG43129	32B1-32B1	-	10854603	10851332	7142		
CG6627	32B1-32B2	DNZDHHC/NEW1 zinc finger protein 11	10856669	10854433	7142		
CG6620	32B2-32B2	IpIl-aurora-like kinase	10858082	10856788	7142		
CG6521	32B2-32B3	Signal transducing adaptor molecule	10862015	10858528	7142		
CG12517	32B3-32B3	-	10870722	10870167	7142		
CG14071	32B3-32B3	-	10888903	10887645	7142		
CG14070	32B4-32B4	-	10901765	10900648	7142		
CG7309	32B4-32B4	-	10908812	10906270	7142		
CG14069	32B4-32B4	-	10910535	10910230	7142		
CG33507	32B4-32C1	-	10964128	10917139	7142		
CG14072	32C1-32C1	-	10937931	10936662	7142		
CG33129	32C1-32C1	-	10970275	10964903	7142		
CG4621	32C1-32C1	YL-1	10971870	10970438	7142		
CG16743	32C1-32C1	-	10973339	10972580	7142		
CG6093	32C1-32C1	abnormal oocyte	10975273	10973443	7142		
CG6105	32C1-32C1	lethal (2) 06225	10976422	10975778	7142		
CG4636	32C1-32C1	SCAR	10982397	10976774	7142		
CG6122	32C1-32C1	piwi	10987416	10982205	7142		
CG12253	32C1-32C1	-	10989241	10987817	7142		
CG16833	32C1-32C1	-	10997700	10989305	7142		
CG6137	32C1-32C1	aubergine	11001489	10997819	7142		
CG16834	32C1-32C1	lectin-33A	11002740	11002072	7142		
CG6141	32C1-32C1	Ribosomal protein L9	11004189	11002833	7142		
CG4579	32C1-32C1	Nucleoporin 154	11009878	11004823	7142		
CG16840	32C1-32C1	Arginine methyltransferase 8	11011085	11009821	7142		
CG4584	32C1-32C1	Deoxyuridine triphosphatase	11012138	11011332	7142		
CG4605	32C1-32C1	Accessory gland-specific peptide 32CD	11016573	11015642	7142		
CG14913	32C1-32C1	-	11018739	11017172	7142		

CG31868	32C1-32D1	SAM-motif ubiquitously expressed punctatedly localized protein	11066997	11013221	7142	5869
CG18666	32D1-32D1	-	11035308	11034849	7142	5869
CG14915	32D2-32D2	-	11071532	11071027		5869
CG14919	32D2-32D2	Allatostatin C	11081402	11076165		5869
CG14920	32D2-32D2	Allatostatin double C	11085243	11083459		5869
CG16854	32D2-32D2	-	11090782	11086721		5869
CG4705	32D2-32D3	-	11095001	11091442		5869
CG6181	32D3-32D3	-	11100866	11095353		5869
CG6192	32D3-32D3	-	11106652	11100963		5869
CG4713	32D3-32D4	lethal (2) giant discs 1	11110851	11106912		5869
CG6201	32D4-32D4	-	11113063	11110557		5869
CG14916	32D4-32D4	Gustatory receptor 32a	11115755	11114183		5869
CG6230	32D4-32D4	-	11120314	11115636		5869
CG14921	32D4-32D4	-	11121683	11120641		5869
CG6249	32D4-32D4	Csl4	11123792	11122564		5869
CG4738	32D4-32D4	Nucleoporin 160	11129335	11123779		5869
CG6258	32D4-32D4	Replication factor C 38kD subunit	11130645	11128930		5869
CG4751	32D4-32D5	-	11136003	11130741		5869
CG4779	32D5-32D5	homogentisate 1,2-dioxygenase	11138567	11136395		5869
CG31867	32D5-32D5	-	11145417	11144579		5869
CG33114	32D5-32D5	Guanyl cyclase at 32E	11148875	11138801		5869
CG6287	32D5-32D5	-	11155716	11151506		5869
CG42403	32D5-32E1	Ca2+-channel-protein-beta-subunit	11170471	11159270		5869
CG16874	32E1-32E1	Vitelline membrane 32E	11171665	11171229		5869
CG4788	32E1-32E1	-	11180436	11179041		5869
CG4807	32E1-32E2	abrupt	11261080	11210681		5869
CR34664	32E2-32E2	-	11234912	11234835		5869
CG32830	32E2-32E2	-	11256577	11254574		5869
CG6392	32E2-32E2	CENP-meta	11269179	11260823		5869
CG33694	32E2-32E2	CENP-ana	11279847	11269727		5869
CG33695	32E2-32E2	-	11279847	11269727		5869
CG4851	32E2-32E2	Palmitoyl-protein Thioesterase 2	11281929	11280314		5869
CG16928	32E2-32E2	meiotic recombination 11	11284337	11282093		5869
CG14925	32E2-32E2	Osiris 21	11285603	11284586		5869
CG43268	32E3-32E3	-	11307993	11307784		5869
CG14926	32E4-32E4	-	11343263	11342313		5869
CG4881	32E4-32F1	spalt-related	11373397	11365305		5869
CG6464	32F1-32F2	spalt major	11445603	11434311	3079	5869
CG43355	32F2-32F2	-	11485783	11484706	3079	5869
CG4922	32F2-32F2	spalt-adjacent	11486955	11486189	3079	5869
CG6488	32F2-32F2	-	11499119	11496794	3079	5869
CG14928	32F2-32F2	spatzle 4	11508650	11501751	3079	5869
CG6509	32F2-32F2	-	11517057	11508399	3079	5869

CG4970	32F2-32F2	-	11519783	11517404	3079	5869		
CG14930	32F2-32F2	-	11521285	11520358	3079	5869		
CG14929	32F2-32F2	-	11521444	11519819	3079	5869		
CG43153	32F2-32F2	-	11522379	11521807	3079	5869		
CG31705	32F2-32F2	-	11528201	11523300	3079	5869		
CG31706	32F2-32F2	-	11531049	11529524	3079	5869		
CG34162	32F2-32F2	-	11533720	11531881	3079	5869		
CR42743	32F2-32F2	-	11534547	11532824	3079	5869		
CG6541	32F3-32F3	Mst33A	11586833	11585433	3079	5869		
CG6555	32F3-32F3	-	11591678	11591339	3079	5869		
CG15841	32F3-32F3	-	11591678	11591339	3079	5869		
CG6589	32F4-32F4	sperm-associated antigen 4	11611772	11610550	3079			
CG4977	32F4-32F4	kekkon-2	11626124	11606514	3079			
CG6614	32F4-32F4	-	11648839	11645133	3079			
CG12307	32F4-32F4	-	11652010	11651331	3079			
CG4983	32F4-32F4	-	11653837	11652448	3079			
CG43167	32F4-32F4	-	11657992	11657460	3079			
CG4988	33A1-33A1	-	11696072	11694856	3079			
CG12602	33A1-33A1	Vacuolar H[+] ATPase subunit 100-5	11744161	11738952	3079			
CG42470	33A1-33A1	-	11753530	11753199	3079			
CG42471	33A1-33A1	-	11754022	11753640	3079			
CG42472	33A1-33A1	Seminal fluid protein 33A1	11754502	11754085	3079			
CG14931	33A1-33A1	-	11789475	11788461	3079			
CG14932	33A1-33A1	-	11791015	11789604	3079			
CG14936	33A1-33A1	Tetraspanin 33B	11792365	11791025	3079			
CG14937	33A1-33A1	-	11794083	11792412	3079			
CR34665	33A1-33A1	-	11798195	11798105	3079			
CG14938	33A1-33A2	crooked legs	11809433	11794327	3079			
CG14939	33A2-33A2	Cyclin Y	11813800	11810497	3079			
CG14941	33A2-33A2	extra sexcombs	11829377	11827204	3079			
CG42604	33A3-33A3	Seminal fluid protein 33A4	11837411	11837259	3079			
CG42473	33A3-33A3	Seminal fluid protein 33A2	11838049	11837713	3079			
CG42474	33A3-33A3	Seminal fluid protein 33A3	11840332	11839912	3079			
CG31704	33A3-33A3	-	11841012	11840691	3079			
CG14933	33A3-33A3	-	11844012	11843137	3079			
CG42486	33A3-33A3	-	11844012	11843137	3079			
CG14934	33A3-33A4	-	11849169	11847226	3079			
CG14935	33A4-33A4	-	11852881	11849963	3079			
CG42751	33A4-33A4	-	11853925	11853430	3079			
CG42325	33A8-33B1	Phosphodiesterase 1c	11928570	11814930	3079			
CG6766	33B10-33B10	-	12040682	12038613	3079			
CG6785	33B10-33B11	-	12045200	12041049	3079			
CG6770	33B11-33B11	-	12046100	12045346	3079			

CG6792	33B11-33B11	-	12048918	12046854	3079		
CG14945	33B11-33B11	-	12052049	12049423	3079		
CG12317	33B11-33C1	Jhl-21	12056042	12051755	3079		
CG16960	33B2-33B2	Odorant receptor 33a	11935716	11934505	3079		
CG16961	33B2-33B2	Odorant receptor 33b	11937501	11936181	3079		
CG5006	33B2-33B2	Odorant receptor 33c	11939202	11937969	3079		
CG16963	33B2-33B2	Crystallin	11946805	11944141	3079		
CG16964	33B2-33B2	-	11948638	11947965	3079		
CR42938	33B2-33B3	bereft	11953503	11953410	3079	3344	
CR43314	33B2-33B3	-	11971094	11952200	3079	3344	
CG16965	33B5-33B5	-	11984380	11981616	3079	3344	
CG6686	33B5-33B5	-	11988035	11984327	3079	3344	
CG34163	33B5-33B5	-	11988801	11988270	3079	3344	
CG16969	33B5-33B5	dim gamma-tubulin 2	11990834	11989938	3079	3344	
CG5202	33B5-33B5	escl	11992848	11990927	3079	3344	
CG31866	33B5-33B5	Ada1-2	11994049	11992906	3079	3344	
CG18789	33B5-33B5	-	11995428	11994066	3079	3344	
CG31864	33B5-33B5	Quetzalcoatl	11996471	11995792	3079	3344	
CG31865	33B5-33B5	Ada1-1	11997960	11996811	3079	3344	
CG18787	33B5-33B5	-	11999317	11997895	3079	3344	
CG12264	33B5-33B5	-	12001244	11999654	3079	3344	
CG6746	33B5-33B6	-	12002276	12001234	3079	3344	
CG12314	33B5-33F2	zucchini	11989861	11988735	3079	3344	
CG5279	33B8-33B8	Rhodopsin 5	12009846	12008376	3079	3344	
CG6734	33B8-33B9	-	12020938	12014304	3079	3344	
CG6756	33B9-33B10	Translocase of outer membrane 70	12038543	12035995	3079	3344	
CG5304	33B9-33B9	lethal (2) 01810	12034123	12027440	3079	3344	
CG18788	33B9-33B9	-	12036137	12034190	3079	3344	
CG5317	33C1-33C1	Ribosomal protein L7-like	12057416	12056324	3079	3344	
CG34164	33C1-33C1	-	12058251	12057393	3079	3344	
CG7061	33C1-33C2	rab3-GAP	12063171	12058304	3079	3344	
CG14946	33C2-33C2	-	12066772	12063523	3079	3344	
CG14947	33C2-33C2	-	12077635	12076823	3079	3344	
CG6716	33C3-33C3	paired	12085792	12082997	3079	3344	
CG5325	33C4-33C4	-	12095250	12093771	3079	3344	
CG6712	33C4-33C4	-	12096510	12095176	3079	3344	
CG10692	33C4-33C4	Methyltransferase 2	12097694	12096586	3079	3344	
CG5336	33C4-33C4	Ced-12	12100839	12097843	3079	3344	
CG6618	33C4-33C4	Patsas	12103285	12100765	3079	3344	
CG5353	33C4-33C4	Threonyl-tRNA synthetase	12106894	12103734	3079	3344	
CG6601	33C4-33C4	Rab-protein 6	12109124	12107287	3079	3344	
CG16996	33C4-33C4	-	12110522	12109457	3079	3344	
CG16997	33C4-33C4	-	12111995	12111133	3079	3344	

CG17211	33D2-33D2	-	12129629	12125098	3079	3344
CG17212	33D2-33D2	rhomboid-6	12133367	12130516	3079	3344
CG17213	33D2-33D2	Gustatory receptor 33a	12140392	12138065	3079	3344
CG31861	33D2-33D2	-	12162607	12161795	3079	3344
CG31860	33D2-33D2	-	12166723	12164241	3079	3344
CG31760	33D2-33D2	-	12170217	12142784	3079	3344
CG17217	33D2-33D2	-	12171232	12170586	3079	3344
CG6583	33D2-33D2	-	12172569	12171204	3079	3344
CG17218	33D2-33D2	crooked	12174091	12172984	3079	3344
CR43356	33D2-33D2	-	12174638	12174090	3079	3344
CG6579	33D2-33D3	atilla	12177886	12175448	3079	3344
CG31759	33D3-33D3	-	12210110	12207627	3079	3344
CG31762	33D3-33D5	arrest	12312795	12205843	3079	3344
CG31862	33E1-33E1	-	12339418	12338870	3079	3344
CG17010	33E1-33E1	-	12357906	12356441	3079	3344
CG43065	33E1-33E3	bruno-2	12397528	12344381	3079	3344
CG6504	33E3-33E3	Polycystic kidney disease gene-2	12402023	12398300	3079	3344
CG31764	33E3-33E4	virus-induced RNA 1	12423421	12403270	3079	3344
CG6405	33E4-33E4	-	12426440	12424904	3079	3344
CG5446	33E4-33E4	-	12427663	12426899	3079	3344
CG6388	33E4-33E4	-	12430021	12428032	3079	3344
CG5435	33E4-33E4	-	12430892	12429827	3079	3344
CG5442	33E4-33E4	SC35	12434665	12431075	3079	3344
CG6382	33E4-33E5	Ef1alpha-like factor	12440605	12434432	3079	3344
CG5427	33E5-33E5	Organic anion transporting polypeptide 33Ea	12445922	12441475	3079	3344
CG5421	33E5-33E5	-	12448113	12446224	3079	3344
CG6417	33E5-33E5	Organic anion transporting polypeptide 33Eb	12452053	12448486	3079	3344
CG5418	33E5-33E5	-	12453230	12452061	3079	3344
CG17024	33E5-33E5	-	12454951	12453664	3079	3344
CR42910	33E5-33E5	mir-967 stem loop	12460100	12460004	3079	3344
CG42281	33E5-33E9	bunched	12546630	12456577	3079	3344
CG31858	33E7-33E7	tetleys-cup	12497333	12496616	3079	3344
CG42754	33E7-33E7	-	12507868	12507612	3079	3344
CG43051	33E7-33E7	-	12508504	12507928	3079	3344
CR42746	33E9-33E9	-	12544343	12543176	3079	3344
CG17031	33F1-33F1	ref2	12611451	12610515	3079	3344
CG34395	33F1-33F1	nubbin	12628143	12587871	3079	3344
CG15485	33F2-33F2	-	12669714	12667243		3344
CG12287	33F2-33F3	POU domain protein 2	12686313	12657829		3344
CG5525	33F3-33F3	-	12692937	12690336		3344
CG6153	33F3-33F3	-	12693892	12692986		3344
CG5780	33F3-33F3	-	12694982	12693872		3344
CG5781	33F3-33F3	-	12697323	12696426		3344

CG6167	33F3-33F3	PICK1	12698917	12695038	3344	
CG17036	33F3-33F3	-	12700640	12698918	3344	
CG5776	33F3-33F3	-	12704423	12701426	3344	
CG12292	33F3-33F3	spichthyin	12706683	12704724	3344	
CG15484	33F3-33F3	-	12707590	12706799	3344	
CG6180	33F3-33F3	-	12708680	12707661	3344	
CG5787	33F3-33F3	-	12712468	12708792	3344	
CG5792	33F3-33F4	-	12721957	12713276	3344	
CG6214	33F3-33F4	Multidrug-Resistance like Protein 1	12744809	12719071	3344	
CG15483	33F5-33F5	-	12761840	12760346	3344	
CR31854	34A10-34A10	small nuclear RNA U2 at 34ABb	13216030	13215839		
CG9426	34A10-34A10	-	13219933	13216290		
CG5705	34A10-34A10	-	13221401	13219988		
CG15481	34A10-34A10	Ski6	13222315	13221394		
CG16812	34A10-34A10	-	13224550	13222561		
CG15480	34A10-34A10	-	13225206	13224706		
CG16813	34A10-34A10	-	13228407	13227853		
CG16815	34A11-34A11	-	13230720	13229642		
CG5648	34A11-34A11	Proteasome alpha6T subunit	13233059	13232039		
CG15479	34A11-34A11	-	13234633	13233796		
CG5867	34A11-34A11	-	13239296	13236493		
CG5945	34A11-34B1	-	13241763	13240133		
CG12283	34A1-34A1	kekkon-1	12822787	12818930		
CG5983	34A2-34A2	ACXC	12916774	12912530		
CG17174	34A2-34A2	ACXB	12921008	12916814		
CG17176	34A2-34A2	ACXA	12925454	12921091		
CG17178	34A2-34A2	ACXE	12929755	12925619		
CG16800	34A3-34A3	-	12967788	12966749		
CG3762	34A3-34A3	Vacuolar H[+] ATPase subunit 68-2	12978615	12974322		
CG5075	34A3-34A3	Vacuolar H[+] ATPase subunit 68-3	12981301	12978786		
CG12404	34A4-34A4	-	13000631	12993748		
CG12403	34A4-34A4	Vacuolar H[+] ATPase subunit 68-1	13004142	13000765		
CG5092	34A4-34A4	Target of rapamycin	13013201	13004786		
CG9934	34A4-34A4	-	13019434	13013388		
CG9933	34A4-34A4	A16	13021307	13019575		
CG5142	34A5-34A5	-	13109468	13106871		
CG43050	34A5-34A5	-	13120767	13119294		
CG9932	34A5-34A6	-	13060115	13022671		
CG5122	34A5-34A6	-	13134804	13130613		
CG9928	34A6-34A6	-	13142902	13142481		
CG16978	34A6-34A6	-	13144490	13143307		
CG5182	34A7-34A7	Pk34A	13160173	13158810		
CG5204	34A7-34A7	-	13163153	13160527		

CG9828	34A7-34A7	DnaJ homolog	13166072	13163291
CG5216	34A7-34A7	Sir2	13169551	13165551
CG16975	34A7-34A8	Scm-related gene containing four mbt domains	13176783	13169643
CG5439	34A8-34A8	-	13178978	13177172
CG31849	34A8-34A8	-	13182593	13180397
CG5287	34A8-34A8	-	13183498	13179245
CG5458	34A8-34A8	-	13184882	13183450
CG16974	34A8-34A8	-	13191949	13184942
CG5682	34A8-34A9	Edem2	13197281	13192206
CG9431	34A9-34A10	kekkon4	13215152	13212335
CG16972	34A9-34A9	-	13203269	13197092
CG5547	34A9-34A9	Phosphoethanolamine cytidylyltransferase	13210848	13203768
CG15482	34A9-34A9	-	13211814	13210773
CR31850	34A9-34A9	small nuclear RNA U2 at 34ABa	13212116	13211925
CG9282	34B10-34B10	Ribosomal protein L24	13395115	13394123
CG16957	34B10-34B10	-	13396184	13395360
CG10859	34B10-34B10	-	13398664	13396392
CG7110	34B10-34B11	-	13411152	13398989
CG9271	34B11-34B11	Vitelline membrane 34Ca	13411631	13411177
CG16848	34B11-34B11	-	13413718	13412519
CG16956	34B11-34B11	-	13414516	13413861
CR33788	34B1-34B1	small nuclear RNA U2 at 34ABc	13244561	13244370
CR31853	34B1-34B1	small nuclear RNA U5 at 34AB	13244974	13244848
CG16820	34B1-34B1	-	13250193	13246231
CG31728	34B2-34B2	-	13257426	13251509
CG31851	34B2-34B2	-	13258336	13257477
CG31730	34B3-34B3	-	13259641	13259064
CG31848	34B3-34B3	-	13265876	13264996
CG6108	34B3-34B4	-	13281617	13277376
CG6043	34B3-34B4	-	13284043	13261010
CG9414	34B4-34B4	DNA fragmentation factor-related protein 4	13286409	13283893
CG6116	34B4-34B4	-	13289561	13286790
CG16824	34B4-34B4	-	13293415	13293009
CG31729	34B4-34B5	-	13301668	13290006
CG15639	34B5-34B5	-	13306755	13304865
CG16825	34B5-34B5	-	13307807	13306588
CG16970	34B5-34B6	-	13331100	13307814
CG16826	34B6-34B6	-	13348959	13347791
CG9395	34B6-34B7	-	13355073	13349823
CG9377	34B7-34B7	-	13361527	13359901
CG12396	34B7-34B7	Nnp-1	13366188	13363300
CG6523	34B7-34B7	-	13367410	13366466
CG31852	34B7-34B8	Two A-associated protein of 42kDa	13369021	13367616

CG31855	34B8-34B8	-	13370334	13369193
CG9306	34B8-34B8	-	13371083	13370219
CG9305	34B8-34B8	-	13373853	13371427
CG6565	34B8-34B8	-	13376182	13374179
CG9302	34B8-34B9	-	13378546	13376449
CG7099	34B9-34B10	-	13393962	13387636
CG6699	34B9-34B9	beta'-coatomer protein	13382382	13378897
CG6866	34B9-34B9	loquacious	13385671	13382648
CG9293	34B9-34B9	-	13387299	13385848
CG7121	34C1-34C1	Tehao	13440955	13435637
CG9267	34C1-34C1	-	13445649	13444097
CG16954	34C1-34C1	Hsp60D	13449497	13447538
CG42809	34C1-34C1	-	13458073	13457636
CG42810	34C1-34C1	-	13460190	13459773
CR31846	34C2-34C2	-	13485098	13461781
CG42784	34C3-34C3	-	13500427	13475160
CG9239	34C3-34C4	B4	13549323	13502656
CG33640	34C4-34C4	-	13528537	13527841
CG33641	34C4-34C4	-	13529821	13529042
CG33642	34C4-34C4	-	13530736	13529975
CG33643	34C4-34C4	-	13531662	13531074
CG33644	34C4-34C4	-	13532636	13532085
CG33645	34C4-34C4	-	13533454	13532872
CG15638	34C4-34C4	-	13535782	13535295
CG16852	34C4-34C4	-	13541647	13540751
CG9263	34C4-34C4	-	13542576	13541675
CG16853	34C4-34C4	-	13543560	13542268
CG7147	34C4-34C6	kuzbanian	13638238	13550141
CG9254	34C5-34C5	-	13597186	13595503
CR42901	34C5-34C5	mir-2489 stem loop	13610068	13609974
CG9031	34C6-34C6	icarus	13642360	13639519
CG18507	34C6-34C6	-	13670854	13665528
CG31814	34C6-34D1	-	13717310	13676860
CG7311	34D1-34D1	-	13710592	13708215
CG9014	34D1-34D1	-	13723642	13722170
CG31813	34D1-34D1	-	13736793	13736140
CR42979	34D1-34D1	mir-1002 stem loop	13747697	13747609
CR43039	34D1-34D1	mir-968 stem loop	13747839	13747748
CG7364	34D1-34D1	-	13773905	13771087
CG31845	34D1-34D1	-	13778125	13777195
CG9008	34D1-34D1	-	13780163	13774340
CG7393	34D1-34D1	p38b	13782611	13780695
CG16890	34D1-34D1	-	13783457	13782229

CG31731	34D1-34D1	-	13790562	13784089
CG16863	34D1-34D1	-	13793264	13790963
CG7578	34D1-34D1	sec71	13799681	13793547
CG7820	34D1-34D1	Carbonic anhydrase 1	13809994	13803628
CG16889	34D1-34D1	adat	13811472	13808360
CG16865	34D1-34D1	-	13812682	13811526
CG16888	34D1-34D1	-	13813234	13812700
CG7793	34D1-34D1	Son of sevenless	13819826	13813828
CG7811	34D1-34D1	black	13823894	13821203
CG8987	34D1-34D1	tamas	13827793	13823980
CG8978	34D1-34D1	Suppressor of profilin 2	13829739	13827932
CG7833	34D1-34D1	Origin recognition complex subunit 5	13831576	13829691
CG33650	34D1-34D1	DNA polymerase gamma 35kD	13833167	13831480
CG33649	34D1-34D1	-	13833167	13831480
CG7885	34D1-34D6	RNA polymerase II 33kD subunit	13834306	13833339
CG31842	34D6-34D6	mitochondrial Ribosomal protein S23	13835038	13834250
CG31811	34D6-34E2	centaurin gamma 1A	13898715	13835567
CG33307	34D7-34D7	-	13841509	13840806
CG33306	34D7-34D7	-	13843742	13842888
CG8997	34D7-34D7	-	13845309	13844377
CG7916	34D7-34D7	-	13847799	13846758
CG7953	34D7-34D8	-	13849165	13847940
CG7968	34D8-34D8	-	13850327	13849412
CG8954	34E2-34E2	Smg5	13904659	13899353
CG8827	34E2-34E2	Angiotensin converting enzyme	13909172	13905645
CG16869	34E2-34E2	Ance-2	13911640	13909640
CG16870	34E2-34E2	Acylphosphatase	13912596	13912139
CG17988	34E3-34E5	Ance-3	13955757	13914725
CG16886	34E4-34E4	-	13923549	13920712
CG42711	34E4-34E4	-	13931224	13930593
CG16885	34E4-34E4	-	13934690	13932559
CG16884	34E4-34E4	-	13947472	13944752
CG42282	34E5-34E5	nimrod A	13963381	13957539
CG33119	34E5-34E5	nimrod B1	13965088	13963546
CG31839	34E5-34E5	nimrod B2	13967022	13965012
CG34003	34E5-34E5	nimrod B3	13967966	13967464
CG33115	34E5-34E5	nimrod B4	13969973	13968280
CG16873	34E5-34E5	nimrod B5	13972173	13970529
CG31770	34E5-34E5	Hemese	13972947	13972094
CG8942	34E5-34E5	nimrod C1	13976753	13974117
CG8864	34E5-34E5	Cyp28a5	13979573	13977303
CG18146	34E5-34E5	nimrod C2	13982952	13980146
CG8930	34E5-34E6	rickets	14001252	13982726

CG42692	34F1-34F1	-	14008820	14008127						
CR31838	34F1-34F1	tRNA:Q:34E	14010636	14010565						
CG4501	34F1-34F1	bubblegum	14019328	14013748						
CG16880	34F1-34F1	nimrod C3	14020208	14018734						
CG4500	34F1-34F1	-	14029368	14027010						
CG4501	34F1-34F1	bubblegum	14019328	14013748						
CG18095	34F1-34F2	-	14031539	14029262						
CG16876	34F2-34F2	nimrod C4	14048863	14047584						
CG32975	34F2-34F4	nicotinic Acetylcholine Receptor alpha 34E	14089437	14040171						
CG16879	34F4-34F4	-	14106684	14104654						
CG15293	34F4-34F4	-	14109304	14108057						
CG31769	34F4-34F5	-	14110739	14109597						
CG17341	35A1-35A1	-	14159075	14134917						
CG43332	35A1-35A1	-	14163222	14161181						
CG43333	35A1-35A1	-	14180681	14161235						
CG43333	35A1-35A1	-	14180681	14163508						
CG4551	35A1-35A2	smell impaired 35A	14234108	14184478						
CG32971	35A3-35A3	-	14278002	14274795						
CG42677	35A3-35A4	wing blister	14328262	14263522						
CG15287	35A4-35A4	male sterile (2) 34Fe	14333867	14328429						
CG15286	35A4-35A4	-	14340080	14338240						
CG33090	35A4-35A4	-	14345802	14334160						
CG18125	35A4-35A4	-	14346688	14345915						
CG18124	35A4-35A4	mitochondrial transcription termination factor	14348818	14347239						
CG7532	35A4-35A4	lethal (2) 34Fc	14351510	14349114						
CG43052	35A4-35A4	-	14352619	14352156						
CG7516	35A4-35A4	lethal (2) 34Fd	14355080	14352594						
CG4212	35A4-35A4	Rab-protein 14	14358400	14355147						
CG7480	35A4-35A4	Polypeptide N-acetylgalactosaminyltransferase 35A	14361411	14359218						
CG4215	35A4-35B1	spellchecker1	14365568	14362068				6084	6085	
CG3710	35B10-35B10	RNA polymerase II elongation factor	15060753	15058919	3588		6244			
CG3478	35B1-35B1	pickpocket	14381170	14378218				6084	6085	
CG4220	35B1-35B1	elbow B	14409547	14390625				6084	6085	
CG15284	35B1-35B1	partner of burs	14417318	14416835				6084	6085	
CG3474	35B1-35B1	Cuticular protein 35B	14425131	14424413				6084	6085	
CG15283	35B1-35B1	-	14450922	14450282				6084	6085	
CG4491	35B2-35B2	no ocelli	14494019	14490862				6084	6085	
CR31985	35B2-35B2	tRNA:P:35Bd	14495949	14495878				6084	6085	
CR31977	35B2-35B2	transfer RNA:gly3:35Ba	14518161	14518091				6084	6085	
CR31978	35B2-35B2	transfer RNA:gly3:35Bb	14518377	14518307				6084	6085	
CR31982	35B2-35B2	transfer RNA:gly3:35Bc	14518691	14518621				6084	6085	
CG33648	35B2-35B2	-	14525625	14524926				6084	6085	
CR31981	35B2-35B2	transfer RNA:gly3:35Bd	14530616	14530546				6084	6085	

CR31980	35B2-35B2	transfer RNA:gly3:35Be	14530924	14530854						6084	6085		
CG4218	35B2-35B2	-	14549075	14547520						6084	6085		
CG3473	35B3-35B3	-	14563726	14563072							6085		
CG42680	35B3-35B3	-	14588234	14587988							6085		
CR31983	35B3-35B3	tRNA:P:35Ba	14598930	14598859							6085		
CR31979	35B3-35B3	tRNA:P:35Bb	14599467	14599396							6085		
CR31984	35B3-35B3	tRNA:P:35Bc	14599745	14599674							6085		
CG3481	35B3-35B3	Alcohol dehydrogenase	14618902	14615555							6085		
CG3484	35B3-35B3	Adh-related	14618902	14615555							6085		
CG3479	35B3-35B4	outspread	14689325	14599776	3588		6244				6085		
CG15282	35B4-35B4	-	14713266	14712665	3588		6244				6085		
CG34165	35B4-35B4	-	14714355	14713777	3588		6244				6085		
CG42685	35B5-35B5	-	14730001	14724658	3588		6244						
CG31835	35B5-35B5	-	14737067	14735843	3588		6244						
CG31775	35B5-35B5	-	14737766	14737097	3588		6244						
CG42585	35B5-35B5	-	14741138	14739914	3588		6244						
CG42586	35B5-35B5	-	14741837	14741168	3588		6244						
CG34166	35B5-35B5	-	14743859	14743253	3588		6244						
CG42681	35B5-35B5	-	14744817	14744435	3588		6244						
CG42587	35B5-35B5	-	14745210	14744897	3588		6244						
CG4691	35B5-35B5	-	14761924	14760767	3588		6244						
CG4697	35B5-35B5	COP9 complex homolog subunit 1 a	14764065	14762765	3588		6244						
CG4701	35B5-35B5	-	14767225	14765908	3588		6244						
CG4650	35B5-35B5	-	14774981	14773810	3588		6244						
CR15280	35B5-35B5	-	14783110	14781715	3588		6244						
CG18636	35B5-35B5	-	14784586	14783342	3588		6244						
CG18420	35B6-35B6	-	14796537	14795368	3588		6244						
CG33308	35B6-35B6	-	14803299	14802334	3588		6244						
CG33309	35B6-35B6	-	14812585	14810788	3588		6244						
CG42682	35B6-35B6	-	14843101	14842128	3588		6244						
CG15279	35B6-35B6	-	14851749	14844993	3588		6244						
CG4480	35B6-35B6	-	14872022	14870371	3588		6244						
CG15278	35B6-35B6	-	14876236	14875114	3588		6244						
CG4479	35B6-35B7	Male-specific-transcript-35Ba	14881652	14879045	3588		6244						
CG4478	35B7-35B7	Male-specific-transcript-35Bb	14883715	14882101	3588		6244						
CG3491	35B7-35B7	-	14930576	14924735	3588		6244						
CG42313	35B7-35B7	-	14972300	14907570	3588		6244						
CG4482	35B7-35B8	moladietz	14997556	14975747	3588		6244						
CG4103	35B8-35B4	lethal (2) 35Bc	15009724	15008489	3588		6244						
CG10846	35B8-35B8	dynactin-subunit-p25	15006607	15005739	3588		6244						
CG4140	35B8-35B8	lethal (2) 35Be	15007404	15006583	3588		6244						
CG4185	35B8-35B8	NC2beta	15008538	15007806	3588		6244						
CG3688	35B8-35B8	lethal (2) 35Bd	15011764	15009941	3588		6244						

CG33310	35B8-35B8	-	15029513	15026909	3588		6244							
CG31832	35B8-35B8	-	15031720	15031156	3588		6244							
CG15274	35B8-35B8	metabotropic GABA-B receptor subtype 1	15034704	15017154	3588		6244							
CG4182	35B8-35B8	yellow-c	15037842	15035471	3588		6244							
CG4180	35B8-35B8	lethal (2) 35Bg	15038857	15036293	3588		6244							
CG3497	35B8-35B8	Suppressor of Hairless	15043335	15039496	3588		6244							
CG7595	35B8-35B9	crinkled	15057848	15044963	3588		6244							
CG33679	35B9-35B10	-	15059120	15058303	3588		6244							
CG4170	35C1-35C1	vasa intronic gene	15070316	15064198	3588		6244							
CG43081	35C1-35C1	vasa	15074311	15061656	3588		6244							
CG15270	35C1-35C2	-	15096915	15075645	3588		6244							
CG15269	35C2-35C2	-	15112914	15109585	3588		6244							
CG3647	35C2-35C2	shuttle craft	15118070	15113482	3588		6244							
CR31831	35C2-35C2	tRNA:L:35C	15132389	15132306	3588		6244							
CG4168	35C3-35C3	-	15178320	15162107	3588		6244							
CG42475	35C3-35C3	Seminal fluid protein 35C	15202092	15201613	3588		6244							
CR43357	35C3-35C3	-	15203713	15202259	3588		6244							
CG43230	35C4-35C4	-	15216160	15215222	3588		6244							
CG3994	35C4-35C5	-	15247832	15228728	3588		6244							
CG15267	35C5-35C5	down and out	15253607	15248885	3588		6244							
CG3975	35C5-35C5	-	15256304	15252388	3588		6244							
CG15266	35C5-35C5	lethal (2) 35Cc	15257642	15256609	3588		6244							
CG31732	35C5-35C5	yuri gagarin	15264690	15257267	3588		6244	7830						
CG42616	35C5-35C5	Cullin-3	15272011	15266029	3588		6244	7830						
CG15261	35D1-35D1	UK114	15275060	15274230	3588	1491	6244	7830	6086	6084	6085			
CG15263	35D1-35D1	-	15285905	15285027	3588	1491	6244	7830	6086	6084	6085			
CG15260	35D1-35D1	-	15292239	15291426	3588	1491	6244	7830	6086	6084	6085			
CG31733	35D1-35D1	ms(2)35Ci	15293774	15292545	3588	1491	6244	7830	6086	6084	6085			
CG15262	35D1-35D1	-	15299367	15297808	3588	1491	6244	7830	6086	6084	6085			
CG15259	35D1-35D1	no hitter	15318901	15317954	3588	1491	6244	7830	6086	6084	6085			
CG3758	35D2-35D2	escargot	15336150	15333864	3588	1491	6244	7830	6086	6084	6085			
CG15258	35D2-35D2	-	15361627	15360921	3588	1491	6244	7830	6086	6084	6085			
CG4158	35D2-35D2	worniu	15425585	15423293	3588	1491	6244	7830	6086	6084	6085			
CG4161	35D2-35D2	-	15435250	15433362	3588	1491	6244	7830	6086	6084	6085	7831		
CG3956	35D2-35D2	snail	15478269	15476593	3588	1491	6244		6086	6084	6085	7831		
CG15257	35D2-35D2	Translocase inner membrane 17	15485490	15484768	3588	1491	6244		6086	6084	6085	7831		
CG4162	35D2-35D2	lace	15505018	15499110	3588	1491	6244		6086	6084	6085	7831		
CG42448	35D3-35D3	-	15548243	15547519	3588	1491	6244		6086	6084	6085	7831		
CG15256	35D3-35D3	-	15552029	15550410	3588	1491	6244		6086	6084	6085	7831		
CG4192	35D3-35D3	kekkon-3	15583579	15552723	3588	1491	6244		6086	6084	6085	7831		
CG15255	35D3-35D3	-	15611969	15610732	3588	1491	6244		6086	6084	6085	7831		
CG11864	35D3-35D3	-	15613335	15612494	3588	1491	6244		6086	6084	6085	7831		
CG15254	35D3-35D3	-	15614824	15613948	3588	1491	6244		6086	6084	6085	7831		

CG15253	35D3-35D3	-	15616333	15615519	3588	1491	6244		6086	6084	6085	7831	
CG11865	35D3-35D3	-	15617794	15617002	3588	1491	6244		6086	6084	6085	7831	
CG17868	35D3-35D3	Odorant receptor 35a	15623558	15622128	3588	1491	6244		6086	6084	6085	7831	
CG7631	35D3-35D3	-	15629552	15628684	3588	1491	6244		6086	6084	6085	7831	
CG18480	35D3-35D3	-	15632618	15630084	3588	1491	6244		6086	6084	6085	7831	
CG18477	35D3-35D3	-	15662753	15661041	3588	1491	6244		6086	6084	6085	7831	
CG18478	35D3-35D3	-	15671223	15670239	3588	1491	6244		6086	6084	6085	7831	
CG31780	35D3-35D3	-	15697750	15696038	3588	1491	6244		6086	6084	6085	7831	
CG31827	35D3-35D3	-	15706220	15705236	3588	1491	6244		6086	6084	6085	7831	
CG4587	35D3-35D3	-	15714237	15647835	3588	1491	6244		6086	6084	6085	7831	
CG3938	35D4-35D4	Cyclin E	15748155	15727762	3588	1491	6244		6086	6084	6085	7831	
CG13240	35D4-35D4	lethal (2) 35Di	15751054	15749601	3588	1491	6244		6086	6084	6085		
CR32877	35D4-35D4	small nuclear RNA U5 at 35EF	15751682	15751557	3588	1491	6244		6086	6084	6085		
CG4152	35D4-35D4	lethal (2) 35Df	15755905	15752253	3588	1491	6244		6086	6084	6085		
CG3903	35D4-35D4	Gliotactin	15762755	15756001	3588	1491	6244		6086	6084	6085		
CG3793	35D4-35D4	-	15766128	15764230	3588	1491	6244		6086	6084	6085		
CG4148	35D4-35D4	weckle	15768317	15766475	3588	1491	6244		6086	6084	6085		
CG18801	35D4-35D4	Ku80	15771280	15768512	3588	1491	6244		6086	6084	6085		
CG31826	35D4-35D4	-	15773119	15771259	3588	1491	6244		6086	6084	6085		
CG18109	35D4-35D4	-	15790050	15784108	3588	1491	6244		6086	6084	6085		
CG42876	35D4-35D4	-	15812141	15810980	3588	1491	6244		6086	6084	6085		
CG18518	35D4-35D4	-	15835658	15834569	3588	1491	6244		6086	6084	6085		
CR31822	35D4-35D4	-	15837444	15836725	3588	1491	6244		6086	6084	6085		
CG13243	35D4-35D5	-	15854064	15852673	3588	1491	6244		6086	6084	6085		
CG4767	35D5-35D5	Tektin A	15856450	15854268	3588	1491	6244		6086	6084	6085		
CG42791	35D5-35D5	-	15863663	15863262	3588	1491	6244		6086	6084	6085		
CG42792	35D5-35D5	-	15865423	15865092	3588	1491	6244		6086	6084	6085		
CG7653	35D5-35D5	-	15880065	15877055	3588	1491	6244		6086	6084	6085		
CR31824	35D6-35D6	-	15888583	15887905	3588	1491				6084	6085		
CG18096	35D6-35D6	Thiolester containing protein I	15893811	15888639	3588	1491				6084	6085		
CG31735	35D6-35D6	-	15897071	15895560	3588	1491				6084	6085		
CG31823	35D6-35D6	-	15900487	15898920	3588	1491				6084	6085		
CG31821	35D6-35D6	-	15902377	15900985	3588	1491				6084	6085		
CG13244	35D6-35D6	-	15917607	15916888	3588	1491				6084	6085		
CG4793	35D6-35D6	-	15926203	15923395	3588	1491				6084	6085		
CG7644	35D6-35D7	beaten path Ib	15962432	15905134	3588	1491				6084	6085		
CG12448	35D7-35D7	-	15942854	15941441	3588	1491				6084	6085		
CG18063	35D7-35D7	-	15959431	15957858	3588	1491				6084	6085		
CG10839	35E1-35E1	-	15981455	15979535	3588	1491	6915			6084	6085		
CG34167	35E1-35E1	-	16003641	16002981	3588	1491	6915			6084	6085		
CG13245	35E1-35E1	-	16005461	16004572	3588	1491	6915			6084	6085		
CG31820	35E1-35E1	-	16006279	16005789	3588	1491	6915			6084	6085		
CG4838	35E1-35E1	beaten path Ic	16040407	16000537	3588	1491	6915			6084	6085		

CG4824	35E2-35E2	Bicaudal C	16048626	16042032	3588	1491	6915			6085	
CG4846	35E2-35E2	beaten path Ia	16081688	16049995	3588	1491	6915			6085	
CG4891	35E2-35E2	-	16095944	16095009	3588	1491	6915			6085	
CG4892	35E3-35E3	-	16134412	16133508		1491	6915				
CG34168	35E3-35E3	-	16135237	16134707		1491	6915				
CG4894	35E5-35E6	Ca[2+]-channel protein alpha[[1]] subunit D	16190086	16170657		1491	6915				
CG4455	35F12-35F12	-	16354549	16352936		1491	6915				
CG5809	35F12-35F12	CaBP1	16356761	16354939		1491	6915				
CG17330	35F12-35F12	juvenile hormone acid methyltransferase	16366977	16365919		1491	6915				
CG5888	35F12-36A1	-	16448465	16400169		1491	6915				
CG31819	35F1-35F1	-	16213307	16211459		1491	6915				
CG42817	35F1-35F1	-	16241432	16231477		1491	6915				
CG42818	35F1-35F1	-	16245459	16242081		1491	6915				
CG4993	35F1-35F1	PRL-1	16257603	16245826		1491	6915				
CG4930	35F1-35F1	Endonuclease G inhibitor	16259433	16257993		1491	6915				
CG4965	35F1-35F1	twine	16261875	16259416		1491	6915				
CG4935	35F1-35F1	-	16263483	16262123		1491	6915				
CG7664	35F1-35F1	cropped	16287728	16264061		1491	6915				
CG4132	35F1-35F1	pkaap	16291197	16288292		1491	6915				
CG17329	35F1-35F1	-	16291948	16291284		1491	6915				
CG13258	35F1-35F1	-	16292970	16292127		1491	6915				
CG4163	35F1-35F1	Cyp303a1	16295997	16294207		1491	6915				
CG5876	35F1-35F1	heixuedian	16299875	16296049		1491	6915				
CG17328	35F1-35F1	-	16301765	16300253		1491	6915				
CG5869	35F1-35F1	-	16302952	16301656		1491	6915				
CG4249	35F1-35F1	crossover suppressor on 2 of Manheim	16305941	16303260		1491	6915				
CG5861	35F1-35F1	-	16307275	16305786		1491	6915				
CG4214	35F1-35F1	Syntaxin 5	16309273	16307359		1491	6915				
CG5855	35F1-35F1	cornichon	16310736	16309594		1491	6915				
CG4274	35F1-35F1	fizzy	16313097	16310929		1491	6915				
CG5848	35F1-35F1	cactus	16326101	16313029		1491	6915				
CG4278	35F1-35F1	-	16328131	16327071		1491	6915				
CG5818	35F1-35F1	mitochondrial ribosomal protein L4	16329128	16328053		1491	6915				
CG4440	35F1-35F1	-	16330369	16329927		1491	6915				
CG31817	35F1-35F1	-	16337807	16330623		1491	6915				
CG42266	35F1-35F1	-	16340368	16337986		1491	6915				
CG42231	35F1-35F12	-	16352093	16342423	2583	1491	6915				
CG5813	35F1-35F12	chiffon	16352600	16342428	2583	1491	6915				
CR42898	36A10-36A10	mir-2497 stem loop	16678335	16678240	2583						
CG4694	36A10-36A10	hermaphrodite	16679383	16677210	2583						
CG4711	36A10-36A10	squash	16681655	16680056	2583						
CG31807	36A10-36A10	-	16682402	16681691	2583						
CG33552	36A10-36A10	-	16683092	16682619	2583						

CR42985	36A10-36A10	mir-9c stem loop	16698015	16697924	2583		
CR42914	36A10-36A10	mir-306 stem loop	16698488	16698404	2583		
CR43019	36A10-36A10	mir-79 stem loop	16698650	16698554	2583		
CR42960	36A10-36A10	mir-9b stem loop	16698834	16698744	2583		
CG17161	36A10-36A11	grapes	16699930	16680046	2583		
CG31782	36A10-36A12	-	16729636	16699377	2583		
CG31808	36A11-36A11	-	16716191	16704286	2583		
CG13263	36A11-36A11	Cytochrome c distal	16719635	16715858	2583		
CG17903	36A11-36A12	Cytochrome c proximal	16722659	16719874	2583		
CR42999	36A12-36A12	mir-1006 stem loop	16724858	16724795	2583		
CG17332	36A12-36A12	Vacuolar H[+]-ATPase SFD subunit	16727825	16723138	2583		
CG17996	36A12-36A12	-	16731039	16730458	2583		
CG31812	36A12-36A12	-	16731199	16729778	2583		
CG17331	36A12-36A12	-	16732129	16731221	2583		
CG17904	36A12-36A12	-	16733624	16732564	2583		
CG11397	36A12-36A13	gluon	16738372	16733617	2583		
CG17905	36A13-36A14	ChLD3	16742614	16738852	2583		
CR34666	36A1-36A1	-	16417884	16417750	2583	1491	6915
CG4472	36A1-36A1	Imaginal disc growth factor 1	16446793	16445280	2583	1491	6915
CG4475	36A1-36A1	Imaginal disc growth factor 2	16450508	16447338	2583	1491	6915
CG4559	36A1-36A1	Imaginal disc growth factor 3	16453176	16450907	2583	1491	6915
CG4952	36A1-36A2	dachshund	16485984	16466512	2583	1491	6915
CG13277	36A14-36A14	-	16743089	16742326	2583		
CG17912	36A14-36A14	-	16749609	16743404	2583		
CG17914	36A14-36A14	yellow-b	16758283	16754336	2583		
CG13278	36A14-36A14	-	16760138	16758184	2583		
CG4580	36A2-36A2	-	16490115	16488203	2583	1491	
CG4599	36A2-36A2	Tetratricopeptide repeat protein 2	16507352	16491542	2583	1491	
CG5953	36A2-36A3	-	16532877	16509120	2583	1491	
CR34667	36A3-36A3	-	16528922	16528823	2583	1491	
CG31816	36A4-36A4	-	16543263	16542546	2583	1491	
CG5968	36A4-36A4	-	16549959	16549323	2583	1491	
CG31815	36A6-36A7	-	16607277	16605945	2583	1491	
CG4631	36A7-36A7	-	16610037	16607423	2583	1491	
CG42389	36A7-36A9	-	16662012	16545033	2583	1491	
CG5996	36A9-36A10	trpgamma	16676666	16664767	2583		
CG17927	36B1-36B1	Myosin heavy chain	16788766	16766737	2583		
CG13279	36B1-36B1	Cytochrome b5-related	16790718	16788857	2583		
CG17928	36B1-36B1	-	16793444	16791053	2583		
CG13270	36B1-36B1	Ugt36Ba	16795827	16794211	2583		
CG13271	36B1-36B1	Ugt36Bb	16798273	16796595	2583		
CG17932	36B1-36B1	Ugt36Bc	16801585	16799029	2583		
CG13272	36B1-36B1	-	16816072	16807318	2583		

CG13280	36B1-36B1	-	16821093	16802021	2583		
CG13281	36B1-36B2	CAS/CSE1 segregation protein	16825206	16821150	2583		
CG31991	36B1-36B2	midway	16826991	16816665	2583		
CG31739	36B2-36B2	-	16831705	16827098	2583		
CG13282	36B2-36B2	-	16833998	16832065	2583		
CG13283	36B2-36B2	-	16837258	16835136	2583		
CR31696	36B2-36B2	putative noncoding RNA 003:2L	16841887	16838593	2583		
CG13284	36B2-36B2	-	16848713	16843192	2583		
CG31810	36B2-36B2	-	16852366	16849018	2583		
CG31809	36B2-36B2	-	16858453	16853619	2583		
CG6012	36B2-36B2	-	16861419	16860073	2583		
CG31781	36B3-36B3	-	16878300	16869487	2583		
CG32832	36B3-36B3	-	16879275	16878601	2583		
CG31743	36B3-36B3	-	16886323	16879517	2583		
CG34313	36B3-36B3	-	16886323	16879517	2583		
CG6115	36B3-36B3	-	16887962	16887125	2583		
CG42556	36B3-36B3	-	16891239	16889908	2583		
CG31805	36B4-36B4	-	16900431	16898174	2583		
CG12288	36B4-36B4	-	16902189	16900535	2583		
CG6291	36B4-36B4	Aminopeptidase P	16910431	16908229	2583		
CG42555	36B4-36B4	tweek	16917052	16888490	2583		
CG43053	36B5-36B5	-	16945374	16944723	2583		
CG33179	36B5-36B6	beat-IIIb	16993999	16973091	2583		
CG31806	36B6-36B6	-	16985583	16985054	2583		
CG6304	36B6-36B6	-	17013054	17011547	2583		
CG15136	36B6-36B6	-	17048068	17047161	2583		
CG12620	36B8-36B8	-	17088824	17087641	2583		
CG6549	36C10-36C10	four way stop	17481212	17478442	2583		
CG5110	36C10-36C10	-	17482037	17481211	2583		
CG6453	36C10-36C10	-	17484302	17481988	2583		
CG5131	36C10-36C10	-	17485624	17484518	2583		
CG43221	36C10-36C10	-	17486005	17485791	2583		
CG43220	36C10-36C10	-	17486779	17486597	2583		
CG6433	36C10-36C10	quail	17497203	17486806	2583		
CG15142	36C10-36C10	-	17498787	17497994	2583		
CG6412	36C10-36C10	-	17501114	17499268	2583		
CG15143	36C10-36C10	-	17524549	17520892	2583		
CG5526	36C10-36C10	Dynein heavy chain at 36C	17525515	17501467	2583		
CG15144	36C10-36C11	-	17529070	17525585	2583		
CG15145	36C11-36C11	-	17532234	17529311	2583		
CR43304	36C11-36C11	-	17542383	17541854	2583		
CG31784	36C1-36C1	-	17125961	17123307	2583		
CG12621	36C1-36C2	beat-IIIa	17170519	17133618	2583		

CG34106	36C2-36C2	-	17171967	17171412	2583		
CG42757	36C2-36C2	-	17173112	17172147	2583		
CG34169	36C2-36C2	-	17174105	17173481	2583		
CG31747	36C2-36C2	Gustatory receptor 36a	17177921	17176618	2583		
CG31744	36C2-36C2	Gustatory receptor 36b	17180064	17178772	2583		
CG31748	36C2-36C2	Gustatory receptor 36c	17181632	17180338	2583		
CG31750	36C2-36C2	Gr36d	17183654	17181938	2583		
CG15138	36C2-36C4	beat-IIIc	17260732	17189810	2583		
CG15139	36C3-36C3	-	17239550	17239359	2583		
CG15140	36C5-36C5	-	17287459	17286294	2583		
CG6380	36C5-36C5	-	17292202	17291134	2583		
CG34170	36C5-36C5	-	17311820	17311507	2583		
CR43239	36C6-36C6	-	17354668	17353903	2583		
CG31804	36C6-36C6	-	17364351	17363496	2583		
CG6860	36C7-36C7	-	17384147	17367509	2583		
CG5020	36C7-36C7	Cytoplasmic linker protein 190	17409698	17384739	2583		
CG6840	36C7-36C7	Rpb11	17410401	17409698	2583		
CG31803	36C7-36C7	-	17412633	17411649	2583		
CG15141	36C7-36C7	-	17413499	17410657	2583		
CG6794	36C7-36C8	Dorsal-related immunity factor	17439923	17413248	2583		
CG5043	36C8-36C8	-	17435800	17433862	2583		
CG33928	36C8-36C8	-	17436600	17435891	2583		
CG6667	36C8-36C9	dorsal	17450360	17436830	2583		
CG6582	36C9-36C10	Aac11	17477886	17474912	2583		
CG6639	36C9-36C9	-	17455917	17454263	2583		
CG18563	36C9-36C9	-	17458025	17456670	2583		
CG5050	36C9-36C9	-	17458776	17452924	2583		
CG6605	36C9-36C9	Bicaudal D	17473255	17460817	2583		
CG5094	36C9-36C9	small glutamine-rich tetratricopeptide containing protein	17474773	17471668	2583		
CG7094	36D1-36D1	-	17555765	17554353	2583		
CR42937	36D1-36D1	mir-124 stem loop	17566469	17566370	2583		
CR42939	36D1-36D1	mir-287 stem loop	17574702	17574610	2583		
CG5545	36D1-36D1	Olig family	17591267	17589407	2583		
CG6870	36D1-36D1	-	17592298	17591448	2583		
CG15147	36D1-36D1	-	17626346	17625746	2583		
CG43054	36D1-36D1	-	17628389	17627859	2583		
CG43231	36D2-36D2	-	17705202	17704681	2583		
CG7100	36D2-36D3	Cadherin-N	17752346	17647305	2583		
CG42830	36D3-36D3	-	17812604	17812041	2583		
CG42829	36D3-36E1	Cadherin-N2	17843608	17788305	2583		
CG5559	36D-36D	Synaptotagmin alpha	17603640	17592260	2583		
CG43271	36E2-36E2	-	17915023	17914508			
CR43274	36E2-36E2	-	17919131	17918552			

CG5674	36E3-36E3	-	17974870	17963338
CG15148	36E3-36E3	beethoven	17982472	17962735
CG5681	36E3-36E3	-	17988218	17986399
CG31742	36E3-36E3	-	17991501	17990418
CG5693	36E3-36E3	-	18007216	18006679
CG42659	36E3-36E3	-	18007843	18007360
CG42634	36E3-36E3	-	18008962	18007935
CG42635	36E3-36E3	-	18008962	18007935
CG31740	36E3-36E3	-	18009694	18008788
CG15150	36E3-36E3	elfless	18011475	18009643
CG15151	36E3-36E3	reduced ocelli	18070249	18012407
CG5711	36E3-36E3	Arrestin 1	18080423	18078266
CG31783	36E3-36E3	neither inactivation nor afterpotential D	18083608	18081630
CG31741	36E3-36E3	-	18086156	18084268
CG15153	36E3-36E3	-	18092238	18090941
CG5755	36E4-36E4	-	18098066	18096568
CG15152	36E5-36E5	-	18115220	18114547
CG31785	36E5-36E5	-	18125435	18124128
CG5758	36E5-36E5	-	18129864	18120027
CG7210	36E5-36E6	kelch	18138210	18129330
CG15154	36E6-36E6	Suppressor of cytokine signaling at 36E	18152410	18138668
CG17681	36E6-36E6	-	18154516	18153123
CG15155	36E6-36E6	-	18155942	18154864
CG5783	36E6-36E6	-	18157162	18156043
CG7200	36E6-36E6	-	18158686	18157110
CG7180	36E6-36E6	-	18184630	18180996
CG43338	36F10-36F10	-	18671187	18666892
CG43339	36F10-36F10	-	18673285	18671647
CG42626	36F10-36F10	Male-specific transcript 36Fb	18675094	18673363
CG31801	36F10-36F10	Male-specific transcript 36Fa	18676998	18675197
CG31751	36F10-36F11	-	18683717	18677203
CG10387	36F11-36F11	tosca	18682155	18679630
CG10385	36F11-37A1	male-specific lethal 1	18688796	18683720
CG31802	36F1-36F1	-	18209237	18208415
CG31788	36F1-36F1	-	18257902	18257494
CG42750	36F1-36F2	-	18275770	18160421
CG31787	36F2-36F2	-	18285684	18284845
CG43362	36F2-36F2	-	18291462	18291253
CG42605	36F2-36F2	Seminal fluid protein 36F	18292713	18292548
CR43358	36F2-36F2	-	18294029	18293733
CG5790	36F2-36F2	-	18297277	18294904
CG43353	36F2-36F2	-	18308684	18308088
CG43354	36F2-36F2	-	18309407	18309187

CG5803	36F2-36F4	Fasciclin 3	18393441	18320101
CG10305	36F2-36F6	Ribosomal protein S26	18443237	18442498
CG7157	36F3-36F3	Accessory gland peptide 36DE	18359026	18356125
CG34171	36F3-36F3	-	18379909	18378626
CG12750	36F5-36F5	nucampholin	18448996	18444507
CG10302	36F5-36F5	bicoid stability factor	18454587	18449514
CG10174	36F5-36F5	Nuclear transport factor-2-related	18455332	18454722
CR43044	36F5-36F5	mir-100 stem loop	18471533	18471434
CR42949	36F5-36F5	let-7	18472111	18472034
CR43029	36F5-36F5	mir-125 stem loop	18472424	18472315
CR43344	36F5-36F5	-	18472900	18455717
CG10283	36F5-36F5	-	18484438	18472964
CG10176	36F5-36F5	-	18487710	18485454
CG10275	36F5-36F6	kon-tiki	18503975	18487746
CG10178	36F6-36F6	-	18513513	18509572
CG10211	36F6-36F6	-	18531782	18517493
CG34341	36F6-36F6	Phosphodiesterase 11	18571648	18532728
CG15160	36F6-36F6	-	18595431	18590897
CG10393	36F6-36F6	absent MD neurons and olfactory sensilla	18597200	18596047
CG10413	36F7-36F7	-	18605021	18599749
CG31789	36F7-36F7	-	18606523	18605942
CG10333	36F7-36F7	-	18609558	18606833
CG10414	36F7-36F7	-	18612242	18609572
CG15161	36F7-36F7	-	18616067	18614339
CG15162	36F7-36F9	Misexpression suppressor of ras 3	18661787	18617257
CG10391	36F8-36F8	Cyp310a1	18652984	18651057
CG42490	36F9-36F10	-	18666863	18665232
CG10336	37A1-37A1	-	18690906	18689581
CG10383	37A1-37A1	-	18695422	18690902
CG10338	37A1-37A1	-	18698571	18695733
CG10341	37A1-37A1	-	18700645	18698719
CG10376	37A1-37A1	-	18703118	18700605
CG10343	37A1-37A1	-	18704457	18703467
CG10373	37A1-37A1	-	18705699	18704570
CG10372	37A1-37A1	Fas-associated factor	18708688	18706261
CG10346	37A1-37A1	Grip71	18711297	18708849
CG10369	37A1-37A1	Inwardly rectifying potassium channel 3	18713763	18711071
CG10348	37A1-37A2	-	18731419	18714615
CG42752	37A2-37A2	-	18740006	18739518
CG15167	37A2-37A2	-	18740807	18740358
CG31753	37A2-37A4	hamlet	18787500	18762874
CG10570	37A4-37A4	-	18810986	18810036
CG42502	37A4-37A4	-	18810986	18810036

CG17325	37A4-37A5	-	18813941	18813010
CG42305	37A4-37A5	-	18813941	18813010
CG17324	37A6-37B1	-	18822573	18819344
CG10653	37B10-37B10	hook	19033495	19030838
CG31800	37B10-37B10	-	19034456	19033657
CG17492	37B10-37B11	mind bomb 2	19041541	19034444
CG10449	37B11-37B11	Catecholamines up	19043614	19041714
CG15173	37B11-37B11	-	19045146	19043535
CG10473	37B11-37B12	hook-like	19048633	19045361
CG10470	37B12-37B12	-	19049886	19049079
CG10655	37B12-37B12	lethal (2) 37Bb	19051606	19049843
CG42641	37B12-37B12	Regulatory particle non-ATPase 3	19053681	19051830
CG10492	37B12-37B12	-	19058823	19054081
CG10493	37B12-37B13	PH domain leucine-rich repeat protein phosphatase	19063049	19059647
CG10495	37B13-37B13	-	19064726	19063325
CG17343	37B13-37B13	-	19069673	19064977
CG10702	37B13-37B13	-	19069850	19065272
CG17572	37B13-37B13	-	19074146	19071131
CR33315	37B13-37B13	-	19075412	19074992
CG10700	37B13-37B13	-	19079028	19077276
CG10699	37B13-37C1	Lim3	19108108	19079234
CG17323	37B1-37B1	-	18826553	18823574
CG17322	37B1-37B1	-	18829064	18826772
CG17597	37B1-37B1	-	18831141	18829006
CG17320	37B1-37B1	Sterol carrier protein X-related thiolase	18833630	18831185
CG10600	37B1-37B1	-	18839667	18834498
CG31752	37B1-37B1	-	18841168	18839929
CG33120	37B1-37B1	-	18844557	18841399
CG17321	37B1-37B1	-	18855118	18845184
CG10603	37B1-37B1	mitochondrial ribosomal protein L13	18859190	18858023
CG10602	37B1-37B1	-	18859212	18855124
CG10619	37B1-37B1	tailup	18881256	18859500
CG18397	37B5-37B6	short spindle 3	18943948	18916525
CG42848	37B6-37B6	-	18947088	18946305
CG10428	37B6-37B7	-	18950973	18948897
CG10679	37B7-37B7	Nedd8	18951845	18951147
CG10621	37B7-37B7	-	18954425	18952206
CG10623	37B7-37B7	-	18957169	18955481
CG10637	37B7-37B7	Numb-associated kinase	18968721	18957900
CG18398	37B7-37B8	Transport and Golgi organization 6	18972004	18969032
CG10639	37B8-37B8	-	18974448	18971991
CG10431	37B8-37B8	-	18978190	18974710
CG10641	37B8-37B8	-	18987276	18977748

CG15168	37B8-37B8	-	18988331	18987727
CG15170	37B8-37B8	-	18990233	18988268
CG15169	37B8-37B8	-	18992409	18991057
CG10650	37B8-37B8	-	18995930	18993617
CG10446	37B9-37B10	similar to Deadpan	19030787	19027712
CG31792	37B9-37B9	-	19002483	18997995
CG31793	37B9-37B9	-	19008231	19003410
CR34668	37B9-37B9	-	19008683	19008611
CG10652	37B9-37B9	Ribosomal protein L30	19009273	19008233
CG15171	37B9-37B9	robl37BC	19011532	19010916
CG15172	37B9-37B9	-	19023650	19023164
CG17344	37C1-37C1	-	19102909	19102044
CG10501	37C1-37C1	alpha methyl dopa-resistant	19114110	19110159
CG10561	37C1-37C1	-	19116571	19114401
CG10697	37C1-37C1	Dopa decarboxylase	19120300	19116480
CG10691	37C1-37C1	lethal (2) 37Cc	19123866	19122040
CG10719	37C1-37C6	brain tumor	19177972	19133806
CG10689	37C5-37C5	lethal (2) 37Cb	19126973	19123998
CG10563	37C5-37C5	lethal (2) 37Cd	19129326	19127262
CG10687	37C5-37C5	Asparaginyl-tRNA synthetase	19131960	19129862
CG17347	37C5-37C5	lethal (2) 37Ce	19133097	19132329
CG10685	37C5-37C5	lethal (2) 37Cg	19133483	19133023
CG17568	37C6-37C6	-	19181702	19179749
CG42688	37C6-37C7	-	19182659	19182184
CG17567	37C7-37C7	-	19183613	19183091
CG17566	37C7-37C7	gamma-Tubulin at 37C	19185724	19183970
CG10739	37C7-37C7	pigeon	19189938	19186036
CG17348	37C7-37C7	derailed	19208615	19190346
CG31797	37D1-37D1	-	19262133	19259527
CG17564	37D2-37D2	-	19299851	19298345
CG10750	37D2-37D2	-	19301600	19300306
CG17559	37D2-37D2	doughnut on 2	19363224	19338676
CG13086	37D2-37D2	-	19365397	19364394
CG17349	37D3-37D3	-	19372712	19370478
CG17350	37D3-37D3	-	19383271	19380930
CG15825	37D3-37D3	fondue	19386202	19383387
CG17549	37D4-37D4	-	19390070	19387050
CG31798	37D4-37D4	-	19396190	19394160
CG17544	37D4-37D5	-	19398492	19390369
CR33712	37D5-37D5	small non-messenger RNA 359	19403568	19403535
CG31794	37D5-37D7	Paxillin	19426424	19400781
CG9976	37D6-37D6	Galactose-specific C-type lectin	19418274	19417447
CG33532	37D6-37D6	lectin-37Da	19419029	19418317

CG33533	37D6-37D6	lectin-37Db	19419767	19419075
CG16771	37D7-37E1	-	19429224	19424090
CG13085	37D7-37E1	-	19430270	19426322
CG9987	37E1-37E1	-	19432444	19430657
CG9994	37E1-37E1	Rab9	19435841	19432593
CG10237	37E1-37E1	-	19441278	19435844
CG10234	37E1-37E1	heparan sulfate 2-O-sulfotransferase	19444761	19442830
CG9999	37E1-37E1	Ran GTPase activating protein	19447322	19442041
CG10223	37E1-37E1	Topoisomerase 2	19453507	19447362
CG10026	37E1-37E1	-	19457726	19454256
CG10034	37E3-37E3	traffic jam	19467758	19464580
CG10195	37E3-37E3	-	19484702	19482877
CG13084	37E3-37E4	-	19486532	19484930
CG13083	37E4-37E4	-	19488691	19487490
CG10194	37E4-37E4	-	19490083	19488682
CG18094	37E4-37E4	-	19491679	19490486
CG10189	37E4-37E4	-	19492927	19491647
CG10084	37E4-37E4	second mitotic wave missing	19497987	19493258
CG10123	37E4-37E4	Topoisomerase 3alpha	19502268	19498179
CG10188	37E4-37E5	-	19508760	19502334
CG10186	37E5-37E5	-	19517201	19508953
CR43363	37E5-37E5	-	19518565	19518109
CG10132	37E5-37E5	-	19525454	19518787
CG10166	37E5-37E5	-	19526347	19525434
CG10165	37E5-37E5	-	19530301	19527281
CG10137	37E5-37F1	-	19532992	19526686
CG31697	37F1-37F1	-	19536107	19535448
CG33116	37F1-37F1	-	19537365	19533473
CG13082	37F1-37F1	-	19539910	19538429
CG13081	37F1-37F1	-	19541343	19540693
CG10360	37F1-37F1	refractory to sigma P	19545548	19542446
CG10337	37F1-37F1	-	19546914	19545376
CG10363	37F1-37F1	Thiolester containing protein IV	19556455	19549793
CG13079	37F1-37F1	-	19563049	19558047
CG13078	37F1-37F1	-	19565158	19563930
CG13077	37F1-37F2	-	19567359	19565863
CR43035	37F2-37F2	mir-2a-2 stem loop	19569561	19569490
CR42899	37F2-37F2	mir-2a-1 stem loop	19569972	19569897
CR43016	37F2-37F2	mir-2b-2 stem loop	19570264	19570182
CG10334	37F2-37F2	spitz	19577324	19567900
CG10364	37F2-37F2	msb1l	19579131	19577707
CG10268	37F2-37F2	-	19580346	19579093
CG10263	37F2-37F2	Hakai	19582497	19580608

CG10262	37F2-37F2	-	19584021	19582823
CG10366	37F2-37F2	-	19586440	19584245
CG10443	37F2-38A2	Leukocyte-antigen-related-like	19731561	19606569
CG31695	38A1-38A1	screw	19701035	19699627
CG10462	38A2-38A2	-	19735954	19732080
CG10447	38A2-38A2	Nuclear factor Y-box B	19737088	19736042
CG10631	38A2-38A2	-	19756867	19742814
CG10628	38A2-38A2	-	19758613	19757243
CG10463	38A2-38A2	-	19760986	19758879
CG31692	38A2-38A3	fructose-1,6-bisphosphatase	19764134	19761579
CG10604	38A3-38A3	brain-specific homeobox	19769067	19765776
CG10538	38A3-38A3	CdGAPr	19791900	19775110
CG10466	38A3-38A3	-	19792846	19792190
CG10528	38A3-38A3	female sterile (2) ltoPP43	19795849	19792902
CR32879	38A4-38A4	small nuclear RNA U4 at 38AB	19810875	19810734
CR32881	38A4-38A4	snRNA:U5:38ABa	19812074	19811948
CR32878	38A4-38A4	small nuclear RNA U2 at 38ABb	19812836	19812646
CG13962	38A4-38A4	-	19814536	19813745
CR32882	38A4-38A4	small nuclear RNA U2 at 38ABa	19815805	19815614
CR32880	38A4-38A4	snRNA:U5:38ABb	19816540	19816414
CG13958	38A4-38A4	-	19828890	19827274
CG10481	38A6-38A6	-	19892529	19890247
CG43097	38A7-38A7	-	19911811	19910648
CG31691	38A7-38A7	Turandot F	19912377	19911863
CG33117	38A7-38A7	Victoria	19913516	19912847
CG42589	38A8-38A8	sickie	19957767	19856184
CG10664	38A8-38A8	-	19960004	19958707
CG34051	38A8-38A8	-	19961030	19960069
CG42866	38A8-38A8	-	19961662	19961251
CG13965	38A8-38A8	-	19962298	19961837
CG16772	38A8-38A8	-	19963844	19962678
CG10680	38A8-38A8	-	19965493	19964173
CG18806	38A8-38A8	-	19967140	19965555
CG10658	38A8-38A8	Helical Factor	19967683	19966727
CG12508	38A8-38A8	-	19969964	19969743
CG13966	38A8-38B1	-	20017282	19969484
CG10659	38B1-38B1	-	20025811	20024975
CG13968	38B1-38B1	short neuropeptide F precursor	20056375	20027915
CG10726	38B1-38B2	barren	20060975	20058163
CG10895	38B2-38B2	loki	20064381	20061477
CG10728	38B2-38B2	valois	20065675	20064261
CG10730	38B2-38B2	-	20072209	20070077
CG13969	38B2-38B3	brain washing	20073725	20066370

CG16784	38B3-38B3	purple	20075467	20073719
CG10718	38B3-38B5	nebbish	20089698	20075757
CG42849	38B4-38B4	-	20080196	20079275
CG10746	38B4-38B4	fledgling of Klp38B	20085064	20081606
CG10747	38B5-38B5	-	20091220	20089636
CG10721	38B6-38B6	-	20093152	20091661
CG10756	38B6-38B6	TBP-associated factor 13	20093846	20093088
CG10722	38B6-38B6	nessun dorma	20096253	20093964
CG10757	38B6-38B6	mitochondrial ribosomal protein S18B	20098065	20096431
CG10723	38C1-38C1	Kua	20103375	20097858
CG13970	38C1-38C1	-	20104063	20103446
CG10651	38C2-38C2	-	20134923	20133805
CG40341	38C3-38C3	-	20248617	20248223
CG40172	38C3-38C3	-	20249371	20249162
CR40465	38C3-38C3	-	20254397	20253808
CG17571	38C3-38C3	-	20257035	20255988
CG17570	38C3-38C3	-	20264299	20263895
CG12617	38C4-38C4	-	20295320	20294707
CG10076	38C5-38C5	spire	20348386	20311219
CG10922	38C5-38C5	La autoantigen-like	20350328	20348393
CR34669	38C5-38C5	-	20353582	20353482
CG10043	38C5-38C5	rho-type guanine exchange factor	20365254	20350436
CG11012	38C5-38C5	UDP-glycosyltransferase 37a1	20373967	20372473
CG16798	38C5-38C5	-	20382355	20376983
CG10947	38C6-38C6	-	20399394	20385293
CG10949	38C6-38C6	-	20416918	20415171
CR34570	38C6-38C6	snoRNA:Psi18S-525a	20418481	20418348
CR34571	38C6-38C6	snoRNA:Psi18S-640a	20418654	20418523
CR34572	38C6-38C6	snoRNA:Psi18S-525b	20418804	20418670
CR34573	38C6-38C6	snoRNA:Psi18S-525c	20418967	20418834
CR34574	38C6-38C6	snoRNA:Psi18S-640b	20419133	20418997
CR34575	38C6-38C6	snoRNA:Psi18S-525d	20419281	20419145
CR34576	38C6-38C6	snoRNA:Psi18S-640c	20419430	20419303
CR34577	38C6-38C6	snoRNA:Psi18S-525e	20419585	20419456
CR34578	38C6-38C6	snoRNA:Psi18S-640d	20419756	20419626
CR34579	38C6-38C6	snoRNA:Psi18S-525f	20419908	20419774
CR34580	38C6-38C6	snoRNA:Psi18S-525g	20420065	20419932
CR34581	38C6-38C6	snoRNA:Psi18S-640e	20421274	20421151
CR34582	38C6-38C6	snoRNA:Psi18S-525h	20421438	20421304
CR34583	38C6-38C6	snoRNA:Psi18S-640f	20421600	20421475
CR34584	38C6-38C6	snoRNA:Psi18S-525i	20421752	20421617
CR34585	38C6-38C6	snoRNA:Psi18S-640g	20421909	20421781
CR34586	38C6-38C6	snoRNA:Psi18S-525j	20422063	20421928

CG10954	38C6-38C6	Arc-p34	20423034	20417061
CG15130	38C6-38C6	-	20424599	20423185
CG11019	38C6-38C6	-	20427375	20426407
CG31688	38C6-38C7	-	20443945	20429027
CG31683	38C7-38C7	-	20449973	20447734
CG31687	38C7-38C7	-	20452538	20450207
CG18858	38C7-38C7	-	20459082	20457057
CG2508	38C7-38C8	cdc23	20461729	20459395
CG2493	38C8-38C8	-	20463449	20461585
CG43233	38C8-38C8	-	20473339	20472793
CG43234	38C8-38C8	-	20477549	20477307
CR43027	38C8-38C8	mir-1 stem loop	20487531	20487441
CG34007	38C8-38C8	-	20495448	20495106
CG31677	38D1-38D1	-	20604196	20603589
CG15475	38D1-38D1	-	20615559	20614618
CR43011	38D1-38D1	mir-133 stem loop	20616714	20616617
CR42978	38D1-38D1	mir-288 stem loop	20618462	20618366
CG17472	38D1-38D1	-	20635167	20634557
CR43158	38D1-38D1	-	20639578	20639015
CG31680	38D1-38D1	-	20640718	20640146
CG42606	38D1-38D1	Seminal fluid protein 38D	20641622	20640917
CG17470	38D2-38D2	-	20643244	20642306
CG2488	38D2-38D2	(6-4)-photolyase	20645789	20643351
CG2608	38D2-38D2	-	20647381	20645826
CR34587	38D2-38D2	-	20647891	20647817
CR34588	38D2-38D2	-	20648125	20648051
CR34589	38D2-38D2	-	20648356	20648282
CR32957	38D2-38D2	Uhg3	20648848	20647533
CG18810	38D2-38D2	-	20650079	20649022
CG2611	38D2-38D2	-	20650898	20650194
CG2478	38D2-38D2	brunelleschi	20656176	20650755
CG2614	38D2-38D2	-	20659218	20656428
CG31678	38D2-38D4	-	20675941	20659128
CG2615	38D4-38E2	IkappaB kinase-like 2	20679308	20676234
CG1962	38D5-38D5	-	20681844	20678921
CG2617	38D5-38D5	-	20683629	20682370
CG1864	38D5-38E3	Hormone receptor-like in 38	20714589	20683462
CG9324	38E10-38E10	Pomp	20789100	20787649
CG9328	38E10-38F1	-	20814030	20797717
CG9316	38E4-38E4	-	20726551	20724209
CG9317	38E4-38E4	-	20730309	20727151
CG9318	38E4-38E5	-	20734310	20730645
CG2637	38E5-38E6	Female sterile (2) Ketel	20750941	20734710

CG9319	38E6-38E6	-	20752341	20750934
CG9320	38E6-38E7	nucleostemin 4	20754657	20752400
CG9323	38E7-38E7	-	20757991	20754579
CG1768	38E7-38E8	diaphanous	20767536	20758147
CG1759	38E9-38E10	caudal	20783135	20770736
CG33322	38F1-38F1	-	20816240	20814337
CG33321	38F1-38F1	Chemosensory protein B 38b	20817270	20816456
CG33320	38F1-38F1	Chemosensory protein B 38a	20818532	20817816
CG14405	38F1-38F1	Chemosensory protein B 38c	20820867	20820089
CG9331	38F1-38F1	-	20827724	20824436
CG31673	38F1-38F1	-	20831063	20829608
CG31674	38F1-38F1	-	20832859	20831262
CG9333	38F1-38F1	Oseg5	20835607	20832858
CG9334	38F1-38F2	Serine protease inhibitor 3	20838179	20836621
CG31676	38F2-38F2	-	20849182	20840800
CG14402	38F2-38F2	-	20850988	20849357
CG9335	38F2-38F3	-	20857113	20852581
CG14400	38F3-38F3	-	20857891	20856987
CG9336	38F3-38F3	-	20861017	20859169
CR9337	38F3-38F3	-	20863775	20862547
CG9338	38F3-38F3	-	20867311	20865227
CG31675	38F3-38F3	-	20869650	20867757
CG14401	38F3-38F3	-	20871565	20869848
CG9339	38F3-38F5	-	20918928	20871335
CR33317	38F4-38F4	-	20901524	20901134
CG9342	38F5-38F5	Microsomal triacylglycerol transfer protein	20922850	20919094
CR33318	38F6-38F6	-	20924534	20923955
CG9273	38F6-38F6	Replication protein A2	20926144	20924975
CG9272	38F6-38F6	-	20927874	20926448
CR33319	38F6-38F6	-	20929525	20928824
CG9270	38F6-38F6	-	20934113	20929456
CG42238	38F6-39A1	-	21051954	20965520
CG1762	39A1-39A1	beta[nu] integrin	21058044	21052832
CG9265	39A1-39A1	-	21069891	21057702
CG9264	39A1-39A1	torn and diminished rhabdomeres	21081053	21071009
CG33511	39A1-39A1	-	21082494	21081127
CG33510	39A1-39A1	-	21084287	21082889
CG33509	39A1-39A1	-	21086506	21084605
CG33508	39A1-39A1	pickpocket 13	21088730	21086900
CG9259	39A1-39A1	-	21090999	21089565
CG14397	39A1-39A1	-	21094864	21091241
CG34136	39A1-39A1	-	21098932	21096922
CG12050	39A1-39A1	-	21102392	21094961

CG9257	39A2-39A2	-	21104329	21102739
CG9256	39A2-39A3	Na[+]/H[+] hydrogen exchanger 2	21134255	21104599
CG1099	39A4-39A4	Dynamin associated protein 160	21142353	21133941
CR34670	39A4-39A4	-	21143941	21143854
CG9253	39A4-39A4	-	21145147	21143227
CG9252	39A4-39A5	deadlock	21148546	21145134
CG1071	39A5-39A6	E2F transcription factor 2	21156245	21154293
CG9250	39A6-39A6	M-phase phosphoprotein 6	21157685	21156874
CG9249	39A6-39A6	-	21158588	21157433
CG9248	39A6-39A7	-	21160783	21158878
CG9247	39A6-39A7	-	21163087	21160636
CG9246	39A7-39A7	-	21166101	21163611
CG43345	39A7-39A7	-	21168344	21166046
CG43346	39A7-39A7	-	21168344	21166046
CG9244	39A7-39A7	Aconitase	21173017	21168356
CG31627	39A7-39A7	-	21174179	21173267
CG9242	39A7-39B1	burgundy	21179697	21174383
CG9241	39B1-39B1	Sensitized chromosome inheritance modifier 19	21182812	21179941
CG14396	39B1-39B1	Ret oncogene	21198745	21182394
CG31624	39B1-39B1	-	21200263	21199187
CG31988	39B1-39B2	-	21202742	21201535
CG8681	39B2-39B3	clumsy	21211820	21206520
CR31625	39B3-39B3	small nuclear RNA U4 at 39B	21215178	21215036
CG8679	39B3-39B3	-	21218527	21216004
CG8678	39B3-39B3	-	21220567	21212693
CG8677	39B3-39B4	-	21234035	21221336
CG31626	39B3-39B4	-	21236733	21232484
CG8674	39C1-39C1	lethal (2) k14505	21262287	21261159
CG8671	39C1-39C1	-	21281575	21262961
CR31621	39C1-39C1	Cyp6t2Psi	21284273	21282811
CG31622	39C1-39C1	Gustatory receptor 39a	21297686	21290734
CG18362	39C1-39C2	Mlx interactor	21310032	21286078
CG8669	39C2-39C3	cryptocephal	21319536	21310854
CG42696	39C4-39C4	-	21327114	21326660
CG8676	39C-60	Hormone receptor-like in 39	21259675	21237237
CG8667	39D1-39D1	dimmed	21340780	21339110
CG8666	39D1-39D1	Tetraspanin 39D	21358273	21344603
CG31623	39D1-39D2	defective transmitter release	21367297	21361216
CG31620	39D2-39D2	Gustatory receptor 39b	21369706	21367908
CG8665	39D2-39D2	-	21377995	21371232
CG8663	39D2-39D2	nervana 3	21390347	21380000
CR31616	39D3-39D3	His-Psi:CR31616	21404579	21404115
CR31615	39D3-39D3	His-Psi:CR31615	21405361	21404963

CR31754	39D3-39D3	His-Psi:CR31754	21405970	21405657
CG33801	39D3-39D3	His1:CG33801	21417975	21417078
CG33910	39D3-39D3	His2B:CG33910	21418843	21418259
CR33802	39D3-39D3	His-Psi:CR33802	21419260	21418852
CG33909	39D3-39D3	His4:CG33909	21420103	21419530
CG33803	39D3-39D3	His3:CG33803	21420596	21420129
CG31617	39D3-39D3	His1:CG31617	21422877	21421980
CG17949	39D3-39D3	His2B:CG17949	21423745	21423125
CR33727	39D3-39D3	snmRNA:430:CR33727	21423911	21423876
CG31618	39D3-39D3	His2A:CG31618	21424322	21423754
CG31611	39D3-39D3	His4:CG31611	21425167	21424592
CG31613	39D3-39D3	His3:CG31613	21425660	21425193
CG33804	39D3-39D3	His1:CG33804	21427938	21427041
CG33908	39D3-39D3	His2B:CG33908	21428666	21428252
CR33805	39D3-39D3	His-Psi:CR33805	21429382	21428850
CG33907	39D3-39D3	His4:CG33907	21430229	21429700
CG33806	39D3-39D3	His3:CG33806	21430722	21430255
CG33807	39D3-39D3	His1:CG33807	21432985	21432088
CG33906	39D3-39D3	His2B:CG33906	21433853	21433299
CR33728	39D3-39D3	snmRNA:430:CR33728	21434019	21433984
CG33808	39D3-39D3	His2A:CG33808	21434430	21433862
CG33905	39D3-39D3	His4:CG33905	21435273	21434748
CG33809	39D3-39D3	His3:CG33809	21435766	21435299
CG33810	39D3-39D3	His1:CG33810	21438033	21437136
CG33904	39D3-39D3	His2B:CG33904	21438901	21438347
CR33811	39D3-39D3	His-Psi:CR33811	21439318	21438910
CG33903	39D3-39D3	His4:CG33903	21440161	21439634
CG33812	39D3-39D3	His3:CG33812	21440654	21440187
CG9326	39D3-40B1	varicose	20797040	20788659
CG33813	39D4-39D4	His1:CG33813	21452074	21451177
CG33902	39D4-39D4	His2B:CG33902	21452942	21452388
CR33729	39D4-39D4	snmRNA:430:CR33729	21453108	21453073
CG33814	39D4-39D4	His2A:CG33814	21453519	21452951
CG33901	39D4-39D4	His4:CG33901	21454362	21453835
CG33815	39D4-39D4	His3:CG33815	21454855	21454388
CG33816	39D4-39D4	His1:CG33816	21457135	21456238
CG33900	39D4-39D4	His2B:CG33900	21458003	21457449
CR33730	39D4-39D4	snmRNA:430:CR33730	21458169	21458134
CG33817	39D4-39D4	His2A:CG33817	21458580	21458012
CG33899	39D4-39D4	His4:CG33899	21459421	21458898
CG33818	39D4-39D4	His3:CG33818	21459914	21459447
CG33819	39D4-39D4	His1:CG33819	21462195	21461298
CG33898	39D4-39D4	His2B:CG33898	21463063	21462509

CR33731	39D4-39D4	snmRNA:430:CR33731	21463229	21463194
CG33820	39D4-39D4	His2A:CG33820	21463640	21463072
CG33897	39D4-39D4	His4:CG33897	21464481	21463958
CG33821	39D4-39D4	His3:CG33821	21464974	21464507
CG33822	39D4-39D4	His1:CG33822	21467238	21466341
CG33896	39D4-39D4	His2B:CG33896	21468106	21467552
CR33732	39D4-39D4	snmRNA:430:CR33732	21468272	21468237
CG33823	39D4-39D4	His2A:CG33823	21468683	21468115
CG33895	39D4-39D4	His4:CG33895	21469524	21469001
CG33824	39D4-39D4	His3:CG33824	21470017	21469550
CG33825	39D4-39D5	His1:CG33825	21472281	21471384
CG33894	39D5-39D5	His2B:CG33894	21473149	21472595
CR33733	39D5-39D5	snmRNA:430:CR33733	21473315	21473280
CG33826	39D5-39D5	His2A:CG33826	21473726	21473158
CG33893	39D5-39D5	His4:CG33893	21474567	21474044
CG33827	39D5-39D5	His3:CG33827	21475060	21474593
CG33828	39D5-39D5	His1:CG33828	21477324	21476427
CG33892	39D5-39D5	His2B:CG33892	21478192	21477638
CR33734	39D5-39D5	snmRNA:430:CR33734	21478358	21478323
CG33829	39D5-39D5	His2A:CG33829	21478769	21478201
CG33891	39D5-39D5	His4:CG33891	21479610	21479087
CG33830	39D5-39D5	His3:CG33830	21480103	21479636
CG33831	39D5-39D5	His1:CG33831	21482367	21481470
CG33890	39D5-39D5	His2B:CG33890	21483235	21482681
CR33735	39D5-39D5	snmRNA:430:CR33735	21483401	21483366
CG33832	39D5-39D5	His2A:CG33832	21483812	21483244
CG33889	39D5-39D5	His4:CG33889	21484655	21484130
CG33833	39D5-39D5	His3:CG33833	21485148	21484681
CG33834	39D5-39D5	His1:CG33834	21487518	21486621
CG33888	39D5-39D5	His2B:CG33888	21488386	21487832
CR33736	39D5-39D5	snmRNA:430:CR33736	21488552	21488517
CG33835	39D5-39D5	His2A:CG33835	21488963	21488395
CG33887	39D5-39D5	His4:CG33887	21489804	21489279
CG33836	39D5-39D5	His3:CG33836	21490297	21489830
CG33837	39D5-39D5	His1:CG33837	21492563	21491666
CG33886	39D5-39D5	His2B:CG33886	21493431	21492877
CR33737	39D5-39D5	snmRNA:430:CR33737	21493597	21493562
CG33838	39D5-39D5	His2A:CG33838	21494008	21493440
CG33885	39D5-39D5	His4:CG33885	21494849	21494324
CG33839	39D5-39D5	His3:CG33839	21495342	21494875
CG33840	39D5-39D5	His1:CG33840	21497608	21496711
CG33884	39D5-39D5	His2B:CG33884	21498476	21497922
CR33738	39D5-39D5	snmRNA:430:CR33738	21498642	21498607

CG33841	39D5-39D5	His2A:CG33841	21499053	21498485
CG33883	39D5-39D5	His4:CG33883	21499894	21499369
CG33842	39D5-39D5	His3:CG33842	21500387	21499920
CG33843	39D5-39D5	His1:CG33843	21502655	21501758
CG33882	39D5-39D5	His2B:CG33882	21503529	21502975
CR33739	39D5-39D5	snmRNA:430:CR33739	21503695	21503660
CG33844	39D5-39D5	His2A:CG33844	21504106	21503538
CG33881	39D5-39D5	His4:CG33881	21504947	21504422
CG33845	39D5-39D5	His3:CG33845	21505440	21504973
CG33846	39D5-39D5	His1:CG33846	21507706	21506809
CG33880	39D5-39D5	His2B:CG33880	21508574	21508020
CR33740	39D5-39D5	snmRNA:430:CR33740	21508740	21508705
CG33847	39D5-39D5	His2A:CG33847	21509151	21508583
CG33879	39D5-39D5	His4:CG33879	21509992	21509467
CG33848	39D5-39D5	His3:CG33848	21510485	21510018
CG33849	39D5-39E1	His1:CG33849	21512750	21511853
CG33878	39E1-39E1	His2B:CG33878	21513618	21513064
CR33741	39E1-39E1	snmRNA:430:CR33741	21513784	21513749
CG33850	39E1-39E1	His2A:CG33850	21514195	21513627
CG33877	39E1-39E1	His4:CG33877	21515036	21514511
CG33851	39E1-39E1	His3:CG33851	21515529	21515062
CG33852	39E1-39E1	His1:CG33852	21517795	21516898
CG33876	39E1-39E1	His2B:CG33876	21518663	21518109
CR33742	39E1-39E1	snmRNA:430:CR33742	21518829	21518794
CG33853	39E1-39E1	His2A:CG33853	21519240	21518672
CG33875	39E1-39E1	His4:CG33875	21520083	21519556
CG33854	39E1-39E1	His3:CG33854	21520576	21520109
CG33855	39E1-39E1	His1:CG33855	21522638	21521741
CG33874	39E1-39E1	His2B:CG33874	21523506	21522952
CR33743	39E1-39E1	snmRNA:430:CR33743	21523672	21523637
CG33856	39E1-39E1	His2A:CG33856	21524083	21523515
CG33873	39E1-39E1	His4:CG33873	21524926	21524399
CG33857	39E1-39E1	His3:CG33857	21525419	21524952
CG33858	39E1-39E1	His1:CG33858	21527481	21526584
CG33872	39E1-39E1	His2B:CG33872	21528349	21527795
CR33744	39E1-39E1	snmRNA:430:CR33744	21528515	21528480
CG33859	39E1-39E1	His2A:CG33859	21528926	21528358
CG33871	39E1-39E1	His4:CG33871	21529769	21529242
CG33860	39E1-39E1	His3:CG33860	21530262	21529795
CG33861	39E1-39E1	His1:CG33861	21532324	21531427
CG33870	39E1-39E1	His2B:CG33870	21533192	21532638
CR33745	39E1-39E1	snmRNA:430:CR33745	21533358	21533323
CG33862	39E1-39E1	His2A:CG33862	21533769	21533201

CG33869	39E1-39E1	His4:CG33869	21534610	21534085
CG33863	39E1-39E1	His3:CG33863	21535103	21534636
CG33864	39E1-39E1	His1:CG33864	21537368	21536471
CG33868	39E1-39E1	His2B:CG33868	21538236	21537682
CR33746	39E1-39E1	snmRNA:430:CR33746	21538402	21538367
CG33865	39E1-39E1	His2A:CG33865	21538813	21538245
CR33867	39E1-39E1	His-Psi:CR33867	21541127	21539129
CG33866	39E1-39E1	His3:CG33866	21541620	21541153
CR31614	39E1-39E1	His-Psi:CR31614	21543706	21542989
CG3305	39E2-39E2	Lamp1	21577103	21573378
CR42545	39E2-39E2	-	21577534	21577205
CG12548	39E2-39E2	no mechanoreceptor potential B	21589355	21578319
CR42546	39E2-39E2	-	21590593	21589784
CG2201	39E3-39E3	-	21623623	21614232
CR43148	39E3-39E3	-	21625388	21624679
CG2207	39E3-39E3	Decondensation factor 31	21629930	21626590
CG1506	39E3-39E3	Ac3	21647967	21632599
CG43144	39E3-39E3	-	21658249	21657659
CG1512	39E3-39E6	Cullin-2	21663218	21658752
CG2225	39E6-39E7	-	21677530	21663792
CR33705	39E7-39E7	small non-messenger RNA 254	21680700	21680670
CG2238	39E7-39E7	Elongation factor 2b	21682150	21678097
CG31619	39F1-39F3	-	21729051	21684536
CG11628	40A1-39F3	steppke	21757461	21741254
CG1416	40A2-40A2	-	21760915	21758002
CG31612	40A2-40A3	-	21795445	21762314
CG11630	40A3-40A3	-	21784013	21782118
CG1374	40A5-40A5	teashirt	21837013	21828595
CG11629	40B3-40B3	-	21898289	21896666
CG1421	40B4-40B4	-	21903739	21903062
CG1428	40B4-40B4	-	21908332	21906289
CG31600	40B4-40B4	-	21915358	21914269
CG11634	40B4-40B4	-	21917450	21916361
CG2528	40D1-40D2	-	21992933	21981572
CG31693	40D3-40D3	-	22017334	22015231
CR33987	40D3-40D3	-	22020254	22019316
CG12630	40D3-40D3	tiptop	22024313	22020035
CG41434	40D4-40D4	-	22038970	22038032
CG31601	40D4-40D4	-	22043034	22040790
CG34173	40D5-40D5	-	22054245	22053883
CG42597	40E1-40E1	-	22065193	22064693
CR31700	40E1-40E1	-	22067170	22066517
CG31702	40E1-40E1	-	22072902	22071153

CG6691	40E2-40E2	tiny tim 3	22080742	22079672
CG31703	40E3-40E3	-	22104401	22102626
CG15219	40E3-40E3	-	22105512	22104891
CG10834	40E3-40E3	-	22107279	22106862
CG6675	40E3-40E3	-	22110449	22108964
CG3651	40E4-40E4	-	22125142	22121836
CG15218	40E4-40E4	Cyclin K	22130142	22128264
CR43240	40E5-40E5	-	22131127	22131026
CR43241	40E5-40E5	-	22132435	22131221
CG34137	40F1-40F1	-	22152640	22151623
CG42748	40F1-40F1	-	22164838	22134351
CG1832	40F2-40F2	-	22169191	22165966
CG3635	40F2-40F3	-	22183991	22175415
CG42352	40F4-40F4	Ionotropic receptor 40a	22214265	22189526
CR12628	40F5-40F5	Microsomal glutathione S-transferase-like pseudogene	22226771	22226151
CG3262	40F6-40F6	-	22240881	22239906
CG12775	40F6-40F6	Ribosomal protein L21	22247833	22247111
CG3278	40F6-40F7	Tif-IA	22258260	22249878
CR43359	40F7-40F7	-	22341291	22340622
CG17018	40F7-40F7	-	22368796	22311931
CG17489	40F7-40F7	Ribosomal protein L5	22429419	22427533
CG17490	40F7-40F7	-	22441190	22430964
CG17493	40F7-40F7	-	22444394	22442846
CG17494	40F7-40F7	-	22478851	22471796

ANNOTATION SYMBOL	CYTOGENETIC MAP	NAME	LOCATION MAX	LOCATION MIN	COVERED BY DELETION STOCK NUMBER	COVERED BY DELETION STOCK NUMBER 2	COVERED BY DELETION STOCK NUMBER 3	COVERED BY DELETION STOCK NUMBER 4	COVERED BY DELETION STOCK NUMBER 5	COVERED BY DELETION STOCK NUMBER 6	COVERED BY DELETION STOCK NUMBER 7	TOTAL COVERAGE
CG17683	-	-	20468	18442								
CG40127	-	-	75661	74991								
CR30260	41A2-41A2	transfer RNA:CR30260	397573	397503								
CR30505	41A2-41A2	transfer RNA:CR30505	398106	398036								
CG18001	41A2-41A2	Ribosomal protein L38	403961	403502								
CG40293	41A3-41A3	Ste20-like kinase	452786	434209								
CG17484	41B1-41B1	Adherens junction protein p120	496995	482798								
CG17486	41B1-41B1	-	508338	506534								
CG17883	41B3-41B3	-	561145	559362								
CG17704	41B3-41C1	Nipped-B	616515	579177								
CG40129	41B3-41C2	G protein-coupled receptor kinase 1	358573	209942								
CR40282	41C1-41C1	-	619068	618351								
CR41440	41C1-41C1	-	619416	619019								
CG17082	41C1-41C1	-	645548	631836								
CG10392	41C1-41C2	super sex combs	1216986	1194756								
CR43281	41C2-41C2	-	671151	668032								
CG12547	41C2-41C2	-	676143	673803								
CG17528	41C2-41C2	-	711821	704674								
CG14464	41C3-41C3	-	717440	716725								
CG17665	41C-41C	-	130444	123268								
CG33492	41C6-41D1	Ionotropic receptor 41a	909460	837172								
CG2981	41D1-41D1	Troponin C at 41C	957715	953796								
CR43360	41D2-41D3	-	969936	969389								
CG3107	41D3-41D3	-	982595	978092								
CG2944	41D3-41D3	gustavus	1015817	1004715								
CR43256	41D3-41D3	-	1016809	1014754								
CG3136	41D4-41E1	Atf6	1042266	1032202								
CG33554	41E1-41E3	Nipped-A	1138553	1065506								
CG41443	41E3-41E3	-	1142800	1141450								
CG2682	41E3-41E4	d4	1183475	1147484								
CG10465	41E5-41E5	-	1228496	1227207								
CG10395	41E5-41E5	-	1239477	1237998								
CG30441	41E5-41E5	-	1239627	1239218								
CG10396	41E5-41E5	-	1242231	1241499								
CG10417	41E5-41E5	-	1250608	1247831								
CR42646	41E5-41E6	-	1254863	1250758								

CG11163	41F10-41F11	-	1670360	1662279
CG17250	41F11-41F11	Odorant receptor 42a	1680472	1678946
CG14468	41F11-41F11	Tetraspanin 42A	1683853	1682918
CG12754	41F11-41F11	Odorant receptor 42b	1686017	1684700
CG42345	41F1-41F1	-	1342518	1301241
CG30440	41F2-41F2	-	1383341	1355819
CG12408	41F2-41F3	Troponin C isoform 4	1395371	1390942
CG30438	41F2-41F3	-	1437059	1384184
CG17510	41F5-41F5	-	1492333	1491091
CG17508	41F5-41F5	-	1499094	1496129
CG11665	41F6-41F6	-	1540288	1529160
CG1344	41F6-41F6	-	1543453	1541144
CG8426	41F6-41F6	lethal (2) NC136	1550725	1544423
CG8245	41F6-41F6	-	1557491	1555898
CG1298	41F6-41F6	kune-kune	1560302	1559277
CG11066	41F6-41F8	scarface	1579200	1564254
CG8376	41F8-41F8	apterous	1614335	1593707
CG7897	41F9-41F10	gp210	1660077	1648373
CG17337	41F9-41F11	-	1587725	1585359
CG8390	41F9-41F8	vulcan	1592944	1589612
CG12792	41F9-41F9	lethal (2) 09851	1643558	1642033
CG34200	41F9-41F9	-	1645572	1645198
CG7791	41F9-41F9	-	1647896	1645560
CG14589	42A11-42A11	-	2025925	2024808
CR30304	42A11-42A11	transfer RNA:arg2:42Ad	2029742	2029670
CR32837	42A11-42A11	transfer RNA:lys2:42Ae	2029949	2029877
CR30513	42A12-42A12	transfer RNA:asn5:42Ah	2040181	2040108
CR33972	42A12-42A12	transfer RNA:asn5:42Ag	2040764	2040691
CR33973	42A12-42A12	transfer RNA:asn5:42Af	2041084	2041011
CR30512	42A12-42A12	transfer RNA:arg2:42Ac	2049112	2049040
CR30518	42A12-42A12	transfer RNA:asn5:42Ac	2049601	2049528
CR30511	42A12-42A12	transfer RNA:asn5:42Ab	2049775	2049702
CR30510	42A12-42A12	transfer RNA:asn5:42Aa	2050097	2050024
CR30517	42A12-42A12	transfer RNA:lys2:42Ac	2050258	2050186
CR30516	42A12-42A12	transfer RNA:lys2:42Ab	2052453	2052381
CR30312	42A12-42A12	transfer RNA:lys2:42Aa	2053561	2053489
CR30313	42A12-42A12	transfer RNA:ile:42A	2053729	2053656
CR30314	42A12-42A12	transfer RNA:arg2:42Ab	2057184	2057112
CR30515	42A12-42A12	transfer RNA:lys2:42Ad	2059073	2059001
CR30316	42A12-42A12	transfer RNA:CR30316	2059264	2059192
CG8345	42A12-42A12	Cyp6w1	2062936	2061189
CR30514	42A12-42A12	transfer RNA:arg2:42Aa	2066161	2066089
CG8343	42A13-42A13	-	2067873	2067231

CG11211	42A13-42A13	-	2069131	2068431
CR30519	42A13-42A13	transfer RNA:asn5:42Ae	2077707	2077634
CR30319	42A13-42A13	transfer RNA:asn5:42Ad	2077950	2077877
CG11212	42A13-42A13	Patched-related	2083512	2069253
CG30432	42A13-42A13	-	2085847	2084892
CG8335	42A13-42A13	-	2089461	2088300
CG30431	42A13-42A13	-	2092729	2090248
CG17994	42A13-42A13	-	2096813	2094724
CG8325	42A13-42A13	lethal (2) k14710	2101623	2097287
CG8276	42A13-42A14	bicoid-interacting protein 3	2127321	2102078
CG34385	42A1-42A1	dpr12	1747693	1734194
CG8330	42A14-42A14	tomboy40	2114389	2113132
CG12110	42A14-42A14	Phospholipase D	2142771	2129529
CG43366	42A3-42A4	-	1818868	1781429
CG7882	42A4-42A4	-	1847322	1845360
CG7881	42A4-42A4	-	1854341	1848503
CG7838	42A5-42A6	Bub1-related kinase	1862122	1856600
CG11680	42A6-42A6	maleless	1868277	1862243
CG7873	42A6-42A7	Src oncogene at 42A	1900039	1868785
CG14471	42A7-42A7	-	1888932	1885303
CG12051	42A7-42A7	Actin 42A	1903190	1901415
CG7865	42A7-42A8	PNGase-like	1907660	1901327
CG7863	42A8-42A8	dream	1910711	1908372
CG33131	42A8-42A8	SCAP	1923922	1913778
CG14591	42A8-42A8	-	1928087	1924063
CG7861	42A8-42A8	tubulin-specific chaperone E	1932469	1930160
CG34211	42A8-42A8	-	1935243	1934675
CG34212	42A8-42A8	-	1937791	1937412
CG7856	42A8-42A9	-	1947063	1944862
CG14593	42A8-42A9	CCHamide-2 receptor	1956185	1938477
CG1765	42A9-42A12	Ecdysone receptor	2056681	1977924
CG7845	42A9-42A9	-	1963882	1961976
CG7849	42A9-42A9	-	1965593	1964415
CG14590	42A9-42A9	-	1968077	1966146
CG7843	42A9-42A9	-	1973125	1968333
CG15233	42B2-42B2	-	2488483	2487549
CG33919	42B2-42B2	-	2512082	2511337
CG3161	42B2-42B2	Vacuolar H[+] ATPase subunit 16-1	2520633	2512747
CG3152	42B2-42B2	Trap1	2523767	2521152
CG3274	42B2-42B2	Brahma associated protein 170kD	2529866	2524023
CG3174	42B2-42B2	Flavin-containing monooxygenase 2	2532585	2529922
CG33134	42B2-42C1	death executioner Bcl-2 homologue	2540347	2536160
CG9397	42C1-42B2	jing	2506901	2389764

CG30443	42C1-42C2	Optix-binding protein	2542772	2540738
CG3183	42C2-42C2	geminin	2543955	2542968
CG3273	42C2-42C3	scrambled	2548129	2544833
CG3189	42C3-42C3	DNA polymerase interacting tpr containing protein of 47kD	2549623	2548155
CG15845	42C3-42C3	Adh transcription factor 1	2555592	2549774
CG15908	42C3-42C4	-	2557581	2555655
CG9410	42C3-42C4	-	2557581	2555655
CG3194	42C4-42C4	-	2560850	2557659
CG3271	42C4-42C4	-	2562566	2561114
CG17266	42C4-42C4	-	2563465	2562533
CG30445	42C4-42C4	Tyrosine decarboxylase 1	2567891	2564506
CG15909	42C4-42C4	-	2571862	2570697
CG30446	42C4-42C4	Tyrosine decarboxylase 2	2577467	2572250
CG9422	42C4-42C5	-	2580095	2563333
CG3270	42C5-42C5	-	2582692	2580935
CG3403	42C5-42C5	-	2584130	2582619
CG3269	42C5-42C5	Rab-protein 2	2587441	2584227
CG3409	42C5-42C6	-	2603370	2587200
CG9428	42C6-42C6	Zinc/iron regulated transporter-related protein 1	2605312	2603847
CG9430	42C6-42C6	-	2607038	2605785
CG9432	42C6-42C7	lethal (2) 01289	2628149	2608606
CG3268	42C7-42C7	phtf	2633649	2629372
CG3267	42C8-42C8	-	2636459	2633890
CG3265	42C8-42C8	Eb1	2643542	2636697
CG3420	42C8-42C8	-	2644714	2643801
CG9436	42C8-42C8	-	2646404	2645106
CG9438	42D1-42D1	Cytochrome P450-6a2	2668960	2667220
CG34392	42D1-42D1	Epac	2684421	2649417
CG3283	42D3-42D4	Succinate dehydrogenase B	2696677	2695117
CG15237	42D4-42D4	-	2697252	2696549
CG3450	42D4-42D4	ubiquitin like	2698019	2697516
CG3287	42D4-42D4	-	2702317	2698525
CG18584	42D4-42D4	klaroid	2705704	2702565
CG34215	42D4-42D4	-	2719296	2718802
CG15236	42D4-42D6	-	2725865	2715863
CG9445	42D6-42D6	-	2726432	2725579
CG9446	42D6-42D6	coro	2760274	2749506
CG9447	42D6-42D6	-	2763118	2760837
CG9453	42D6-42D6	Serine protease inhibitor 4	2766428	2763409
CG9454	42D6-42D6	Serpin 42Db	2768220	2766823
CG9455	42D6-42D6	Serpin 42Dc	2770912	2768501
CG9456	42D6-42D6	Serine protease inhibitor 1	2772378	2770508
CG9460	42D6-42D6	Serpin 42De	2775767	2773910

CG30158	42D6-42E1	-	2810118	2779268	3368		
CG3358	42E1-42E1	-	2812434	2810875	3368		
CG33351	42E1-42E1	Chemosensory protein B 42b	2831491	2830675	3368		
CG33350	42E1-42E1	Chemosensory protein B 42c	2832912	2832119	3368		
CR30300	42E1-42E1	transfer RNA:lys2:42Ea	2834385	2834313	3368		
CR30301	42E1-42E1	transfer RNA:lys2:42Eb	2835315	2835243	3368		
CR30302	42E1-42E1	transfer RNA:lys2:42Ec	2835861	2835789	3368		
CR30303	42E1-42E1	transfer RNA:lys2:42Ed	2836710	2836638	3368		
CG33348	42E1-42E1	Chemosensory protein B 42a	2837789	2836854	3368		
CG33349	42E1-42E1	pickpocket 25	2839663	2837890	3368		
CG33558	42E1-42E1	missing-in-metastasis	2859139	2813207	3368		
CG3567	42E1-42E1	Cyp6u1	2862514	2859617	3368		
CG30157	42E1-42E1	-	2862638	2861543	3368		
CG30156	42E1-42E1	-	2870491	2868951	3368		
CG3572	42E1-42E1	visceral mesodermal armadillo-repeats	2873214	2862787	3368		
CG17002	42E1-42E1	-	2876427	2873568	3368		
CG30159	42E4-42E4	-	2881811	2880191	3368		
CG18816	42E4-42E4	Tetraspanin 42Eb	2887353	2886358	3368		
CR42785	42E4-42E4	-	2889059	2887656	3368		
CG18817	42E4-42E4	Tetraspanin 42Ea	2891766	2880181	3368		
CG30160	42E4-42E5	-	2893641	2892662	3368		
CG12847	42E5-42E5	Tetraspanin 42Ec	2896127	2893952	3368		
CG12846	42E5-42E5	Tetraspanin 42Ed	2899359	2897365	3368		
CG10106	42E5-42E5	Tetraspanin 42Ee	2905869	2899761	3368		
CG12845	42E5-42E5	Tetraspanin 42Ef	2915587	2912517	3368		
CG12142	42E5-42E5	Tetraspanin 42Eg	2920738	2916418	3368		
CG12844	42E5-42E5	Tetraspanin 42Eh	2922424	2921068	3368		
CG12843	42E5-42E5	Tetraspanin 42Ei	2924454	2922632	3368		
CG33914	42E5-42E5	-	2925174	2924437	3368		
CR12842	42E5-42E5	-	2927318	2926635	3368		
CG12143	42E5-42E5	Tetraspanin 42Ej	2930267	2927644	3368		
CG12841	42E5-42E5	Tetraspanin 42Ek	2932215	2930161	3368		
CG12840	42E5-42E5	Tetraspanin 42El	2936050	2933278	3368		
CG2374	42E6-42E6	late bloomer	2939470	2937301	3368		
CG12839	42E7-42E7	Tetraspanin 42En	2941548	2940279	3368		
CG12838	42E7-42E7	Tetraspanin 42Eo	2944087	2942218	3368		
CG4471	42E7-42E7	Tetraspanin 42Ep	2945040	2943902	3368		
CG4445	42E7-42E7	polypeptide GalNAc transferase 3	2949224	2945156	3368		
CG12832	42E7-42E7	Tetraspanin 42Eq	2951071	2949612	3368		
CG12837	42E7-42E7	Tetraspanin 42Er	2953618	2951921	3368		
CG12836	42E7-42E7	-	2957322	2955752	3368		
CR30298	42E7-42E7	transfer RNA:CR30298	2957548	2957475	3368		
CR30299	42E7-42E7	transfer RNA:CR30299	2958338	2958265	3368		

CG12831	42E7-42E7	-	2961621	2960550	3368		
CG12835	42F1-42F1	-	2995433	2994447	3368		
CG12833	42F1-42F2	espinas	3015375	2973819	3368		
CG4485	42F2-42F2	Cytochrome P450-9b1	3017312	3015343	3368		
CG4486	42F2-42F2	Cytochrome P450-9b2	3019640	3017782	3368		
CG12172	42F2-42F3	Serine protease inhibitor 43Aa	3036757	3035203	3368		
CG12828	42F3-42F3	-	3037142	3036793	3368		
CG1865	42F3-42F3	Serine protease inhibitor 43Ab	3041188	3039170	3368		
CG1859	42F3-42F3	Spn43Ad	3042927	3041242	3368		
CG1857	42F3-42F3	necrotic	3045733	3043981	3368		
CG11060	42F3-42F3	-	3065793	3063391	3368		
CG33140	42F3-42F3	-	3068165	3065895	3368		
CG11084	42F3-43A1	prickle	3110885	3038207	3368		
CG30385	43A1-43A1	-	3070542	3068831	3368		
CG30384	43A1-43A1	-	3072808	3070502	3368		
CG1854	43A1-43A1	Odorant receptor 43a	3122418	3120344	3368		
CG1851	43A1-43A2	Ady43A	3133263	3130529	3368		
CG11086	43A2-43A2	Gadd45	3138160	3136668	3368		
CG1850	43A2-43A2	-	3148756	3146372	3368		
CG1845	43A2-43A2	-	3165580	3160037	3368		
CG12165	43A2-43A3	Inner centromere protein	3169066	3165972	3368		
CG11101	43A3-43A3	pawn	3187907	3182813	3368		
CG12164	43A4-43A4	-	3200855	3198913	3368		
CG17800	43A4-43B1	Down syndrome cell adhesion molecule	3269374	3207059	3368		
CG1708	43B1-43B2	costa	3274617	3269669	3368		
CG11107	43B2-43B2	-	3278529	3274719	3368		
CG1712	43B2-43B2	Gustatory receptor 43a	3280666	3278374	3368		
CG1707	43B2-43B2	-	3283453	3281051	3368		
CG11112	43B2-43B2	-	3288991	3288292	3368		
CG11113	43B2-43B2	-	3289870	3289373	3368		
CG43123	43B2-43B2	-	3291572	3290285	3368		
CG43267	43B2-43B2	-	3291860	3291563	3368		
CG11166	43B2-43B2	ELL-associated factor	3295326	3285731	3368		
CG1701	43B2-43B2	-	3296865	3296398	3368		
CG11145	43B3-43C1	-	3316098	3315409	3368		
CG11121	43B3-43C1	sine oculis	3322377	3306537	3368		
CG11123	43C1-43C1	-	3330390	3328198	3368		
CG11124	43C1-43C1	secretory Phospholipase A2	3331347	3330369	3368		
CG1669	43C1-43C1	kappaB-Ras	3333266	3331329	3368		
CG30503	43C1-43C1	-	3333266	3331329	3368		
CG11125	43C1-43C1	-	3336915	3334984	3368		
CG30502	43C1-43C1	-	3339056	3333694	3368		
CG11143	43C3-43C3	Inos	3346373	3342427	3368		

CG11141	43C3-43C3	-	3350900	3347936	3368
CG11127	43C3-43C3	-	3352492	3350876	3368
CG11139	43C3-43C4	p47	3354236	3352523	3368
CG11140	43C4-43C4	Aldehyde dehydrogenase type III	3364667	3354384	3368
CG42396	43C5-43C5	wech	3377368	3369381	3368
CG1621	43C5-43C5	-	3380084	3378341	3368
CG1620	43C5-43C6	-	3383971	3381311	3368
CG1616	43C6-43C7	disc proliferation abnormal	3387394	3384207	3368
CG2146	43C7-43D1	dilute class unconventional myosin	3396130	3387660	3368
CG12736	43D1-43D1	-	3397959	3396032	3368
CG1605	43D1-43D1	az2	3400229	3398116	3368
CG1603	43D1-43D1	-	3403875	3401575	3368
CG1602	43D1-43D1	-	3406426	3404426	3368
CG2144	43D1-43D1	-	3410051	3406785	3368
CG10667	43D1-43D2	Origin recognition complex subunit 1	3413213	3409940	3368
CG1600	43D2-43D3	-	3420487	3413623	3368
CG2140	43D3-43D3	Cyt-b5	3423441	3421013	3368
CG2137	43D3-43D3	-	3425802	3423424	3368
CG1598	43D3-43D3	-	3427201	3425737	3368
CG2105	43D3-43D6	Corin	3448759	3433167	3368
CG30499	43D7-43D7	-	3453254	3451937	3368
CG30498	43D7-43D7	boca	3454240	3453375	3368
CG2093	43D7-43E1	Vacuolar protein sorting 13	3468180	3454770	3368
CG30496	43E11-43E11	-	3589383	3587009	3368
CG30493	43E11-43E11	-	3591006	3586786	3368
CG34216	43E11-43E12	-	3592442	3591320	3368
CG1389	43E11-43E12	torso	3597042	3590680	3368
CG1941	43E12-43E12	-	3599494	3597379	3368
CG1942	43E12-43E12	-	3601695	3600128	3368
CG1946	43E12-43E12	-	3604286	3602445	3368
CG18812	43E12-43E13	-	3623124	3605784	3368
CG30497	43E13-43E16	-	3670119	3625273	3368
CG1363	43E1-43E3	blown fuse	3474581	3467993	3368
CG1555	43E16-43E16	cinnabar	3672711	3670302	3368
CG11217	43E16-43E16	Calcineurin B2	3675640	3673517	3368
CG12825	43E16-43E16	-	3677496	3676719	3368
CG12824	43E16-43E16	-	3678676	3677896	3368
CG12055	43E17-43E17	Glyceraldehyde 3 phosphate dehydrogenase 1	3680885	3679403	3368
CG1925	43E17-43E17	mutagen-sensitive 205	3688549	3680757	3368
CG1553	43E17-43E18	-	3693904	3688286	3368
CG1891	43E18-43E18	saxophone	3697575	3693983	3368
CG1550	43E18-43E18	-	3699540	3697580	3368
CG1882	43E18-43E18	-	3702250	3700011	3368

CG1548	43E18-43E18	cathD	3711073	3709615	3368		
CG30383	43E18-43E18	-	3712646	3711448	3368		
CG11205	43E18-43E18	photorepair	3714824	3712997	3368		
CG18495	43E18-43E18	Proteasome alpha1 subunit	3716181	3714808	3368		
CG18853	43E18-43E18	-	3717934	3716562	3368		
CG30382	43E18-43E18	-	3719276	3717918	3368		
CG12822	43E18-43E18	-	3721346	3719672	3368		
CG12821	43E18-43E18	-	3723579	3719704	3368		
CG34361	43E18-43F1	Diacyl glycerol kinase	3773487	3723747	3368		
CG1360	43E3-43E3	-	3477611	3475278	3368		
CG1358	43E3-43E5	-	3508216	3483240	3368		
CG2092	43E4-43E6	scraps	3482759	3477624	3368		
CG43341	43E6-43E6	-	3521386	3520346	3368		
CG43340	43E6-43E7	-	3539292	3510749	3368		
CG1341	43E7-43E7	Rpt1	3541453	3539945	3368		
CG17985	43E7-43E7	-	3542816	3539130	3368		
CG30491	43E7-43E7	-	3544275	3542633	3368		
CG30495	43E7-43E8	-	3546269	3544701	3368		
CG1339	43E8-43E8	Gr43b	3548123	3546761	3368		
CG2070	43E8-43E8	-	3550764	3549487	3368		
CG2065	43E8-43E9	-	3552774	3551292	3368		
CG1399	43E9-43E11	-	3586395	3564045	3368		
CG2064	43E9-43E9	-	3554848	3553338	3368		
CG12042	43E9-43E9	-	3556534	3554753	3368		
CG12826	43E9-43E9	-	3558608	3557832	3368		
CG1577	43E9-43E9	mitochondrial ribosomal protein L52	3561908	3561226	3368		
CG12107	43E9-43E9	-	3562867	3561951	3368		
CG1406	43E9-43E9	U2A	3563857	3562867	3368		
CG30377	43F1-43F1	-	3802537	3777580	3368	198	
CG12159	43F1-43F1	-	3803968	3802532	3368	198	
CG1877	43F1-43F2	lin-19-like	3808560	3804361	3368	198	
CG17853	43F2-43F2	Odorant receptor 43b	3810109	3808340	3368	198	
CG15835	43F2-43F2	Histone demethylase 4A	3812488	3810280	3368	198	
CG8791	43F2-43F2	-	3817427	3814182	3368	198	
CG30381	43F2-43F2	-	3818521	3817163	3368	198	
CG8729	43F2-43F2	ribonuclease H1	3819891	3818559	3368	198	
CG8730	43F2-43F3	drosha	3824360	3819931	3368	198	
CG8728	43F3-43F4	-	3826674	3824362	3368	198	6090
CG30380	43F4-43F4	-	3827144	3826706	3368	198	6090
CG30379	43F4-43F4	-	3829375	3827461	3368	198	6090
CG14764	43F4-43F7	-	3843377	3829545	3368	198	6090
CG34430	43F5-43F5	-	3831980	3830947	3368	198	6090
CG34431	43F5-43F5	-	3834487	3832343	3368	198	6090

CG11165	43F6-43F6	-	3837970	3837344	3368	198	6090	
CG30378	43F6-43F6	-	3838997	3837844	3368	198	6090	
CG2906	43F7-43F7	-	3845762	3843655	3368	198	6090	
CG2915	43F7-43F8	-	3847532	3845712	3368	198	6090	
CG2916	43F8-43F8	Sep-05	3849427	3847638	3368	198	6090	
CG2910	43F8-43F9	spenito	3857320	3849991	3368	198	6090	
CG14763	43F9-43F9	-	3855529	3854283	3368	198	6090	
CG8726	43F9-43F9	-	3859554	3855634	3368	198	6090	
CG8725	43F9-44A1	COP9 complex homolog subunit 4	3861604	3859680	3368	198	6090	
CG11198	44A1-44A2	Acetyl-CoA carboxylase	3874729	3861620	3368	198		
CG8722	44A2-44A2	Nucleoporin 44A	3878789	3875967	3368	198		
CG11196	44A2-44A2	-	3882473	3881295	3368	198		
CG11194	44A2-44A2	Hairy/E(spl)-related with YRPW motif	3886078	3882941	3368	198		
CG11191	44A2-44A2	-	3889625	3888154	3368	198		
CG8721	44A2-44A2	Ornithine decarboxylase 1	3894177	3892308	3368	198		
CG8719	44A2-44A2	Ornithine decarboxylase 2	3896567	3894769	3368	198		
CG14762	44A2-44A2	-	3901259	3896624	3368	198		
CG18455	44A3-44A3	Optix	3930041	3919138	3368	198		
CG12769	44A4-44A4	-	3953056	3941331	3368	198		
CG17977	44A4-44A4	-	3955157	3954114	3368	198		
CG8715	44A4-44A4	lingerer	3966320	3955460	3368	198		
CG12770	44A4-44A4	Vacuolar protein sorting 28	3967561	3966742	3368	198		
CG8717	44A4-44A4	saliva	3969875	3968064	3368	198		
CG8714	44A4-44A4	sugar transporter 1	3974654	3970483	3368	198		
CG17975	44A4-44A4	sugar transporter 2	3976802	3974921	3368	198		
CG17976	44A4-44A4	sugar transporter 3	3978802	3976981	3368	198		
CG8713	44A4-44A4	-	3984450	3979203	3368	198		
CG8712	44A4-44A4	-	3985959	3984442	3368	198		
CG11210	44A4-44A4	-	3989811	3986182	3368	198		
CG8711	44A4-44A4	Cullin-4	3993819	3989765	3368	198		
CG18316	44A4-44A4	-	3994878	3993931	3368	198		
CG30372	44B2-44B2	-	4010357	4001791	3368	198		
CG2158	44B2-44B3	Nucleoporin 50	4012563	4010521	3368	198		
CG8710	44B3-44B3	coilin	4014747	4012486	3368	198		
CG2160	44B3-44B3	Suppressor of Cytokine Signaling at 44A	4016981	4015136	3368	198		
CG42515	44B3-44B3	PSEA-binding protein 49kD	4018837	4016859	3368	198		
CG42516	44B3-44B3	-	4018837	4016859	3368	198		
CG2163	44B3-44B3	Pabp2	4021879	4018938	3368	198		
CG2297	44B3-44B3	Obp44a	4022588	4021875	3368	198		
CG8709	44B4-44B5	Lipin	4044128	4024824	3368	198		
CG11546	44B5-44B5	kermit	4044126	4034423	3368	198		
CR30374	44B5-44B5	-	4045419	4044762	3368	198		
CR30297	44B5-44B5	transfer RNA:CR30297	4046033	4045960	3368	198		

CG8708	44B5-44B7	-	4048739	4046911	3368	198		
CG8707	44B7-44B7	-	4051018	4049184	3368	198		
CG30373	44B7-44B7	-	4052171	4051505	3368	198		
CR34650	44B7-44B7	-	4053553	4053455	3368	198		
CG2173	44B7-44B7	Rs1	4055274	4052390	3368	198		
CG2183	44B7-44B8	-	4057596	4055452	3368	198		
CG11482	44B8-44B8	Mlh1	4059907	4057541	3368	198		
CG14757	44B8-44B8	-	4061118	4059969	3368	198		
CG14756	44C1-44C1	-	4093211	4092393	3368	198		
CG33087	44C1-44C2	LDL receptor protein 1	4113243	4094023	3368	198		
CG34217	44C2-44C2	-	4116229	4115704		198		
CG8704	44C2-44C2	deadpan	4119832	4116476		198		
CG8705	44C2-44C2	peanut	4127835	4124774		198		
CG14760	44C2-44C2	-	4144241	4141761		198		
CG30369	44C3-44C3	-	4147289	4146816		198		
CG14759	44C3-44C3	-	4147988	4147469		198		
CG2291	44C3-44C3	-	4148968	4148152		198		
CG12126	44C3-44C3	-	4150783	4150179		198		
CG30376	44C3-44C3	-	4151931	4150991		198		
CG30375	44C3-44C3	-	4154787	4153387		198		
CG30371	44C3-44C3	-	4156839	4155148		198		
CR43002	44C4-44C4	mir-280 stem loop	4185705	4185611		198		
CG11635	44C4-44C4	-	4246977	4246043		198		
CG30365	44C4-44C4	spacewatch	4248522	4246971		198		
CG30364	44C4-44C4	hug-bell	4249661	4248728		198		
CG34218	44C4-44C4	whipple	4250723	4249864		198		
CG30363	44C4-44C4	comas sola	4252850	4250776		198		
CG30366	44C4-44C4	swift-tuttle	4252850	4250776		198		
CG30362	44C4-44C4	borrelly	4254165	4253054		198		
CG18449	44C4-44C4	-	4255432	4254666		198		
CG2127	44C4-44C4	-	4257543	4255847		198		
CG8701	44C4-44C4	-	4259656	4258578		198		
CG42698	44C4-44C4	pou domain motif 3	4283785	4215005		198		
CG2121	44C4-44C6	-	4299228	4283898		198		
CG43296	44C6-44C6	-	4305211	4304681		198		
CG2038	44C6-44C6	COP9 complex homolog subunit 7	4316089	4308493		198		
CG11650	44C6-44C6	Larval cuticle protein 1	4318737	4318139		198		
CR30367	44C6-44C6	Larval cuticle protein 1 pseudogene	4320889	4320391		198		
CG8697	44C6-44C6	Larval cuticle protein 2	4322080	4321472		198		
CG2043	44C6-44C6	Larval cuticle protein 3	4323523	4322949		198		
CG2044	44D1-44D1	Larval cuticle protein 4	4325908	4325162	201	198		
CG2110	44D1-44D1	Cyp4ad1	4330284	4326898	201	198		
CR43023	44D1-44D1	mir-986 stem loop	4332586	4332487	201	198		

CG2060	44D1-44D1	Cytochrome P450-4e2	4334676	4332217	201	198	
CG2062	44D1-44D1	Cytochrome P450-4e1	4337250	4334974	201	198	
CG8696	44D1-44D1	Larval visceral protein H	4339404	4337166	201	198	
CG8694	44D1-44D1	Larval visceral protein D	4343291	4341137	201	198	
CG8695	44D1-44D1	Larval visceral protein L	4345390	4343414	201	198	
CG8693	44D1-44D1	-	4348389	4346329	201	198	
CG30359	44D1-44D1	-	4352597	4350278	201	198	
CG30360	44D1-44D1	-	4354701	4352675	201	198	
CG11669	44D1-44D1	-	4359154	4357054	201	198	
CG8690	44D1-44D1	-	4361466	4359488	201	198	
CG30361	44D1-44D2	mangetout	4419420	4361933	201	198	
CG12780	44D2-44D2	-	4439758	4439364	201	198	
CR8687	44D3-44D3	Cyp6a14	4453481	4451798	201	198	
CR14753	44D3-44D3	Cyp6a15Psi	4457652	4456874	201	198	
CG2397	44D3-44D3	Cyp6a13	4459650	4458007	201	198	
CG42326	44D3-44D3	-	4471147	4460868	201	198	
CG8732	44D3-44D6	Acyl-CoA synthetase long-chain	4570296	4553360	201	198	
CG14752	44D4-44D4	-	4479452	4478001	201	198	
CG43183	44D4-44D4	-	4480474	4479757	201	198	
CG8736	44D4-44D4	-	4482506	4481533	201	198	
CG8735	44D4-44D4	-	4487436	4485033	201	198	
CG8643	44D4-44D4	regular	4498743	4487938	201	198	
CG8642	44D4-44D4	-	4501416	4499399	201	198	
CG8639	44D4-44D5	Cirl	4512708	4502296	201	198	
CG14750	44D5-44D5	Vacuolar protein sorting 25	4513685	4512956	201	198	
CG8734	44D5-44D5	Galactosyltransferase II	4515089	4513686	201	198	
CG14749	44D5-44D5	-	4517691	4515382	201	198	
CG8635	44D5-44D5	-	4519467	4517699	201	198	
CG2411	44D5-44E1	patched	4552728	4537140	201	198	
CG30354	44E2-44E2	-	4565166	4564730	201		
CG30355	44E2-44E2	-	4567453	4566644	201		
CR30292	44E2-44E2	transfer RNA:leu2:44EF	4570802	4570720	201		
CG8579	44E2-44E2	Jonah 44E	4579856	4578955	201		
CG8586	44E2-44E2	-	4583301	4581244	201		
CG8738	44E2-44E2	-	4586088	4583931	201		
CG8584	44E2-44E2	-	4589299	4588197	201		
CG12376	44E2-44E2	-	4592007	4589340	201		
CG14744	44E2-44E2	-	4596737	4594583	201		
CG14746	44E2-44E2	PGRP-SC1a	4597825	4597268	201		
CG14743	44E2-44E2	-	4600222	4597903	201		
CG8577	44E2-44E2	PGRP-SC1b	4601587	4600949	201		
CG14745	44E2-44E2	PGRP-SC2	4605026	4604472	201		
CG14767	44E2-44E3	-	4611342	4605522	201		

CG30357	44E3-44E3	-	4609129	4607605	201				
CG8411	44E3-44E3	germ cell-less	4616509	4611765	201				
CG30356	44E3-44E3	-	4617007	4616465	201				
CG8739	44E3-44E3	stambha A	4621809	4617003	201				
CG42615	44E3-44E3	-	4625295	4624875	201				
CG8740	44E3-44E4	-	4647095	4623324	201				
CG33199	44F11-44F11	-	4838609	4835938	201				
CG8229	44F11-44F11	-	4838609	4835618	201				
CG8226	44F11-44F11	Translocase of outer membrane 7	4839694	4839193	201				
CG8224	44F11-44F12	baboon	4850301	4839846	201	3591			
CG8216	44F12-44F12	-	4855687	4850669	201	3591			
CG8213	44F12-45A1	-	4873063	4856841	201	3591			
CG8746	44F1-44F1	-	4681282	4680138	201				
CG30350	44F1-44F1	-	4715268	4713896	201				
CG33141	44F1-44F1	sticks and stones	4743142	4686022	201				
CG10844	44F1-44F2	Ryanodine receptor 44F	4775602	4747869	201				
CG8272	44F2-44F3	-	4778941	4775909	201				
CG8269	44F3-44F3	Dynamitin	4780844	4779345	201				
CG8266	44F3-44F3	sec31	4786303	4781129	201				
CG8262	44F3-44F3	anastral spindle 2	4787706	4786228	201				
CG13751	44F3-44F3	-	4788122	4787746	201				
CG13746	44F3-44F3	MrgBP	4788877	4788071	201				
CG8261	44F3-44F5	G protein gamma 1	4792296	4788908	201				
CG8258	44F5-44F5	-	4794506	4792347	201				
CG30349	44F5-44F6	-	4798390	4795025	201				
CG8252	44F6-44F6	-	4797854	4796935	201				
CG8251	44F6-44F6	Phosphoglucose isomerase	4801631	4798407	201				
CG11770	44F6-44F7	lines	4805739	4802033	201				
CG34219	44F7-44F7	-	4806474	4805213	201				
CG8248	44F7-44F7	-	4807871	4806445	201				
CG8247	44F7-44F7	-	4810256	4807775	201				
CG8243	44F7-44F8	-	4812851	4810293	201				
CG8237	44F8-44F8	-	4814395	4813194	201				
CG8235	44F8-44F8	-	4815605	4814519	201				
CG8232	44F8-44F9	-	4820608	4815679	201				
CG8230	44F9-44F10	-	4834866	4831801	201				
CG13749	44F9-44F9	-	4821950	4820928	201				
CG13745	44F9-44F9	Fanconi anemia complementation group I homologue	4827299	4822078	201				
CG13748	44F9-44F9	-	4828641	4827920	201				
CG8058	45A11-45A11	alpha/beta hydrolase 1	5022958	5019992	201	3591		6246	6247
CG8788	45A11-45A12	-	5029486	5025979	201	3591		6246	6247
CG8057	45A11-45B1	alicorn	5025455	5022880	201	3591		6246	6247
CG30342	45A12-45A12	pre-mRNA processing factor 38	5032656	5031464	201	3591		6246	6247

CG30344	45A12-45A13	-	5036017	5032754	201	3591		6246	6247	
CG8055	45A12-45E	shrub	5031415	5029651	201	3591		6246	6247	
CG30345	45A13-45A13	-	5039397	5036190	201	3591		6246	6247	
CG34350	45A1-45A1	-	4892622	4881047	201	3591				
CG8172	45A1-45A1	-	4901013	4894739	201	3591				
CG13744	45A1-45A1	-	4904184	4902011	201	3591				
CG13747	45A1-45A1	-	4906539	4905360	201	3591				
CG8170	45A1-45A1	-	4918546	4906530	201	3591				
CG8196	45A1-45A1	Ance-4	4929647	4927225	201	3591				
CG8193	45A1-45A1	-	4932213	4929765	201	3591				
CG13743	45A1-45A1	-	4947411	4932355	201	3591				
CG8197	45A1-45A1	-	4949429	4948068	201	3591				
CG8084	45A1-45A1	anachronism	4965059	4956606	201	3591				
CG8083	45A1-45A1	-	4969879	4966232	201	3591				
CG11778	45A1-45A1	-	4973222	4969942	201	3591				
CG13742	45A1-45A1	-	4975062	4972098	201	3591				
CG12759	45A1-45A2	DEAD box protein 45A	4977304	4975358	201	3591				
CG8080	45A2-45A2	-	4980474	4977279		3591				
CG13741	45A2-45A2	-	4982173	4980008		3591				
CR34525	45A2-45A2	snoRNA:Psi28S-2949	4983031	4982877		3591				
CR33637	45A2-45A3	snoRNA:Or-aca5	4983337	4983190		3591				
CR42451	45A2-45A3	Uhg4	4984817	4982803		3591				
CR34526	45A3-45A3	snoRNA:Me28S-G3255a	4983585	4983501		3591				
CR34527	45A3-45A3	snoRNA:Me28S-A982a	4983818	4983742		3591				
CR34528	45A3-45A3	snoRNA:Me28S-A982b	4984087	4984011		3591				
CR34529	45A3-45A3	snoRNA:Me28S-G3255b	4984349	4984268		3591				
CR33636	45A3-45A3	-	4984674	4984535		3591				
CG8078	45A3-45A3	-	4985972	4984436		3591				
CG8777	45A3-45A4	-	4990658	4986075		3591				
CG8075	45A4-45A6	Van Gogh	4994301	4990749	4966	3591	6227			
CG8073	45A6-45A7	Phosphomannomutase 45A	4997228	4994647	4966	3591	6227			
CG8781	45A7-45A7	tsunagi	4999087	4998306	4966	3591	6227			
CG8070	45A7-45A8	Mystery 45A	5001458	4999010	4966	3591	6227			
CG8069	45A8-45A8	Phosphorylated adaptor for RNA export	5003535	5001768	4966	3591	6227			
CG8068	45A8-45A9	Suppressor of variegation 2-10	5009507	5003631	4966	3591	6227	6246	6247	
CG18659	45A9-45A10	-	5019486	5010809	4966	3591	6227	6246	6247	
CG11784	45A9-45A9	-	5010814	5009630	4966	3591	6227	6246	6247	
CG8008	45B1-45B1	-	5048940	5045412	4966	3591		6246	6247	
CG8046	45B1-45B1	-	5052455	5049542	4966	3591		6246	6247	
CG2412	45B1-45B1	Rad51C	5054371	5053240	4966	3591		6246	6247	
CG42382	45B1-45B1	-	5055023	5054071	4966	3591		6246	6247	
CG8014	45B1-45B2	Receptor mediated endocytosis 8	5064685	5055261	4966	3591		6246	6247	
CG8024	45B2-45B3	lightoid	5073866	5065369	4966	3591		6246	6247	

CG8026	45B3-45B3	-	5079600	5074175	4966	3591		6246	6247				
CG1650	45B3-45B3	unplugged	5087377	5082719	4966	3591		6246	6247				
CG8027	45B3-45B4	-	5094626	5091913	4966	3591		6246	6247				
CG8029	45B4-45B4	Vacuolar H[+] ATPase accessory protein AC45	5097169	5095067	4966	3591		6246	6247				
CG1944	45B7-45B7	Cyp4p2	5127338	5125035	4966	3591		6246	6247				
CG10842	45B7-45B7	Cytochrome P450-4p1	5129642	5127548	4966	3591		6246	6247				
CG10843	45B7-45B7	Cyp4p3	5131915	5129846	4966	3591		6246	6247				
CG2040	45B7-45B8	hikaru genki	5134752	5115286	4966	3591		6246	6247				
CG30343	45C1-45C1	-	5140760	5139518	4966	3591		6246	6247				
CG34141	45C1-45C1	-	5151476	5147783	4966	3591		6246	6247				
CG2049	45C1-45C1	Protein kinase related to protein kinase N	5172602	5139815	4966	3591		6246	6247				
CG2063	45C1-45C1	-	5174134	5172815	4966	3591		6246	6247				
CG1968	45C1-45C4	-	5176531	5174341	4966	3591		6246	6247				
CG2072	45C4-45C4	-	5179059	5176462	4966	3591		6246	6247				
CG1975	45C4-45C5	DNA fragmentation factor-related protein 2	5189715	5179362	4966	3591		6246	6247				
CG2078	45C5-45C5	Myd88	5196181	5191183	4966	3591		6246	6247				
CR42927	45C6-45C6	mir-987 stem loop	5200621	5200528	4966	3591		6246	6247				
CG13739	45C6-45D1	-	5239139	5205046	4966	3591	68	6246	6247	6245			
CG1978	45D1-45D1	Odorant receptor 45a	5234117	5232927	4966	3591	68	6246	6247	6245			
CG12158	45D1-45D1	-	5250411	5250076	4966	3591	68	6246	6247	6245			
CG13954	45D1-45D1	-	5261741	5257635	4966	3591	68	6246	6247	6245			
CG8799	45D1-45D1	lethal (2) 03659	5282705	5277963	4966	3591	68	6246	6247	6245			
CG8800	45D1-45D2	-	5283602	5282834	4966	3591	68	6246	6247	6245			
CG8801	45D2-45D3	-	5286255	5283865	4966	3591	68	6246	6247	6245	6917		
CG13951	45D3-45D3	lethal (2) k10201	5287404	5286594	4966	3591	68	6246	6247	6245	6917		
CG33774	45D3-45D3	-	5287809	5287258	4966	3591	68	6246	6247	6245	6917		
CG8804	45D3-45D4	wunen	5300965	5288036	4966	3591	68	6246	6247	6245	6917		
CG8805	45D4-45D5	wunen-2	5305351	5301849	4966	3591	68	6246	6247	6245	6917		
CG13955	45D5-45D5	-	5311127	5309923	4966	3591	68	6246	6247	6245	6917		
CG8806	45D5-45D5	preli-like	5313612	5311576	4966	3591	68	6246	6247	6245	6917		
CG8808	45D5-45D7	Pyruvate dehydrogenase kinase	5321930	5313947	4966	3591	68	6246	6247	6245	6917		
CG11804	45D7-45D8	ced-6	5332439	5322174	4966	3591	68	6246	6247	6245	6917		
CG33758	45D8-45D8	-	5341560	5340914	4966	3591	68	6246	6247	6245	6917		
CG33757	45D8-45D8	-	5342453	5341802	4966	3591	68	6246	6247	6245	6917		
CG42332	45E1-45E1	Calmodulin-binding transcription activator	5365595	5333551	4966	3591				6245	6917		
CG1916	45E1-45E1	Wnt oncogene analog 2	5390695	5381674	4966	3591				6245	6917		
CG42344	45E3-45F1	bruchpilot	5424980	5391293	4966	3591					6917		
CG1888	45F1-45F1	-	5434459	5432677							6917		
CR43013	45F1-45F1	mir-14 stem loop	5441329	5441267							6917		
CG12931	45F1-45F1	Odorant receptor 45b	5448573	5447103							6917		
CG1809	45F1-45F1	-	5451378	5449154							6917		
CG34407	45F4-45F4	Not1	5465985	5453651							6917		
CG1814	45F4-45F4	-	5469352	5464932							6917		

CG1868	45F4-45F5	-	5472050	5469261		6917	
CG1818	45F5-45F5	Updo	5473623	5472172		6917	
CG12929	45F5-45F5	-	5474180	5473615		6917	
CG1821	45F5-45F5	Ribosomal protein L31	5475505	5474688		6917	
CG1827	45F5-45F5	-	5477948	5476611		6917	
CG42600	45F5-45F5	closca	5487237	5475458		6917	
CG1825	45F5-45F6	Microtubule-associated protein 60	5480249	5478331		6917	
CG30338	45F6-45F6	-	5487010	5481552		6917	
CG30340	45F6-45F6	-	5488716	5487414		6917	
CG30339	45F6-45F6	-	5490406	5488936		6917	
CG1902	45F6-45F6	-	5493129	5481588		6917	
CG30000	45F6-45F6	-	5494689	5493495		6917	
CG30005	45F6-45F6	-	5495855	5494797		6917	
CG12926	45F6-45F6	-	5497792	5495633		6917	
CG1794	45F6-46A1	Matrix metalloproteinase 2	5571356	5498644		6917	
CR42913	45F8-45F8	mir-307 stem loop	5508843	5508756			
CR42879	45F8-45F8	mir-307-as stem loop	5508858	5508739			
CR30003	46A1-46A1	transfer RNA:met3:46A	5548801	5548730	1743		
CG1782	46A1-46A1	Ubiquitin activating enzyme 1	5580833	5575792	1743		
CG30002	46A1-46A1	-	5593652	5591888	1743		
CG1773	46A1-46A1	-	5595085	5593789	1743		
CG10459	46A1-46A1	-	5596227	5595076	1743		
CG1772	46B1-46B1	dacapo	5603607	5599828	1743		
CG42347	46B2-46B2	-	5632778	5603981	1743		
CG33800	46B2-46B2	Chemosensory protein A 46a	5636894	5636305	1743		
CG1690	46B2-46B2	-	5645573	5644433	1743		
CG18345	46B2-46B2	trp-like	5653023	5641202	1743		
CG1688	46B2-46B4	-	5694370	5653867	1743		
CG1698	46B3-46B3	-	5685512	5680848	1743		
CG1652	46B4-46B4	lectin-46Cb	5704105	5700867	1743		
CG1656	46B4-46B4	lectin-46Ca	5706040	5704805	1743		
CG1648	46B4-46B4	-	5707556	5698890	1743		
CG34033	46B4-46B4	-	5708691	5708068	1743		
CG30001	46B4-46B4	-	5710539	5708668	1743		
CG1625	46B4-46B4	-	5714988	5710582	1743		
CG1623	46B4-46B4	hebe	5724147	5715606	1743		
CG1663	46B4-46B4	-	5725986	5724535	1743		
CG12924	46B4-46B4	Lsm11	5727005	5725939	1743		
CG1665	46B4-46B4	-	5728667	5727283	1743		
CG1599	46B4-46B4	-	5730014	5728585	1743		
CG1667	46B4-46B4	-	5733017	5730192	1743		
CG1584	46B4-46B4	Origin recognition complex subunit 6	5733964	5732964	1743		
CG1519	46B4-46B4	Proteasome alpha7 subunit	5735339	5734141	1743		

CG1671	46B4-46B4	-	5738323	5735568	1743			
CG30010	46B4-46B4	-	5752081	5751325	1743			
CG1675	46B4-46B4	-	5754189	5753154	1743			
CG1516	46B4-46B4	-	5757853	5738208	1743			
CG10536	46B4-46C1	crossbronx	5762577	5752015	1743			
CG2328	46C10-46C10	even skipped	5868284	5866746	1743			
CG18446	46C1-46C1	-	5761151	5758977	1743			
CG12744	46C1-46C1	-	5763747	5762789	1743			
CG1472	46C1-46C2	sec24	5769858	5763737	1743	1702		
CG12923	46C2-46C2	-	5776386	5775153	1743	1702		
CG30008	46C2-46C2	-	5778625	5777403	1743	1702		
CG1513	46C2-46C2	-	5779183	5770077	1743	1702		
CG30007	46C2-46C4	-	5786018	5779496	1743	1702		
CG1441	46C4-46C4	-	5790788	5786523	1743	1702		
CG2346	46C4-46C4	FMRFamide-related	5797969	5793796	1743	1702		
CG12140	46C4-46C4	-	5800993	5798398	1743	1702		
CG1429	46C4-46C7	Myocyte enhancer factor 2	5846313	5801001	1743	1702		
CG15863	46C7-46C7	-	5848459	5846624	1743	1702		
CG12130	46C7-46C7	Peptidyl-alpha-hydroxyglycine-alpha-amidating lyase 1	5851358	5847054	1743	1702		
CG1418	46C7-46C8	-	5852567	5851342	1743	1702		
CG12133	46C8-46C8	-	5855941	5854737	1743	1702		
CG12131	46C8-46C9	Adam	5858410	5856465	1743	1702		
CG12134	46C9-46C9	-	5860295	5858654	1743	1702		
CG15862	46D1-46D4	cAMP-dependent protein kinase R2	5913540	5883325		1702		
CG12128	46D4-46D6	-	5918173	5914346		1702		
CG2331	46D-46D1	TER94	5881072	5876666		1702		
CG1407	46D5-46D7	-	5920393	5915948		1702	447	
CG12129	46D7-46D7	-	5922203	5920799		1702	447	
CG34220	46D7-46D7	-	5930995	5928701		1702	447	
CG18445	46D7-46D8	oysgedart	5936123	5923268		1702	447	
CG2249	46D8-46D9	-	5938379	5936985		1702	447	
CG12918	46D9-46D9	-	5939682	5938367		1702	447	
CG1385	46D9-46D9	Defensin	5942081	5941683		1702	447	
CG2264	46D9-46E1	magu	5951218	5940048		1702	447	
CG2292	46E1-46E1	-	5954060	5950890		1702	447	
CG12921	46E1-46E1	mitochondrial ribosomal protein L42	5954747	5954154		1702	447	
CG1362	46E1-46E1	cdc2-related-kinase	5956206	5954722		1702	447	
CG12920	46E1-46E1	-	5958572	5956614		1702	447	
CG1371	46E1-46E1	-	5963147	5958476		1702	447	
CG12919	46E1-46E3	eiger	5971715	5965870		1702	447	
CG1380	46E3-46E4	sugar transporter 4	5974568	5972947		1702	447	
CG2269	46E4-46E4	-	5983921	5972774		1702	447	
CG2275	46E4-46E5	Jun-related antigen	5986061	5983985		1702	447	

CG1381	46E5-46E6	Ribosomal protein LP0-like	5987091	5986023		1702	447	
CG17870	46E6-46E8	14-3-3zeta	5997192	5987184		1702	447	
CG4001	46E8-46F1	Phosphofructokinase	6004962	5997245	596	1702	447	
CG11866	46F1-46F1	-	6008956	6005198	596	1702	447	
CG17753	46F1-46F1	CCS	6010067	6009077	596	1702	447	
CG30011	46F1-46F2	gemini	6024977	6011793	596	1702	447	
CG12917	46F2-46F2	-	6026772	6025161	596	1702	447	
CG33478	46F2-46F2	Odorant receptor 46a	6029579	6026769	596	1702	447	
CG18011	46F2-46F3	-	6033711	6029845	596	1702	447	
CG12214	46F3-46F3	-	6046385	6043875	596	1702	447	
CG33135	46F3-46F5	KCNQ potassium channel	6079899	6033402	596	1702	447	
CG34221	46F5-46F5	-	6087196	6085053	596	1702	447	
CG33183	46F5-46F7	Hormone receptor-like in 46	6124853	6091773	596	1702	447	
CG12912	46F7-46F7	-	6122081	6120971	596	1702	447	
CG3454	46F7-46F7	Histidine decarboxylase	6133588	6128374	596	1702	447	
CG12209	46F7-46F7	-	6134977	6133576	596	1702	447	
CG12914	46F7-46F8	-	6136909	6135319	596	1702	447	
CG12210	46F8-46F8	Synaptobrevin	6139914	6136940	596	1702	447	
CG12913	46F8-46F9	-	6142479	6136762	596	1702	447	
CG12911	46F9-46F9	-	6148781	6144194	596	1702	447	
CR30009	46F9-46F9	-	6151331	6148820	596	1702	447	
CG12910	46F9-46F9	-	6156710	6154217	596	1702	447	
CG18408	46F9-47A1	CAP	6194529	6156528	596	1702	447	
CG11761	47A11-47A11	translin	6367612	6366516	596	1702	447	
CG17765	47A11-47A11	-	6369391	6367665	596	1702	447	
CG12052	47A11-47A13	longitudinals lacking	6430794	6369712	596	1702	447	
CG2368	47A13-47B1	pipsqueak	6503753	6445409	596	1702	447	
CG3298	47A1-47A1	Juvenile hormone-inducible protein 1	6197276	6194535	596	1702	447	
CG12909	47A1-47A1	-	6198648	6197629	596	1702	447	
CG12905	47A1-47A1	Odorant-binding protein 46a	6199528	6198677	596	1702	447	
CG34222	47A1-47A1	-	6208005	6207349	596	1702	447	
CG12908	47A1-47A1	Nidogen/entactin	6209405	6201423	596	1702	447	
CG42732	47A1-47A7	-	6304502	6211164	596	1702	447	
CG43172	47A2-47A2	-	6239666	6239038	596		447	
CG43200	47A2-47A2	-	6239666	6239038	596		447	
CG43171	47A2-47A2	-	6240587	6239961	596		447	
CG43178	47A2-47A2	-	6240587	6239961	596		447	
CG43201	47A2-47A2	-	6240587	6239957	596		447	
CG12907	47A2-47A2	-	6241889	6240873	596		447	
CG12902	47A2-47A2	-	6243336	6242229	596		447	
CG42733	47A2-47A2	-	6244305	6243676	596		447	
CG12906	47A2-47A2	Gustatory receptor 47a	6251089	6249810	596		447	
CG12900	47A2-47A2	Ionotropic receptor 47a	6267614	6264633	596		447	

CG12898	47A6-47A6	-	6294950	6294480	596		447		
CG43177	47A6-47A6	-	6296279	6296025	596		447		
CG33477	47A6-47A6	-	6297256	6296660	596		447		
CG33476	47A6-47A6	-	6298075	6297490	596		447		
CG33475	47A6-47A6	-	6298718	6298275	596		447		
CG42236	47A7-47A5	Ran-binding protein M	6324086	6317217	596		447		
CG11765	47A7-47A7	Peroxiredoxin 2540-2	6307266	6306225	596		447		
CG11825	47A7-47A7	-	6309413	6307919	596		447		
CG33474	47A7-47A7	-	6310343	6309738	596		447		
CG12405	47A7-47A7	Peroxiredoxin 2540-1	6312976	6311941	596		447		
CG12896	47A7-47A7	-	6315418	6314385	596		447		
CG12895	47A7-47A7	-	6324864	6324177	596		447		
CG18377	47A7-47A9	Cyp49a1	6346393	6336855	596		447		
CG2204	47A7-47A9	G protein oalpha 47A	6351297	6325466	596		447		
CG12891	47A9-47A11	withered	6366073	6356978	596		447		
CG12892	47A9-47A9	Caf1-105	6355994	6353518	596		447		
CG11777	47A9-47A9	-	6357148	6356105	596		447		
CG30018	47B13-47B13	methuselah-like 13	6680614	6678964	596		447		
CG11883	47B1-47B1	-	6528718	6505169	596		447		
CG16728	47B1-47B1	-	6532925	6529323	596		447		
CG11887	47B1-47B1	Elongator complex protein 2	6536139	6533230	596		447		
CG12934	47B2-47B2	-	6537250	6536388	596		447		
CG11895	47B4-47B7	starry night	6608643	6561061	596		447		
CG12309	47B7-47B7	-	6614783	6612775	596		447		
CG7576	47B7-47B7	Rab-protein 3	6616695	6608833	596		447		
CG12338	47B7-47B7	-	6618419	6617080	596		447		
CG7220	47B7-47B9	-	6626116	6618861	596		447		
CG33144	47B9-47B13	-	6681852	6627901	596		447		
CG7614	47B9-47B9	Mat1	6627339	6626122	596		447		
CG12340	47C1-47C1	windei	6696430	6687924			447		
CG12935	47C1-47C1	-	6698160	6696898			447		
CG7637	47C1-47C1	-	6698395	6698057			447		
CG12936	47C1-47C1	-	6699729	6698599			447		
CG12341	47C1-47C1	-	6700835	6699621			447		
CG7222	47C1-47C1	-	6703287	6701056			447		
CG12342	47C1-47C1	diego	6707378	6703531			447		
CG12323	47C1-47C1	Proteasome beta5 subunit	6708685	6707469			447		
CG12938	47C1-47C1	Lsm10	6709145	6708690			447		
CG12324	47C1-47C1	Ribosomal protein S15Ab	6709914	6709176			447		
CG12343	47C1-47C1	-	6710826	6709743			447		
CG12325	47C1-47C1	-	6715149	6711105			447		
CG12344	47C1-47C2	-	6721741	6714934			447		
CG7686	47C3-47C3	-	6726231	6724514			447		

CG30015	47C3-47C5	-	6762229	6726607	447		
CG30016	47C5-47C5	-	6762897	6762397	447		
CG6751	47C5-47C5	-	6764801	6763259	447		
CG7704	47C5-47C5	TBP-associated factor 5	6767175	6764817	447		
CG11919	47C5-47C5	-	6772441	6767458	447		
CG18003	47C5-47C5	-	6772441	6767458	447		
CR42957	47C5-47C5	mir-1008 stem loop	6773094	6773038	447		
CG18004	47C5-47C5	-	6773880	6772524	447		
CG30020	47C5-47C5	-	6780696	6774320	447		
CG12346	47C5-47C6	cag	6781865	6780528	447		
CG12942	47C6-47C6	-	6784727	6782016	447		
CG7712	47C6-47C6	-	6785388	6784641	447		
CG11979	47C6-47C6	Rpb5	6786563	6785747	447		
CG12943	47C6-47C6	-	6793068	6791075	447		
CG12944	47C6-47C6	Odorant-binding protein 47a	6797990	6797428	447		
CG7722	47C7-47C7	Serpin 47C	6829206	6827693	447		
CG33473	47D1-47D4	luna	6994321	6870299	447		
CG43189	47D3-47D3	-	6974144	6973968	447		
CG43188	47D3-47D3	-	6975805	6973091	447		
CG30489	47D4-47D4	Cyp12d1-p	7009353	7007610	447		
CG33503	47D4-47D4	Cyp12d1-d	7013119	7011159	447		
CG13232	47D5-47D5	BBS4	7026766	7023433	447		
CG13229	47D5-47D5	-	7031176	7027374	447		
CG13231	47D5-47D5	-	7034308	7033873	447		
CG12391	47D5-47D5	-	7037561	7035102	447		
CG13230	47D5-47D5	-	7042731	7042433	447		
CG7734	47D6-47D7	schnurri	7104918	7061325	447		
CG9084	47D7-47D7	-	7106718	7104918	447		
CG7736	47D7-47E1	Syntaxin 6	7109987	7107046	447		
CG7737	47E1-47E1	-	7114251	7110376	447		
CG30021	47E1-47E1	menage a trois	7120056	7113962	447		
CG13218	47E1-47E1	-	7121209	7120769	447		
CG13228	47E1-47E1	-	7121915	7121508	447		
CG13227	47E1-47E1	-	7123260	7122759	447		
CG34223	47E1-47E1	-	7123709	7123365	447		
CG13217	47E1-47E1	-	7124188	7123708	447		
CG34224	47E1-47E1	-	7125129	7124677	447		
CG13216	47E1-47E1	-	7126499	7125613	447		
CG13215	47E1-47E1	-	7127619	7126999	447		
CG9080	47E1-47E1	Listericin	7129700	7129250	447		
CG13226	47E1-47E1	-	7132508	7131795	447		
CG34225	47E1-47E1	-	7133263	7132949	447		
CR30029	47E1-47E1	-	7134161	7133622	447		

CG34227	47E1-47E1	-	7136117	7135631	447		
CG43112	47E1-47E1	-	7137438	7137099	447		
CG13225	47E1-47E3	Odorant receptor 47a	7139420	7137873	447		
CG9079	47E3-47E3	Cuticular protein 47Ea	7140903	7139256	447		
CG13224	47E3-47E3	Cuticular protein 47Eb	7143488	7142674	447		
CG13223	47E3-47E3	-	7146272	7144012	447		
CG9077	47E3-47E3	Cuticular protein 47Ec	7147344	7146822	447		
CG9076	47E4-47E4	Cuticular protein 47Ed	7149295	7148818	447		
CG13222	47E4-47E4	Cuticular protein 47Ee	7154361	7152631	447		
CG13214	47E4-47E5	Cuticular protein 47Ef	7160019	7154420	447		
CG9073	47E5-47E5	Troponin C at 47D	7162796	7161540	447		
CG9070	47E5-47E5	Cuticular protein 47Eg	7165946	7165461	447		
CG9067	47E5-47E5	-	7167106	7166398	447		
CG13221	47E5-47E6	von Hippel-Lindau	7168538	7167231	447		
CG9062	47E5-47E6	-	7171461	7167982	447		
CG13220	47E6-47E6	-	7172605	7171921	447		
CG13213	47E6-47F1	-	7177253	7172653	447		
CG7759	47F10-47F10	-	7295584	7293191	447		
CG30026	47F10-47F10	-	7296936	7296081	447		
CG34054	47F11-47F11	-	7297943	7297315	447		
CG7763	47F11-47F11	-	7302842	7302015	447		
CG9023	47F11-47F11	Drip	7317146	7299447	447		
CG7777	47F12-47F13	-	7329720	7323751	447		
CG33472	47F13-47F13	quiver	7339109	7330031	447		
CG7776	47F13-47F14	Enhancer of Polycomb	7351535	7339722	447		
CG18335	47F1-47F1	-	7178541	7177193	447		
CG12390	47F1-47F1	defective in the avoidance of repellents	7180676	7178499	447		
CG30033	47F1-47F1	-	7181096	7180036	447		
CG18336	47F1-47F1	-	7182091	7181281	447		
CG42336	47F1-47F1	-	7185041	7182041	447		
CG13208	47F1-47F1	Odorant-binding protein 47b	7190492	7189752	447		
CG7741	47F1-47F1	-	7193112	7189426	447		
CG12389	47F1-47F1	Farnesyl pyrophosphate synthase	7195070	7193016	447		
CG7745	47F1-47F1	-	7197334	7195389	447		
CG43114	47F1-47F1	-	7198670	7198361	447		
CG13207	47F1-47F1	no mechanoreceptor potential A	7206180	7197953	447		
CG13206	47F1-47F1	Odorant receptor 47b	7208817	7207215	447		
CG17835	47F15-47F17	invected	7394688	7361970	447		
CG9015	47F17-48A1	engrailed	7415715	7411509	447		
CG13209	47F2-47F3	shavenoid	7223632	7211819	447		
CG12350	47F3-47F3	lambdaTry	7225296	7224353	447		
CG12388	47F3-47F3	kappaTry	7226282	7225302	447		
CG12387	47F3-47F3	zetaTrypsin	7227633	7226691	447		

CG12386	47F3-47F3	etaTrypsin	7228928	7228018		447	
CG12385	47F3-47F4	thetaTrypsin	7230261	7229219		447	
CG18444	47F4-47F4	alphaTrypsin	7232620	7231756		447	
CG18681	47F4-47F4	epsilonTrypsin	7233567	7232734		447	
CG18211	47F4-47F4	betaTrypsin	7234641	7233844		447	
CG30028	47F4-47F4	gammaTrypsin	7237374	7236566		447	
CG30031	47F4-47F4	-	7239126	7238318		447	
CG30025	47F4-47F5	-	7241864	7241103		447	
CG12351	47F5-47F5	deltaTrypsin	7243633	7242838		447	
CG13202	47F5-47F5	-	7243998	7243619		447	
CG7754	47F5-47F5	iotaTrypsin	7245041	7244227		447	
CR30024	47F5-47F5	transfer RNA:SeCys	7245155	7245069		447	
CG12384	47F5-47F5	-	7246674	7245407		447	
CG13201	47F5-47F5	intersex	7247668	7246942		447	
CG12352	47F5-47F5	separation anxiety	7249376	7248213		447	
CG30030	47F5-47F5	Gustatory receptor 47b	7250774	7249405		447	
CG13204	47F6-47F7	-	7257789	7254216		447	
CG9035	47F7-47F7	Translocon-associated protein delta	7258675	7257805		447	
CG13203	47F7-47F7	-	7264614	7261112		447	
CG9033	47F7-47F7	Tetraspanin 47F	7266682	7264967		447	
CG9027	47F7-47F8	-	7271613	7267849		447	
CG30022	47F8-47F8	-	7276282	7274663		447	
CR30257	47F8-47F8	transfer RNA:CR30257	7281929	7281858		447	
CG30023	47F8-47F8	sprite	7284935	7272238		447	
CR30506	47F9-47F9	transfer RNA:CR30506	7287346	7287275		447	
CG10897	48A2-48A3	toutatis	7503336	7466385	1145		
CR34530	48A3-48A3	snoRNA:Psi28S-1936	7475836	7475688	1145		
CR33661	48A3-48A3	snoRNA:Psi28S-1180	7478990	7478846	1145		
CG9006	48A3-48A3	Enigma	7506515	7504374	1145		
CG9005	48A3-48B2	-	7528197	7506984	1145		
CG9003	48B2-48B4	-	7539127	7529772	1145		
CG34228	48B4-48B4	-	7539844	7539382	1145		
CR30254	48B4-48B4	transfer RNA:CR30254	7539944	7539872	1145		
CR30255	48B4-48B4	transfer RNA:met2:48Ba	7540226	7540154	1145		
CG8998	48B4-48C1	Roc2	7566857	7540261	1145		
CG13198	48B5-48B5	-	7543267	7542403	1145		
CR32844	48B5-48B5	transfer RNA:met2:48Bb	7548140	7548068	1145		
CG30035	48B6-48B7	Trehalose transporter 1-1	7562287	7553259	1145		
CG8234	48B8-48C1	Trehalose transporter 1-2	7565519	7563465	1145		
CG13196	48C1-48C1	-	7573937	7571654	1145		
CG8238	48C1-48C1	Buffy	7576264	7566978	1145		
CG8996	48C1-48C2	walrus	7578380	7576432	1145		
CG13197	48C2-48C2	-	7582958	7578801	1145		

CR33471	48C2-48C2	Ionotropic receptor 48a	7587822	7586597	1145		
CG13195	48C2-48C2	Ionotropic receptor 48b	7589954	7588152	1145		
CG13194	48C2-48C2	pyramus	7613850	7599767	1145		
CG13193	48C2-48C2	-	7657066	7655958	1145		
CG42493	48C2-48C2	-	7666740	7666083	1145		
CG12444	48C3-48C3	Transport and Golgi organization 3	7676998	7675313	1145		
CG12443	48C3-48C4	thisbe	7701667	7658042	1145		
CG13192	48C4-48C4	-	7714602	7712870	1145		
CG8991	48C4-48C4	Sine oculis-binding protein	7727035	7714668	1145		
CG34229	48C4-48C4	-	7729669	7729113	1145		
CG8988	48C4-48C4	site-2 protease	7731743	7729608	1145		
CG43190	48C4-48C4	-	7732421	7732019	1145		
CG8271	48C4-48C5	Silnoon	7739829	7732831	1145		
CG8274	48C5-48C5	Megator	7748364	7740124	1145		
CG34230	48C5-48C5	-	7749520	7748815	1145		
CG8986	48C5-48C5	TwdlBeta	7750753	7750042	1145		
CG42531	48C5-48C5	-	7752444	7751709	1145		
CG18188	48C5-48C5	Death associated molecule related to Mch2	7753888	7752681	1145		
CR42532	48C5-48C5	-	7755084	7754448	1145		
CG13185	48C5-48C5	-	7772951	7755381	1145		
CG13190	48C5-48C5	cutoff	7775108	7773572	1145		
CG8983	48C5-48C5	ERp60	7778520	7775073	1145		
CR32905	48C5-48C5	-	7780700	7780628	1145		
CG8280	48C5-48C5	Elongation factor 1alpha48D	7783025	7779597	1145		
CG13189	48C5-48C5	-	7788899	7787024	1145		
CG42572	48C5-48C5	Microcephalin	7791429	7783499	1145		
CG13183	48C5-48D2	-	7800280	7791828	1145		
CG13188	48D3-48D5	-	7854942	7826989			
CG8979	48D5-48D5	-	7856348	7854841			
CG8290	48D5-48D5	-	7865236	7858179			
CG30036	48D5-48D5	-	7866454	7865038			
CG30037	48D5-48D5	-	7867990	7866598			
CG33145	48D5-48D5	-	7870457	7868086			
CG8975	48D5-48D5	Ribonucleoside diphosphate reductase small subunit	7872948	7870650			
CG34231	48D5-48D5	-	7874487	7873513			
CG8972	48D5-48D5	rhomboid-7	7876261	7874223			
CG8298	48D5-48D5	-	7879471	7876638			
CG8967	48D6-48D7	off-track	7907329	7888983			
CG17509	48D7-48D6	-	7921230	7915484			
CG8964	48D7-48D7	-	7912775	7910651			
CG8889	48D7-48D7	-	7915212	7913004			
CG8321	48D8-48D8	-	7923765	7921453			
CG43191	48D8-48D8	-	7924670	7923426			

CG8340	48D8-48D8	upstream of RpIII128	7926356	7924811		
CG8344	48D8-48D8	RNA polymerase III 128kD subunit	7930138	7926595		
CG8357	48D8-48D8	DNA fragmentation factor-related protein 1	7937678	7932119		
CG30039	48D8-48D8	-	7939260	7938480		
CG8364	48D8-48D8	DNA fragmentation factor-related protein 3	7950374	7940449		
CG8888	48D8-48E1	-	7967046	7952068		
CG8856	48E10-48E10	Scavenger receptor class C, type II	8098730	8096359		
CG13171	48E10-48E10	-	8101900	8101509		
CG8854	48E10-48E10	-	8114351	8111964		
CG13186	48E1-48E1	-	7969562	7968781		
CG30040	48E1-48E2	jelly belly	8006377	7978127		
CG18343	48E2-48E2	-	8026781	8026307		
CG8881	48E2-48E2	skpB	8027567	8026800		
CG8378	48E2-48E2	-	8030834	8028110		
CG13178	48E2-48E2	-	8032038	8030696		
CG8878	48E2-48E3	-	8038562	8033524		
CG12367	48E2-48E3	-	8040259	8033231		
CG8407	48E3-48E3	-	8041767	8040576		
CG8877	48E3-48E4	pre-mRNA processing factor 8	8050496	8041763		
CR43007	48E4-48E4	mir-988 stem loop	8046475	8046377		
CG13177	48E4-48E4	-	8051898	8051180		
CG34232	48E4-48E4	-	8053224	8052416		
CG8427	48E4-48E4	Small ribonucleoprotein particle protein SmD3	8057514	8056231		
CR42975	48E4-48E4	mir-281-2 stem loop	8057749	8057658		
CR42931	48E4-48E4	mir-281-1 stem loop	8057967	8057878		
CG16747	48E4-48E4	Ornithine decarboxylase antizyme	8061767	8054077		
CG8439	48E4-48E4	T-complex Chaperonin 5	8065039	8062281		
CG8862	48E4-48E4	Endonuclease G	8066035	8064950		
CG8860	48E6-48E6	-	8067392	8066988		
CG13176	48E6-48E6	washout	8069878	8068145		
CG16792	48E6-48E7	Small ribonucleoprotein particle protein SmF	8071778	8071349		
CG13175	48E6-48E7	-	8073011	8070144		
CG33964	48E6-48E7	-	8073011	8070144		
CG8453	48E7-48E7	Cyp6g1	8075936	8073168		
CG8859	48E7-48E7	Cyp6g2	8077882	8075843		
CG8457	48E7-48E8	Cyp6t3	8079941	8078187		
CG8858	48E8-48E8	-	8086343	8079872		
CR34153	48E8-48E8	snoRNA:Me28S-C3420b	8086778	8086688		
CG8857	48E8-48E9	Ribosomal protein S11	8088333	8086524		
CR34152	48E9-48E9	snoRNA:Me28S-C3420a	8087257	8087167		
CR30249	48F10-48F10	transfer RNA:CR30249	8221502	8221431	5879	
CR30250	48F10-48F10	transfer RNA:CR30250	8221810	8221739	5879	
CR30251	48F10-48F10	transfer RNA:CR30251	8222571	8222500	5879	

CG8490	48F10-48F10	-	8223710	8222822	5879		
CR30252	48F10-48F10	transfer RNA:his:48F	8223994	8223923	5879		
CR30253	48F10-48F10	transfer RNA:his:pseudogene	8224309	8224238	5879		
CG34021	48F10-48F10	-	8225223	8224487	5879		
CG8493	48F10-48F10	Deneddylase 1	8227050	8225307	5879		
CG8839	48F10-48F11	-	8232118	8227115	5879		
CG13162	48F11-49A1	anastral spindle 3	8238583	8232591	5879		
CG13170	48F1-48F1	-	8128267	8127914	5879		
CG43315	48F1-48F1	-	8129264	8128723	5879		
CG43316	48F1-48F1	-	8130778	8130051	5879		
CG43244	48F1-48F1	-	8132167	8131576	5879		
CG13168	48F1-48F1	-	8143197	8141497	5879		
CG13167	48F1-48F1	Vacuolar H[+] ATPase subunit 36-2	8146157	8144787	5879		
CG8472	48F1-48F1	Calmodulin	8164709	8146913	5879		
CG42700	48F6-48F6	-	8185752	8167278	5879		
CG8850	48F6-48F6	-	8189741	8186283	5879		
CG13164	48F6-48F6	Syntaxin Interacting Protein 2	8193774	8190042	5879		
CG17739	48F6-48F7	-	8197917	8194029	5879		
CG30203	48F7-48F7	-	8201340	8198194	5879		
CG30046	48F7-48F7	-	8204736	8201624	5879		
CG13163	48F7-48F8	-	8210017	8208798	5879		
CG8487	48F8-48F10	gartenzwerg	8221324	8214179	5879		
CG8841	48F8-48F8	-	8213763	8210012	5879		
CG8821	49A10-49A10	vismay	8398311	8395396	5879		
CG8819	49A10-49A10	achintya	8402556	8399035	5879		
CG13151	49A10-49A10	-	8404789	8402884	5879		
CG8818	49A10-49A10	-	8406423	8404760	5879		
CG8569	49A10-49A10	-	8409131	8406654	5879		
CG33632	49A10-49A10	-	8410236	8409528	5879		
CG8581	49A10-49B3	frazzled	8451691	8416561	5879		
CG30047	49A1-49A1	-	8242918	8239298	5879		
CG30049	49A1-49A1	-	8246592	8243176	5879		
CG30043	49A1-49A1	-	8250670	8246958	5879		
CG33013	49A1-49A1	-	8253889	8250877	5879		
CG33012	49A1-49A1	-	8258338	8254903	5879		
CG13160	49A1-49A1	-	8262597	8259101	5879		
CG13159	49A1-49A1	-	8263183	8262794	5879		
CG30045	49A1-49A1	Cuticular protein 49Aa	8264883	8264175	5879		
CG30042	49A1-49A1	Cuticular protein 49Ab	8266901	8265962	5879		
CG13155	49A1-49A1	-	8267931	8267119	5879		
CG8501	49A1-49A1	-	8272025	8271125	5879		
CG8502	49A2-49A2	Cuticular protein 49Ac	8277562	8274472	5879		
CG8836	49A2-49A2	Cuticular protein 49Ad	8279159	8278538	5879		

CG13158	49A2-49A2	Odorant receptor 49a	8282347	8280988	5879
CG30048	49A2-49A2	-	8286611	8282447	5879
CG8505	49A2-49A2	Cuticular protein 49Ae	8292620	8289720	5879
CG8510	49A2-49A3	Cuticular protein 49Af	8293948	8293510	5879
CG8511	49A3-49A3	Cuticular protein 49Ag	8296038	8295341	5879
CG30050	49A3-49A3	-	8297218	8296459	5879
CG33626	49A3-49A3	-	8298201	8297584	5879
CG33627	49A3-49A3	-	8299183	8298516	5879
CG8515	49A3-49A3	Cuticular protein 49Ah	8302675	8301467	5879
CG13157	49A3-49A4	-	8305647	8303960	5879
CG42782	49A4-49A4	-	8306799	8306619	5879
CG8834	49A4-49A4	-	8310040	8307316	5879
CG8520	49A4-49A4	-	8312964	8310490	5879
CG8525	49A4-49A4	-	8314480	8312988	5879
CG13154	49A4-49A4	-	8315366	8314388	5879
CG8831	49A4-49A4	Nucleoporin 54	8318600	8315954	5879
CG43204	49A4-49A4	-	8318801	8318100	5879
CG8830	49A4-49A6	-	8324082	8319407	5879
CG30051	49A6-49A6	-	8324495	8323602	5879
CG30334	49A6-49A6	-	8328778	8328138	5879
CG8529	49A6-49A6	Dystrobrevin-like	8340421	8324840	5879
CG12369	49A6-49A7	Lachesin	8353154	8340696	5879
CG8545	49A7-49A7	-	8359227	8356145	5879
CG8828	49A7-49A7	dim gamma-tubulin 5	8359280	8353177	5879
CG8550	49A7-49A7	-	8361321	8359420	5879
CG12370	49A7-49A9	-	8375491	8361949	5879
CG30044	49A9-49A10	stanley-cup	8388972	8383030	5879
CG8824	49A9-49A10	fused lobes	8394841	8375253	5879
CG34234	49A9-49A9	-	8374883	8374224	5879
CG8811	49B10-49B10	muskelin	8519883	8516472	754
CG33792	49B10-49B10	-	8520959	8520179	754
CG12372	49B10-49B10	spt4	8523546	8521122	754
CG33671	49B10-49B10	-	8523666	8521668	754
CG33672	49B10-49B10	-	8523666	8521668	754
CG8625	49B10-49B10	Imitation SWI	8528133	8524123	754
CG8785	49B10-49B11	-	8535718	8528195	754
CG8778	49B11-49B11	-	8539987	8538806	754
CG8632	49B11-49B11	-	8543248	8540312	754
CG8646	49B11-49B11	-	8546846	8543461	754
CG42708	49B12-49B12	-	8567094	8557988	754
CG8771	49B12-49B12	-	8573670	8567472	754
CG13148	49B12-49B12	-	8576291	8574114	754
CG30053	49B12-49B12	-	8577381	8576238	754

CG30052	49B12-49B12	Odorant-binding protein 49a	8578460	8577564	754	
CG8776	49B12-49C1	no extended memory	8557722	8547002	754	442
CG33752	49B3-49B3	-	8433806	8433194	754	442
CG30056	49B3-49B3	-	8450160	8449590	754	442
CG33775	49B3-49B3	-	8452406	8451729	754	442
CG8587	49B4-49B5	Cyp301a1	8456566	8453692	754	442
CG8816	49B5-49B5	Adenylate kinase 6	8457372	8456518	754	442
CG8592	49B5-49B5	stand still	8459388	8457861	754	442
CG8594	49B5-49B5	Chloride channel-b	8462801	8459617	754	442
CG8815	49B5-49B7	Sin3A	8480397	8462745	754	442
CR30055	49B7-49B7	-	8478387	8476808	754	442
CG8604	49B7-49B8	Amphiphysin	8499578	8481088	754	442
CG17759	49B8-49B9	G protein alpha49B	8510272	8500246	754	442
CG17760	49B9-49B10	-	8516124	8513338	754	442
CG30054	49B9-49B9	-	8512857	8511231	754	442
CG8768	49C1-49C1	-	8580193	8578813	754	442
CG12442	49C1-49C1	-	8588356	8587586	754	442
CG42663	49C2-49C2	-	8639050	8592679	754	442
CG8767	49C2-49C2	mos	8640441	8638988	754	442
CG8766	49C2-49C2	Tafazzin	8643915	8640531	754	442
CG12373	49C2-49C2	mitochondrial ribosomal protein L18	8644678	8643904	754	442
CG8764	49C2-49C2	oxen	8645028	8644644	754	442
CG8657	49C2-49C2	Diacyl glycerol kinase epsilon	8647226	8645051	754	442
CG8759	49C2-49C3	Nascent polypeptide associated complex protein alpha subunit	8648377	8647198	754	442
CG12374	49C3-49C3	-	8651330	8649617	754	442
CG17579	49C3-49D3	scabrous	8689515	8668049	754	442
CG13345	49C-50C6	tumbleweed	9746222	9743655	754	442
CG17580	49D3-49D3	-	8695316	8694182	754	442
CG17577	49D4-49D4	Cyp9h1	8730063	8728318	754	442
CG17584	49D4-49D4	Odorant receptor 49b	8732214	8730170	754	442
CG17575	49D4-49D4	-	8734101	8733049	754	442
CG30488	49D4-49D4	-	8735509	8734353	754	442
CG30486	49D4-49D4	-	8736481	8735539	754	442
CG17574	49D4-49D6	-	8756922	8736863	754	442
CG3644	49D6-49D6	bicaudal	8759299	8757742	754	442
CG3790	49D6-49D6	-	8762518	8760289	754	442
CG3814	49D6-49D6	-	8764471	8762663	754	442
CG3798	49D6-49D6	N-methyl-D-aspartate receptor-associated protein	8767328	8764596	754	442
CG3821	49D7-49D7	Aspartyl-tRNA synthetase	8770675	8767824	754	442
CG3830	49E1-49E1	vestigial	8786900	8771794	754	442
CG3845	49E1-49E1	NAT1	8810745	8803502	754	442
CG13319	49E1-49E1	-	8812169	8811409	754	442
CG3850	49E1-49E1	sugarbabe	8818151	8816368	754	442

CG17019	49E1-49E1	-	8821550	8818417	754	442		
CG13322	49E1-49E1	-	8824032	8821739	754	442		
CG30487	49E1-49E1	-	8825848	8825121	754	442		
CG13320	49E1-49E1	Sans ortholog	8827917	8824400	754	442		
CG3879	49E1-49E4	Multi drug resistance 49	8833850	8827828	754	442		
CG3884	49E4-49E4	-	8839791	8835853		442		
CG13321	49E4-49E4	-	8842675	8841061		442		
CG3886	49E6-49E6	Posterior sex combs	8868494	8853815		442		
CG33798	49E7-49E7	-	8882127	8881402		442		
CG3905	49E7-49E7	Suppressor of zeste 2	8895307	8884030		442		
CG34438	49E7-49F7	-	9030325	9020624		442		
CG4627	49F10-49F10	-	9103265	9102238		442		
CG4630	49F10-49F10	-	9106752	9103159		442		
CG4646	49F10-49F10	-	9107730	9106995		442		
CG17059	49F10-49F10	-	9108523	9107829		442		
CG4643	49F10-49F10	-	9109964	9108444		442		
CG4654	49F10-49F11	DP transcription factor	9115714	9109902		442		
CG4663	49F11-49F11	peroxin 13	9117733	9115772		442		
CG12765	49F11-49F11	fates-shifted	9119170	9118088		442		
CG4670	49F11-49F11	-	9122547	9119263		442		
CG4676	49F11-49F11	-	9124560	9123367		442		
CG4679	49F11-49F11	-	9126972	9124761		442		
CG4688	49F12-49F12	-	9128518	9127234		442		
CG4696	49F13-49F13	Muscle protein 20	9135278	9134157		442		
CG4712	49F13-49F13	-	9139214	9136399		442		
CG4714	49F13-49F13	-	9141842	9139351		442		
CG4716	49F13-49F13	-	9144951	9144088		442		
CG10799	49F13-49F13	-	9145997	9145391		442		
CG42319	49F14-49F15	-	9153843	9147617		442		
CG13323	49F1-49F1	-	8934793	8934238		442		
CG13324	49F1-49F1	-	8937123	8936647		442		
CG3915	49F1-49F1	Derailed 2	8967043	8944081		442		
CG32843	49F15-50A1	Diuretic hormone 31 receptor 1	9183429	9155302		442		
CG13325	49F2-49F2	-	9013285	9003810		442		
CG3955	49F2-49F2	-	9016559	9015417		442		
CG13326	49F2-49F2	-	9019960	9017016		442		
CG33007	49F3-49F3	-	9035785	9033718		442		
CG3969	49F3-49F4	Fak-like tyrosine kinase	9040161	9030337		442		
CG3991	49F4-49F4	tripeptidyl-peptidase II	9046595	9040393		442		
CG34439	49F4-49F4	-	9047695	9046118		442		
CG4007	49F4-49F4	Neurospecific receptor kinase	9050989	9047554		442		
CG15870	49F4-49F4	-	9051348	9050868		442		
CG4604	49F4-49F4	Glial Lazarillo	9054111	9051559		442		

CG4016	49F4-49F4	Serine palmitoyltransferase subunit I	9058249	9056005	442		
CG33138	49F4-49F4	-	9062305	9058906	442		
CG33137	49F4-49F4	-	9063580	9062699	442		
CG17724	49F4-49F7	-	9073317	9063597	442		
CG32904	49F4-49F7	sequoia	9077579	9067187	442		
CG33182	49F7-49F7	Histone demethylase 4B	9085869	9073242	442		
CG4062	49F7-49F7	Valyl-tRNA synthetase	9090217	9086356	442		
CG34315	49F7-49F8	-	9094027	9090248	442		
CG4088	49F7-49F8	latheo	9094027	9090248	442		
CG4616	49F8-49F9	FLASH ortholog	9097974	9094261	442		
CG12251	49F9-49F10	aquaporin	9102005	9099837	442		
CG30058	49F9-49F9	-	9099680	9097314	442		
CG34235	49F9-49F9	-	9099680	9097314	442		
CG34312	49F9-49F9	-	9099680	9097314	442		
CG43192	50A11-50A11	-	9365584	9364847	442		
CG5970	50A11-50A11	crowded by cid	9372901	9371017	442		
CG13329	50A11-50A11	centromere identifier	9374136	9373106	442		
CG6016	50A11-50A13	bb in a boxcar	9382374	9374139	442		
CG6033	50A13-50A13	downstream of receptor kinase	9390342	9382727	442		
CG17064	50A13-50A14	mars	9393516	9390080	442		
CG6050	50A14-50A14	Elongation factor Tu mitochondrial	9396837	9395063	442		
CG6061	50A14-50A14	Myb-interacting protein 120	9400617	9393947	442		
CG13330	50A14-50A15	-	9404951	9402764	442		
CG4734	50A1-50A1	-	9185972	9184707	442		
CG17047	50A1-50A1	-	9189045	9187107	442		
CR42925	50A1-50A1	mir-184 stem loop	9217006	9216907	442		
CG13331	50A15-50A15	-	9410806	9409269	442		
CG17048	50A3-50A3	-	9241973	9241231	442		
CG10814	50A3-50A3	-	9265219	9263476	442		
CG17050	50A3-50A3	-	9279139	9277358	442		
CG17049	50A3-50A3	-	9280723	9280035	442		
CG4740	50A3-50A3	Attacin-C	9282172	9281210	442		
CG4744	50A3-50A3	-	9286873	9282120	442		
CG18279	50A5-50A5	Immune induced molecule 10	9295608	9294511	442		
CG18278	50A5-50A5	-	9297458	9295547	442		
CG33470	50A5-50A5	-	9300590	9299244	442		
CG30059	50A5-50A5	-	9302119	9300274	442		
CG30060	50A7-50A7	-	9311152	9310483	442		
CR32842	50A7-50A7	transfer RNA:ile:49Fa	9317860	9317787	442		
CR32841	50A7-50A7	transfer RNA:leu:49Fa	9318320	9318200	442		
CR30244	50A7-50A7	transfer RNA:ile:49Fb	9318562	9318489	442		
CR30521	50A7-50A7	transfer RNA:ile:49Fc	9318863	9318790	442		
CR30246	50A7-50A7	transfer RNA:ile:49Fd	9319355	9319282	442		

CR30247	50A7-50A7	transfer RNA:ile:49Fe	9319671	9319598	442		
CR30508	50A7-50A7	transfer RNA:leu:49Fb	9320299	9320173	442		
CG30065	50A8-50A8	-	9321265	9320600	442		
CG4812	50A8-50A8	Ser8	9322539	9321712	442		
CR30509	50A8-50A8	transfer RNA:CR30509	9325444	9325371	442		
CG42321	50A8-50A8	-	9326550	9302483	442		
CG4832	50A8-50A9	centrosomin	9337990	9326819	442		
CG5912	50A9-50A11	arrow	9370723	9341159	442		
CG30062	50A9-50A9	-	9333814	9333205	442		
CG4840	50A9-50A9	centrosomin's beautiful sister	9340898	9338169	442		
CG13332	50B1-50B1	-	9413953	9412882	442		
CR30507	50B1-50B1	transfer RNA:lys2:50C	9423622	9423550	442		
CG6145	50B1-50B1	-	9435082	9424893	442		
CG33156	50B1-50B1	-	9440666	9434650	442		
CG6155	50B1-50B1	Roe1	9443111	9441587	442		
CG13333	50B1-50B1	-	9444847	9443398	442		
CR34531	50B1-50B1	snoRNA:Psi28S-1153	9445191	9445044	442		
CG13334	50B1-50B2	-	9448273	9446050	442		
CG42807	50B2-50B2	-	9460045	9459029	442		
CG42808	50B2-50B2	-	9461747	9461123	442		
CG33528	50B2-50B3	Vesicular monoamine transporter	9420494	9400632	442		
CG6191	50B3-50B4	-	9480841	9468091	442		
CG6197	50B4-50B4	-	9484068	9481154	442		
CG18369	50B4-50B5	-	9486255	9484182	442		
CG43058	50B5-50B5	-	9488517	9488215	442		
CG34236	50B5-50B5	-	9492910	9492079	442		
CG12464	50B5-50B6	-	9496683	9496178	442		
CG17716	50B6-50C3	faint sausage	9636872	9510593	442		
CG6209	50B9-50B9	-	9551103	9549000	442		
CG13337	50C1-50C1	-	9555184	9552619	442		
CG18368	50C1-50C1	-	9558824	9555241	442		
CG30481	50C16-50C16	mitochondrial ribosomal protein L53	9843174	9841704	442		
CG33155	50C16-50C16	-	9843174	9841704	442		
CG13349	50C17-50C18	-	9847909	9846033	442		
CG6692	50C18-50C20	Cysteine proteinase-1	9855486	9848164	442		
CG42806	50C19-50C20	-	9852879	9852173	442		
CG13348	50C20-50C20	Phenylalanyl-tRNA synthetase	9857407	9855852	442		
CG6704	50C20-50C20	-	9858662	9857415	442		
CG18568	50C21-50C22	-	9860336	9859106	442		
CG6701	50C22-50C23	-	9867670	9860504	442		
CG13350	50C23-50C23	-	9870979	9867867	442		
CG8067	50C23-50C23	-	9872398	9871157	442		
CG8085	50C23-50C23	tre oncogene-related protein	9878191	9872320	442		

CG8118	50C23-50D3	mastermind	9947861	9878686		442			
CG6220	50C2-50C2	-	9580874	9579212		442			
CG6280	50C3-50C3	-	9646362	9642849		442			
CG13338	50C3-50C5	Cuticular protein 50Ca	9675310	9657420		442			
CG13340	50C5-50C5	-	9667750	9665629		442			
CG6305	50C5-50C5	Cuticular protein 50Cb	9692741	9682308		442			
CG12295	50C5-50C6	straightjacket	9707076	9692979		442			
CG6315	50C6-50C6	female lethal d	9712054	9707129		442			
CG13339	50C6-50C6	-	9713082	9712397		442			
CG6329	50C6-50C6	-	9720419	9713880		442			
CG6337	50C6-50C6	-	9722593	9721359		442			
CG6347	50C6-50C6	-	9726869	9723926		442			
CG6357	50C6-50C6	-	9729248	9727581		442			
CG10808	50C6-50C6	synaptogyrin	9733757	9729255		442			
CG30484	50C6-50C6	-	9736994	9734358		442			
CG30485	50C6-50C6	-	9740488	9737387		442			
CG6543	50C6-50C6	-	9741879	9740452		442			
CG6553	50C6-50C6	-	9743270	9742083		442			
CG13343	50C6-50C6	-	9747937	9746462		442			
CG16935	50C6-50C6	-	9749507	9747854		442			
CG13344	50C6-50C6	-	9751661	9749517		442			
CG18076	50C6-50C9	short stop	9829615	9751742		442			
CG6671	50C9-50C17	Argonaute-1	9845594	9830892		442			
CG6646	50C9-50C9	DJ-1alpha	9830882	9830039		442			
CG18371	50D2-50D2	-	9916611	9916123	6516	442			
CG30483	50D3-50E1	Prosap	10028403	9947961	6516	442			
CG42287	50D5-50D5	-	9978479	9977840	6516	442			
CG42288	50D5-50D5	-	9979310	9978536	6516	442			
CR42922	50E1-50E1	mir-989 stem loop	10033029	10032856					
CG8233	50E1-50E1	Reduction in Cnn dots 1	10040624	10035763					
CG8241	50E1-50E1	peanuts	10044611	10040661					
CG13018	50E1-50E1	-	10044984	10044555					
CG13016	50E1-50E1	-	10046939	10045276					
CG8257	50E1-50E1	-	10048754	10046896					
CG12366	50E1-50E1	O-fucosyltransferase 1	10050326	10048940					
CG8309	50E1-50E1	Transport and Golgi organization 7	10052374	10050571					
CG8323	50E1-50E1	-	10054496	10052560					
CG18327	50E1-50E1	-	10055738	10054487					
CG18324	50E1-50E1	-	10057738	10056361					
CG8331	50E1-50E1	-	10060503	10057971					
CG8338	50E1-50E1	mitochondrial ribosomal protein S16	10061041	10060485					
CG8367	50E1-50E1	combgap	10070345	10061175					
CG30069	50E1-50E3	-	10085730	10073324					

CG8394	50E4-50E4	Vesicular GABA Transporter	10088226	10086505
CG8404	50E4-50E4	Sox box protein 15	10099914	10088888
CR42951	50E4-50E4	mir-308 stem loop	10103369	10103307
CG8415	50E4-50E4	Ribosomal protein S23	10104132	10102740
CG8468	50E4-50E4	-	10118131	10107425
CR42981	50E4-50E4	mir-1016 stem loop	10120692	10120635
CG8485	50E4-50E4	-	10127203	10123286
CG8479	50E4-50E5	optic atrophy 1-like	10122953	10118125
CG8494	50E4-50E5	-	10131167	10127442
CG8503	50E5-50E6	-	10133571	10131192
CG8523	50E6-50E6	Multi drug resistance 50	10140102	10134471
CG8542	50E6-50E6	Heat shock protein cognate 5	10143697	10140103
CG8531	50E6-50E6	-	10146292	10143966
CG8536	50E6-50E6	beta4GalNAcTA	10148655	10146537
CG8547	50E6-50E6	-	10155419	10148711
CG8561	50E6-50E6	convoluted	10162377	10158306
CR30068	50E6-50E6	-	10166920	10163569
CG8585	50E6-50F1	I[[h]] channel	10186413	10166938
CG8553	50E8-50E8	Selenide,water dikinase	10158159	10156275
CG8589	50F1-50F1	tejas	10189858	10187605
CG34379	50F4-50F6	Shroom	10239312	10195667
CG8613	50F6-50F6	-	10243180	10239744
CG8617	50F6-50F6	-	10244789	10243274
CG12505	50F6-50F6	Activity-regulated cytoskeleton associated protein 1	10247799	10245432
CR10102	50F6-50F6	-	10249285	10247938
CG13941	50F6-50F6	Arc2	10250330	10249449
CG8151	50F6-50F6	Tfb1	10252978	10250548
CG34184	50F6-50F6	-	10254163	10253161
CG34442	50F6-50F6	-	10255379	10254337
CG34443	50F6-50F6	-	10256554	10255536
CG34444	50F6-50F6	-	10257824	10256747
CG30067	50F6-50F6	Odorant-binding protein 50a	10258621	10257836
CG30072	50F6-50F6	Odorant-binding protein 50c	10260511	10258691
CG30073	50F6-50F6	Odorant-binding protein 50b	10260511	10258691
CG30074	50F6-50F6	Odorant-binding protein 50d	10261264	10260629
CG34185	50F6-50F6	-	10261838	10261341
CG13939	50F6-50F6	Odorant-binding protein 50e	10262836	10262077
CG30075	50F7-50F7	-	10264182	10263426
CG8422	50F8-50F9	Diuretic hormone 44 receptor 1	10272864	10265630
CG10104	51A1-51A1	-	10279831	10278291
CG17385	51A1-51A2	-	10299077	10297522
CG10105	51A2-51A2	SAPK-interacting protein 1	10301356	10299316
CG17386	51A2-51A2	-	10312099	10307846

CG10108	51A2-51A2	phyllopod	10319840	10314841
CG42702	51A4-51A4	O/E-associated zinc finger protein	10352962	10323623
CG10109	51A4-51A4	Lobe	10384817	10368708
CG10110	51A4-51A4	Cleavage and polyadenylation specificity factor 160	10390978	10386194
CG8787	51A5-51A6	Additional sex combs	10399951	10391514
CG30197	51A6-51A6	-	10402500	10401539
CG10112	51A6-51A6	Cuticular protein 51A	10402713	10400047
CG10117	51A7-51B4	tout-velu	10472826	10414076
CG30076	51A8-51A8	-	10433264	10431942
CG30479	51B10-51B10	-	10562558	10561970
CG30480	51B10-51B10	-	10565638	10562676
CG10119	51B1-51B1	Lamin C	10463307	10458309
CG12869	51B4-51B4	-	10483126	10478708
CG10122	51B4-51B6	RNA polymerase I subunit	10488702	10483112
CG30077	51B6-51B6	BLOC-1 subunit 1	10489515	10488769
CG10128	51B6-51B6	transformer 2	10491857	10489509
CG12868	51B6-51B6	-	10492840	10492052
CG33469	51B6-51B6	-	10493774	10493157
CG33468	51B6-51B6	-	10494466	10493812
CG12864	51B6-51B6	Su(var)2-HP2	10505550	10494659
CG10130	51B6-51B6	Sec61beta	10507186	10506235
CG12863	51B6-51B6	-	10508820	10507303
CR34532	51B6-51B6	snoRNA:Me18S-C1366	10509386	10509287
CR34533	51B6-51B6	snoRNA:Me28S-C3227a	10509672	10509593
CR34534	51B6-51B6	snoRNA:Me28S-C3227b	10509914	10509835
CR34535	51B6-51B6	snoRNA:Me28S-U1848	10510154	10510075
CR34536	51B6-51B6	snoRNA:Me18S-G1952	10510382	10510307
CR34537	51B6-51B6	snoRNA:Me18S-A1061	10510622	10510547
CR34538	51B6-51B6	snoRNA:Me28S-A992	10510851	10510781
CR34539	51B6-51B6	snoRNA:Me28S-G2703a	10511112	10511022
CR34540	51B6-51B6	snoRNA:Me28S-G2703b	10511355	10511269
CR34541	51B6-51B6	snoRNA:Me28S-G2703c	10511596	10511512
CR34542	51B6-51B6	-	10511835	10511758
CR42452	51B6-51B6	Uhg5	10512013	10509111
CG10131	51B6-51B6	-	10518526	10517418
CG43236	51B7-51B7	-	10526280	10526063
CG42715	51B7-51B7	-	10527268	10526710
CG12862	51B7-51B7	-	10528131	10527719
CG10139	51B7-51B7	-	10533676	10532776
CG10143	51B7-51B8	Adenosine deaminase-related growth factor E	10546260	10544303
CG12861	51B9-51B9	-	10552856	10551751
CG12860	51B9-51B9	-	10554322	10553146
CG12866	51B9-51B9	-	10559180	10555896

CG10145	51B9-51C1	M-spondin	10601126	10559440	
CG12865	51C1-51C1	-	10626793	10626224	
CG12858	51C1-51C1	-	10632834	10627871	
CG10816	51C1-51C1	Drosocin	10633821	10633461	
CG10146	51C1-51C1	Attacin-A	10635699	10634867	
CG18372	51C1-51C1	Attacin-B	10637670	10636728	
CG10149	51C1-51C2	Proteasome p44.5 subunit	10640415	10637671	
CG30476	51C2-51C2	aveugle	10640774	10640031	
CG10151	51C2-51C2	-	10643793	10640842	
CG12859	51C2-51C2	-	10644577	10644026	
CG10153	51C2-51C2	-	10645334	10644569	
CG12857	51C2-51C2	-	10647099	10645557	
CG10155	51C2-51C2	Sprouty-related protein with EVH-1 domain	10656927	10648661	
CG42254	51C2-51C2	-	10658762	10657104	
CG10159	51C2-51C2	Boundary element-associated factor of 32kD	10660135	10657939	
CG10197	51C2-51C3	knot	10694566	10660152	6380
CG10200	51C3-51C4	-	10697436	10695929	6380
CG10202	51C4-51C4	-	10707492	10705365	6380
CG10205	51C4-51C4	-	10721460	10720338	6380
CG10207	51C5-51C5	Na[+]-dependent inorganic phosphate cotransporter	10733379	10730216	6380
CG10209	51C5-51C5	-	10735864	10733562	6380
CG10212	51C5-51C5	SMC2	10740155	10736094	6380
CG10215	51C5-51C5	Ercc1	10741453	10740470	6380
CG12797	51C5-51C5	Ciao1	10742573	10741368	6380
CG12855	51C5-51C5	Hermansky-Pudlak Syndrome 1 ortholog	10745007	10742947	6380
CG33506	51C5-51C5	-	10746138	10744952	6380
CG33505	51C5-51C5	U3 small nuclear riboprotein factor 55K	10748250	10746350	6380
CG10228	51C5-51C7	Pcf11	10758575	10748661	6380
CG10240	51C7-51D1	Cyp6a22	10760970	10759178	6380
CG10241	51D1-51D1	Cyp6a17	10763063	10761459	6380
CG10242	51D1-51D1	Cyp6a23	10765159	10763338	6380
CG10243	51D1-51D1	Cyp6a19	10767257	10765293	6380
CG10246	51D1-51D1	Cytochrome P450-6a9	10768877	10766861	6380
CG10245	51D1-51D1	Cyp6a20	10771551	10769625	6380
CG10247	51D1-51D1	Cyp6a21	10774456	10772769	6380
CG10248	51D1-51D1	Cytochrome P450-6a8	10776514	10774676	6380
CG17453	51D2-51D2	Cyp317a1	10788556	10787000	6380
CG10249	51D2-51D2	-	10815585	10788975	6380
CG12853	51D3-51D3	-	10821418	10821020	6380
CG10253	51D3-51D3	-	10822366	10817588	6380
CG10255	51D4-51D4	Lap1	10827807	10823182	6380
CG10257	51D5-51D5	-	10831974	10830116	6380
CG42783	51D5-51D5	atypical protein kinase C	10850451	10831963	6380

CG12424	51D6-51D6	-	10868089	10850819	6380	
CG7761	51D6-51D7	parcas	10878841	10868782	6380	
CR30241	51D7-51D7	transfer RNA:CR30241	10871913	10871832		
CG7639	51D7-51D7	-	10879728	10875170		
CG10265	51D7-51D7	-	10881336	10879837		
CG43101	51D8-51D8	-	10901004	10900604		
CG30473	51D8-51D8	Odorant-binding protein 51a	10912344	10911880		
CG7449	51D8-51D8	hibris	10928901	10898903		
CG33467	51D9-51D9	-	10943746	10943008		
CG8095	51E10-51E11	scab	11146003	11136290		
CG16827	51E11-51E11	alphaPS4	11150371	11146272		
CG34123	51E11-51F2	-	11180386	11150309		
CG11798	51E1-51E2	charlatan	11032288	11002762		
CG34186	51E2-51E2	Rpb12	11033003	11032473		
CG8089	51E2-51E2	-	11035329	11033330		
CG7544	51E2-51E2	-	11037214	11035382		
CG18285	51E3-51E5	igloo	11077797	11042944		
CG43068	51E5-51E5	-	11073408	11072663		
CG42476	51E5-51E5	Seminal fluid protein 51E	11080733	11080133		
CG8090	51E5-51E5	-	11088681	11086570		
CG42391	51E5-51E5	-	11090492	11089698		
CG11807	51E5-51E5	-	11091971	11089029		
CR12953	51E5-51E5	Ionotropic receptor 51a	11093839	11092159		
CG8092	51E5-51E7	relative of woc	11101137	11094028		
CG30081	51E6-51E7	Ionotropic receptor 51b	11097291	11095498		
CG33466	51E7-51E10	Follistatin	11129084	11111061		
CG8093	51E7-51E7	-	11103191	11101786		
CG11808	51E7-51E7	-	11104575	11103716		
CG12954	51E7-51E7	mitochondrial ribosomal protein L41	11105118	11104529		
CG8094	51E7-51E7	Hexokinase C	11107917	11106342		
CG8079	51E7-51E7	-	11111329	11105886		
CG8169	51F11-51F11	Pms2	11259021	11255577		
CR43276	51F11-51F11	-	11261255	11260745		
CR43275	51F11-51F11	-	11262226	11261395		
CR43105	51F11-51F11	-	11263204	11262351		
CR43186	51F11-51F11	-	11263986	11263339		
CG8171	51F11-51F11	double parked	11268465	11264124		
CG8174	51F11-51F12	SRPK	11275362	11268223		
CG34187	51F2-51F3	-	11182593	11180439		
CG8102	51F3-51F4	-	11185834	11184269		
CG8152	51F4-51F4	-	11198634	11197436		
CG8153	51F4-51F5	mutagen-sensitive 210	11205347	11198991		
CG8155	51F5-51F6	-	11209674	11205349		

CG8156	51F6-51F6	ADP ribosylation factor 51F	11212399	11209979		
CG8157	51F6-51F6	-	11213888	11213338		
CG8160	51F6-51F7	-	11215770	11214638		
CG16801	51F7-51F7	Hormone receptor 51	11226825	11219106		
CG8166	51F9-51F11	unc-5	11255807	11237659		
CG30471	52A10-52A10	-	11425155	11422700	3517	
CG30467	52A10-52A10	-	11427520	11425718	3517	
CG8187	52A10-52A10	-	11428840	11427057	3517	
CG8186	52A10-52A10	Vacuolar H[+] ATPase subunit 36-1	11430003	11428922	3517	
CG8190	52A10-52A10	eIF2B-gamma	11431922	11430175	3517	
CG8192	52A10-52A10	-	11437485	11431820	3517	
CG12963	52A11-52A12	-	11449941	11443303	3517	
CG8195	52A12-52A13	-	11453291	11450201	3517	
CG8200	52A13-52A13	flotillin	11456907	11453772	3517	
CG8203	52A13-52A13	Cyclin-dependent kinase 5	11458918	11457035	3517	
CG30466	52A13-52A13	-	11460676	11458973	3517	
CG8204	52A13-52A13	-	11461496	11460641	3517	
CG8175	52A1-52A1	Metchnikowin	11296621	11296351	3517	
CG30472	52A1-52A1	-	11311597	11310693	3517	
CG34188	52A1-52A1	-	11315528	11314596	3517	
CG43223	52A3-52A4	-	11351351	11297677	3517	
CG34318	52A3-52A4	-	11358596	11346436	3517	
CG8179	52A3-52A4	-	11358613	11346436	3517	
CG8180	52A4-52A4	-	11370338	11359970	3517	
CG12964	52A4-52A6	-	11384712	11373457	3517	
CG8183	52A6-52A10	Kinesin-73	11419743	11403283	3517	
CG12960	52A6-52A6	Ionotropic receptor 52a	11388936	11387137	3517	
CG30469	52A6-52A6	Ionotropic receptor 52b	11391115	11389325	3517	
CG30468	52A6-52A6	Ionotropic receptor 52c	11393505	11391706	3517	
CG30464	52A6-52A6	Ionotropic receptor 52d	11395871	11394087	3517	
CG8182	52A6-52A6	GalNAc-T1	11403102	11399218	3517	
CG42524	52B2-52B3	-	11537815	11501607	3517	
CR42945	52B3-52B3	mir-278 stem loop	11544668	11544571	3517	
CG8205	52B3-52B5	fusilli	11564198	11544823	3517	
CG8210	52B5-52B2	Vacuolar H[+] ATPase subunit 14-1	11567585	11566931	3517	
CG8207	52B5-52B5	-	11566444	11564723	3517	
CG30091	52B5-52B5	-	11569908	11568076	3517	
CG30082	52B5-52B5	-	11573587	11572509	3517	
CG33139	52B5-52B5	Ranbp11	11574925	11570221	3517	
CG8214	52B5-52C1	-	11576490	11574893	3517	
CG30090	52C1-52C1	-	11578519	11577348	3517	
CG30088	52C1-52C1	-	11579680	11578657	3517	
CG30087	52C1-52C1	-	11581256	11579953	3517	

CG33460	52C1-52C1	-	11582737	11581597	3517		
CG33461	52C1-52C1	-	11583983	11582891	3517		
CG33462	52C1-52C1	-	11585515	11584309	3517		
CG30080	52C1-52C1	-	11589199	11586231	3517		
CG42662	52C1-52C1	-	11589199	11586231	3517		
CG30083	52C2-52C2	-	11600149	11599102	3517		
CG30089	52C2-52C4	-	11649549	11614903	3517		
CG30084	52C4-52C7	Z band alternatively spliced PDZ-motif protein 52	11704314	11650070	3517		
CG33465	52C7-52C7	-	11708600	11706619	3517		
CG8246	52C7-52C7	Pox neuro	11722280	11714198	3517		
CG8249	52C8-52C8	-	11734865	11731595	3517		
CG8253	52C8-52C8	tungus	11741092	11736111	3517		
CG12970	52C8-52C8	-	11745027	11743466	3517		
CG8256	52C8-52C8	Glycerophosphate oxidase-1	11750251	11745256	3517		
CG30085	52C8-52C8	-	11756650	11751809	3517		
CG33464	52C9-52C9	-	11760649	11758924	3517		
CG8355	52C9-52D2	slit	11809623	11760176	3517		
CG8370	52D11-52D12	-	11894413	11888628	3517		
CG8386	52D12-52D12	-	11895160	11894396	3517		
CG8388	52D12-52D13	-	11898850	11896906	3517		
CG8389	52D12-52D13	-	11901329	11895877	3517		
CG8392	52D13-52D14	Proteasome beta1 subunit	11902285	11901309	3517		
CG8395	52D14-52D14	Rrp42	11903559	11902483	3517		
CG8397	52D14-52D14	-	11904679	11903546	3517		
CG8399	52D14-52D14	-	11912139	11905244	3517		
CG8400	52D14-52D15	caspar	11915666	11912133	3517		
CG33463	52D1-52D1	-	11783932	11783334	3517		
CG8401	52D15-52D15	-	11917596	11916108	3517		
CG8403	52D15-52E1	SP2353	11933760	11919465	3517		
CG8291	52D2-52D2	bedraggled	11819434	11810545	3517		
CG8293	52D2-52D2	Inhibitor of apoptosis 2	11822330	11819675	3517		
CG8297	52D2-52D2	-	11823443	11822373	3517		
CG8295	52D2-52D3	Myelodysplasia/myeloid leukemia factor	11827578	11823398	3517		
CG8299	52D3-52D3	-	11828988	11828206	3517		
CG30093	52D3-52D4	-	11832072	11831548	3517		
CG8302	52D3-52D4	Cyp4aa1	11834772	11830386	3517		
CG18255	52D4-52D9	Stretchin-Mlck	11873458	11834431	3517		
CG8366	52D6-52D6	-	11844143	11842547	3517		
CG8320	52D9-52D10	-	11881212	11879915	3517		
CG8322	52D9-52D11	ATP citrate lyase	11888765	11879931	3517		
CG15699	52D9-52D9	-	11875349	11875071	3517		
CG8314	52D9-52D9	-	11878787	11877188	3517		
CG8315	52D9-52D9	-	11879856	11878872	3517		

CG30094	52E10-52E11	-	12030443	12029737	3517		3520		
CG8431	52E11-52E11	Cysteinyl-tRNA synthetase	12033415	12030655	3517		3520		
CG10731	52E11-52E11	-	12037121	12033411	3517		3520		
CG8433	52E11-52E11	Ext2	12037121	12033411	3517		3520		
CG8405	52E1-52E1	-	11946972	11935177	3517		3520		
CR43012	52E1-52E1	mir-137 stem loop	11952849	11952759	3517		3520		
CG18250	52E2-52E4	Dystroglycan	11986045	11968681	3517		3520		
CG34147	52E4-52E4	mitochondrial ribosomal protein L34	11986842	11986498	3517		3520		
CG8414	52E4-52E5	-	11990108	11986811	3517		3520		
CG8416	52E5-52E5	Rho1	11994734	11990191	3517	3176	3520		
CG8418	52E5-52E5	Ras which interacts with Calmodulin	11997520	11994945	3517		3520		
CG8421	52E5-52E5	Aspartyl beta-hydroxylase	12004501	11997990	3517		3520		
CG8424	52E5-52E5	Juvenile hormone esterase duplication	12006654	12004616	3517		3520		
CG8425	52E5-52E5	Juvenile hormone esterase	12010278	12007311	3517		3520		
CG30095	52E5-52E5	-	12012082	12010989	3517		3520		
CG8428	52E6-52E	spinster	12025743	12012488	3517		3520		
CG8430	52E7-52E10	Glutamate oxaloacetate transaminase 1	12029439	12025857	3517		3520		
CR30238	52F11-52F11	transfer RNA:CR30238	12106950	12106879	3517		3520		
CR30239	52F11-52F11	transfer RNA:CR30239	12107214	12107143	3517		3520		
CR30240	52F11-52F11	transfer RNA:CR30240	12107628	12107557	3517		3520		
CG7798	52F11-52F11	-	12110132	12109686	3517		3520		
CG3666	52F11-52F11	Transferrin 3	12117379	12114031	3517		3520		
CG15706	52F11-52F11	-	12118189	12110719	3517		3520		
CG15701	52F11-53A1	-	12121591	12117722	3517		3520		
CG10734	52F1-52F1	-	12046299	12044772	3517		3520		
CG8434	52F2-52F3	lambik	12057024	12037628	3517		3520		
CG8435	52F3-52F3	-	12058365	12057105	3517		3520		
CG18243	52F3-52F4	Ptp52F	12065812	12058747	3517		3520		
CG8440	52F4-52F5	Lissencephaly-1	12072608	12066309	3517		3520		
CG8441	52F5-52F5	-	12074011	12072627	3517		3520		
CG8443	52F5-52F7	clueless	12081754	12074090	3517		3520		
CG8445	52F7-52F7	calypso	12083807	12081562	3517		3520		
CG42837	52F7-52F8	-	12086883	12084553	3517		3520		
CG8446	52F7-52F8	-	12086883	12083891	3517		3520		
CG8448	52F8-52F11	mrj	12109308	12090834	3517		3520		
CG18247	52F8-52F8	SH2 ankyrin repeat kinase	12090388	12086931	3517		3520		
CR30237	52F9-52F9	transfer RNA:CR30237	12095211	12095140			3521		
CG7786	53A1-53A1	-	12122441	12121863			3520		
CG3687	53A1-53A1	-	12124986	12124277			3520		
CG15707	53A1-53A1	krimper	12128222	12125608			3520		
CG15708	53A1-53A1	-	12129439	12128441			3520		
CG42701	53A2-53A2	Cyclic-nucleotide-gated ion channel protein	12147000	12130650			3520		
CG7773	53A2-53A3	fidipidine	12152126	12149789			3520		

CG3730	53A3-53A3	capsuleen	12154464	12152180	3520		
CG7765	53A3-53A4	Kinesin heavy chain	12159483	12154465	3520		
CG33017	53A4-53A4	-	12164840	12159817	3520		
CG7760	53A4-53A4	cousin of atonal	12165863	12165294	3520		
CG15704	53A4-53A4	-	12167975	12167519	3520		
CG15705	53A5-53A5	-	12169134	12168455	3520		
CG7755	53A5-53A5	-	12170451	12169135	3520		
CG9068	53A5-53B1	-	12174955	12170940	3520		
CG30324	53B1-53B1	-	12175738	12175091	3520		
CG30099	53B1-53B1	-	12176474	12175713	3520		
CG3767	53B1-53B1	Juvenile hormone-inducible protein 26	12178838	12176830	3520		
CG30100	53B1-53B1	-	12179774	12178958	3520		
CG42372	53B1-53B1	-	12179774	12178958	3520		
CG7747	53B1-53B1	-	12181631	12179769	3520		
CG3615	53B1-53B2	Autophagy-specific gene 9	12184737	12181903	3520		
CG43265	53B2-53B2	-	12186099	12185359	3520		
CG34399	53B3-53B4	NADPH oxidase	12203725	12197072	3520		
CG8060	53B4-53B4	-	12208222	12203817	3520		
CG30096	53B4-53B5	-	12209577	12208320	3520		
CG4282	53B5-53B5	-	12212306	12209693	3520		
CG8048	53B5-53C1	Vacuolar H[+] ATPase 44kD C subunit	12224142	12212318	3520		
CG5065	53C11-53C12	-	12512223	12495175			
CG8250	53C12-53C13	Alk	12525279	12513590			
CG18471	53C13-53C14	gprs	12536284	12528745			
CG8221	53C14-53C14	Amyrel	12540204	12538597			
CG8178	53C14-53C14	Nach	12542551	12540710			
CG4311	53C1-53C1	HMG Coenzyme A synthase	12228760	12223595	3520		
CG7997	53C1-53C1	-	12231684	12228756	3520		
CG6251	53C1-53C1	Nucleoporin 62	12233333	12231882	3520		
CG7989	53C1-53C1	wicked	12235003	12233343	3520		
CG15710	53C1-53C1	-	12236032	12235119	3520		
CG8098	53C15-53D1	Picot	12555183	12542820			
CG30098	53C2-53C2	-	12242720	12241729			
CG6262	53C2-53C2	-	12251029	12247235			
CG15711	53C2-53C2	-	12251812	12251056			
CG43187	53C3-53C3	-	12268657	12268063			
CG7964	53C4-53C4	Malic enzyme like-1	12306903	12302320			
CG7969	53C4-53C4	Malic enzyme like-2	12306903	12302320			
CG33960	53C4-53C4	-	12318273	12274053			
CG4398	53C4-53C4	-	12320682	12319678			
CG7848	53C4-53C4	-	12323459	12321353			
CG4409	53C4-53C4	-	12332350	12330741			
CG15925	53C4-53C5	-	12335019	12333491			

CG33550	53C5-53C5	Chemosensory protein B 53a	12355027	12354214
CG33524	53C5-53C5	Chemosensory protein B 53b	12356439	12355714
CG15712	53C6-53C6	-	12373057	12372346
CG33458	53C6-53C6	-	12375306	12374179
CG33459	53C6-53C6	-	12376687	12375558
CG4439	53C6-53C6	-	12380738	12378605
CG7813	53C6-53C6	-	12386934	12384394
CG4700	53C6-53C7	Sema-2a	12420934	12387701
CG4905	53C7-53C7	Syntrophin-like 2	12445991	12439765
CG8380	53C7-53C8	Dopamine transporter	12452763	12446072
CG4945	53C8-53C8	-	12457625	12453552
CG8332	53C8-53C8	Ribosomal protein S15	12458756	12457618
CG4927	53C8-53C8	-	12461659	12459604
CG8317	53C8-53C8	-	12464087	12462084
CG4750	53C9-53C10	loopin-1	12424591	12422455
CG8303	53C9-53C10	-	12492716	12482533
CG5072	53C9-53C9	Cyclin-dependent kinase 4	12472953	12466981
CG4918	53C9-53C9	Ribosomal protein LP2	12474237	12473599
CG8311	53C9-53C9	-	12476686	12474550
CG8306	53C9-53C9	-	12482218	12477023
CG5089	53C9-53C9	-	12487916	12486253
CG5550	53D10-53D10	-	12705086	12704096
CG34459	53D11-53D11	-	12714153	12713037
CG34460	53D11-53D11	-	12715310	12714402
CR42988	53D11-53D11	mir-8 stem loop	12719023	12718937
CG8652	53D12-53D12	UDP-glycosyltransferase 37c1	12732392	12730935
CG5859	53D13-53D13	-	12741606	12737963
CG8648	53D13-53D14	Flap endonuclease 1	12742843	12741482
CG5935	53D14-53D14	Dek	12747861	12743726
CG8912	53D14-53D14	P-element somatic inhibitor	12755218	12750470
CG6341	53D14-53D14	Elongation factor 1 beta	12756681	12755698
CG6426	53D14-53D14	-	12759359	12756897
CG34457	53D1-53D1	-	12559341	12557831
CG34458	53D1-53D1	-	12560330	12559557
CG30463	53D1-53D4	-	12618889	12560966
CG6421	53D15-53D15	-	12760413	12759755
CG6429	53D15-53D15	-	12761266	12760522
CG6435	53D15-53D15	-	12762453	12761284
CG6472	53D15-53E1	-	12772005	12767778
CG8910	53D15-53E1	-	12783156	12762229
CG5210	53D2-53D2	-	12581260	12579203
CG43104	53D5-53D5	-	12625355	12624316
CG42477	53D5-53D5	Seminal fluid protein 53D	12632609	12632055

CG15617	53D5-53D5	-	12634067	12632728			
CG8626	53D5-53D5	Acp53C14a	12636077	12635565			
CG15616	53D6-53D6	Acp53C14b	12636952	12636411			
CG8622	53D6-53D6	Accessory gland-specific peptide 53Ea	12637827	12637308			
CG33530	53D6-53D6	Acp53C14c	12638974	12638281			
CG34189	53D6-53D6	-	12642380	12642012			
CG5267	53D6-53D6	-	12643328	12642606			
CG8566	53D6-53D7	unc-104	12660002	12639008			
CG42392	53D7-53D7	-	12653433	12652866			
CG5348	53D7-53D7	-	12656743	12654342			
CG8905	53D8-53D8	Superoxide dismutase 2 (Mn)	12661440	12660376			
CG5409	53D8-53D8	Actin-related protein 53D	12663179	12661811			
CG33544	53D8-53D8	Vitamin-K epoxide reductase	12666499	12665870			
CG15920	53D8-53D8	resilin	12670676	12667410			
CG5522	53D8-53D9	-	12679981	12671196			
CG15919	53D9-53D9	-	12680585	12680162			
CG15615	53D9-53D9	-	12683912	12680621			
CG43327	53E10-53E11	-	12921432	12919992			
CG43328	53E10-53E11	-	12921432	12919992			
CG43371	53E11-53E11	-	12922017	12921589			
CR43014	53E1-53E1	mir-990 stem loop	12782813	12782728	6404		
CG6518	53E1-53E1	inactivation no afterpotential C	12789083	12786088	6404		
CG6622	53E2-53E2	Protein C kinase 53E	12830668	12812430	6404		
CG34190	53E2-53E2	-	12835018	12834710	6404		
CG9013	53E2-53E2	Vacuolar H[+] ATPase subunit 16-4	12835729	12835163	6404		
CG15614	53E2-53E2	-	12836060	12833060	6404		
CG34191	53E2-53E2	-	12840086	12839510	6404		
CG34415	53E2-53E2	muscle wasted	12842770	12835802	6404		
CG6657	53E2-53E2	vegetable	12844826	12842969	6404		
CG6665	53E2-53E3	-	12846436	12845007	6404		
CG9010	53E3-53E3	-	12847652	12846448	6404		
CR30236	53E3-53E3	transfer RNA:gly3:53E	12855583	12855513	6405		
CG6702	53E4-53E4	Calbindin 53E	12883566	12861465	6404		
CG30461	53E4-53E4	-	12886099	12883494	6404		
CG9002	53E4-53E4	ste24c prenyl protease type I	12886099	12883498	6404		
CG9001	53E4-53E4	ste24b prenyl protease type I	12887631	12886115	6404		
CG9000	53E4-53E4	prenyl protease type I	12889431	12887745	6404		
CG6796	53E4-53E4	-	12891107	12889519	6404		
CG8980	53E4-53E4	Nuclear inhibitor of Protein phosphatase 1	12892658	12891068	6404		
CG6805	53E4-53E4	-	12895006	12892958	6404		
CG15609	53E4-53E4	-	12903391	12895411	6404		
CG8963	53E4-53E4	-	12907057	12903851	6404		
CG6829	53E4-53E4	Apaf-1-related-killer	12914208	12907549	6404		

CG9635	53E4-53F1	RhoGEF2	12932158	12914746	6404	
CG15611	53F10-53F11	-	13001866	12996352	6404	
CG18730	53F12-53F12	Amylase proximal	13007808	13006211		
CG10956	53F12-53F12	Serpin 53F	13011742	13010398		
CG17876	53F12-53F12	Amylase distal	13013887	13012267		
CG15605	53F12-53F12	-	13014528	13013912		
CG15918	53F13-53F13	Chitin deacetylase-like 9	13017839	13016338		
CG9640	53F1-53F1	-	12934273	12932461	6404	
CG9642	53F1-53F2	-	12936012	12934350	6404	
CG9646	53F2-53F2	-	12941360	12936380	6404	
CG6953	53F2-53F3	fat-spondin	12946810	12941508	6404	
CG8961	53F2-53F5	teflon	12944329	12942048	6404	
CG8950	53F3-53F4	-	12950139	12947213	6404	
CG6967	53F4-53F4	-	12954051	12950282	6404	
CG30460	53F4-53F6	-	12974747	12953476	6404	
CG8946	53F6-53F7	Sphingosine-1-phosphate lyase	12979462	12975939	6404	
CG6984	53F7-53F7	-	12980575	12979515	6404	
CG8938	53F7-53F8	Glutathione S transferase S1	12984935	12980758	6404	
CG30456	53F8-53F9	-	12995047	12990372	6404	
CG34098	54A1-54A1	Acp54A1	13021255	13020963		
CG11400	54A1-54A1	-	13022357	13021662		
CG15917	54A1-54A1	-	13024408	13023962		
CG11395	54A1-54A1	-	13026337	13024746		
CG43103	54A1-54A1	-	13027430	13026956		
CG43107	54A1-54A1	-	13028384	13028000		
CR33921	54A2-54A2	snoRNA:U3:54Aa	13031198	13031026		
CR30234	54A2-54A2	transfer RNA:CR30234	13031551	13031470		
CR30235	54A2-54A2	transfer RNA:CR30235	13032886	13032805		
CR33628	54A2-54A2	snoRNA:U3:54Ab	13033331	13033159		
CG17290	54A2-54A2	-	13042815	13042204		
CG17287	54A2-54A2	-	13045821	13044039		
CG30458	54A2-54A2	-	13046536	13045830		
CG30457	54A2-54A2	-	13048330	13047659		
CG10953	54A2-54A2	-	13054006	13052966		
CG10950	54A2-54A2	-	13084664	13082708		
CG43237	54A3-54A3	-	13093248	13092713		
CG33197	54A-54A	muscleblind	13266470	13153058		
CG18467	54B14-54B15	-	13329994	13328109		
CG18469	54B1-54B1	-	13133782	13133274		
CG12699	54B1-54B1	-	13134888	13134035		
CG43272	54B1-54B1	-	13143242	13142746		
CG43108	54B1-54B1	-	13145391	13144661		
CG6536	54B15-54B15	methuselah-like 4	13334988	13332688		

CG6530	54B16-54B16	methuselah-like 3	13340099	13336038		5574	
CG10764	54B16-54B16	-	13343234	13340924		5574	
CG34192	54B16-54B16	-	13343666	13343269		5574	
CG10751	54B16-54B16	roadblock	13344634	13343979		5574	
CG14478	54B16-54B16	-	13353085	13345186		5574	
CG6522	54B16-54B16	-	13356681	13353384		5574	
CG4816	54B16-54B16	quaking related 54B	13362153	13357131		5574	
CG6520	54B16-54B16	-	13363566	13362719		5574	
CG4827	54B16-54B17	veil	13369633	13366629	5680	5574	
CG43110	54B17-54B17	-	13371531	13369501	5680		
CG30104	54B17-54B17	-	13380680	13372502	5680		
CG30103	54B17-54B17	-	13383504	13381267	5680		
CG43164	54B18-54C1	-	13396150	13389862	5680		
CR30232	54B5-54B5	transfer RNA:CR30232	13279350	13279279	5681		
CR30233	54B5-54B5	transfer RNA:his:56E	13279791	13279720	5682		
CG10939	54B6-54B7	SRY interacting protein 1	13292678	13282101	5680		
CG6542	54B7-54B15	Egg-derived tyrosine phosphatase	13332443	13319615	5680		
CG6568	54B7-54B7	-	13294930	13292809	5680		
CG30101	54B7-54B7	-	13297705	13295763	5680		
CG10938	54B7-54B7	Proteasome alpha5 subunit	13301274	13300269	5680		
CG6556	54B7-54B7	connector enhancer of ksr	13307104	13301476	5680		
CG4798	54B7-54B7	lethal (2) k01209	13313192	13307938	5680		
CG6550	54B7-54B7	-	13314984	13313168	5680		
CG4802	54B7-54B7	-	13316816	13315225	5680		
CG6546	54B7-54B7	Brahma associated protein 55kD	13318440	13316854	5680		
CG18468	54B7-54B7	Lethal hybrid rescue	13319728	13318556	5680		
CG6493	54C10-54C10	Dicer-2	13469011	13462484			
CG6484	54C10-54C10	-	13471514	13469512			
CG14483	54C11-54C11	-	13473659	13473140			
CG6477	54C11-54C12	RhoGAP54D	13478387	13473930			
CG4924	54C12-54C12	icln	13479386	13478471			
CG30105	54C12-54C12	-	13479999	13479309			
CG11423	54C12-54C12	-	13484914	13482772			
CG42649	54C12-54C12	-	13487112	13486645			
CG4943	54C12-54D1	lethal with a checkpoint kinase	13491489	13480319			
CG34193	54C1-54C1	-	13398303	13397449	5680		
CG4847	54C1-54C1	-	13401364	13399028	5680		
CG4853	54C1-54C1	-	13404950	13401710	5680		
CG11419	54C1-54C1	Anaphase promoting complex subunit 10	13405688	13404766	5680		
CG4866	54C1-54C1	-	13406577	13405728	5680		
CG33130	54C1-54C3	short spindle 4	13422942	13406523	5680		
CG4878	54C3-54C3	eIF3-S9	13426647	13423718	5680		
CG43370	54C3-54C3	-	13431858	13426827			

CG34194	54C3-54C3	-	13432555	13431833	5680	
CG4886	54C3-54C3	cyclophilin-33	13433906	13432397	5680	
CG6510	54C3-54C3	Ribosomal protein L18A	13434999	13433895	5680	
CG4903	54C3-54C5	Misexpression suppressor of ras 4	13443644	13435329		
CG43323	54C5-54C8	Kinesin-like protein at 54D	13450790	13444560		
CG43324	54C8-54C8	-	13451570	13451111		
CG14480	54C8-54C8	-	13453357	13451845		
CG6501	54C8-54C9	nucleostemin 2	13455950	13453284		
CG4921	54C9-54C10	Rab-protein 4	13462484	13460579		
CG4909	54C9-54C9	Plenty of SH3s	13459827	13456243		
CG14482	54C9-54C9	-	13460259	13459837		
CG42239	54C9-54C9	-	13460984	13460335		
CR30333	54D1-54D1	transfer RNA:CR30333	13492112	13492040		
CR30231	54D1-54D1	transfer RNA:CR30231	13492348	13492276		
CR34543	54D1-54D1	snoRNA:Or-aca4	13504422	13504261		
CG10936	54D1-54D2	-	13526639	13492456		
CG10683	54D2-54D2	rhino	13521018	13515994		
CG18186	54D2-54D2	-	13521680	13521302		
CG30106	54D3-54D3	CCHamide-1 receptor	13541801	13535037		
CG4954	54D4-54D4	eIF3-S8	13556749	13553183		
CG30108	54D4-54D4	-	13557505	13556905		
CG30109	54D4-54D4	-	13558253	13556910		
CG6459	54D4-54D4	-	13560148	13558814		
CG6446	54D4-54D5	Sema-1b	13571000	13560344		
CG42561	54D5-54D5	-	13573053	13572223		
CG42562	54D5-54D5	-	13573915	13573348		
CG4966	54D5-54D5	Hermansky-Pudlak Syndrome 4 ortholog	13578327	13571102		
CG14485	54D5-54D6	swi2	13582856	13577779		
CG17818	54D6-54D6	rdgBbeta	13585866	13583281		
CR32887	54D6-54D6	-	13586781	13586713		
CR32888	54D6-54D6	-	13587293	13587207		
CR32889	54D6-54D6	-	13587509	13587437		
CR32890	54D6-54D6	snoRNA:U29:54Eb	13587810	13587725		
CR32894	54D6-54D6	snoRNA:U29:54Ec	13588064	13587977		
CR32891	54D6-54D6	snoRNA:U76:54Eb	13588318	13588246		
CR32895	54D6-54D6	snoRNA:U29:54Ed	13588567	13588481		
CR32892	54D6-54D6	snoRNA:U27:54Ea	13588802	13588734		
CR32893	54D6-54E1	-	13589028	13588952	3064	
CR32886	54D6-54E1	U snoRNA host gene 1	13590827	13586602	3064	
CG42311	54E10-54F1	grainy head	13729584	13690294	3064	
CR32896	54E1-54E1	snoRNA:snR38:54Eb	13589269	13589194	3064	
CR32897	54E1-54E1	snoRNA:U31:54Eb	13589507	13589441	3064	
CR32898	54E1-54E1	snoRNA:U31:54Ec	13589743	13589677	3064	

CR32899	54E1-54E1	snoRNA:U31:54Ed	13589982	13589916	3064		
CR32900	54E1-54E1	snoRNA:U27:54Eb	13590213	13590142	3064		
CR32901	54E1-54E1	snoRNA:snR38:54Ec	13590454	13590378	3064		
CR32902	54E1-54E1	-	13590673	13590607	3064		
CG6424	54E1-54E1	-	13606832	13590840	3064		
CG10934	54E1-54E2	-	13610886	13609844	3064		
CG10933	54E2-54E2	-	13612561	13610818	3064		
CG6410	54E2-54E2	-	13614305	13612535	3064		
CG4975	54E2-54E4	-	13620492	13614443	3064		
CG4984	54E2-54E4	-	13620492	13614477	3064		
CG34195	54E4-54E4	-	13621988	13620760	3064		
CG6406	54E4-54E4	-	13624769	13621924	3064		
CG6401	54E4-54E5	-	13627162	13625357	3064		
CG4996	54E5-54E7	-	13631480	13627398	3064		
CG14487	54E7-54E7	Ionotropic receptor 54a	13633366	13631606	3064		
CG12298	54E7-54E7	subito	13635616	13633000	3064		
CG10931	54E7-54E8	-	13637644	13636440	3064		
CG5002	54E8-54E8	-	13640719	13637803	3064		
CG6385	54E8-54E8	-	13643923	13641052	3064		
CG5005	54E8-54E8	HLH54F	13648022	13644922	3064		
CG5009	54E8-54E8	-	13652065	13648438	3064		
CG6370	54E8-54E8	-	13654712	13652077	3064		
CG14488	54E8-54E8	-	13655263	13654670	3064		
CG18635	54E8-54E8	-	13657411	13655313	3064		
CG6362	54E8-54E8	-	13660057	13657910	3064		
CG33981	54E9-54E9	-	13669417	13661469	3064		
CG6355	54E9-54E9	-	13669417	13661469	3064		
CR42964	54E9-54E9	mir-31a stem loop	13671391	13671300	3064		
CG5032	54E9-54E9	adrift	13676072	13673642	3064		
CG5788	54E9-54E9	Ubiquitin conjugating enzyme 10	13676914	13675912	3064		
CG5033	54E9-54E9	-	13679953	13677197	3064		
CG5036	54E9-54E9	-	13685633	13680387	3064		
CG14489	54F1-54F1	olf186-M	13735949	13734206	3064		
CG30323	54F1-54F1	-	13741766	13740846	3064		
CG11430	54F1-54F3	olf186-F	13748075	13730950	3064		
CG14490	54F3-54F3	-	13749018	13748304	3064		
CG5785	54F3-54F4	three rows	13753397	13748998	3064		
CG5784	54F4-54F4	Mapmodulin	13759515	13753827	3064		
CG5076	54F4-55A2	eag-like K[+] channel	13813097	13761452	3064		
CG30325	54F5-54F5	-	13767362	13765110	3064		
CG30110	54F5-54F5	-	13769719	13767812	3064		
CG42639	54F6-54F6	prophenol oxidase A1	13777477	13774718	3064		
CG14492	55A1-55A1	-	13781847	13781187	3064		

CG14491	55A1-55A1	-	13783083	13782583	3064		
CG10930	55A2-55A2	Protein phosphatase Y at 55A	13844075	13842900	3064		
CG33996	55A3-55A3	dpr13	13895370	13862622	3064		
CG5733	55B10-55B11	Nucleoporin 75	14054634	14052193	3064		
CG42517	55B11-55B11	Mediator complex subunit 9	14055885	14054782	3064		
CG42518	55B11-55B11	-	14055885	14054732	3064		
CG5729	55B11-55B11	Dgp-1	14060112	14055913	3064		
CG10916	55B11-55B12	-	14062195	14061176	3064		
CG5726	55B12-55B12	-	14067674	14062783	3064		
CG5140	55B12-55B12	no poles	14070024	14068001	3064		
CG5721	55B12-55B12	-	14071618	14069934	3064		
CR14499	55B12-55B12	-	14075794	14075227	3064		
CG14500	55B12-55B12	-	14077159	14076484	3064		
CG33958	55B12-55B12	-	14080341	14071886	3064		
CG30114	55B12-55B12	-	14096483	14095260	3064		
CG5084	55B1-55B1	-	13907297	13906171	3064		
CG10910	55B1-55B1	-	13909911	13907754	3064		
CG5773	55B1-55B1	-	13931249	13930409	3064		
CG5770	55B1-55B1	-	13932565	13931551	3064		
CG5767	55B1-55B2	-	13934989	13933903	3064		
CG34005	55B2-55B2	-	13936417	13935617	3064		
CG14495	55B2-55B2	-	13937230	13936309	3064		
CG5765	55B2-55B2	Mucin 55B	13939610	13937731	3064		
CG10911	55B2-55B2	-	13941569	13940052	3064		
CG10912	55B2-55B2	-	13944564	13943568	3064		
CG34386	55B2-55B4	-	13981138	13950209	3064		
CG5757	55B4-55B4	-	13982212	13981233	3064		
CG5098	55B4-55B5	-	13988618	13982523	3064		
CG5756	55B5-55B5	-	13995891	13988555	3064		
CG34196	55B5-55B5	-	13997744	13997505	3064		
CG5753	55B5-55B7	staufen	14013337	14005401	3064		
CG10913	55B7-55B7	Serine protease inhibitor 6	14015715	14013810	3064		
CG12767	55B7-55B7	Dorsal interacting protein 3	14017751	14016005	3064		
CG5748	55B7-55B8	Heat shock factor	14022136	14017808	3064		
CG5109	55B8-55B8	Polycomblike	14026947	14022934	3064		
CG5119	55B8-55B9	polyA-binding protein	14033740	14027583	3064		
CG10915	55B9-55B10	-	14051719	14048222	3064		
CR34544	55B9-55B9	snoRNA:Psi18S-1347a	14030443	14030307	3064		
CR34545	55B9-55B9	snoRNA:Psi18S-1347b	14030647	14030505	3064		
CR33633	55B9-55B9	snoRNA:Psi18S-1347c	14030829	14030684	3064		
CG17680	55B9-55B9	-	14035499	14034802	3064		
CG5742	55B9-55B9	-	14038892	14035969	3064		
CG5124	55B9-55B9	adipose	14041565	14039209	3064		

CG5738	55B9-55B9	lola like	14045697	14042350	3064	
CG10914	55B9-55B9	-	14047815	14045772	3064	
CG30116	55C10-55D1	-	14385516	14344467		
CG10917	55C1-55C1	four-jointed	14123816	14120268	3064	
CG5581	55C2-55C2	Otefin	14164698	14163112		
CG33198	55C2-55C2	presenilin enhancer	14165658	14165031		
CG14502	55C2-55C2	-	14182217	14176593		
CG18536	55C2-55C2	-	14183163	14176597		
CG18537	55C2-55C2	-	14184138	14183450		
CG18538	55C2-55C2	-	14185256	14184575		
CG18539	55C2-55C2	-	14186506	14185683		
CG18540	55C2-55C2	-	14187539	14186963		
CG14505	55C2-55C2	-	14191482	14190450		
CG14503	55C2-55C2	Transport and Golgi organization 8	14199503	14199327		
CG5580	55C2-55C4	scribbler	14244766	14166570		
CG42736	55C4-55C4	-	14265301	14264992		
CG43202	55C4-55C4	-	14269349	14268914		
CG15066	55C4-55C4	Immune induced molecule 23	14270737	14270209		
CG18108	55C4-55C4	Immune induced molecule 1	14271883	14271457		
CG18107	55C4-55C4	-	14272416	14272070		
CG15067	55C4-55C4	-	14273093	14272417		
CG18106	55C4-55C4	Immune induced molecule 2	14274535	14274102		
CG16844	55C4-55C4	Immune induced molecule 3	14275995	14275625		
CG16836	55C4-55C4	-	14276963	14276600		
CG15065	55C4-55C4	-	14277752	14277463		
CG15068	55C4-55C4	-	14278114	14277847		
CG5154	55C4-55C6	Imaginal disc growth factor 5	14282787	14281170		
CG17522	55C6-55C6	Glutathione S transferase E10	14285031	14284143		
CG5164	55C6-55C6	Glutathione S transferase E1	14286728	14285898		
CG17523	55C6-55C7	Glutathione S transferase E2	14287880	14286998		
CG17524	55C7-55C7	Glutathione S transferase E3	14288972	14288222		
CG17525	55C7-55C7	Glutathione S transferase E4	14291591	14290780		
CG17527	55C7-55C7	Glutathione S transferase E5	14292843	14292125		
CG17530	55C7-55C7	Glutathione S transferase E6	14294266	14293518		
CG17531	55C7-55C7	Glutathione S transferase E7	14295193	14294425		
CG17533	55C7-55C8	Glutathione S transferase E8	14296067	14295339		
CG17534	55C8-55C8	Glutathione S transferase E9	14297340	14296516		
CG5576	55C8-55C8	immune deficiency	14299024	14297296		
CG5170	55C8-55C8	Dodeca-satellite-binding protein 1	14308629	14299511		
CG5174	55C8-55C9	-	14313732	14308915		
CG12263	55C9-55C9	-	14317838	14313935		
CG30118	55C9-55C9	-	14327986	14318031		
CG30120	55C9-55C9	-	14336925	14334075		

CG5189	55C9-55C9	-	14336925	14334075		
CG5190	55C9-55C9	-	14340241	14338773		
CG17669	55C9-55C9	-	14341967	14340242		
CG5186	55C9-56F12	scruin like at the midline	14333037	14328462		
CG5519	55D1-55C9	Prp19	14338545	14334860		
CG5224	55D1-55D1	-	14392349	14391115		
CG43066	55D1-55D1	-	14412922	14402081		
CG10924	55D1-55D2	-	14423263	14414937		
CG17725	55D3-55D3	Phosphoenolpyruvate carboxykinase	14426924	14424272		
CG34390	55D3-55D3	Rgk2	14436472	14427090		
CG30115	55D3-55E1	-	14499260	14441624		
CG15088	55E10-55E10	-	14617763	14615328		
CG33998	55E11-55E11	-	14626648	14625997		
CG30121	55E11-55E11	-	14629163	14626632		
CG18609	55E11-55E11	-	14631121	14630022		
CG17821	55E11-55E11	-	14632501	14631311		
CG42697	55E1-55E1	-	14500235	14499149		
CG10927	55E1-55E2	-	14501759	14500587		
CG5497	55E2-55E2	mitochondrial ribosomal protein S28	14502521	14501715		
CG5323	55E2-55E2	-	14503504	14502587		
CG5493	55E2-55E2	-	14505517	14504199		
CG5327	55E2-55E2	-	14505823	14503493		
CG5335	55E2-55E2	-	14510475	14509050		
CG5489	55E2-55E2	Autophagy-specific gene 7	14512553	14507961		
CG5341	55E2-55E2	sec6	14515249	14512772		
CG5345	55E2-55E2	Eip55E	14516784	14515399		
CG5482	55E2-55E3	-	14519403	14517420		
CG30122	55E3-55E3	-	14526773	14519833		
CR30227	55E3-55E3	transfer RNA:CR30227	14527133	14527062		
CR30228	55E3-55E3	transfer RNA:gly3:55E	14527301	14527231		
CG33724	55E3-55E3	Chemosensory protein A 56a	14528307	14527699		
CG5473	55E3-55E5	SP2637	14545706	14528476		
CG42306	55E5-55E5	-	14549053	14545920		
CG5469	55E5-55E5	GDI interacting protein 3	14549053	14545920		
CG33136	55E6-55E6	-	14553250	14552467	757	
CG15085	55E6-55E6	ETS-domain lacking	14561037	14555026	757	
CG15086	55E6-55E6	-	14574280	14566185	757	
CG42855	55E6-55E6	-	14576146	14574877	757	
CG15071	55E8-55E8	-	14584759	14584139	757	
CG42856	55E8-55E9	-	14593310	14575637	757	
CG15073	55E9-55E9	-	14595728	14593487	757	
CG15087	55E9-55E9	-	14598365	14595652	757	
CR33942	55E9-55E9	putative noncoding RNA 016:2R	14599457	14598896	757	

CG33147	55E9-55F1	Heparan sulfate 3-O sulfotransferase-A	14642026	14605634	757		
CR34651	55F11-55F11	-	14787042	14786934	757		
CG30329	55F11-55F11	Vacuolar H[+] ATPase subunit 100-3	14799219	14796505	757		
CG15077	55F1-55F1	Cyp12b2	14644588	14642500	757		
CG42351	55F1-55F1	-	14648577	14644579	757		
CG15078	55F1-55F2	Multiple C2 domain and transmembrane region protein	14662174	14649487	757		
CR30229	55F2-55F2	transfer RNA:CR30229	14657717	14657636	757		
CG15093	55F2-55F2	-	14664481	14663174	757		
CG15080	55F3-55F3	-	14682105	14670806	757		
CG15094	55F3-55F3	-	14684181	14682123	757		
CG15095	55F3-55F4	lethal (2) 08717	14691232	14684769	757		
CG15096	55F5-55F5	-	14702514	14695841	757		
CG15081	55F5-55F6	lethal (2) 03709	14709755	14706972	757		
CG15097	55F6-55F6	-	14717180	14709693	757		
CG15082	55F6-55F6	-	14720746	14718598	757		
CG15098	55F6-55F6	-	14722276	14720877	757		
CG15083	55F6-55F6	-	14724347	14722770	757		
CG15099	55F6-55F7	-	14733368	14724326	757		
CG15100	55F7-55F7	-	14738184	14734363	757		
CG15084	55F7-55F7	-	14739468	14738366	757		
CG18190	55F7-55F7	-	14740494	14739390	757		
CG15101	55F7-55F8	Juvenile hormone epoxide hydrolase 1	14742614	14740939	757		
CG15102	55F8-55F8	Juvenile hormone epoxide hydrolase 2	14745443	14743272	757		
CG15106	55F8-55F8	Juvenile hormone epoxide hydrolase 3	14749576	14747880	757		
CG43069	55F8-55F8	-	14750765	14750367	757		
CG43070	55F8-55F8	-	14752038	14751497	757		
CG43071	55F8-55F8	-	14752677	14752429	757		
CG12763	55F8-55F8	Diptericin	14753765	14753270	757		
CG10794	55F8-55F8	Diptericin B	14755400	14754895	757		
CG43109	55F8-55F8	-	14755672	14755351	757		
CG12758	55F8-56A1	serrano	14847000	14765899	757		
CG18608	56A2-56A2	proliferation disrupter	14858656	14856910	757		
CG15107	56A2-56A2	-	14859943	14858814	757		
CG15104	56A2-56A2	Topoisomerase I-interacting protein	14864767	14860449	757		
CG18605	56A2-56A2	-	14866784	14865040	757		
CG15105	56A2-56A3	another B-box affiliate	14896469	14874846	757		
CG43351	56B1-56B1	-	14917741	14917523	757		
CG15113	56B1-56B1	Serotonin receptor 1B	14920128	14909830	757		
CG15115	56B1-56B1	-	14923892	14922997	757		
CG15116	56B2-56B2	-	14943429	14942736	757		
CG15109	56B2-56B2	-	14948575	14946926	757		
CG16720	56B2-56B5	Serotonin receptor 1A	15009463	14954664	757		
CG30125	56B3-56B3	Ionotropic receptor 56a	14983679	14981772	757		

CG15117	56B5-56B5	-	15016746	15009735	757	
CG15110	56B5-56B5	brother of tout-velu	15021223	15017099	757	
CG15111	56B5-56B5	-	15028543	15024882	757	
CG15118	56B5-56B6	-	15031646	15021222	757	
CG15112	56B5-56C1	enabled	15050124	15029140	757	
CG9834	56C10-56C10	endophilin B	15198197	15194952		
CG9811	56C10-56C11	Rgk1	15212994	15199898		
CG30127	56C11-56D1	-	15218595	15213378		
CG10737	56C1-56C1	-	15065728	15051652	757	
CG7097	56C1-56C4	happyhour	15114705	15066259	757	
CG7137	56C4-56C4	-	15116118	15114835		
CG11949	56C4-56C4	coracle	15131256	15116570		
CG7225	56C4-56C4	windbeutel	15138419	15137266		
CG33454	56C4-56C4	-	15139171	15138532		
CG33453	56C5-56C5	-	15140690	15140050		
CG7229	56C6-56C6	-	15149744	15147419		
CG7230	56C6-56C6	ribbon	15168901	15163231		
CG11906	56C6-56C6	-	15171476	15168923		
CG10476	56C6-56C6	-	15172724	15172056		
CG10474	56C7-56C7	-	15174235	15172900		
CG18606	56C8-56C8	-	15176500	15175488		
CG18607	56C8-56C8	-	15177305	15176631		
CG11001	56C8-56C8	FK506-binding protein 2	15178467	15177610		
CG15119	56C8-56C8	Myb-interacting protein 40	15179708	15178610		
CG7417	56C8-56C9	TAK1-associated binding protein 2	15191529	15180073		
CG7461	56C9-56C10	-	15194689	15192668		
CG11242	56D11-56D12	-	15374340	15372999		
CG11237	56D12-56D12	Oseg6	15379241	15374549		
CG8432	56D13-56D13	Rab escort protein	15381630	15379596		
CG11228	56D13-56D13	hippo	15384372	15381802		
CG15120	56D13-56D14	-	15387877	15385259		
CG16926	56D14-56D14	-	15388823	15387800		
CG11007	56D14-56D14	-	15391773	15390563		
CR30223	56D14-56D14	transfer RNA:CR30223	15393915	15393844		
CG15121	56D15-56D15	Ionotropic receptor 56b	15396949	15395672		
CG15122	56D15-56D15	Ionotropic receptor 56c	15398976	15397273		
CG15904	56D15-56D15	Ionotropic receptor 56d	15401076	15399178		
CG43111	56D15-56D15	-	15440183	15439576		
CR33535	56D15-56D15	transfer RNA:CR33535	15452449	15452378		
CG9218	56D15-56E1	smooth	15519007	15417414		
CG34045	56D1-56D1	-	15222693	15218394		
CG9975	56D1-56D1	-	15233067	15229314		
CG11961	56D1-56D2	-	15249878	15245236		

CG10051	56D2-56D2	-	15254799	15251150
CG9416	56D2-56D2	-	15260747	15254746
CG10062	56D2-56D2	-	15267679	15263230
CG10073	56D2-56D2	-	15272470	15269121
CG10081	56D2-56D3	-	15276823	15273429
CG11257	56D3-56D3	-	15279405	15277633
CG17246	56D3-56D3	Succinate dehydrogenase A	15283477	15279368
CG10460	56D3-56D3	crammer	15284279	15283720
CG34197	56D3-56D3	-	15292897	15289403
CR30224	56D3-56D3	transfer RNA:ser4:56D	15302184	15302103
CR30225	56D3-56D3	transfer RNA:CR30225	15302422	15302350
CR30326	56D3-56D3	transfer RNA:CR30326	15302848	15302776
CG9325	56D3-56D5	hu li tai shao	15312454	15284840
CG7563	56D5-56D5	Calpain-A	15318068	15312578
CG10023	56D5-56D5	Focal Adhesion Kinase	15324774	15318164
CG7626	56D5-56D7	Spt5	15329403	15324991
CR34546	56D7-56D7	snoRNA:Psi28S-2444	15330761	15330632
CG7726	56D7-56D7	Ribosomal protein L11	15331014	15329854
CG7735	56D7-56D7	-	15332563	15331687
CG9291	56D7-56D7	Elongin C	15333797	15332590
CG9277	56D7-56D8	beta-Tubulin at 56D	15339122	15334824
CG7744	56D8-56D9	-	15343032	15340014
CG7753	56D9-56D9	meiotic W68	15347029	15343700
CG8201	56D9-57D12	par-1	15373193	15343679
CG42878	56E1-56E1	-	15475145	15474877
CG16716	56E1-56E1	-	15484371	15481295
CG42753	56E1-56E1	-	15523245	15522784
CG18367	56E1-56E1	-	15524905	15524165
CG43277	56E1-56E1	-	15525431	15525068
CG15124	56E1-56E1	-	15531203	15530452
CG15905	56E1-56E1	-	15535150	15533988
CG15125	56E1-56E1	-	15547163	15545263
CR42966	56E1-56E1	mir-6-3 stem loop	15548300	15548221
CR42954	56E1-56E1	mir-6-2 stem loop	15548447	15548374
CR43047	56E1-56E1	mir-6-1 stem loop	15548589	15548508
CR42952	56E1-56E1	mir-5 stem loop	15548731	15548663
CR42961	56E1-56E1	mir-4 stem loop	15548874	15548794
CR43006	56E1-56E1	mir-286 stem loop	15549026	15548927
CR42890	56E1-56E1	mir-3 stem loop	15549168	15549100
CR42903	56E1-56E1	mir-309 stem loop	15549279	15549211
CG11018	56E1-56E1	-	15551243	15549941
CG9854	56E1-56E1	hiiragi	15557326	15551422
CG11025	56E1-56E1	isopeptidase-T-3	15560982	15558124

CG15127	56E1-56E1	-	15568878	15568272
CG34198	56E1-56E1	-	15570478	15570029
CG15128	56E2-56E2	-	15575583	15573111
CG15126	56E2-56E2	-	15578511	15578350
CG11797	56E2-56E2	Odorant-binding protein 56a	15586016	15585228
CG30129	56E2-56E2	Odorant-binding protein 56b	15586822	15586347
CG30128	56E2-56E2	Odorant-binding protein 56c	15588573	15587678
CG11218	56E2-56E2	Odorant-binding protein 56d	15591300	15590635
CG8462	56E2-56E2	Odorant-binding protein 56e	15600461	15599850
CG30450	56E2-56E2	Odorant-binding protein 56f	15601481	15600919
CG8517	56E2-56E2	-	15602373	15601581
CR30215	56E2-56E2	transfer RNA:CR30215	15603143	15603070
CR30452	56E2-56E2	transfer RNA:CR30452	15613196	15613125
CR30218	56E2-56E2	transfer RNA:CR30218	15613481	15613410
CR30451	56E2-56E2	transfer RNA:glu4:56Fc	15613718	15613647
CR33930	56E2-56E2	snoRNA:185	15614657	15614603
CR30455	56E2-56E2	transfer RNA:glu4:56Fb	15615036	15614965
CR30453	56E2-56E2	transfer RNA:glu4:56Fa	15615557	15615486
CR30454	56E2-56E2	transfer RNA:CR30454	15615764	15615693
CR30220	56E2-56E2	transfer RNA:CR30220	15616463	15616392
CR30449	56E2-56E2	transfer RNA:CR30449	15616858	15616787
CR33452	56E2-56E2	5SrRNA:CR33452	15617201	15617067
CR33451	56E2-56E2	5SrRNA:CR33451	15617560	15617426
CR33450	56E2-56E2	5SrRNA:CR33450	15617943	15617809
CR33449	56E2-56E2	5SrRNA:CR33449	15618309	15618175
CR33448	56E2-56E2	5SrRNA:CR33448	15618682	15618548
CR33447	56E2-56E2	5SrRNA:CR33447	15619048	15618914
CR33446	56E2-56E2	5SrRNA:CR33446	15619407	15619273
CR33445	56E2-56E2	5SrRNA:CR33445	15619809	15619675
CR33444	56E2-56E2	5SrRNA:CR33444	15620189	15620055
CR33443	56E2-56E2	5SrRNA:CR33443	15620565	15620431
CR33442	56E2-56E2	5SrRNA:CR33442	15620927	15620793
CR33441	56E2-56E2	5SrRNA:CR33441	15621310	15621176
CR33440	56E2-56E2	5SrRNA:CR33440	15621676	15621542
CR33439	56E2-56E2	5SrRNA:CR33439	15622035	15621901
CR33438	56E2-56E2	5SrRNA:CR33438	15622411	15622277
CR33437	56E2-56E2	5SrRNA:CR33437	15622780	15622646
CR33436	56E2-56E2	5SrRNA:CR33436	15623149	15623015
CR33435	56E2-56E2	5SrRNA:CR33435	15623518	15623384
CR33434	56E2-56E2	5SrRNA:CR33434	15623887	15623753
CR33433	56E2-56E2	5SrRNA:CR33433	15624256	15624122
CR33432	56E2-56E2	5SrRNA:CR33432	15624625	15624491
CR33431	56E2-56E2	5SrRNA:CR33431	15624994	15624860

CR33430	56E2-56E2	5SrRNA:CR33430	15625363	15625229
CR33429	56E2-56E2	5SrRNA:CR33429	15625725	15625591
CR33428	56E2-56E2	5SrRNA:CR33428	15626091	15625957
CR33427	56E2-56E2	5SrRNA:CR33427	15626457	15626323
CR33426	56E2-56E2	5SrRNA:CR33426	15626833	15626699
CR33425	56E2-56E2	5SrRNA:CR33425	15627209	15627075
CR33424	56E2-56E2	5SrRNA:CR33424	15627575	15627441
CR33423	56E2-56E2	5SrRNA:CR33423	15627944	15627810
CR33422	56E2-56E2	5SrRNA:CR33422	15628303	15628169
CR33421	56E2-56E2	5SrRNA:CR33421	15628679	15628545
CR33420	56E2-56E2	5SrRNA:CR33420	15629045	15628911
CR33419	56E2-56E2	5SrRNA:CR33419	15629407	15629273
CR33418	56E2-56E2	5SrRNA:CR33418	15629776	15629642
CR33417	56E2-56E2	5SrRNA:CR33417	15630142	15630008
CR33416	56E2-56E2	5SrRNA-Psi:CR33416	15630523	15630381
CR33415	56E2-56E2	5SrRNA:CR33415	15630892	15630758
CR33414	56E2-56E2	5SrRNA:CR33414	15631268	15631134
CR33413	56E2-56E2	5SrRNA:CR33413	15631634	15631500
CR33412	56E2-56E2	5SrRNA:CR33412	15632000	15631866
CR33411	56E2-56E2	5SrRNA:CR33411	15632359	15632225
CR33410	56E2-56E2	5SrRNA:CR33410	15632735	15632601
CR33409	56E2-56E2	5SrRNA:CR33409	15633101	15632967
CR33408	56E2-56E2	5SrRNA:CR33408	15633467	15633333
CR33407	56E2-56E2	5SrRNA:CR33407	15633840	15633706
CR33406	56E2-56E2	5SrRNA:CR33406	15634213	15634079
CR33405	56E2-56E2	5SrRNA:CR33405	15634581	15634448
CR33404	56E2-56E2	5SrRNA:CR33404	15634957	15634823
CR33403	56E2-56E2	5SrRNA:CR33403	15635316	15635182
CR33402	56E2-56E2	5SrRNA:CR33402	15635682	15635548
CR33401	56E2-56E2	5SrRNA:CR33401	15636044	15635910
CR33400	56E2-56E2	5SrRNA:CR33400	15636413	15636279
CR33399	56E2-56E2	5SrRNA:CR33399	15636782	15636648
CR33398	56E2-56E2	5SrRNA:CR33398	15637151	15637017
CR33397	56E2-56E2	5SrRNA:CR33397	15637517	15637383
CR33396	56E2-56E2	5SrRNA:CR33396	15637890	15637756
CR33395	56E2-56E2	5SrRNA:CR33395	15638259	15638125
CR33394	56E2-56E2	5SrRNA:CR33394	15638628	15638494
CR33393	56E2-56E2	5SrRNA:CR33393	15638997	15638863
CR33392	56E2-56E2	5SrRNA:CR33392	15639366	15639232
CR33391	56E2-56E2	5SrRNA:CR33391	15639734	15639601
CR33390	56E2-56E2	5SrRNA:CR33390	15640096	15639962
CR33389	56E2-56E2	5SrRNA:CR33389	15640455	15640321
CR33388	56E2-56E2	5SrRNA:CR33388	15640828	15640694

CR33387	56E2-56E2	5SrRNA:CR33387	15641197	15641063
CR33386	56E2-56E2	5SrRNA:CR33386	15641566	15641432
CR33385	56E2-56E2	5SrRNA:CR33385	15641935	15641801
CR33384	56E2-56E2	5SrRNA:CR33384	15642304	15642170
CR33383	56E2-56E2	5SrRNA:CR33383	15642673	15642539
CR33382	56E2-56E2	5SrRNA:CR33382	15643042	15642908
CR33381	56E2-56E2	5SrRNA:CR33381	15643411	15643277
CR33380	56E2-56E2	5SrRNA:CR33380	15643780	15643646
CR33379	56E2-56E2	5SrRNA:CR33379	15644149	15644015
CR33378	56E2-56E2	5SrRNA:CR33378	15644518	15644384
CR33377	56E2-56E2	5SrRNA:CR33377	15644894	15644760
CR33376	56E2-56E2	5SrRNA:CR33376	15645263	15645129
CR33375	56E2-56E2	5SrRNA:CR33375	15645632	15645498
CR33374	56E2-56E2	5SrRNA:CR33374	15646001	15645867
CR33373	56E2-56E2	5SrRNA:CR33373	15646374	15646240
CR33372	56E2-56E2	5SrRNA:CR33372	15646740	15646606
CR33371	56E2-56E2	5SrRNA-Psi:CR33371	15647115	15646979
CR33370	56E2-56E2	5SrRNA:CR33370	15647481	15647347
CR33369	56E2-56E2	5SrRNA:CR33369	15647854	15647720
CR33368	56E2-56E2	5SrRNA:CR33368	15648230	15648096
CR33367	56E2-56E2	5SrRNA:CR33367	15648606	15648472
CR33366	56E2-56E2	5SrRNA:CR33366	15648982	15648848
CR33365	56E2-56E2	5SrRNA:CR33365	15649341	15649207
CR33364	56E2-56E2	5SrRNA:CR33364	15649707	15649573
CR33363	56E2-56E2	5SrRNA-Psi:CR33363	15650075	15649932
CR33362	56E2-56E2	5SrRNA:CR33362	15650441	15650307
CR33361	56E2-56E2	5SrRNA:CR33361	15650814	15650680
CR33360	56E2-56E2	5SrRNA:CR33360	15651183	15651049
CR33359	56E2-56E2	5SrRNA:CR33359	15651552	15651418
CR33358	56E2-56E2	5SrRNA:CR33358	15651928	15651794
CR33357	56E2-56E2	5SrRNA:CR33357	15652287	15652153
CR33356	56E2-56E2	5SrRNA-Psi:CR33356	15652668	15652526
CR33355	56E2-56E2	5SrRNA:CR33355	15653048	15652914
CR33354	56E2-56E2	5SrRNA:CR33354	15653414	15653280
CR33353	56E2-56E2	5SrRNA:CR33353	15653783	15653649
CG12501	56E2-56E2	Odorant receptor 56a	15658738	15656966
CG13873	56E3-56E3	Odorant-binding protein 56g	15671525	15670989
CR30520	56E3-56E3	transfer RNA:lys2:56EF	15690168	15690096
CG13874	56E4-56E4	Odorant-binding protein 56h	15703709	15703059
CG8595	56E4-56E4	Toll-7	15720473	15714410
CG30448	56E4-56E4	Odorant-binding protein 56i	15756219	15752222
CG13872	56E4-56E4	-	15768425	15766333
CG43195	56E5-56E5	-	15832444	15831779

CG42690	56E5-56E5	-	15833194	15832463		
CG42691	56E5-56E5	-	15834254	15833236		
CG30447	56E5-56E5	-	15835585	15834726		
CG10822	56E5-56E5	-	15839456	15838938		
CR30214	56F10-56F10	transfer RNA:gly3:56EFa	16117056	16116986	543	
CR30138	56F10-56F10	transfer RNA:gly3:56EFb	16120372	16120302	543	
CG11044	56F10-56F10	-	16122438	16119336	543	
CG11099	56F10-56F11	-	16126706	16123740	543	
CG13869	56F10-56F11	-	16126904	16126075	543	
CG11048	56F11-56F11	-	16130387	16127492	543	
CG11208	56F11-56F11	-	16132904	16130256	543	
CG11209	56F11-56F11	pickpocket 6	16135078	16133276	543	
CG9864	56F11-56F11	-	16141444	16135635	543	
CG9204	56F11-56F11	Ate1	16144886	16141297	543	
CG11055	56F11-56F11	-	16149241	16145157	543	
CG9193	56F11-56F11	mutagen-sensitive 209	16150362	16149257	543	
CG9183	56F11-56F11	plutonium	16151224	16150463	543	
CG8900	56F11-56F11	Ribosomal protein S18	16152399	16151477	543	
CG8908	56F11-56F11	-	16158290	16152437	543	
CG10444	56F11-56F11	-	16162030	16159156	543	
CG11788	56F11-56F14	-	16163648	16162191	543	
CG9143	56F14-56F15	-	16166501	16163475	543	
CG9090	56F15-56F16	-	16168629	16166561	543	
CG16868	56F16-56F16	-	16174584	16169134		
CG34199	56F16-56F16	-	16175851	16175120		
CG8914	56F16-56F16	Casein kinase II beta2 subunit	16178056	16177132		
CG9036	56F16-56F16	Cuticular protein 56F	16179448	16175860		
CG11200	56F16-56F16	Carbonyl reductase	16196170	16192022		
CG13868	56F16-56F16	-	16204415	16196217		
CG13871	56F16-56F16	-	16206544	16204828		
CG8920	56F16-56F16	-	16213478	16193796		
CG13867	56F16-56F16	Mediator complex subunit 8	16214311	16213346		
CG8929	56F16-56F16	-	16218226	16214772		
CG16739	56F17-56F17	-	16230279	16229533		
CG13870	56F17-56F17	-	16233384	16231350		
CG16741	56F17-56F17	-	16235101	16234541		
CG11192	56F17-56F17	-	16242558	16241610		
CG8654	56F4-56F4	-	15872255	15866749		
CR30212	56F4-56F4	transfer RNA:CR30212	15887873	15887801		
CR33538	56F4-56F4	transfer RNA:CR33538	15888396	15888324		
CG16898	56F4-56F4	-	15892492	15891124		
CG8896	56F8-56F8	18 wheeler	16004437	15999016	543	
CG11041	56F8-56F8	-	16034329	16033638	543	

CG16894	56F9-56F9	-	16100124	16099109	543
CG30152	57A10-57A10	-	16560059	16558708	
CG12484	57A3-57A3	-	16366459	16311840	
CG13421	57A4-57A4	Odorant-binding protein 57c	16392296	16391061	
CG30142	57A4-57A4	Odorant-binding protein 57b	16392322	16391755	
CG30141	57A4-57A4	Odorant-binding protein 57a	16393265	16392672	
CG13426	57A4-57A4	-	16400674	16400199	
CG13422	57A4-57A4	-	16414331	16413832	
CG30151	57A4-57A4	-	16416969	16416009	
CG30154	57A5-57A5	-	16421441	16420879	
CG18067	57A5-57A5	-	16422860	16422015	
CG13423	57A5-57A5	-	16425767	16424083	
CG13427	57A5-57A5	-	16426819	16426382	
CG13428	57A5-57A5	-	16427953	16427016	
CG30148	57A5-57A5	-	16435186	16434535	
CG30145	57A5-57A5	Odorant-binding protein 57e	16435796	16435321	
CG18066	57A5-57A5	Cuticular protein 57A	16437597	16435872	
CG30150	57A5-57A5	Odorant-binding protein 57d	16437597	16435872	
CG13430	57A5-57A5	-	16439591	16437838	
CG18065	57A5-57A5	-	16439591	16437838	
CG13424	57A5-57A5	lateral muscles scarcer	16447458	16444364	
CG13431	57A5-57A5	UDP-GlcNAc:a-3-D-mannoside-beta-1,2-N-acetylglucosaminyltransferase I	16449834	16446661	
CG43308	57A5-57A5	-	16450506	16449968	
CG13432	57A5-57A6	lethal (2) 05510	16469633	16450540	
CR42995	57A6-57A6	mir-310 stem loop	16471345	16471257	
CR42943	57A6-57A6	mir-311 stem loop	16471465	16471382	
CR43017	57A6-57A6	mir-312 stem loop	16471626	16471561	
CR43003	57A6-57A6	mir-313 stem loop	16471765	16471695	
CR42918	57A6-57A6	mir-2498 stem loop	16472325	16472214	
CR42934	57A6-57A6	mir-991 stem loop	16472800	16472705	
CR43041	57A6-57A6	mir-992 stem loop	16472910	16472819	
CG13434	57A6-57A6	Nnf1a	16474758	16473727	
CG13425	57A6-57A7	bancal	16494359	16475010	
CR42883	57A7-57A7	mir-7 stem loop	16493659	16493572	
CG30147	57A7-57A7	Hillarin	16505719	16494386	
CG9945	57A7-57A7	-	16508586	16506008	
CG11180	57A7-57A8	-	16510808	16508419	
CG16742	57A8-57A8	-	16515820	16511079	
CG11175	57A8-57A8	Reduction in Cnn dots 6	16521007	16515691	
CG13436	57A8-57A8	-	16525928	16523897	
CG30149	57A8-57A8	rigor mortis	16528191	16521381	
CG9954	57A8-57A8	maf-S	16529173	16528476	
CG11110	57A8-57A8	-	16530063	16529255	

CG33785	57A8-57A9	-	16531285	16529971		
CG33786	57A8-57A9	-	16531285	16529971		
CG8994	57A9-57A10	exuperantia	16558379	16554924		
CG11132	57A9-57A9	DMAP1	16533370	16531536		
CG16799	57A9-57A9	-	16542596	16540630		
CG11159	57A9-57A9	-	16544114	16543261		
CR30155	57A9-57A9	transfer RNA:CR30155	16545467	16545396		
CR30211	57A9-57A9	transfer RNA:CR30211	16545680	16545609		
CG11136	57A9-57A9	Leucine-rich tendon-specific protein	16548432	16534113		
CG13437	57A9-57A9	-	16549932	16549254		
CG9025	57A9-57A9	Fem-1	16554748	16549979		
CG9350	57B12-57B12	-	16913591	16912585		
CG3722	57B15-57B16	shotgun	16944664	16938107		
CG13441	57B1-57B1	Gustatory receptor 57a	16574415	16573110		
CG13438	57B1-57B1	-	16581114	16580375		
CG13442	57B1-57B1	-	16618115	16615329		
CG13439	57B1-57B2	defective proboscis extension response	16637949	16586355		
CG10540	57B16-57B16	capping protein alpha	16947388	16945276		
CG15653	57B16-57B16	-	16948014	16947285		
CG9353	57B16-57B16	mitochondrial ribosomal protein L54	16949092	16948284		
CG9357	57B16-57B16	Cht8	16950717	16949151		
CG30293	57B16-57B16	Cht12	16952491	16950683		
CG3986	57B16-57B16	Chitinase 4	16954592	16952885		
CG10531	57B16-57B16	Cht9	16956813	16955487		
CG10527	57B16-57B16	-	16960290	16957568		
CG9364	57B16-57B19	Trehalase	16975734	16961530	3467	
CG4030	57B19-57B19	-	16978507	16975888	3467	
CG4038	57B20-57B20	-	16984808	16983447	3467	
CG34396	57B20-57B20	-	16988961	16979743	3467	
CG9398	57B20-57C2	king tubby	17011220	16989435	3467	
CG34201	57B2-57B2	-	16639628	16638452	3467	
CG34202	57B2-57B2	-	16641244	16640110	3467	
CG13443	57B2-57B2	-	16662618	16661234	3467	
CG15226	57B2-57B2	-	16679643	16675822	3467	
CG15225	57B2-57B2	-	16681191	16680472	3467	
CG9985	57B3-57B3	skittles	16719919	16714916	3467	
CG11312	57B3-57B3	inscuteable	16723569	16708771	3467	
CG17999	57B3-57B3	-	16737424	16735485	3467	
CG9993	57B3-57B3	-	16739626	16737651	3467	
CG15227	57B3-57B3	-	16754481	16753606	3467	
CG15231	57B3-57B3	Immune induced molecule 4	16756826	16756341	3467	
CG33990	57B3-57B3	Immune induced molecule 14	16758134	16757930	3467	
CG30295	57B3-57B4	Ipk1	16766632	16758311	3467	

CG9236	57B4-57B4	-	16770168	16767435	3467		
CR43160	57B4-57B4	-	16786134	16784499	3467		
CG10036	57B4-57B4	orthopedia	16790900	16771116	3467		
CG9235	57B4-57B4	-	16798313	16797209	3467		
CG10052	57B4-57B4	Retinal Homeobox	16824537	16804285	3467		
CG9327	57B5-57B	Proteasome 29kD subunit	16883616	16882372	3467		
CR33780	57B5-57B5	snoRNA:660	16833570	16833475	3467		
CG10067	57B5-57B5	Actin 57B	16833945	16831533	3467		
CG33704	57B5-57B5	-	16838599	16837607	3467		
CG33152	57B5-57B5	homeobrain	16848414	16842169	3467		
CG15649	57B5-57B5	-	16861502	16860421	3467		
CG34115	57B5-57B5	-	16864439	16863005	3467		
CG9344	57B5-57B5	-	16865105	16864561	3467		
CG15650	57B5-57B5	-	16865742	16865233	3467		
CG9313	57B5-57B5	-	16871548	16866849	3467		
CG15651	57B5-57B5	-	16874000	16871339	3467		
CG3216	57B5-57B5	-	16878676	16874338	3467		
CG3221	57B5-57B5	dim gamma-tubulin 3	16881841	16879781	3467		
CG10543	57B5-57B5	-	16894146	16883790	3467		
CG30291	57B5-57B9	-	16897078	16895260	3467		
CG30296	57B9-57B12	-	16912423	16905290	3467		
CG33133	57B9-57B9	grauzone	16899424	16897274	3467		
CG9346	57B9-57B9	-	16903133	16899477	3467		
CG3295	57B9-57B9	-	16904951	16903099	3467		
CG9394	57C1-57C1	-	17008214	17005899	3467		
CG4050	57C2-57C2	-	17015995	17011233	3467		
CG9401	57C2-57C2	mago nashi	17017245	17016084	3467		
CG30388	57C2-57C3	Magi	17030067	17016968	3467		
CG9406	57C3-57C3	-	17030766	17029873	3467		
CG9415	57C3-57C4	X box binding protein-1	17033255	17031050	3467		
CG9418	57C4-57C4	-	17035113	17033713	3467		
CG15657	57C4-57C4	-	17035658	17034983	3467		
CG30389	57C4-57C6	-	17048050	17036238	3467	3469	
CR30206	57C6-57C6	transfer RNA:CR30206	17048639	17048568	3467	3469	
CR30207	57C6-57C6	transfer RNA:gly3:57BCa	17048931	17048861	3467	3469	
CR30208	57C6-57C6	transfer RNA:CR30208	17049102	17049031	3467	3469	
CG4266	57C6-57C7	-	17056163	17049218	3467	3469	
CG9433	57C7-57C6	Xeroderma pigmentosum D	17062009	17058460	3467	3469	
CG9437	57C7-57C7	-	17057515	17056465	3467	3469	
CG4279	57C7-57C7	-	17058150	17057474	3467	3469	
CG4286	57C7-57C7	-	17066141	17065259	3467	3469	
CG9441	57C7-57C8	Punch	17070121	17062822	3467	3469	
CR33539	57C8-57C8	transfer RNA:CR33539	17068860	17068789	3467	3469	

CR30209	57C8-57C8	transfer RNA:CR30209	17070254	17070183	3467	3469	
CR30210	57C8-57C8	transfer RNA:gly3:57BCb	17070431	17070361	3467	3469	
CG9450	57C8-57C9	tudor	17079903	17070937	3467	3469	
CG15658	57C9-57D1	-	17086941	17081078	3467	3469	
CG9754	57D11-57D11	-	17199853	17197873	3467	3469	
CG9485	57D11-57D11	-	17207074	17200185	3467	3469	
CG33655	57D11-57D11	-	17207522	17206941	3467	3469	
CG30394	57D11-57D11	-	17211056	17207543	3467	3469	
CR34652	57D11-57D11	-	17212828	17212723	3467	3469	
CR34547	57D11-57D11	snoRNA:Psi28S-3316a	17214375	17214244	3467	3469	
CR34548	57D11-57D12	snoRNA:Psi28S-3316b	17214527	17214387	3467	3469	
CG9696	57D11-57D12	domino	17229352	17210949	3467	3469	
CR33765	57D12-57D12	snoRNA:Psi18S-841a	17214704	17214561	3467	3469	
CR34653	57D12-57D12	-	17215876	17215768	3467	3469	
CR34549	57D12-57D12	snoRNA:Psi28S-3378	17217352	17217203	3467	3469	
CR34550	57D12-57D12	snoRNA:Psi28S-3316c	17217764	17217632	3467	3469	
CR34551	57D12-57D12	snoRNA:Psi18S-841b	17217918	17217781	3467	3469	
CR34552	57D12-57D12	snoRNA:Psi28S-3316d	17218070	17217939	3467	3469	
CR34553	57D12-57D12	snoRNA:Psi18S-841c	17218220	17218088	3467	3469	
CR34554	57D12-57D12	snoRNA:Psi28S-3316e	17218372	17218241	3467	3469	
CR34555	57D12-57D12	snoRNA:Psi18S-841d	17218548	17218411	3467	3469	
CR34654	57D12-57D12	-	17219184	17219078	3467	3469	
CR34556	57D12-57D12	snoRNA:Psi18S-1389a	17221597	17221439	3467	3469	
CR34557	57D12-57D12	snoRNA:Psi18S-1389b	17221804	17221650	3467	3469	
CR34655	57D12-57D12	-	17222961	17222888	3467	3469	
CR33916	57D12-57D12	small non-messenger RNA 184	17223049	17223015	3467	3469	
CG15666	57D12-57D12	-	17233113	17229490	3467	3469	
CG9822	57D12-57D12	-	17235356	17234380	3467	3469	
CG17974	57D12-57D12	-	17238349	17235692	3467	3469	
CG15671	57D12-57E1	crossveinless 2	17266967	17242520	3467	3469	
CG9480	57D1-57D1	Glycogenin	17100474	17087979	3467	3469	
CG4302	57D1-57D2	-	17102485	17100385	3467	3469	
CG15661	57D2-57D2	-	17105258	17102940	3467	3469	
CG18375	57D2-57D4	Ankyrin-repeat, SH3-domain, and Proline-rich-region containing Protein	17138458	17105361	3467	3469	
CG30391	57D4-57D4	-	17153847	17152344	3467	3469	
CG30393	57D4-57D5	-	17155084	17153869	3467	3469	
CG34397	57D5-57D6	Rgk3	17167878	17143319	3467	3469	
CG34203	57D6-57D7	-	17169161	17168568	3467	3469	
CG10069	57D7-57D7	-	17173174	17169805	3467	3469	
CG10505	57D7-57D8	-	17177833	17173225	3467	3469	
CG42672	57D8-57D11	-	17197916	17183178	3467	3469	
CG30392	57D8-57D8	-	17179683	17178419	3467	3469	
CG30390	57D8-57D8	-	17180981	17179744	3467	3469	

CG10071	57D8-57D8	Ribosomal protein L29	17181909	17181274	3467	3469		
CG9752	57D8-57D8	-	17183092	17181907	3467	3469		
CG30287	57E10-57E11	-	17425520	17424399		3469	6276	
CG33226	57E11-57E11	-	17426798	17425755		3469	6276	
CG30283	57E11-57E11	-	17428078	17427089		3469	6276	
CG10795	57E1-57E1	-	17271846	17270732	3467	3469	6276	
CG9841	57E1-57E1	EfSec	17273720	17272060	3467	3469	6276	
CG9707	57E1-57E1	acyl-Coenzyme A oxidase at 57D proximal	17276788	17273859	3467	3469	6276	
CG9709	57E1-57E1	acyl-Coenzyme A oxidase at 57D distal	17279944	17276901	3467	3469	6276	
CG10497	57E1-57E6	Syndecan	17368680	17280111	3467	3469	6276	
CG15667	57E6-57E6	Smad anchor for receptor activation	17374618	17369424	3467	3469	6276	
CG9847	57E6-57E6	Fkbp13	17385431	17374670	3467	3469	6276	
CG10496	57E6-57E8	-	17389475	17386408	3467	3469	6276	
CG15669	57E8-57E9	Misexpression suppressor of KSR 2	17404747	17389591		3469	6276	
CG30286	57E9-57E10	-	17424300	17423221		3469	6276	
CG10494	57E9-57E9	-	17406611	17403601		3469	6276	
CG30288	57E9-57E9	-	17407874	17406840		3469	6276	
CG30289	57E9-57E9	-	17409338	17407960		3469	6276	
CG10079	57E9-57F1	Epidermal growth factor receptor	17446932	17410510		3469	6276	
CG30403	57F10-57F10	-	17599114	17596955	6859		6276	
CG17950	57F10-57F10	High mobility group protein D	17604230	17600836	6859		6276	
CG30398	57F10-57F10	-	17606337	17605338	6859		6276	
CG30404	57F10-57F10	Transport and Golgi organization 11	17607466	17604285	6859		6276	
CG17952	57F10-57F11	Lamin B receptor	17611564	17608002	6859		6276	
CG7975	57F11-57F11	Grx-1	17645483	17644932	6859			
CG10440	57F1-57F1	-	17458957	17447751		3469	6276	
CG30222	57F2-57F2	-	17472873	17470997		3469	6276	
CG33225	57F2-57F2	-	17479089	17477891		3469	6276	
CG10433	57F3-57F3	-	17494458	17493181		3469	6276	
CG43243	57F3-57F3	-	17495982	17495192		3469	6276	
CG15673	57F3-57F4	-	17500594	17495898		3469	6276	
CG18870	57F4-57F4	-	17504398	17502268		3469	6276	
CG9858	57F4-57F4	cricklet	17506564	17504566		3469	6276	
CG9856	57F4-57F4	Protein tyrosine phosphatase-ERK/Enhancer of Ras1	17511947	17506889		3469	6276	
CG10080	57F4-57F5	mahjong	17518927	17512543		3469	6276	
CR42547	57F5-57F5	-	17521545	17518926		3469	6276	
CG15674	57F5-57F5	-	17521675	17519791		3469	6276	
CG10321	57F5-57F5	-	17525906	17522173		3469	6276	
CG30284	57F6-57F6	-	17539504	17538330		3469	6276	
CG10082	57F6-57F6	-	17544944	17533683		3469	6276	
CG10320	57F6-57F6	-	17546282	17545580		3469	6276	
CG9862	57F6-57F6	Rae1	17547508	17546261		3469	6276	
CG15678	57F6-57F6	poor Imd response upon knock-in	17549749	17548472		3469	6276	

CG42362	57F7-57F7	-	17553613	17551938		6276	
CG42363	57F7-57F7	-	17553613	17551938		6276	
CG42364	57F7-57F7	-	17554084	17553445		6276	
CG42365	57F7-57F7	-	17555099	17554252		6276	
CG42379	57F7-57F7	-	17557560	17555046		6276	
CG42380	57F7-57F7	-	17557560	17555046		6276	
CG42381	57F7-57F7	-	17557560	17555046		6276	
CG9865	57F7-57F7	-	17557560	17555046		6276	
CG10318	57F7-57F7	NC2alpha	17559098	17557673		6276	
CG15676	57F8-57F8	-	17559850	17559205		6276	
CG30263	57F8-57F8	-	17572505	17563826		6276	
CG10306	57F8-57F8	-	17573709	17572775		6276	
CG9874	57F8-57F8	TATA binding protein	17575145	17573705		6276	
CG30285	57F8-57F8	-	17576026	17575408		6276	
CG10307	57F8-57F8	-	17577758	17576417		6276	
CG42497	57F8-57F8	-	17578643	17577720		6276	
CG9878	57F8-57F8	Translocase of inner membrane 10	17578643	17577720		6276	
CG30290	57F8-57F9	Phosphopantothenoylcysteine decarboxylase	17580269	17579095	6859	6276	
CG42496	57F8-57F9	-	17580269	17579095	6859	6276	
CG17922	57F9-57F9	-	17584657	17580191	6859	6276	
CG17921	57F9-57F9	HMG protein Z	17591993	17585056	6859	6276	
CG30395	58A1-58A1	-	17657701	17653030	6859		
CG4021	58A1-58A1	-	17662381	17660852	6859		
CG4402	58A1-58A1	lysyl oxidase-like 2	17679160	17677121	6859		
CG34204	58A1-58A1	-	17684446	17683956	6859		
CG18735	58A1-58A1	-	17686671	17685577	6859		
CG4386	58A1-58A1	-	17688405	17686835	6859		
CG9284	58A2-58A2	-	17691846	17690929	6859		
CG13492	58A2-58A2	-	17718853	17708349	6859		
CG34040	58A2-58A2	-	17721012	17720006	6859		
CG4363	58A2-58A2	-	17722534	17721735	6859		
CG4377	58A2-58A2	-	17723835	17722953	6859		
CG4372	58A2-58A2	-	17726303	17725110	6859		
CR30407	58A2-58A2	transfer RNA:CR30407	17730673	17730602	6859		
CR30406	58A3-58A3	transfer RNA:CR30406	17735983	17735912	6859		
CG9294	58A3-58A3	-	17749469	17748356	6859		
CG13493	58A3-58A3	cookie monster	17754364	17752372	6859		
CG3245	58A3-58A3	Protein phosphatase N at 58A	17770038	17768857	6859		
CG34368	58A3-58A4	Fish-lips	17833769	17759537	6859		
CG13488	58A4-58A4	-	17840068	17839196	6859		
CG13494	58A4-58A4	-	17842350	17841743	6859		
CG34369	58A4-58A4	-	17858169	17851678	6859		
CG34029	58A4-58A4	-	17858693	17858266	6859		

CG9304	58A4-58A4	-	17863701	17860631	6859		
CG13491	58A4-58A4	Gustatory receptor 58c	17865462	17864167	6859		
CG11061	58B10-58B10	GM130	18015002	18012075	6859		
CG6698	58B10-58C1	NtR	18017693	18015313	6859		
CG13495	58B1-58B1	Gustatory receptor 58b	17867190	17865720	6859		
CG30396	58B1-58B1	Gustatory receptor 58a	17868604	17867365	6859		
CG30401	58B1-58B1	-	17874149	17873267	6859		
CG9308	58B1-58B1	-	17923173	17922349	6859		
CG34370	58B1-58B1	-	17927063	17874573	6859		
CG10138	58B1-58B1	Protein phosphatase D5	17930387	17929172	6859		
CG13500	58B1-58B1	-	17945186	17943972	6859		
CG13501	58B1-58B1	-	17948215	17946409	6859		
CG42257	58B1-58B2	Snipper	17957262	17948458	6859		
CG11475	58B2-58B2	-	17958791	17957230	6859		
CG11474	58B2-58B3	-	17960948	17958739	6859		
CG2921	58B3-58B3	-	17962842	17961043	6859		
CG6437	58B3-58B3	GlcT-1	17966886	17963547	6859		
CG6562	58B4-58B4	synaptojanin	17973272	17967676	6859		
CG13502	58B4-58B5	-	17976084	17973174	6859		
CG11073	58B5-58B7	-	17987231	17978994	6859		
CG6613	58B7-58B8	-	17993468	17990693	6859		
CG30280	58B8-58B9	-	18002346	18001094	6859		
CG13503	58B8-58B9	Verprolin 1	18010053	17994243	6859		
CG5303	58B9-58B10	meiotic from via Salaria 332	18012071	18009606	6859		
CG30281	58B9-58B9	-	18003694	18002502	6859		
CG34205	58C1-58C1	-	18018715	18017834	6859		
CG11269	58C1-58C1	-	18026770	18026447	6859		
CG6727	58C1-58C1	gomdanji	18028842	18027440	6859		
CG6741	58C1-58C5	arc	18060346	18024494	6859		
CG34206	58C4-58C4	-	18052099	18051272	6859		
CG3045	58C5-58C5	-	18062243	18060308	6859		
CG6758	58C5-58C5	-	18064933	18062413	6859		
CG30279	58C5-58C5	-	18067033	18066686	6859		
CG11275	58C5-58C5	-	18070147	18067199	6859		
CG11170	58C5-58C5	-	18070337	18064924	6859		
CG5465	58C5-58C7	Mediator complex subunit 16	18073397	18070652	6859		
CG5625	58C7-58C7	Vacuolar protein sorting 35	18077392	18073483	6859		
CG3074	58C7-58D1	-	18090178	18077326	6859		
CR34656	58D1-58D1	-	18084879	18084774	6859		
CG3292	58D1-58D1	-	18093081	18091199	6859		
CG3290	58D1-58D1	-	18095492	18093510	6859		
CG3264	58D1-58D1	-	18098247	18096412	6859		
CG11291	58D1-58D1	-	18100209	18098946	6859		

CG5709	58D1-58D2	ariadne 2	18104769	18100346	6859	
CG30278	58D2-58D2	-	18106003	18105022	6859	
CG30277	58D2-58D2	Organic anion transporting polypeptide 58Da	18108393	18105961	6859	
CG3382	58D2-58D2	Organic anion transporting polypeptide 58Db	18111095	18108685	6859	
CG3380	58D2-58D2	Organic anion transporting polypeptide 58Dc	18116073	18111186	6859	
CG5799	58D2-58D2	defective proventriculus	18173982	18131468	6859	
CG5819	58D3-58D3	-	18184463	18180964		
CG3413	58D3-58D3	windpipe	18199425	18185718		
CG5820	58D3-58D3	Gp150	18216933	18205167		
CG34207	58D3-58D3	-	18217225	18216920		
CG3425	58D3-58D3	Type III alcohol dehydrogenase	18219562	18217231		
CG32885	58D3-58D3	polar granule component	18220320	18217658		
CG34208	58D3-58D3	-	18221010	18220631		
CG11206	58D3-58D4	Liprin-gamma	18260610	18221009		
CG11298	58D4-58D4	-	18236387	18235812		
CG10955	58D4-58D4	Rtf1	18265352	18262597		
CG10382	58D4-58D4	wrapper	18270191	18267017		
CG13506	58D4-58D4	-	18281527	18270641		
CG3624	58D4-58D4	-	18289561	18281567		
CG6044	58D4-58D7	-	18295880	18291678		
CG33200	58D7-58D7	ventrally-expressed-protein-D	18296693	18296156		
CG3584	58D7-58D8	quaking related 58E-3	18299049	18297009		
CG11301	58D8-58D8	Mes4	18300087	18299312		
CG3613	58D8-58D8	quaking related 58E-1	18303047	18300422		
CG5821	58D8-58E1	quaking related 58E-2	18306209	18303318		
CG3633	58E1-58E1	mitochondrial ribosomal protein S29	18307882	18306442		
CG6339	58E1-58E1	rad50	18312979	18308544		
CG10344	58E1-58E1	-	18314470	18313238		
CG10972	58E1-58E1	pickpocket 12	18317089	18314984		
CG10384	58E2-58E2	-	18359160	18353994		
CG3701	58E3-58E3	-	18364775	18360786		
CG4752	58E3-58E3	-	18370559	18365892		
CG4554	58E3-58E3	-	18379538	18370846		
CG4610	58E3-58E4	-	18381800	18379719		
CG4444	58E4-58E8	plexus	18449569	18384003		
CG6018	58E8-58E8	-	18439618	18437605		
CG11362	58E8-58E8	-	18450358	18449865		
CG12489	58E9-58F1	defense repressor 1	18480473	18451012		
CG3927	58F1-58F1	-	18483858	18482193		
CG4269	58F1-58F1	-	18487861	18486860		
CG4294	58F1-58F1	-	18493140	18487910		
CR34657	58F1-58F1	-	18494366	18494300		
CR34558	58F1-58F1	snoRNA:Psi28S-1175a	18494725	18494590		

CR34559	58F1-58F1	snoRNA:Psi28S-1175b	18494877	18494737
CR34560	58F1-58F1	snoRNA:Psi28S-1175c	18495025	18494890
CR34561	58F1-58F1	snoRNA:Or-aca1	18495183	18495049
CG4046	58F1-58F1	Ribosomal protein S16	18495506	18493626
CG4071	58F1-58F2	Vacuolar protein sorting 20	18496936	18496038
CG4329	58F2-58F2	-	18500881	18496838
CG33143	58F2-58F2	-	18521590	18501835
CG17807	58F2-58F2	-	18523435	18521524
CG5179	58F2-58F3	Cyclin-dependent kinase 9	18525228	18523568
CG4207	58F3-58F3	bonsai	18526373	18525277
CG3732	58F3-58F3	-	18527668	18526310
CG3751	58F3-58F3	Ribosomal protein S24	18528923	18528026
CG4414	58F3-58F3	Ugt58Fa	18531420	18529401
CG2852	58F3-58F3	-	18533851	18532448
CG30195	58F3-58F3	-	18534746	18534118
CG34446	58F3-58F3	-	18535268	18535083
CG34445	58F3-58F3	-	18535978	18535397
CG3746	58F4-58F4	-	18537251	18536621
CG3875	58F4-58F4	novel spermatogenesis regulator	18539812	18538079
CG4373	58F4-58F4	Cyp6d2	18542032	18540078
CG30196	58F4-58F4	-	18542896	18542310
CG43325	58F4-58F4	-	18544499	18543054
CG43326	58F4-58F4	-	18544499	18543054
CG13510	58F4-58F4	-	18546638	18545410
CG13511	58F4-58F4	-	18547643	18547217
CG42565	58F4-58F4	-	18548894	18547988
CG42566	58F4-58F4	-	18550746	18549439
CG4250	58F4-58F4	-	18551979	18551193
CG42867	58F4-58F4	-	18553634	18553052
CG42868	58F4-58F4	-	18554269	18553789
CG30273	58F4-58F4	-	18555445	18554661
CG30269	58F4-58F6	-	18556352	18555447
CG13516	58F7-58F7	-	18558127	18556961
CG12190	58F7-58F7	Ring and YY1 Binding Protein	18560717	18558257
CG9952	59A1-59A2	partner of paired	18576478	18573030
CG13521	59A2-59A3	roundabout	18588467	18580029
CG13517	59A3-59A3	Odorant-binding protein 59a	18591291	18590222
CG30259	59A3-59A3	-	18591952	18588949
CG13518	59A3-59A3	Odorant-binding protein 58b	18593144	18592215
CG13524	59A3-59A3	Odorant-binding protein 58c	18594165	18593450
CG13519	59A3-59A3	Odorant-binding protein 58d	18595219	18594453
CG30275	59A3-59A3	-	18600255	18595299
CG30268	59A3-59A3	-	18604752	18600206

CG30092	59A3-59A3	jitterbug	18624550	18604826
CG13526	59A4-59A4	-	18643401	18642745
CG13527	59A4-59A4	-	18652362	18651239
CG30270	59B1-59B1	-	18672441	18671809
CG42260	59B1-59B1	-	18684614	18631377
CG3612	59B1-59B2	bellwether	18689685	18686561
CG3510	59B2-59B2	Cyclin B	18694490	18691026
CG3622	59B2-59B2	stall	18703498	18695809
CG30271	59B2-59B2	-	18709279	18703979
CG30274	59B2-59B2	-	18714350	18712713
CG42284	59B2-59B2	-	18716429	18710231
CG30272	59B2-59B2	-	18719248	18717220
CG30265	59B2-59B2	-	18722103	18719979
CG12490	59B2-59B2	-	18724224	18722170
CG9825	59B2-59B2	-	18726814	18724886
CG9826	59B2-59B2	-	18729988	18728358
CG3649	59B2-59B2	-	18735434	18733524
CG13531	59B2-59B3	-	18741220	18735355
CG3661	59B3-59B3	Ribosomal protein L23	18743211	18741898
CG3504	59B3-59B3	inactivation no afterpotential D	18746317	18743211
CG3668	59B4-59B4	forkhead domain 59A	18758229	18754044
CG13532	59B4-59B4	-	18761950	18758818
CG3682	59B4-59B4	PIP5K59B	18768959	18762294
CG3501	59B4-59B4	-	18770210	18768845
CG3499	59B4-59B4	-	18773855	18770499
CG13533	59B4-59B4	asrij	18775105	18773921
CG3495	59B4-59B4	GDP-4-keto-6-deoxy-D-mannose 3,5-epimerase/4-reductase	18776374	18775095
CG3695	59B4-59B4	Mediator complex subunit 23	18783261	18776507
CG3700	59B4-59B4	-	18783269	18776507
CG12781	59B4-59B4	nahoda	18804242	18783696
CG30187	59B4-59B4	-	18806289	18804366
CG3820	59B4-59B6	Nucleoporin 214	18812255	18806459
CG42678	59B6-59B6	-	18819567	18812613
CG3788	59B6-59B6	-	18821208	18819558
CG3800	59B6-59B6	-	18824453	18822092
CG9849	59B6-59B6	-	18826548	18824802
CG3831	59B6-59B7	-	18828467	18826510
CG42694	59B7-59B7	-	18832673	18830732
CG32835	59B7-59B7	-	18841323	18838671
CR43305	59C1-59C1	-	18871427	18870109
CG32834	59C1-59C1	-	18871798	18870128
CG32833	59C1-59C1	-	18872837	18871796
CG9897	59C1-59C1	-	18873851	18872946

CR42742	59C1-59C1	-	18874062	18872908		
CG9896	59C1-59C1	-	18886406	18881186		
CG42741	59C2-59C2	-	18929143	18899290		
CG2956	59C2-59C2	twist	18935849	18933631		
CG30194	59C2-59C2	-	18949074	18943019		
CG9893	59C2-59C3	lethal (2) 06496	18950125	18948943		
CG9890	59C3-59C3	-	18951787	18950270		
CG42640	59C3-59C3	-	18954706	18952307		
CG3082	59C3-59C3	lethal (2) k09913	18959404	18954725		
CR30201	59C3-59C3	transfer RNA:CR30201	18959623	18959542		
CR30202	59C3-59C3	transfer RNA:CR30202	18960185	18960104		
CR33684	59C3-59C3	snoRNA:229	18961491	18961352		
CG9888	59C3-59C3	Fibrillarin	18962243	18960414		
CG3085	59C3-59C3	-	18964381	18962592		
CG9882	59C3-59C3	Arginine methyltransferase 7	18966559	18964207		
CG30189	59C3-59C3	Gustatory receptor 59a	18969248	18968084		
CG30191	59C3-59C3	Gustatory receptor 59b	18970889	18969726		
CG9877	59C3-59C3	-	18973784	18973402		
CG13538	59C3-59C3	-	18975688	18974785		
CG9876	59C3-59C3	-	18981785	18977626		
CG9873	59C4-59C4	Ribosomal protein L37b	18987982	18987580		
CG42703	59C4-59C4	-	18989224	18988755		
CG30186	59C4-59C4	Gustatory receptor 59c	18991256	18990000		
CG30330	59C4-59C4	Gustatory receptor 59d	18992692	18991464		
CG3219	59C4-59C4	Klp59C	19013565	19011517		
CG3215	59C4-59C4	-	19017712	19016126		
CG30192	59C5-59D1	-	19026612	19026103		
CG3530	59D10-59D10	-	19284202	19276524	1682	
CG3520	59D10-59D10	-	19289832	19284289	1682	
CG30411	59D11-59D11	-	19304761	19303468	1682	
CG9812	59D11-59D11	-	19307207	19299859	1682	
CG9815	59D11-59D11	-	19313420	19309031	1682	
CG13544	59D1-59D1	-	19028107	19026599		
CG12192	59D1-59D1	Klp59D	19032022	19029522		
CG43207	59D1-59D1	-	19040841	19040317		
CG13545	59D1-59D1	-	19045708	19045105		
CG9899	59D1-59D1	-	19049553	19046429		
CG34371	59D1-59D2	-	19091494	19050535		
CG13539	59D2-59D2	-	19072811	19071931		
CG3162	59D2-59D2	-	19099062	19097648		
CG3092	59D3-59D3	-	19121451	19120149		
CG13549	59D3-59D3	yippee interacting protein 3	19132809	19131556		
CG9871	59D3-59D3	Ribosomal protein L22-like	19135360	19134115		

CG12782	59D4-59D4	-	19153057	19151792			
CG13540	59D4-59D4	-	19158590	19158107			
CG3134	59D4-59D4	orientation disruptor	19161798	19158778			
CG3124	59D4-59D4	-	19171636	19170265			
CG13541	59D4-59D4	-	19172799	19171803			
CG9868	59D6-59D6	Proteasome beta5R subunit	19197339	19196177	1682		
CG43352	59D6-59D6	-	19201377	19200540	1682		
CG30412	59D6-59D6	-	19206871	19205712	1682		
CG30416	59D6-59D6	-	19210922	19209003	1682		
CG9861	59D6-59D6	-	19214268	19211182	1682		
CG30417	59D6-59D6	-	19215104	19214262	1682		
CG30413	59D6-59D6	-	19217593	19217066	1682		
CG3502	59D7-59D7	-	19235160	19230928	1682		
CG9863	59D7-59D7	-	19235291	19234158	1682		
CG34210	59D7-59D8	-	19239667	19239107	1682		
CG30409	59D8-59D8	-	19242755	19241983	1682		
CG30410	59D8-59D8	-	19243964	19242706	1682		
CG3500	59D8-59D8	-	19245088	19243895	1682		
CG9875	59D8-59D8	-	19246419	19245183	1682		
CG34423	59D8-59D8	-	19246988	19246241	1682		
CG34424	59D8-59D8	-	19247796	19246742	1682		
CG3496	59D8-59D9	virilizer	19253777	19247786	1682		
CG10315	59D9-59D10	eIF2B-delta	19276575	19274016	1682		
CG13550	59D9-59D9	-	19258984	19254412	1682		
CG3493	59D9-59D9	-	19264535	19258874	1682		
CG9889	59D9-59D9	yellow-d	19267961	19266056	1682		
CG9891	59D9-59D9	yellow-d2	19270114	19268722	1682		
CG13551	59D9-59D9	-	19270944	19265383	1682		
CG30414	59D9-59D9	-	19272978	19271166	1682		
CG30415	59D9-59D9	-	19273969	19273201	1682		
CG9820	59E1-59E1	Odorant receptor 59a	19328588	19327391	1682		
CG5357	59E1-59E1	-	19346133	19343498	1682		
CG12227	59E1-59E1	skpF	19346282	19345586	1682		
CG3569	59E1-59E1	Odorant receptor 59b	19359233	19357925	1682		
CG17226	59E1-59E1	Odorant receptor 59c	19361126	19359836	1682		
CG13557	59E1-59E1	-	19363941	19363221	1682		
CG34372	59E2-59E2	-	19379520	19351816	1682		
CG13558	59E2-59E2	-	19387842	19387255	1682		
CG13559	59E2-59E2	-	19391197	19390853	1682		
CG3906	59E2-59E2	-	19399747	19398809	1682		
CG3870	59E2-59E2	chrowded	19411096	19407362	1682		
CG5360	59E2-59E3	minus	19415788	19411381	1682		
CG17632	59E2-59E3	brown	19426016	19415328	1682		

CG30181	59E3-59E3	-	19428296	19426154	1682		
CG33151	59E3-59E3	Gustatory receptor 59e	19429902	19428577	1682		
CG33150	59E3-59E3	Gustatory receptor 59f	19431408	19430033	1682		
CG30185	59E3-59E3	-	19432422	19431564	1682		
CG3957	59E3-59E3	wing morphogenesis defect	19435603	19432342	1682		
CG17280	59E3-59E3	levy	19436505	19435763	1682		
CG5370	59E3-59E3	Death caspase-1	19441079	19438838	1682		
CG3941	59E3-59E3	pita	19442241	19436488	1682		
CG3931	59E3-59E3	Rrp4	19443724	19442541	1682		
CG5372	59E4-59E4	alphaPS5	19447720	19444333	1682		
CG5373	59E4-59F1	Phosphotidylinositol 3 kinase 59F	19451558	19447961	1682		
CG30184	59F1-59F1	-	19452303	19451552	1682		
CG5393	59F1-59F4	apontic	19487049	19452377	1682		
CG42559	59F4-59F4	-	19488310	19487051	1682		
CG42560	59F4-59F4	-	19488310	19487046	1682		
CG10332	59F4-59F4	-	19489296	19488437	1682		
CG33706	59F4-59F4	Immune induced molecule 18	19489296	19488437	1682		
CG43209	59F4-59F4	-	19489979	19489504	1682		
CG5398	59F4-59F4	-	19491164	19490108	1682		
CG17664	59F4-59F4	-	19492676	19491249	1682		
CG17662	59F4-59F4	-	19494177	19493281	1682		
CG4019	59F4-59F4	-	19502269	19495115	1682		
CG5403	59F5-59F5	retained	19542343	19520135	1682		
CG42241	59F5-59F5	-	19561421	19560399	1682		
CG5411	59F5-59F6	Phosphodiesterase 8	19568368	19545099	1682		
CG5428	59F6-59F6	-	19570475	19569147	1682		
CG5431	59F6-59F6	-	19572251	19570904	1682		
CG4533	59F6-59F6	lethal (2) essential for life	19573063	19572174	1682		
CG11293	59F6-59F6	-	19575503	19573202	1682		
CG5472	59F6-59F6	Peptidyl-alpha-hydroxyglycine-alpha-amidating lyase 2	19578107	19575681	1682		
CG12273	59F6-59F6	angel	19582755	19581521	1682		
CG30183	59F6-59F6	-	19585198	19578314	1682		
CG5479	59F6-59F6	mitochondrial ribosomal protein L43	19586537	19585631	1682		
CG4091	59F6-59F6	-	19589924	19586469	1682		
CG11295	59F6-59F6	lethal-(2)-denticleless	19592926	19590002	1682		
CG5504	59F6-59F6	lethal (2) tumorous imaginal discs	19596549	19594385	1682		
CG4084	59F6-59F6	lethal (2) neighbor of tid	19597311	19592962	1682		
CG18128	59F6-59F6	-	19607459	19606320	1682		
CG11299	59F6-59F7	Sestrin	19620706	19601425	1682		
CG4051	59F7-59F7	egalitarian	19634348	19622427	1682		
CG13560	59F7-59F7	-	19635741	19635096	1682		
CG34105	59F7-59F7	-	19637375	19636759	1682		
CG12491	59F7-59F7	-	19638824	19638208	1682		

CG11300	59F7-59F7	-	19640018	19639438	1682		
CG5532	59F7-59F7	-	19640929	19640264	1682		
CG9850	59F7-60A1	-	19685240	19641218	1682		
CG2812	60A11-60A11	-	19814433	19812762	1682		
CG3725	60A11-60A12	Calcium ATPase at 60A	19823408	19814479	1682		
CG3735	60A12-60A12	-	19827274	19824909	1682		
CG2827	60A12-60A12	Tal	19829637	19827936	1682		
CG2835	60A12-60A13	G protein salpha 60A	19834459	19830064	1682		
CG13565	60A13-60A13	-	19836137	19834482	1682		
CG16783	60A13-60A13	fizzy-related 2	19839622	19838029	1682		
CG2970	60A13-60A13	-	19839984	19836724	1682		
CG3803	60A13-60A13	-	19841538	19840040	1682		
CG2980	60A13-60A13	thoc5	19843930	19841616	1682		
CG16787	60A13-60A14	-	19844926	19843858	1682		
CG2987	60A14-60A14	alpha-catenin related	19849148	19845630	1682		
CG13566	60A14-60A14	-	19850034	19849178	1682		
CG3006	60A14-60A14	Flavin-containing monooxygenase 1	19852175	19850498	1682		
CG3017	60A14-60A14	Aminolevulinate synthase	19854271	19852224	1682		
CG34213	60A14-60A14	-	19855239	19854647	1682		
CG3029	60A14-60A14	orange	19856467	19855467	1682		
CG10904	60A14-60A14	-	19857592	19856584	1682		
CG3065	60A14-60A15	-	19859756	19857830	1682		
CG3060	60A15-60A15	morula	19862935	19859956	1682		
CG3825	60A15-60A16	-	19864801	19863124	1682		
CG15800	60A1-60A1	-	19678715	19678241	1682		
CG30177	60A1-60A1	-	19690593	19689065	1682		
CG5539	60A1-60A2	-	19693411	19692334	1682		
CG13561	60A1-60A2	-	19693772	19691838	1682		
CG3090	60A16-60A16	Sox box protein 14	19872700	19866744	1682		
CG30178	60A16-60A16	-	19874832	19874197	1682		
CG3832	60A16-60A16	Peptidylglycine-alpha-hydroxylating monooxygenase	19875990	19872750	1682		
CG3105	60A16-60B1	PAS kinase	19879573	19876240	1682		
CG4817	60A2-60A2	Structure specific recognition protein	19696518	19693884	1682		
CG5543	60A2-60A2	-	19698907	19696768	1682		
CG12752	60A2-60A2	NTF2-related export protein 1	19699496	19698844	1682		
CG4797	60A2-60A2	-	19705849	19699704	1682		
CG4763	60A2-60A2	-	19712391	19710880	1682		
CG5549	60A2-60A3	-	19724863	19707893	1682		
CR33913	60A3-60A3	snoRNA:Psi18S-176	19727587	19727434	1682		
CG4735	60A3-60A3	shutdown	19730802	19728984	1682		
CG11173	60A3-60A3	ubisnap	19732248	19731006	1682		
CG5554	60A3-60A3	-	19734547	19732415	1682		
CG17611	60A3-60A3	eIF6	19737822	19736769	1682		

CG18426	60A3-60A3	yantar	19738619	19734693	1682		
CG5562	60A3-60A4	glass bottom boat	19740772	19739106	1682		
CG30176	60A4-60A4	within bgcn	19744457	19743478	1682		
CG30170	60A4-60A4	benign gonial cell neoplasm	19746314	19740801	1682		
CG10327	60A4-60A5	TBPH	19750135	19746590	1682		
CG4585	60A5-60A5	-	19752917	19750485	1682		
CG5569	60A5-60A5	-	19754177	19752944	1682		
CG4581	60A5-60A5	Thiolase	19756139	19754124	1682		
CG5575	60A6-60A7	ken and barbie	19764965	19757798	1682		
CG11303	60A7-60A7	Transmembrane 4 superfamily	19768383	19765982	1682		
CG4882	60A7-60A7	-	19769954	19768340	1682		
CG11182	60A7-60A8	Putative homeodomain protein	19771835	19770708	1682		
CG5597	60A8-60A8	-	19776300	19774497	1682		
CG11183	60A8-60A8	Decapping protein 1	19777788	19776465	1682		
CG5602	60A8-60A8	DNA ligase I	19780700	19778061	1682		
CG11184	60A8-60A9	Upf3	19782510	19780589	1682		
CG5594	60A9-60A11	kazachoc	19812619	19795651	1682		
CG17658	60A9-60A9	-	19784520	19782601	1682		
CG5339	60A9-60A9	-	19785757	19784419	1682		
CG5591	60A9-60A9	-	19791187	19786102	1682		
CG13562	60A9-60A9	-	19792792	19791352	1682		
CG5330	60A9-60A9	Nucleosome assembly protein 1	19794837	19792698	1682		
CG11290	60B10-60B10	enoki mushroom	19994557	19987404	1682		
CG4049	60B10-60B10	-	20001793	19995429			
CG3253	60B10-60B11	-	20003882	20001921			
CG3257	60B11-60B11	-	20010786	20004295			
CG13569	60B11-60B11	-	20014153	20010690			
CG4057	60B11-60B11	tamo	20021074	20014161			
CG3260	60B11-60B12	Zinc finger protein RP-8	20022928	20021528			
CG4065	60B12-60B12	-	20025561	20022696			
CG3318	60B12-60C1	Dopamine N acetyltransferase	20045285	20027108			
CR42994	60B1-60B1	mir-1009 stem loop	19880637	19880577	1682		
CG3860	60B1-60B1	-	19882573	19879661	1682		
CG33519	60B1-60B2	Unc-89	19901384	19883066	1682		
CG4324	60B2-60B3	-	19904719	19902433	1682		
CG3121	60B3-60B3	-	19907418	19904944	1682		
CG3907	60B3-60B4	-	19909779	19907421	1682		
CG11388	60B4-60B4	-	19911507	19909896	1682		
CG3140	60B4-60B4	Adenylate kinase-2	19913400	19911721	1682		
CG11390	60B4-60B4	Ejaculatory bulb protein III	19915040	19914056	1682		
CG30173	60B4-60B4	-	19916325	19915474	1682		
CG3163	60B4-60B5	-	19918078	19916844	1682		
CG30172	60B5-60B5	-	19918724	19918165	1682		

CG3924	60B5-60B5	Chip	19921459	19919062	1682		
CG3167	60B5-60B5	MAN1	19924231	19921732	1682		
CG13567	60B5-60B5	-	19925322	19924243	1682		
CG3173	60B5-60B5	-	19931981	19925507	1682		
CG4254	60B5-60B5	twinstar	19934359	19931971	1682		
CG3988	60B5-60B5	gamma-soluble NSF attachment protein	19936412	19934668	1682		
CG3182	60B5-60B6	seizure	19940562	19936728	1682		
CG13568	60B6-60B6	-	19944656	19940438	1682		
CG13563	60B6-60B7	-	19945128	19942829	1682		
CG3186	60B7-60B7	eIF-5A	19947002	19945347	1682		
CG3195	60B7-60B7	Ribosomal protein L12	19949039	19947923	1682		
CG3997	60B7-60B7	Ribosomal protein L39	19949952	19949373	1682		
CG3204	60B7-60B7	Ras-associated protein 2-like	19952928	19950576	1682		
CG4005	60B7-60B8	yorkie	19956008	19953498	1682		
CG3209	60B8-60B8	-	19961075	19956433	1682		
CG42309	60B8-60B8	Muscle LIM protein at 60A	19965746	19962536	1682		
CG10339	60B8-60B8	-	19967999	19965757	1682		
CG13564	60B8-60B8	-	19968915	19968448	1682		
CG16786	60B8-60B9	-	19973683	19969255	1682		
CG4012	60B9-60B10	genghis khan	19986157	19979600			
CG3231	60B9-60B11	something that sticks like glue	19979542	19974129			
CG42567	60C1-60C1	DnaJ-like-60	20046819	20045189			
CG42568	60C1-60C1	-	20046819	20045189			
CG13570	60C1-60C1	spaghetti	20049021	20046888			
CG3328	60C1-60C1	-	20061150	20050013			
CG4326	60C1-60C1	mitochondrial ribosomal protein S17	20061958	20061187			
CG3333	60C1-60C2	Nucleolar protein at 60B	20073866	20062248			
CR32884	60C2-60C2	-	20063890	20063751			
CR34562	60C2-60C2	snoRNA:Me28S-G1083a	20072446	20072363			
CR34563	60C2-60C2	snoRNA:Me28S-G1083b	20072692	20072610			
CR34564	60C2-60C2	snoRNA:Me28S-G1083c	20072928	20072846			
CR34565	60C2-60C2	snoRNA:Me28S-G1083d	20073167	20073085			
CR42804	60C2-60C2	-	20073445	20073348			
CR42805	60C2-60C2	-	20073675	20073585			
CG3363	60C2-60C2	-	20082813	20074226			
CG3362	60C2-60C2	-	20084550	20083065			
CG3356	60C2-60C2	-	20089710	20085405			
CG11406	60C2-60C2	-	20095726	20089614			
CG30419	60C2-60C3	-	20117311	20100014			
CG30418	60C3-60C4	nord	20142617	20130786			
CG13576	60C4-60C4	Ionotropic receptor 60a	20138826	20136578			
CR34658	60C4-60C4	-	20138907	20138792		7561	
CG13575	60C4-60C4	-	20144937	20142168			

CG3376	60C4-60C4	-	20152746	20145552		7561			
CG13577	60C4-60C4	-	20156686	20154899	2604	7561			
CG3385	60C5-60C6	nervy	20178611	20163260	2604	7561			
CG3394	60C6-60C6	-	20185646	20181621	2604	7561			
CG3401	60C6-60C6	beta-Tubulin at 60D	20200626	20193405	2604	7561			
CG4354	60C6-60C6	slow border cells	20221829	20219045	2604	7561			
CG3411	60C6-60C7	blistered	20263998	20231236	2604	7561			
CR33537	60C7-60C7	transfer RNA:asn5:60C	20261659	20261586	2604	7914			
CG13578	60C7-60C7	-	20266263	20265354	2604	7914			
CG4356	60C7-60C7	muscarinic Acetylcholine Receptor 60C	20277235	20266159	2604	7914			
CG4527	60C7-60C8	Sterile20-like kinase	20290245	20279652	2604	7914			
CG3416	60C8-60C8	Mov34	20292050	20290494	2604	7914	8028	9068	
CG4545	60C8-60C8	Serotonin transporter	20298070	20292118	2604	7914	8028	9068	
CG3419	60C8-60C8	-	20302820	20299414	2604	7914	8028	9068	
CG42383	60C8-60C8	-	20312625	20311449	2604	7914	8028	9068	
CG42310	60C8-60C8	prominin	20315910	20302931	2604	7914	8028	9068	
CG15873	60C8-60C8	-	20318136	20317096	2604	7914	8028	9068	
CG15874	60C8-60C8	Phosphoglycerate mutase 5-2	20320256	20318867	2604	7914	8028	9068	
CG3483	60C8-60C8	-	20334362	20333023	2604	7914	8028	9068	
CR34659	60D10-60D10	-	20516267	20516150			8028	9068	
CG3616	60D10-60D10	Cytochrome P450-9c1	20520455	20518598			8028	9068	
CG3640	60D10-60D10	-	20528279	20527211			8028	9068	
CG4781	60D10-60D10	-	20529760	20528206			8028	9068	
CG3663	60D13-60D13	-	20549940	20549047			8028	9068	
CG30163	60D13-60D13	Cuticular protein 60D	20550929	20550374			8028	9068	
CG30161	60D13-60D13	-	20551880	20551055			8028	9068	
CG3683	60D13-60D13	-	20552962	20551921			8028	9068	
CG34214	60D13-60D13	-	20553543	20552950			8028	9068	
CG4806	60D13-60D13	-	20555853	20553681			8028	9068	
CG33228	60D13-60D13	-	20556853	20555934			8028	9068	
CG3691	60D13-60D13	Painting of fourth	20559041	20556901			8028	9068	
CG4859	60D13-60D14	Matrix metalloproteinase 1	20575704	20558817			8028	9068	
CG4871	60D14-60D14	Sialyltransferase	20581071	20578938			8028		
CG33988	60D14-60D16	-	20624176	20586468			8028		
CG4563	60D1-60D1	-	20340560	20338605	2604	7914	8028	9068	
CG3492	60D1-60D1	-	20361756	20360235	2604	7914	8028	9068	
CG3494	60D1-60D1	-	20362704	20361822	2604	7914	8028	9068	
CG16837	60D1-60D1	-	20363544	20362949	2604	7914	8028	9068	
CG13579	60D1-60D1	-	20376970	20342831	2604	7914	8028	9068	
CG13589	60D1-60D1	-	20380378	20379737	2604	7914	8028	9068	
CG13590	60D1-60D1	-	20381471	20380779	2604	7914	8028	9068	
CG13580	60D1-60D1	Caldesmon-related protein	20384550	20382041	2604	7914	8028	9068	
CR42645	60D1-60D1	Yu	20386192	20385606	2604	7914	8028	9068	

CG13591	60D1-60D1	Suppressor of Stellate-like	20387754	20386766	2604	7914	8028	9068		
CG4569	60D1-60D1	Proteasome 28kD subunit 1B	20389757	20388387	2604	7914	8028	9068		
CG30421	60D16-60E1	-	20644501	20631335			8028			
CG13581	60D3-60D3	-	20395236	20394398	2604	7914	8028	9068		
CG4589	60D3-60D3	Letm1	20402813	20397285	2604	7914	8028	9068		
CG42289	60D3-60D3	Ionotropic receptor 60b	20404981	20403248	2604	7914	8028	9068		
CR42290	60D3-60D3	Ionotropic receptor 60c	20406675	20405347	2604	7914	8028	9068		
CG42291	60D3-60D3	Ionotropic receptor 60d	20408670	20406946	2604	7914	8028	9068		
CG4612	60D3-60D4	-	20413647	20409463	2604	7914	8028	9068		
CG30169	60D4-60D4	Breast cancer 2, early onset homolog	20417104	20413724	2604		8028	9068		
CG13592	60D4-60D4	Ionotropic receptor 60e	20418795	20417140	2604		8028	9068		
CG13585	60D4-60D4	-	20420915	20419123	2604		8028	9068		
CG11413	60D4-60D4	-	20424314	20423713	2604		8028	9068		
CG4622	60D4-60D5	-	20443759	20420897	2604		8028	9068		
CG13586	60D4-60D5	ion transport peptide	20446273	20427465	2604		8028	9068		
CG4634	60D5-60D5	Nucleosome remodeling factor - 38kD	20448610	20446490	2604		8028	9068		
CG11414	60D5-60D5	-	20452581	20449132	2604		8028	9068		
CG11416	60D5-60D5	unconventional prefoldin RPB5 interactor	20455605	20453082	2604		8028	9068		
CG12252	60D5-60D5	-	20459106	20455510	2604		8028	9068		
CG3511	60D5-60D5	-	20462027	20459192	2604		8028	9068		
CG3522	60D5-60D5	Start1	20465199	20462079	2604		8028	9068		
CG33527	60D5-60D5	IFamide	20465657	20465089	2604		8028	9068		
CG4681	60D5-60D7	-	20467304	20465770	2604		8028	9068		
CG3541	60D7-60D8	piopio	20485385	20468772	2604		8028	9068		
CG13587	60D8-60D9	-	20486614	20485518	2604		8028	9068		
CG13594	60D9-60D10	-	20526110	20502944			8028	9068		
CG4692	60D9-60D9	-	20487344	20486611	2604		8028	9068		
CG3548	60D9-60D9	-	20489890	20487489	2604		8028	9068		
CG3565	60D9-60D9	-	20491011	20489995	2604		8028	9068		
CG3570	60D9-60D9	-	20492194	20491135	2604		8028	9068		
CG4707	60D9-60D9	-	20494541	20492117	2604		8028	9068		
CG42361	60D9-60D9	-	20496311	20495216	2604		8028	9068		
CG42360	60D9-60D9	-	20498049	20494812	2604		8028	9068		
CG3608	60D9-60D9	-	20501430	20499228	2604		8028	9068		
CG4741	60D9-60D9	-	20502663	20498324	2604		8028	9068		
CG2765	60E10-60E11	-	20852606	20847361		4961				
CG30424	60E11-60E11	-	20854808	20852797		4961				
CG2746	60E11-60E11	Ribosomal protein L19	20857070	20855968		4961				
CG3776	60E11-60E11	-	20858383	20857296		4961				
CG9358	60E11-60E11	Pherokine 3	20859365	20858366		4961				
CG2736	60E11-60E11	-	20862894	20860954		4961				
CG2727	60E11-60E11	epithelial membrane protein	20872321	20863979		4961				
CG3829	60E11-60E11	-	20878012	20873478		4961				

CG15792	60E11-60E12	zipper	20899488	20878093	11215	4961		
CG3533	60E12-60F1	unzipped	20917609	20899573		4961		
CG9196	60E1-60E1	spatzle 6	20647989	20644903			8028	
CG3880	60E1-60E1	-	20650069	20648286			8028	
CG12848	60E1-60E1	-	20650605	20650089			8028	
CG3894	60E1-60E1	-	20654273	20650687			8028	
CG16936	60E1-60E1	-	20655697	20654241			8028	
CG16932	60E1-60E1	Epidermal growth factor receptor pathway substrate clone 15	20662788	20655837			8028	
CG12196	60E1-60E1	eggless	20667437	20663057			8028	
CG16914	60E1-60E1	Larval cuticle protein 9	20667892	20667558			8028	
CG3594	60E1-60E1	Exu-associated protein	20669307	20668468			8028	
CG16912	60E1-60E1	-	20671018	20669244			8028	
CG3589	60E1-60E1	-	20673065	20671095			8028	
CG16910	60E1-60E1	kenny	20674932	20673037			8028	
CG2928	60E1-60E1	Rhythmically expressed gene 5	20680929	20675531			8028	
CG18105	60E1-60E1	Ecdysis triggering hormone	20682981	20682193			8028	
CR43257	60E1-60E1	-	20683295	20681330			8028	
CG2917	60E1-60E2	Origin recognition complex subunit 4	20684927	20683013			8028	
CG12849	60E2-60E2	-	20686136	20685448			8028	
CG3611	60E2-60E2	-	20687085	20686321			8028	
CG42851	60E2-60E2	-	20697212	20696871			8028	
CG3629	60E2-60E2	Distal-less	20722686	20702353			8028	
CG3650	60E3-60E3	-	20737284	20736499			8028	
CG16896	60E4-60E4	-	20762420	20758929			8028	
CG30423	60E4-60E4	-	20763359	20762499			8028	
CG30420	60E4-60E5	Activating transcription factor-2	20767817	20757590			8028	
CG34413	60E5-60E5	Na,K-ATPase Interacting	20776138	20769075			8028	
CG10142	60E5-60E5	Ance-5	20778545	20776151			8028	
CG9083	60E5-60E5	-	20787028	20785801			8028	
CG2857	60E5-60E5	Thiamine pyrophosphate carrier protein 2	20788191	20785425			8028	
CG30425	60E5-60E5	Ribosomal protein L41	20791452	20790940			8028	
CG34405	60E5-60E5	Na channel protein 60E	20807788	20779163			8028	
CG15860	60E5-60E5	painless	20815794	20809028			8028	
CG30427	60E5-60E5	-	20824994	20816270			8028	
CG3760	60E5-60E5	-	20827292	20825862			8028	
CG2811	60E5-60E5	-	20827993	20827229			8028	
CG2803	60E5-60E8	Troponin C-akin-1	20829932	20828148			8028	
CG15861	60E8-60E8	-	20832120	20830914				
CG3770	60E8-60E8	-	20834159	20832666				
CG2790	60E8-60E8	-	20835898	20834084				
CG12851	60E8-60E9	-	20842004	20836170				
CG3441	60F1-60F1	Neuropeptide-like precursor 1	20927520	20919903		4961		
CG2692	60F1-60F2	gooseberry-neuro	20939850	20927905		4961		

CG3388	60F2-60F2	gooseberry	20952166	20949502	4961		
CR30198	60F3-60F3	transfer RNA:CR30198	20963599	20963528	4962		
CR30199	60F3-60F3	transfer RNA:CR30199	20964359	20964288	4963		
CR30200	60F3-60F3	transfer RNA:CR30200	20964642	20964571	4964		
CG2679	60F3-60F3	goliath	20971843	20960150	4961		
CG16778	60F3-60F5	-	20986688	20973303	4961		
CG30430	60F5-60F5	-	21017435	21016955	4961		
CG43106	60F5-60F5	-	21027064	21026184	4961		
CG34038	60F5-60F5	-	21057283	21055457	4961		
CG42478	60F5-60F5	Seminal fluid protein 60F	21060218	21059768	4961		
CG2665	60F5-60F5	Protein ejaculatory bulb II	21061729	21061320	4961		
CG2668	60F5-60F5	Protein ejaculatory bulb	21064238	21062864	4961		
CG9380	60F5-60F5	-	21076360	21071152	4961		
CG3340	60F5-60F5	Kruppel	21117057	21114138	4961		
CG30429	60F5-60F5	-	21135109	21133990	4961		
CG33680	60F5-60F5	-	21137839	21136529	4961		
CG30428	60F5-60F5	-	21142371	21140837	4961		

Appendix 2: Detail of deficiency overlaps for the five deficiencies that had a dendritic phenotype when removed. Different identified deficiencies are found on different sheets

Colours distinguish between deficiencies. Only those genes deleted by *Df(2L)al* are depicted, other deficiencies may extend outside the region shown. Horizontal shading = screen result was negative for a phenotype; diagonal shading = screening not complete.

Annotation ID	Cytological location	Name	Overlaps					
CG4574	21B8-21C1	*Phospholipase C at 21C*	***Df(2L)BSC4***	***Df(2L)al***	***Df(2L)net-PMF***			
CG33992	21C1-21C1	-	***Df(2L)BSC4***	***Df(2L)al***				
CG31920	21C1-21C1	-	***Df(2L)BSC4***	***Df(2L)al***				
CG31921	21C1-21C1	-	***Df(2L)BSC4***	***Df(2L)al***				
CG11907	21C1-21C1	*Equilibrative nucleoside transporter 1*	***Df(2L)BSC4***	***Df(2L)al***				
CG3935	21C1-21C1	*aristaless*	***Df(2L)BSC4***	***Df(2L)al***				
CG4213	21C2-21C2	-	***Df(2L)BSC4***	***Df(2L)al***				
CG4033	21C2-21C2	*RNA polymerase I 135kD subunit*	***Df(2L)BSC4***	***Df(2L)al***				
CG4260	21C2-21C2	*alpha-Adaptin*	***Df(2L)BSC4***	***Df(2L)al***				
CG4063	21C2-21C2	*ebi*	***Df(2L)BSC4***	***Df(2L)al***				
CG13690	21C2-21C2	-	***Df(2L)BSC4***	***Df(2L)al***				
CG4087	21C2-21C2	*Ribosomal protein LP1*	***Df(2L)BSC4***	***Df(2L)al***				
CG11885	21C2-21C2	-	***Df(2L)BSC4***	***Df(2L)al***				
CG13692	21C2-21C2	-	***Df(2L)BSC4***	***Df(2L)al***				
CG13691	21C2-21C2	*BBS8*	***Df(2L)BSC4***	***Df(2L)al***				
CG4114	21C2-21C2	*expanded*	***Df(2L)BSC4***	***Df(2L)al***				***Df(2L)BSC107***
CG4280	21C2-21C2	*croquemort*	***Df(2L)BSC4***	***Df(2L)al***				***Df(2L)BSC107***
CG4164	21C2-21C2	-	***Df(2L)BSC4***	***Df(2L)al***				***Df(2L)BSC107***
CR43080	21C2-21C2	-	***Df(2L)BSC4***	***Df(2L)al***				***Df(2L)BSC107***
CG4133	21C2-21C8	-	***Df(2L)BSC4***	***Df(2L)al***		***Df(2L)BSC16***	***Df(2L)S2***	***Df(2L)BSC107***

Colours distinguish between deficiencies. Only those genes deleted by deficiency *Df(2L)TE35BC-24* are depicted. Other deficiencies may extend outside the region shown. Diagonal shading = screening not complete.

Annotation ID	Cytological location	Name	Overlaps								
CG3710	35B10-35B10	*RNA polymerase II elongation factor*	*Df(2L)TE35BC-24*		*Df(2L)TE35BC-34*				*Df(2L) Sco^{rv14}*		
CG3479	35B3-35B4	*outspread*	*Df(2L)TE35BC-24*		*Df(2L)TE35BC-34*				*Df(2L) Sco^{rv14}*		
CG15282	35B4-35B4	-	*Df(2L)TE35BC-24*		*Df(2L)TE35BC-34*				*Df(2L) Sco^{rv14}*		
CG34165	35B4-35B4	-	*Df(2L)TE35BC-24*		*Df(2L)TE35BC-34*				*Df(2L) Sco^{rv14}*		
CG42685	35B5-35B5	-	*Df(2L)TE35BC-24*		*Df(2L)TE35BC-34*						
CG31835	35B5-35B5	-	*Df(2L)TE35BC-24*		*Df(2L)TE35BC-34*						
CG31775	35B5-35B5	-	*Df(2L)TE35BC-24*		*Df(2L)TE35BC-34*						
CG42585	35B5-35B5	-	*Df(2L)TE35BC-24*		*Df(2L)TE35BC-34*						
CG42586	35B5-35B5	-	*Df(2L)TE35BC-24*		*Df(2L)TE35BC-34*						
CG34166	35B5-35B5	-	*Df(2L)TE35BC-24*		*Df(2L)TE35BC-34*						
CG42681	35B5-35B5	-	*Df(2L)TE35BC-24*		*Df(2L)TE35BC-34*						
CG42587	35B5-35B5	-	*Df(2L)TE35BC-24*		*Df(2L)TE35BC-34*						
CG4691	35B5-35B5	-	*Df(2L)TE35BC-24*		*Df(2L)TE35BC-34*						
CG4697	35B5-35B5	*COP9 complex homolog subunit 1 a*	*Df(2L)TE35BC-24*		*Df(2L)TE35BC-34*						
CG4701	35B5-35B5	-	*Df(2L)TE35BC-24*		*Df(2L)TE35BC-34*						
CG4650	35B5-35B5	-	*Df(2L)TE35BC-24*		*Df(2L)TE35BC-34*						
CR15280	35B5-35B5	-	*Df(2L)TE35BC-24*		*Df(2L)TE35BC-34*						
CG18636	35B5-35B5	-	*Df(2L)TE35BC-24*		*Df(2L)TE35BC-34*						
CG18420	35B6-35B6	-	*Df(2L)TE35BC-24*		*Df(2L)TE35BC-34*						
CG33308	35B6-35B6	-	*Df(2L)TE35BC-24*		*Df(2L)TE35BC-34*						
CG33309	35B6-35B6	-	*Df(2L)TE35BC-24*		*Df(2L)TE35BC-34*						
CG42682	35B6-35B6	-	*Df(2L)TE35BC-24*		*Df(2L)TE35BC-34*						
CG15279	35B6-35B6	-	*Df(2L)TE35BC-24*		*Df(2L)TE35BC-34*						
CG4480	35B6-35B6	-	*Df(2L)TE35BC-24*		*Df(2L)TE35BC-34*						
CG15278	35B6-35B6	-	*Df(2L)TE35BC-24*		*Df(2L)TE35BC-34*						
CG4479	35B6-35B7	*Male-specific-transcript-35Ba*	*Df(2L)TE35BC-24*		*Df(2L)TE35BC-34*						
CG4478	35B7-35B7	*Male-specific-transcript-35Bb*	*Df(2L)TE35BC-24*		*Df(2L)TE35BC-34*						
CG3491	35B7-35B7	-	*Df(2L)TE35BC-24*		*Df(2L)TE35BC-34*						
CG42313	35B7-35B7	-	*Df(2L)TE35BC-24*		*Df(2L)TE35BC-34*						
CG4482	35B7-35B8	*moladietz*	*Df(2L)TE35BC-24*		*Df(2L)TE35BC-34*						
CG4103	35B8-35B4	*lethal (2) 35Bc*	*Df(2L)TE35BC-24*		*Df(2L)TE35BC-34*						
CG10846	35B8-35B8	*dynactin-subunit-p25*	*Df(2L)TE35BC-24*		*Df(2L)TE35BC-34*						
CG4140	35B8-35B8	*lethal (2) 35Be*	*Df(2L)TE35BC-24*		*Df(2L)TE35BC-34*						
CG4185	35B8-35B8	*NC2beta*	*Df(2L)TE35BC-24*		*Df(2L)TE35BC-34*						
CG3688	35B8-35B8	*lethal (2) 35Bd*	*Df(2L)TE35BC-24*		*Df(2L)TE35BC-34*						
CG33310	35B8-35B8	-	*Df(2L)TE35BC-24*		*Df(2L)TE35BC-34*						
CG31832	35B8-35B8	-	*Df(2L)TE35BC-24*		*Df(2L)TE35BC-34*						
CG15274	35B8-35B8	*metabotropic GABA-B receptor subtype 1*	*Df(2L)TE35BC-24*		*Df(2L)TE35BC-34*						
CG4182	35B8-35B8	*yellow-c*	*Df(2L)TE35BC-24*		*Df(2L)TE35BC-34*						
CG4180	35B8-35B8	*lethal (2) 35Bg*	*Df(2L)TE35BC-24*		*Df(2L)TE35BC-34*						
CG3497	35B8-35B8	*Suppressor of Hairless*	*Df(2L)TE35BC-24*		*Df(2L)TE35BC-34*						
CG7595	35B8-35B9	*crinkled*	*Df(2L)TE35BC-24*		*Df(2L)TE35BC-34*						
CG33679	35B9-35B10	-	*Df(2L)TE35BC-24*		*Df(2L)TE35BC-34*						
CG4170	35C1-35C1	*vasa intronic gene*	*Df(2L)TE35BC-24*		*Df(2L)TE35BC-34*						
CG43081	35C1-35C1	*vasa*	*Df(2L)TE35BC-24*		*Df(2L)TE35BC-34*						
CG15270	35C1-35C2	-	*Df(2L)TE35BC-24*		*Df(2L)TE35BC-34*						
CG15269	35C2-35C2	-	*Df(2L)TE35BC-24*		*Df(2L)TE35BC-34*						
CG3647	35C2-35C2	*shuttle craft*	*Df(2L)TE35BC-24*		*Df(2L)TE35BC-34*						
CR31831	35C2-35C2	*tRNA:L:35C*	*Df(2L)TE35BC-24*		*Df(2L)TE35BC-34*						
CG4168	35C3-35C3	-	*Df(2L)TE35BC-24*		*Df(2L)TE35BC-34*						
CG42475	35C3-35C3	*Seminal fluid protein 35C*	*Df(2L)TE35BC-24*		*Df(2L)TE35BC-34*						
CR43357	35C3-35C3	-	*Df(2L)TE35BC-24*		*Df(2L)TE35BC-34*						
CG43230	35C4-35C4	-	*Df(2L)TE35BC-24*		*Df(2L)TE35BC-34*						
CG3994	35C4-35C5	-	*Df(2L)TE35BC-24*		*Df(2L)TE35BC-34*						
CG15267	35C5-35C5	*down and out*	*Df(2L)TE35BC-24*		*Df(2L)TE35BC-34*						
CG3975	35C5-35C5	-	*Df(2L)TE35BC-24*		*Df(2L)TE35BC-34*						
CG15266	35C5-35C5	*lethal (2) 35Cc*	*Df(2L)TE35BC-24*		*Df(2L)TE35BC-34*						
CG31732	35C5-35C5	*yuri gagarin*	*Df(2L)TE35BC-24*		*Df(2L)TE35BC-34*	*Df(2L)Exel8034*					
CG42616	35C5-35C5	*Cullin-3*	*Df(2L)TE35BC-24*		*Df(2L)TE35BC-34*	*Df(2L)Exel8034*					
CG15261	35D1-35D1	*UK114*	*Df(2L)TE35BC-24*	*Df(2L)r10*	*Df(2L)TE35BC-34*	*Df(2L)Exel8034*	*Df(2L) Sco^{rv25}*	*Df(2L)Sco^{rv10}*	*Df(2L) Sco^{rv14}*		
CG15263	35D1-35D1	-	*Df(2L)TE35BC-24*	*Df(2L)r10*	*Df(2L)TE35BC-34*	*Df(2L)Exel8034*	*Df(2L) Sco^{rv25}*	*Df(2L)Sco^{rv10}*	*Df(2L) Sco^{rv14}*		
CG15260	35D1-35D1	-	*Df(2L)TE35BC-24*	*Df(2L)r10*	*Df(2L)TE35BC-34*	*Df(2L)Exel8034*	*Df(2L) Sco^{rv25}*	*Df(2L)Sco^{rv10}*	*Df(2L) Sco^{rv14}*		
CG31733	35D1-35D1	*ms(2)35Ci*	*Df(2L)TE35BC-24*	*Df(2L)r10*	*Df(2L)TE35BC-34*	*Df(2L)Exel8034*	*Df(2L) Sco^{rv25}*	*Df(2L)Sco^{rv10}*	*Df(2L) Sco^{rv14}*		
CG15262	35D1-35D1	-	*Df(2L)TE35BC-24*	*Df(2L)r10*	*Df(2L)TE35BC-34*	*Df(2L)Exel8034*	*Df(2L) Sco^{rv25}*	*Df(2L)Sco^{rv10}*	*Df(2L) Sco^{rv14}*		
CG15259	35D1-35D1	*no hitter*	*Df(2L)TE35BC-24*	*Df(2L)r10*	*Df(2L)TE35BC-34*	*Df(2L)Exel8034*	*Df(2L) Sco^{rv25}*	*Df(2L)Sco^{rv10}*	*Df(2L) Sco^{rv14}*		
CG3758	35D2-35D2	*escargot*	*Df(2L)TE35BC-24*	*Df(2L)r10*	*Df(2L)TE35BC-34*	*Df(2L)Exel8034*	*Df(2L) Sco^{rv25}*	*Df(2L)Sco^{rv10}*	*Df(2L) Sco^{rv14}*		
CG15258	35D2-35D2	-	*Df(2L)TE35BC-24*	*Df(2L)r10*	*Df(2L)TE35BC-34*	*Df(2L)Exel8034*	*Df(2L) Sco^{rv25}*	*Df(2L)Sco^{rv10}*	*Df(2L) Sco^{rv14}*		
CG4158	35D2-35D2	*worniu*	*Df(2L)TE35BC-24*	*Df(2L)r10*	*Df(2L)TE35BC-34*	*Df(2L)Exel8034*	*Df(2L) Sco^{rv25}*	*Df(2L)Sco^{rv10}*	*Df(2L) Sco^{rv14}*		
CG4161	35D2-35D2	-	*Df(2L)TE35BC-24*	*Df(2L)r10*	*Df(2L)TE35BC-34*	*Df(2L)Exel8034*	*Df(2L) Sco^{rv25}*	*Df(2L)Sco^{rv10}*	*Df(2L) Sco^{rv14}*	*Df(2L)Exel7063*	
CG3956	35D2-35D2	*snail*	*Df(2L)TE35BC-24*	*Df(2L)r10*	*Df(2L)TE35BC-34*		*Df(2L) Sco^{rv25}*	*Df(2L)Sco^{rv10}*	*Df(2L) Sco^{rv14}*	*Df(2L)Exel7063*	
CG15257	35D2-35D2	*Translocase inner membrane 17*	*Df(2L)TE35BC-24*	*Df(2L)r10*	*Df(2L)TE35BC-34*		*Df(2L) Sco^{rv25}*	*Df(2L)Sco^{rv10}*	*Df(2L) Sco^{rv14}*	*Df(2L)Exel7063*	
CG4162	35D2-35D2	*lace*	*Df(2L)TE35BC-24*	*Df(2L)r10*	*Df(2L)TE35BC-34*		*Df(2L) Sco^{rv25}*	*Df(2L)Sco^{rv10}*	*Df(2L) Sco^{rv14}*	*Df(2L)Exel7063*	
CG42448	35D3-35D3	-	*Df(2L)TE35BC-24*	*Df(2L)r10*	*Df(2L)TE35BC-34*		*Df(2L) Sco^{rv25}*	*Df(2L)Sco^{rv10}*	*Df(2L) Sco^{rv14}*	*Df(2L)Exel7063*	
CG15256	35D3-35D3	-	*Df(2L)TE35BC-24*	*Df(2L)r10*	*Df(2L)TE35BC-34*		*Df(2L) Sco^{rv25}*	*Df(2L)Sco^{rv10}*	*Df(2L) Sco^{rv14}*	*Df(2L)Exel7063*	
CG4192	35D3-35D3	*kekkon-3*	*Df(2L)TE35BC-24*	*Df(2L)r10*	*Df(2L)TE35BC-34*		*Df(2L) Sco^{rv25}*	*Df(2L)Sco^{rv10}*	*Df(2L) Sco^{rv14}*	*Df(2L)Exel7063*	
CG15255	35D3-35D3	-	*Df(2L)TE35BC-24*	*Df(2L)r10*	*Df(2L)TE35BC-34*		*Df(2L) Sco^{rv25}*	*Df(2L)Sco^{rv10}*	*Df(2L) Sco^{rv14}*	*Df(2L)Exel7063*	
CG11864	35D3-35D3	-	*Df(2L)TE35BC-24*	*Df(2L)r10*	*Df(2L)TE35BC-34*		*Df(2L) Sco^{rv25}*	*Df(2L)Sco^{rv10}*	*Df(2L) Sco^{rv14}*	*Df(2L)Exel7063*	
CG15254	35D3-35D3	-	*Df(2L)TE35BC-24*	*Df(2L)r10*	*Df(2L)TE35BC-34*		*Df(2L) Sco^{rv25}*	*Df(2L)Sco^{rv10}*	*Df(2L) Sco^{rv14}*	*Df(2L)Exel7063*	
CG15253	35D3-35D3	-	*Df(2L)TE35BC-24*	*Df(2L)r10*	*Df(2L)TE35BC-34*		*Df(2L) Sco^{rv25}*	*Df(2L)Sco^{rv10}*	*Df(2L) Sco^{rv14}*	*Df(2L)Exel7063*	
CG11865	35D3-35D3	-	*Df(2L)TE35BC-24*	*Df(2L)r10*	*Df(2L)TE35BC-34*		*Df(2L) Sco^{rv25}*	*Df(2L)Sco^{rv10}*	*Df(2L) Sco^{rv14}*	*Df(2L)Exel7063*	
CG17868	35D3-35D3	*Odorant receptor 35a*	*Df(2L)TE35BC-24*	*Df(2L)r10*	*Df(2L)TE35BC-34*		*Df(2L) Sco^{rv25}*	*Df(2L)Sco^{rv10}*	*Df(2L) Sco^{rv14}*	*Df(2L)Exel7063*	
CG7631	35D3-35D3	-	*Df(2L)TE35BC-24*	*Df(2L)r10*	*Df(2L)TE35BC-34*		*Df(2L) Sco^{rv25}*	*Df(2L)Sco^{rv10}*	*Df(2L) Sco^{rv14}*	*Df(2L)Exel7063*	
CG18480	35D3-35D3	-	*Df(2L)TE35BC-24*	*Df(2L)r10*	*Df(2L)TE35BC-34*		*Df(2L) Sco^{rv25}*	*Df(2L)Sco^{rv10}*	*Df(2L) Sco^{rv14}*	*Df(2L)Exel7063*	
CG18477	35D3-35D3	-	*Df(2L)TE35BC-24*	*Df(2L)r10*	*Df(2L)TE35BC-34*		*Df(2L) Sco^{rv25}*	*Df(2L)Sco^{rv10}*	*Df(2L) Sco^{rv14}*	*Df(2L)Exel7063*	
CG18478	35D3-35D3	-	*Df(2L)TE35BC-24*	*Df(2L)r10*	*Df(2L)TE35BC-34*		*Df(2L) Sco^{rv25}*	*Df(2L)Sco^{rv10}*	*Df(2L) Sco^{rv14}*	*Df(2L)Exel7063*	
CG31780	35D3-35D3	-	*Df(2L)TE35BC-24*	*Df(2L)r10*	*Df(2L)TE35BC-34*		*Df(2L) Sco^{rv25}*	*Df(2L)Sco^{rv10}*	*Df(2L) Sco^{rv14}*	*Df(2L)Exel7063*	

CG31827	35D3-35D3	-	Df(2L)TE35BC-24	Df(2L)r10	Df(2L)TE35BC-34		Df(2L) Sco^{rv25}	Df(2L)Sco^{rv10}	Df(2L) Sco^{rv14}	Df(2L)Exel7063
CG4587	35D3-35D3	-	Df(2L)TE35BC-24	Df(2L)r10	Df(2L)TE35BC-34		Df(2L) Sco^{rv25}	Df(2L)Sco^{rv10}	Df(2L) Sco^{rv14}	Df(2L)Exel7063
CG3938	35D4-35D4	Cyclin E	Df(2L)TE35BC-24	Df(2L)r10	Df(2L)TE35BC-34		Df(2L) Sco^{rv25}	Df(2L)Sco^{rv10}	Df(2L) Sco^{rv14}	Df(2L)Exel7063
CG13240	35D4-35D4	lethal (2) 35Di	Df(2L)TE35BC-24	Df(2L)r10	Df(2L)TE35BC-34		Df(2L) Sco^{rv25}	Df(2L)Sco^{rv10}	Df(2L) Sco^{rv14}	
CR32877	35D4-35D4	small nuclear RNA U5 at 35EF	Df(2L)TE35BC-24	Df(2L)r10	Df(2L)TE35BC-34		Df(2L) Sco^{rv25}	Df(2L)Sco^{rv10}	Df(2L) Sco^{rv14}	
CG4152	35D4-35D4	lethal (2) 35Df	Df(2L)TE35BC-24	Df(2L)r10	Df(2L)TE35BC-34		Df(2L) Sco^{rv25}	Df(2L)Sco^{rv10}	Df(2L) Sco^{rv14}	
CG3903	35D4-35D4	Gliotactin	Df(2L)TE35BC-24	Df(2L)r10	Df(2L)TE35BC-34		Df(2L) Sco^{rv25}	Df(2L)Sco^{rv10}	Df(2L) Sco^{rv14}	
CG3793	35D4-35D4	-	Df(2L)TE35BC-24	Df(2L)r10	Df(2L)TE35BC-34		Df(2L) Sco^{rv25}	Df(2L)Sco^{rv10}	Df(2L) Sco^{rv14}	
CG4148	35D4-35D4	weckle	Df(2L)TE35BC-24	Df(2L)r10	Df(2L)TE35BC-34		Df(2L) Sco^{rv25}	Df(2L)Sco^{rv10}	Df(2L) Sco^{rv14}	
CG18801	35D4-35D4	Ku80	Df(2L)TE35BC-24	Df(2L)r10	Df(2L)TE35BC-34		Df(2L) Sco^{rv25}	Df(2L)Sco^{rv10}	Df(2L) Sco^{rv14}	
CG31826	35D4-35D4	-	Df(2L)TE35BC-24	Df(2L)r10	Df(2L)TE35BC-34		Df(2L) Sco^{rv25}	Df(2L)Sco^{rv10}	Df(2L) Sco^{rv14}	
CG18109	35D4-35D4	-	Df(2L)TE35BC-24	Df(2L)r10	Df(2L)TE35BC-34		Df(2L) Sco^{rv25}	Df(2L)Sco^{rv10}	Df(2L) Sco^{rv14}	
CG42876	35D4-35D4	-	Df(2L)TE35BC-24	Df(2L)r10	Df(2L)TE35BC-34		Df(2L) Sco^{rv25}	Df(2L)Sco^{rv10}	Df(2L) Sco^{rv14}	
CG18518	35D4-35D4	-	Df(2L)TE35BC-24	Df(2L)r10	Df(2L)TE35BC-34		Df(2L) Sco^{rv25}	Df(2L)Sco^{rv10}	Df(2L) Sco^{rv14}	
CR31822	35D4-35D4	-	Df(2L)TE35BC-24	Df(2L)r10	Df(2L)TE35BC-34		Df(2L) Sco^{rv25}	Df(2L)Sco^{rv10}	Df(2L) Sco^{rv14}	
CG13243	35D4-35D5	-	Df(2L)TE35BC-24	Df(2L)r10	Df(2L)TE35BC-34		Df(2L) Sco^{rv25}	Df(2L)Sco^{rv10}	Df(2L) Sco^{rv14}	
CG4767	35D5-35D5	Tektin A	Df(2L)TE35BC-24	Df(2L)r10	Df(2L)TE35BC-34		Df(2L) Sco^{rv25}	Df(2L)Sco^{rv10}	Df(2L) Sco^{rv14}	
CG42791	35D5-35D5	-	Df(2L)TE35BC-24	Df(2L)r10	Df(2L)TE35BC-34		Df(2L) Sco^{rv25}	Df(2L)Sco^{rv10}	Df(2L) Sco^{rv14}	
CG42792	35D5-35D5	-	Df(2L)TE35BC-24	Df(2L)r10	Df(2L)TE35BC-34		Df(2L) Sco^{rv25}	Df(2L)Sco^{rv10}	Df(2L) Sco^{rv14}	
CG7653	35D5-35D5	-	Df(2L)TE35BC-24	Df(2L)r10	Df(2L)TE35BC-34		Df(2L) Sco^{rv25}	Df(2L)Sco^{rv10}	Df(2L) Sco^{rv14}	
CR31824	35D6-35D6	-	Df(2L)TE35BC-24	Df(2L)r10				Df(2L)Sco^{rv10}	Df(2L) Sco^{rv14}	
CG18096	35D6-35D6	Thiolester containing protein I	Df(2L)TE35BC-24	Df(2L)r10				Df(2L)Sco^{rv10}	Df(2L) Sco^{rv14}	
CG31735	35D6-35D6	-	Df(2L)TE35BC-24	Df(2L)r10				Df(2L)Sco^{rv10}	Df(2L) Sco^{rv14}	
CG31823	35D6-35D6	-	Df(2L)TE35BC-24	Df(2L)r10				Df(2L)Sco^{rv10}	Df(2L) Sco^{rv14}	
CG31821	35D6-35D6	-	Df(2L)TE35BC-24	Df(2L)r10				Df(2L)Sco^{rv10}	Df(2L) Sco^{rv14}	
CG13244	35D6-35D6	-	Df(2L)TE35BC-24	Df(2L)r10				Df(2L)Sco^{rv10}	Df(2L) Sco^{rv14}	
CG4793	35D6-35D6	-	Df(2L)TE35BC-24	Df(2L)r10				Df(2L)Sco^{rv10}	Df(2L) Sco^{rv14}	
CG7644	35D6-35D7	beaten path Ib	Df(2L)TE35BC-24	Df(2L)r10				Df(2L)Sco^{rv10}	Df(2L) Sco^{rv14}	
CG12448	35D7-35D7	-	Df(2L)TE35BC-24	Df(2L)r10				Df(2L)Sco^{rv10}	Df(2L) Sco^{rv14}	
CG18063	35D7-35D7	-	Df(2L)TE35BC-24	Df(2L)r10				Df(2L)Sco^{rv10}	Df(2L) Sco^{rv14}	
CG10839	35E1-35E1	-	Df(2L)TE35BC-24	Df(2L)r10	Df(2L)RA5			Df(2L)Sco^{rv10}	Df(2L) Sco^{rv14}	
CG34167	35E1-35E1	-	Df(2L)TE35BC-24	Df(2L)r10	Df(2L)RA5			Df(2L)Sco^{rv10}	Df(2L) Sco^{rv14}	
CG13245	35E1-35E1	-	Df(2L)TE35BC-24	Df(2L)r10	Df(2L)RA5			Df(2L)Sco^{rv10}	Df(2L) Sco^{rv14}	
CG31820	35E1-35E1	-	Df(2L)TE35BC-24	Df(2L)r10	Df(2L)RA5			Df(2L)Sco^{rv10}	Df(2L) Sco^{rv14}	
CG4838	35E1-35E1	beaten path Ic	Df(2L)TE35BC-24	Df(2L)r10	Df(2L)RA5			Df(2L)Sco^{rv10}	Df(2L) Sco^{rv14}	
CG4824	35E2-35E2	Bicaudal C	Df(2L)TE35BC-24	Df(2L)r10	Df(2L)RA5				Df(2L) Sco^{rv14}	
CG4846	35E2-35E2	beaten path Ia	Df(2L)TE35BC-24	Df(2L)r10	Df(2L)RA5				Df(2L) Sco^{rv14}	
CG4891	35E2-35E2	-	Df(2L)TE35BC-24	Df(2L)r10	Df(2L)RA5				Df(2L) Sco^{rv14}	

Colours distinguish between deficiencies. Only those genes deleted by deficiency line *Df(2R)Np5* are depicted, other deficiencies may extend outside the region shown. Horizontal shading = screen result was negative for a phenotype; diagonal shading = screening not complete.

Annotation ID	Cytological location	Name	Overlaps				
CG8224	44F11-44F12	*baboon*	*Df(2R)H3E1*	*Df(2R)Np5*			
CG8216	44F12-44F12	-	*Df(2R)H3E1*	*Df(2R)Np5*			
CG8213	44F12-45A1	-	*Df(2R)H3E1*	*Df(2R)Np5*			
CG8058	45A11-45A11	*alpha/beta hydrolase 1*	*Df(2R)H3E1*	*Df(2R)Np5*		*Df(2R)w73-1*	*Df(2R)w73-2*
CG8788	45A11-45A12	-	*Df(2R)H3E1*	*Df(2R)Np5*		*Df(2R)w73-1*	*Df(2R)w73-2*
CG8057	45A11-45B1	*alicorn*	*Df(2R)H3E1*	*Df(2R)Np5*		*Df(2R)w73-1*	*Df(2R)w73-2*
CG30342	45A12-45A12	*pre-mRNA processing factor 38*	*Df(2R)H3E1*	*Df(2R)Np5*		*Df(2R)w73-1*	*Df(2R)w73-2*
CG30344	45A12-45A13	-	*Df(2R)H3E1*	*Df(2R)Np5*		*Df(2R)w73-1*	*Df(2R)w73-2*
CG8055	45A12-45E	*shrub*	*Df(2R)H3E1*	*Df(2R)Np5*		*Df(2R)w73-1*	*Df(2R)w73-2*
CG30345	45A13-45A13	-	*Df(2R)H3E1*	*Df(2R)Np5*		*Df(2R)w73-1*	*Df(2R)w73-2*
CG34350	45A1-45A1	-	*Df(2R)H3E1*	*Df(2R)Np5*			
CG8172	45A1-45A1	-	*Df(2R)H3E1*	*Df(2R)Np5*			
CG13744	45A1-45A1	-	*Df(2R)H3E1*	*Df(2R)Np5*			
CG13747	45A1-45A1	-	*Df(2R)H3E1*	*Df(2R)Np5*			
CG8170	45A1-45A1	-	*Df(2R)H3E1*	*Df(2R)Np5*			
CG8196	45A1-45A1	*Ance-4*	*Df(2R)H3E1*	*Df(2R)Np5*			
CG8193	45A1-45A1	-	*Df(2R)H3E1*	*Df(2R)Np5*			
CG13743	45A1-45A1	-	*Df(2R)H3E1*	*Df(2R)Np5*			
CG8197	45A1-45A1	-	*Df(2R)H3E1*	*Df(2R)Np5*			
CG8084	45A1-45A1	*anachronism*	*Df(2R)H3E1*	*Df(2R)Np5*			
CG8083	45A1-45A1	-	*Df(2R)H3E1*	*Df(2R)Np5*			
CG11778	45A1-45A1	-	*Df(2R)H3E1*	*Df(2R)Np5*			
CG13742	45A1-45A1	-	*Df(2R)H3E1*	*Df(2R)Np5*			
CG12759	45A1-45A2	*DEAD box protein 45A*	*Df(2R)H3E1*	*Df(2R)Np5*			
CG8080	45A2-45A2	-		*Df(2R)Np5*			
CG13741	45A2-45A2	-		*Df(2R)Np5*			
CR34525	45A2-45A2	*snoRNA:Psi28S-2949*		*Df(2R)Np5*			
CR33637	45A2-45A3	*snoRNA:Or-aca5*		*Df(2R)Np5*			
CR42451	45A2-45A3	*Uhg4*		*Df(2R)Np5*			
CR34526	45A3-45A3	*snoRNA:Me28S-G3255a*		*Df(2R)Np5*			
CR34527	45A3-45A3	*snoRNA:Me28S-A982a*		*Df(2R)Np5*			
CR34528	45A3-45A3	*snoRNA:Me28S-A982b*		*Df(2R)Np5*			
CR34529	45A3-45A3	*snoRNA:Me28S-G3255b*		*Df(2R)Np5*			
CR33636	45A3-45A3	-		*Df(2R)Np5*			
CG8078	45A3-45A3	-		*Df(2R)Np5*			
CG8777	45A3-45A4	-		*Df(2R)Np5*			
CG8075	45A4-45A6	*Van Gogh*	*Df(2R)w45-30n*	*Df(2R)Np5*	*Df(2R)G53*		
CG8073	45A6-45A7	*Phosphomannomutase 45A*	*Df(2R)w45-30n*	*Df(2R)Np5*	*Df(2R)G53*		
CG8781	45A7-45A7	*tsunagi*	*Df(2R)w45-30n*	*Df(2R)Np5*	*Df(2R)G53*		
CG8070	45A7-45A8	*Mystery 45A*	*Df(2R)w45-30n*	*Df(2R)Np5*	*Df(2R)G53*		
CG8069	45A8-45A8	*Phosphorylated adaptor for RNA export*	*Df(2R)w45-30n*	*Df(2R)Np5*	*Df(2R)G53*		
CG8068	45A8-45A9	*Suppressor of variegation 2-10*	*Df(2R)w45-30n*	*Df(2R)Np5*	*Df(2R)G53*	*Df(2R)w73-1*	*Df(2R)w73-2*
CG18659	45A9-45A10	-	*Df(2R)w45-30n*	*Df(2R)Np5*	*Df(2R)G53*	*Df(2R)w73-1*	*Df(2R)w73-2*
CG11784	45A9-45A9	-	*Df(2R)w45-30n*	*Df(2R)Np5*	*Df(2R)G53*	*Df(2R)w73-1*	*Df(2R)w73-2*
CG8008	45B1-45B1	-	*Df(2R)w45-30n*	*Df(2R)Np5*		*Df(2R)w73-1*	*Df(2R)w73-2*
CG8046	45B1-45B1	-	*Df(2R)w45-30n*	*Df(2R)Np5*		*Df(2R)w73-1*	*Df(2R)w73-2*
CG2412	45B1-45B1	*Rad51C*	*Df(2R)w45-30n*	*Df(2R)Np5*		*Df(2R)w73-1*	*Df(2R)w73-2*
CG42382	45B1-45B1	-	*Df(2R)w45-30n*	*Df(2R)Np5*		*Df(2R)w73-1*	*Df(2R)w73-2*
CG8014	45B1-45B2	*Receptor mediated endocytosis 8*	*Df(2R)w45-30n*	*Df(2R)Np5*		*Df(2R)w73-1*	*Df(2R)w73-2*
CG8024	45B2-45B3	*lightoid*	*Df(2R)w45-30n*	*Df(2R)Np5*		*Df(2R)w73-1*	*Df(2R)w73-2*
CG8026	45B3-45B3	-	*Df(2R)w45-30n*	*Df(2R)Np5*		*Df(2R)w73-1*	*Df(2R)w73-2*
CG1650	45B3-45B3	*unplugged*	*Df(2R)w45-30n*	*Df(2R)Np5*		*Df(2R)w73-1*	*Df(2R)w73-2*
CG8027	45B3-45B4	-	*Df(2R)w45-30n*	*Df(2R)Np5*		*Df(2R)w73-1*	*Df(2R)w73-2*
CG8029	45B4-45B4	*Vacuolar H[+] ATPase accessory protein AC45*	*Df(2R)w45-30n*	*Df(2R)Np5*		*Df(2R)w73-1*	*Df(2R)w73-2*
CG1944	45B7-45B7	*Cyp4p2*	*Df(2R)w45-30n*	*Df(2R)Np5*		*Df(2R)w73-1*	*Df(2R)w73-2*
CG10842	45B7-45B7	*Cytochrome P450-4p1*	*Df(2R)w45-30n*	*Df(2R)Np5*		*Df(2R)w73-1*	*Df(2R)w73-2*
CG10843	45B7-45B7	*Cyp4p3*	*Df(2R)w45-30n*	*Df(2R)Np5*		*Df(2R)w73-1*	*Df(2R)w73-2*
CG2040	45B7-45B8	*hikaru genki*	*Df(2R)w45-30n*	*Df(2R)Np5*		*Df(2R)w73-1*	*Df(2R)w73-2*
CG30343	45C1-45C1	-	*Df(2R)w45-30n*	*Df(2R)Np5*		*Df(2R)w73-1*	*Df(2R)w73-2*
CG34141	45C1-45C1	-	*Df(2R)w45-30n*	*Df(2R)Np5*		*Df(2R)w73-1*	*Df(2R)w73-2*
CG2049	45C1-45C1	*Protein kinase related to protein kinase N*	*Df(2R)w45-30n*	*Df(2R)Np5*		*Df(2R)w73-1*	*Df(2R)w73-2*
CG2063	45C1-45C1	-	*Df(2R)w45-30n*	*Df(2R)Np5*		*Df(2R)w73-1*	*Df(2R)w73-2*
CG1968	45C1-45C4	-	*Df(2R)w45-30n*	*Df(2R)Np5*		*Df(2R)w73-1*	*Df(2R)w73-2*
CG2072	45C4-45C4	-	*Df(2R)w45-30n*	*Df(2R)Np5*		*Df(2R)w73-1*	*Df(2R)w73-2*
CG1975	45C4-45C5	*DNA fragmentation factor-related protein 2*	*Df(2R)w45-30n*	*Df(2R)Np5*		*Df(2R)w73-1*	*Df(2R)w73-2*
CG2078	45C5-45C5	*Myd88*	*Df(2R)w45-30n*	*Df(2R)Np5*		*Df(2R)w73-1*	*Df(2R)w73-2*

CR42927	45C6-45C6	*mir-987 stem loop*	~~Df(2R)w45-30n~~	Df(2R)Np5		Df(2R)w73-1	Df(2R)w73-2			
CG13739	45C6-45D1	-	~~Df(2R)w45-30n~~	Df(2R)Np5	Df(2R)wun-GL	Df(2R)w73-1	Df(2R)w73-2	Df(2R)w45-19g		
CG1978	45D1-45D1	*Odorant receptor 45a*	~~Df(2R)w45-30n~~	Df(2R)Np5	Df(2R)wun-GL	Df(2R)w73-1	Df(2R)w73-2	Df(2R)w45-19g		
CG12158	45D1-45D1	-	~~Df(2R)w45-30n~~	Df(2R)Np5	Df(2R)wun-GL	Df(2R)w73-1	Df(2R)w73-2	Df(2R)w45-19g		
CG13954	45D1-45D1	-	~~Df(2R)w45-30n~~	Df(2R)Np5	Df(2R)wun-GL	Df(2R)w73-1	Df(2R)w73-2	Df(2R)w45-19g		
CG8799	45D1-45D1	*lethal (2) 03659*	~~Df(2R)w45-30n~~	Df(2R)Np5	Df(2R)wun-GL	Df(2R)w73-1	Df(2R)w73-2	Df(2R)w45-19g		
CG8800	45D1-45D2	-	~~Df(2R)w45-30n~~	Df(2R)Np5	Df(2R)wun-GL	Df(2R)w73-1	Df(2R)w73-2	Df(2R)w45-19g		
CG8801	45D2-45D3	-	~~Df(2R)w45-30n~~	Df(2R)Np5	Df(2R)wun-GL	Df(2R)w73-1	Df(2R)w73-2	Df(2R)w45-19g	Df(2R)BSC29	
CG13951	45D3-45D3	*lethal (2) k10Df(2R)H3E1*	~~Df(2R)w45-30n~~	Df(2R)Np5	Df(2R)wun-GL	Df(2R)w73-1	Df(2R)w73-2	Df(2R)w45-19g	Df(2R)BSC29	
CG33774	45D3-45D3	-	~~Df(2R)w45-30n~~	Df(2R)Np5	Df(2R)wun-GL	Df(2R)w73-1	Df(2R)w73-2	Df(2R)w45-19g	Df(2R)BSC29	
CG8804	45D3-45D4	*wunen*	~~Df(2R)w45-30n~~	Df(2R)Np5	Df(2R)wun-GL	Df(2R)w73-1	Df(2R)w73-2	Df(2R)w45-19g	Df(2R)BSC29	
CG8805	45D4-45D5	*wunen-2*	~~Df(2R)w45-30n~~	Df(2R)Np5	Df(2R)wun-GL	Df(2R)w73-1	Df(2R)w73-2	Df(2R)w45-19g	Df(2R)BSC29	
CG13955	45D5-45D5	-	~~Df(2R)w45-30n~~	Df(2R)Np5	Df(2R)wun-GL	Df(2R)w73-1	Df(2R)w73-2	Df(2R)w45-19g	Df(2R)BSC29	
CG8806	45D5-45D5	*preli-like*	~~Df(2R)w45-30n~~	Df(2R)Np5	Df(2R)wun-GL	Df(2R)w73-1	Df(2R)w73-2	Df(2R)w45-19g	Df(2R)BSC29	
CG8808	45D5-45D7	*Pyruvate dehydrogenase kinase*	~~Df(2R)w45-30n~~	Df(2R)Np5	Df(2R)wun-GL	Df(2R)w73-1	Df(2R)w73-2	Df(2R)w45-19g	Df(2R)BSC29	
CG11804	45D7-45D8	*ced-6*	~~Df(2R)w45-30n~~	Df(2R)Np5	Df(2R)wun-GL	Df(2R)w73-1	Df(2R)w73-2	Df(2R)w45-19g	Df(2R)BSC29	
CG33758	45D8-45D8	-	~~Df(2R)w45-30n~~	Df(2R)Np5	Df(2R)wun-GL	Df(2R)w73-1	Df(2R)w73-2	Df(2R)w45-19g	Df(2R)BSC29	
CG33757	45D8-45D8	-	~~Df(2R)w45-30n~~	Df(2R)Np5	Df(2R)wun-GL	Df(2R)w73-1	Df(2R)w73-2	Df(2R)w45-19g	Df(2R)BSC29	
CG42332	45E1-45E1	*Calmodulin-binding transcription activator*	~~Df(2R)w45-30n~~	Df(2R)Np5				Df(2R)w45-19g	Df(2R)BSC29	
CG1916	45E1-45E1	*Wnt oncogene analog 2*	~~Df(2R)w45-30n~~	Df(2R)Np5				Df(2R)w45-19g	Df(2R)BSC29	
CG42344	45E3-45F1	*bruchpilot*	~~Df(2R)w45-30n~~	Df(2R)Np5					Df(2R)BSC29	

Colours distinguish between deficiencies. Only those genes deleted by deficiency *Df(2R)Px2* are depicted, other deficiencies may extend outside the region shown. Horizontal shading = screen result was negative for a phenotype; diagonal shading = screening not complete.

Annotation ID	Cytological location	Name	Overlaps			
CG3385	60C5-60C6	*nervy*	***Df(2R)Px2***	***Df(2R)Exel6082***		
CG3401	60C6-60C6	*beta-Tubulin at 60D*	***Df(2R)Px2***	***Df(2R)Exel6082***		
CG4354	60C6-60C6	*slow border cells*	***Df(2R)Px2***	***Df(2R)Exel6082***		
CG3394	60C6-60C6	-	***Df(2R)Px2***	***Df(2R)Exel6082***		
CG3411	60C6-60C7	*blistered*	***Df(2R)Px2***	***Df(2R)Exel6082***		
CG4356	60C7-60C7	*muscarinic Acetylcholine Receptor 60C*	***Df(2R)Px2***	***Df(2R)Exel7185***		
CG13578	60C7-60C7	-	***Df(2R)Px2***	***Df(2R)Exel7185***		
CR33537	60C7-60C7	*transfer RNA:asn5:60C*	***Df(2R)Px2***	***Df(2R)Exel7185***		
CG4527	60C7-60C8	*Sterile20-like kinase*	***Df(2R)Px2***	***Df(2R)Exel7185***		
CG3416	60C8-60C8	*Mov34*	***Df(2R)Px2***	***Df(2R)Exel7185***	***Df(2R)ED4071***	***Df(2R)ED4061***
CG4545	60C8-60C8	*Serotonin transporter*	***Df(2R)Px2***	***Df(2R)Exel7185***	***Df(2R)ED4071***	***Df(2R)ED4061***
CG3419	60C8-60C8	-	***Df(2R)Px2***	***Df(2R)Exel7185***	***Df(2R)ED4071***	***Df(2R)ED4061***
CG15873	60C8-60C8	-	***Df(2R)Px2***	***Df(2R)Exel7185***	***Df(2R)ED4071***	***Df(2R)ED4061***
CG15874	60C8-60C8	*Phosphoglycerate mutase 5-2*	***Df(2R)Px2***	***Df(2R)Exel7185***	***Df(2R)ED4071***	***Df(2R)ED4061***
CG3483	60C8-60C8	-	***Df(2R)Px2***	***Df(2R)Exel7185***	***Df(2R)ED4071***	***Df(2R)ED4061***
CG42310	60C8-60C8	*prominin*	***Df(2R)Px2***	***Df(2R)Exel7185***	***Df(2R)ED4071***	***Df(2R)ED4061***
CG42383	60C8-60C8	-	***Df(2R)Px2***	***Df(2R)Exel7185***	***Df(2R)ED4071***	***Df(2R)ED4061***
CG13591	60D1-60D1	*Suppressor of Stellate-like*	***Df(2R)Px2***	***Df(2R)Exel7185***	***Df(2R)ED4071***	***Df(2R)ED4061***
CG4569	60D1-60D1	*Proteasome 28kD subunit 1B*	***Df(2R)Px2***	***Df(2R)Exel7185***	***Df(2R)ED4071***	***Df(2R)ED4061***
CG13580	60D1-60D1	*Caldesmon-related protein*	***Df(2R)Px2***	***Df(2R)Exel7185***	***Df(2R)ED4071***	***Df(2R)ED4061***
CG4563	60D1-60D1	-	***Df(2R)Px2***	***Df(2R)Exel7185***	***Df(2R)ED4071***	***Df(2R)ED4061***
CG3492	60D1-60D1	-	***Df(2R)Px2***	***Df(2R)Exel7185***	***Df(2R)ED4071***	***Df(2R)ED4061***
CG3494	60D1-60D1	-	***Df(2R)Px2***	***Df(2R)Exel7185***	***Df(2R)ED4071***	***Df(2R)ED4061***
CG16837	60D1-60D1	-	***Df(2R)Px2***	***Df(2R)Exel7185***	***Df(2R)ED4071***	***Df(2R)ED4061***
CG13579	60D1-60D1	-	***Df(2R)Px2***	***Df(2R)Exel7185***	***Df(2R)ED4071***	***Df(2R)ED4061***
CG13589	60D1-60D1	-	***Df(2R)Px2***	***Df(2R)Exel7185***	***Df(2R)ED4071***	***Df(2R)ED4061***
CG13590	60D1-60D1	-	***Df(2R)Px2***	***Df(2R)Exel7185***	***Df(2R)ED4071***	***Df(2R)ED4061***
CR42645	60D1-60D1	*Yu*	***Df(2R)Px2***	***Df(2R)Exel7185***	***Df(2R)ED4071***	***Df(2R)ED4061***
CG4589	60D3-60D3	*Letm1*	***Df(2R)Px2***	***Df(2R)Exel7185***	***Df(2R)ED4071***	***Df(2R)ED4061***
CG13581	60D3-60D3	-	***Df(2R)Px2***	***Df(2R)Exel7185***	***Df(2R)ED4071***	***Df(2R)ED4061***
CG42289	60D3-60D3	*Ionotropic receptor 60b*	***Df(2R)Px2***	***Df(2R)Exel7185***	***Df(2R)ED4071***	***Df(2R)ED4061***
CR42290	60D3-60D3	*Ionotropic receptor 60c*	***Df(2R)Px2***	***Df(2R)Exel7185***	***Df(2R)ED4071***	***Df(2R)ED4061***
CG42291	60D3-60D3	*Ionotropic receptor 60d*	***Df(2R)Px2***	***Df(2R)Exel7185***	***Df(2R)ED4071***	***Df(2R)ED4061***
CG4612	60D3-60D4	-	***Df(2R)Px2***	***Df(2R)Exel7185***	***Df(2R)ED4071***	***Df(2R)ED4061***
CG13592	60D4-60D4	*Ionotropic receptor 60e*	***Df(2R)Px2***		***Df(2R)ED4071***	***Df(2R)ED4061***
CG13585	60D4-60D4	-	***Df(2R)Px2***		***Df(2R)ED4071***	***Df(2R)ED4061***
CG11413	60D4-60D4	-	***Df(2R)Px2***		***Df(2R)ED4071***	***Df(2R)ED4061***
CG30169	60D4-60D4	*Breast cancer 2, early onset homolog*	***Df(2R)Px2***		***Df(2R)ED4071***	***Df(2R)ED4061***
CG4622	60D4-60D5	-	***Df(2R)Px2***		***Df(2R)ED4071***	***Df(2R)ED4061***
CG13586	60D4-60D5	*ion transport peptide*	***Df(2R)Px2***		***Df(2R)ED4071***	***Df(2R)ED4061***
CG4634	60D5-60D5	*Nucleosome remodeling factor - 38kD*	***Df(2R)Px2***		***Df(2R)ED4071***	***Df(2R)ED4061***
CG11414	60D5-60D5	-	***Df(2R)Px2***		***Df(2R)ED4071***	***Df(2R)ED4061***
CG11416	60D5-60D5	*unconventional prefoldin RPB5 interactor*	***Df(2R)Px2***		***Df(2R)ED4071***	***Df(2R)ED4061***
CG12252	60D5-60D5	-	***Df(2R)Px2***		***Df(2R)ED4071***	***Df(2R)ED4061***
CG3511	60D5-60D5	-	***Df(2R)Px2***		***Df(2R)ED4071***	***Df(2R)ED4061***
CG3522	60D5-60D5	*Start1*	***Df(2R)Px2***		***Df(2R)ED4071***	***Df(2R)ED4061***
CG33527	60D5-60D5	*IFamide*	***Df(2R)Px2***		***Df(2R)ED4071***	***Df(2R)ED4061***
CG4681	60D5-60D7	-	***Df(2R)Px2***		***Df(2R)ED4071***	***Df(2R)ED4061***
CG3541	60D7-60D8	*piopio*	***Df(2R)Px2***		***Df(2R)ED4071***	***Df(2R)ED4061***
CG13587	60D8-60D9	-	***Df(2R)Px2***		***Df(2R)ED4071***	***Df(2R)ED4061***
CG13594	60D9-60D10	-	***Df(2R)Px2***		***Df(2R)ED4071***	***Df(2R)ED4061***
CG4692	60D9-60D9	-	***Df(2R)Px2***		***Df(2R)ED4071***	***Df(2R)ED4061***
CG3548	60D9-60D9	-	***Df(2R)Px2***		***Df(2R)ED4071***	***Df(2R)ED4061***
CG3565	60D9-60D9	-	***Df(2R)Px2***		***Df(2R)ED4071***	***Df(2R)ED4061***
CG3570	60D9-60D9	-	***Df(2R)Px2***		***Df(2R)ED4071***	***Df(2R)ED4061***
CG4707	60D9-60D9	-	***Df(2R)Px2***		***Df(2R)ED4071***	***Df(2R)ED4061***
CG3608	60D9-60D9	-	***Df(2R)Px2***		***Df(2R)ED4071***	***Df(2R)ED4061***
CG4741	60D9-60D9	-	***Df(2R)Px2***		***Df(2R)ED4071***	***Df(2R)ED4061***
CG42361	60D9-60D9	-	***Df(2R)Px2***		***Df(2R)ED4071***	***Df(2R)ED4061***
CG42360	60D9-60D9	-	***Df(2R)Px2***		***Df(2R)ED4071***	***Df(2R)ED4061***

Colours distinguish between deficiencies. Only those genes deleted by *Df(2L)S2590* are depicted; other deficiencies may extend outside the region shown. Horizontal shading = screen result was negative for a phenotype; diagonal shading = screening not complete; dotted fill = screen result was positive for a matched phenotype. Highlighted in bold and with border is *CG34393*, a candidate gene selected for further study.

Annotation ID	Cytological location	Name	Overlaps			
CG9660	23D1-23D2	toucan	*Df(2L)BSC28*	*Df(2L)JS32*	*Df(2L)S2590*	*Df(2L)BSC162*
CG15403	23D2-23D2	-	*Df(2L)BSC28*	*Df(2L)JS32*	*Df(2L)S2590*	*Df(2L)BSC162*
CG12400	23D3-23D3	-	*Df(2L)BSC28*		*Df(2L)S2590*	*Df(2L)BSC162*
CG12399	23D3-23D3	Mothers against dpp	*Df(2L)BSC28*		*Df(2L)S2590*	*Df(2L)BSC162*
CG8825	23D4-23D4	glaikit	*Df(2L)BSC28*		*Df(2L)S2590*	*Df(2L)BSC162*
CG31953	23D4-23D4	-	*Df(2L)BSC28*		*Df(2L)S2590*	*Df(2L)BSC162*
CG3488	23D4-23D4	alpha/beta hydrolase2	*Df(2L)BSC28*		*Df(2L)S2590*	*Df(2L)BSC162*
CR31734	23D4-23D4	transfer RNA:ser7:23Eb	*Df(2L)BSC28*		*Df(2L)S2590*	
CG34406	23D4-23D4	-	*Df(2L)BSC28*		*Df(2L)S2590*	
CR31951	23D4-23D4	transfer RNA:ser7:23Ea	*Df(2L)BSC28*		*Df(2L)S2590*	
CG31698	23D4-23D4	-	*Df(2L)BSC28*		*Df(2L)S2590*	
CG15404	23D4-23D4	-	*Df(2L)BSC28*		*Df(2L)S2590*	
CG34393	**23D5-23D5**	-	*Df(2L)BSC28*		*Df(2L)S2590*	
CG3347	23E1-23E1	-	*Df(2L)BSC28*		*Df(2L)S2590*	
CG3332	23E1-23E1	-	*Df(2L)BSC28*		*Df(2L)S2590*	
CG9664	23E1-23E1	-	*Df(2L)BSC28*		*Df(2L)S2590*	
CG9663	23E1-23E3	-	*Df(2L)BSC28*		*Df(2L)S2590*	*Df(2L)Exel8008*
CG15406	23E3-23E3	-			*Df(2L)S2590*	*Df(2L)Exel8008*
CG3277	23E3-23E3	-			*Df(2L)S2590*	*Df(2L)Exel8008*
CG3326	23E3-23E3	-			*Df(2L)S2590*	*Df(2L)Exel8008*
CG8837	23E3-23E4	-			*Df(2L)S2590*	*Df(2L)Exel8008*

Deficiency	**No of CNSs examined**	**Total motor neurons examined *n***	**Motor neuron subtype (phenotype observed/total number of subtype examined)**									
			VO4/5	**DO5**	**VL2**	**VT**	**VUM**	**SN1**	**RP4**	**L-type**	**Terminal ganglion**	**Thoracic/unidentifiable**
Df(2L)al	17	20	1/4[a]	1	0	0	1	0	1	1	1/7[b]	5
Overlapping stocks:												
Df(2L)net-PMF	not tested											
Df(2L)BSC4	45	33	2	2	2	3	0	3	2	3	9	7
Df(2L)BSC16	34	30	6	4	4	1	0	1	0	6	6	3
Df(2L)S2	33	10	5	0	1	1	0	0	0	3	0	0
Df(2L)BSC107	not tested											

[a]loss of secondary branching phenotype

[b]blebbing of fine dendrites phenotype

Deficiency	No of CNSs examined	Total motor neurons examined *n*	Motor neuron subtype (phenotype observed/total number of subtype examined)										
			VO4/5	**DO5**	**VL2**	**VT**	**VUM**	**SN1**	**RP4**	**L-type**	**RP5**	**Terminal ganglion**	**Thoracic/unidentifiable**
Df(2L)TE35BC-24	10	13	1/1[a]	1/1[b]	2	0	0	1	0	1	1	3	3[c]
	Overlapping stocks:												
Df(2L)TE35BC-34	not tested												
Df(2L)Sco^{rv14}	not tested												
Df(2L)r10	not tested												
Df(2L)Exel8034	not tested												
Df(2L)Sco^{rv25}	not tested												
Df(2L)Sco^{rv10}	not tested												
Df(2L)Exel7063	not tested												
Df(2L)RA5	not tested												

[a] Reduced anterior-posterior spread

[b] Aberrantly crosses midline

[c] Unidentifiable as their morphology was so unusual in terms of anterior-posterior spread/midline attraction

Deficiency	**No of CNSs examined**	**Total motor neurons examined *n***	**Motor neuron subtype (phenotype observed/total number of subtype examined)**									
			VO4/5	**DO5**	**VL2**	**VT**	**VUM**	**SN1**	**RP4**	**L-type**	**Terminal ganglion**	**Thoracic/unidentifiable**
Df(2R)Np5	12	9	1	0	0	1/1[a]	0	1	0	0	3	3
Overlapping stocks:												
Df(2R)H3E1	18	7	0	0	1		1	0	0	1	1	3
Df(2R)w73-1	not tested											
Df(2R)w73-2	not tested											
Df(2R)w45-30n	18	10	0	0	4	0	0	2	0	1	2	1
Df(2R)G53	31	5	0	0	0	0	0	0	0	0	3	2
Df(2R)wun-GL	not tested											
Df(2R)w45-19g	not tested											
Df(2R)BSC29	not tested											

[a]axon targeting; aberrant dendrite positioning in the mediolateral axis phenotypes

Deficiency	**No of CNSs examined**	**Total motor neurons examined *n***	**Motor neuron subtype (phenotype observed/total number of subtype examined)**									
			VO4/5	**DO5**	**VL2**	**VT**	**VUM**	**SN1**	**RP4**	**L-type**	**Terminal ganglion**	**Thoracic/unidentifiable**
Df(2R)Px2	16	9	0	0	2	1	0	0	0	2	2/2[a]	2
Overlapping stocks:												
Df(2R)Exel6082	12	0										
Df(2R)Exel7185	33	0										
Df(2R)ED4071	1	0										
Df(2R)ED4061	not tested											

[a]one neuron had blebbing and overgrowth of fine dendrites anteriorly while the other had only dendritic overgrowth.

Deficiency	**No of CNSs examined**	**Total motor neurons examined *n***	**Motor neuron subtype (phenotype observed/total number of subtype examined)**									
			VO4/5	**DO5**	**VL2**	**VT**	**VUM**	**SN1**	**RP4**	**L-type**	**Terminal ganglion**	**Thoracic/unidentifiable**
Df(2L)S2590	25	47	2/5[a]	0/3	0/1	0/2	0/1	0/2	0/2	0/1	0	8
Overlapping deficiencies												
Df(2L)JS32	not tested											
Df(2L)BSC162	41	22	1/2[b]	2	3	0	1	0	1	1	4	9
Df(2L)BSC28	12	16	3	0	4	0	1	0	0	2/2[c]	5	1/1
Df(2L)Exel8008	13	14	2	0	2	1	2	1	0	3	1	2

[a]These neurons had a phenotype where dendrites were aberrantly attracted to the midline or failed to cross the midline appropriately.

[b]one neuron seems to have a loss of fine, higher order branching, though it is unclear whether this reflects slight differences in age, GFP expression, image or image processing artefacts.

[c]One neuron was unidentifiable, though its primary branches suggested it was an ‘L-type’ neuron. Both neurons had a phenotype where some dendrites were aberrantly attracted to the midline/crossed the midline.